Report of the
2nd International UV Filter Radiometer comparison
UVC-II

PMOD/WRC, WCC-UV

Davos, Switzerland

25 May to 5 October 2017

G. Hülsen and J. Gröbner

Contents

Summary **4**
1. Introduction **5**
2. Setup and measurements **6**
3. Instrumentation for the absolute calibration **9**
4. Laboratory characterisation **12**
4.1. Relative spectral response facility 12
4.2. Angular response facility 14
5. Calculation of the calibration factors **16**
5.1. Spectral correction function, f_n 16
5.2. Cosine correction function, Coscor 17
5.3. Absolute calibration factor, C 18
6. Uncertainty Budget **19**
6.1. WCCUV broadband radiometer calibration 19
6.2. Manufacturer calibration of broadband radiometers 20
6.3. Reference Spectroradiometer QASUME 20
7. Campaign Results **21**
7.1. Spectroradiometer intercomparison 21
7.2. Radiometer Comparison 24
8. Discussion **27**
8.1. Data processing 27
8.1.1. Neglecting the spectral mismatch between the instrumental spectral response and the nominal response of the desired action spectrum 27
8.1.2. Neglecting the mismatch between the instrumental angular response and the nominal cosine response 28
8.2. Humidity 29
8.3. History 29
8.4. Summary 30
9. Comments **31**
9.1. Radiometer maintenance 31
9.2. Checklist 32
Acknowledgements **33**
References **34**
Annex **35**

Summary

The main task of the WCCUV is to assist WMO members operating WMO/GAW stations to link their UV radiation observations to the WMO/GAW reference scale through comparisons of the station instruments with the standard instruments operated by PMOD/WRC. Therefore an “International UV Filter Radiometer Comparison” was organised at the WCCUV of PMOD/WRC. The campaign lasted from 25th May to 5th October 2017; it is located at 1610 m a.s.l. in the Swiss Alps.

A total of 75 UV filter radiometers from 37 Countries participated at the campaign, of which 22 from Europe. The nine different radiometer types represented at the campaign were Kipp & Zonen / Sintec (28), Yankee UVB-1 (11), analog and digital Solar Light V. 501 (19/9), Delta Ohm LP UVI 02 (2), EKO MS-212W (2) and each one of Indium Sensor 1E.1-081, Genicom GUVB, Eppley TUVR and Middleton Solar UVR1-B2. The filter weighting function were mostly approximating the erythemal action spectrum and some UVB, UVA and UVG. 16 radiometers were not well maintained according to the recommendations of Webb et al. 2007.

The two reference spectroradiometers QASUME and QASUMEII of the WCCUV operated during the campaign agreed within ±2%. The atmospheric conditions during the campaign varied between fully overcast to clear skies and allowed a reliable calibration for all instruments.

The standard calibration methodology, using the instrumental spectral as well as the angular response functions measured in the laboratory, provided remarkable agreement with the reference spectroradiometer, with expanded uncertainties (k=2) of around 6% for most instruments.

The measurements of the broadband radiometers were analysed both with the PMOD/WRC calibration as well as the calibration used by the home institutes. The average date of the user calibration was five years prior to this campaign (e.g. 2012) and 40 out of the 75 instruments used a single calibration factor, instead of the suggested calibration matrix [5, 7, 8]. The relative differences between the measurements using the user calibration and the one from PMOD/WRC varied between 0.04% to differences larger than 50% for specific instruments.

1. Introduction

The international UV filter radiometer comparison was held at the World Calibration Center for UV (WCCUV) of the Physikalisch-Meteorologisches Observatorium Davos, World Radiation Center (PMOD/WRC) from 25th May to 5th October 2017.

The campaign was initiated to fulfil the main task of the WCCUV, which is to assist WMO Members operating WMO/GAW stations to link their UV radiation observations to the WMO/GAW reference scale through comparisons of the station instruments with the standard instruments operated by PMOD/WRC. The absolute calibration of the WCCUV is supported by CMC's within the CIPM MRA[1].

The objective of the campaign was to provide a calibration traceable to the WCCUV reference for all participating radiometers, in view of homogenising UV measurements in all participating countries.

The specific tasks of the campaign were to individually characterise each radiometer with respect to the relative spectral and angular responsivity in the laboratory following the standard operating procedures of the WCCUV. The absolute calibration was obtained by direct comparison of solar irradiance measurements with the WCCUV reference spectroradiometers on the roof platform of PMOD/WRC.

This filter radiometer comparison campaign followed three similar campaigns held in 1995 in Helsinki, Finland [1], in 1999 in Thessaloniki, Greece [2] and in 2006 in Davos, Switzerland [3]. 75 broadband radiometers from 37 Institutions participated at the comparison campaign. The radiometers were for the most part reference instruments within their respective regional or national networks.

In addition, to providing traceability to the solar UV irradiance reference of the World Calibration Center for UV (WCC-UV), a calibration facility intercomparison was organized. A subset of 8 radiometers participated to this activity from the institutions NOAA and ISO-CAL (USA), AEMET and INTA (Spain), LAP (Greece), IBK (Austria), ARPA-Piemonte (Italy) and BIRA-IASB (Belgium). The task of the calibration facility intercomparison was to calibrate and characterize the radiometer before and after the campaign. The outcome of this intercomparison will be discussed in a separate publication.

The measurement campaign at PMOD/WRC allowed comparing the original calibration with the WCCUV-based calibration on the one hand, and to estimate the variability between the UV radiometer measurements based on calibrations originating from different sources (manufacturer or national calibration laboratory) on the other hand.

The result of the campaign was the release of calibration certificates to all participating institutes traceable to the WCCUV reference and thus to the international system of units.

[1] PMOD/WRC follows the requirements for the competence of testing and calibration laboratories according to ISO/IEC 17025. PMOD/WRC is a designated institute of the Swiss Federal Office of Metrology, the Swiss signatory of the CIPM MRA (International Committee for Weights and Measures - Mutual Recognition Arrangement).

2. Setup and measurements

The calibration and intercomparison campaign took place at PMOD/WRC, Switzerland. The period from 19 June to 18 August 2017 was selected for the calibration. The measurement platform is located on the roof of PMOD/WRC at 1610 m a.s.l., latitude 46.8 N, longitude 9.83 E. The measurement site is in the Swiss Alps and its horizon is limited by mountains; the Davos valley runs NE to SW.

Figure 1. Roof platform of PMOD/WRC.

The laboratory characterisations – spectral and angular responsivity measurements – were accomplished during the campaign. Due to the early arrival of 9 radiometers the calibration campaign started on 25th May. The radiometers were installed on the roof platform of PMOD/WRC and acquired enough calibration days before the scheduled start of the campaign. Most radiometers arrived beginning of June. Late arrivals used the last days of the scheduled campaign period. Four radiometers had to be repaired and needed extended measurement days until 5th October.

The QASUME and QASUMEII [4] spectroradiometers were installed in April 2017. QASUMEII operated continuously until beginning of October, whereas QASUME was traveling to site audits in Spain from May 22 till June 14, 2017.

The measurement data used for the calibration were obtained in the period 25th May to 5th October, totalling 134 measurement days. The measurement conditions in summer 2017 were very variable, with periods of clear sky, clouds, rain and snow.

Figure 2. Temperature and precipitation.

Figure 3. UVI index in Davos, 2017.

The total column ozone was obtained from Brewer spectrophotometer #163 located next to QASUME. From 19th May till 30th June this Brewer was participating in the 12th RBCC-E in Spain. Therefore, OMI Ozone data where used in this period. The OMI data were validated using Brewer #072 located around 30 m away from QASUME. The total column ozone varied between 256 DU and 423 DU with a mean value of 304 DU over the measurement period.

Figure 4. Total ozone column over Davos.

3. Instrumentation for the absolute calibration

75 filter radiometers from 58 Institutions of 37 Countries took part in this campaign. Their weighted functions for solar irradiance are: UVE (erythemal) [5], UVB (280nm-315nm), UVB320 (280nm-320nm), UVA (315nm-400nm) and UVG (280nm-400nm).

Table 1. Summary of participating radiometers.

Number	Manufacturer	Type	Weighting
1	Kipp & Zonen	CUV4	UVG
8	Kipp & Zonen	UV-S-AE-T / UV-S-AB-T	UVA+UVE/UVB
3	Kipp & Zonen	UV-S-A-T	UVA
2	Kipp & Zonen	UV-S-B-T	UVB
11	Kipp & Zonen	UV-S-E-T	UVE
2	Sintec	UV-S-E-T	UVE
1	Sintec	UV-S-AE-T	UVA+UVE
16	Solar Light	SL501 (analog)	UVA
3	Solar Light	SL501 (analog)	UVE
9	Solar Light	SL501 (digital)	UVE
11	YES	UVB-1	UVE/UVB
2	Delta Ohm	LP UVI 02 AC/AV	UVE
1	Indium Sensor	1E.1-081	UVE
1	Genicom	GUVB-T12GD-3LWH6	UVE
1	Eppley	TUVR	UVG
2	EKO	MS-212W	UVE
1	Middleton Solar	UVR1-B2	UVB

The analog voltages of the radiometers were acquired with a Campbell CR7 logger (reference: Keysight 34420A Micro-Ohm Meter; calibration date: 9th February 2017) every 10 s. The two EKO systems used their own data acquisition system. The data from the digital SL-501 data acquisition recorders were read out using a custom interface with an interval of 2 s. Their sensitivity factor was set to 10 to improve their resolution.

Figure 5. CR7 logger (left) and connection panel 1 and 2.

The data of the two reference spectroradiometers QASUME and QASUMEII provided the reference for the outdoor measurements. Both spectroradiometers were synchronised and measured solar irradiance spectra in the range 290 nm to 420 nm every 15 or 30 minutes.

Figure 6. Picture of the main set of participating radiometers. SL (front), KZ/Sintec (middle), YES (back), Delta Ohm, Indium Sensor, Genicom, Eppley, EKO and Middleton Solar (last row).

Table 2. List of participating radiometers; PMOD/WRC (blue), laboratory intercomparison (red).

Type	SN	Country	Institute	Calibration Factors
KZ CUV4	080018	USA	National Renewable Energy Lab (NREL)	C
KZ UV-S-AE-T	000526	Italy	ARPA Valle d'Aosta	C, f_n, Coscor
KZ UV-S-AE-T	020614	United Kingdom	Centre for Atmospheric Science, University of Manchester	C, f_n, Coscor
KZ UV-S-AE-T	070635	Germany	DWD/MOL-RAO	C, f_n
KZ UV-S-AE-T	080002	France	Institut Pierre Simon Laplace (IPSL)	C, f_n, Coscor
KZ UV-S-AE-T	080003	Italy	ARPA Piemonte	C, f_n
KZ UV-S-AB-T	110141	USA	ISO-CAL North America	C
KZ UV-S-AE-T	120023	Ecuador	INAMHI (Sistemas Tecnològicos Alcatecni Cìa. Ltda)	C
KZ UV-S-AB-T	120132	Spain	CENER	C
KZ UV-S-E-T	560	Switzerland	PMOD/WRC	C, f_n, Coscor
KZ UV-S-E-T	070642	Hong Kong	Hong Kong Observatory	C
KZ UV-S-E-T	070643	Spain	Universidad de Extremadura	C, Fn
KZ UV-S-A-T	080005	Spain	Izana Atmospheric Research Center (AEMET)	C
KZ UV-S-A-T	100013	Hong Kong	Hong Kong Observatory	C
KZ UV-S-E-T	110042	Hong Kong	Hong Kong Observatory	C
KZ UV-S-A-T	110062	Russia	Lomonosov Moscow State University, Faculty of Geography	C, f_n
KZ UV-S-E-T	120056	Russia	Lomonosov Moscow State University, Faculty of Geography	C, f_n
KZ UV-S-B-T	120076	Denmark	Danish Meteorological Institute	C
KZ UV-S-B-T	120077	France	Institut Pierre Simon Laplace (IPSL)	C
KZ UV-S-E-T	150110	Estonia	Estonian Environment Agency	C
KZ UV-S-E-T	150124	France	Laboratoire de l'Atmosphere et des Cyclones, La Reunion	C
KZ UV-S-E-T	160142	Spain	Agencia Estatal de Meteorologia (AEMET)	C, f_n, Coscor
KZ UV-S-B-T	160158	Taiwan	National Central University	C
KZ UV-S-E-T	160177	Chile	Dirección General de Aeronàutica Civil	C
KZ UV-S-E-T	170204	South Africa	NMISA	C
SCI UV-S-E-T	00341	Germany	Dept. of Dermatology / Medical Fac. TU Dresden	C
SCI UV-S-AE-T	00400	France	Laboratoire d'Optique Atmospherique, University Lille	C, f_n^*
SCI UV-S-E-T	00407	Germany	Meteorologisches Institut München	C, f_n
SL501	1453	Finland	FMI Helsinki	C
SL501	1492	Switzerland	PMOD/WRC	C, f_n, Coscor
SL501	1493	Switzerland	PMOD/WRC	C, f_n, Coscor
SL501	1890	France	Reuniwatt	C
SL501	1903	Switzerland	Federal Office of Meteorology and Climatology MeteoSwiss	C, f_n, Coscor
SL501	2839	France	ASS Sécurité Solaire	C
SL501	2875	Switzerland	PMOD/WRC	C, f_n, Coscor
SL501	3564	USA	Colorado State University - UV-B Program	C
SL501	3860	Switzerland	PMOD/WRC	C, f_n, Coscor
SL501	4402	Lithuania	Lithuanian Hydrometeorological Service	C
SL501	4405	Lithuania	Lithuanian Hydrometeorological Service	C
SL501	4433	USA	Colorado State University - UV-B Program	C
SL501	5760	Luxembourg	Computarium and meteoLCD Classique Diekirch	C
SL501	5790	Italy	CNR-IBIMET	C, f_n, Coscor
SL501	8887	Norway	Norwegian Radiation Protection Authority (NRPA)	C
SL501	19474	Portugal	Instituto Português do Mar e da Atmosfera	C
SL501	19488	México	Instituto de Geofísica, Universidad Nacional Autónoma de	C
SL501	19507	Austria	Innsbruck Medical University, Division for Biomed. Physics	C, f_n^*
SL501	23148	Taiwan	Central Weather Bureau	C
SL501digital	0922	Sweden	Swedish Meteorological and Hydrological Institute (SMHI)	C, f_n, Coscor
SL501digital	0936	Poland	Institute of Meteorology and Water Management National	C, f_n, Coscor
SL501digital	1119	Poland	Research Institute	C, f_n, Coscor
SL501digital	2733	Czech Republic	CHMI	C, f_n, Coscor
SL501digital	4811	Slovak Republic	Slovak Hydrometeorological Institute	C, f_n, Coscor
SL501digital	4834	Peru	National Service of Meteorology and Hidrology of Peru	C, f_n, Coscor
SL501digital	10403	Hungary	Hungarian Meteorological Service, György Observatory	C, f_n, Coscor
SL501digital	14078	Argentina	Servicio Meteorologico Nacional	C, f_n, Coscor
SL501digital	16721	Brazil	Universidade de São Paulo	C
YES UVB-1	000904	USA	National Oceanic and Atmospheric Administration (NOAA)	C, f_n, Coccor
YES UVB-1	010938	Switzerland	PMOD/WRC	C, f_n, Coscor
YES UVB-1	030520	Spain	Agencia Estatal de Meteorologia (AEMET)	C, f_n, Coscor
YES UVB-1	030525	Iceland	Icelandic Meteorological Office	C
YES UVB-1	090703	Argentina	CITEDEF	C
YES UVB-1	921106	USA	National Renewable Energy Lab (NREL)	C
YES UVB-1	921116	Greece	Aristotle Uni. of Thessaloniki, Lab. of Atmos. Physics (LAP)	C, f_n
YES UVB-1	930204	USA	Colorado State University - UV-B Program	C
YES UVB-1	960819	USA	Colorado State University - UV-B Program	C
YES UVB-1	990608	Spain	Instituto Nacional de T´ecnica Aerospacial (INTA)	C, f_n, Coscor
YES UVB-1	990703	Hong Kong	Hong Kong Observatory	C
LP UVI 02 AC	15010872	Italy	Delta Ohm	C, f_n, Coscor
LP UVI 02 AV	17010973	Italy	Delta Ohm	C
Indium Sensor	12688.17	Deutschland	IndiumSensor GmbH	C
Genicom	C-586	Republic of Korea	Genicom	C
Eppley TUVR	26919	Greece	National Observatory of Athens	C
EKO MS-212W	S11132.04	Belgien	Royal Belgian Institute for Space Aeronomy, BIRA-IASB	C, f_n, Coscor
EKO MS-212W	S17008.02	Japan	EKO Instruments	C
MS UVR1-B2	5089	Australia	Middleton Solar	C

4. Laboratory characterisation

The spectral and angular responsivity functions (SRF and ARF) of the radiometers were measured in the WCCUV laboratory at PMOD/WRC. The method is described in the following four quality management documents: QM-PD-UV-0045 and QM-SOP-UV-0062 (SRF); QM-PD-UV-0043 and QM-SOP-UV-0060 (ARF).

4.1. Relative spectral response facility

The relative spectral response facility consists of an Acton SP2500 double monochromator with gratings of 2400 lines/mm. The wavelength can be selected within the range 200 nm to 1200 nm and the chosen slit width yields a triangular slit function with a full width at half maximum of 2.0 nm. The light of a 1000 W Xenon lamp is focused onto the entrance slit. A lens array installed after the exit slit produces a homogeneous 12 mm x 12 mm reference plane.

Behind the lens array a quartz plate mounted at 45° relative to the vertical transmits about 92% of the radiation towards the test detector while about 8% are deflected towards a photodiode, which is used to monitor the stability of the monochromator signal.

Due to the large receiving surfaces of some radiometers only part of those detectors could be illuminated by the monochromatic light source. Thus, spatial inhomogeneities of the receiving surface of the radiometer were not considered during the SRF measurement.

Figure 7. Spectral Response Setup of the WCCUV.

The relative spectral throughput of the setup was determined by measuring the outgoing radiation with a reference silicon diode and was verified using the QASUME spectroradiometer between 270 nm and 420 nm, with a step of 2 nm.

The wavelength scale of the SRF setup was determined by two methods which produced equivalent results:

- A mercury discharge lamp was placed at the entrance of the monochromator and the throughput measured with a photodiode is used to determine the slit function and thus the wavelength offset.
- The slit function measurements of the complete setup (with Xe-Lamp source) with the QASUME spectroradiometer allowed the determination of the wavelength offset.

The variability of the radiometer dark signal was monitored for five minutes prior to the SRF measurement, as indicator for the minimum signal to noise ratio of the radiometer. The SRF measurement itself was obtained over the wavelength range 420 nm down to 270 nm with a step size of 2 nm.

The Solar Light data-loggers of the digital SL501 radiometers were set to a sensitivity of 10 to increase the resolution of the stored measurements. To further increase the signal to noise ratio, the output signal was sampled 10 to 20 times at each wavelength setting of the monochromatic light source.

The SRF was obtained from the measurements by subtracting the dark signal measured before initiating the wavelength scan, and normalising it to the maximum signal.

Figure 8. SRF of a KZ radiometer.

4.2. Angular response facility

The angular response function of the radiometers was measured on a 3 m long optical bench. A 1000 W Xenon lamp was mounted at one end of the optical bench and served as radiation source. The detector was mounted on a goniometer at the other end with the vertical rotation axis passing through the plane of the receiving surface of the radiometer. The resolution of the rotation stage was 29642 steps per degree, or 0.12 arcseconds. The homogeneity of the radiation at the detector reference plane was measured and optimised to better than 1% over the receiving surface area of the detector. A baffle was placed in the beam path to reduce stray light and a WG305 filter with a 50% cut off at 303 nm removed radiation below approx. 300 nm.

Figure 9. Angular response setup of the WCCUV.

The normal alignment of the radiometer is done by a mirror tool, which reflected a laser beam in the optical axis. This method provided an adjustment precision of better than 0.1 degree.

The measurements were performed in two orientations of the detector so that the angular response could be determined for the four quadrants N, S, E, W; the N orientation being defined by the connector of the radiometer.

Figure 10. Mounting of an EKO MS-212W radiometer onto the ARF setup.

The ARF for each quadrant was obtained by normalising the measurements at each angle to the reference measurement at normal incidence. The cosine error of each quadrant was calculated from the ARF by assuming an isotropic radiation distribution and integrating it over the whole hemisphere. The final ARF was obtained by averaging the measurements of the four quadrants. Five instruments show a deviation between the four quadrants, which is an indication of a tilt of the sensor relative to the optical axis. Depending on the mounting of the radiometer this tilt can lead to an azimuth dependence of the solar measurements.

Figure 11. ARF of a KZ radiometer (left) and the corresponding cosine error (right).

5. Calculation of the calibration factors

The absolute calibration measurements were carried out on the roof of PMOD/WRC. The method is described in the two quality management documents QM-PD-UV-0041 and QM-SOP-UV-0058. A detailed description can be found in [6]. In the following the main steps of the procedure are summarized.

The calculation of the weighted irradiance from the radiometer data follows the equation published in [6,7]:

$$E_{CIE} = (U - U_{offset}) \cdot C \cdot f_n(SZA, TO_3) \cdot Coscor \quad \textbf{(1)}$$

where U and U_{offset} are the raw and dark signals from the radiometer respectively; C represents the absolute calibration factor determined for a solar zenith angle, SZA, of 40° and total column ozone, TO_3, of 300 DU. The conversion function, f_n, converts from the detector weighted solar irradiance to erythemal weighted irradiance (or other weighting function, see section 3)[2]. By definition the function is normalised to unity for a total ozone column of 300 DU and a solar zenith angle of 40°. *Coscor* corrects for the detector cosine error. The dark offset, U_{offset}, is determined every day during the night as the average over all measurements between 0 to 4 UT and 20 to 24 UT at PMOD/WRC.

5.1. Spectral correction function, f_n

The conversion function, f_n, accounts for the mismatch of the detector spectral responsivity and the norm weighting function and is calculated as

$$f(SZA, TO_3) = \frac{\int CIE(\lambda) E_{rad}(\lambda) d\lambda}{\int SRF(\lambda) E_{rad}(\lambda) d\lambda} \quad \textbf{(2)}$$

where E_{rad} represents a set of solar spectra calculated with a radiative transfer model for different SZA and TO_3. The SRF is obtained from the laboratory measurement described above, and CIE represents the selected action spectrum.

Figure 12. Spectral correction function of a KZ radiometer.

[2] Some users calculate f_n^* with a cosine correction function included.

Figure 13. Spectral correction function of a KZ radiometer as projections relative to the SZA (left) and TO_3 (right).

5.2. Cosine correction function, Coscor

The angular response of UV radiometers deviates from the nominal cosine response. The cosine correction function, *Coscor,* is used to correct the data. This correction depends on the atmospheric conditions and especially on the relative fraction of direct and diffuse radiation. The cosine correction assumes an isotropic diffuse radiation distribution; the fraction of direct and diffuse radiation is modelled by a radiative transfer model in dependence of the solar zenith angle. For the determination of the calibration factor only two cases were distinguished:

- Clear sky: A cosine correction function $1/f_{glo}$ in dependence on the SZA was used.
- Diffuse sky: Only the diffuse cosine correction factor $1/f_{dif}$ was applied to the calibration.

This simple approximation results in substantial uncertainties especially during rapidly changing cloud conditions. Therefore, only the clear or completely overcasted sky data were used for the calibration. The following equations illustrate the derivation of *Coscor*:

$$f_{dir} = \frac{ARF(\theta)}{\cos(\theta)}, \quad \textbf{(3)}$$

$$f_{dif} = 2 \cdot \int_0^{pi/2} ARF(\theta)\sin(\theta)d\theta, \quad \textbf{(4)}$$

$$f_{glo} = f_{dir}\frac{E_{dir}}{E_{glo}} + f_{dif}\frac{E_{dif}}{E_{glo}}, \quad \textbf{(5)}$$

where f_{dir} is the cosine error of the radiometer, f_{dif} represents the diffuse cosine error and f_{glo} the global cosine error of the radiometer.

Figure 14. Clear sky cosine correction function (f_{glo}) of a KZ (left) and a YES radiometer (right).

5.3. Absolute calibration factor, C

The calibration factor, *C,* is obtained by comparison with the solar spectrum measured by the spectroradiometer weighted with the SRF of the radiometer. Thus,

$$C = \frac{E_{DET}}{U_{DET} - U_{offset}} \cdot \frac{1}{Coscor} \cdot \frac{1}{f(40°, 300DU)}, \quad \textbf{(6)}$$

Figure 15. Calibration factors determined for the campaign period for a KZ radiometer. The plots show the inverse of C as defined in the equation above to facilitate the interpretation. A lower calibration factor means a lower signal measured with the radiometer.

6. Uncertainty Budget

6.1. WCCUV broadband radiometer calibration

The uncertainty budget for the calibration of UV broadband radiometers is defined in the quality management document QM-OA-UV-0036. The expanded uncertainty is composed of the following uncertainty contributions according to equation 6:

- **Ed** is the detector weighted spectrum, recorded by the reference spectroradiometer (see Table 4).
- **Ud** is the signal of the UV radiometer, averaged over the recording time of the spectroradiometer.
- **Uoffset** is the dark signal of the UV radiometer; calculated daily
- **Cd** is the variability of the calibration factor during the calibration periode (see Figure 15 as example).
- **fvar** accounts for the mismatch of the measured and modelled correction function, ***fn***.
- **dSRF**: The uncertainty of the SRF measurement is composed of the extrapolation to 400 nm as well as the measurement uncertainty of the SRF itself.

The uncertainty of the cosine correction (***Coscor***) doesn't add to the total uncertainty because it is included through the diurnal variability of the calibration factor C (**Cd**).
The nominal uncertainty budget is summarized in Table 3. The expanded uncertainties stated on the individual certificates issued for the campaign are calculated from the actual data of the specific radiometer calibration and these deviate slightly from the values shown in Table 3.

Table 3. Uncertainty budget for the calibration UV broadband radiometer.

Quantity	xi	[E]	Typ	Distribution	nui	u(xi)	[E]
Ed	1-10	UVI	B	Normal	inf	2.3	%
Ud	0-1	V	B	Rectangular	inf	0.2	%
Uoffset		V	B	Rectangular	inf	0.25	%
Cd	0.2	$Wm^{-2}nm^{-1}V^{-1}$	A	Normal	~3	1.5	%
fvar			B	Rectangular	inf	0.6	%
dSRF			B	Rectangular	Inf	0.6	%
					u(C)	**2.9**	**%**
					u(C)95	**5.8**	**%**

6.2. Manufacturer calibration of broadband radiometers

Most UV radiometers are delivered to the customers either with a certificate of calibration or their electronic amplifier is adjusted to set a nominal relationship between UV irradiance and radiometer output signal. At the campaign some participants sent the radiometer together with this certificate where the uncertainty of the calibration should be stated.

6.3. Reference Spectroradiometer QASUME

The uncertainty budget for solar UV measurements using QASUME and QASUMEII is summarized in Table 4. The estimation of the various uncertainty components is based on the procedure outlined in Gröbner at al. 2005 [7], with reduced uncertainty values due to the improved characterizations and calibrations developed during the European Joint Research Project "Traceability for surface spectral solar ultraviolet radiation". The uncertainty contributions shown in the table are described in [4].

Table 4. Uncertainty budget for solar UV measurements using QASUME and QASUMEII; wavelength range: 310–400 nm (if not stated otherwise).

	Relative Std Uncertainty /%	
Uncertainty Parameter	**QASUME**	**QASUMEII**
Radiometric calibration (λ≥300 nm)	0.55	
250 W lamp stability (one year)	0.10	
Nonlinearity (PMTor PC)	0.25	0.17
ND filter transmission	n/a	0.3
Stability	0.2	
Temperature dependence	0.2	
Angular response (Clear Sky / Diffuse Sky)	0.6 / 0.3	
Integrated cosine error	0.3	
Measurement noise	0.2	
Measurement noise (λ=300 nm; SZA=75°)	3.5	
Wavelength shift (after matSHIC)	0.1, 0.5 (λ=300 nm)	
Combined uncertainty	0.98	1.01
Combined uncertainty (DS)	0.83	0.86
Combined uncertainty (λ=300 nm)	3.66	3.67
Expanded uncertainty (k=2)	**1.95**	**2.01**
Expanded uncertainty (k=2, DS)	**1.66**	**1.72**
Expanded uncertainty (k=2, λ=300 nm)	**7.32**	**7.34**

7. Campaign Results

7.1. Spectroradiometer intercomparison

The two reference spectroradiometers QASUME and QASUMEII measured synchronised solar irradiance spectra in the range 290 nm to 400 nm every 0.25 nm every 15/30 minutes. The instrument entrance optics were located within less than 50 cm from each other at the same height and distant from the broadband radiometers by 1 m to 12 m.

Figure 16. Entrance optic of QASUME (right) and QASUMEII (left).

The comparison of the solar irradiance spectra followed the standard operating procedure of a QASUME intercomparison, i.e. the spectra were convolved to a 1 nm slit width and wavelength adjusted to a common wavelength scale using the matSHIC algorithm. The comparison of all measurements at selected wavelengths and the average over the measurement period is shown in the figures below.

Figure 17. Mean ratio of QASUMEII / QASUME (clear sky data) at PMOD/WRC, 8th April 2017 (098) to 8th October 2017 (281).

Figure 18. Ratio of QASUMEII / QASUME (clear sky data) at PMOD/WRC, 8th April 2017 (098) to 8th October 2017 (281).

As can be seen in the figure the difference between the two instruments are well within the uncertainty bounds defined in Table 4 with an average offset of 0% and a variability of less than or equal to 3%. The higher ratios for the UVB irradiance for the DOYs 169- till 241 are due to a faster scan frequency of 15 min which resulted in lower calculated QASUME values in this wavelength range. The reason is that the recovery time of the photomultiplier was reduced to a few minutes for these scan settings affecting the stability of the dark current.

The QASUMEII data was used as reference for the calibration of the broadband radiometers. This system was calibrated several times during the comparison period using a portable monitor system with 250 W lamps. The spectroradiometers remained stable within ±1% for the period. The temperature of the monochromator was stabilized to 27.1 ± 0.2 °C and the diffuser head was heated to a temperature of 28.7 ± 0.7 °C.

Figure 19. QASUMEII responsivity change based on T68523, 2017.

Figure 20. QASUMEII temperature stability of the monochromator and the input optic.

7.2. Radiometer Comparison

The raw data of the broadband UV radiometers of the whole campaign (all sky conditions, without precipitation) were converted to weighted solar irradiance using the "PMOD" calibration factors on the one hand, and the "USER" supplied original calibration factors[3] on the other. The figures show an example of the relative ratio between the two data sets with respect to the reference measurements calculated from QASUMEII.

Figure 21. Erythemal weighted broadband irradiance vs. QASUMEII reference data - plotted against the time (left) and as a histogram distribution (right). In this example the data of UVE channel of KZ120023 was used.

Figure 22. Erythemal weighted broadband irradiance vs. QASUMEII reference data - plotted against the solar zenith angle. Left: PMOD calibration; right: USER calibration. In this example the data of UVE channel of KZ120023 was used.

[3] Most calibration factors from the participants entered the database of the WCCUV before the start of the campaign, which enabled a "blind" comparison. Two institutes (LAP and Middleton Solar) delivered the factors after the campaign because of technical problems during their prior-campaign calibration period.

The figure below summarizes the comparison of the PMOD and USER calibration relative to the reference. Displayed is the median of the ratio for the calibration period for each instrument.

Figure 23. Comparison of the original (USER, green) and the new (PMOD, red) calibration.

For some instruments a history of calibrations is available in the WCCUV database. One example is shown here:

Figure 24. History of the calibration factor C for a SL501 radiometer. The grey shaded area represents the expanded uncertainty of the last calibration factor (red point).

Many participants sent the SRF and ARF derived from the manufacturer or from their own measurements. These data where compared - if available. The individual results of all radiometers are listed in the appendix.

8. Discussion

Two factors should be pointed out which dominate the quality of the final product of UV radiometers. First, the maintenance and appearance of the instrument itself and second, the calibration and data processing of the raw data. In the following these two factors are discussed.

8.1. Data processing

Since 2007 several publications give practical guides for broadband instruments measuring solar UV radiation [6,8,9]. The most important point mentioned in these investigation is that using a single calibration factor will result in very high uncertainties of the calculated solar irradiance data. However, the data of most of the participating radiometers (40 out of 75) where processed using a single calibration factor prior to the campaign. The calibration methodology for each participating radiometer can be found in Table 2.
From the variability of the normalized additional factors f_n and *Coscor* the resulting error can be extracted which is the consequence of the neglection of those factors in Equation 1. This will be illustrated in the following two sections.

8.1.1. Neglecting the spectral mismatch between the instrumental spectral response and the nominal response of the desired action spectrum

The three figures below show the diurnal variability on a clear sky day of the ratio broadband radiometer vs. reference data for KZ560, SL1493 and YES010938, representing the three main types of radiometers participating at the campaign. The data of the broadband radiometers were calculated using equation 6 with f_n equal to unity, i.e. neglecting the f_n. The correction function is shown in green. For this typical summer day, the maximal correction is 20% for the KZ, 10% for the SL and 10% for the YES radiometer.

Figure 25. Diurnal variability on DOY 187, 2017, of a KZ (left), SL (middle) and YES (right) radiometer, caused by neglecting the correction matrix f_n. This function is added to the figures in green.

8.1.2. Neglecting the mismatch between the instrumental angular response and the nominal cosine response

Analog to the section before the three figures below show the diurnal variability on a clear sky day of the same data, however the data of the broadband radiometer were now calculated using equation 6 with *Coscor* equal to unity, i.e. neglecting the departure of the instrument angular response function from a Lambertian receiver. The cosine function is shown in green. For this typical summer day, the maximal correction is 3% for the KZ, 6% for the SL and 10% for the YES radiometer. For a diffuse sky day, the corresponding diffuse cosine correction factors are 0.97, 1.09 and 1.21, respectively.

Figure 26. Diurnal variability on DOY 187, 2017, of a KZ (left), SL (middle) and YES (right) radiometer, caused by neglecting the cosine correction function *Coscor*. This function is added to the figures in green.

8.2. Humidity

Humidity is the environmental factor which affects mostly the sensitivity of UV radiometers through the susceptibility of the filters used to produce the desired spectral response function. SL2839 can act as a good example to illustrate the response of an instrument from high to low humidity, i.e. the renewal of the desiccant at the beginning of the period (see Figure below). Within a timescale of 20 days the calibration factor changed by 20%.

Figure 27. The ratio of the SL2839 irradiance data relative to the reference reveals the sensitivity change after the renewal of the desiccant on DOY 180, 2017.

8.3. History

The calibration frequency of an instrument is an essential element in assessing the uncertainty of UV measurements. Only by knowing the instrument calibration before and after a measurement period can the data be quality assessed and produce traceable solar UV irradiance data. From the history of past calibrations, one can estimate typical degradation timescales of radiometers measuring solar UV irradiance. The following radiometers – most belong to PMOD/WRC - have been calibrated annually since 2006: SL1492, SL1493, SL1903, SL3860, KZ560, YES010938. Figure 28 shows that the calibration factors typically increase by 1.5% to 3% per year for the Solar Light radiometers, which means that the responsivity decreases by the same rate. This results in a calibration frequency of at least every four years to achieve an uncertainty less than 10%. The KZ560 shows unpredictable sensitivity changes in the order 10% between subsequent calibrations. This is probably due to high intake of humidity of the radiometer. On the opposite, SL1903 shows only a very small variability of its sensitivity. The reason is very likely the custom-made sealing of the instrument and annual nitrogen purging procedure.

The GAW-COST document from Webb et al. [8] recommends an annual recalibration because of well-known sensitivity changes of UV radiometers. The average of last calibration year for the 75 radiometers is 2012. The oldest calibration is three decades old.

Figure 28. History of calibration.

8.4. Summary

To summarize – one can extract three components affecting the overall measurement uncertainty of solar UV measurements using broadband radiometers on different time scales:

- Short term (diurnal) ➔usage of the correction factors f_n and ***Coscor***
- Mid term (months) ➔Control of the humidity inside the device
- Long term (years) ➔Recalibration frequency

The reported relative expanded uncertainty of measurement of the calibration factor is stated as the standard relative uncertainty of measurement multiplied by the coverage factor k=2, which for a normal distribution corresponds to a coverage probability of approximately 95%. An uncertainty of e.g. 20% (see section 6.2) over or under estimates UV irradiance by up to this amount.

9. Comments

9.1. Radiometer maintenance

The campaign was intended to investigate the performance of “reference” radiometers of UV broadband networks around the globe. In general, most of the participating devices arrived in very good shape at the WCCUV. However, a surprisingly high number of radiometers (16 out of 75) were not well-maintained instruments. In the following a complete list of the observations is given.

1.) High humidity inside the radiometer can cause transmission changes of the filter and is therefore a crucial condition for the radiometers sensitivity.
    a. Very old drying agent found for two radiometers.
    b. Visible humidity inside of one radiometer.
    c. Large sensitivity drift after the renewal of the desiccant found for three radiometers.
2.) UV radiometers are temperature stabilized, because the sensitivity is a function of the filter and sensor temperature.
    a. A bad temperature stability was found for three radiometers.
    b. The temperature regulation of three radiometers didn’t work.
3.) Various:
    a. Cable Code mutation found for one radiometer.
    b. Corrosion was found on
        i. two cables and
        ii. two electronic boards.
    c. A visible filter degradation had three radiometers.
    d. The dome of one radiometer was contaminated on the outside and on the inside of another radiometer.
    e. The mounting of several radiometers could not be performed according to the manufactures manual because:
        i. The mounting feet of one radiometer was missing.
        ii. The level was missing or was opaque for several instruments.
4.) Three radiometers malfunctioned during the campaign and needed to be repaired.

Figure 29. Filter degradation and dome contamination of a YES radiometer.

9.2. Checklist

The following questions follow the observations discussed in the previous sections and are intended as a guideline for improving the solar UV measurements from a UV monitoring station:

1. Data processing:
    - Are you using Equation 1 for the data processing?
        - YES □
        - NO □
    - Name the reasons for using a single calibration factor:
        - Real time processing □
        - Computational power □
        - Uncertainty known and accepted □
        - Unfamiliar with Equation 1 □
        - No TO_3 data available □
        - No algorithm to distinguish between clear and diffuse sky conditions available □
        - …

2. Choose the reasons for the used recalibration frequency:
    - Trust in the factory calibration □
    - Loss of data due to calibration activity □
    - Financial issues □
    - Degradation of the radiometer considered as negligible □
    - Calibration frequency □
    - …

3. Field site environmental condition
    - Harsh (sea site, urban) □
    - Moderate (rural) □
    - Clean (mountain) □

4. Describe your maintenance procedure:
    - Cleaning frequency
        - Daily □
        - Weekly □
        - Monthly □
        - Yearly □
    - Desiccant check and replacement (if required)
        - Daily □
        - Weekly □
        - Monthly □
        - Yearly □

Acknowledgements

We would like to acknowledge the active support of the PMOD/WRC staff in the preparation and organization of the intercomparison campaign. The instrument owners provided the calibrated data for the intercomparison period using their home calibration. Special thanks to Christian Thomann for the help in installing the radiometers and the repair of various KZ radiometers, our electronic civil servants for repairing the broken Solar Light radiometers and the staff of our administrative department for organizing the shipping of the instruments. Finally, we thank Luca Egli for his support in maintaining the reference spectroradiometers.

References

[1] K. Leszczynski, K. Jokela, L. Ylianttila, R. Visuri and M. Blumthaler, “Erythemally weighted radiometers in solar UV monitoring: Results from the WMO/STUK Intercomparison,” Photochem. Photobiol. 67, 212–221, 1998.

[2] WMO/GAW Report No. 141: Report of the LAP/COST/WMO Intercomparison of Erythemal radiometers, Thessaloniki, Greece, 1999. WMO TD {No. 1051}.

[3] J. Gröbner, G. Hülsen, L. Vuilleumier, M. Blumthaler, J. M. Vilaplana, D. Walker, and J. E. Gil, “COST 726 – Report of the PMOD/WRC-COST Calibration and Intercomparison of erythemal Radiometers,” COST Office, 2009.

[4] G. Hülsen, J. Gröbner, S. Nevas, P. Sperfeld, L. Egli, G. Porrovecchio, and M. Smid, “Traceability of solar UV measurements using the Qasume reference spectroradiometer," Appl. Opt. 55, 7265-7275, 2016.

[5] A.R. Webb, H. Slaper, P. Koepke, and A.W. Schmalwieser, “Know your standard: clarifying the CIE erythema action spectrum,” Photochemistry and Photobiology 87: 483-486., 2011.

[6] G. Hülsen, and J. Gröbner, “Characterisation and calibration of ultraviolet broadband radiometers measuring erythemally weighted irradiance,” Appl. Opt. 46, 5877-5886, 2007.

[7] J. Gröbner, J. Schreder, S. Kazadzis, A. F. Bais, M. Blumthaler, P. Görts, R. Tax, T. Koskela, G. Seckmeyer, A. R. Webb, and D. Rembges, “Traveling reference spectroradiometer for routine quality assurance of spectral solar ultraviolet irradiance measurements,” Appl. Opt. 44, 5321–5331, 2005.

[8] A. Webb, J. Gröbner, and M. Blumthaler, “A Practical Guide to Operating Broadband Instruments Measuring Erythemally Weighted Irradiance,” 2007. EUR 22595, ISBN 92-898-0032-1.

[9] G. Seckmeyer, A. F. Bais, G. Bernhard, M. Blumthaler, C. R. Booth, R.L. Lantz, R.L. McKenzie, P. Disterhoft, and A. Webb, “Instruments to measure solar ultraviolet radiation. Part 2: Broadband Instruments Measuring Erythemally Weighted Solar Irradiance,” WMO/GAW No. 164 World Meteorological Organization, Geneva, 2007.

Annex

Individual results for each instrument participating at the calibration and intercomparison campaign at PMOD/WRC, Davos, Switzerland from 25th May to 5th October 2017.

Calibration Results of KZ080018 (UVG)

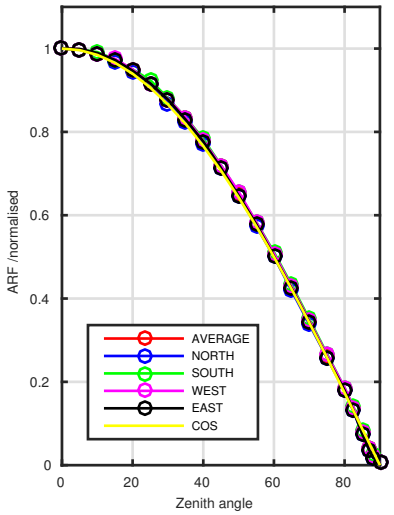

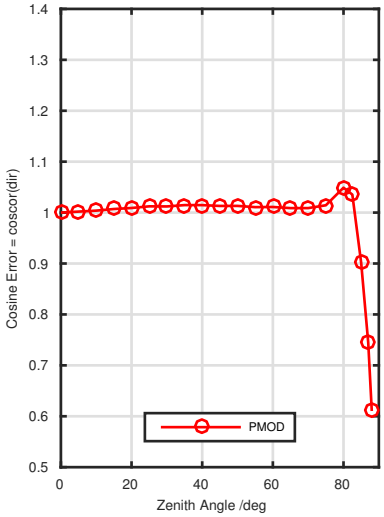

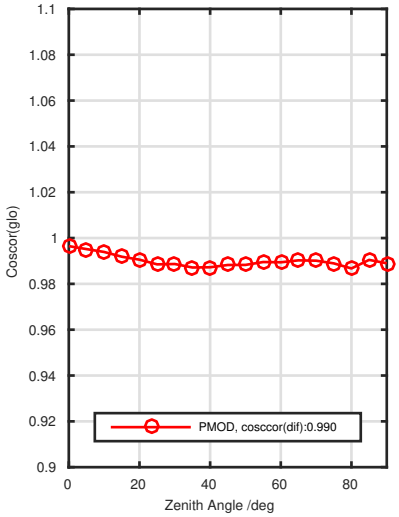

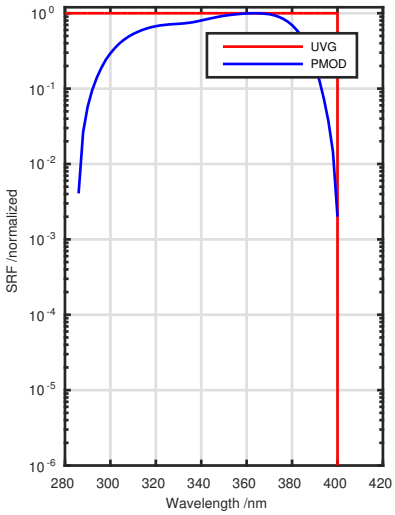

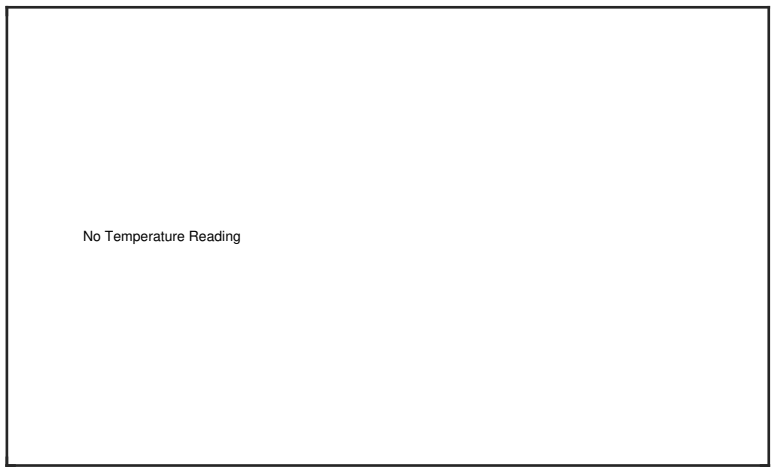

Calibration Matrix fn; Model sdisortREFms2009; f0=1.4684

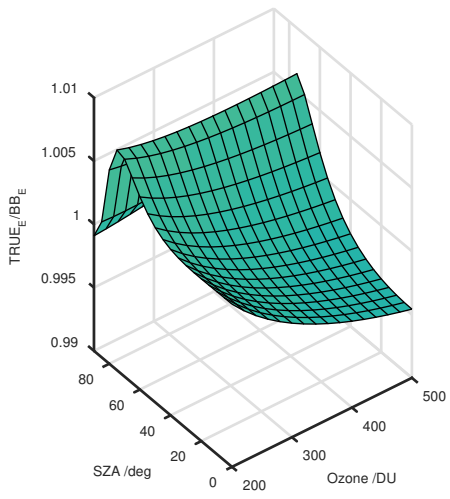

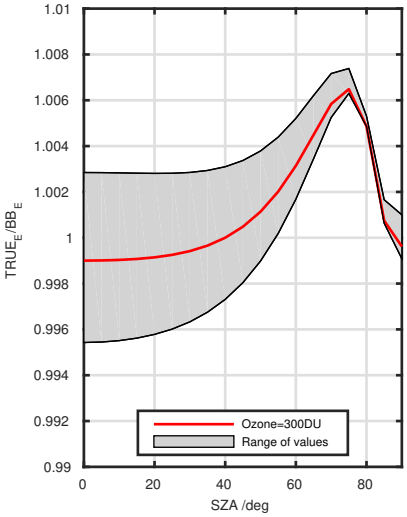

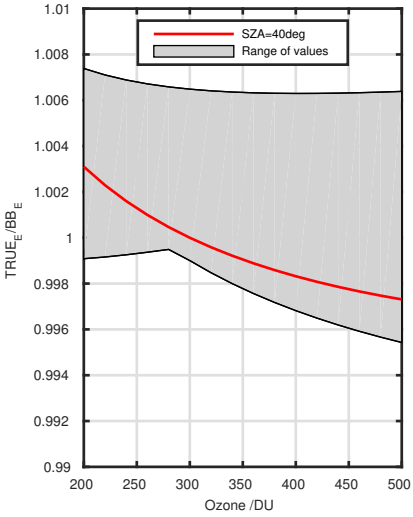

Calibration Results of KZ080018 (UVG)

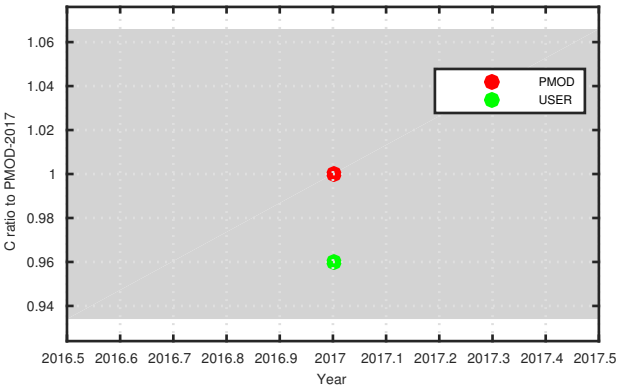

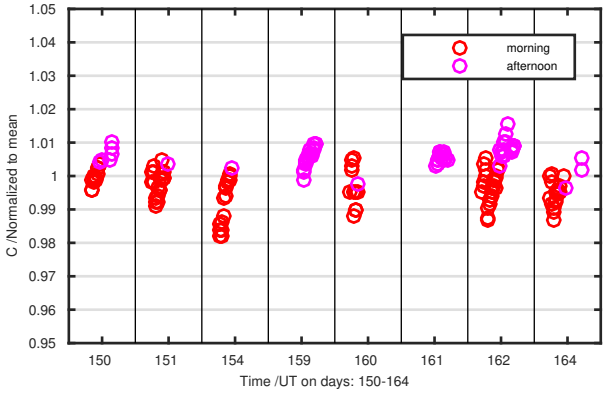

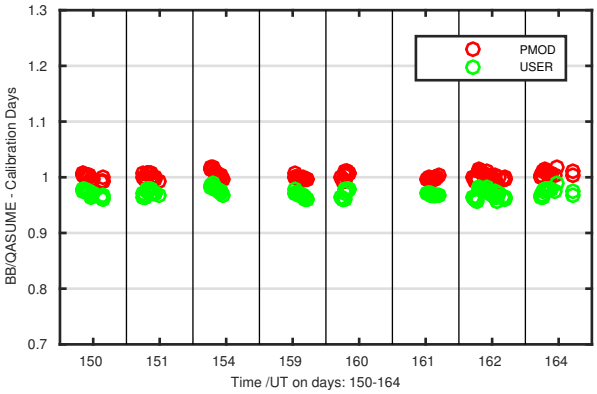

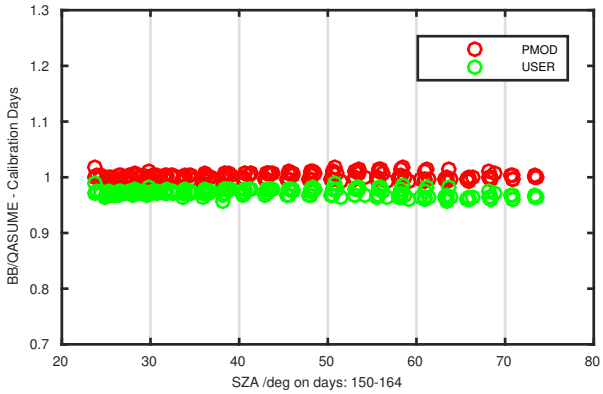

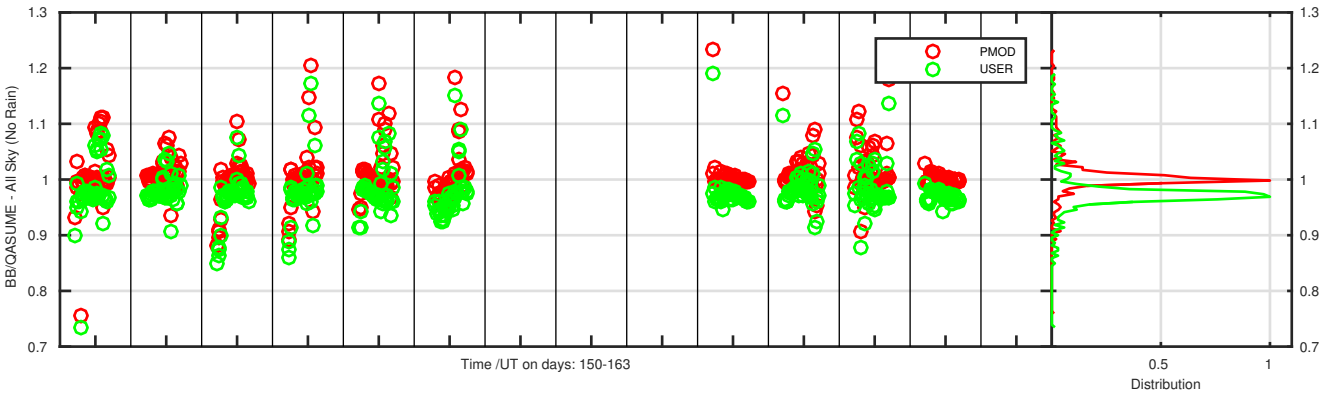

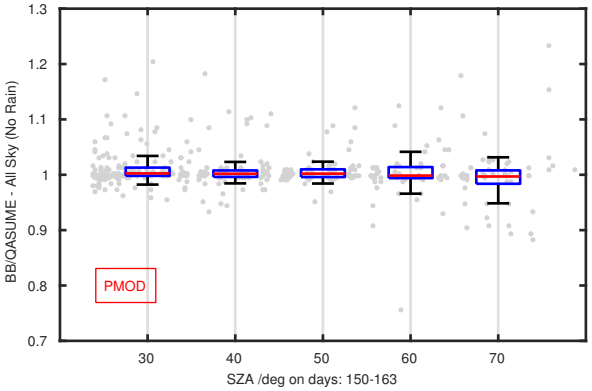

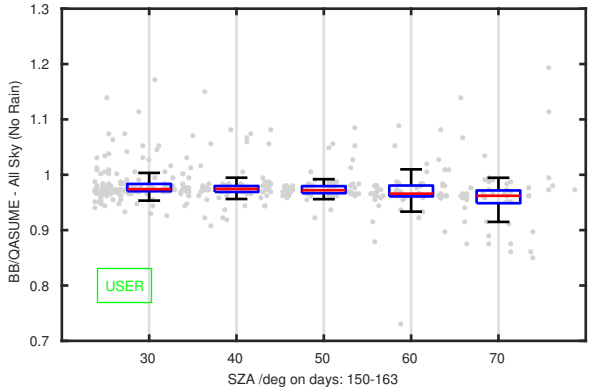

Calibration Results of KZ000526 (UVA)

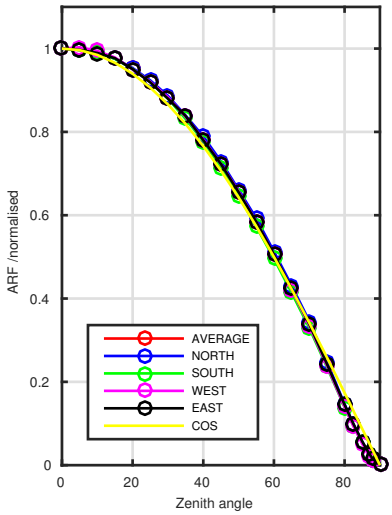

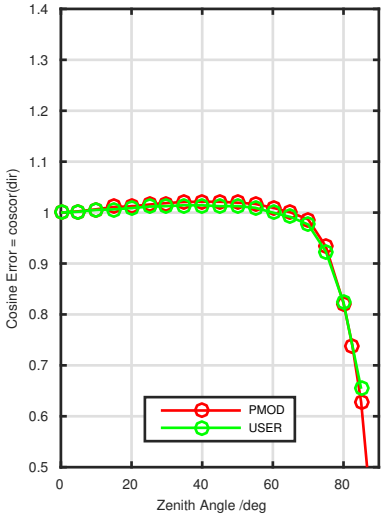

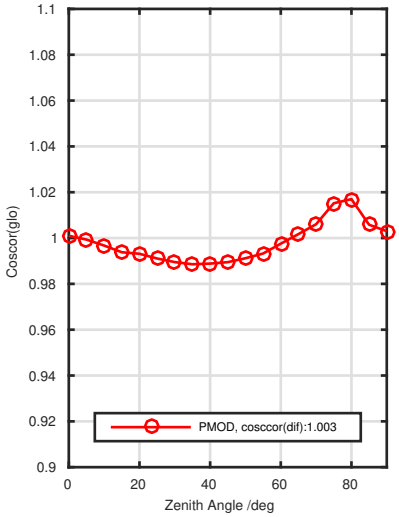

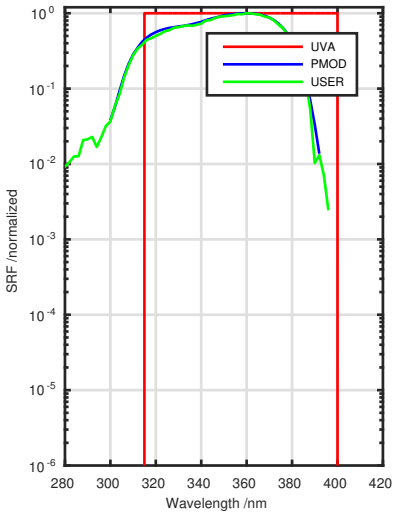

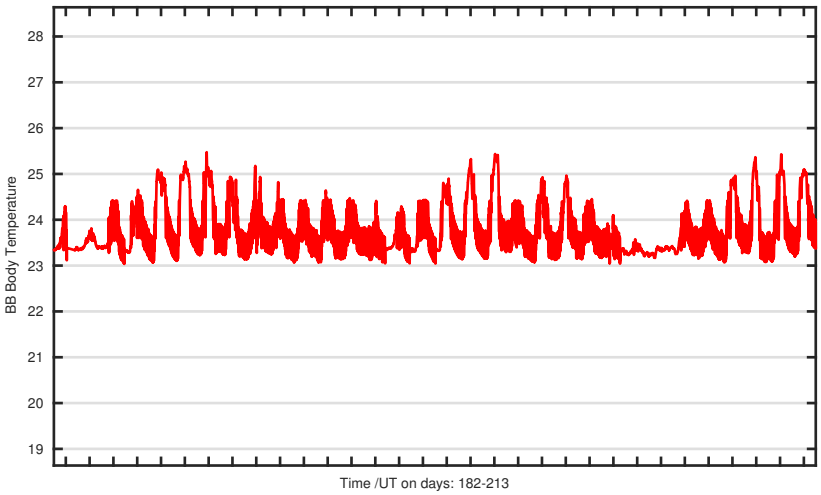

Calibration Matrix fn; Model sdisortREFms2009; f0=1.6581

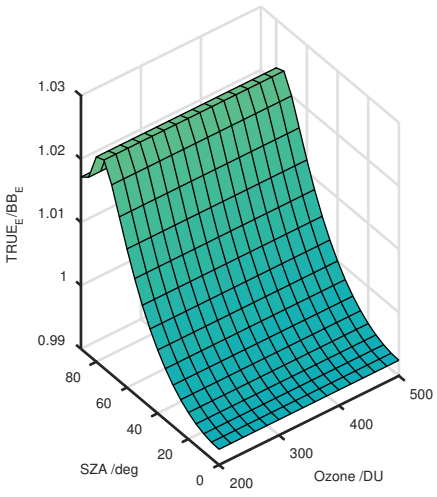

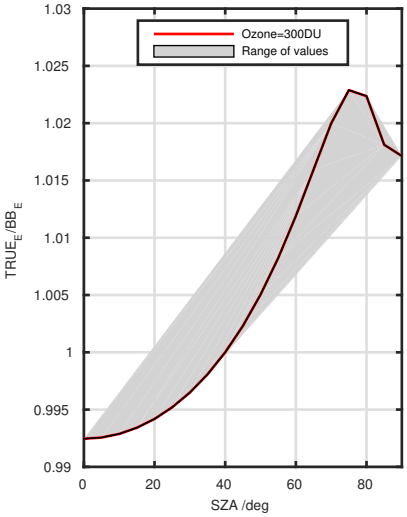

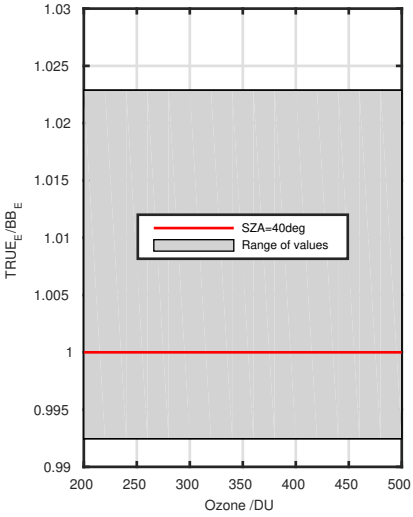

Calibration Results of KZ000526 (UVA)

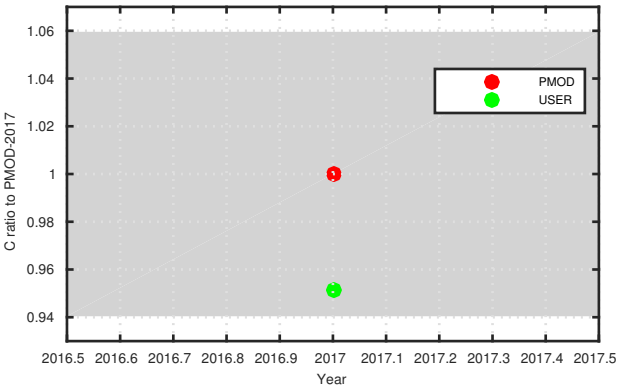

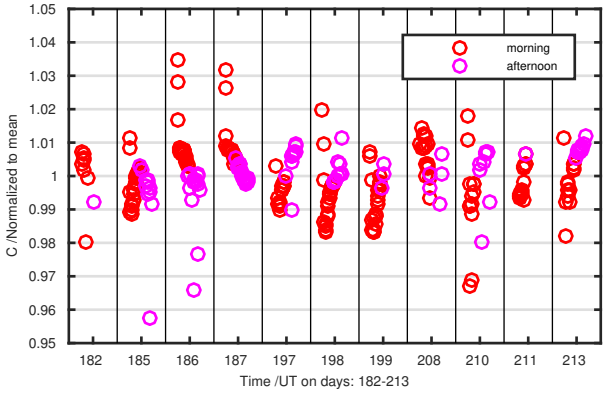

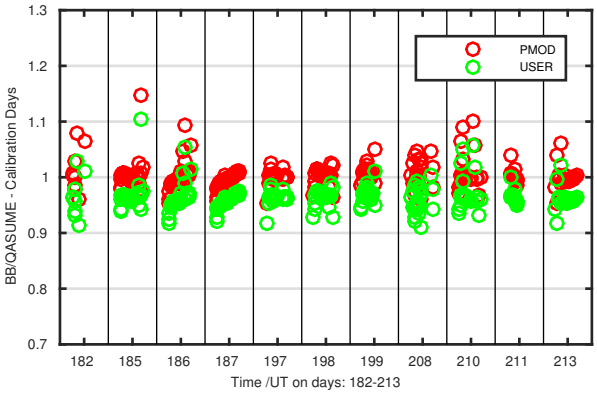

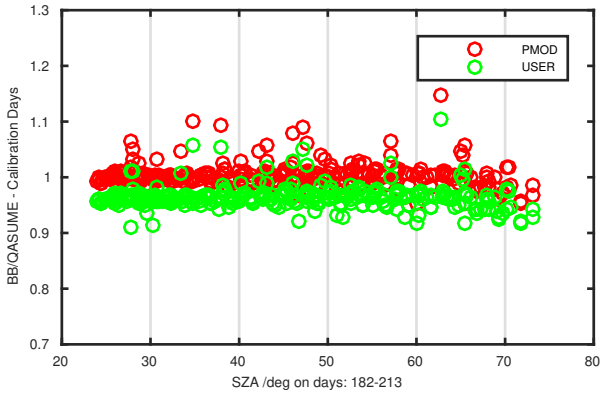

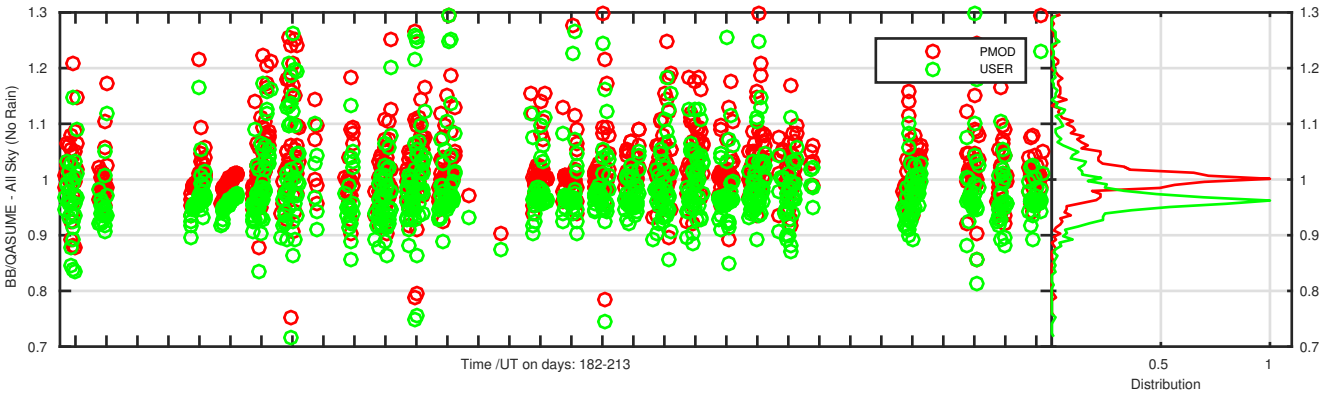

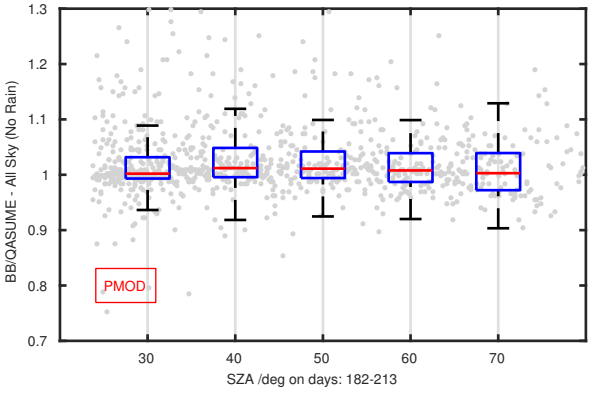

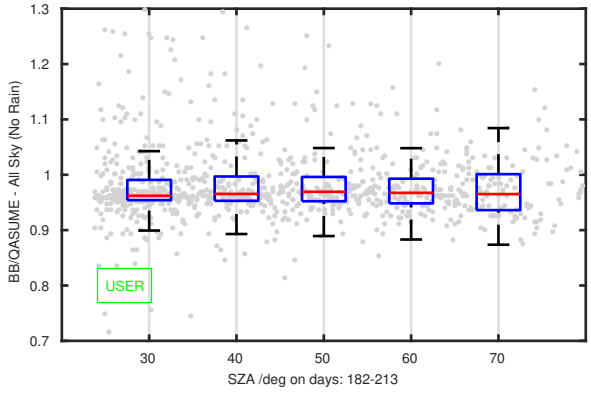

Calibration Results of KZ000526 (UVE)

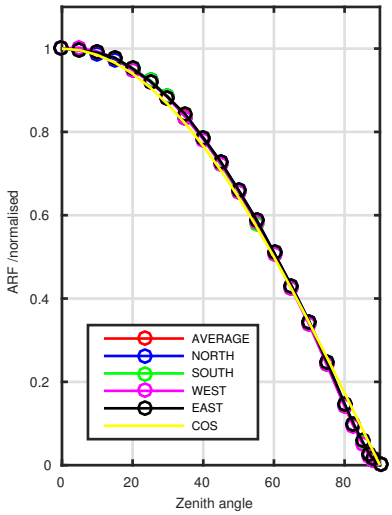

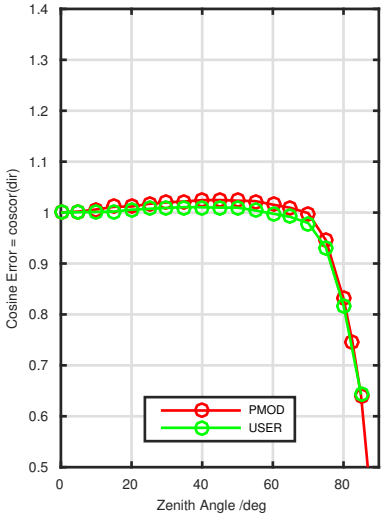

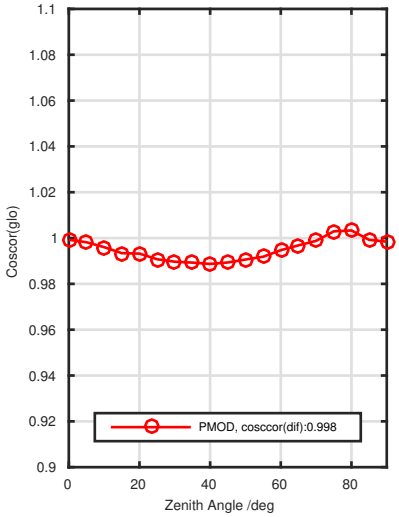

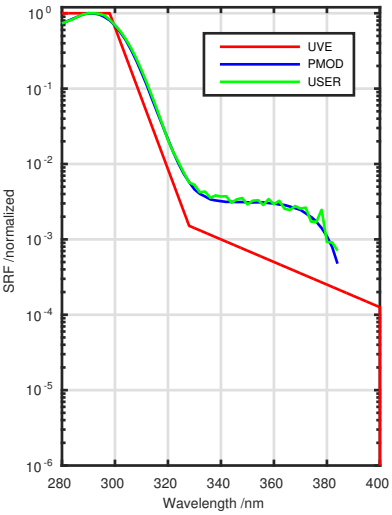

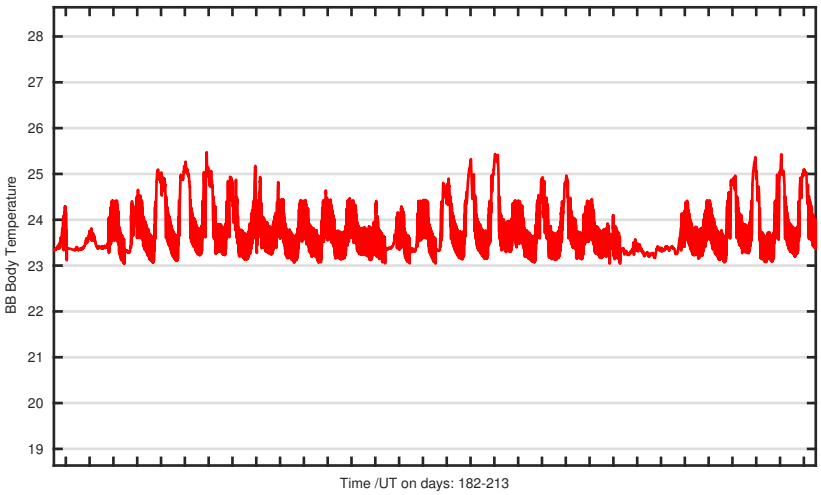

Calibration Matrix fn; Model sdisortREFms2009; f0=0.4348

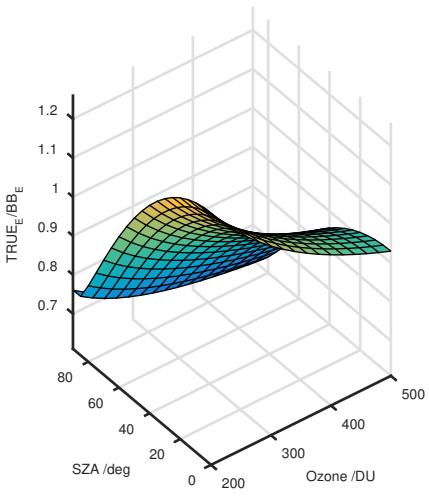

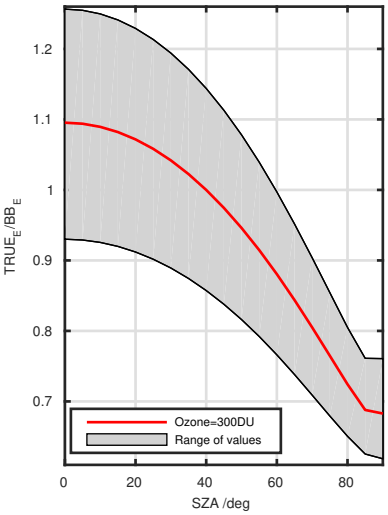

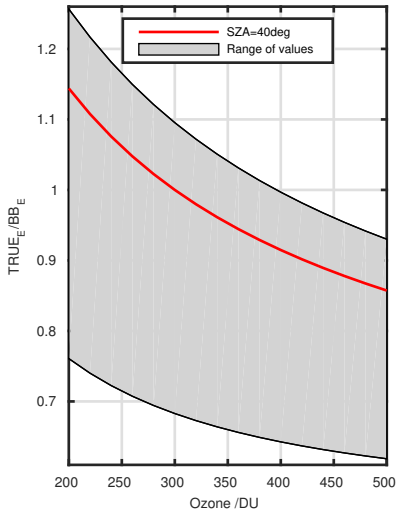

Calibration Results of KZ000526 (UVE)

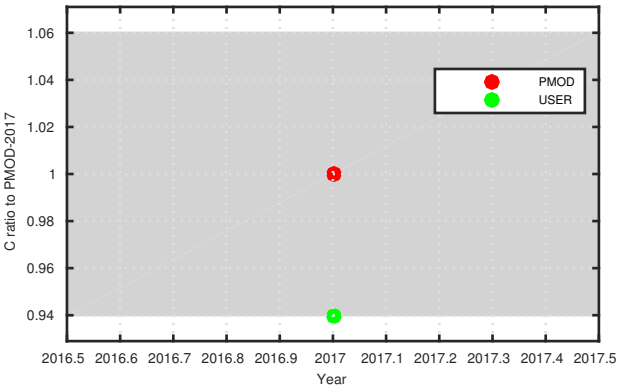

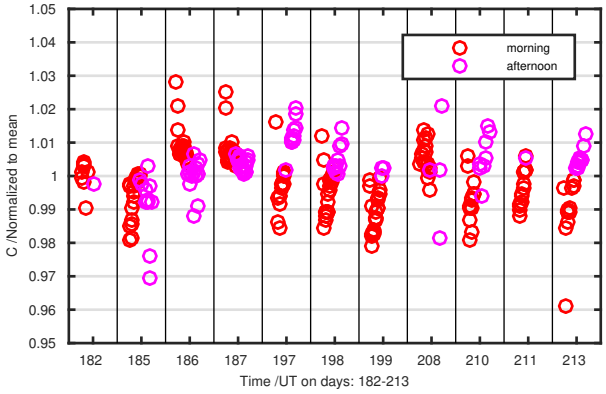

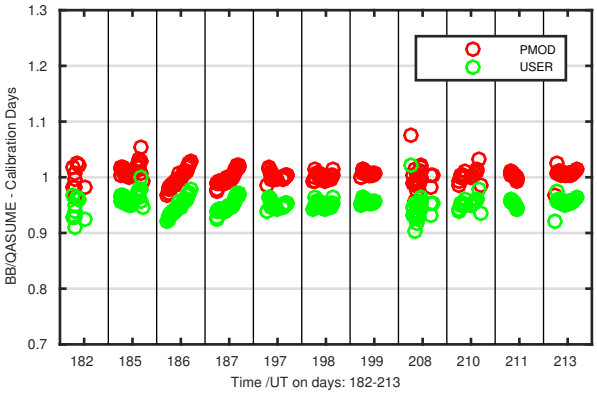

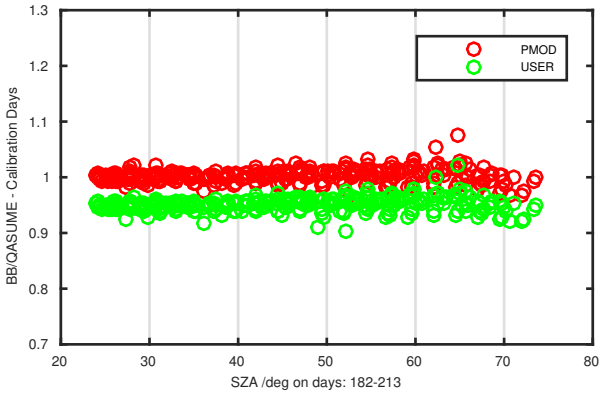

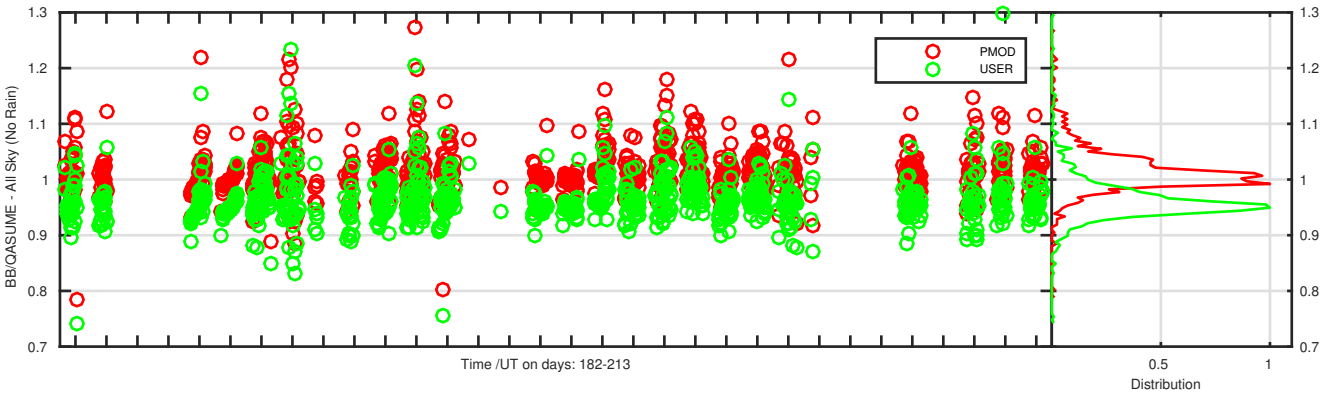

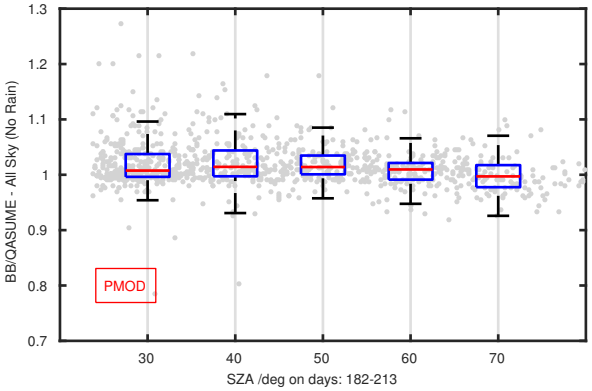

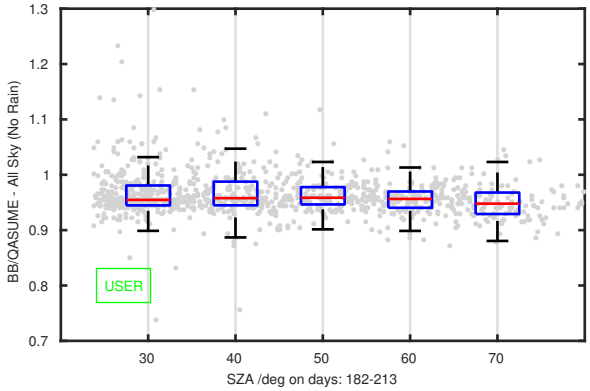

Calibration Results of KZ020614 (UVA)

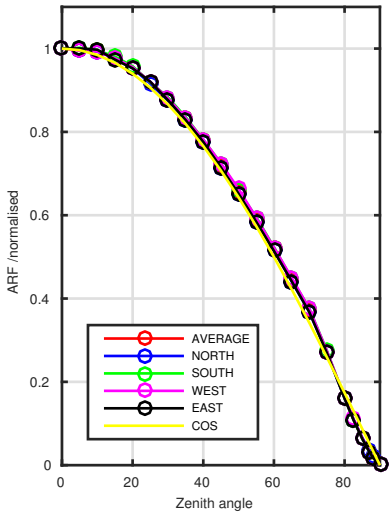

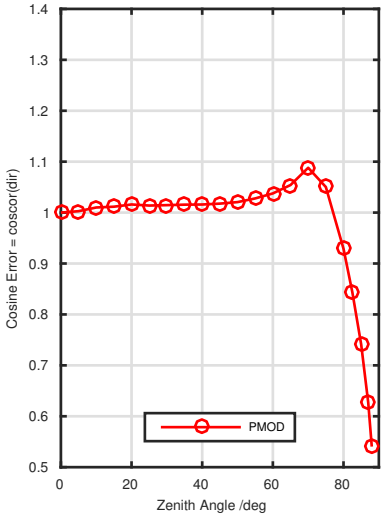

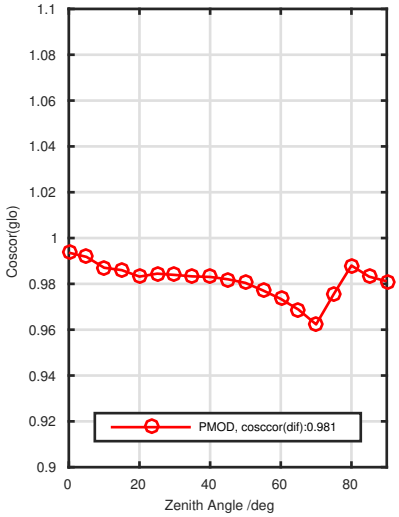

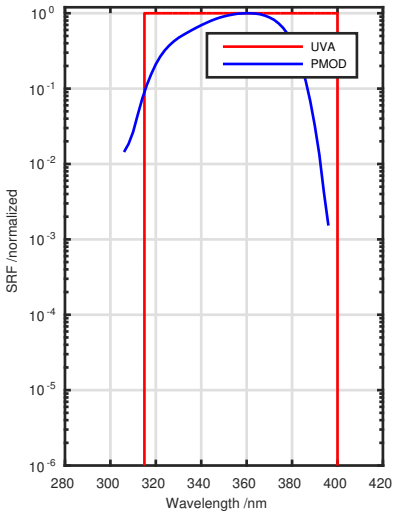

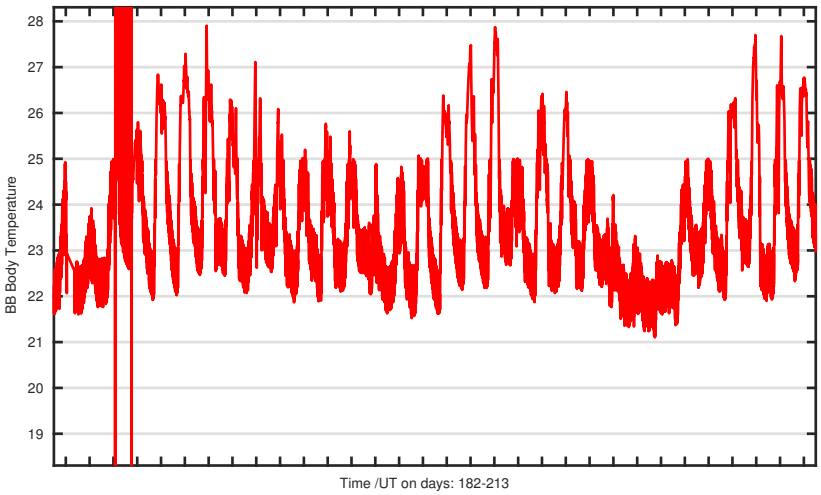

Calibration Matrix fn; Model sdisortREFms2009; f0=1.8252

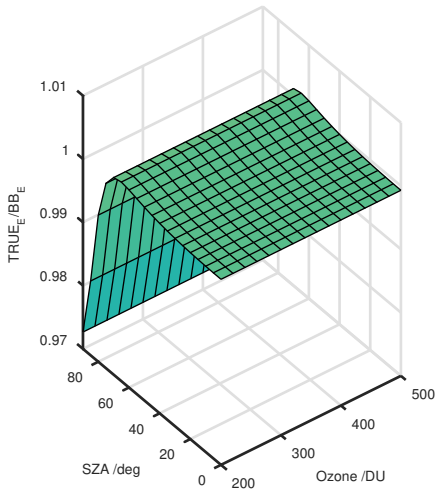

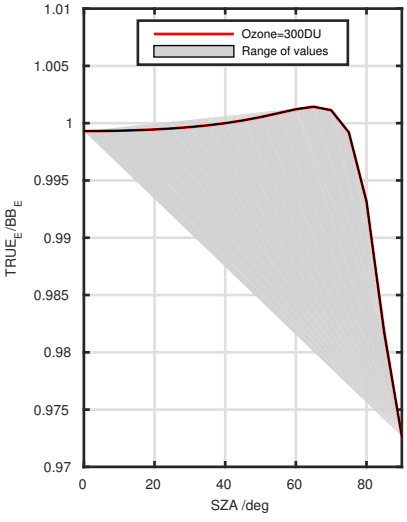

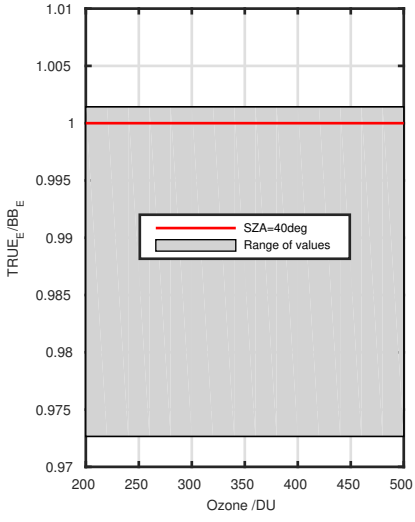

Calibration Results of KZ020614 (UVA)

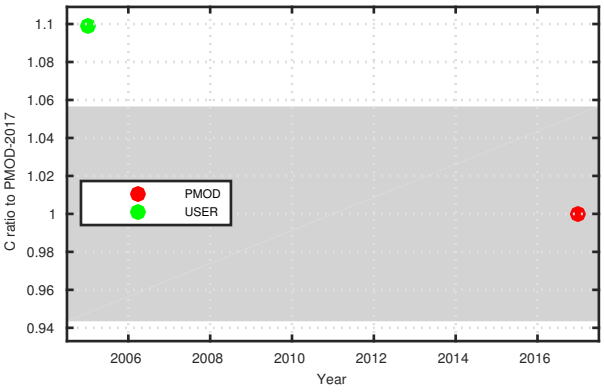

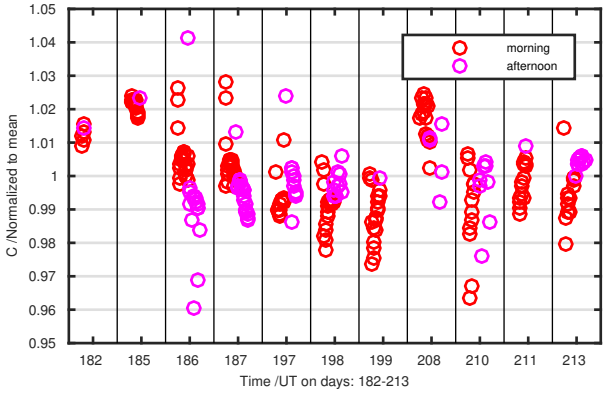

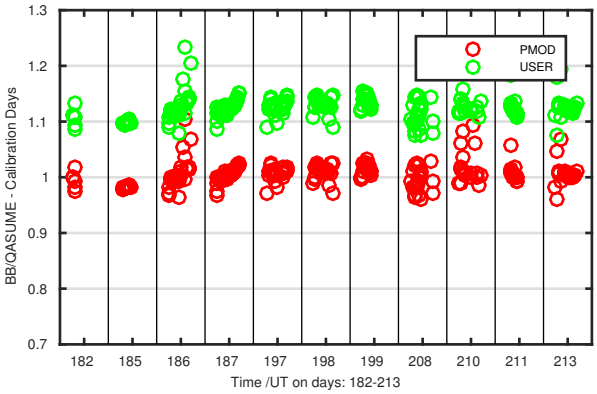

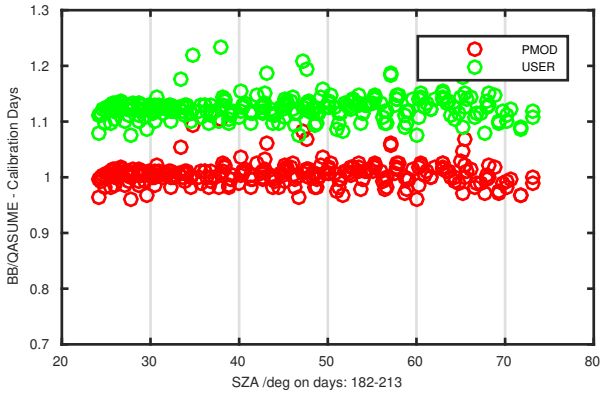

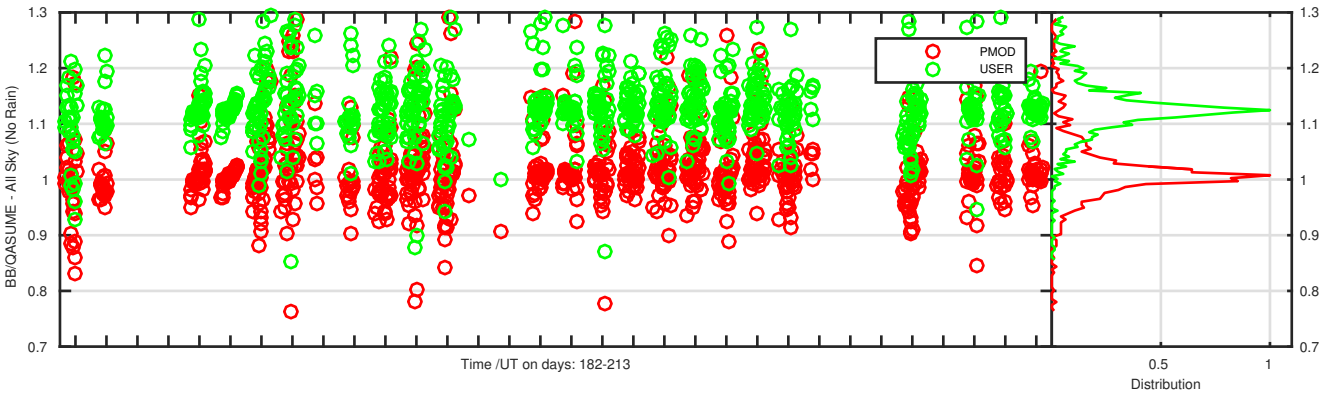

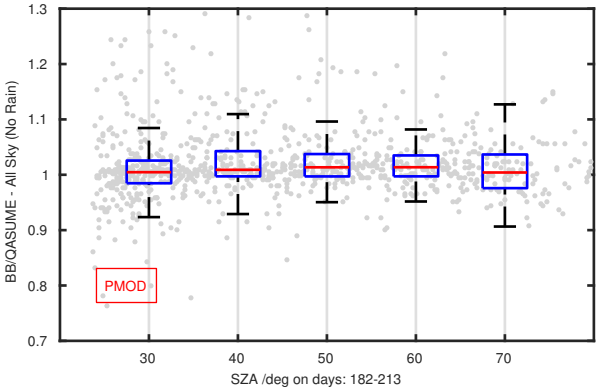

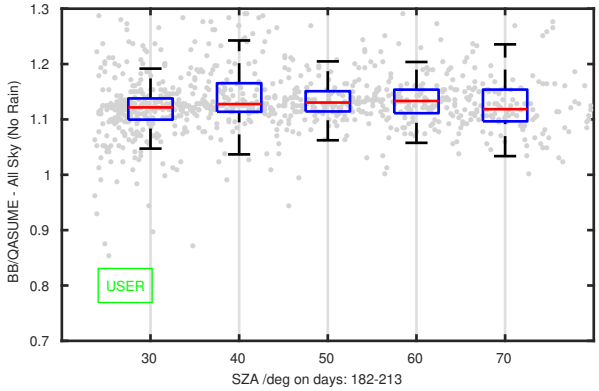

Calibration Results of KZ020614 (UVE)

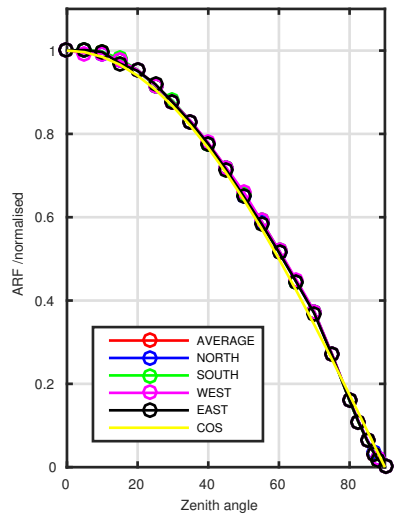

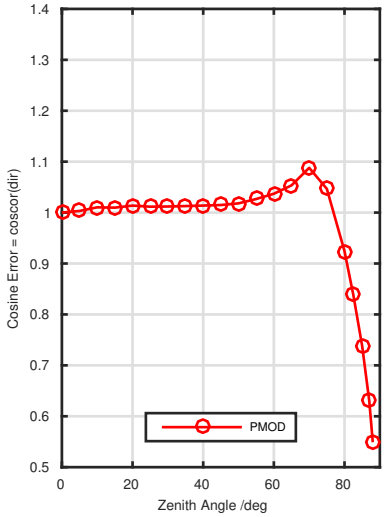

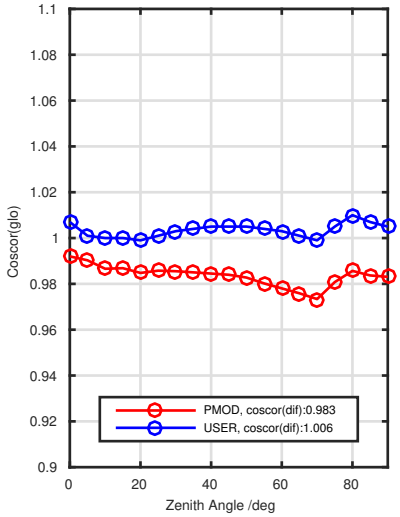

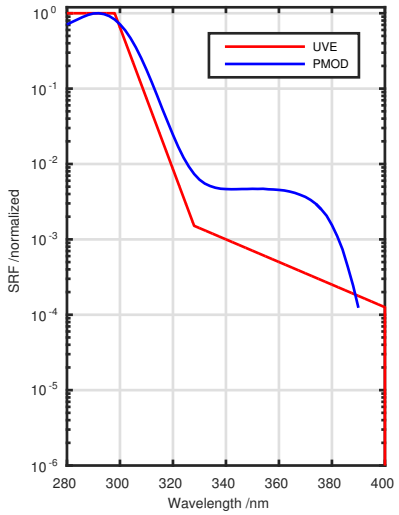

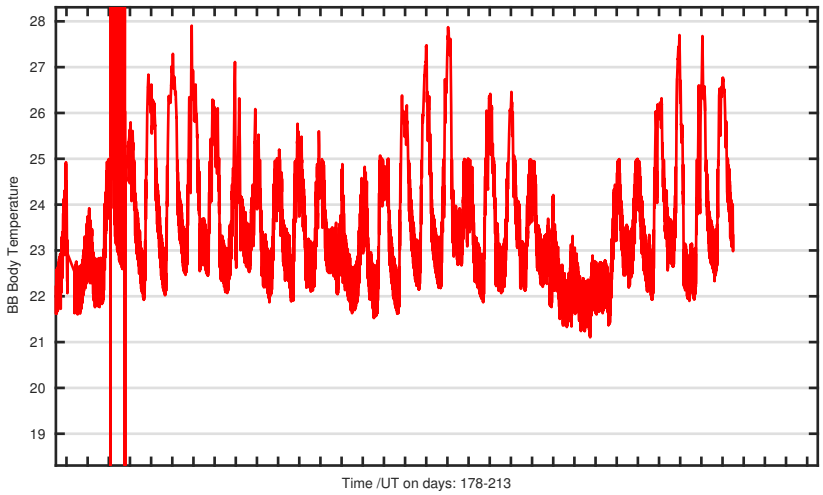

Calibration Matrix fn; Model sdisortREFms2009; f0=0.3668

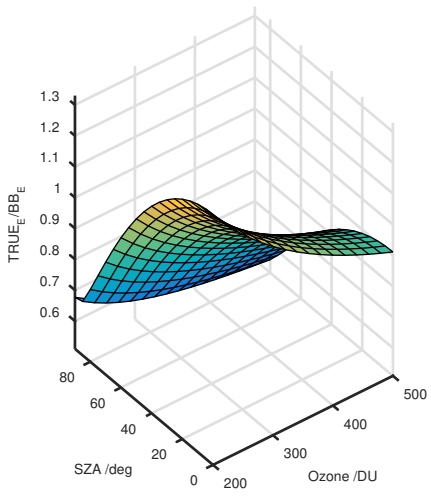

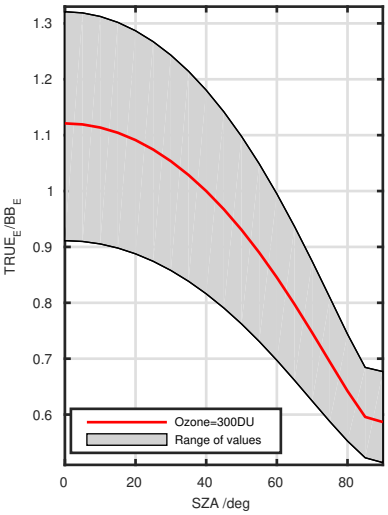

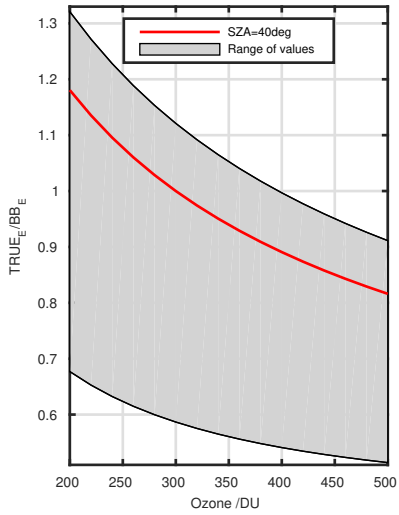

Calibration Results of KZ020614 (UVE)

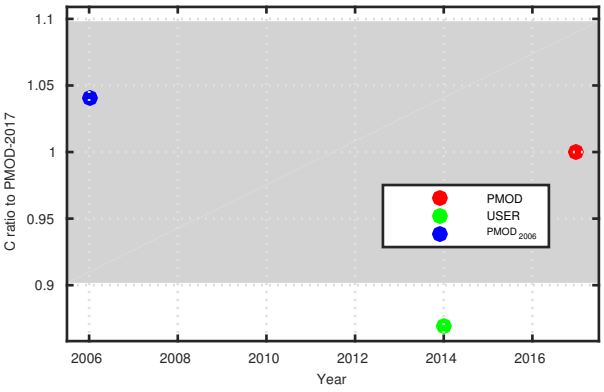

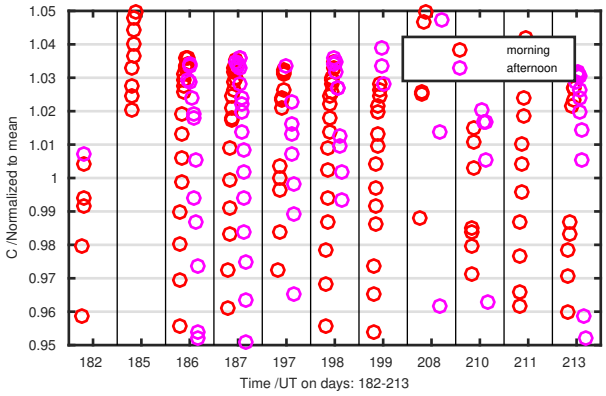

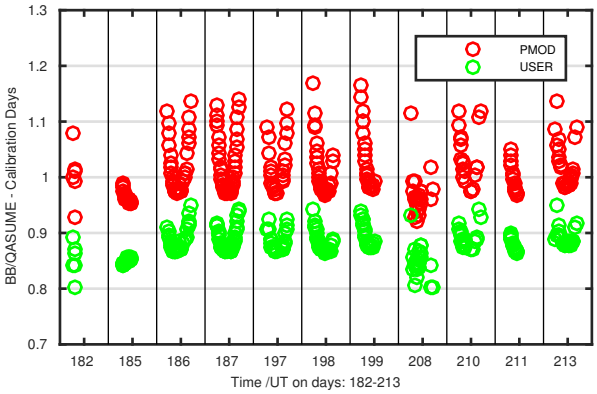

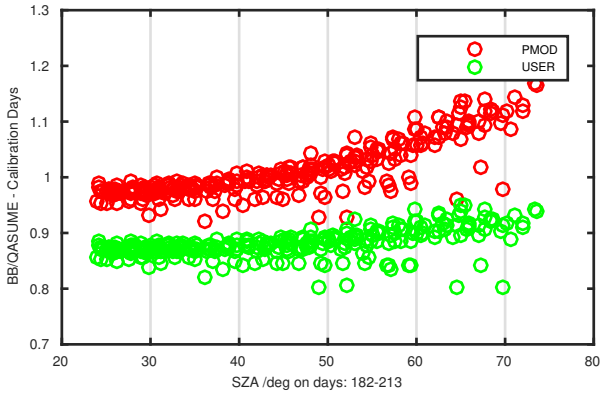

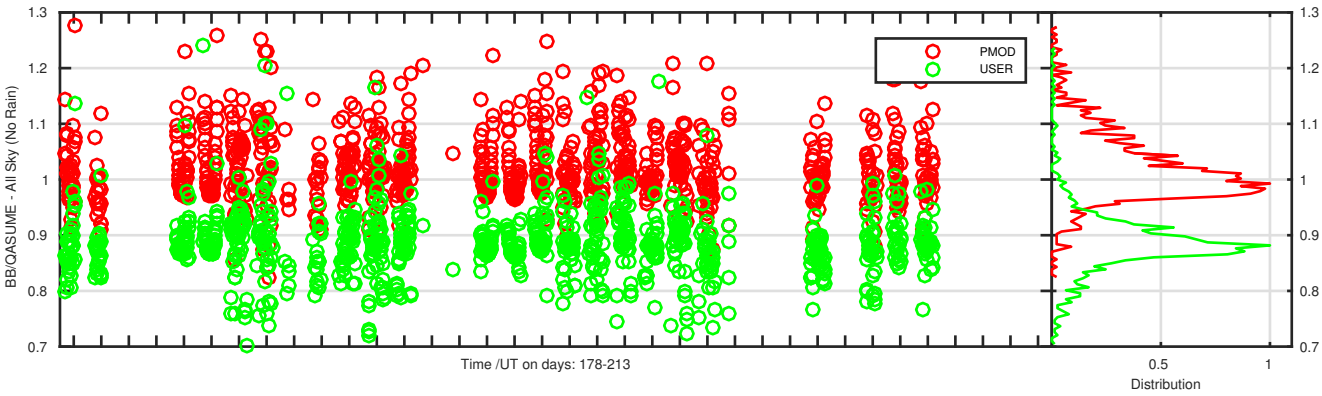

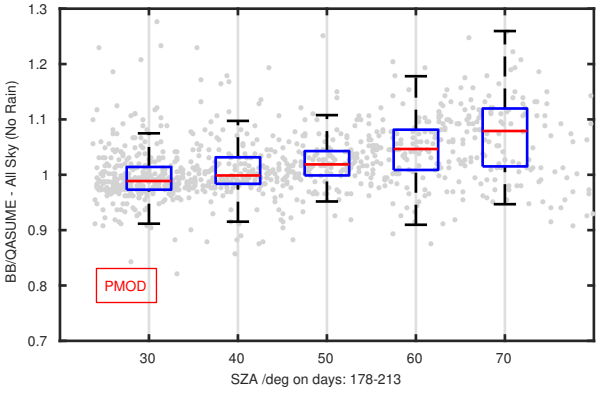

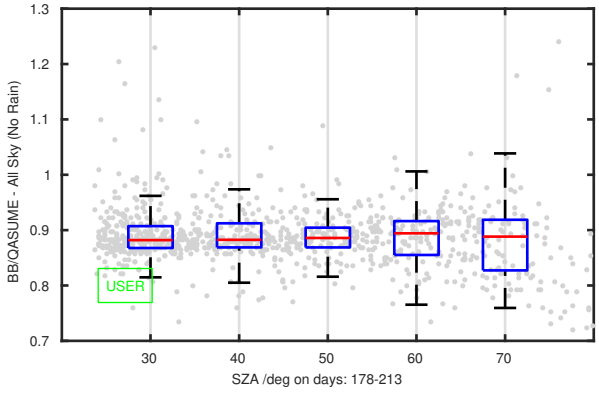

Calibration Results of KZ070635 (UVA)

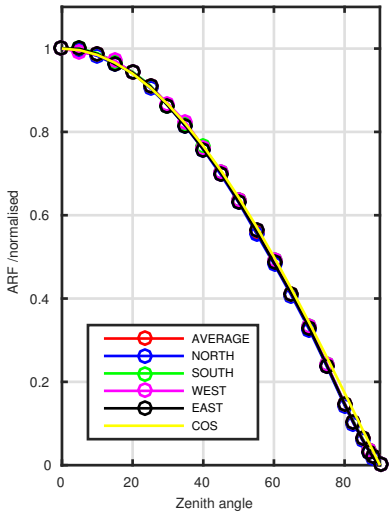

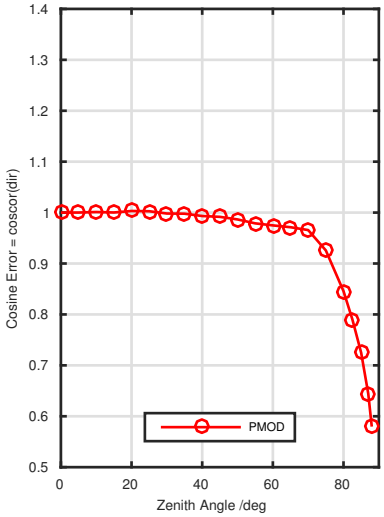

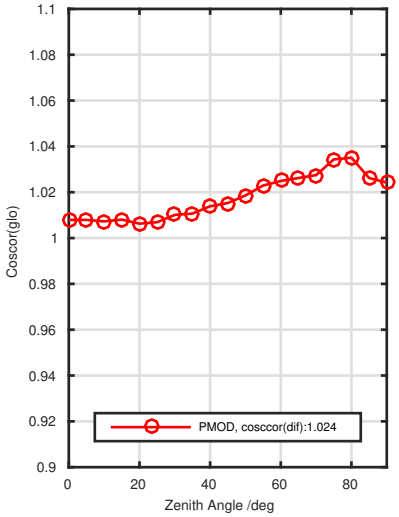

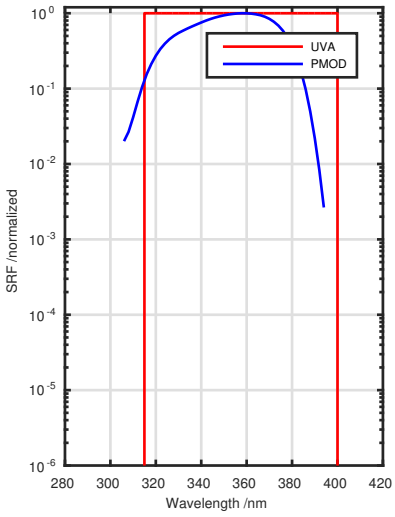

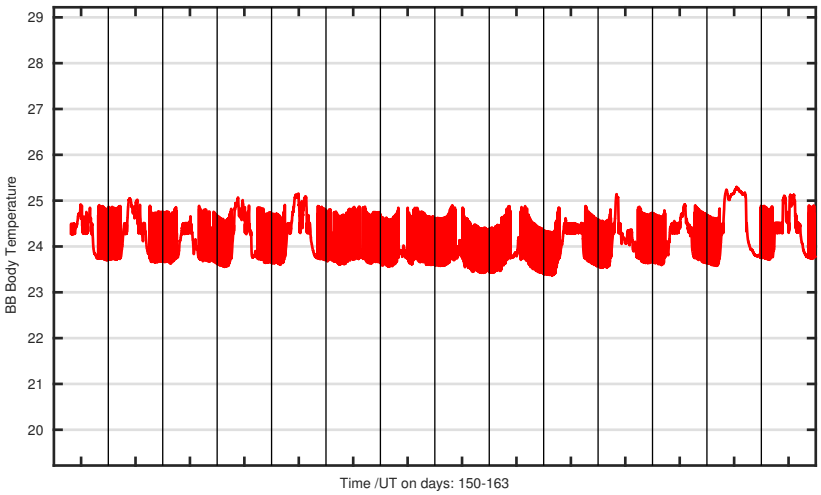

Calibration Matrix fn; Model sdisortREFms2009; f0=1.8047

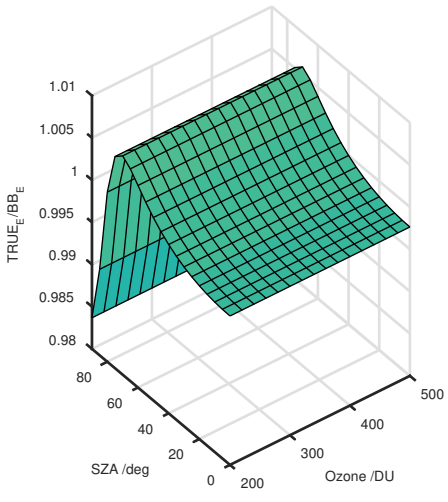

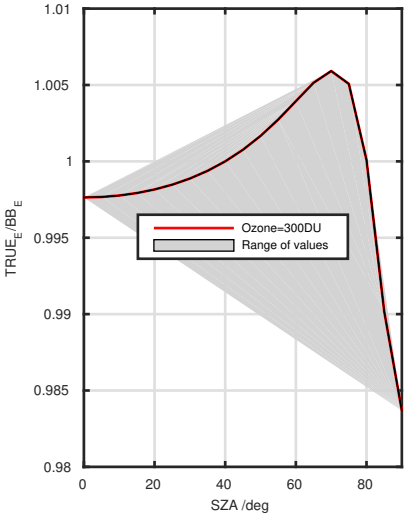

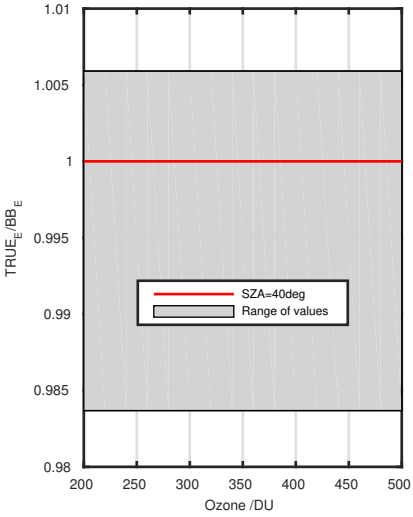

Calibration Results of KZ070635 (UVA)

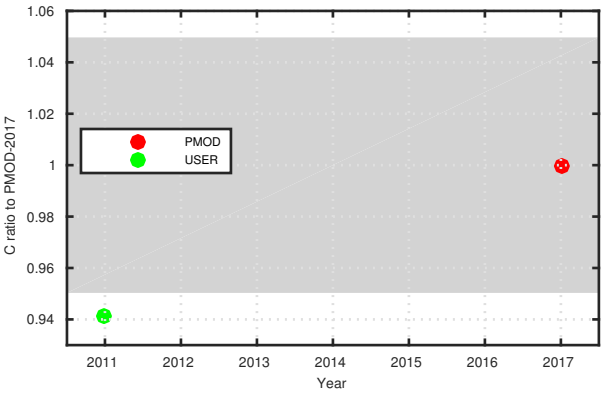

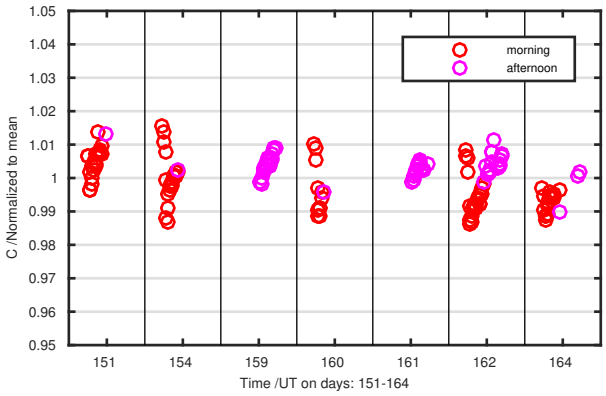

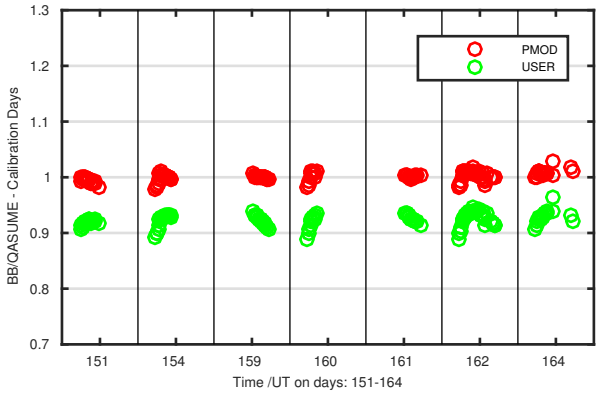

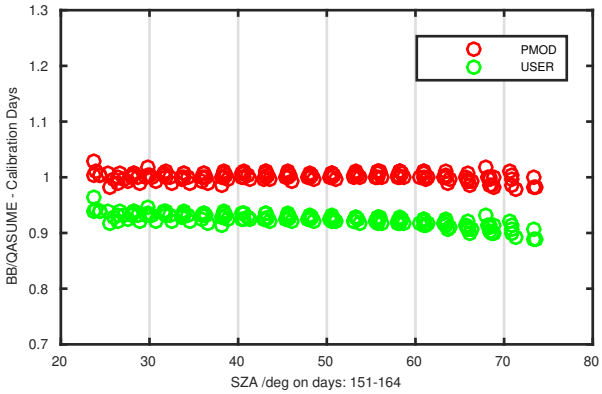

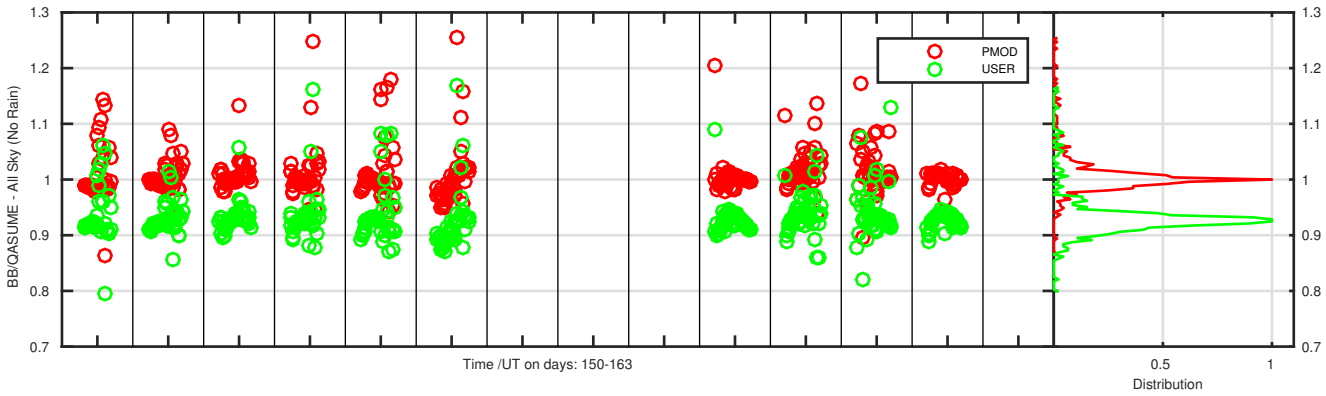

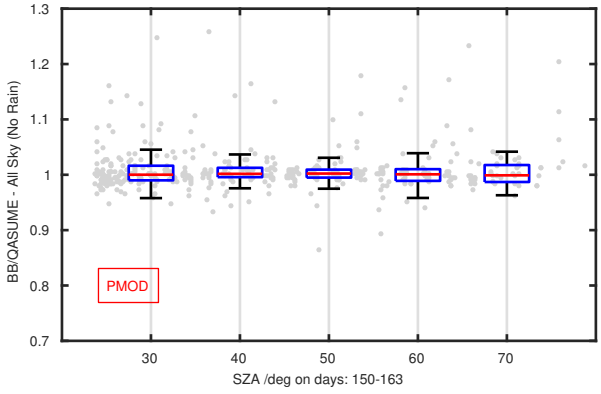

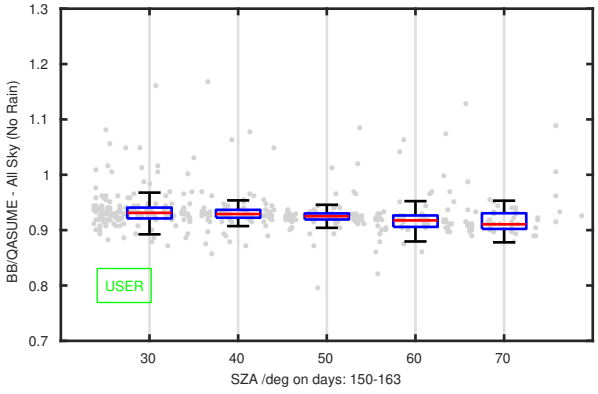

Calibration Results of KZ070635 (UVE)

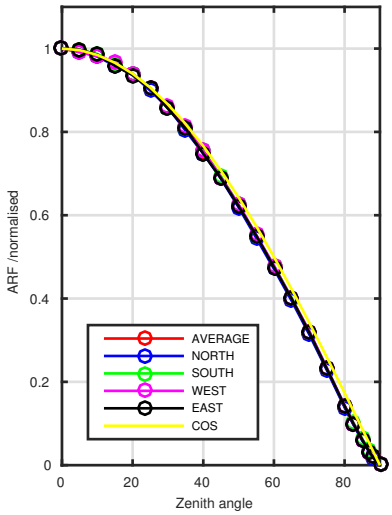

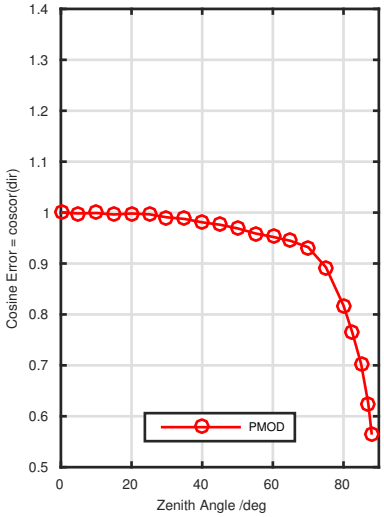

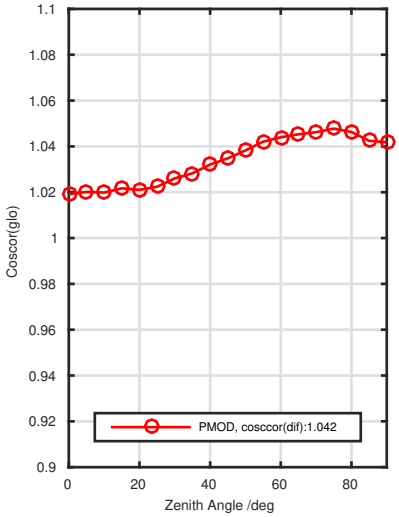

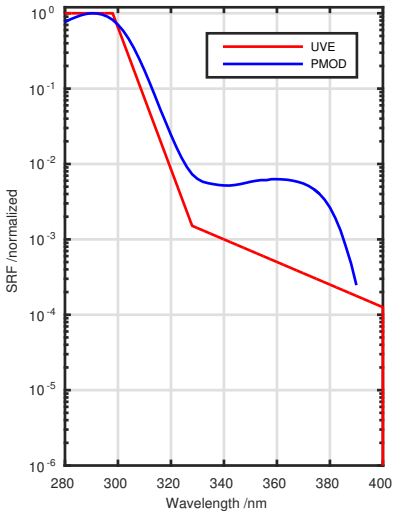

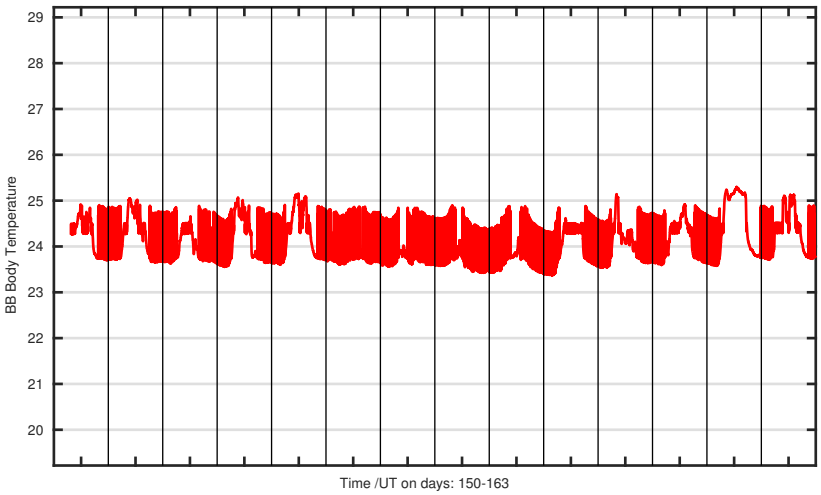

Calibration Matrix fn; Model sdisortREFms2009; f0=0.3430

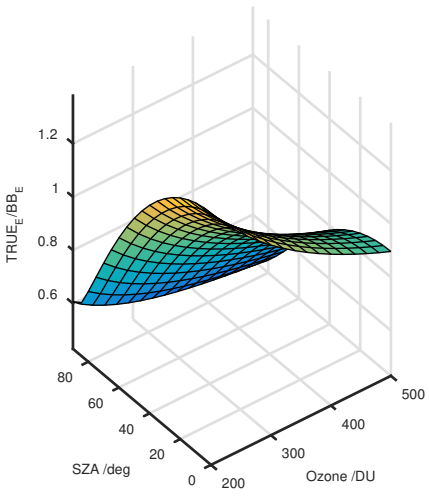

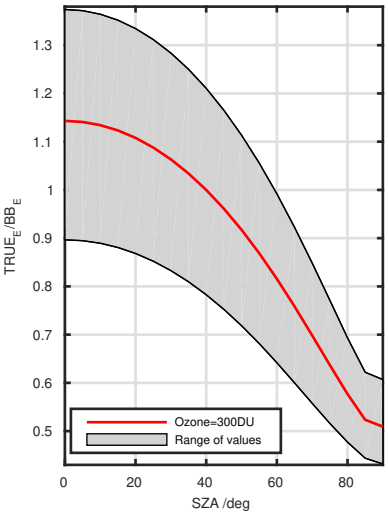

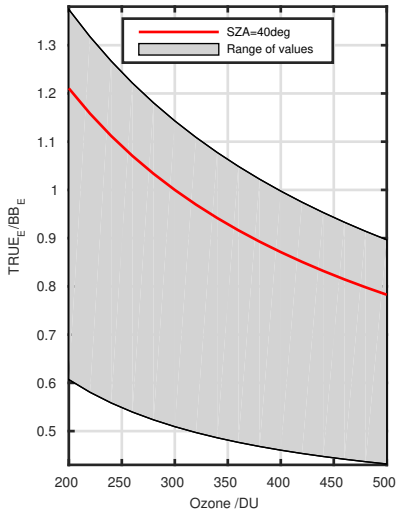

Calibration Results of KZ070635 (UVE)

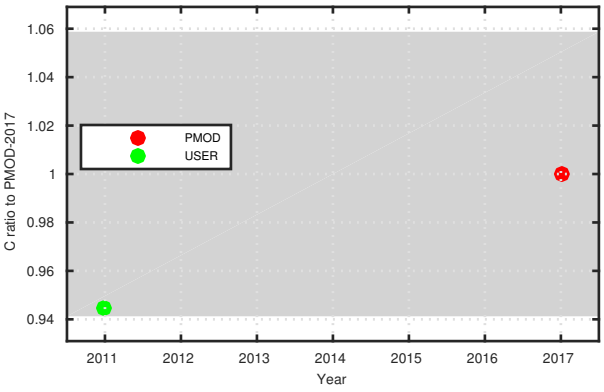

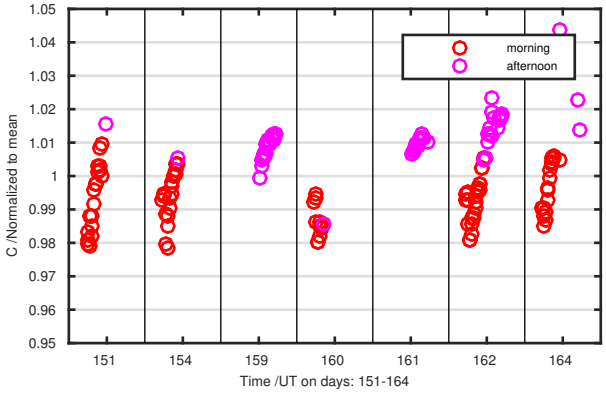

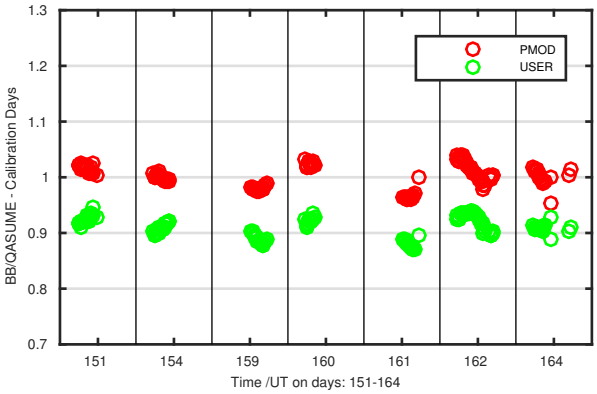

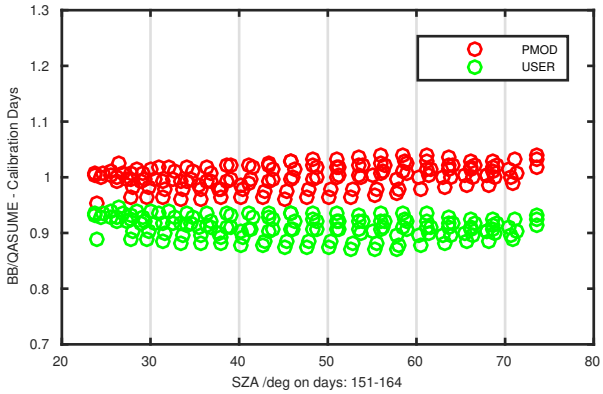

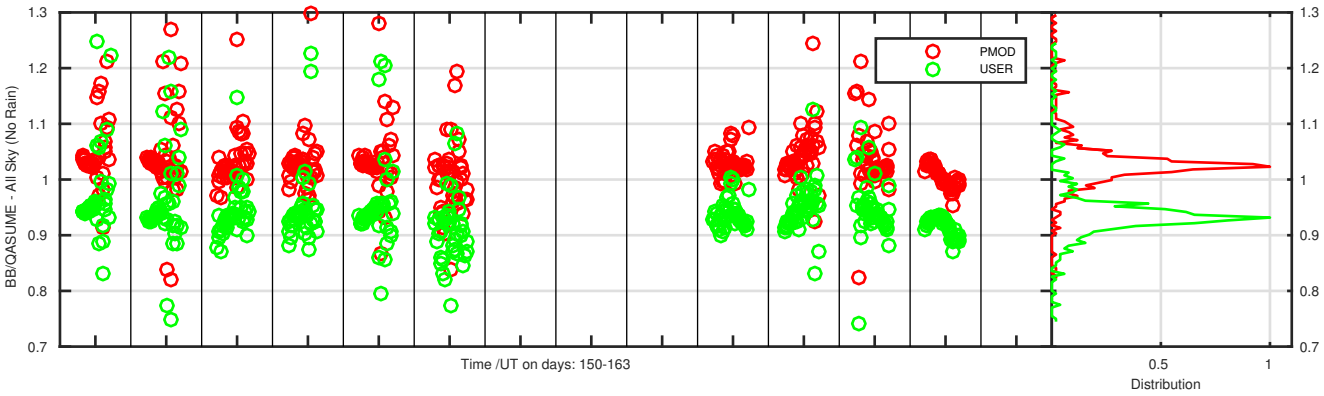

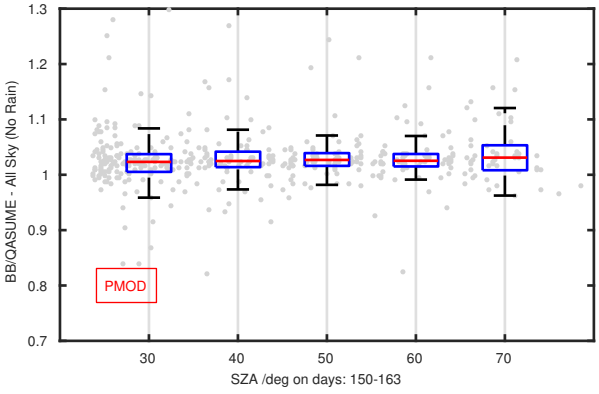

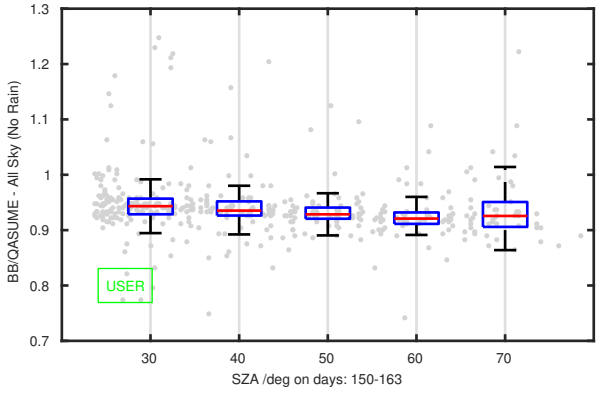

Calibration Results of KZ080002 (UVA)

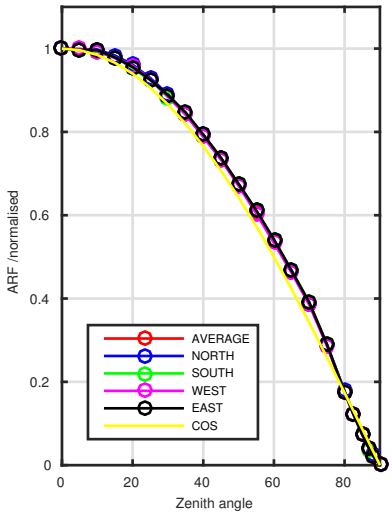

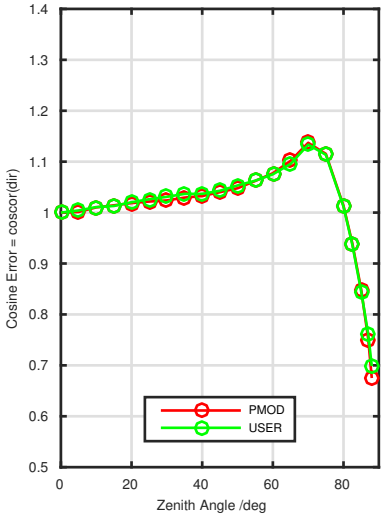

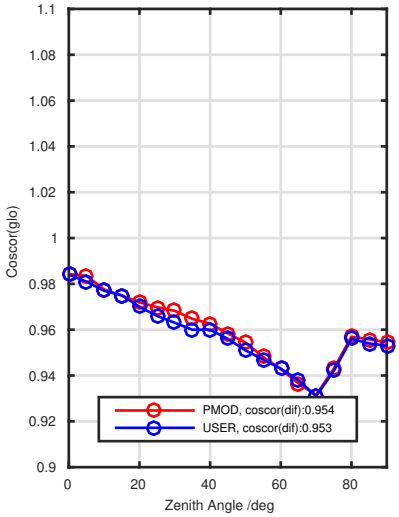

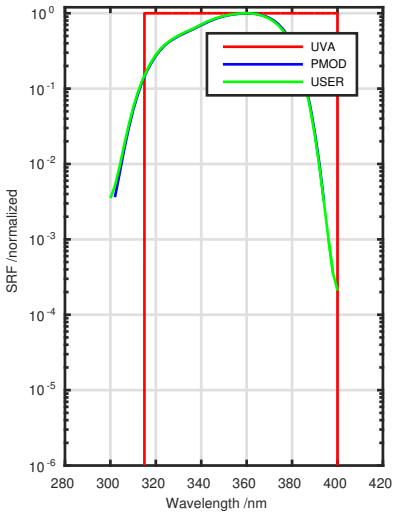

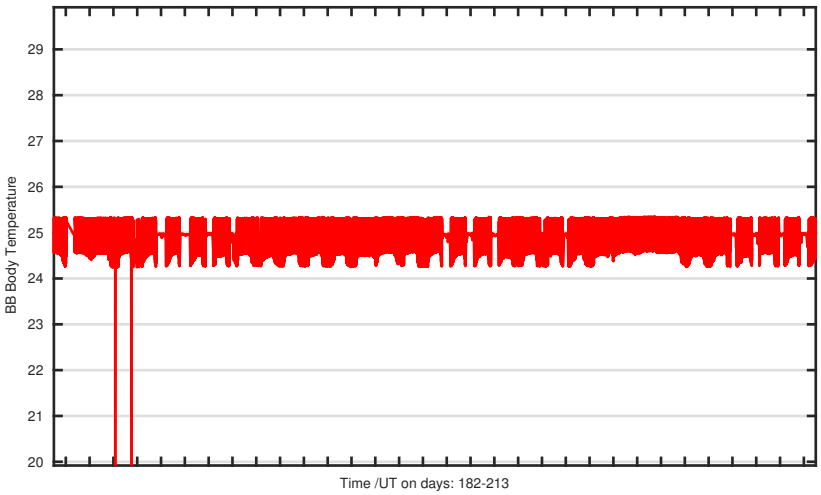

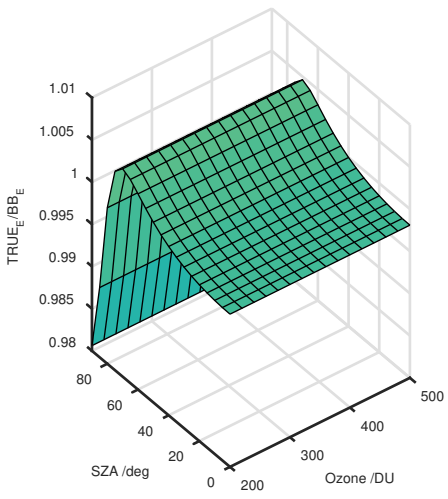

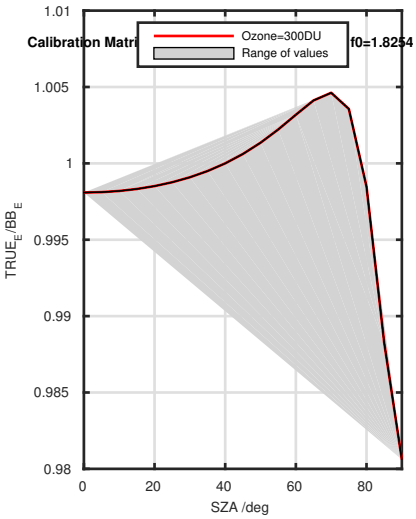

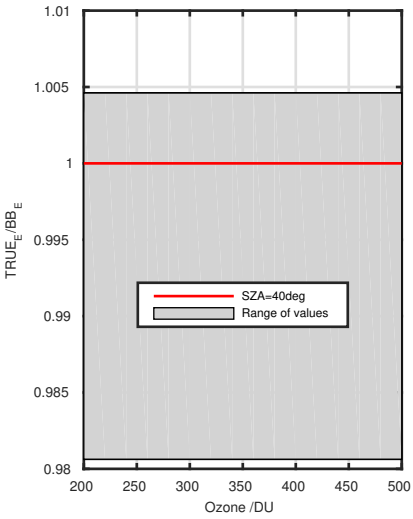

Calibration Results of KZ080002 (UVA)

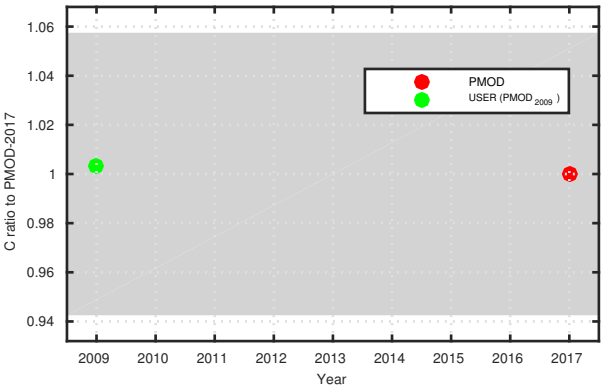

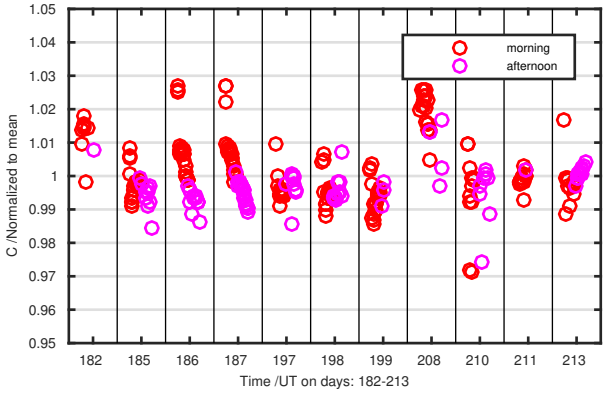

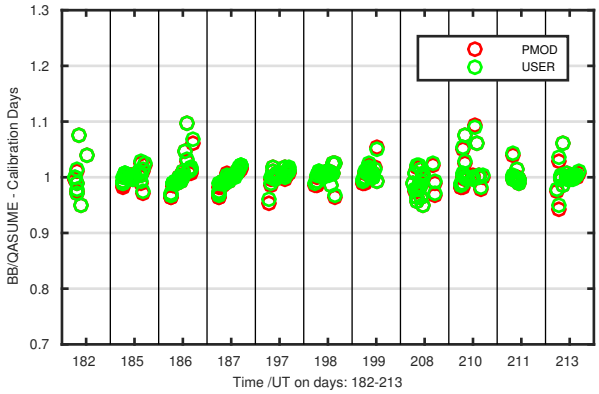

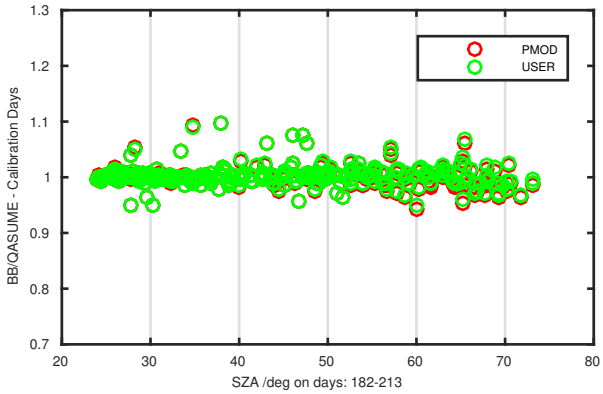

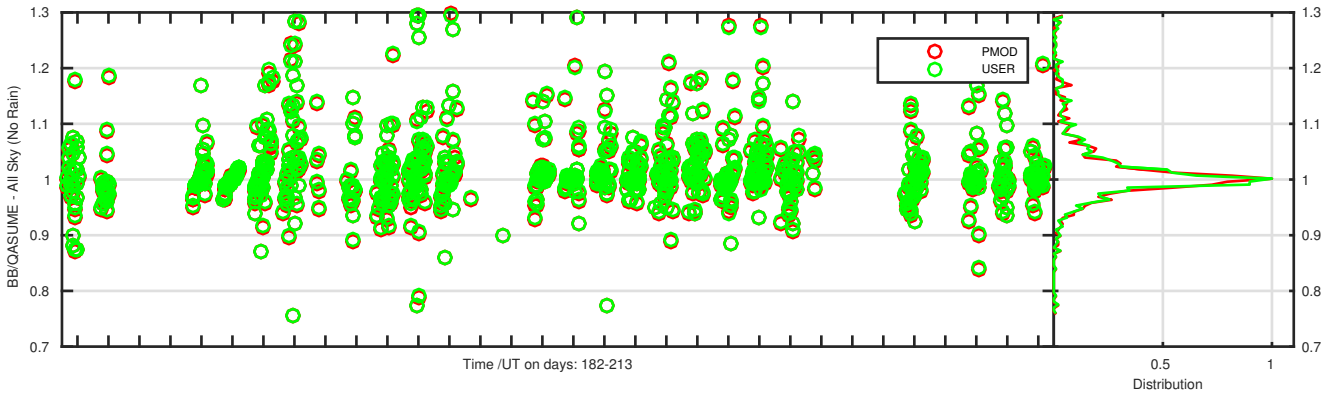

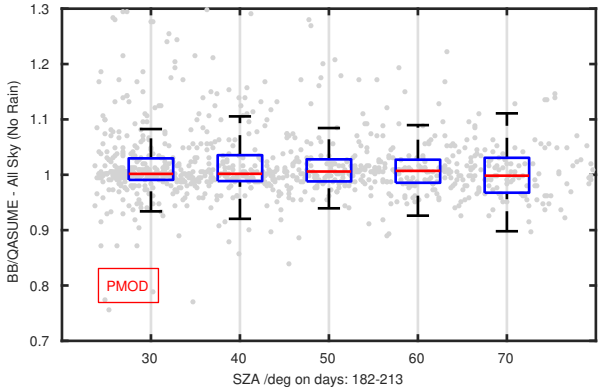

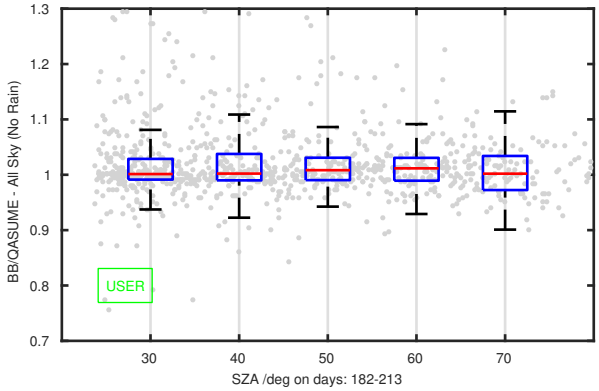

Calibration Results of KZ080002 (UVE)

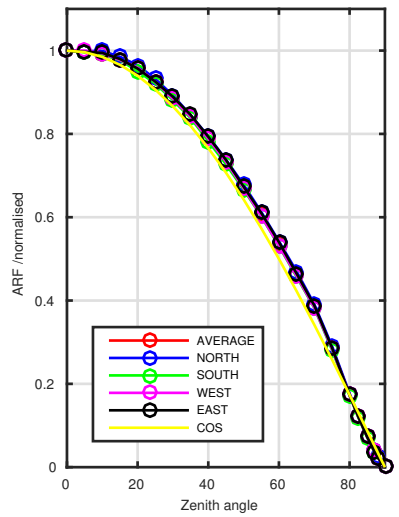

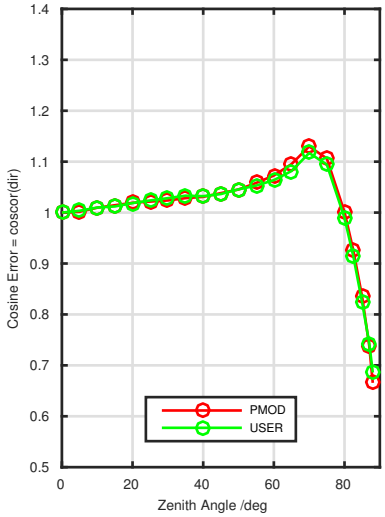

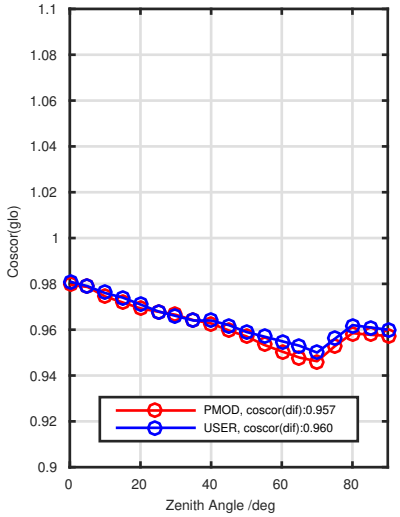

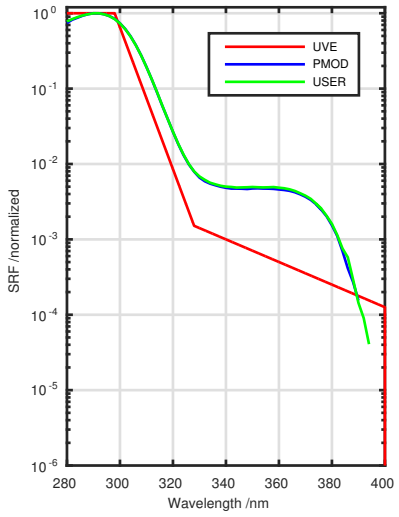

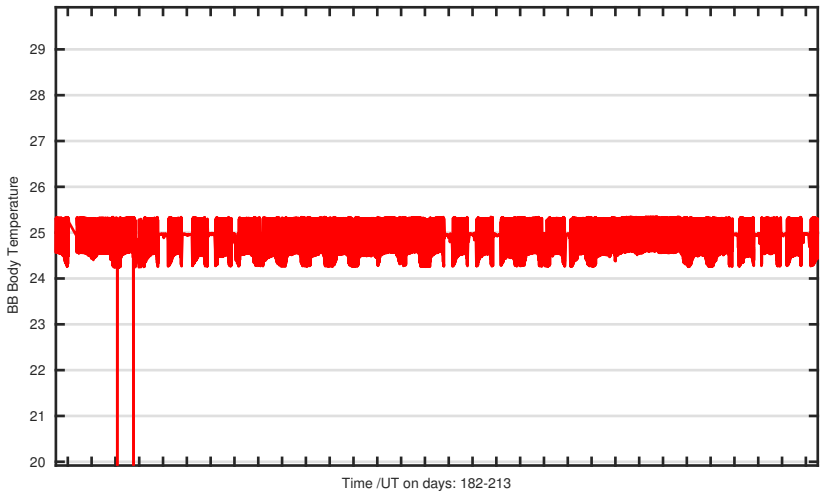

Calibration Matrix fn; Model sdisortREFms2009; f0=0.3445

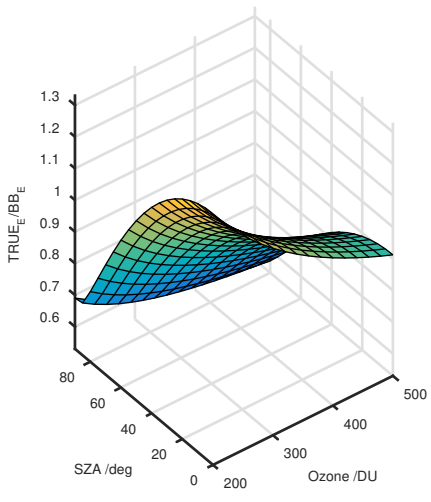

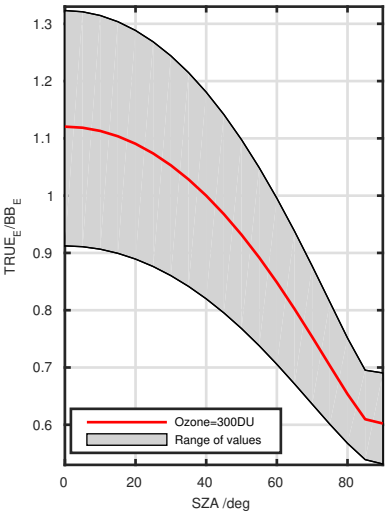

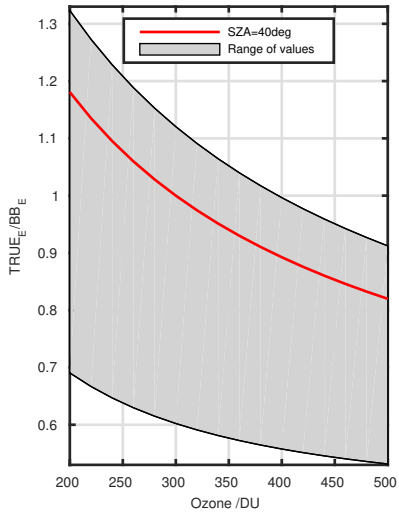

Calibration Results of KZ080002 (UVE)

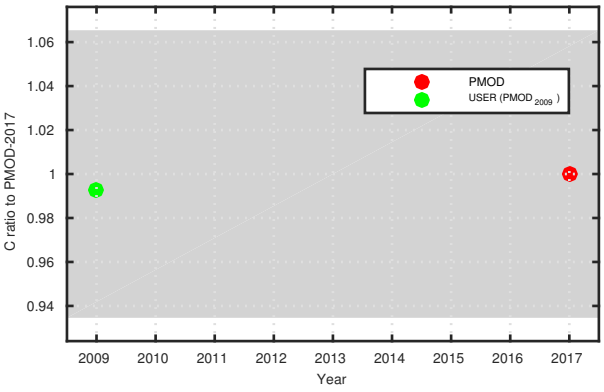

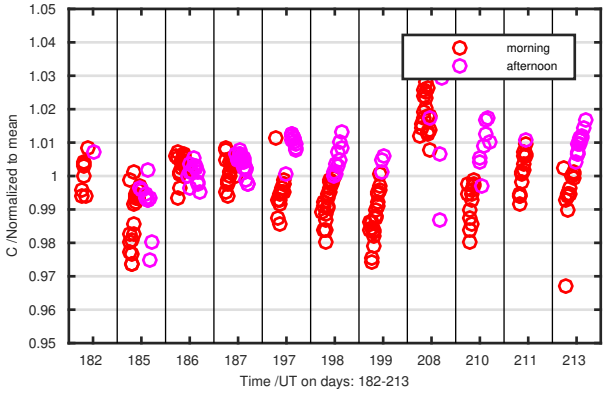

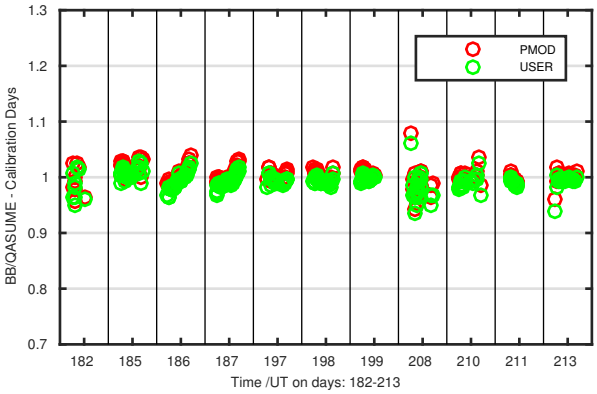

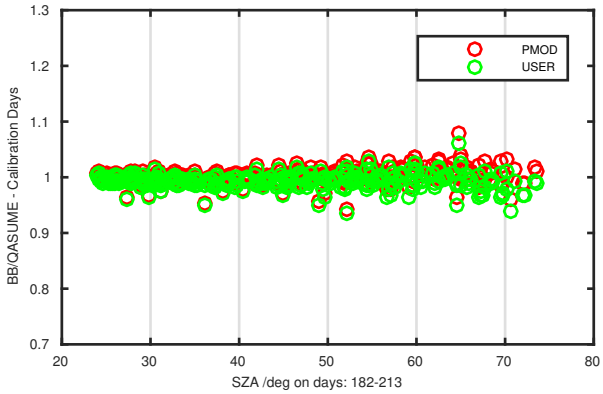

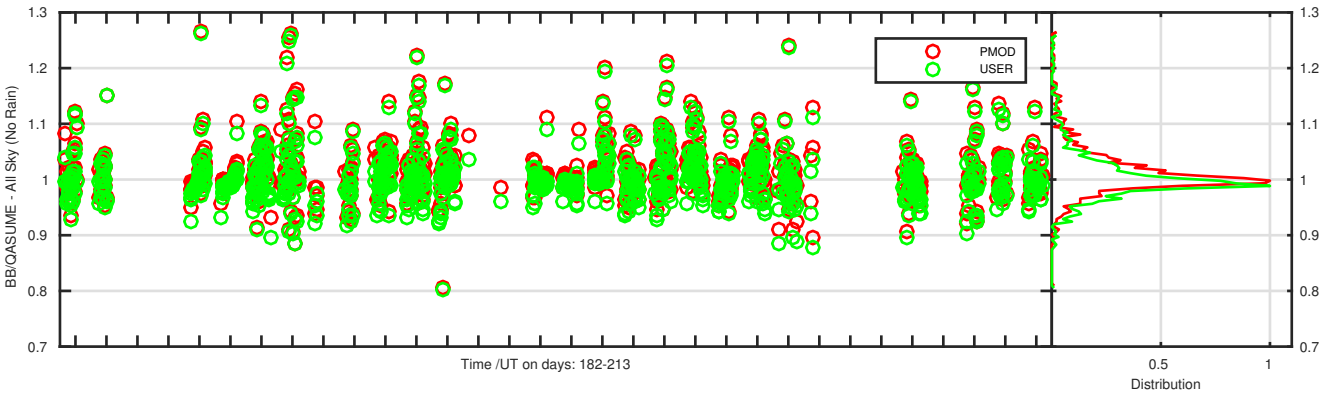

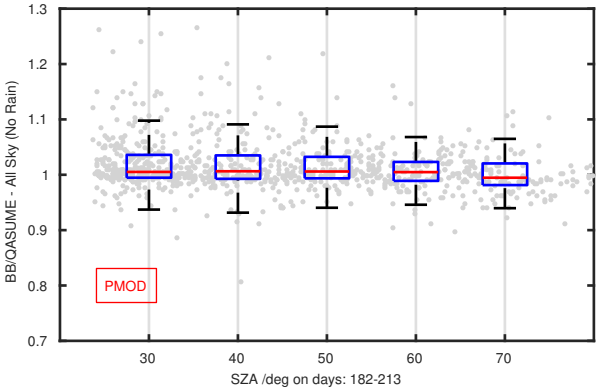

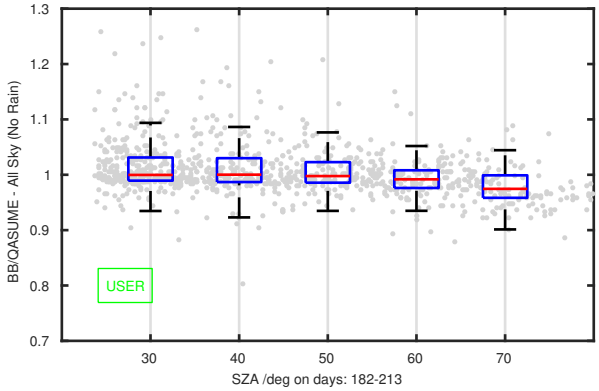

Calibration Results of KZ080003 (UVA)

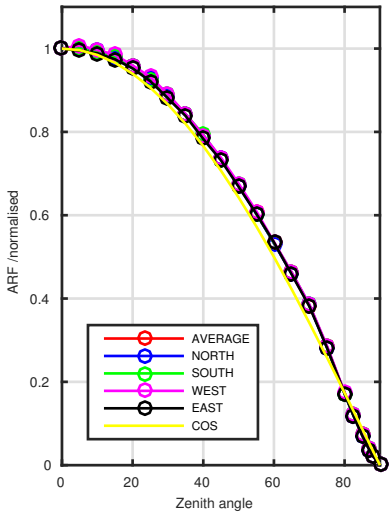

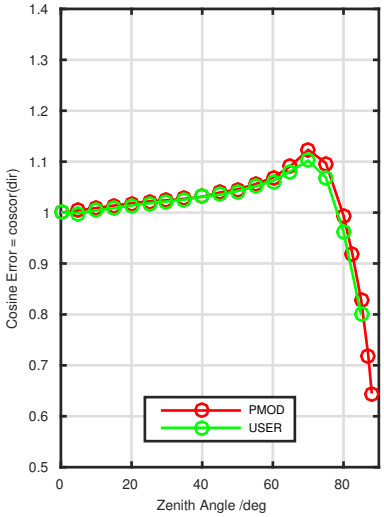

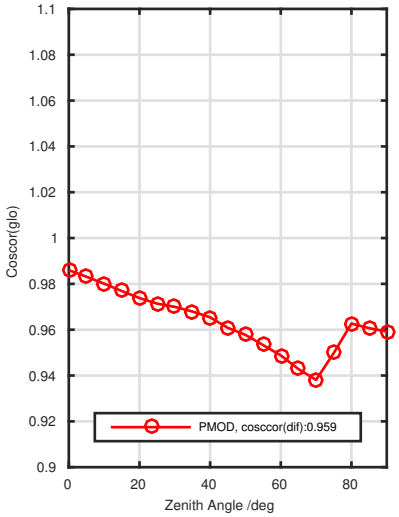

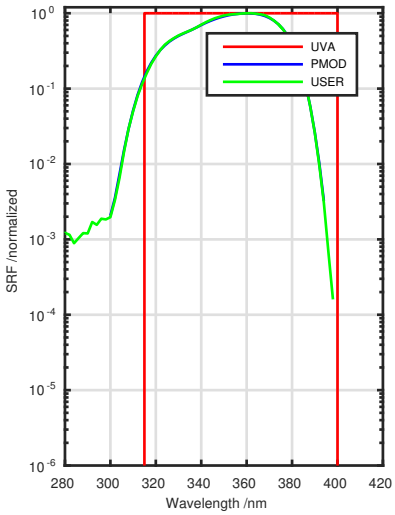

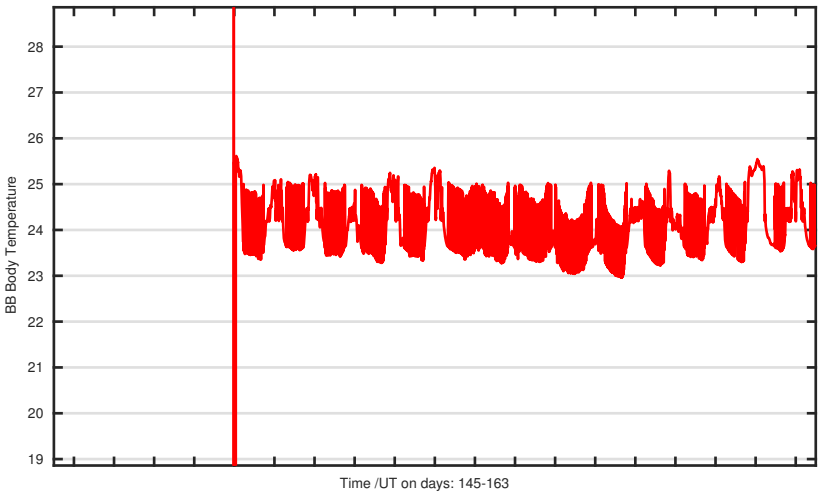

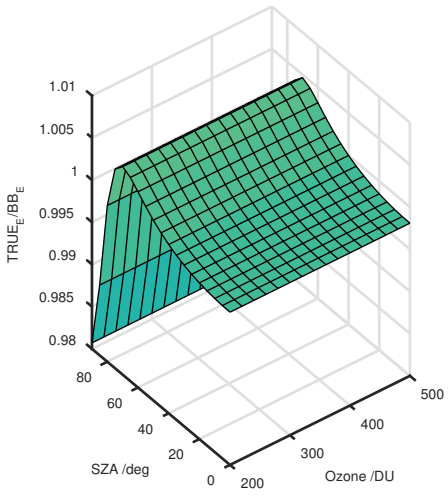

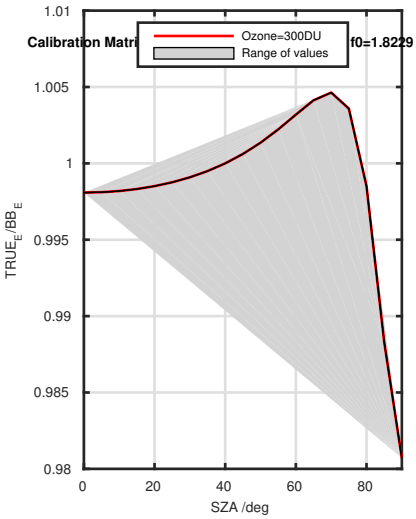

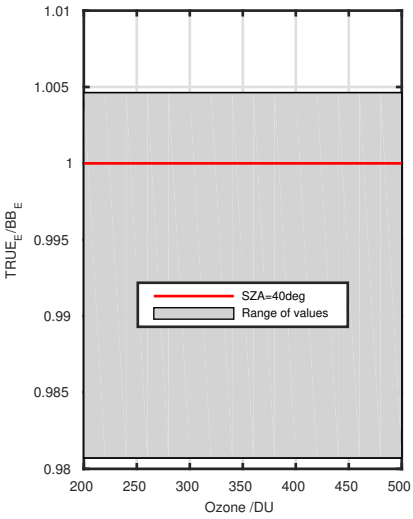

Calibration Results of KZ080003 (UVA)

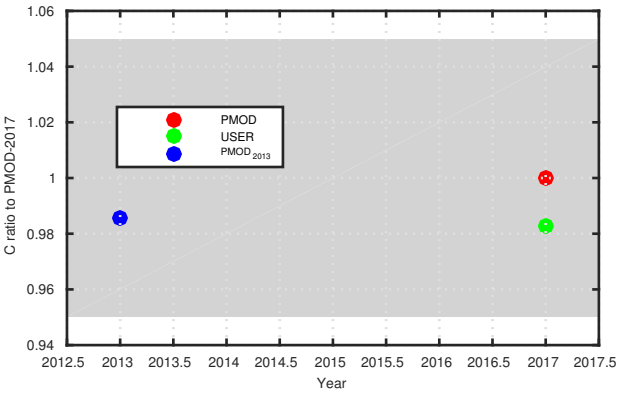

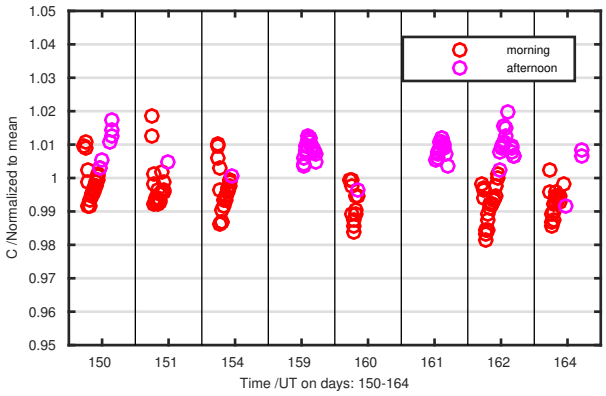

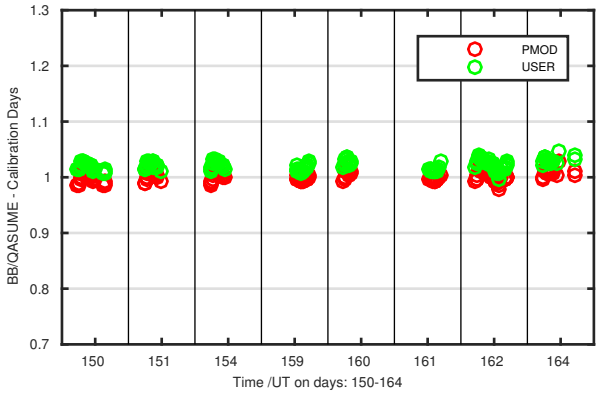

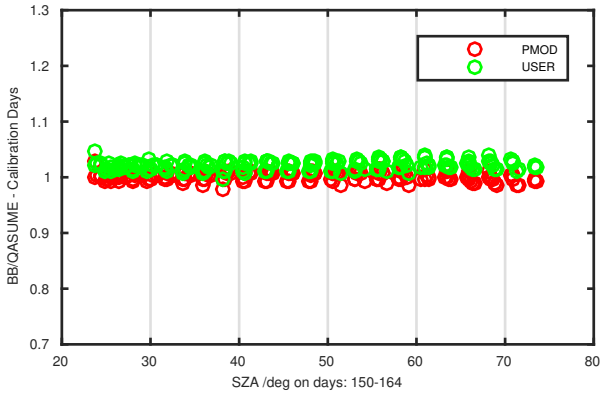

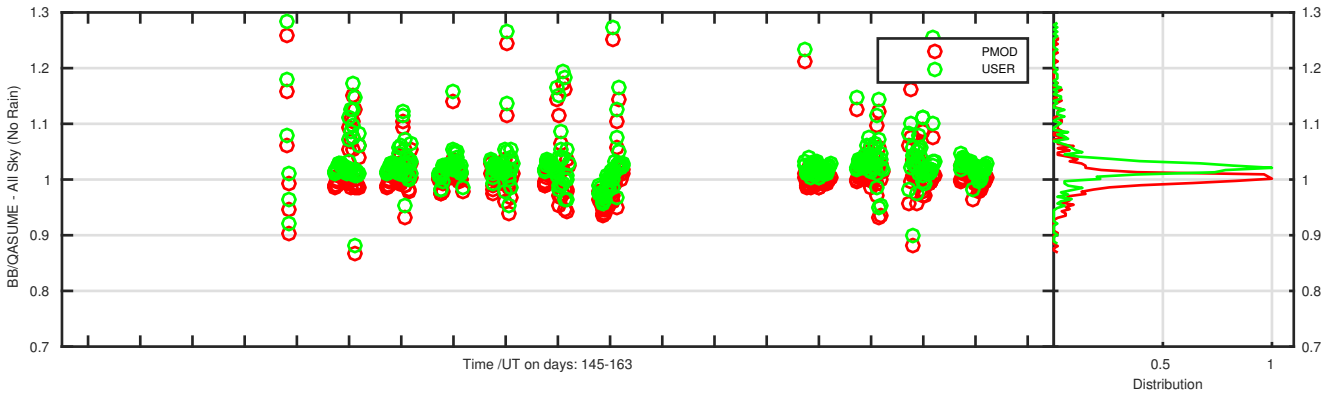

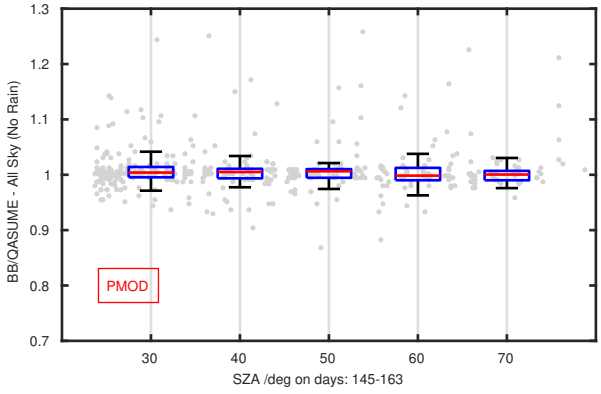

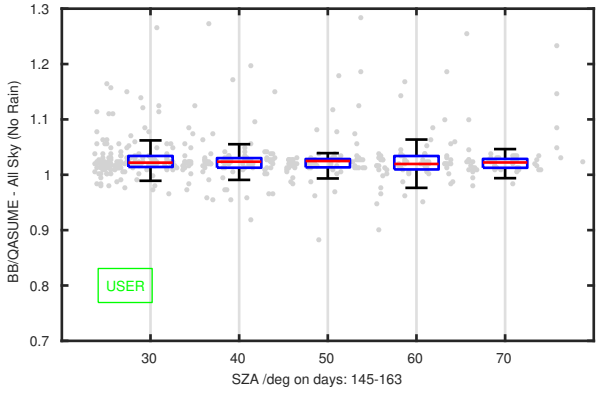

Calibration Results of KZ080003 (UVE)

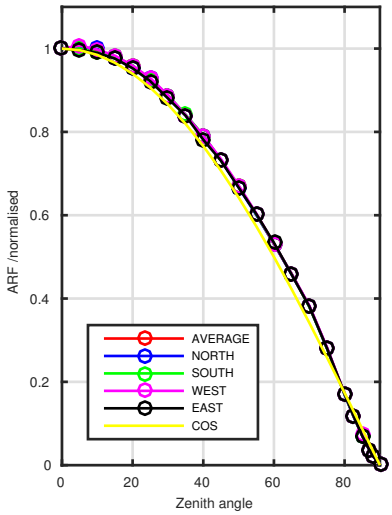

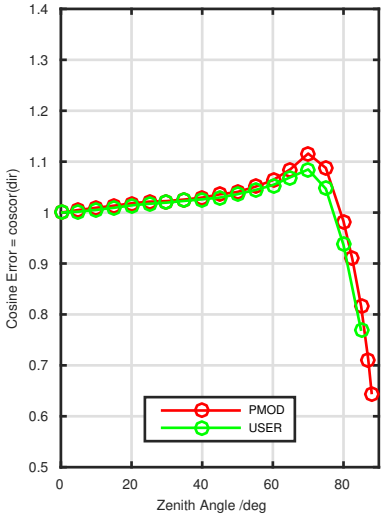

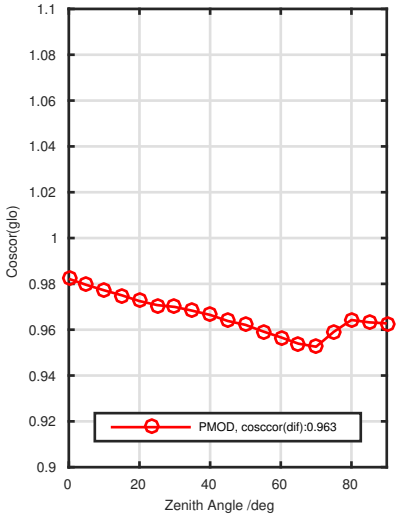

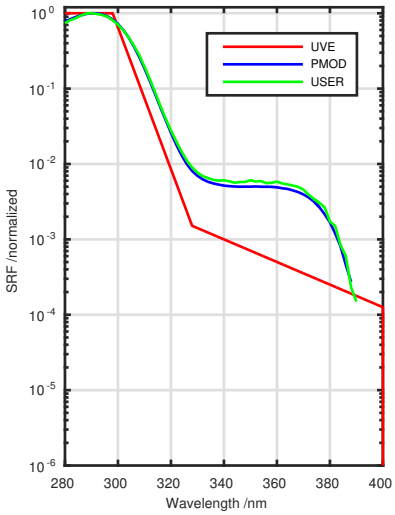

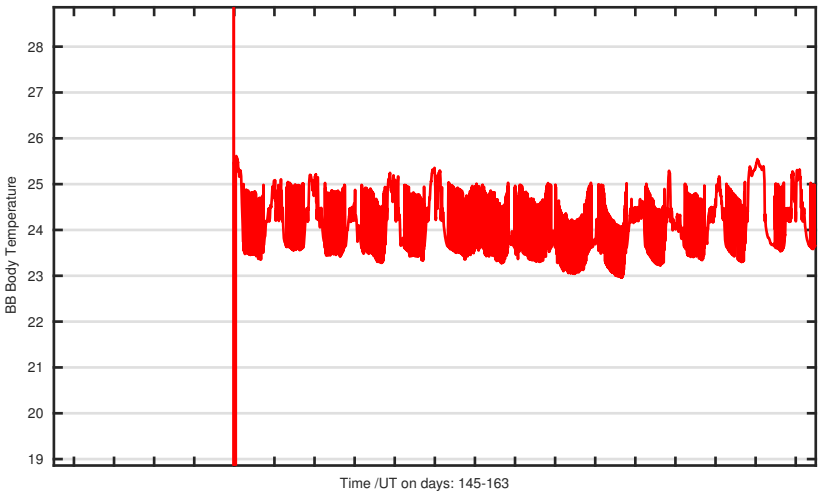

Calibration Matrix fn; Model sdisortREFms2009; f0=0.3485

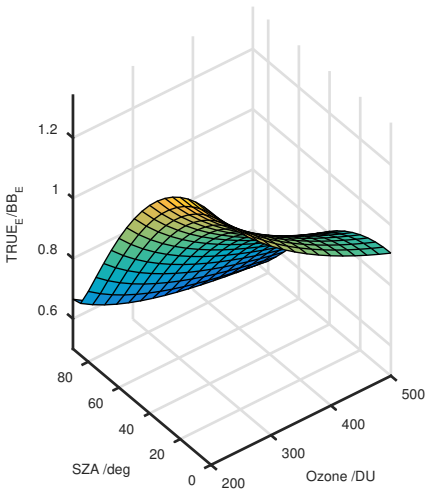

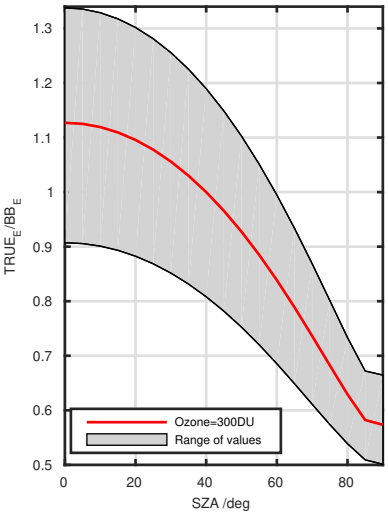

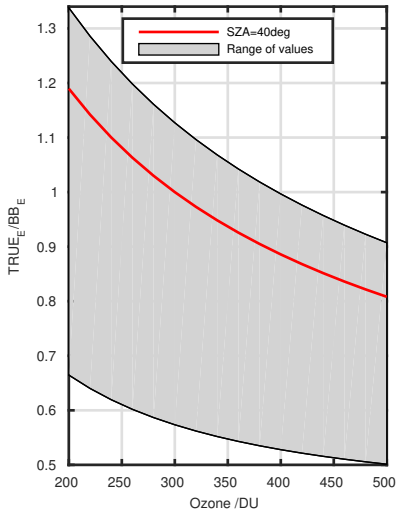

Calibration Results of KZ080003 (UVE)

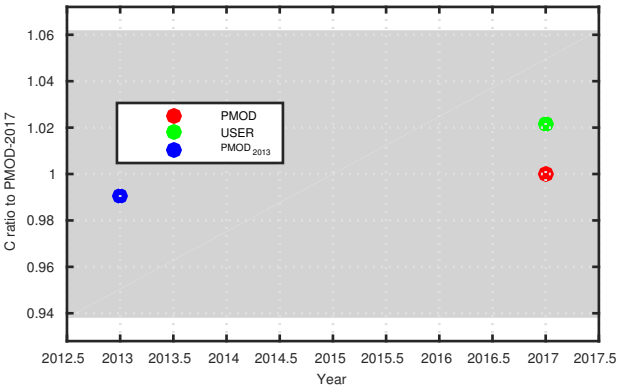

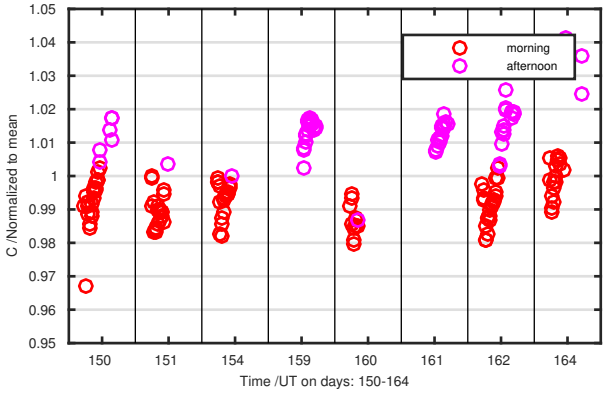

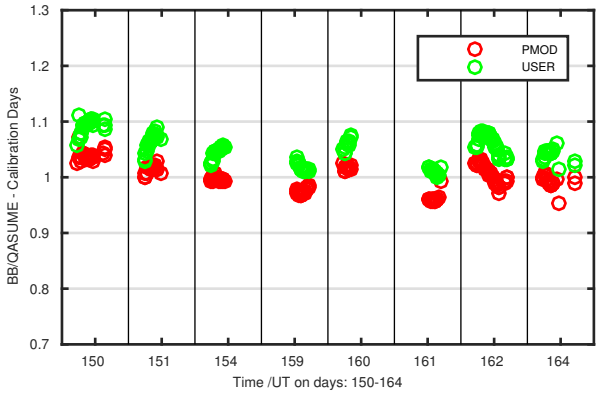

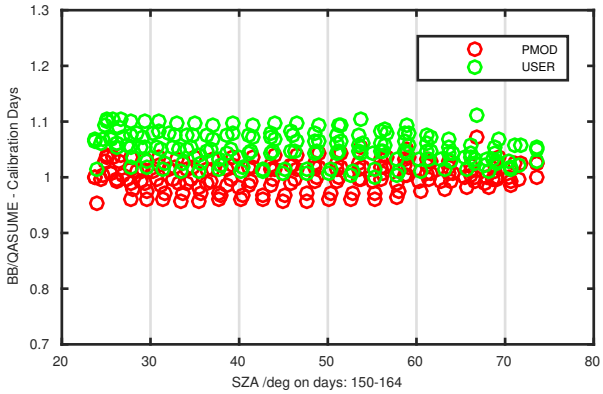

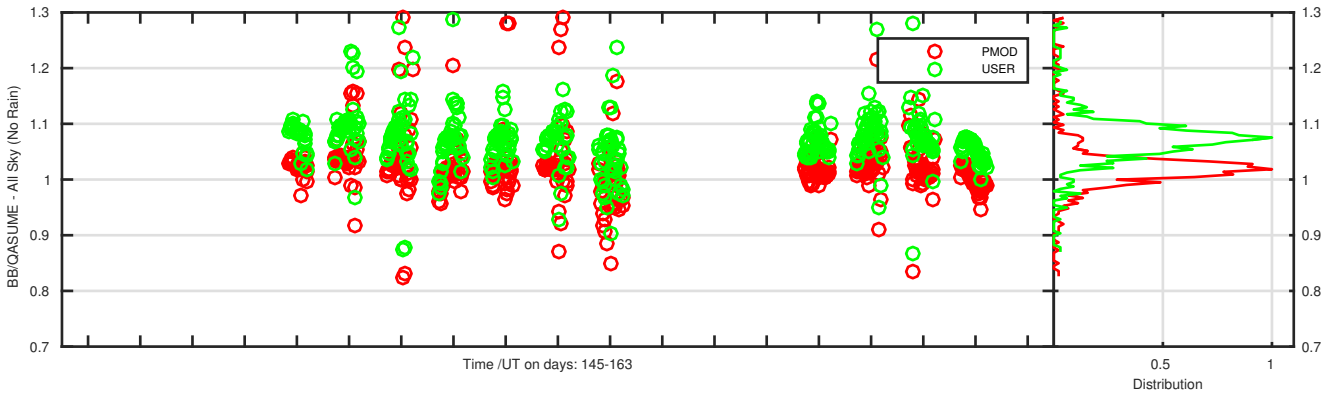

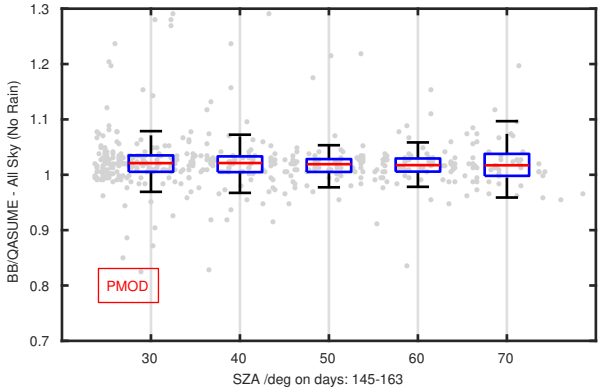

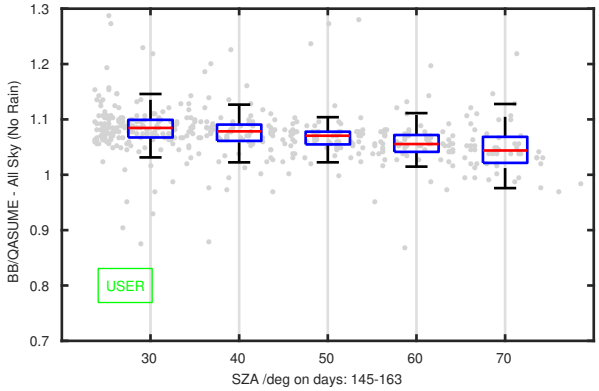

Calibration Results of KZ110141 (UVA)

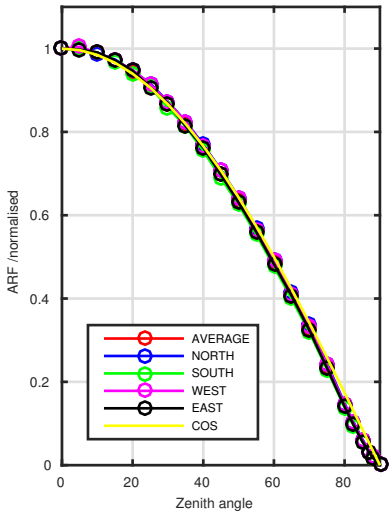

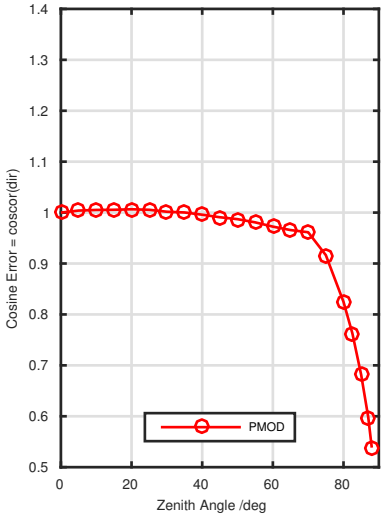

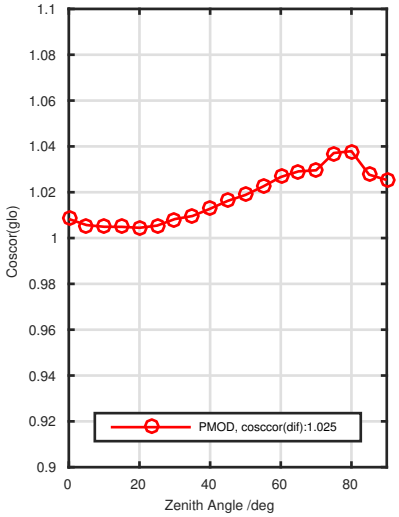

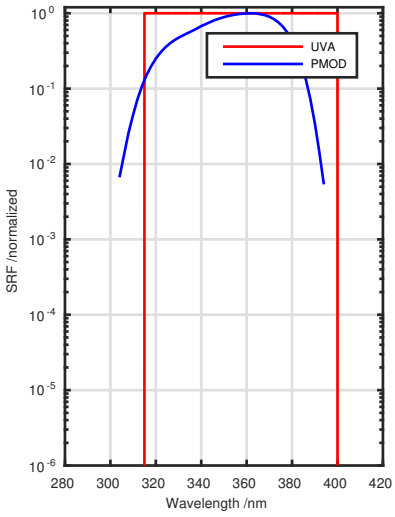

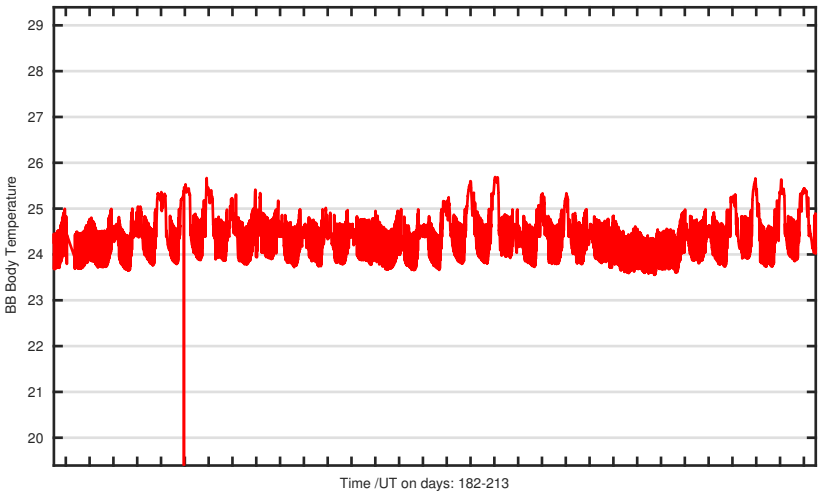

Calibration Matrix fn; Model sdisortREFms2009; f0=1.8171

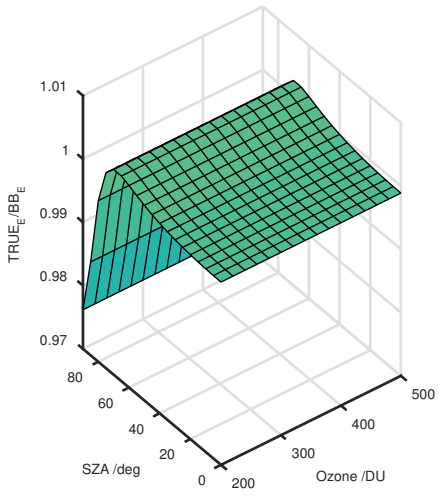

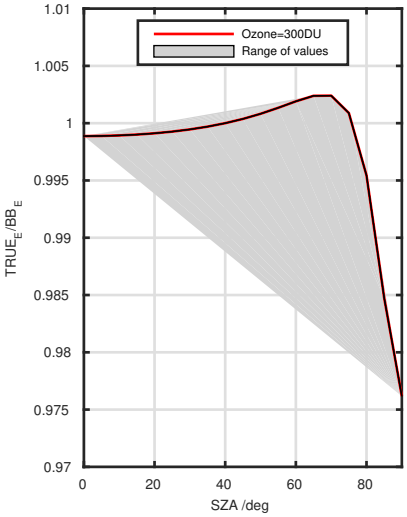

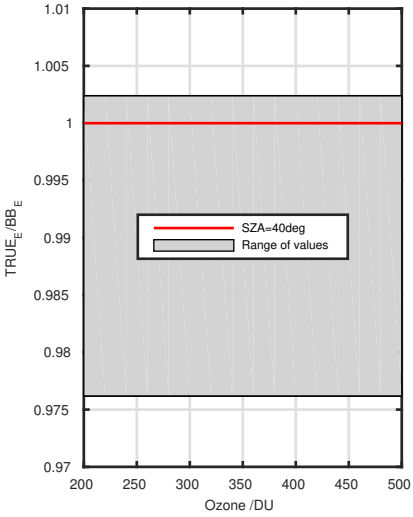

Calibration Results of KZ110141 (UVA)

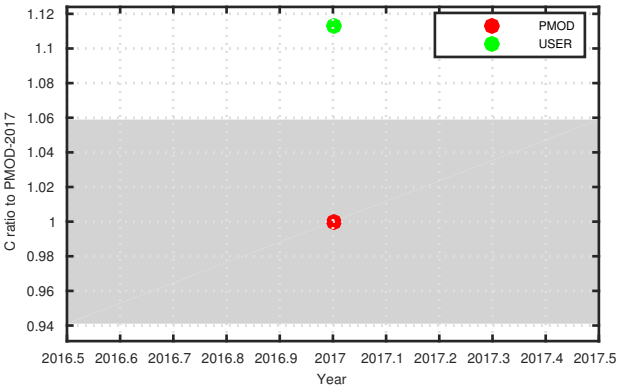

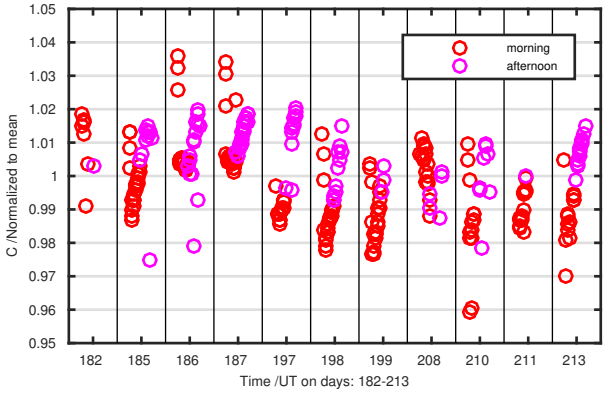

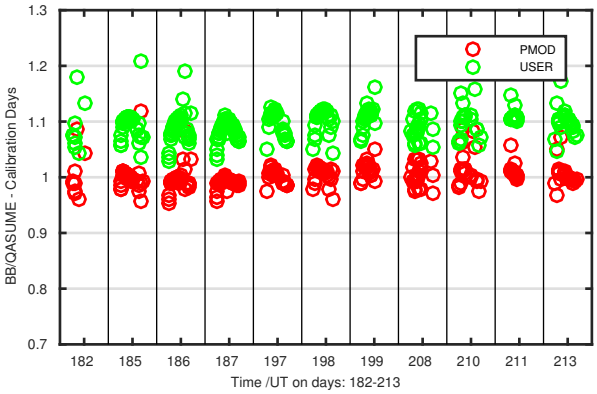

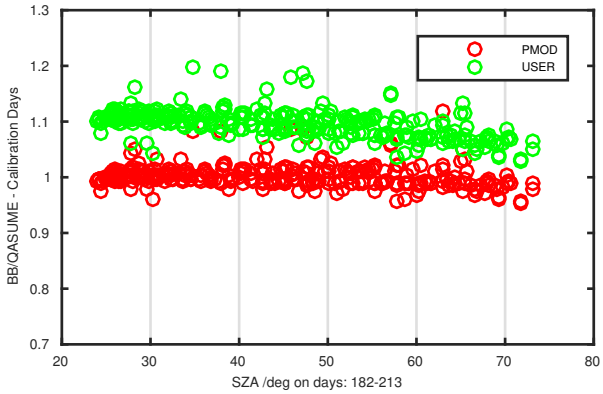

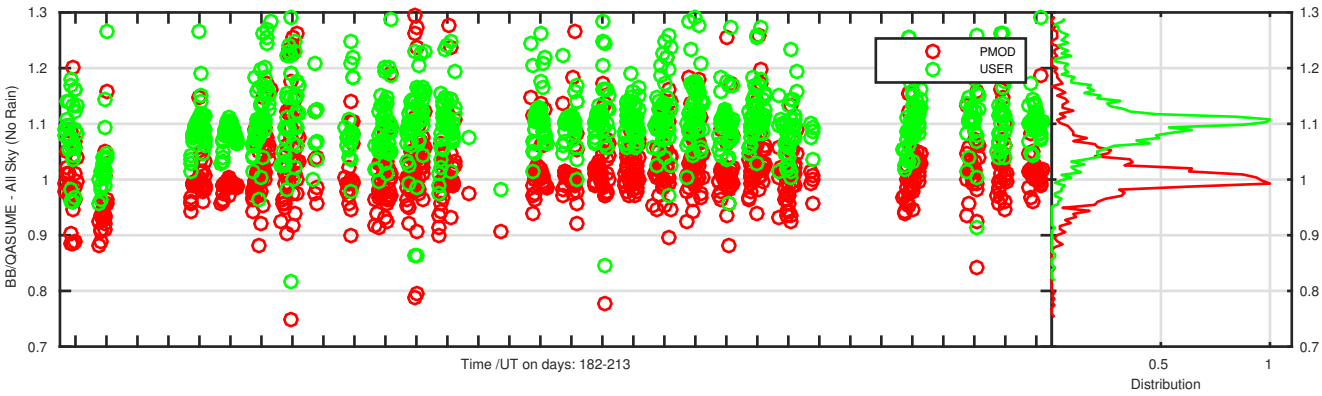

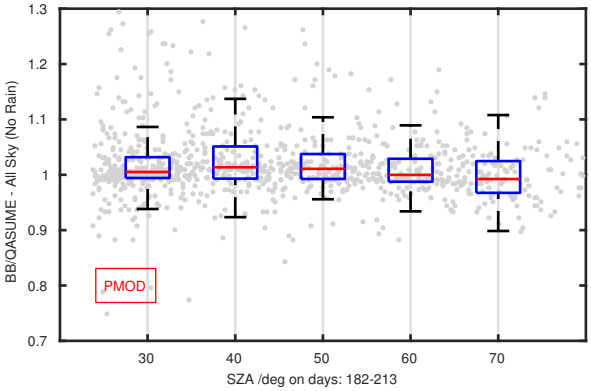

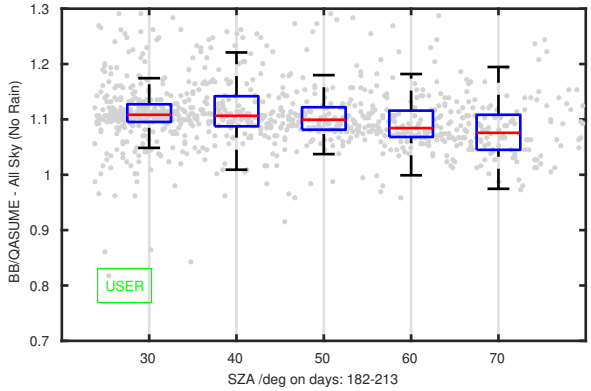

Calibration Results of KZ110141 (UVB)

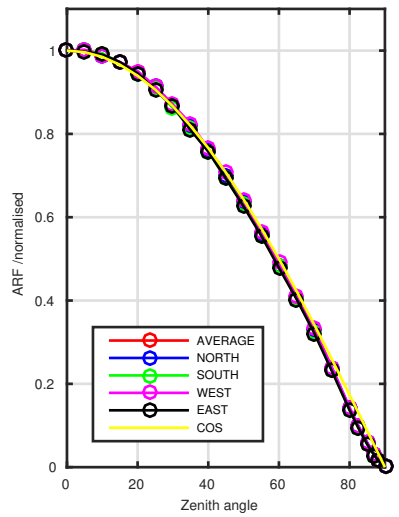

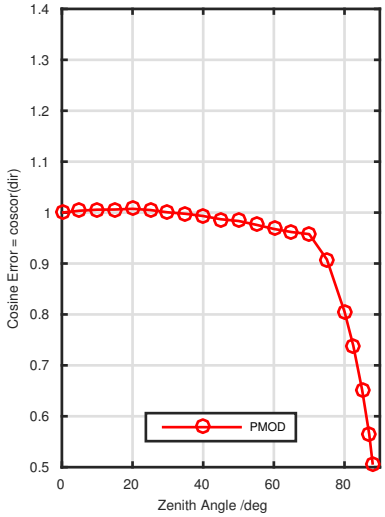

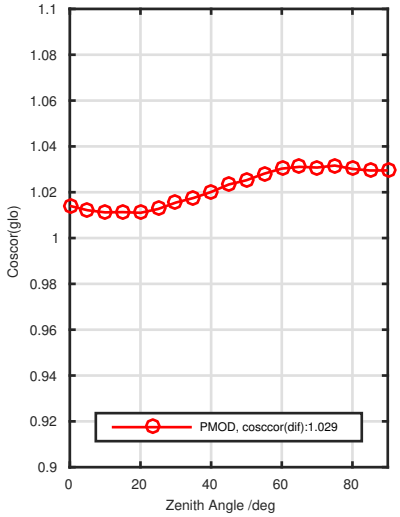

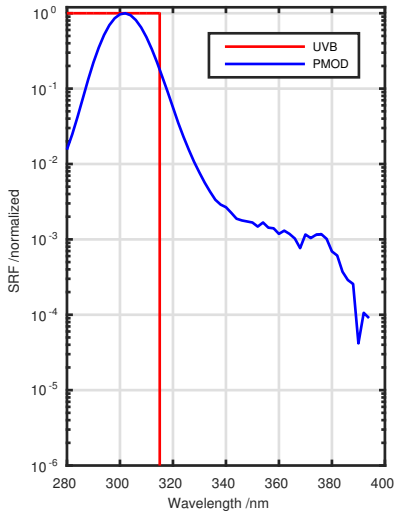

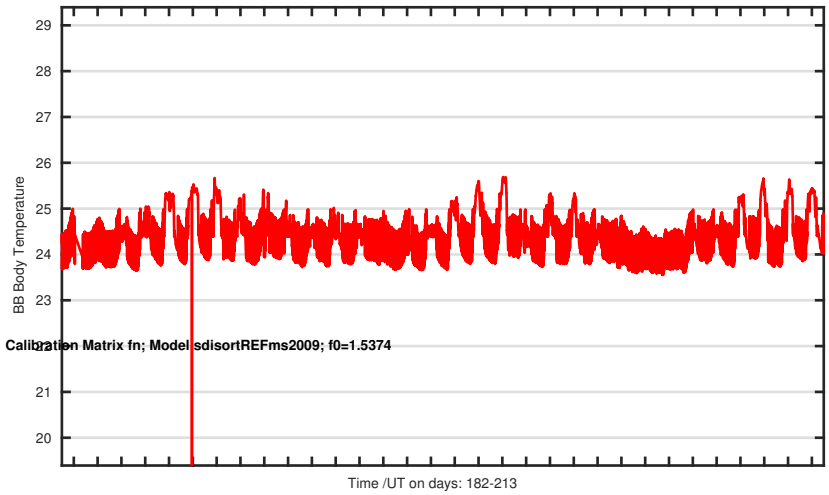

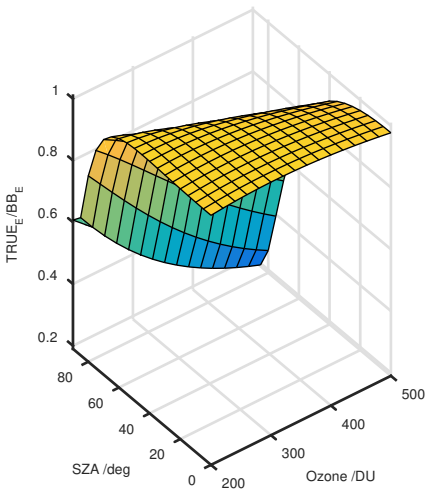

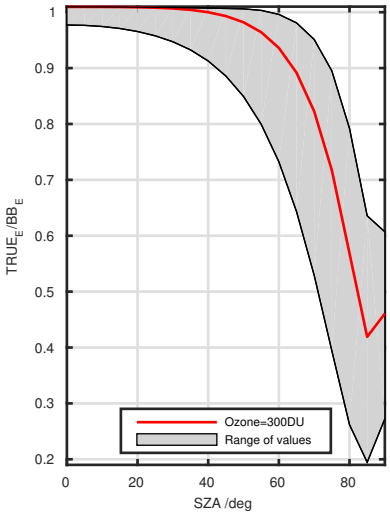

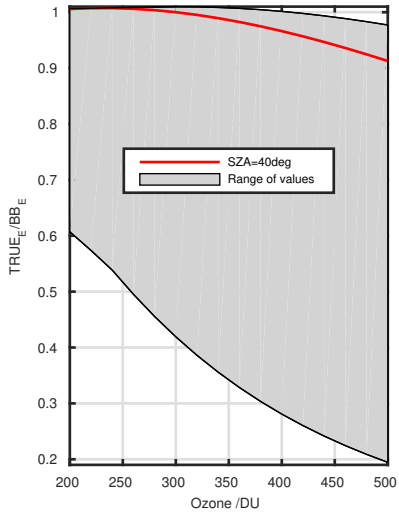

Calibration Results of KZ110141 (UVB)

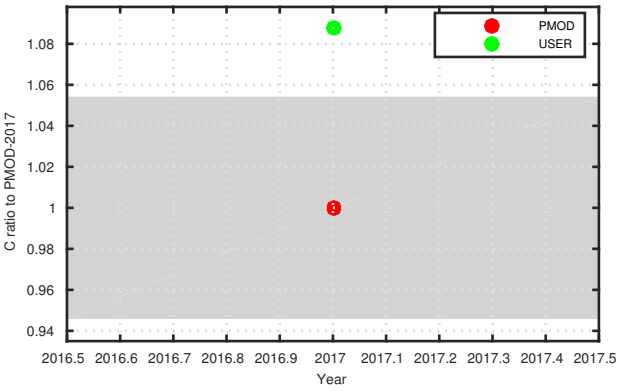

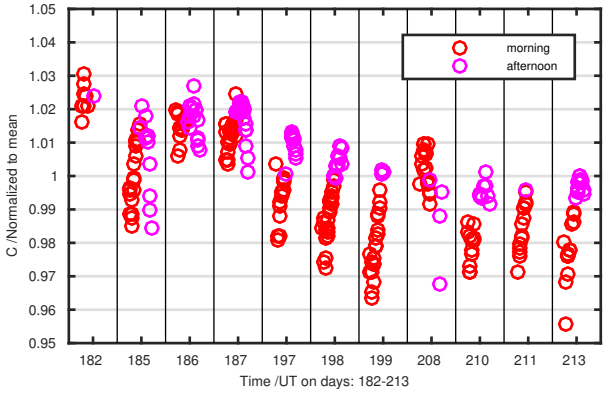

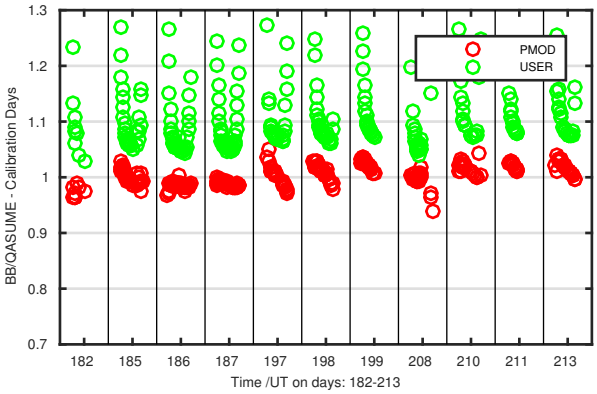

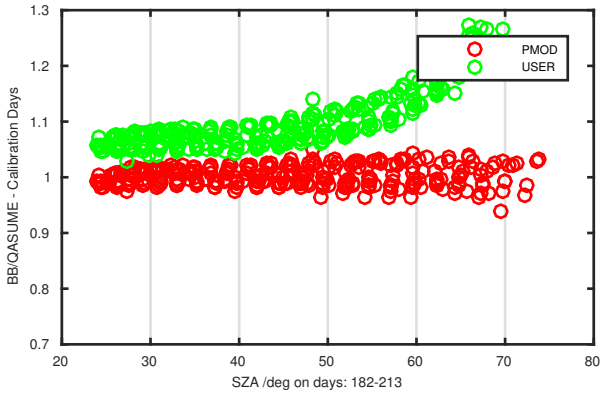

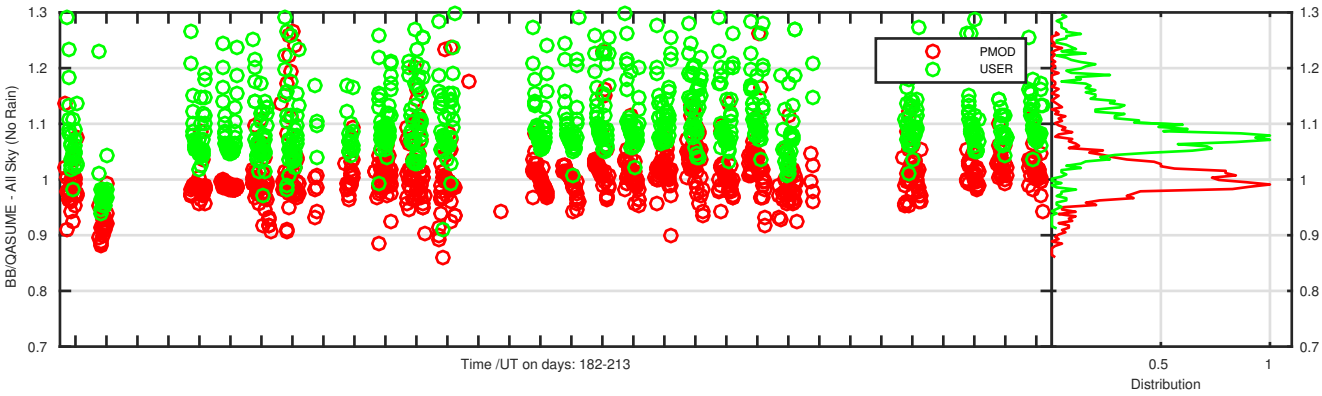

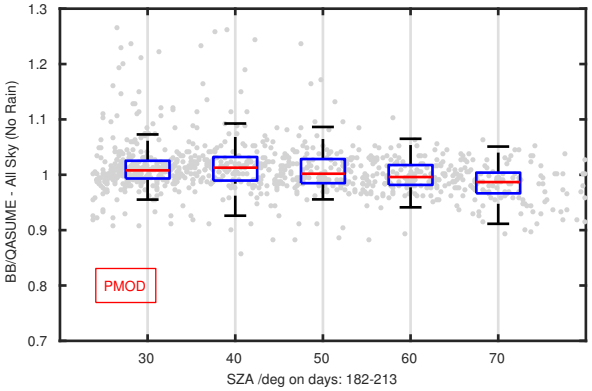

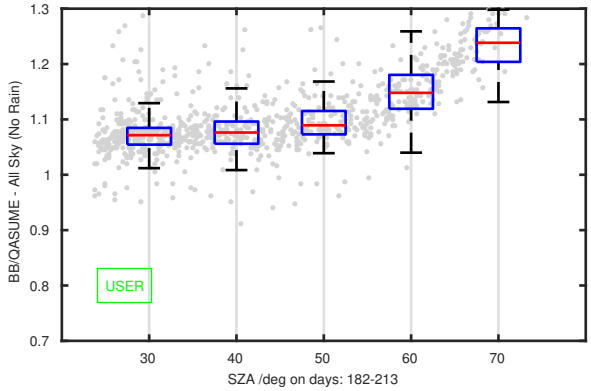

Calibration Results of KZ120023 (UVA)

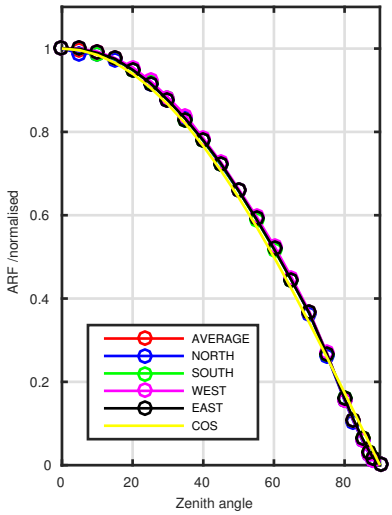

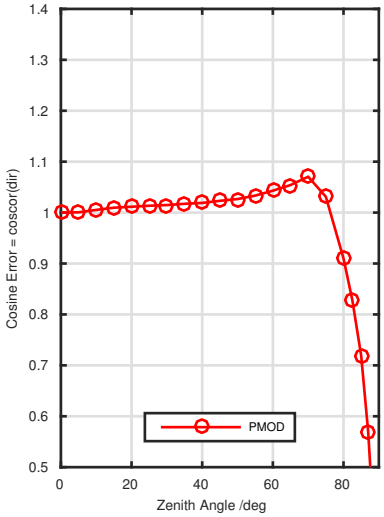

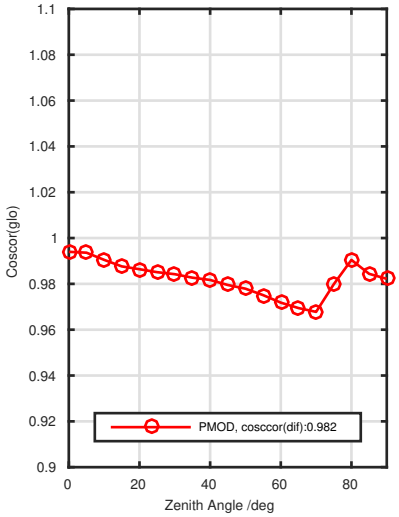

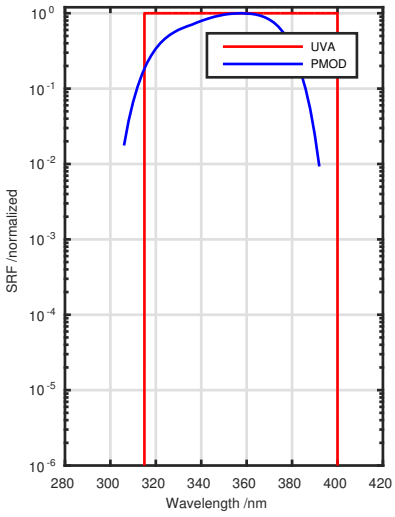

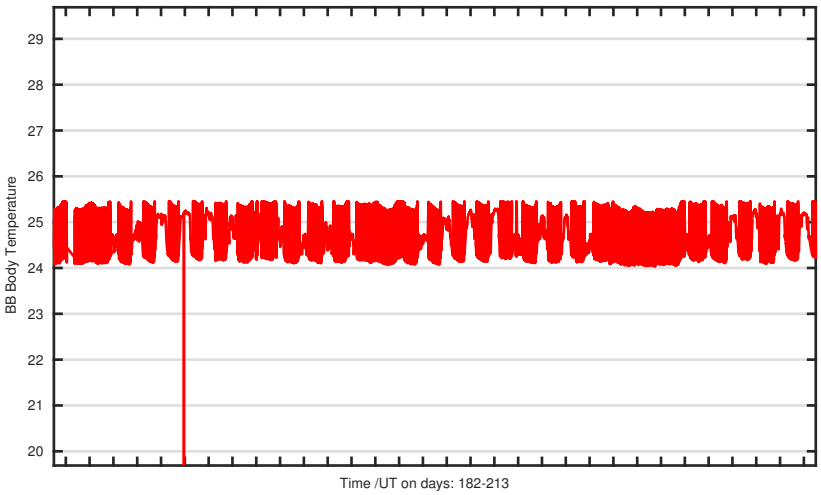

Calibration Matrix fn; Model sdisortREFms2009; f0=1.7733

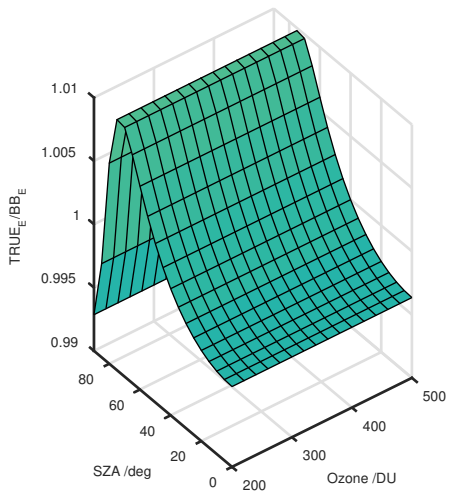

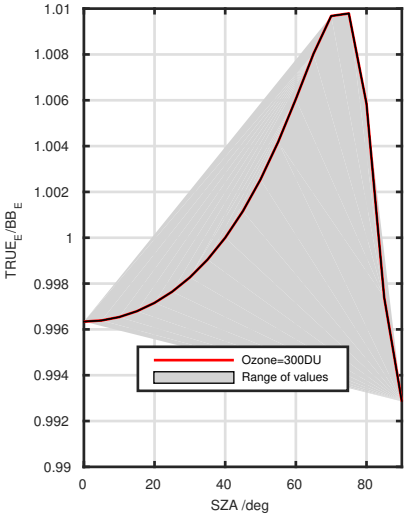

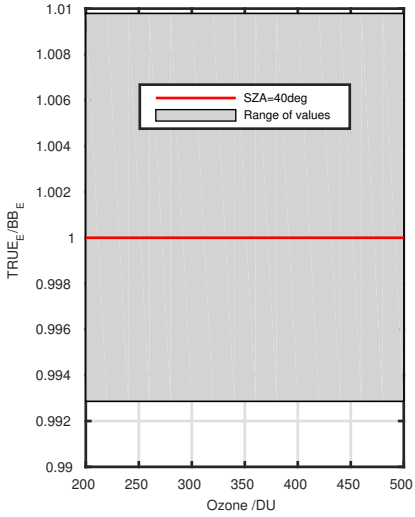

Calibration Results of KZ120023 (UVA)

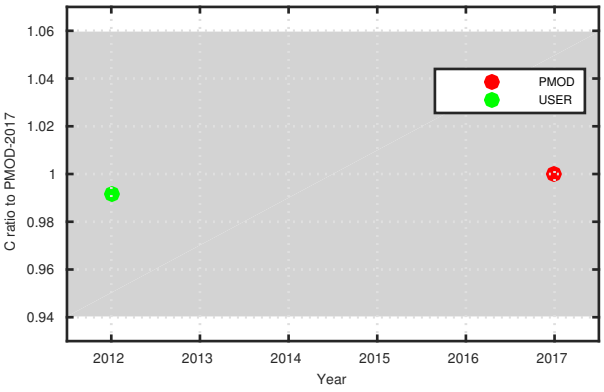

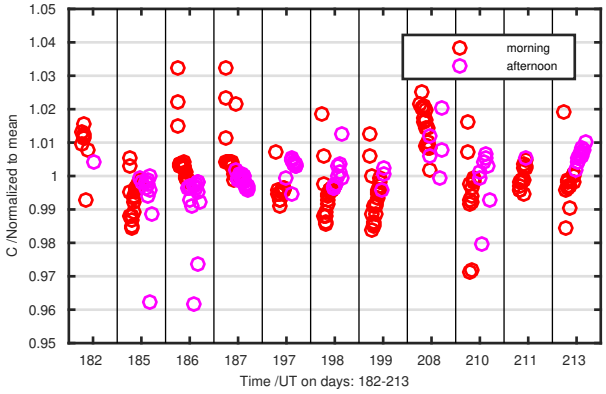

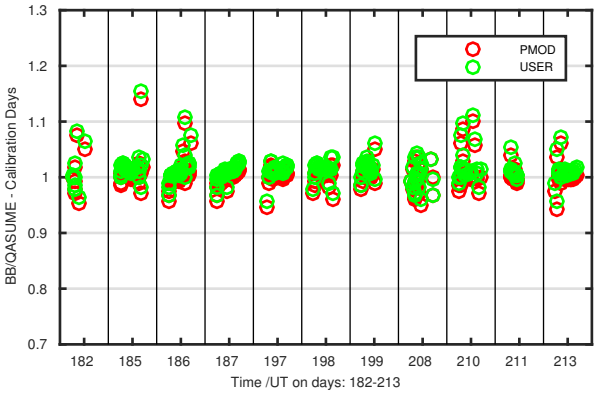

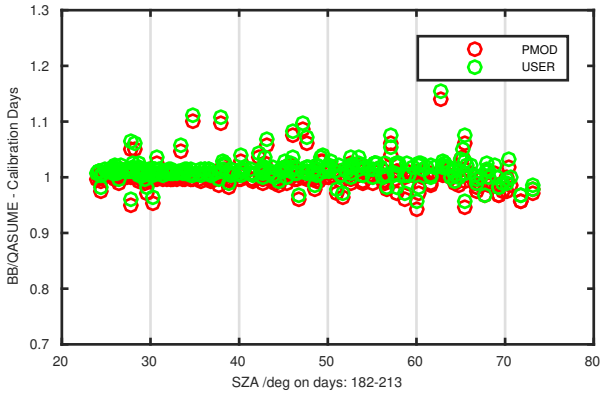

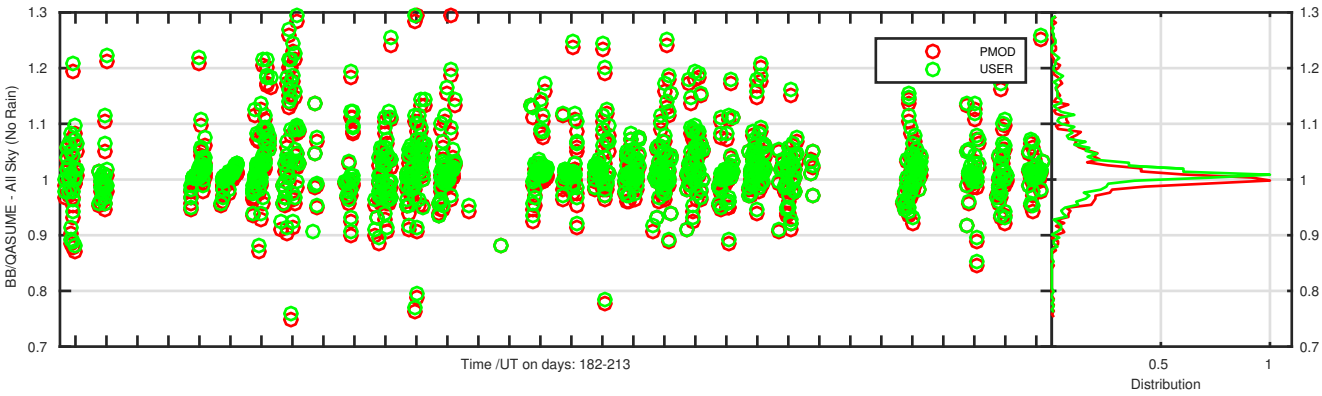

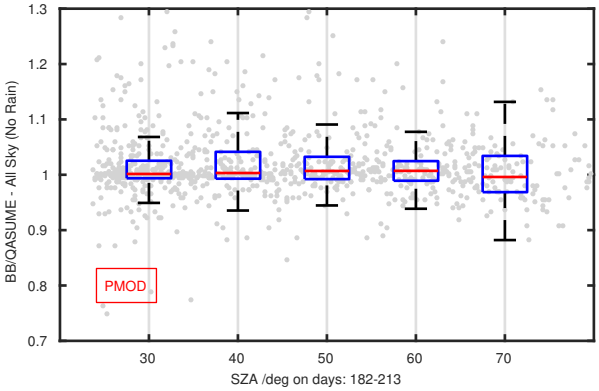

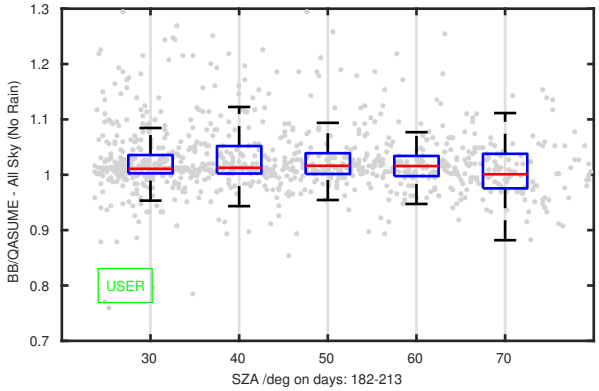

Calibration Results of KZ120023 (UVE)

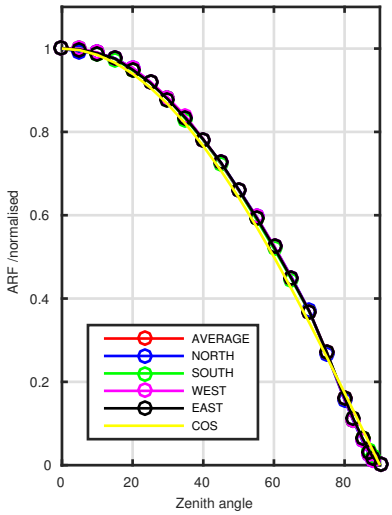

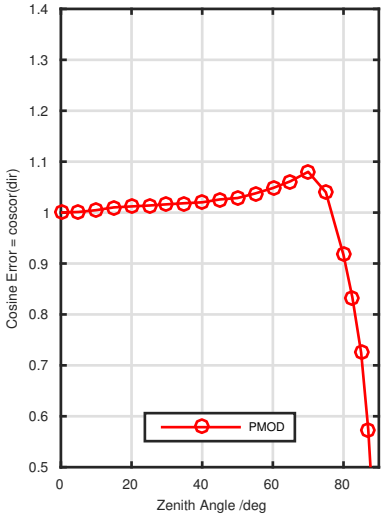

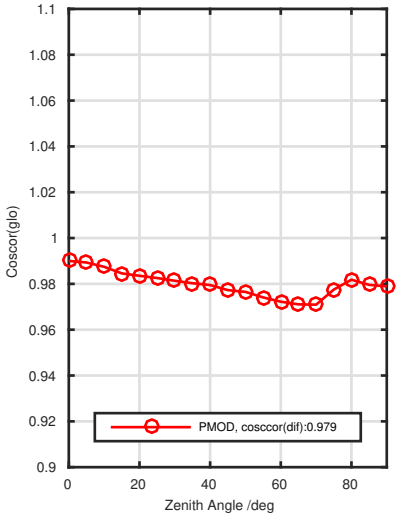

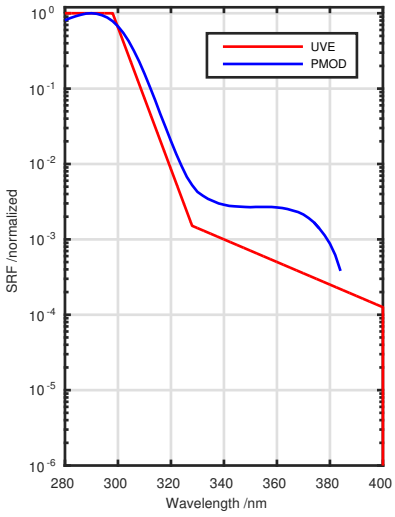

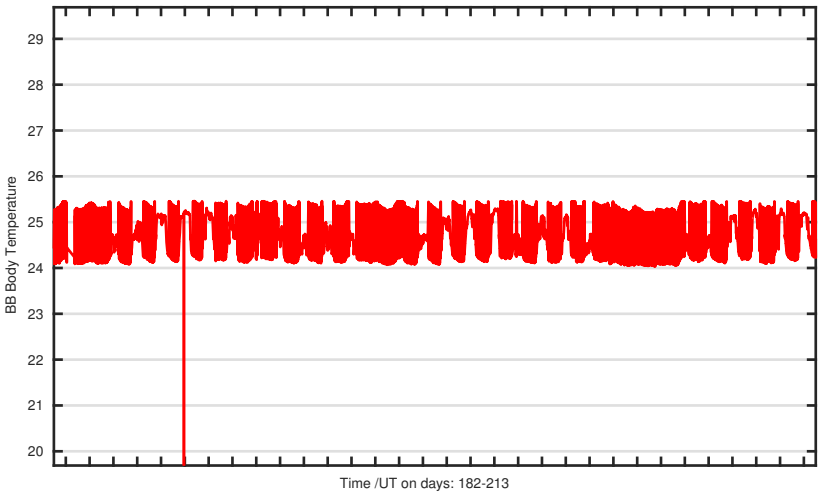

Calibration Matrix fn; Model sdisortREFms2009; f0=0.4617

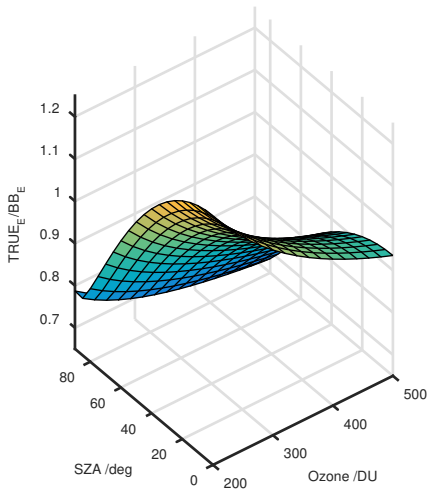

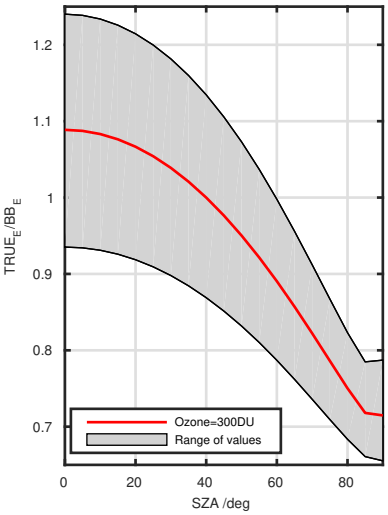

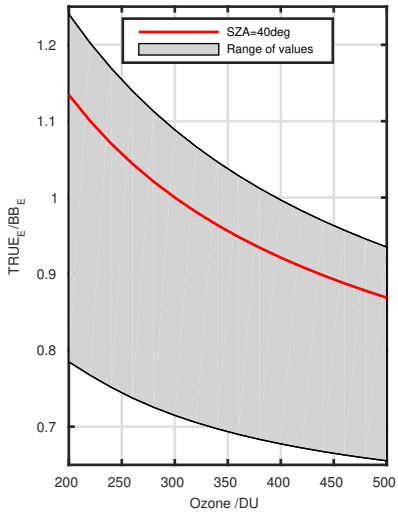

Calibration Results of KZ120023 (UVE)

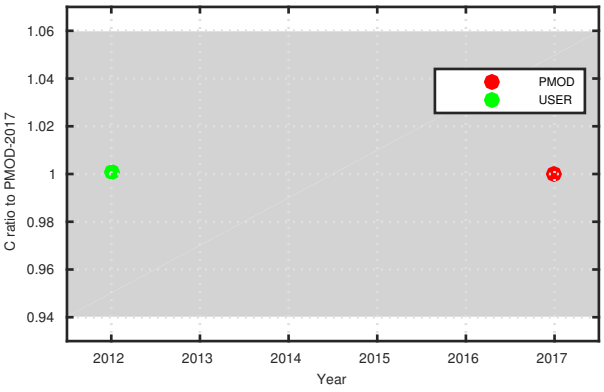

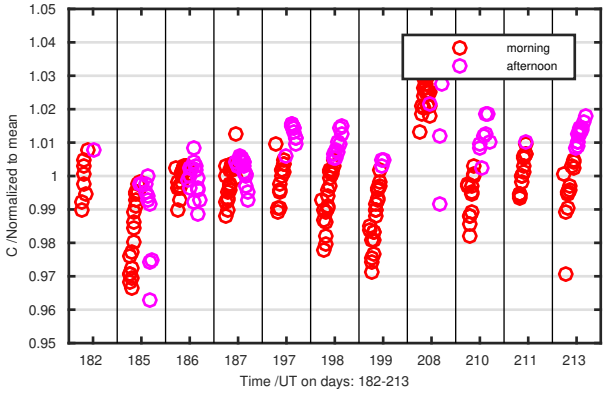

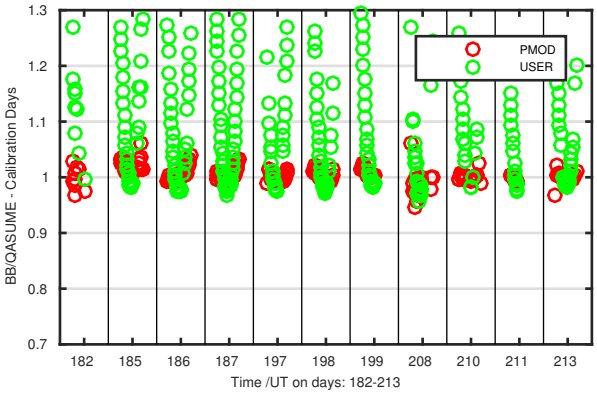

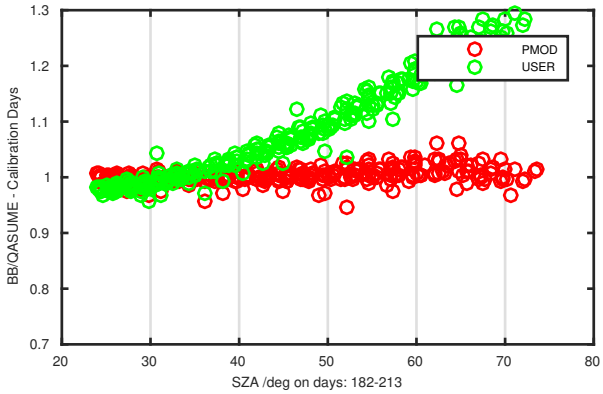

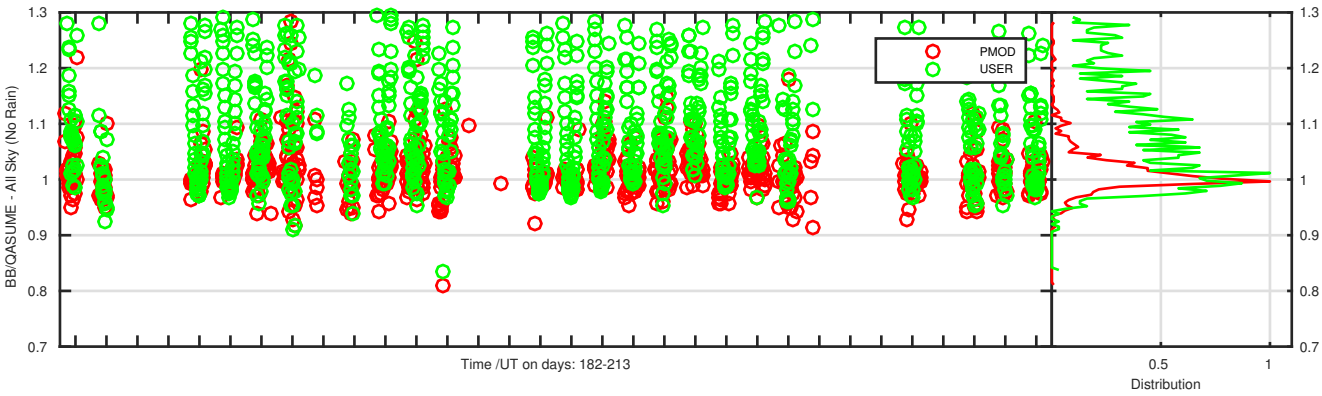

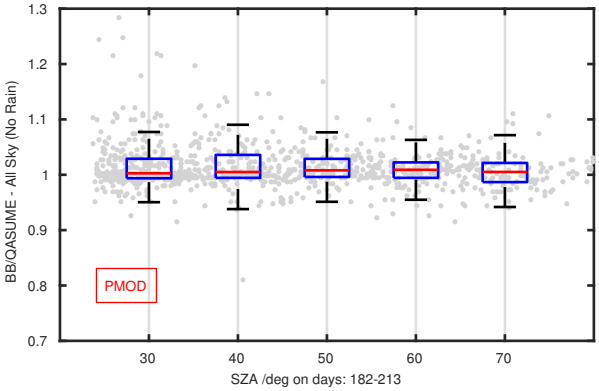

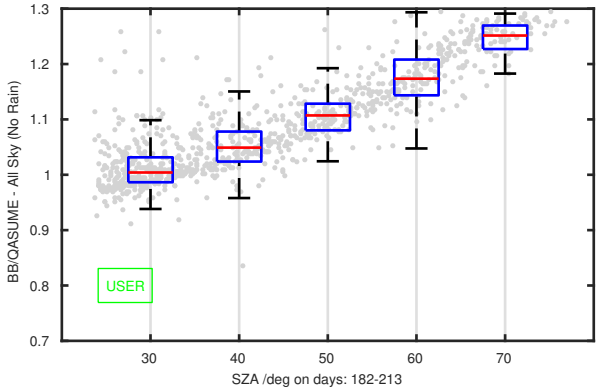

Calibration Results of KZ120132 (UVA)

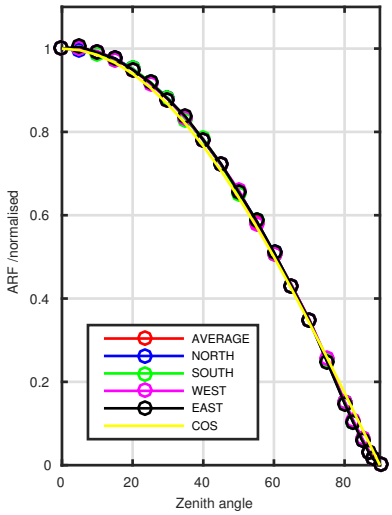

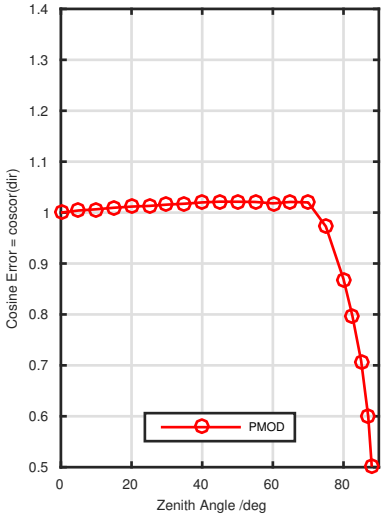

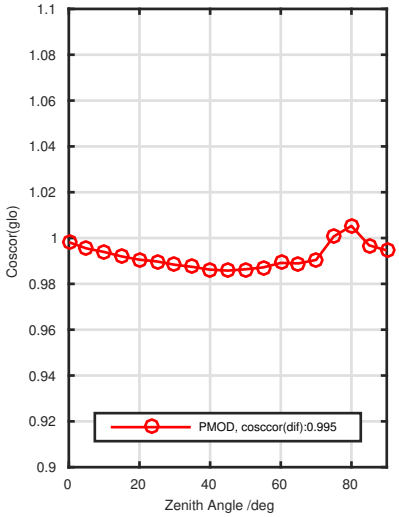

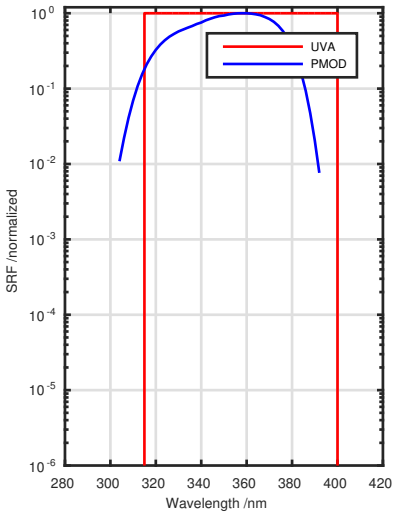

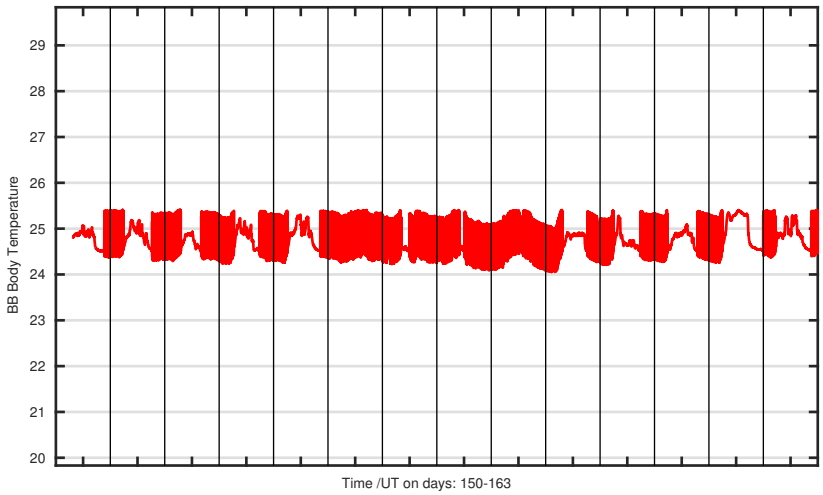

Calibration Matrix fn; Model sdisortREFms2009; f0=1.7866

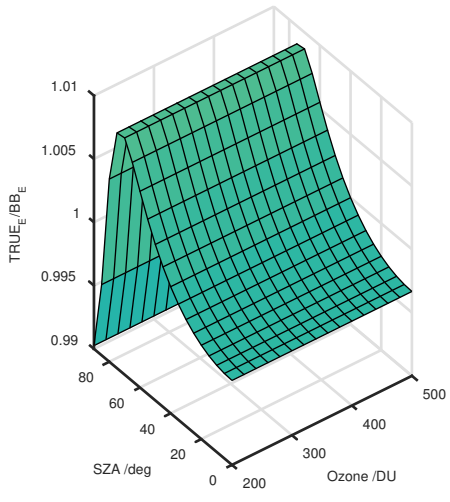

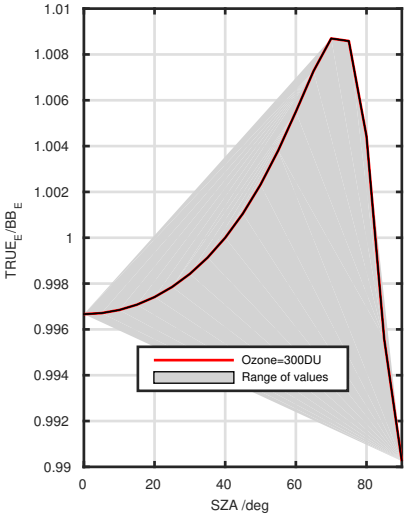

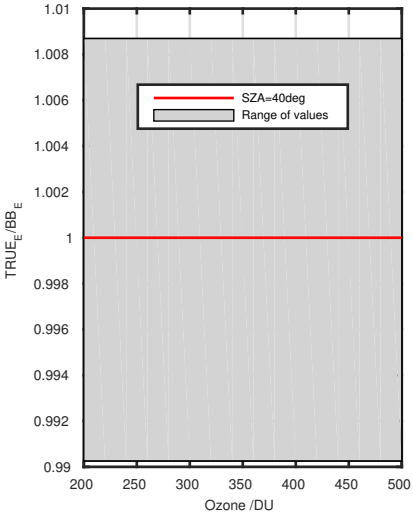

Calibration Results of KZ120132 (UVA)

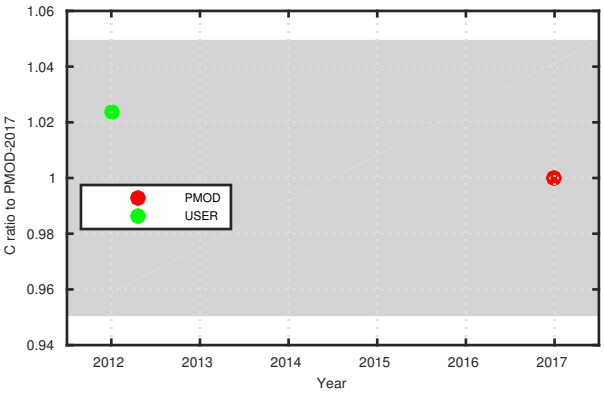

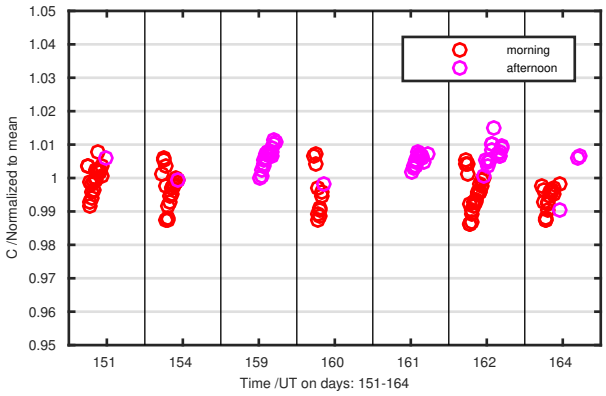

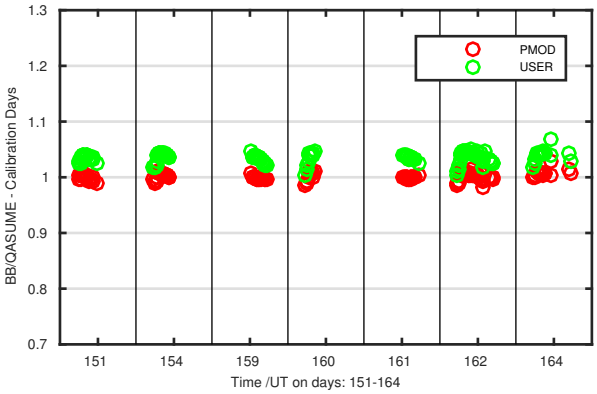

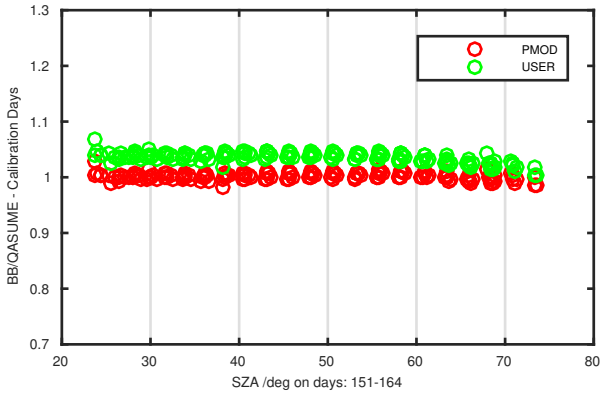

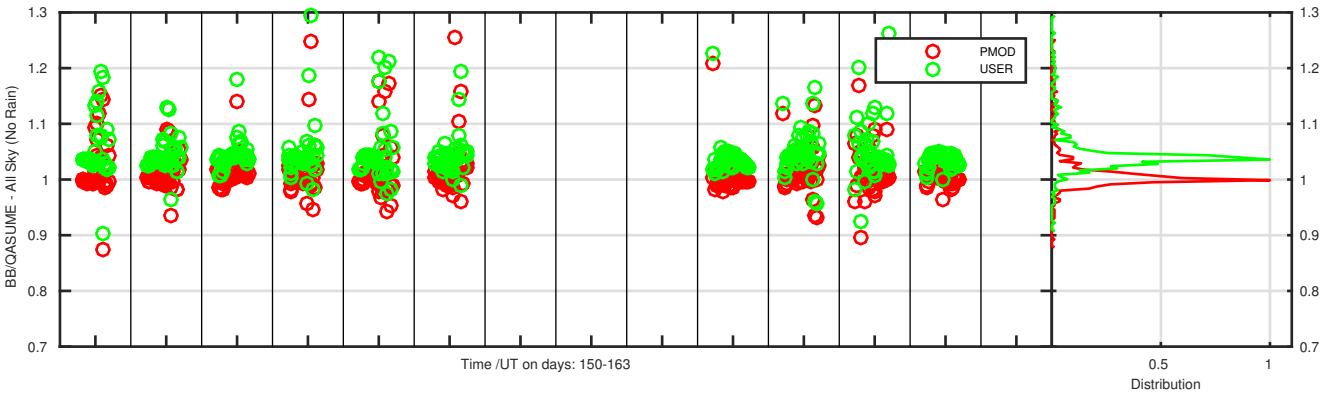

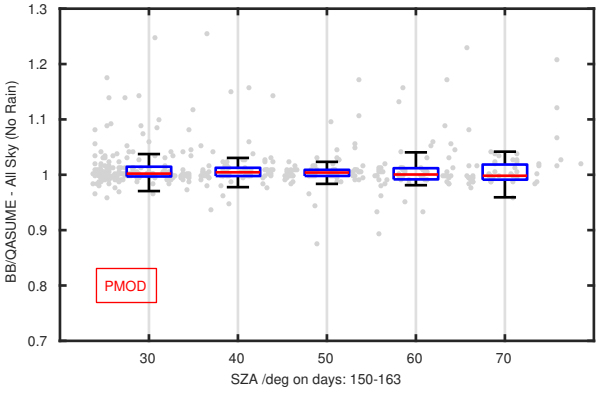

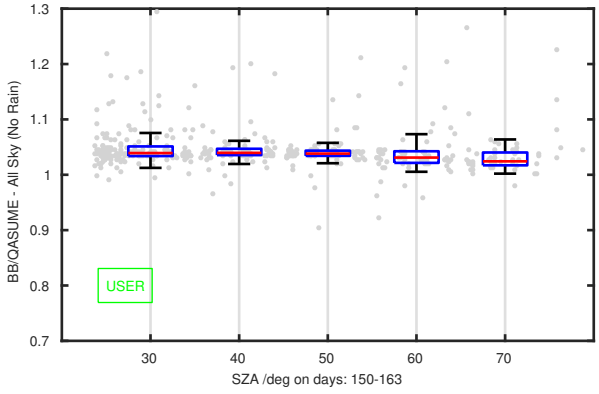

Calibration Results of KZ120132 (UVB)

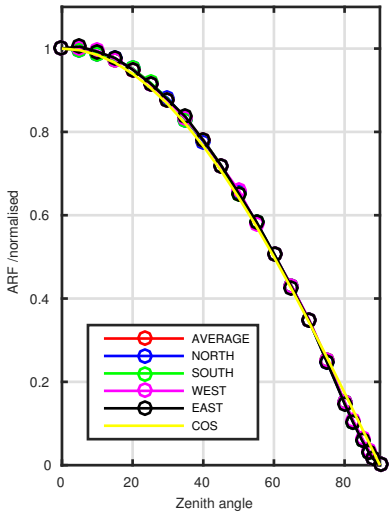

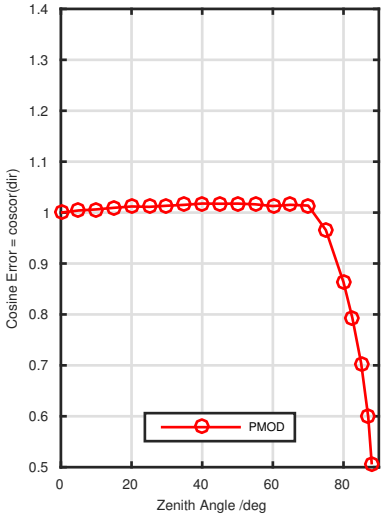

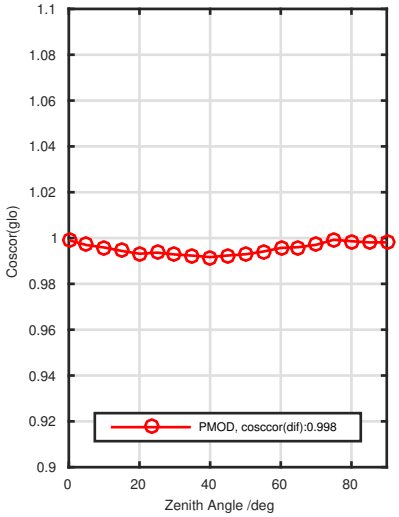

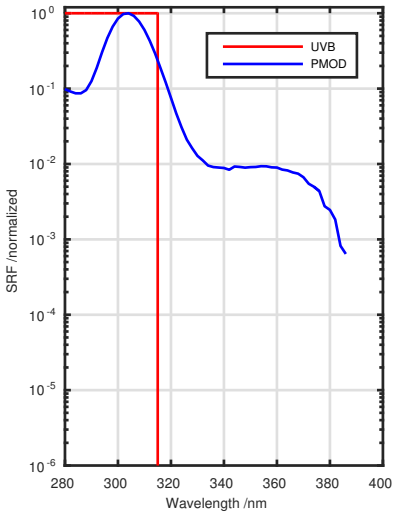

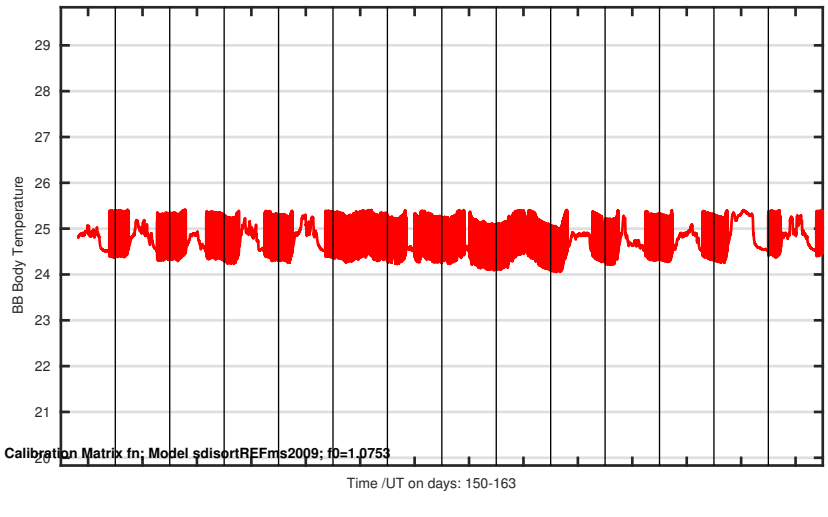

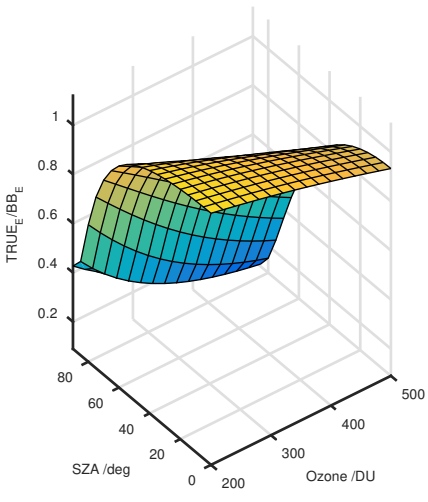

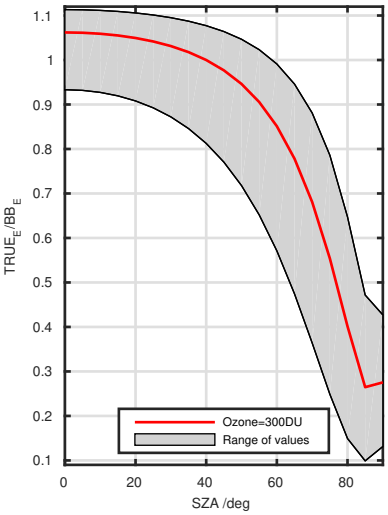

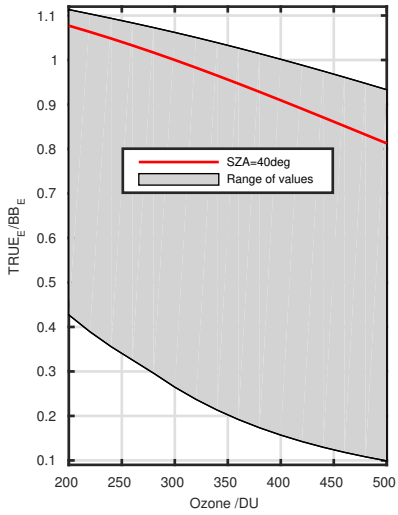

Calibration Results of KZ120132 (UVB)

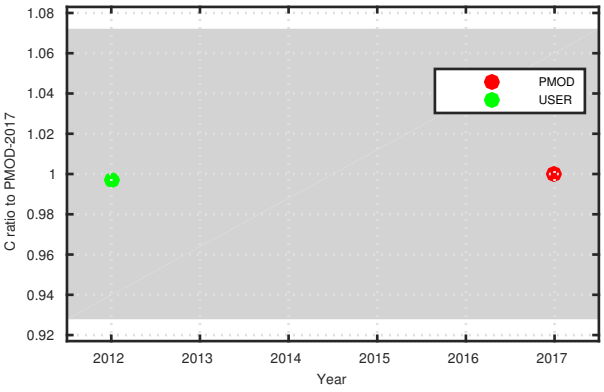

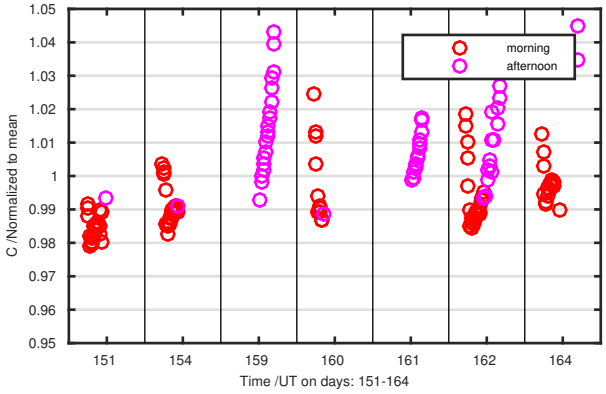

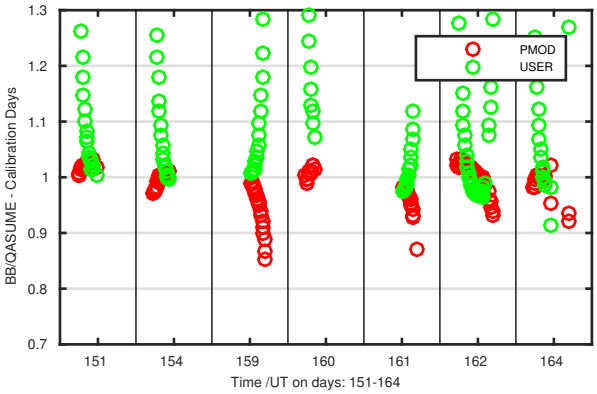

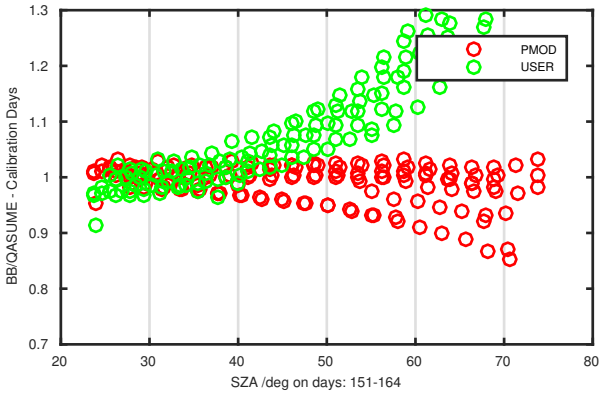

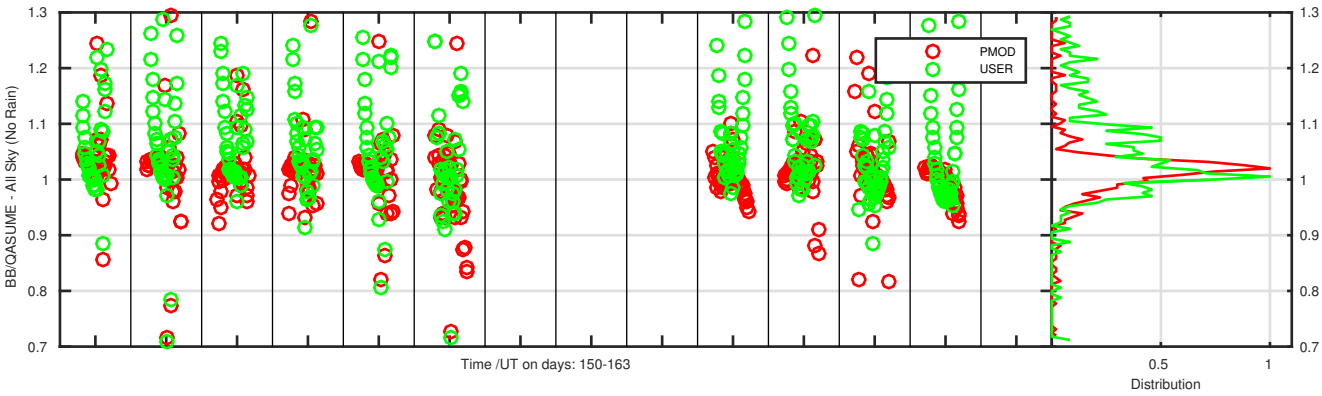

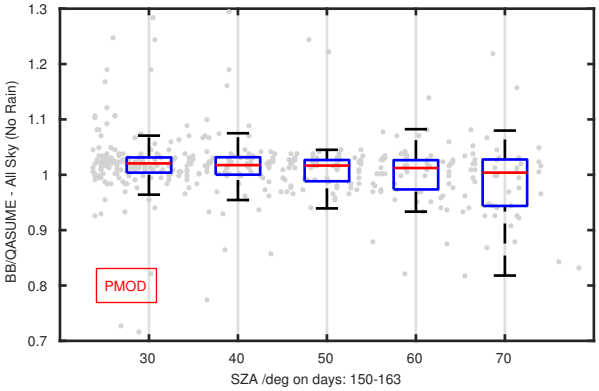

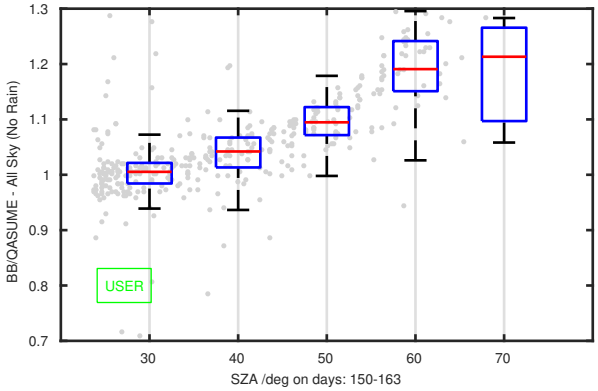

Calibration Results of KZ560 (UVE)

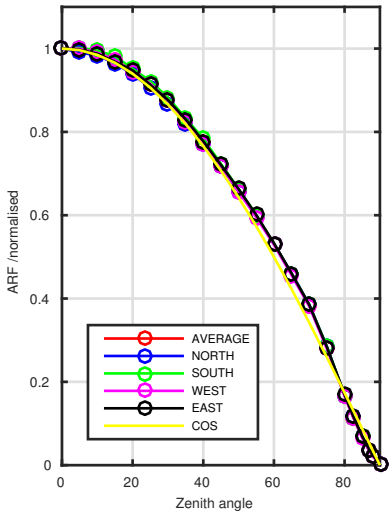

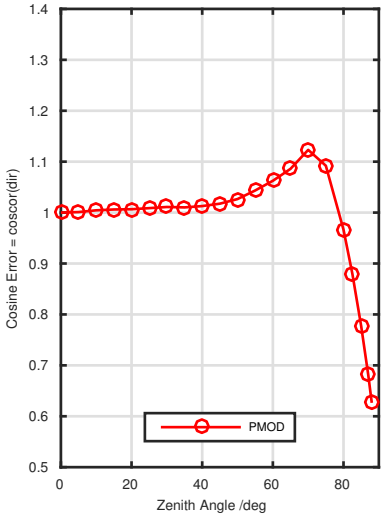

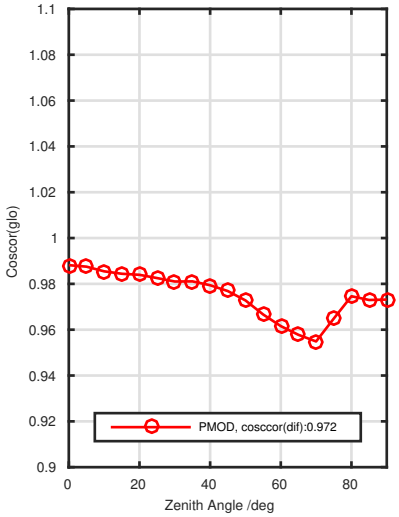

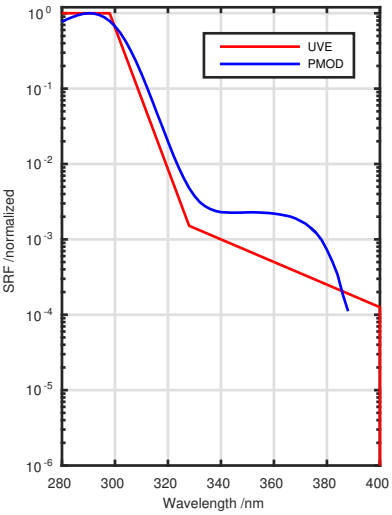

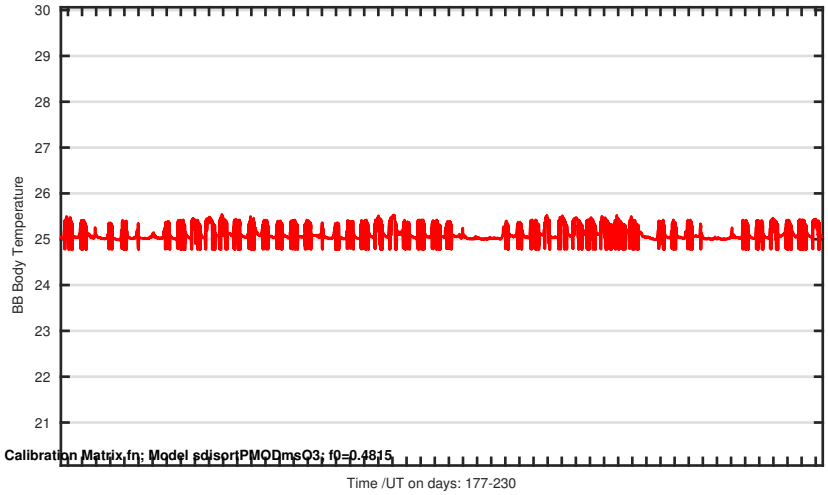

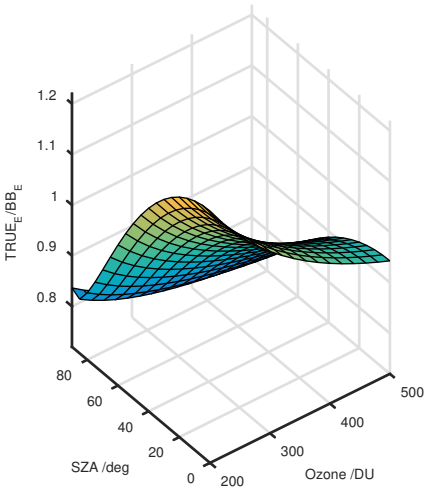

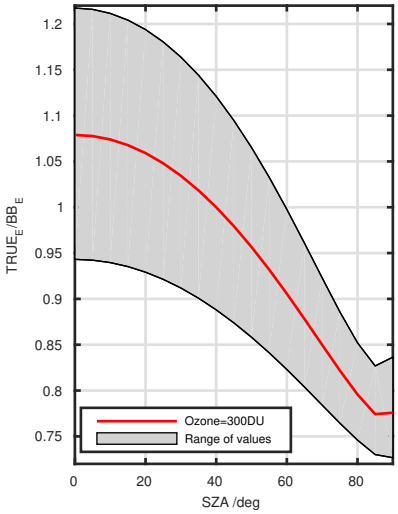

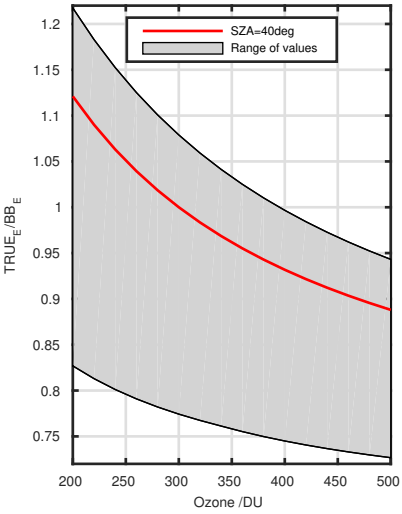

Calibration Results of KZ560 (UVE)

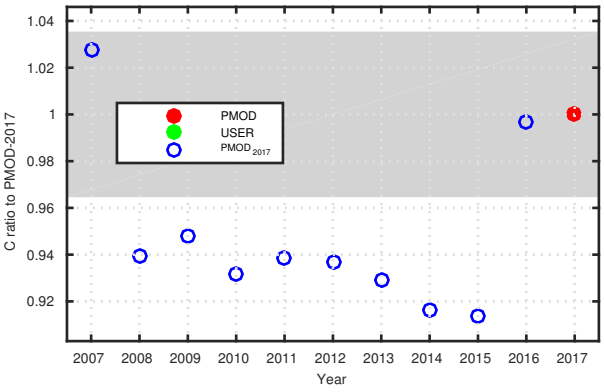

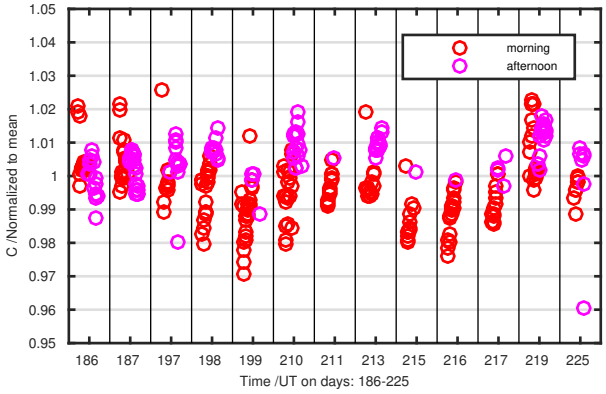

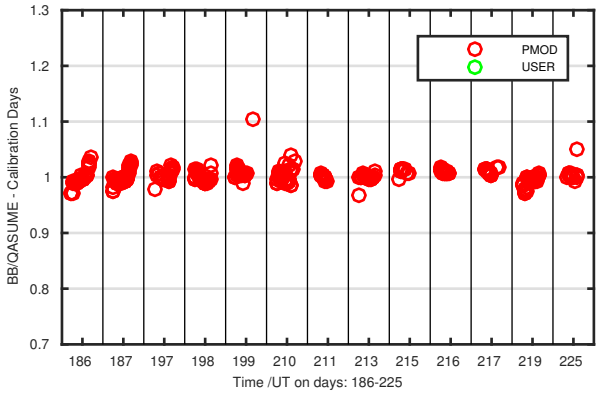

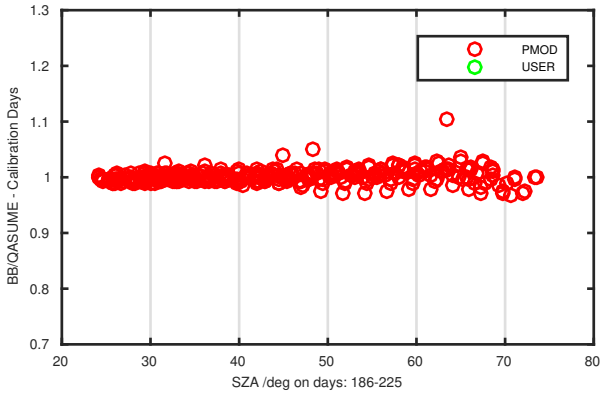

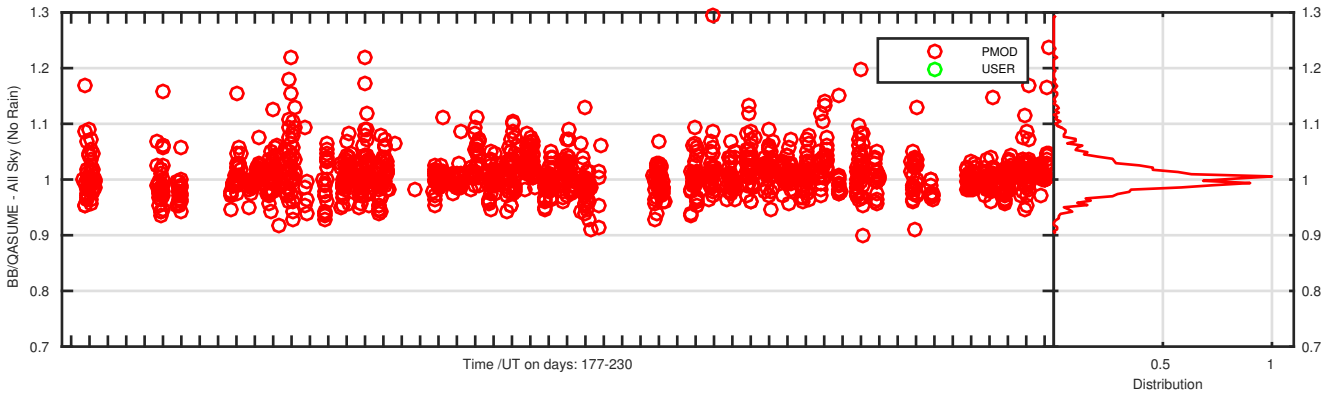

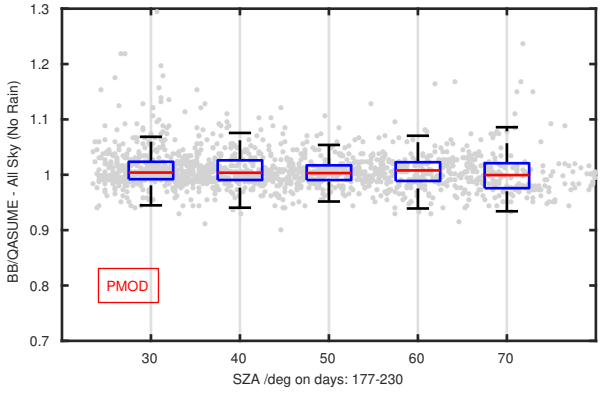

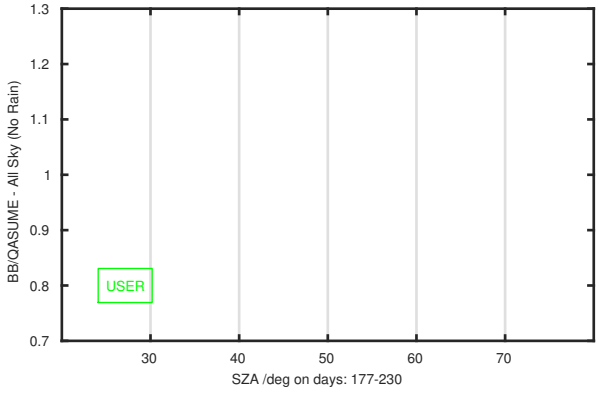

Calibration Results of KZ070642 (UVE)

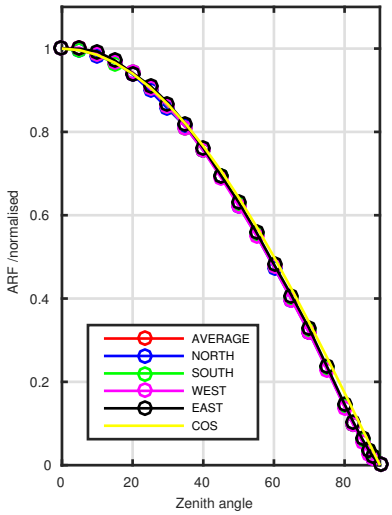

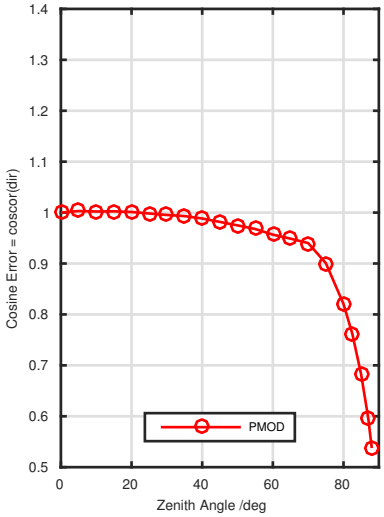

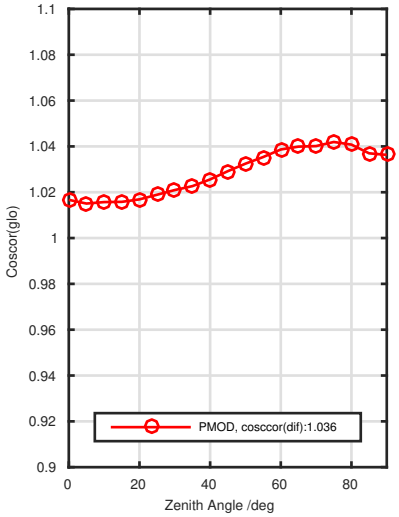

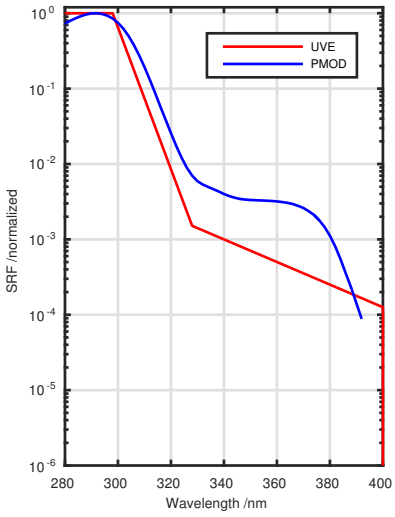

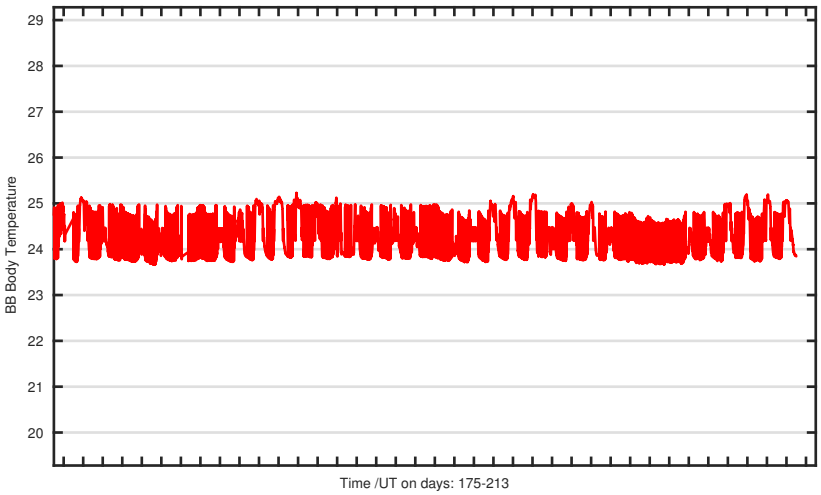

Calibration Matrix fn; Model sdisortREFms2009; f0=0.3730

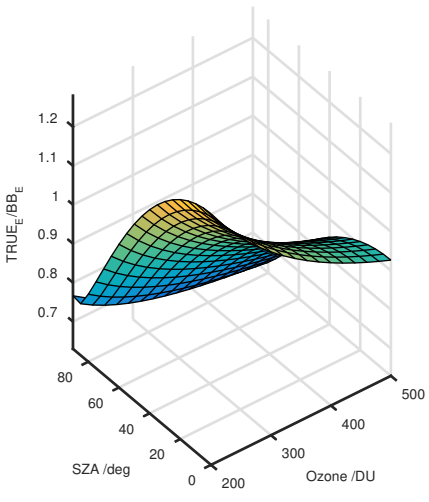

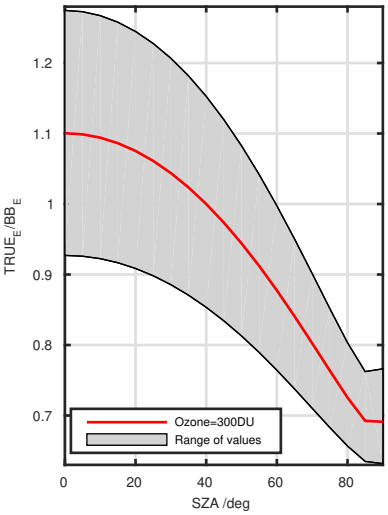

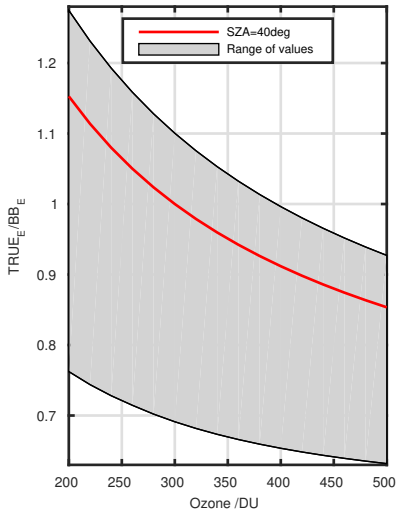

Calibration Results of KZ070642 (UVE)

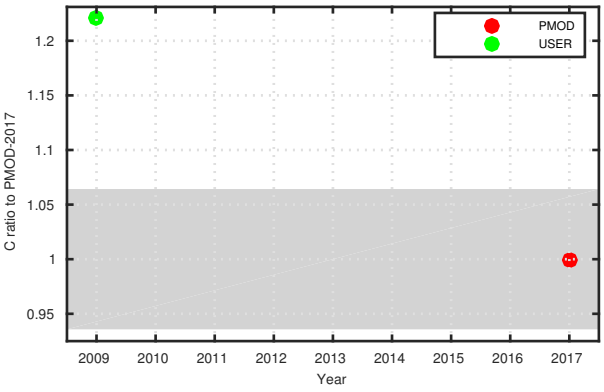

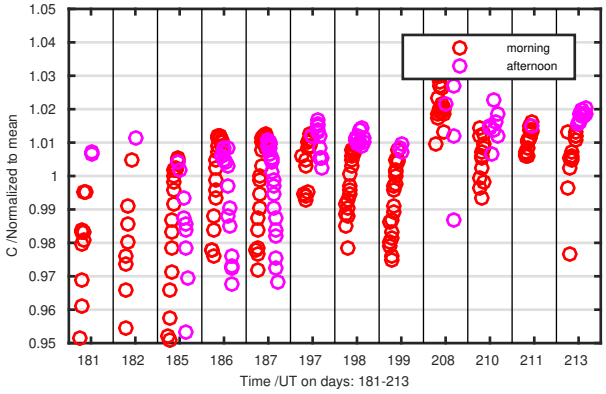

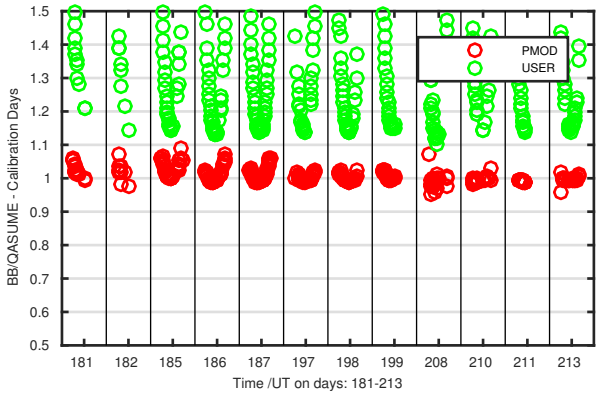

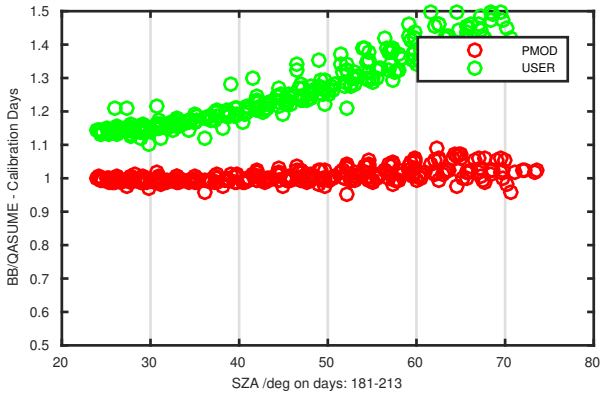

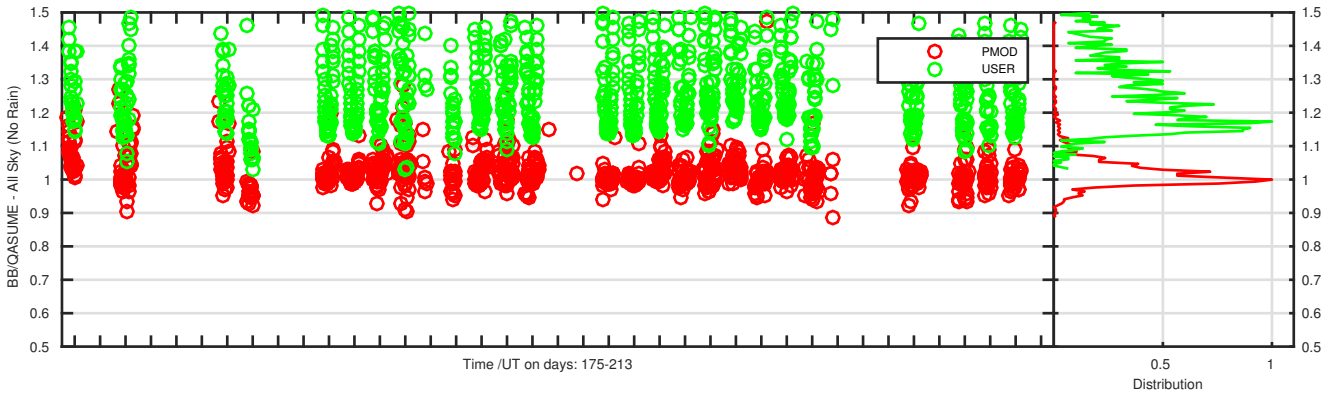

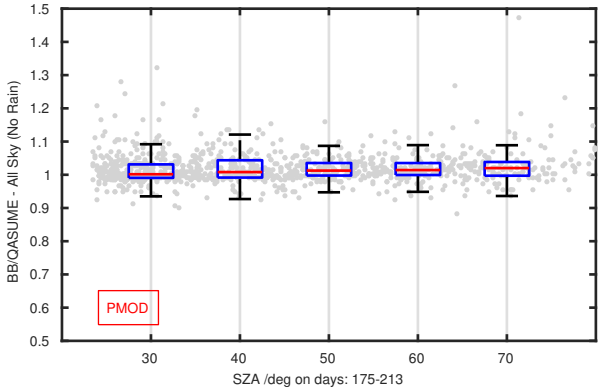

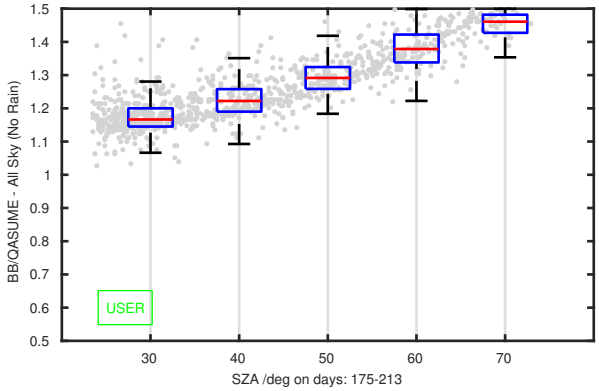

Calibration Results of KZ070643 (UVE)

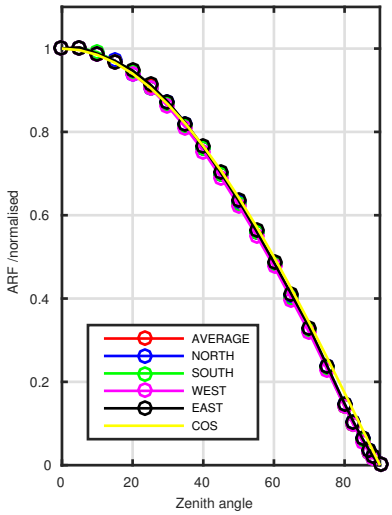

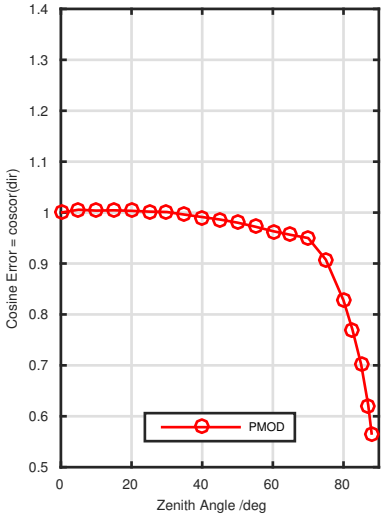

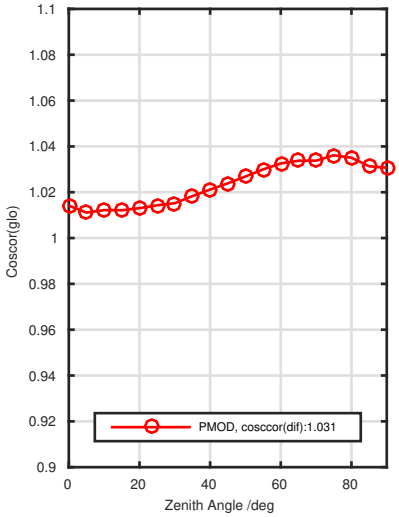

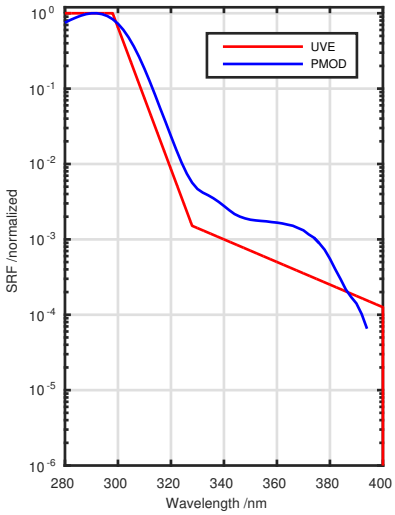

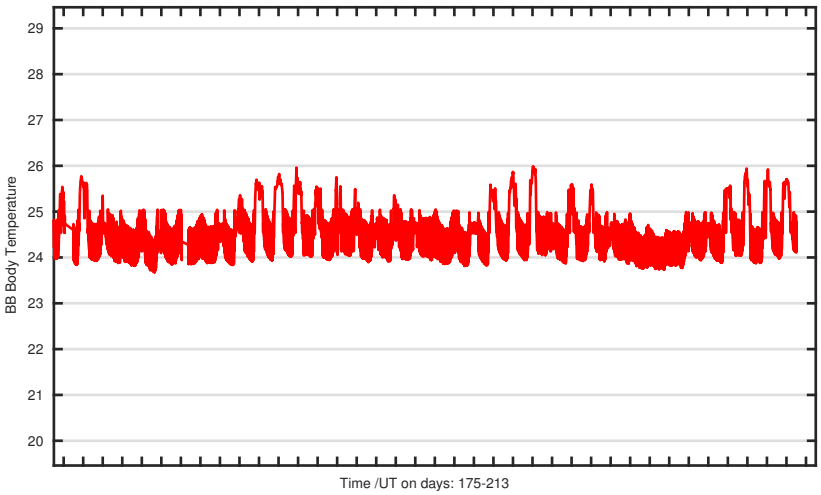

Calibration Matrix fn; Model sdisortREFms2009; f0=0.4320

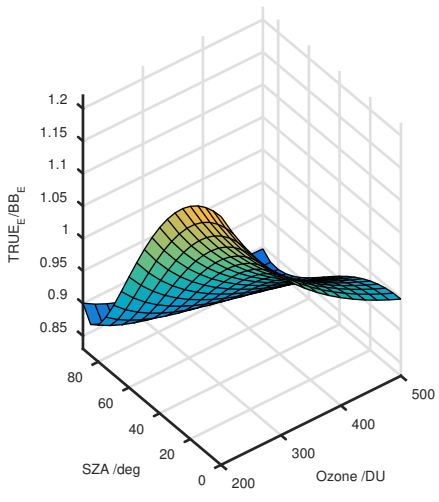

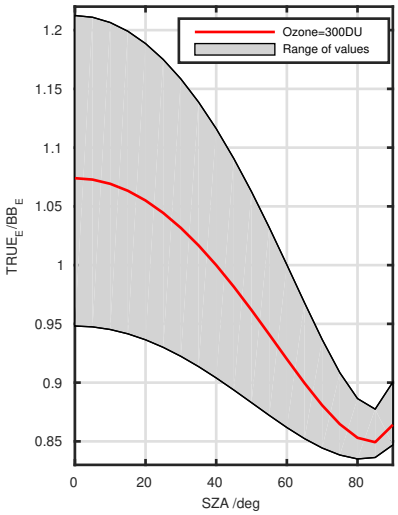

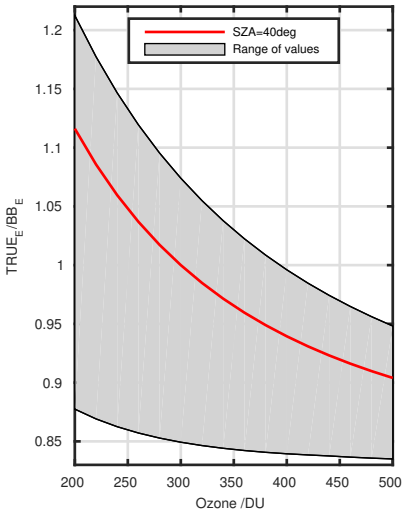

Calibration Results of KZ070643 (UVE)

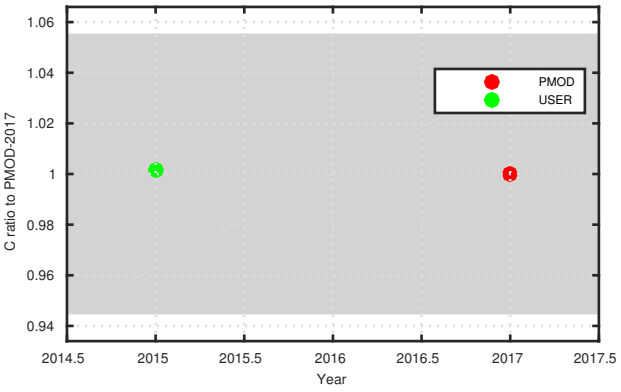

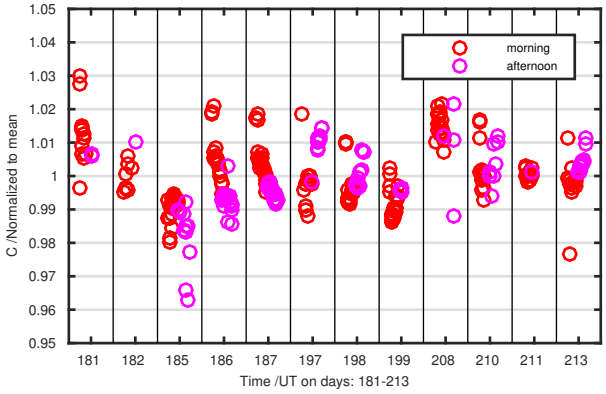

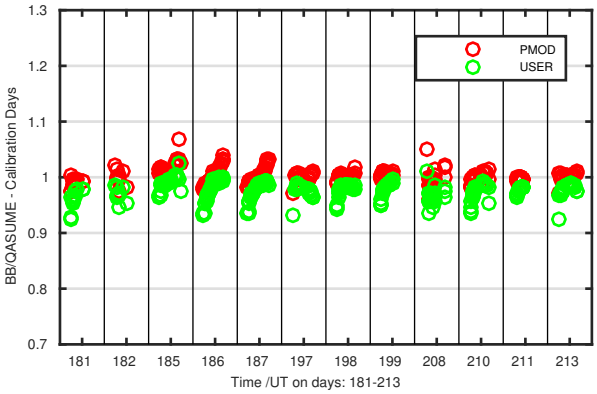

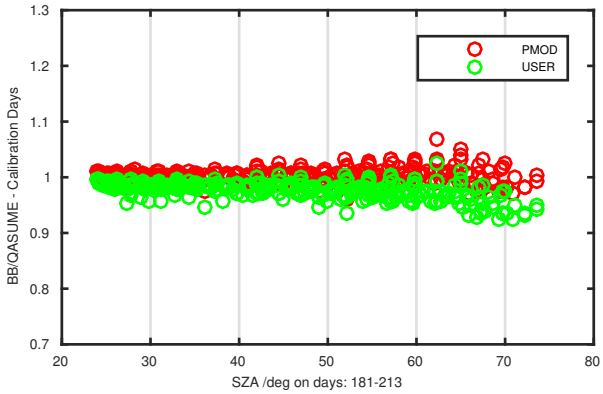

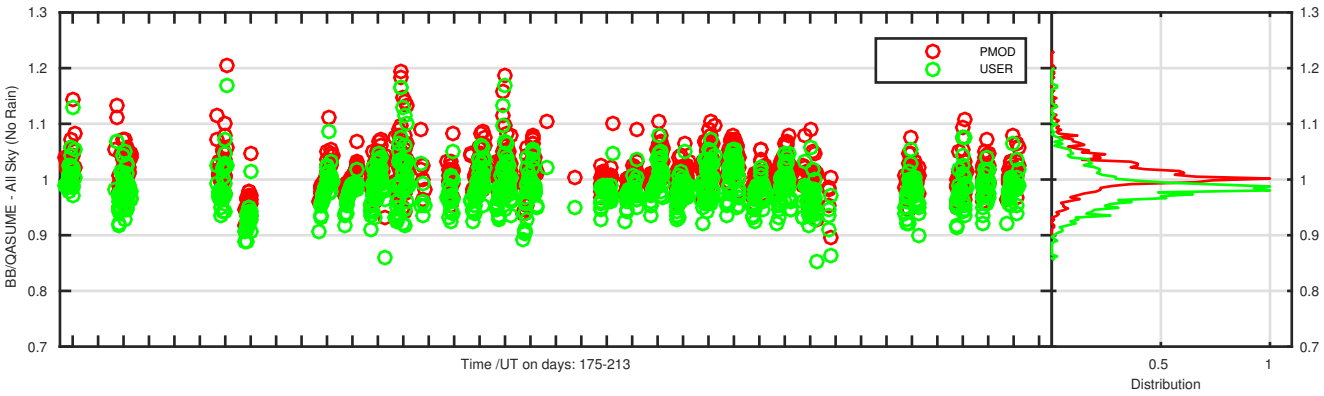

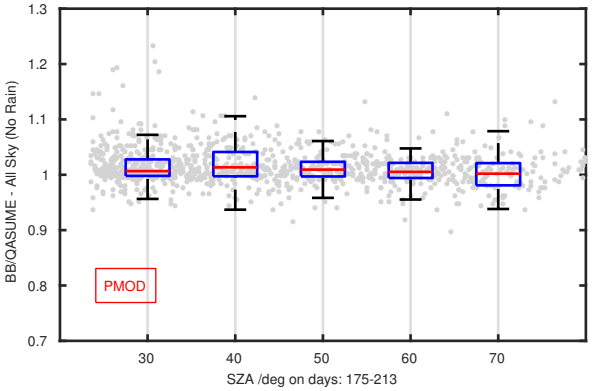

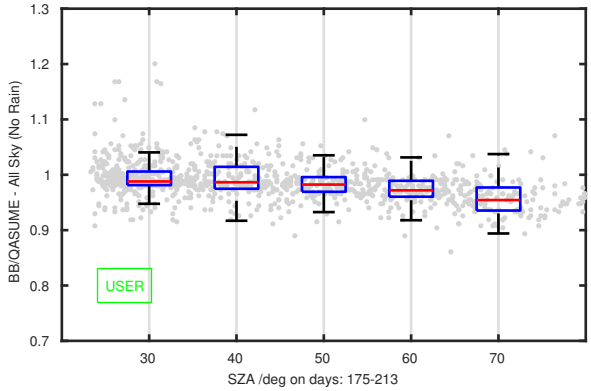

Calibration Results of KZ080005 (UVA)

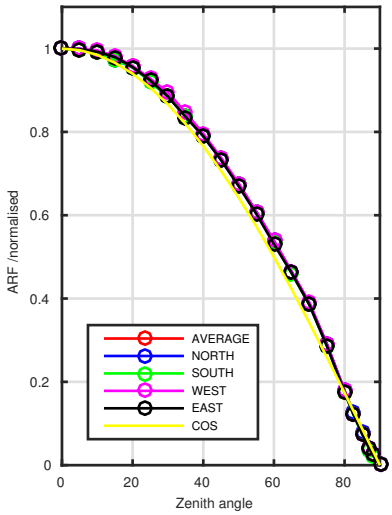

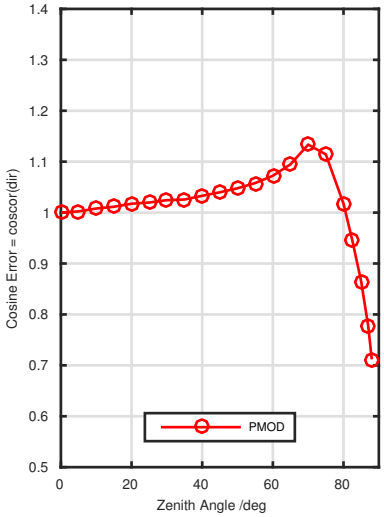

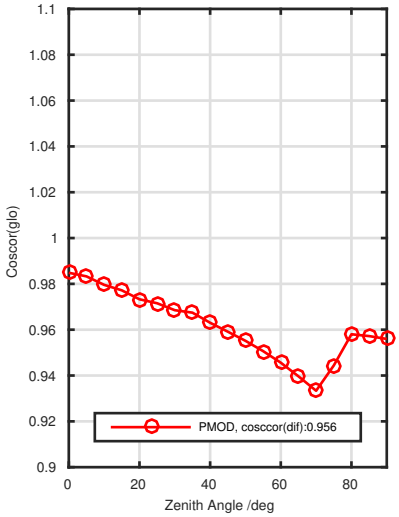

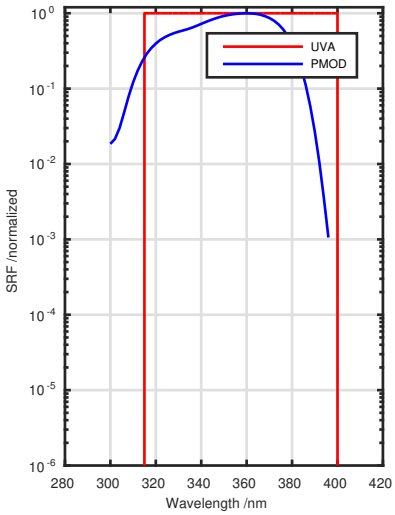

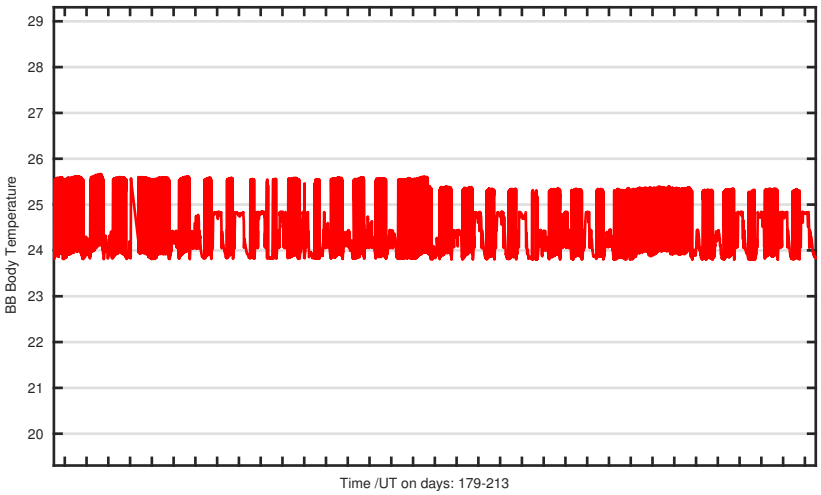

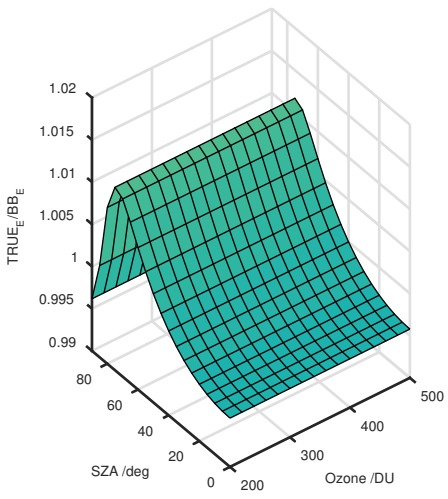

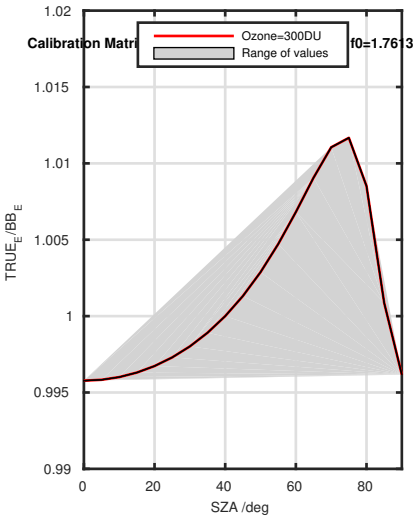

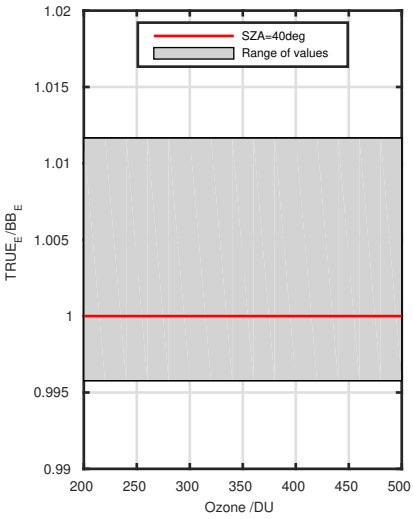

Calibration Results of KZ080005 (UVA)

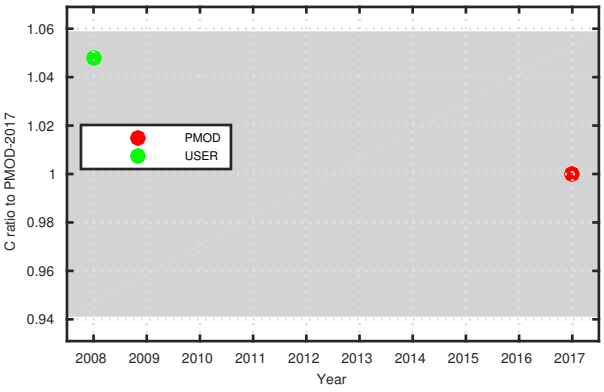

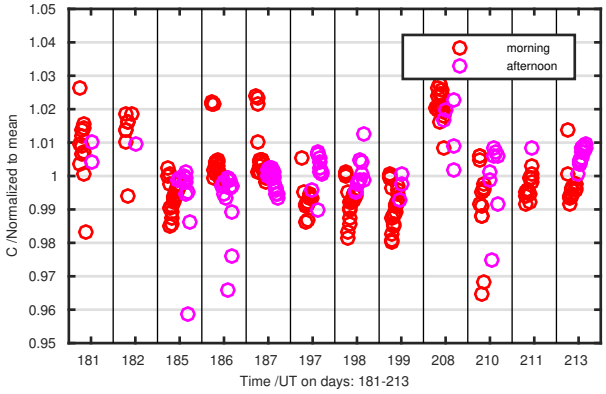

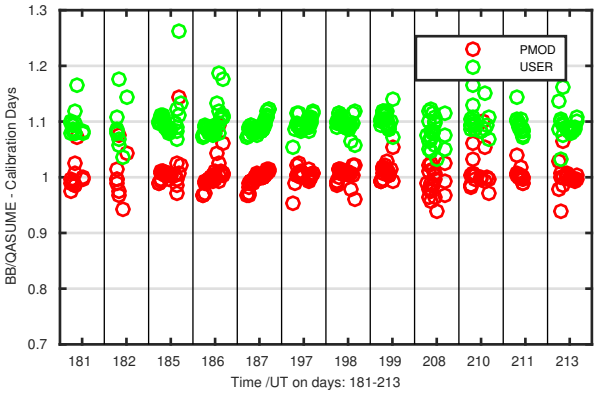

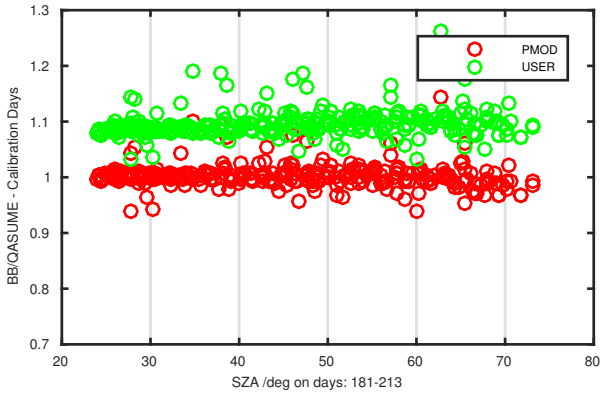

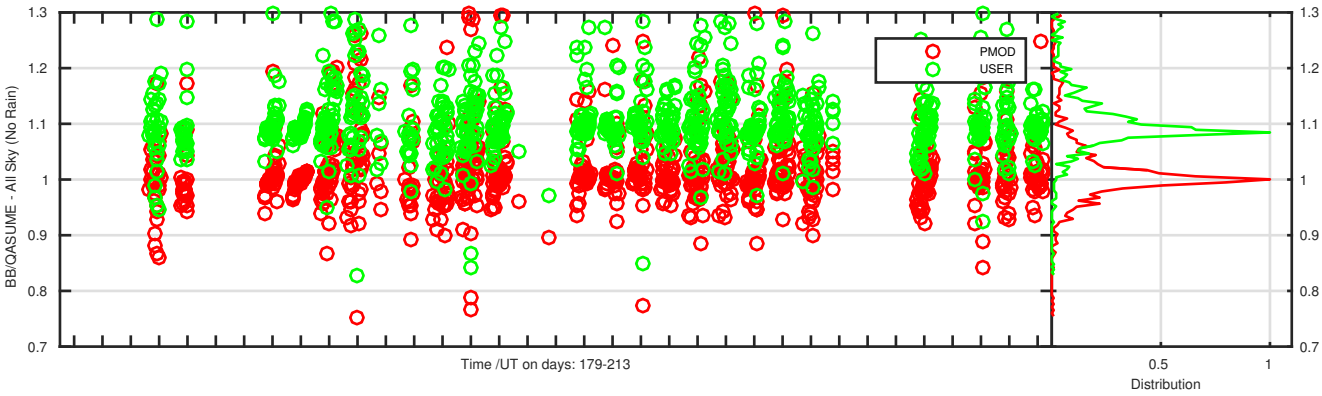

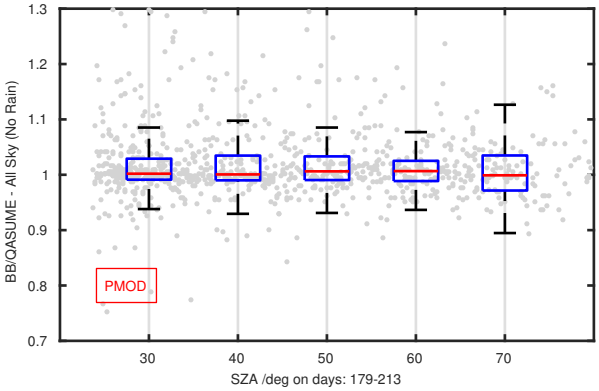

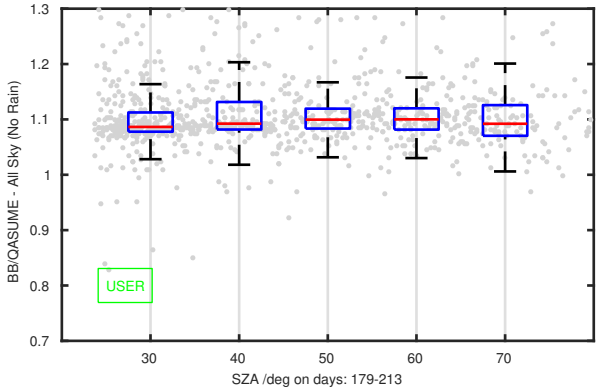

Calibration Results of KZ100013 (UVA)

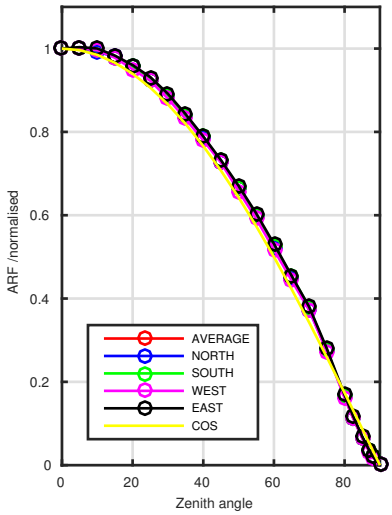

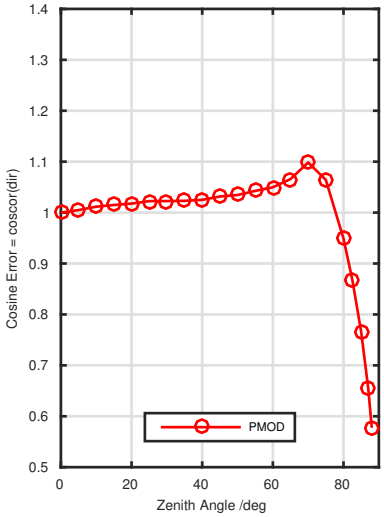

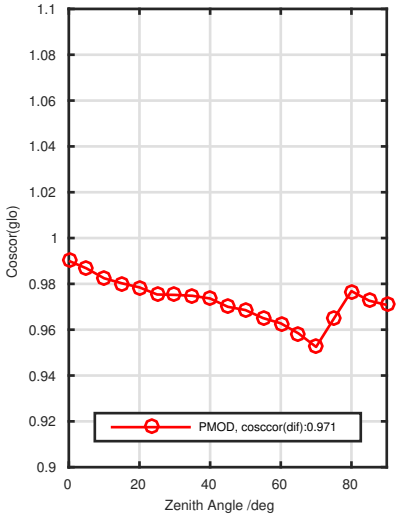

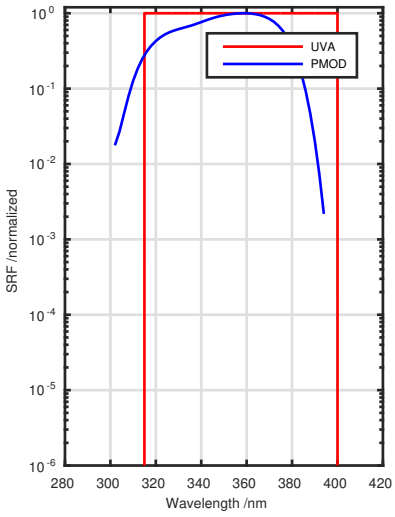

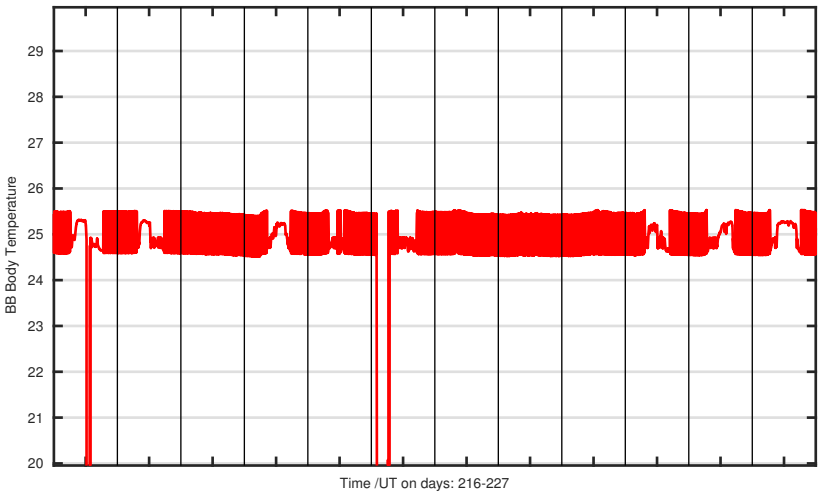

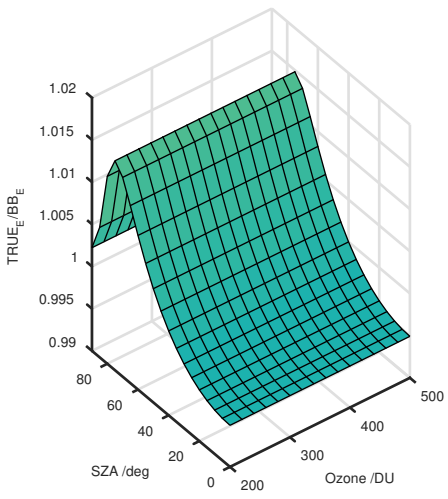

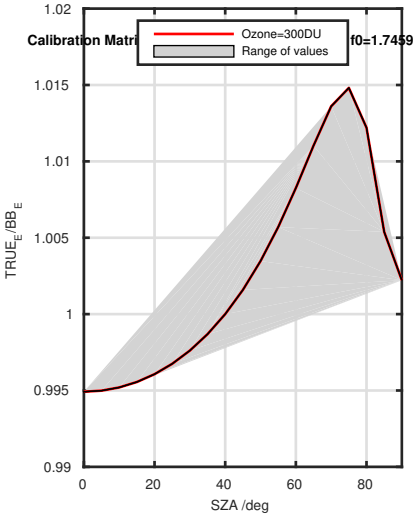

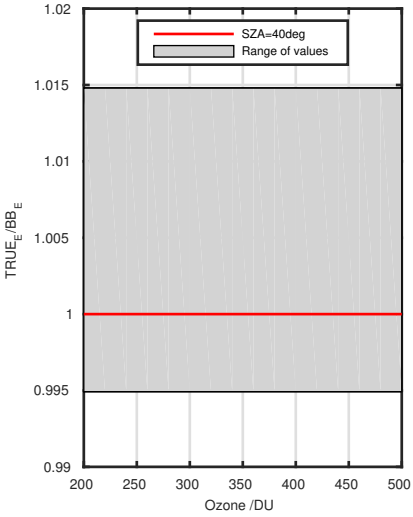

Calibration Results of KZ100013 (UVA)

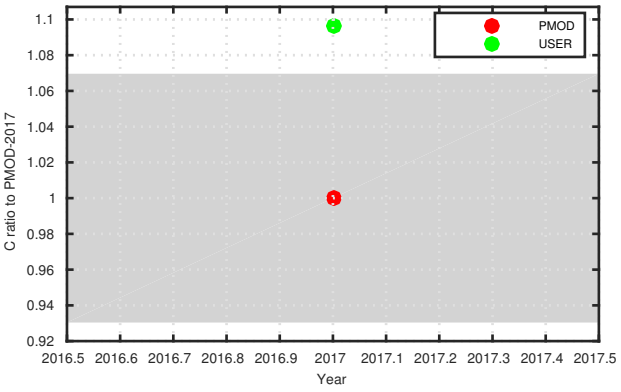

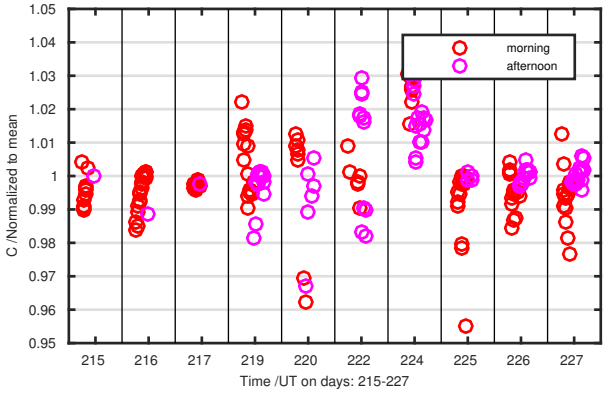

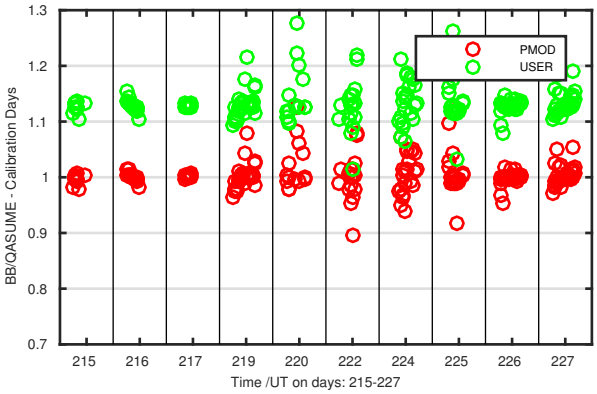

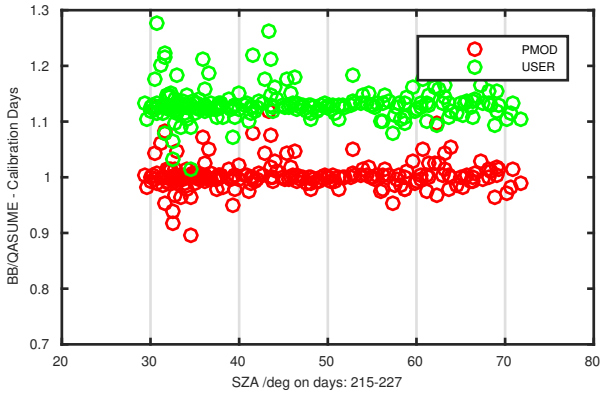

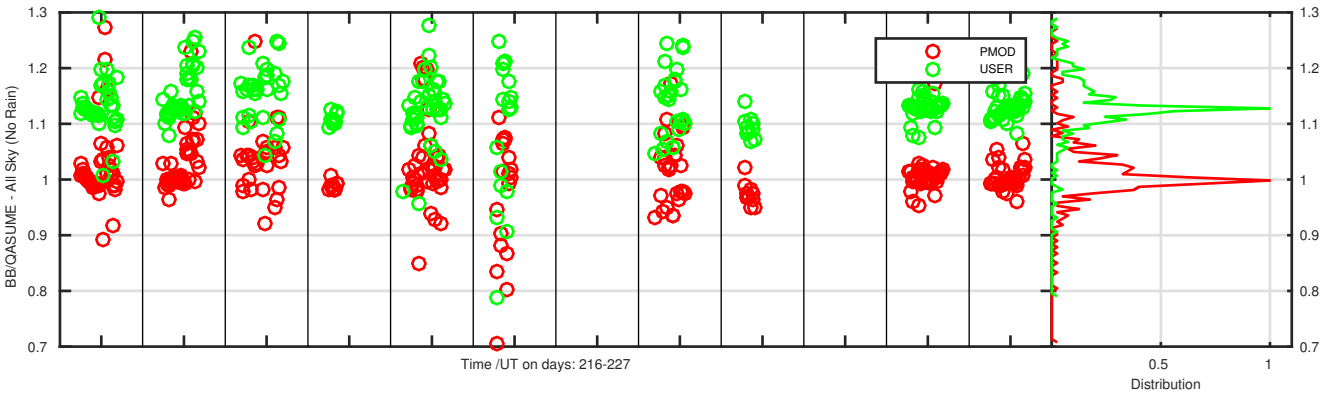

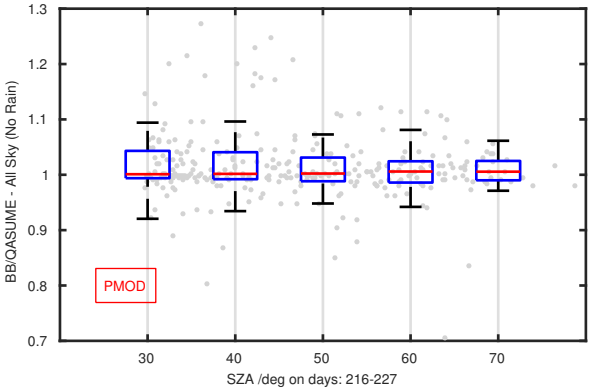

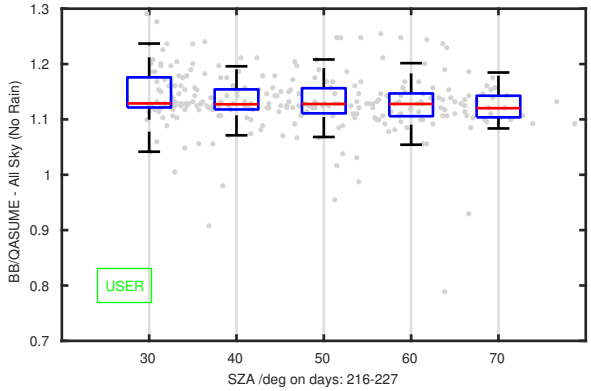

Calibration Results of KZ110042 (UVE)

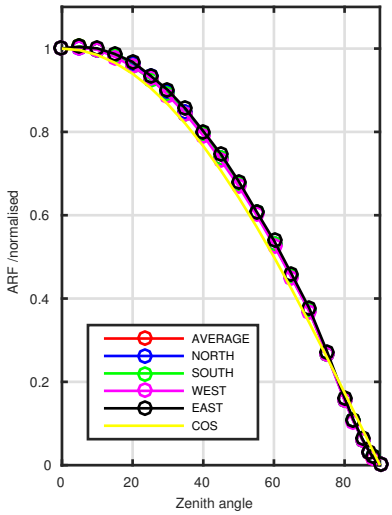

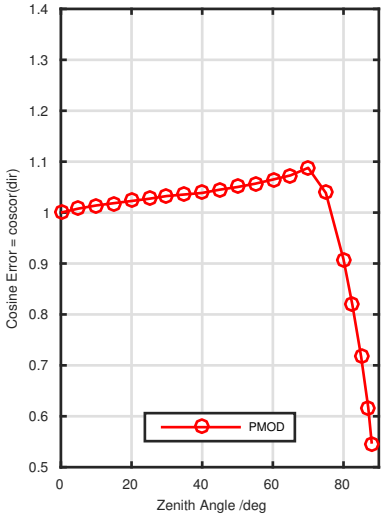

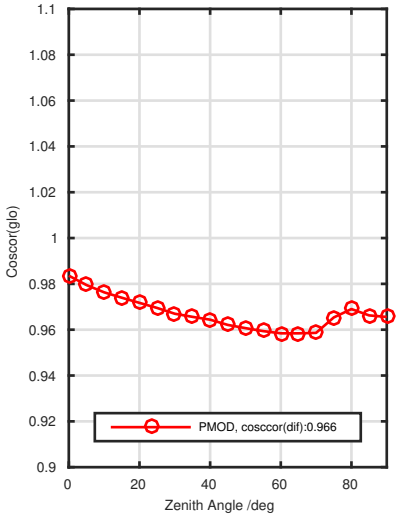

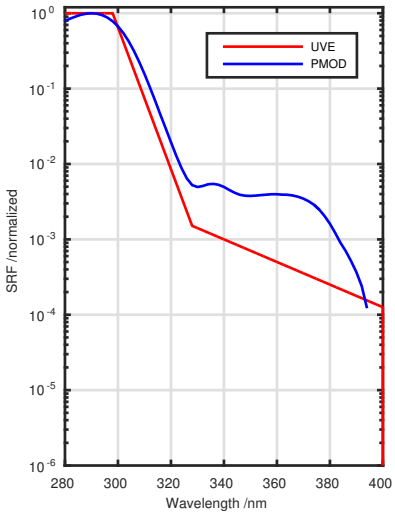

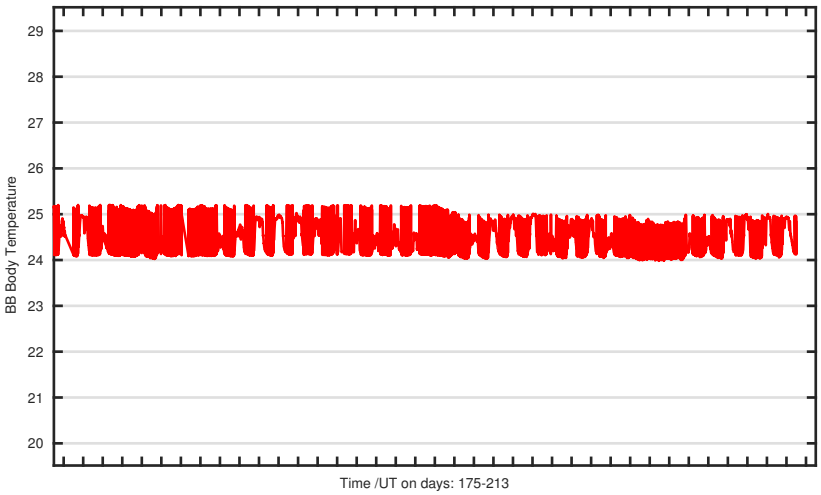

Calibration Matrix fn; Model sdisortREFms2009; f0=0.4150

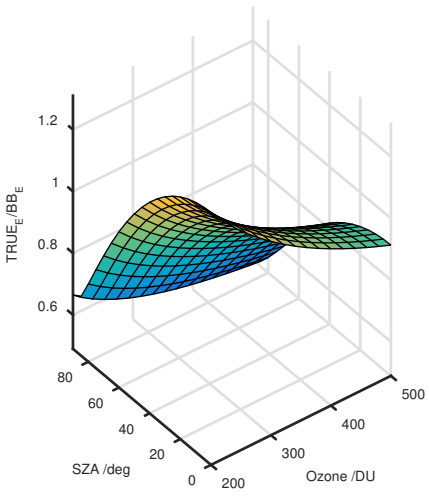

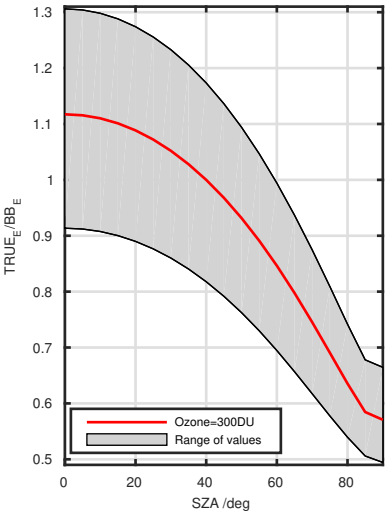

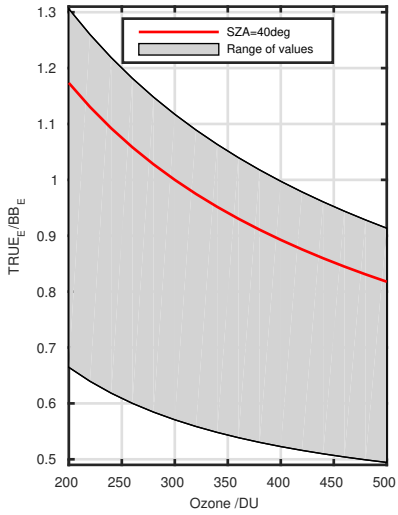

Calibration Results of KZ110042 (UVE)

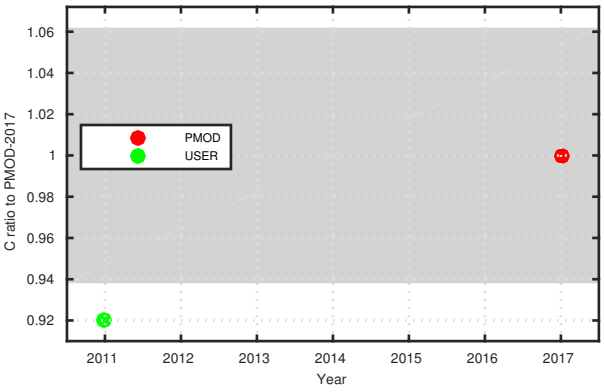

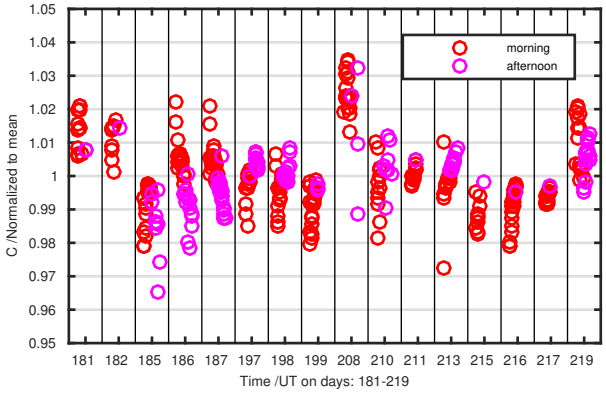

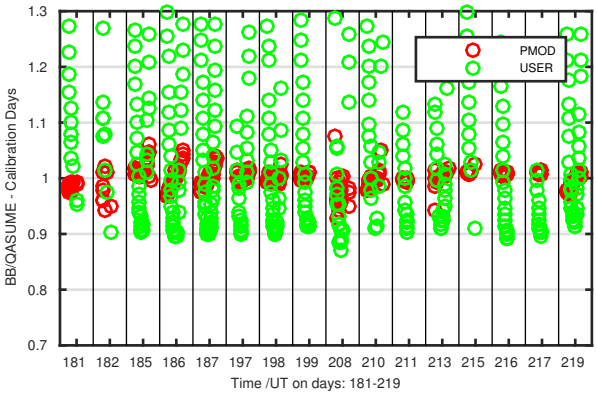

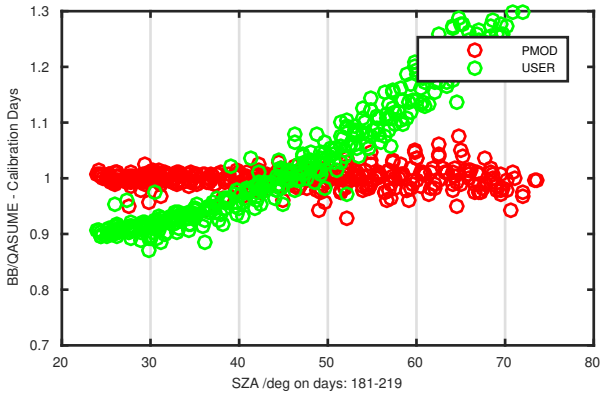

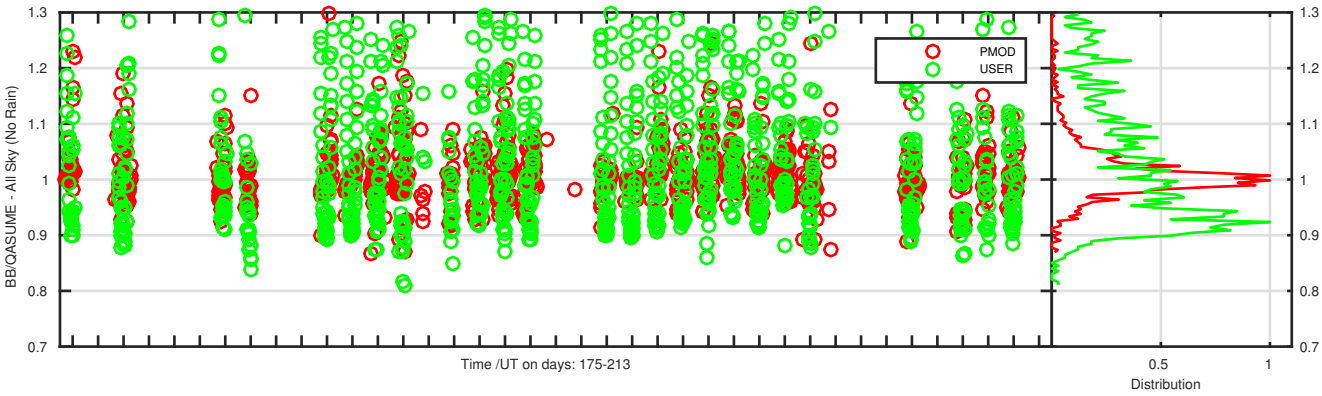

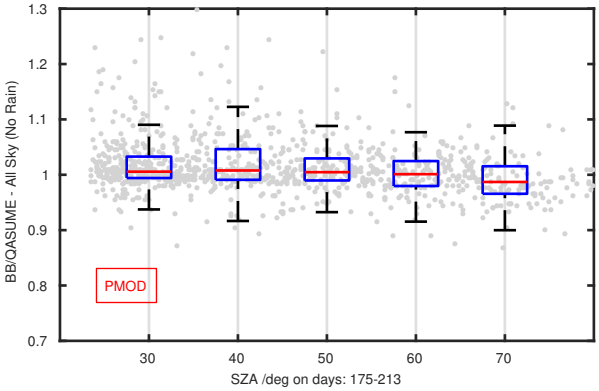

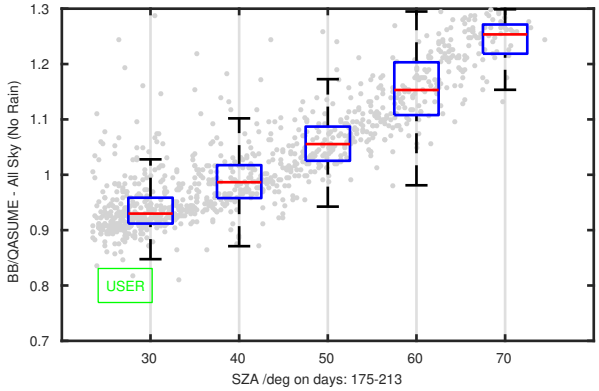

Calibration Results of KZ110062 (UVA)

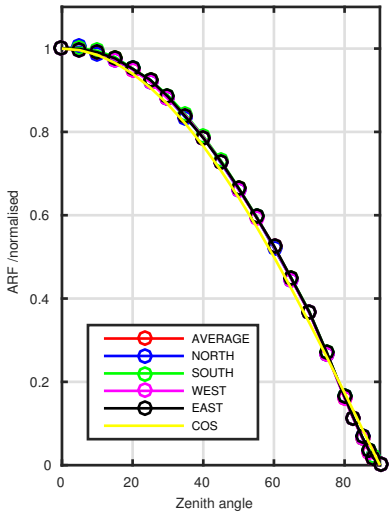

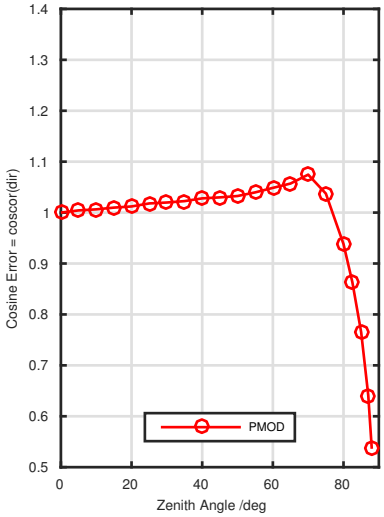

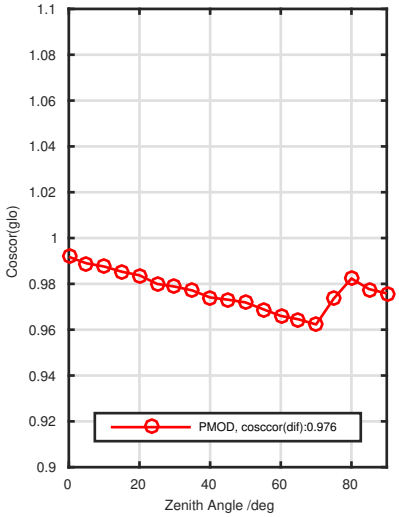

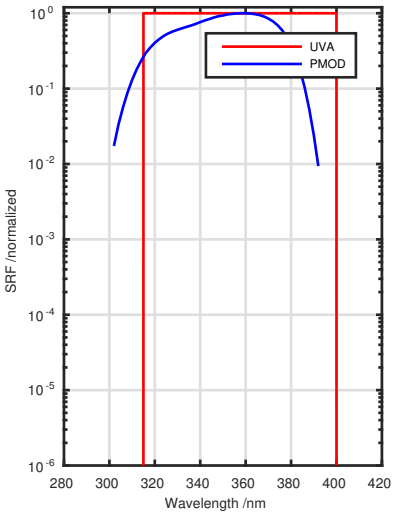

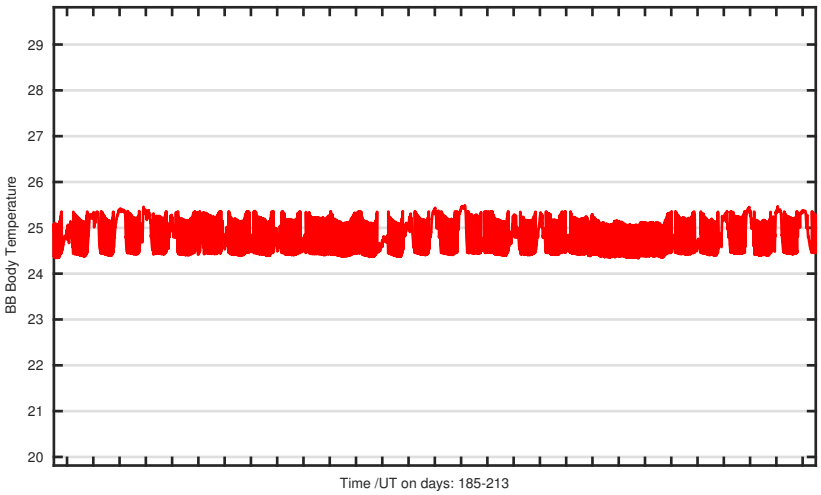

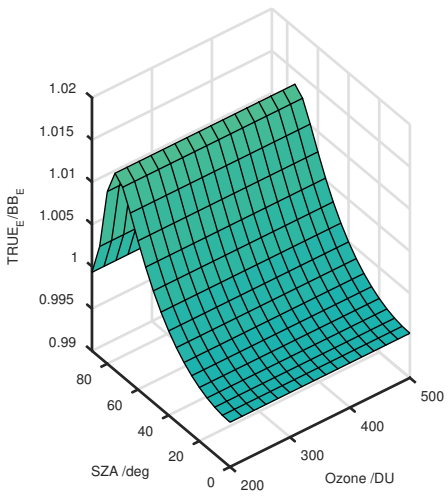

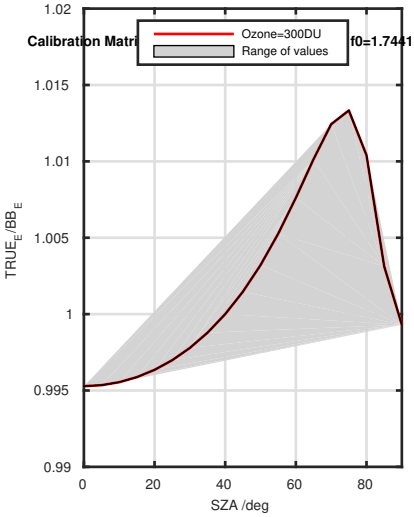

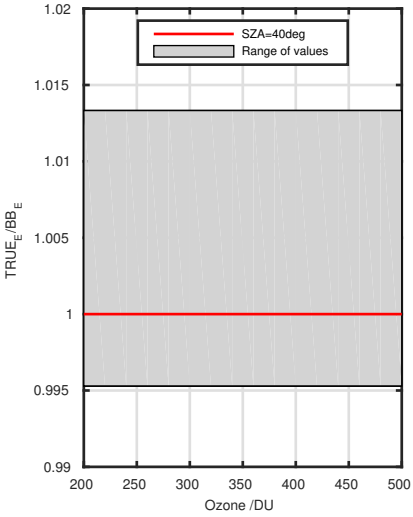

Calibration Results of KZ110062 (UVA)

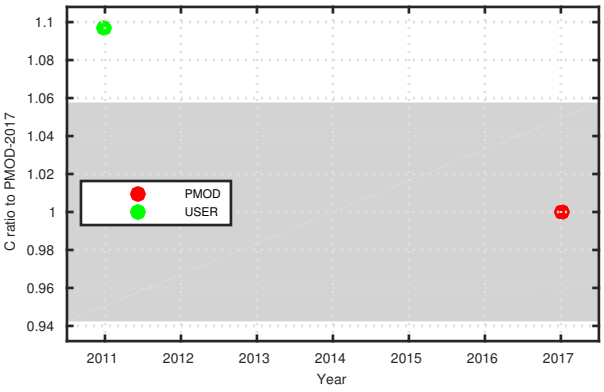

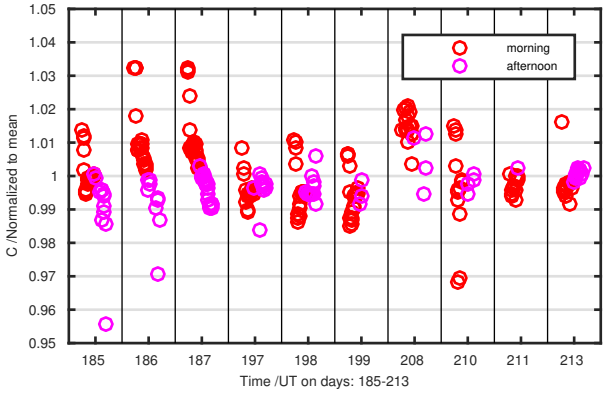

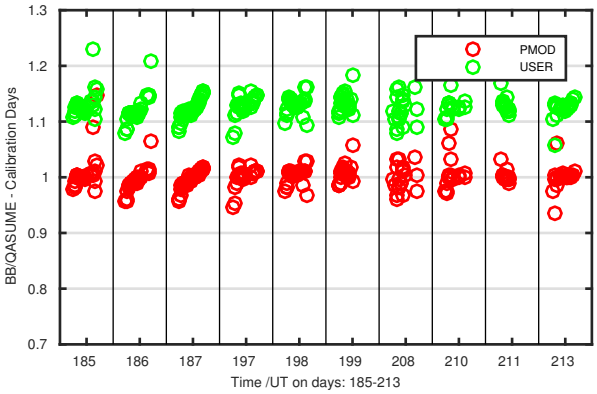

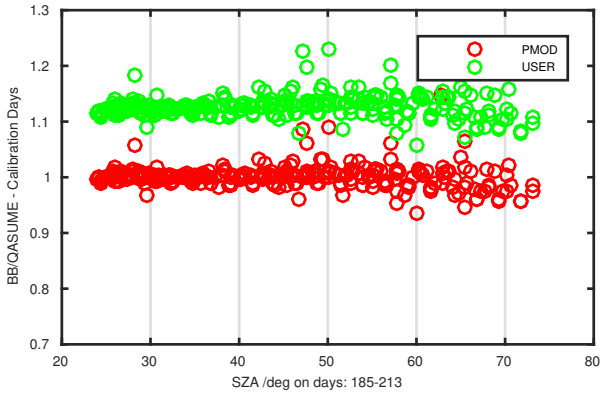

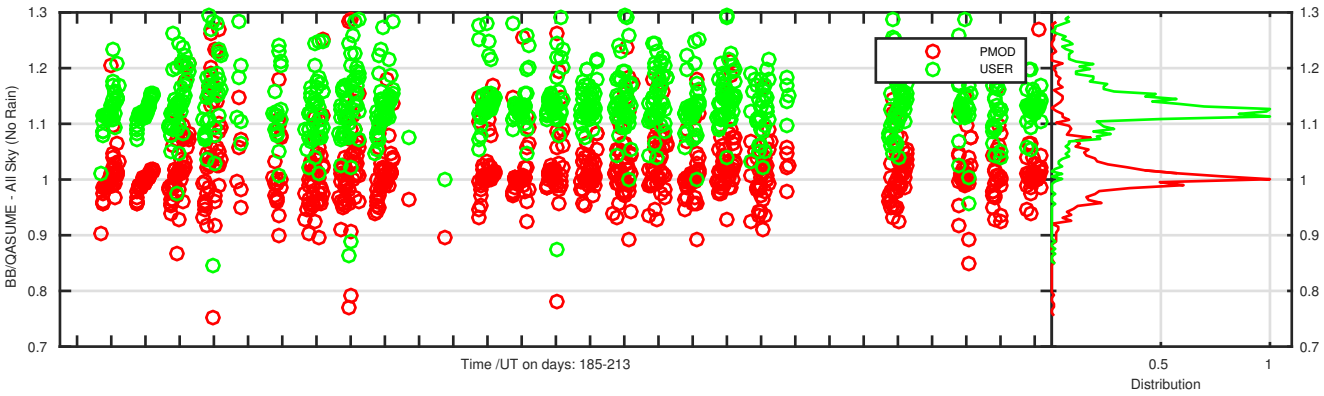

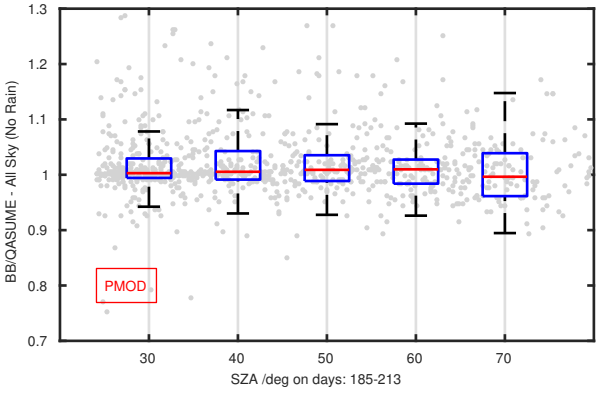

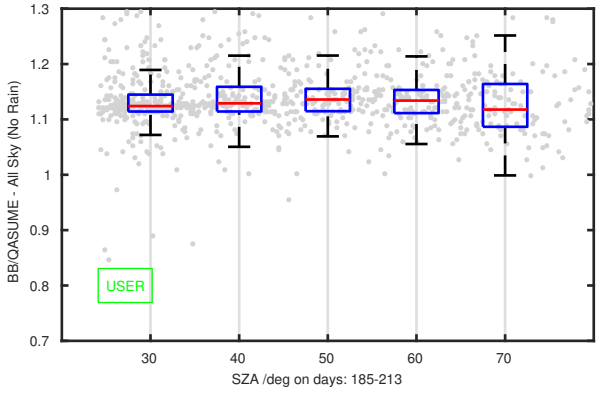

Calibration Results of KZ120056 (UVE)

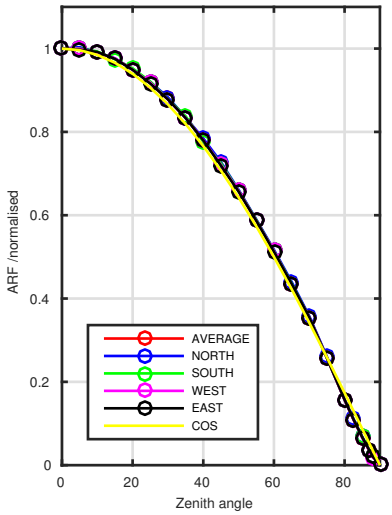

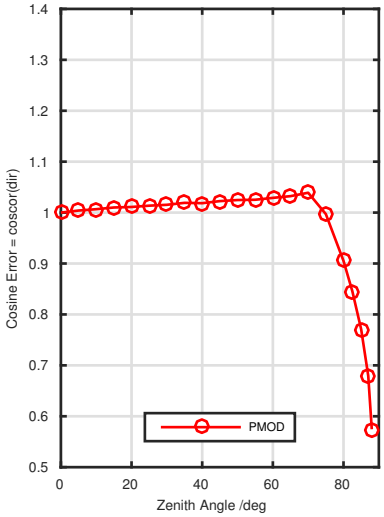

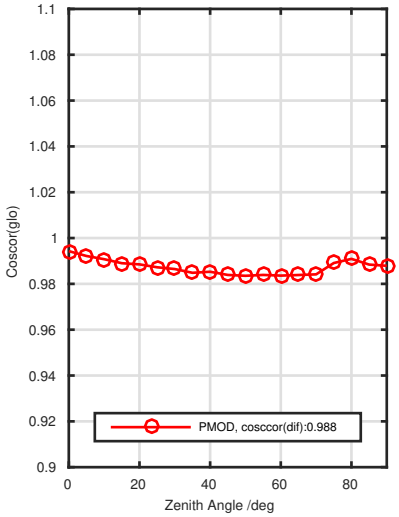

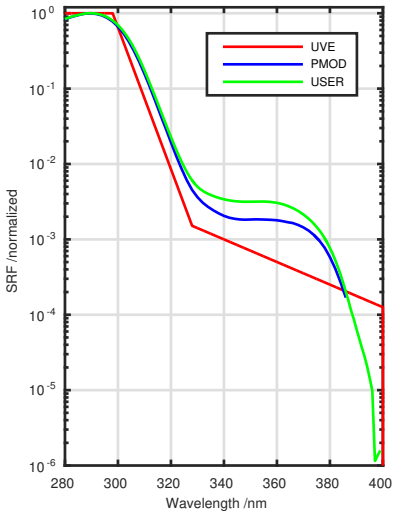

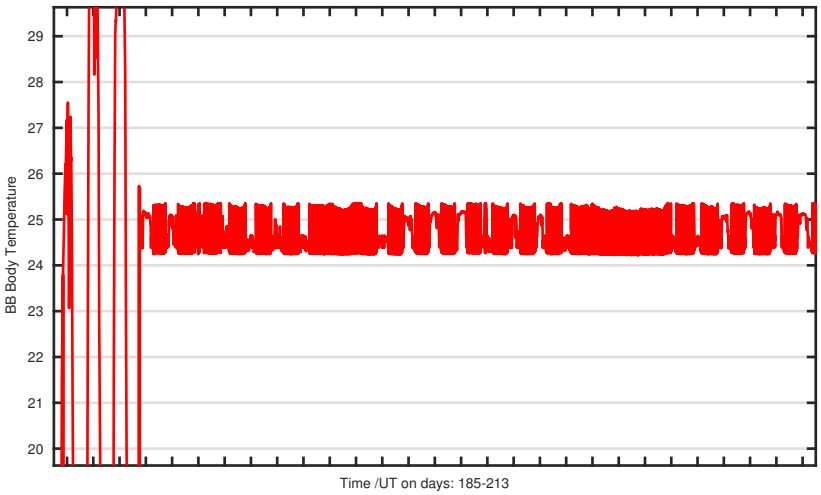

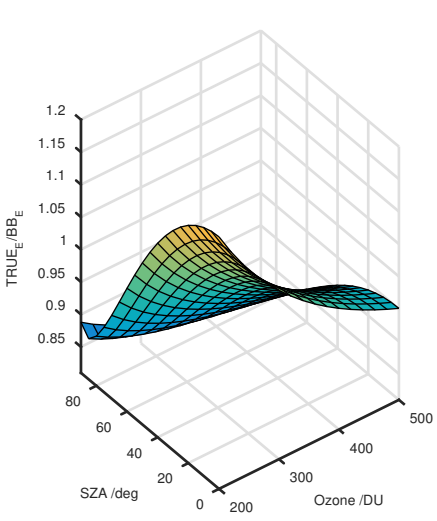

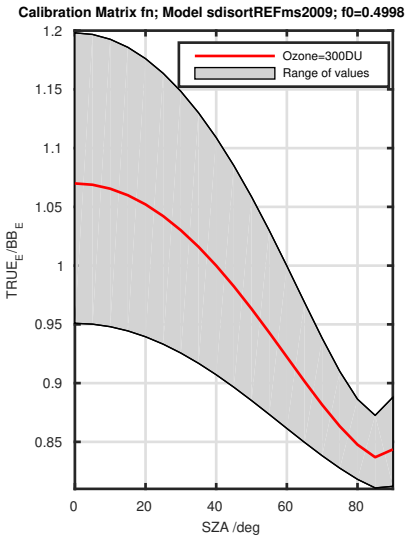

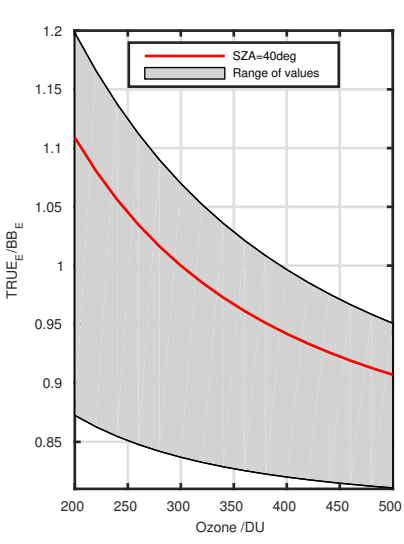

Calibration Results of KZ120056 (UVE)

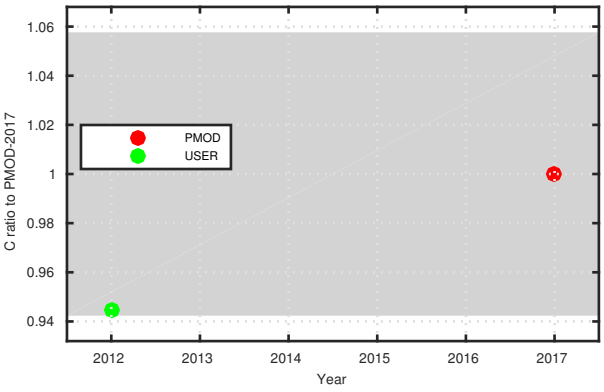

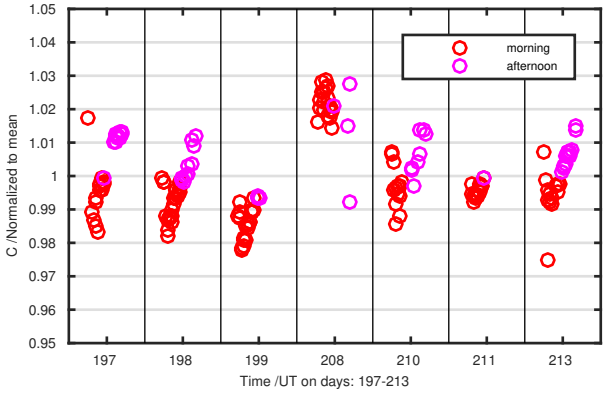

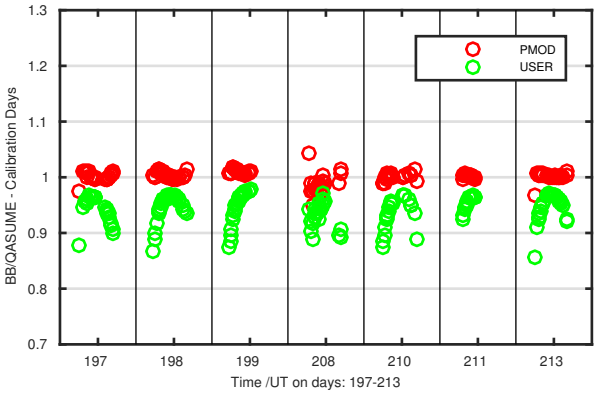

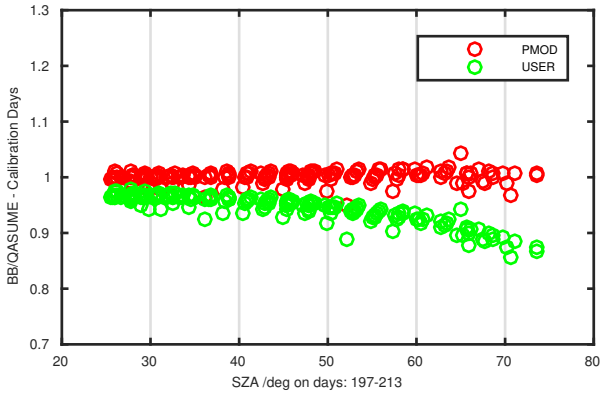

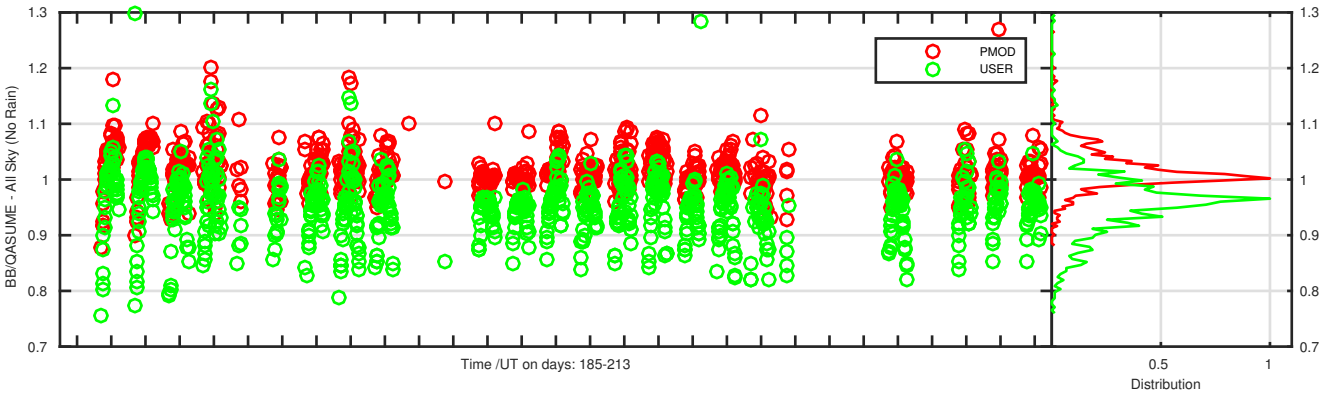

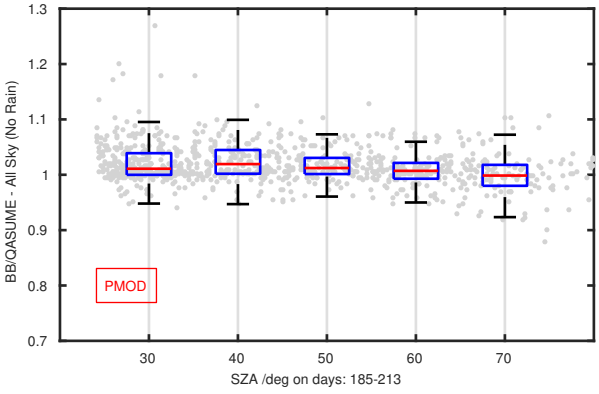

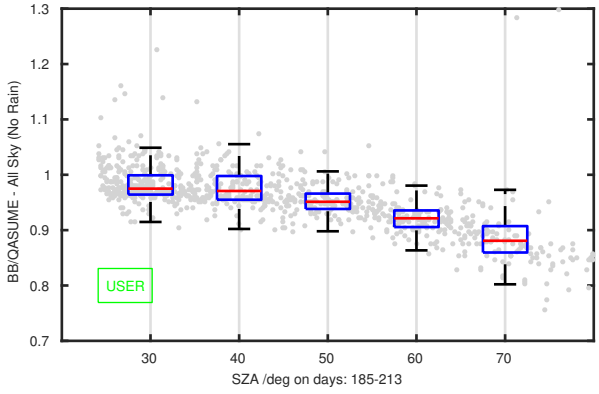

Calibration Results of KZ120076 (UVB)

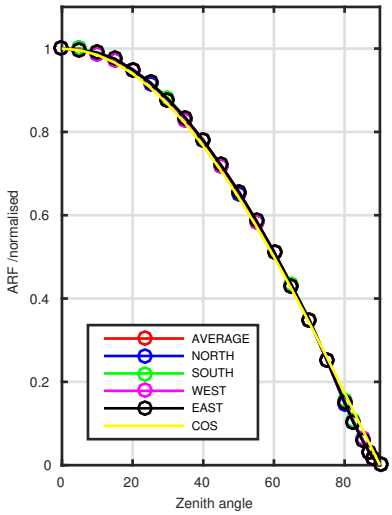

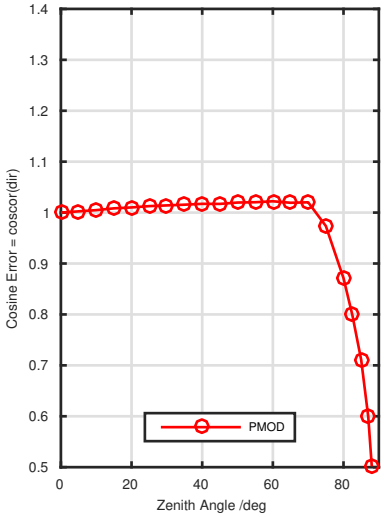

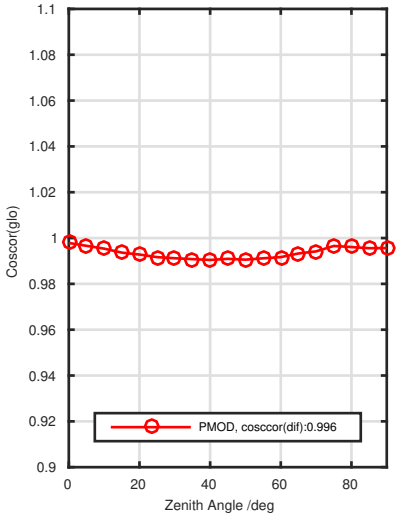

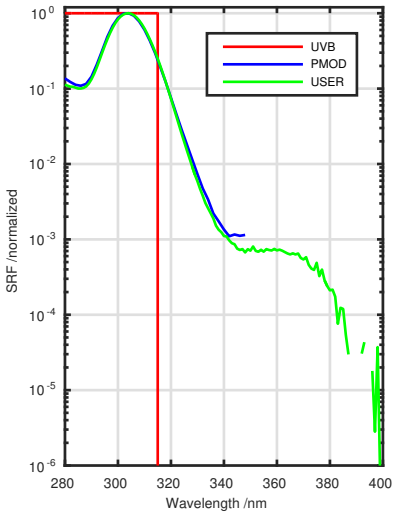

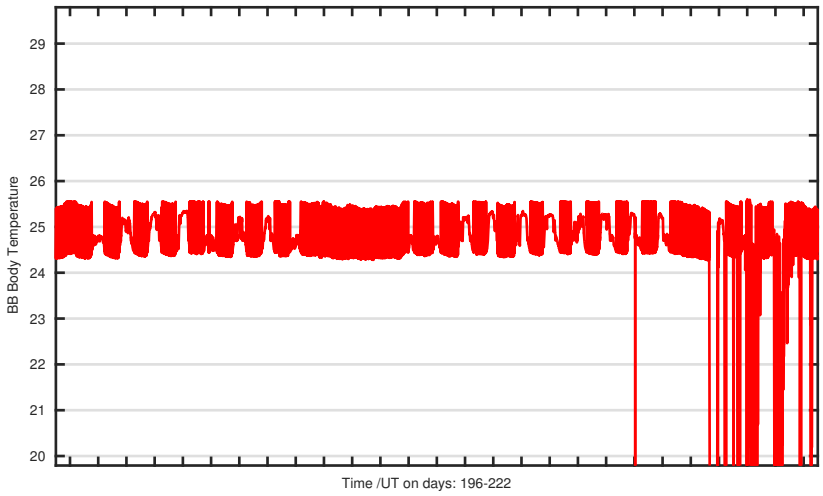

Calibration Matrix fn; Model sdisortREFms2009; f0=1.3040

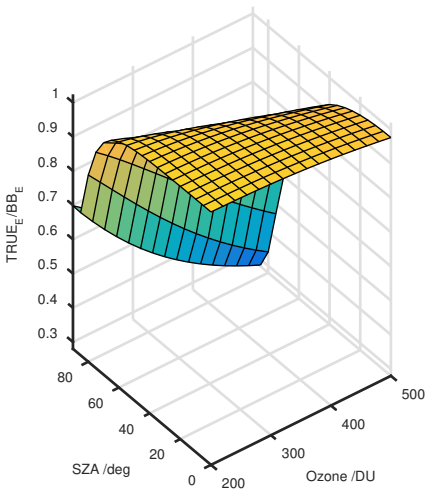

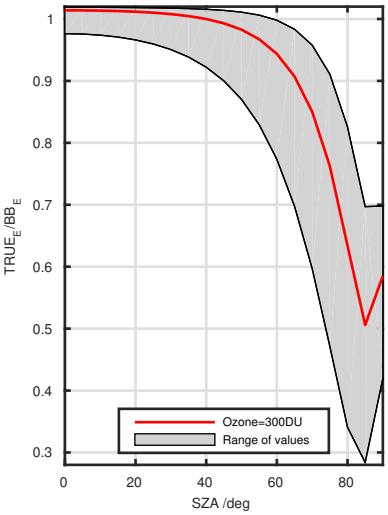

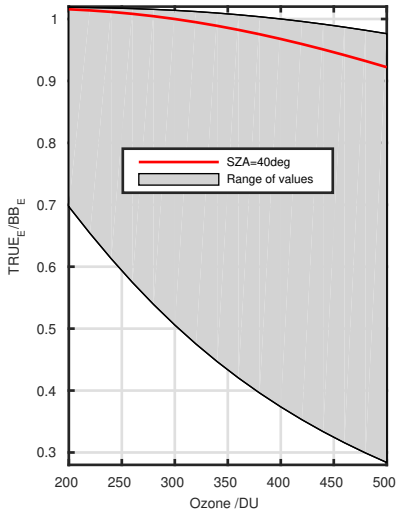

Calibration Results of KZ120076 (UVB)

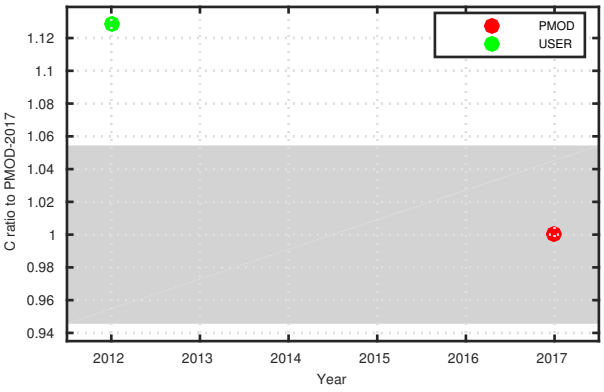

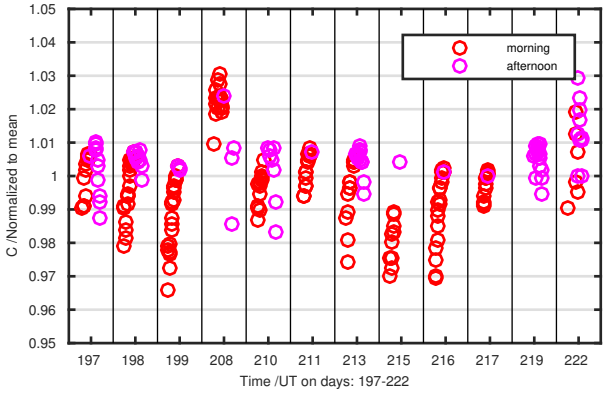

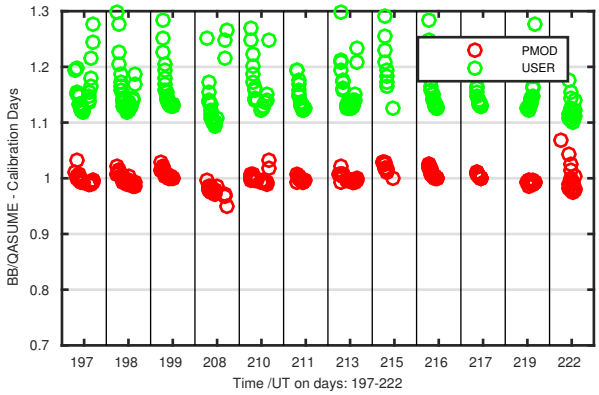

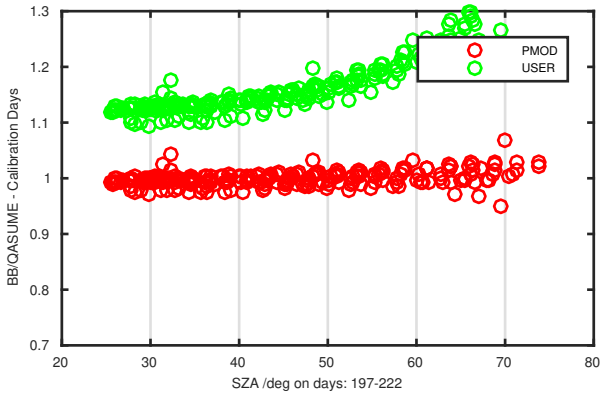

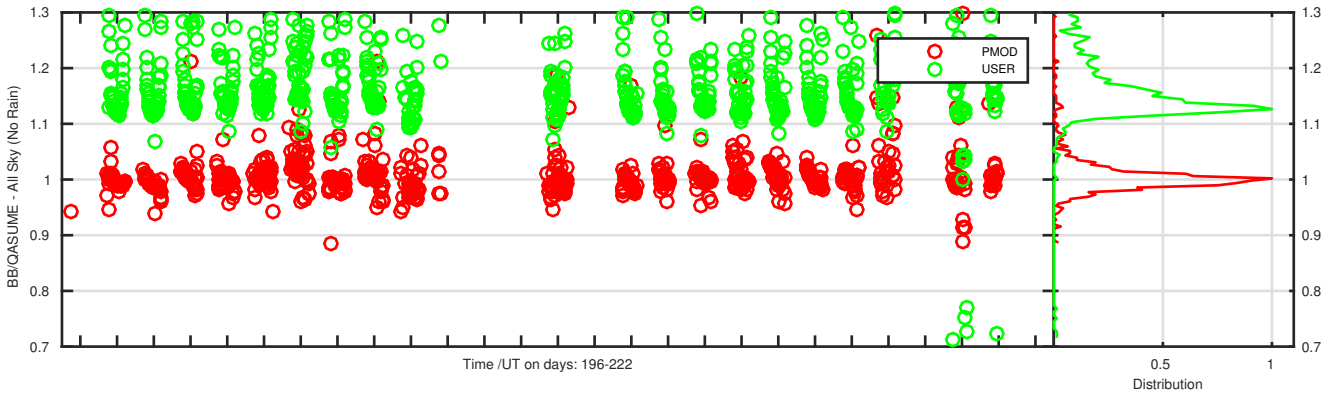

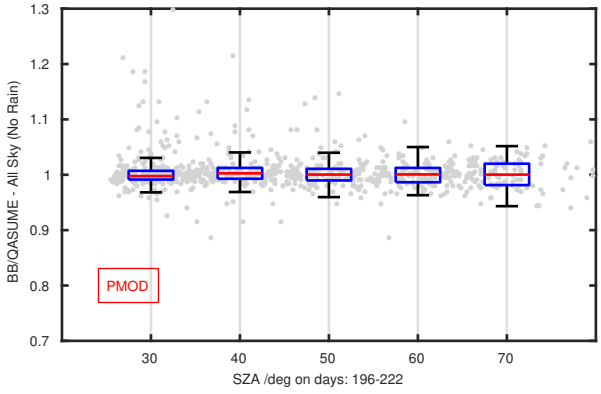

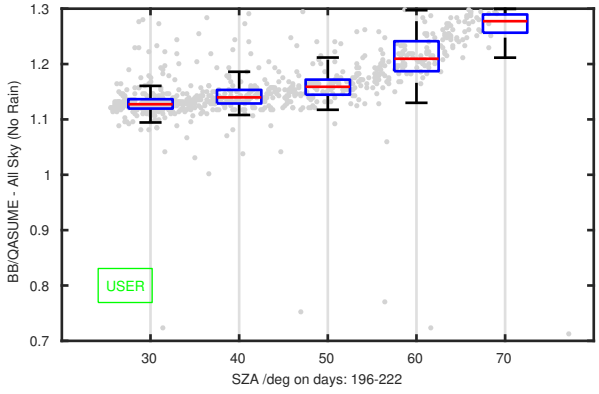

Calibration Results of KZ120077 (UVB)

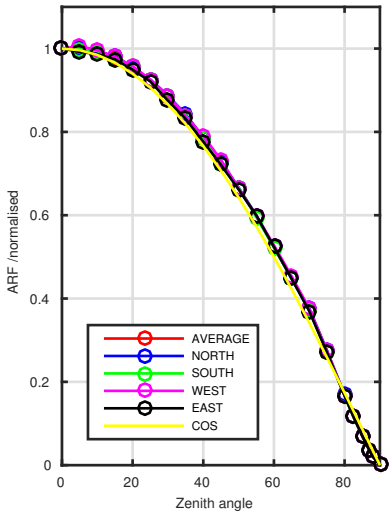

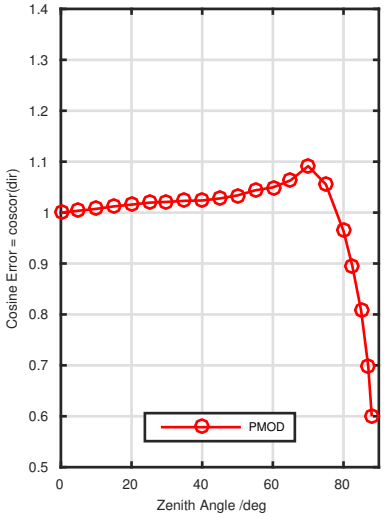

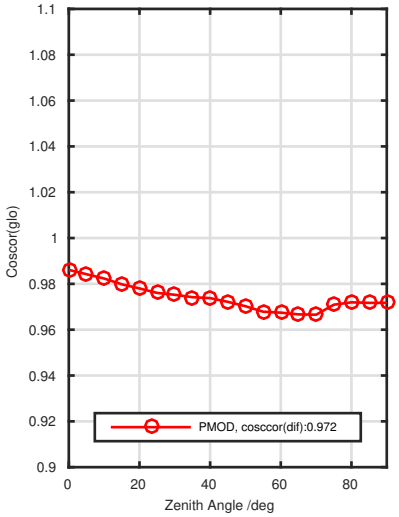

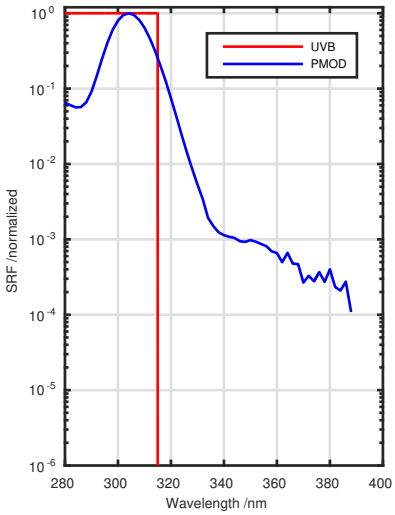

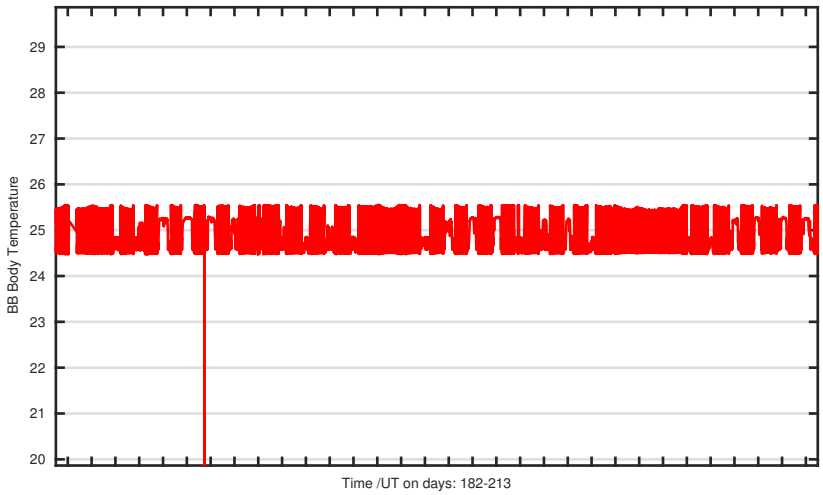

Calibration Matrix fn; Model sdisortREFms2009; f0=1.2652

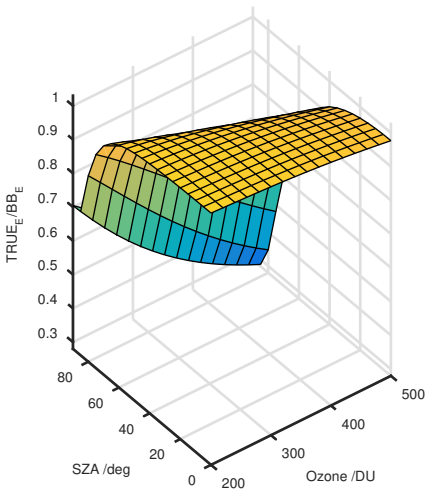

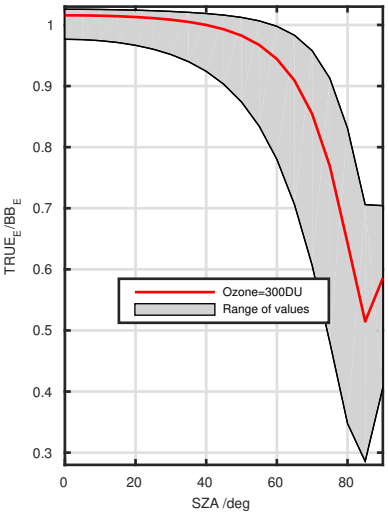

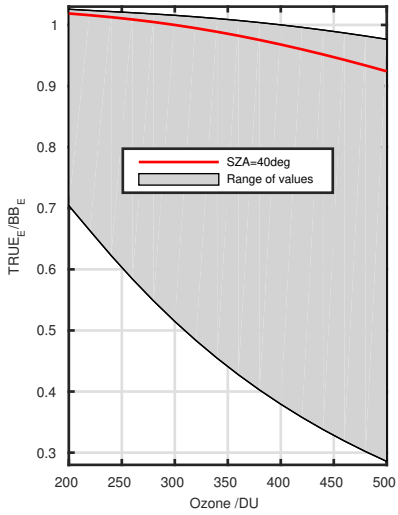

Calibration Results of KZ120077 (UVB)

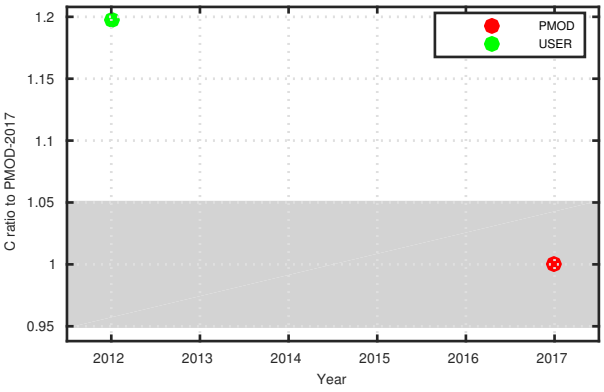

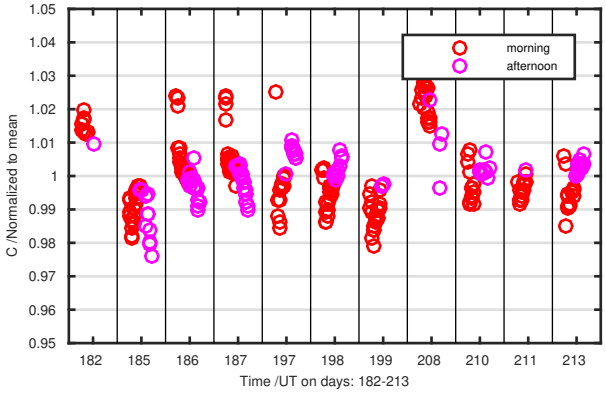

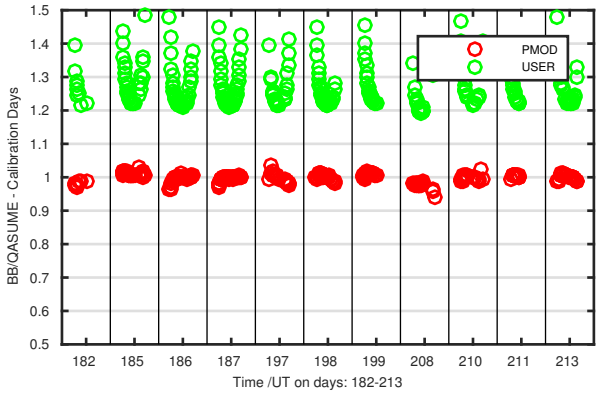

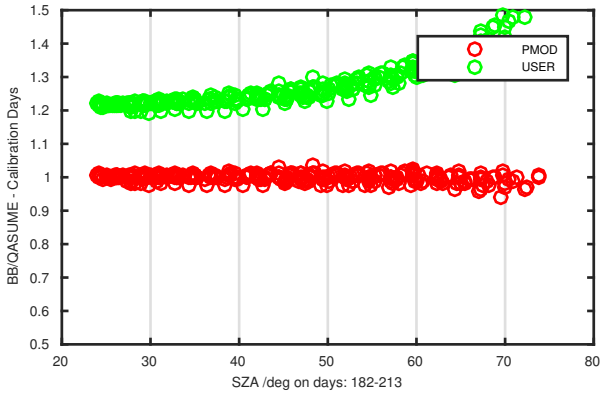

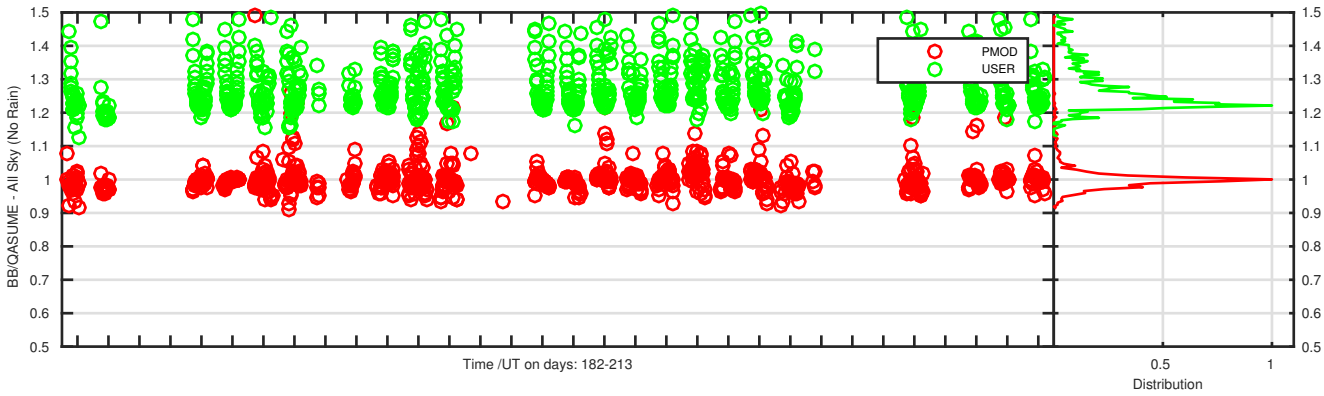

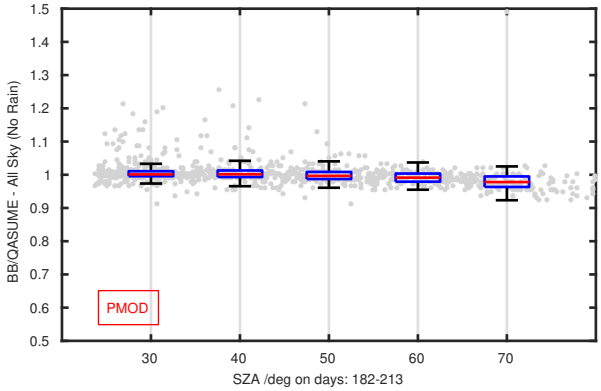

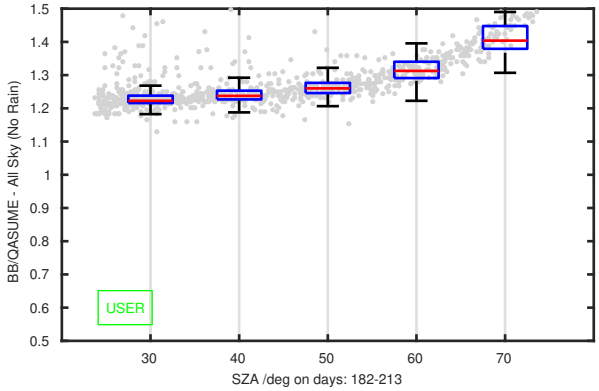

Calibration Results of KZ150110 (UVE)

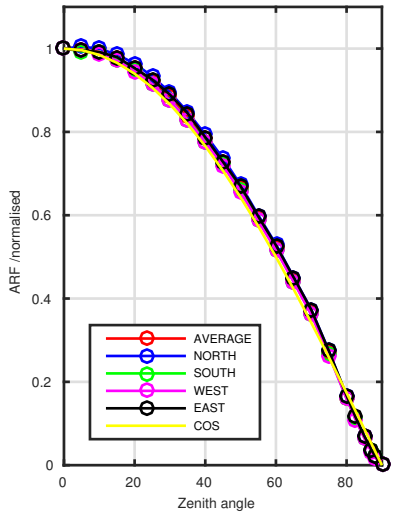

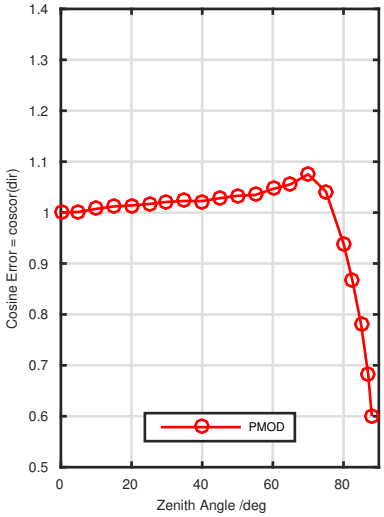

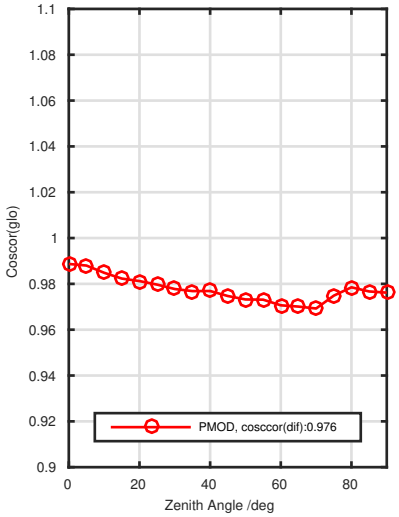

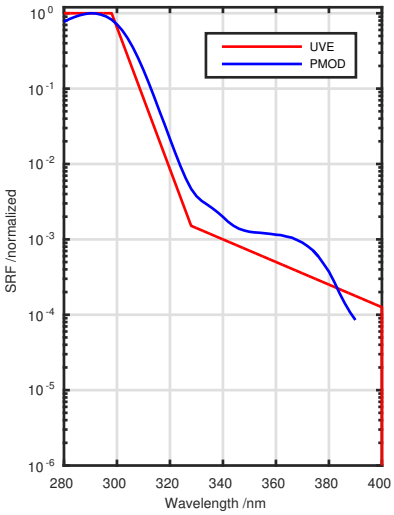

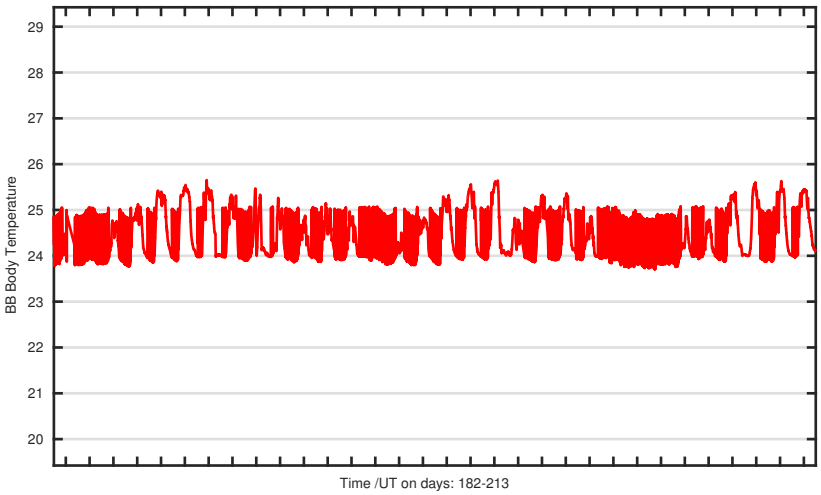

Calibration Matrix fn; Model sdisortREFms2009; f0=0.4722

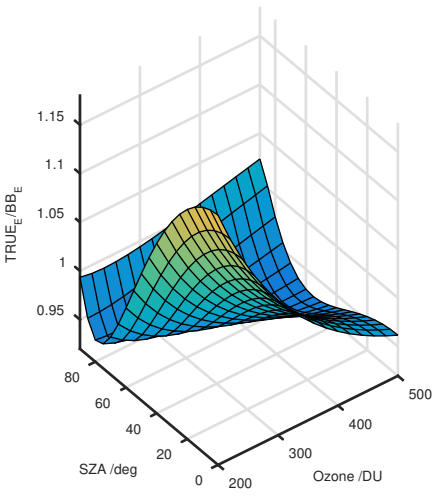

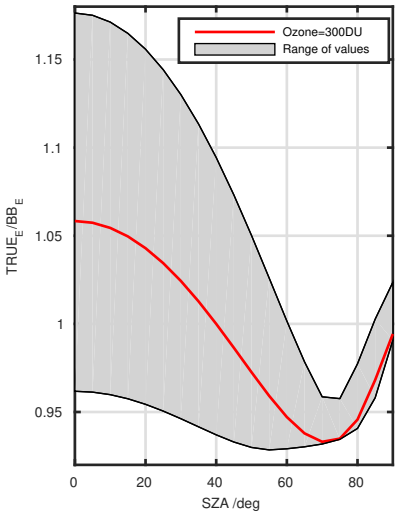

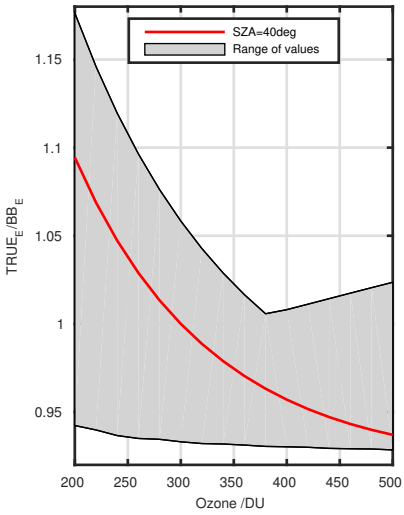

Calibration Results of KZ150110 (UVE)

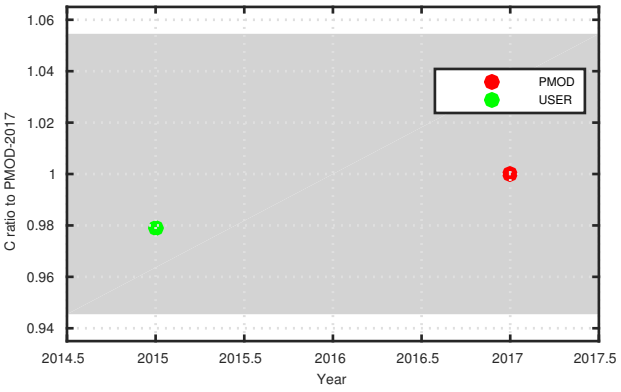

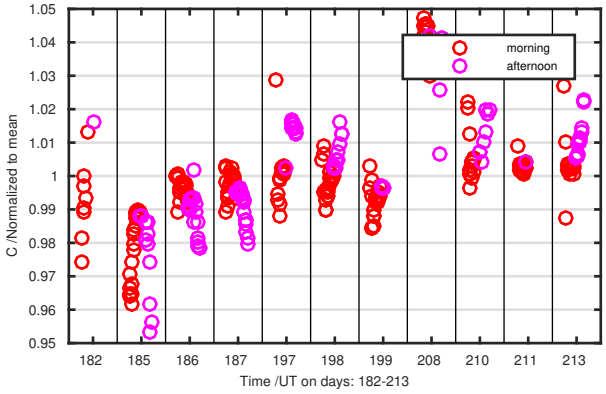

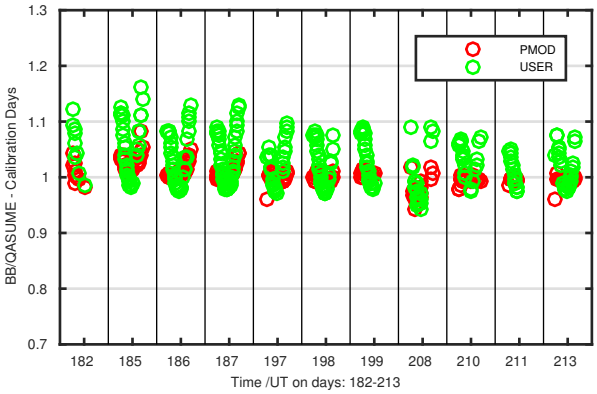

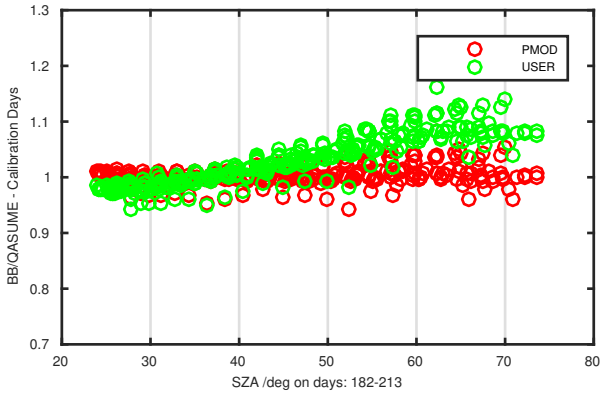

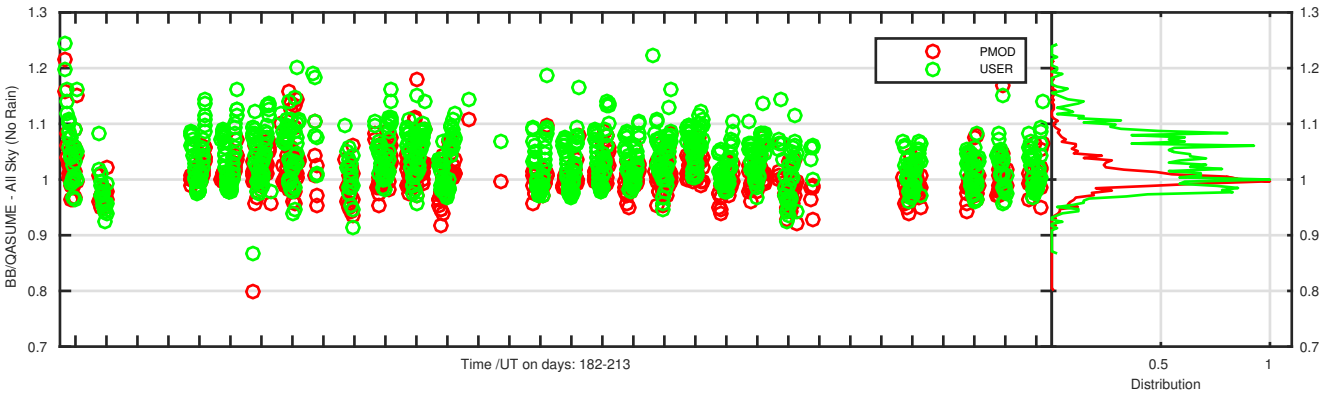

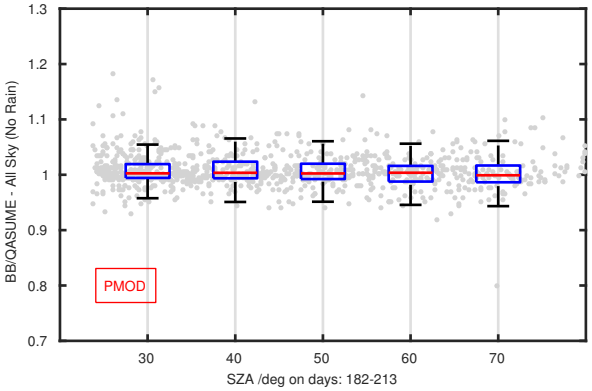

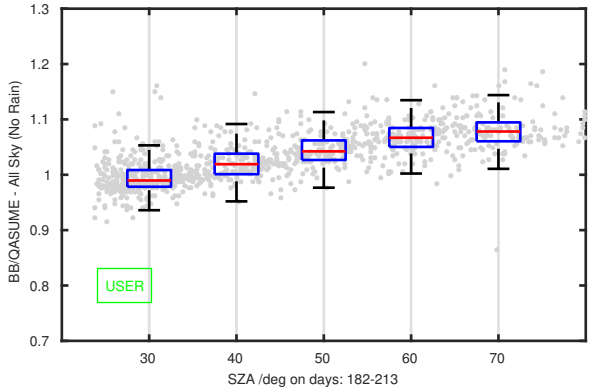

Calibration Results of KZ150124 (UVE)

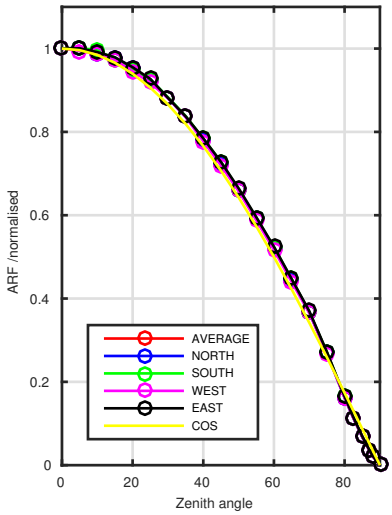

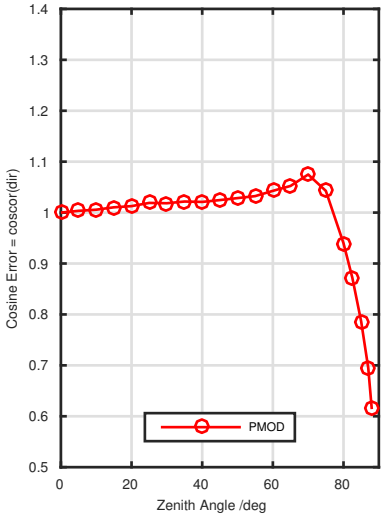

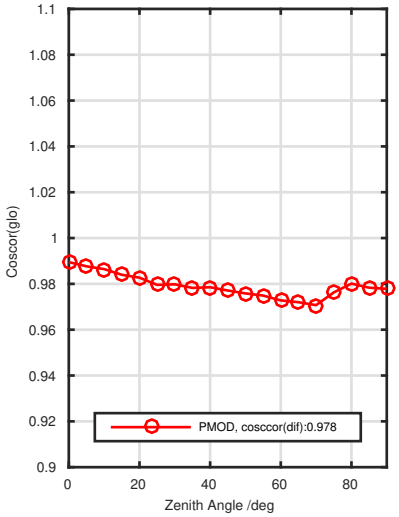

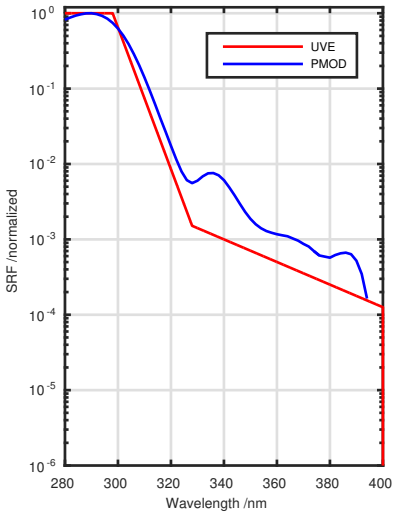

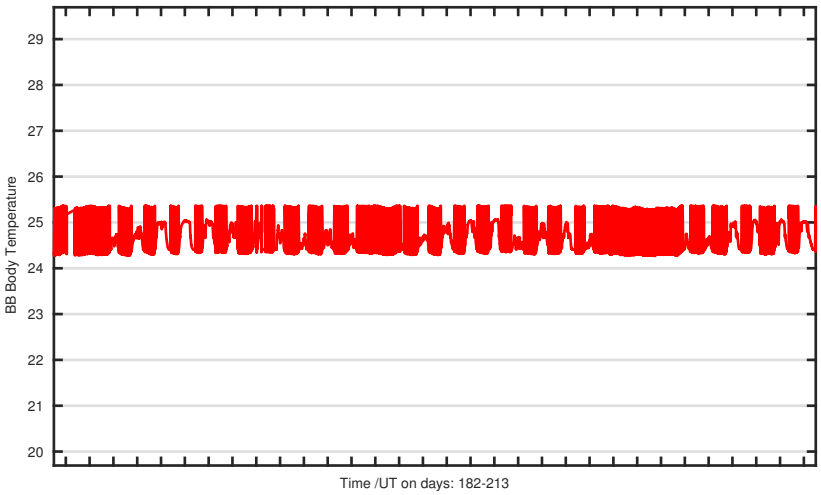

Calibration Matrix fn; Model sdisortREFms2009; f0=0.4977

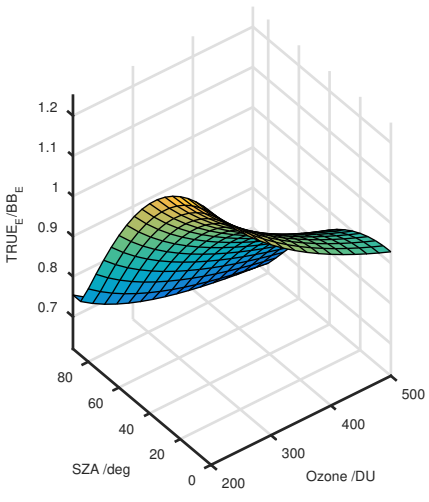

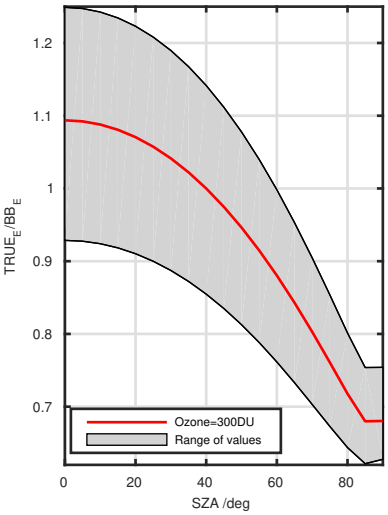

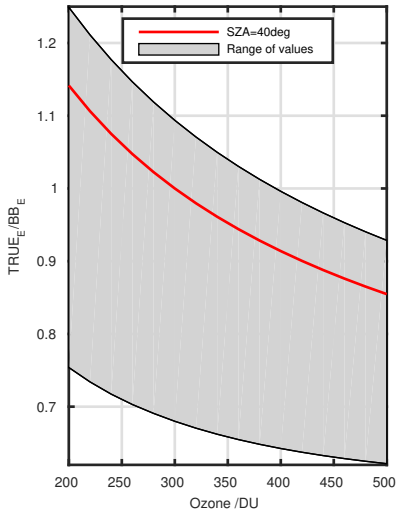

Calibration Results of KZ150124 (UVE)

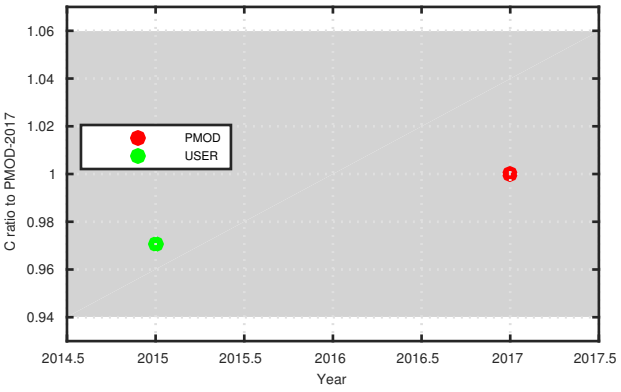

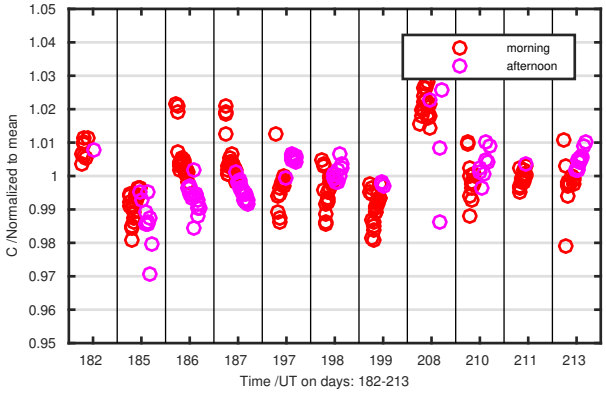

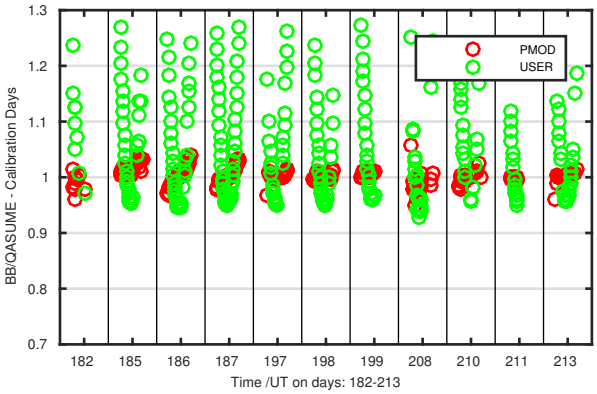

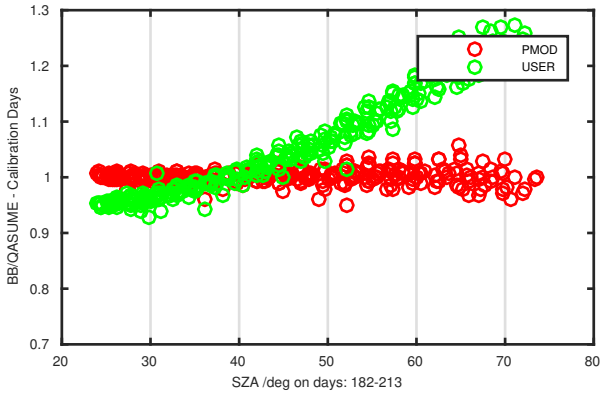

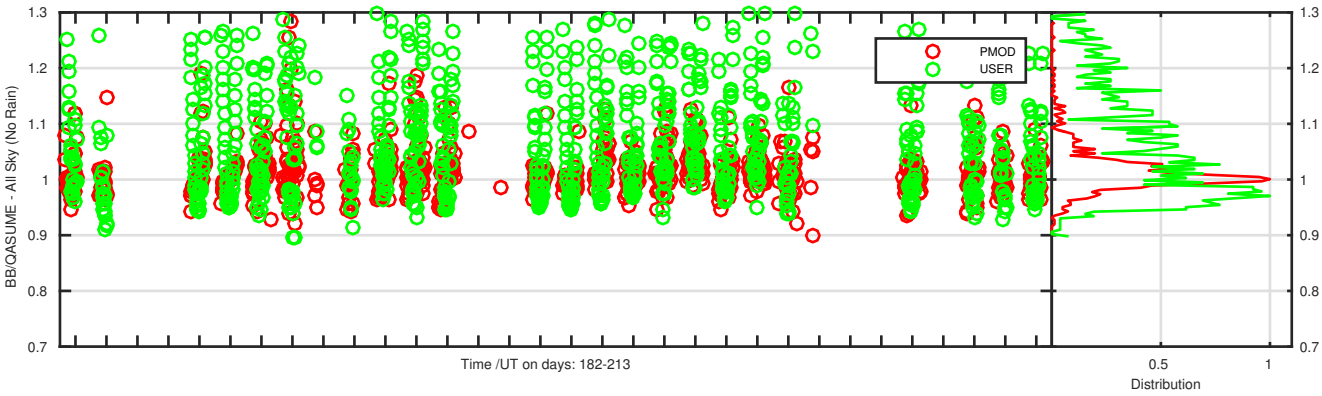

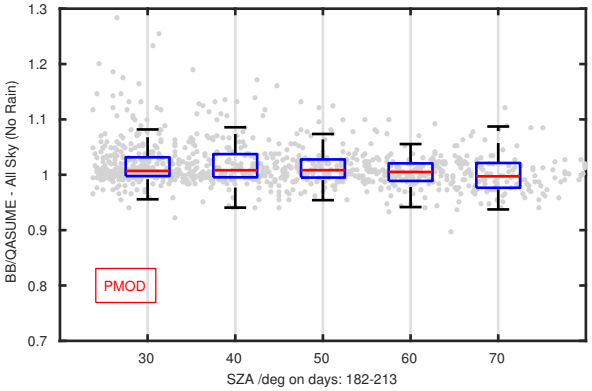

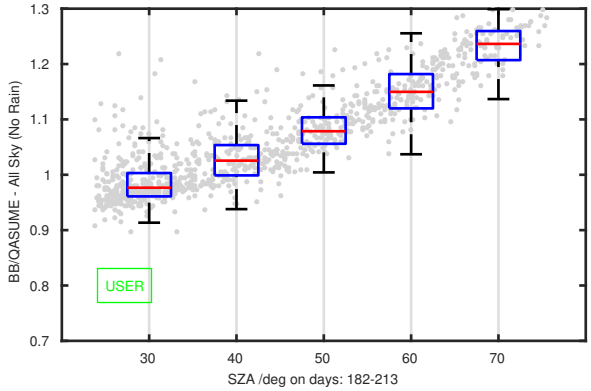

Calibration Results of KZ160142 (UVE)

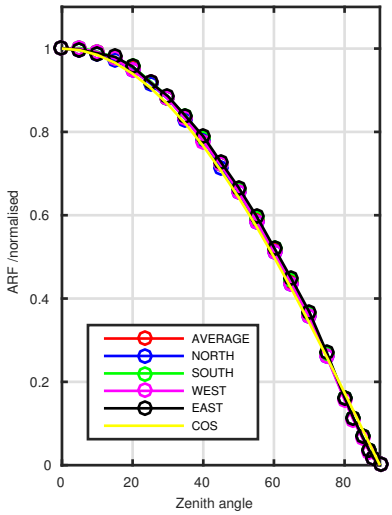

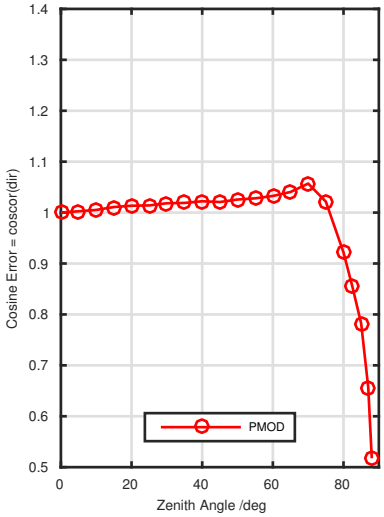

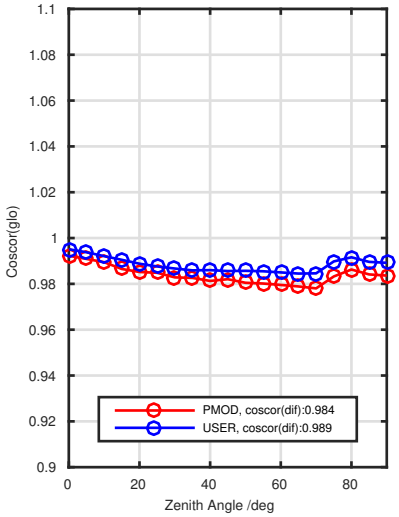

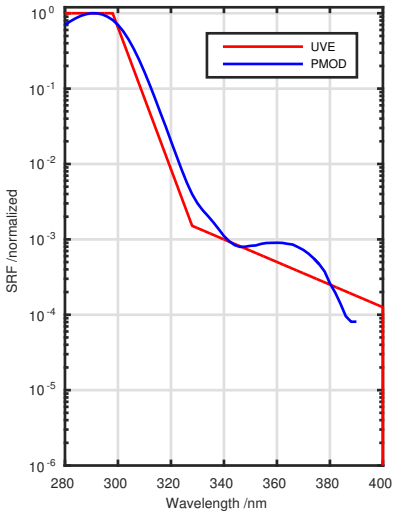

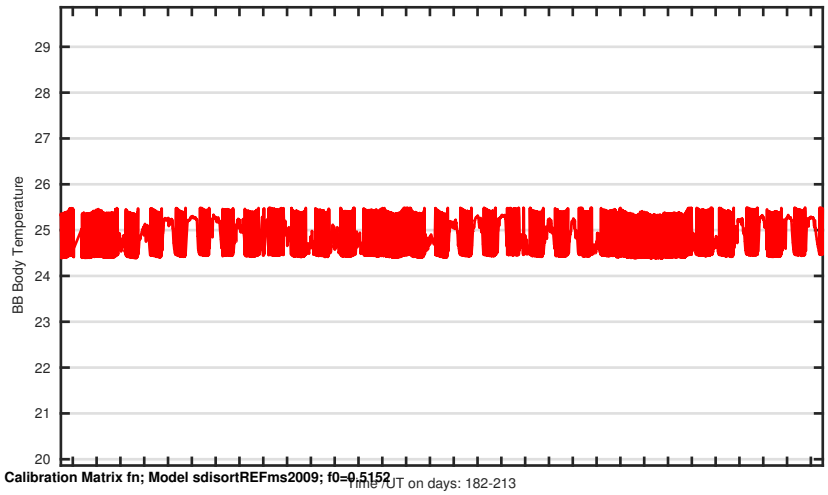

Calibration Matrix fn; Model sdisortREFms2009; f0=0.5152

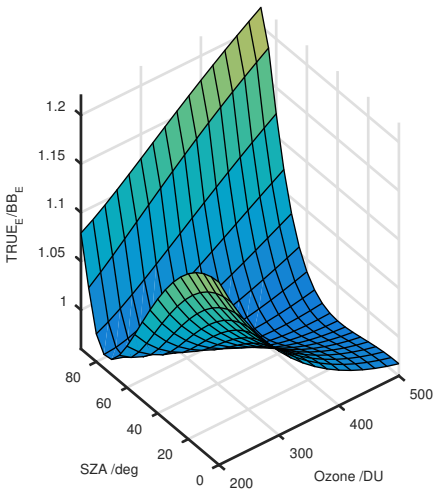

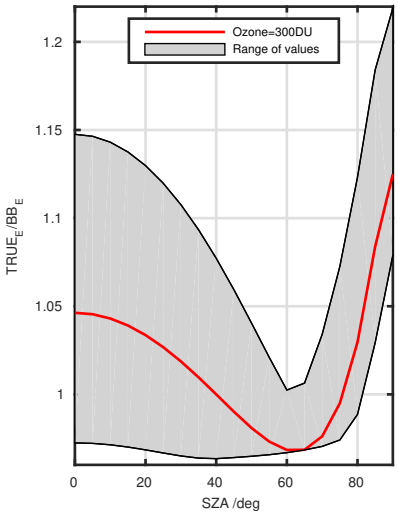

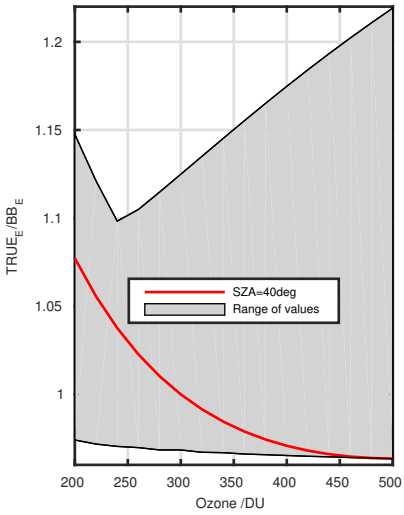

Calibration Results of KZ160142 (UVE)

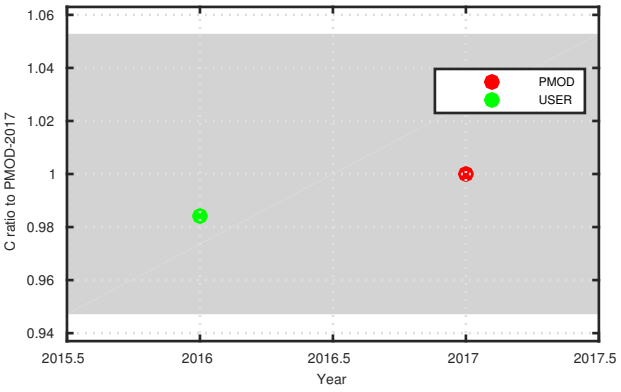

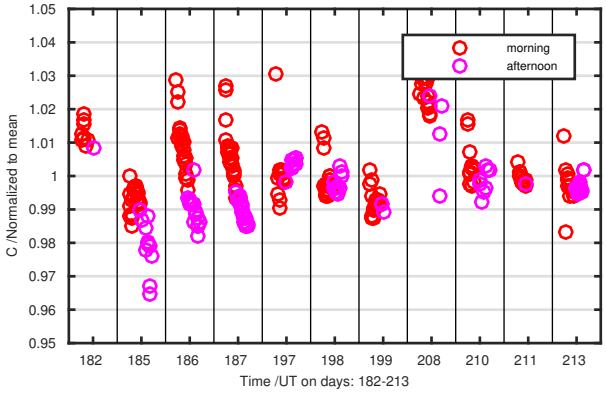

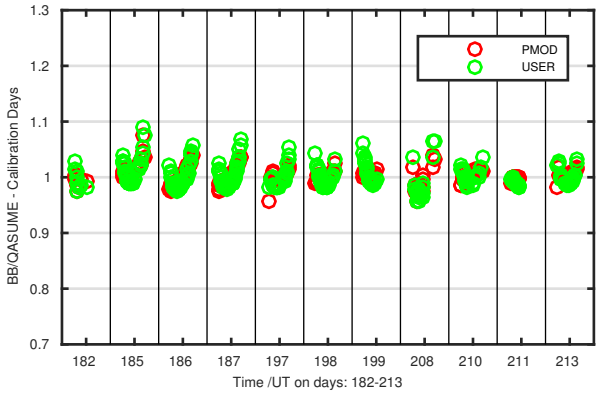

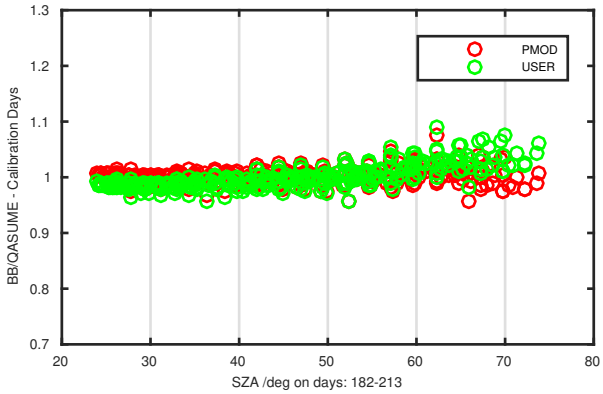

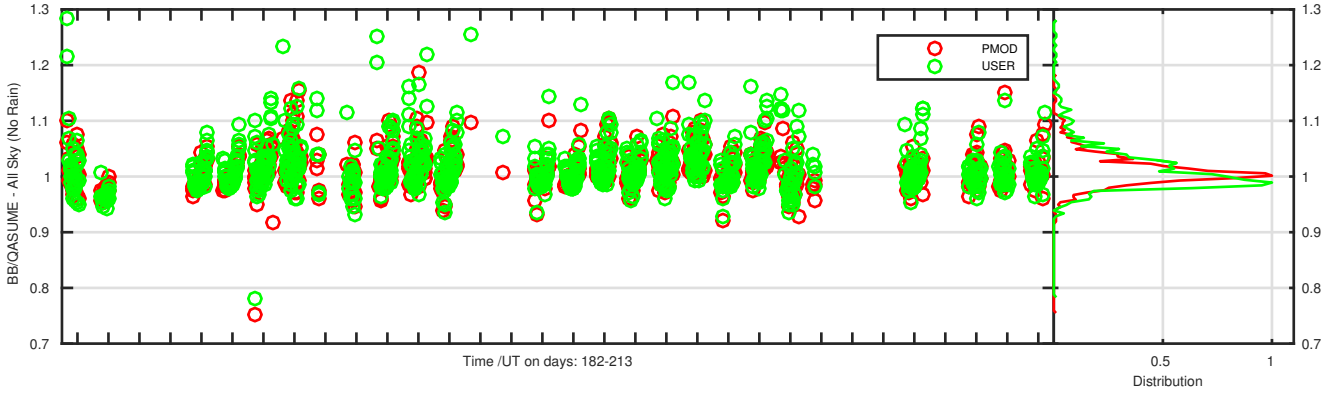

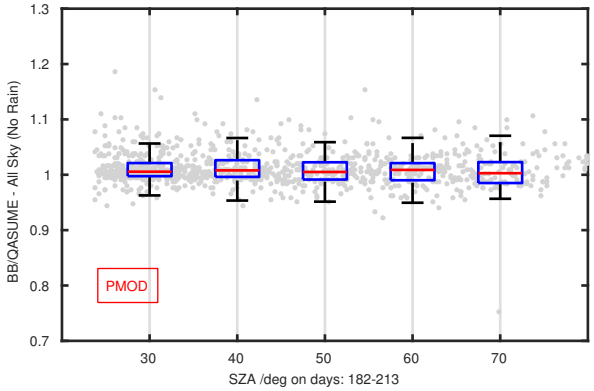

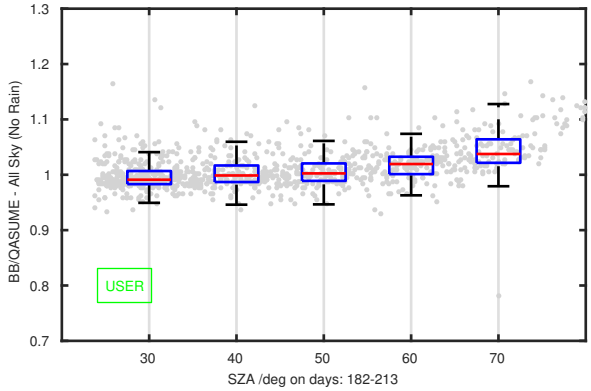

Calibration Results of KZ160158 (UVE)

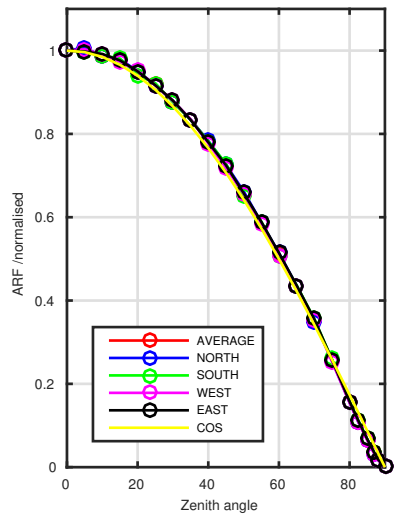

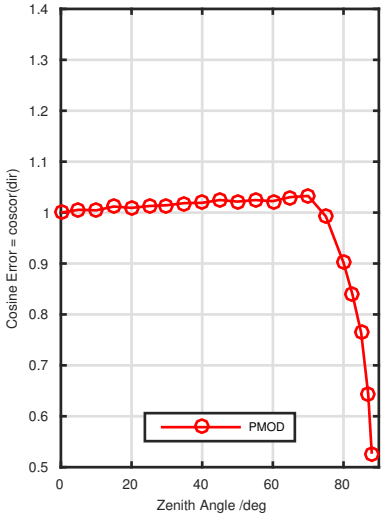

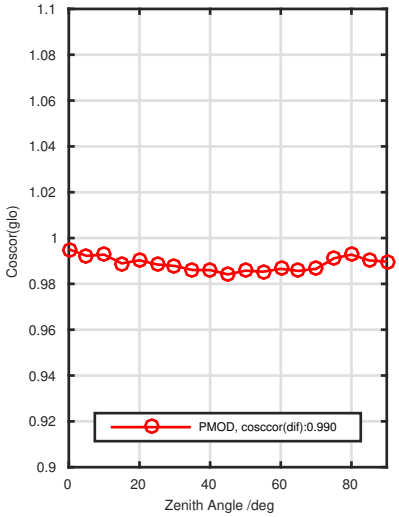

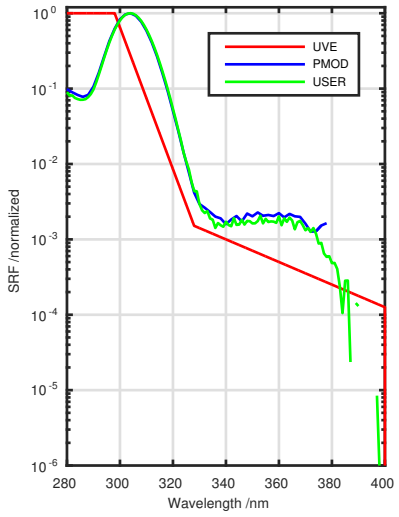

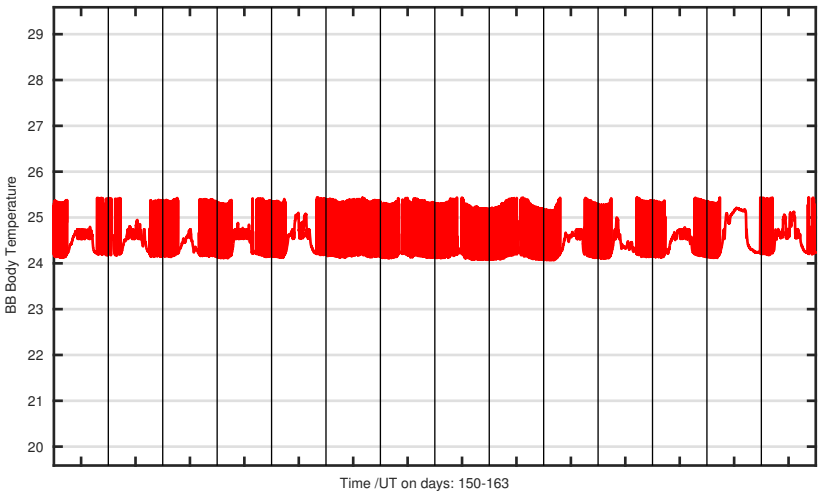

Calibration Matrix fn; Model sdisortREFms2009; f0=0.1830

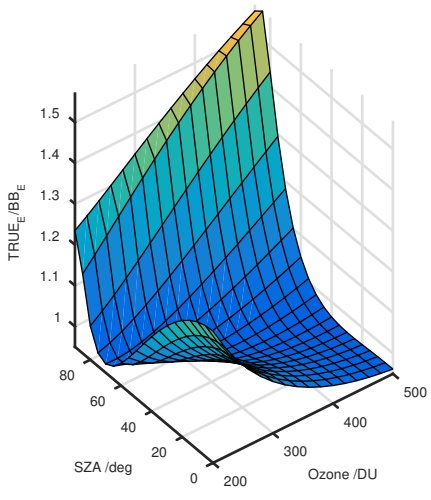

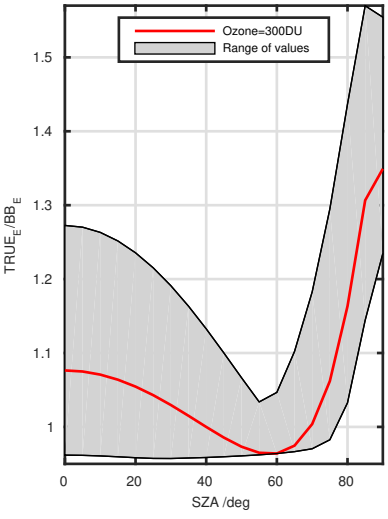

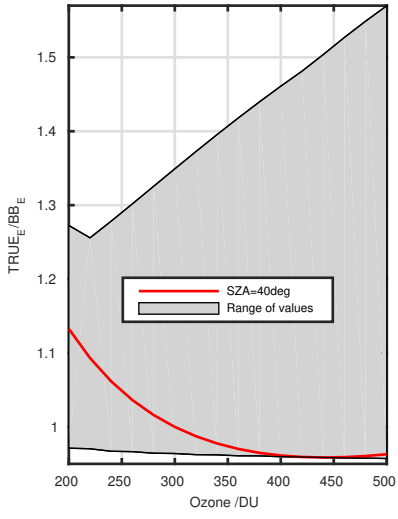

Calibration Results of KZ160158 (UVE)

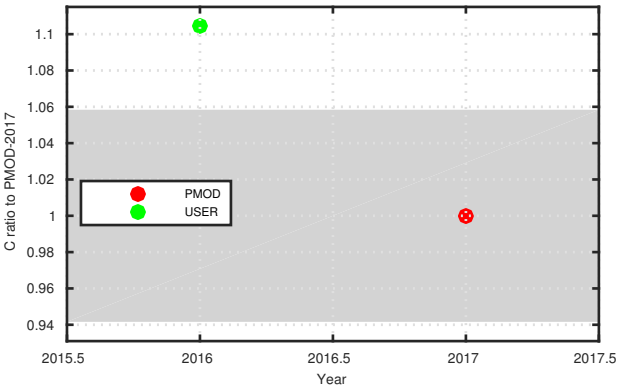

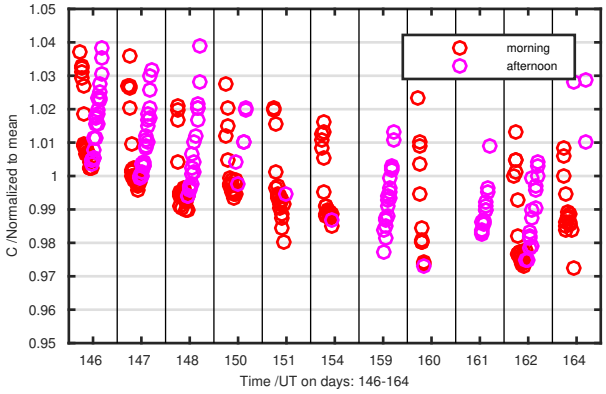

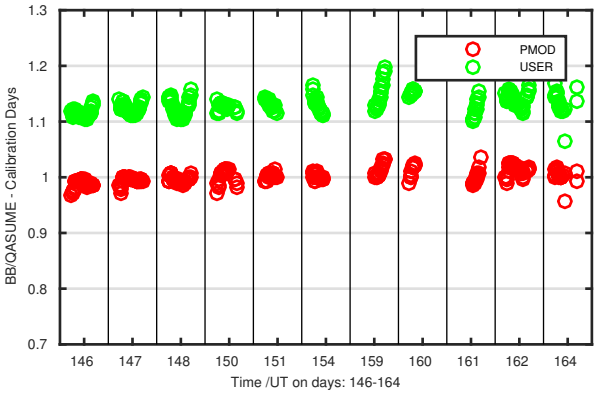

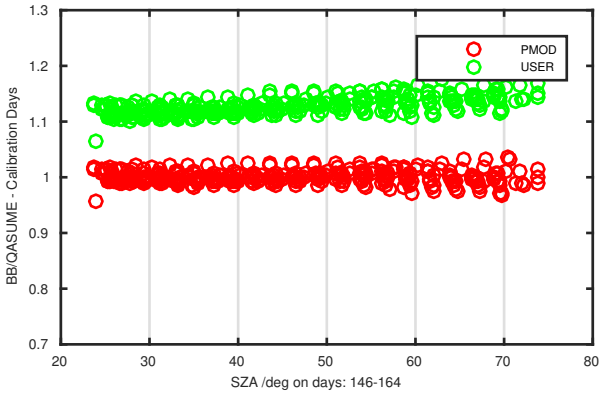

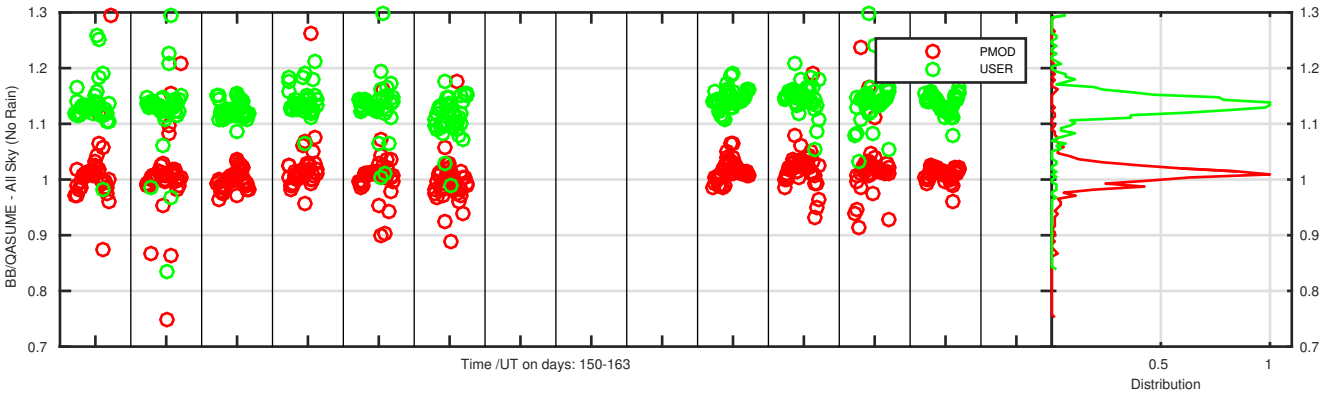

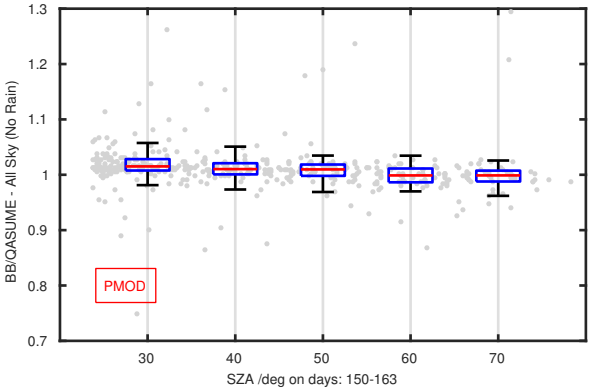

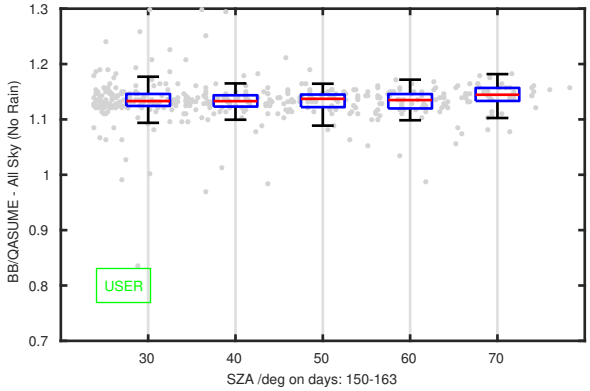

Calibration Results of KZ160177 (UVE)

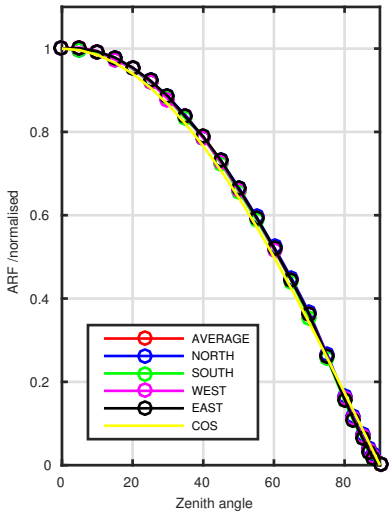

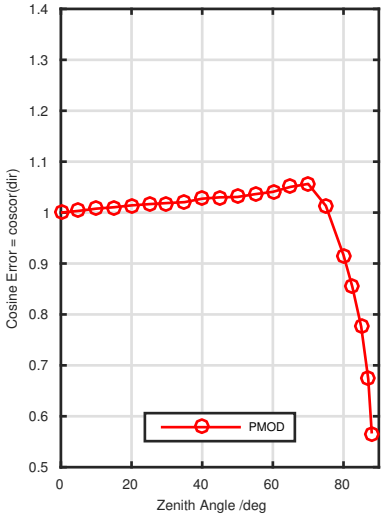

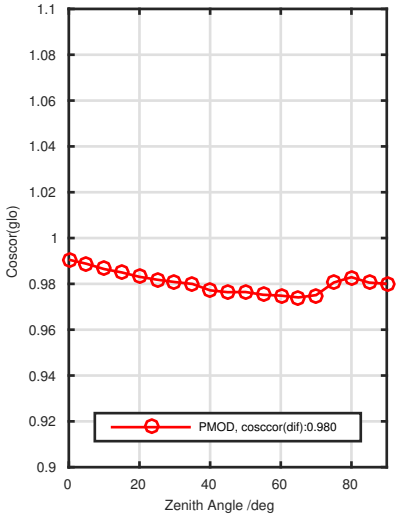

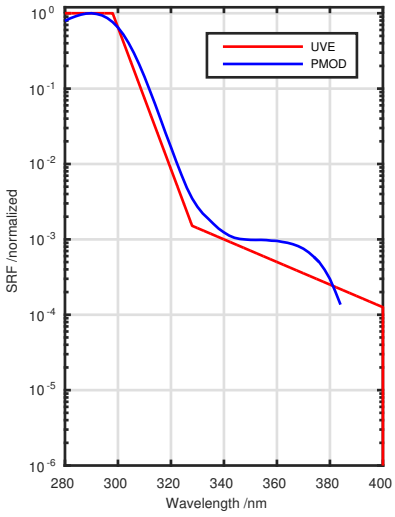

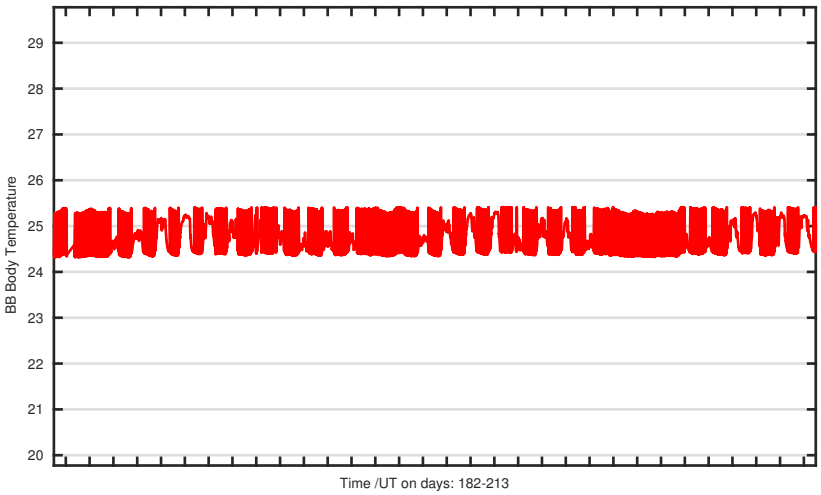

Calibration Matrix fn; Model sdisortREFms2009; f0=0.5855

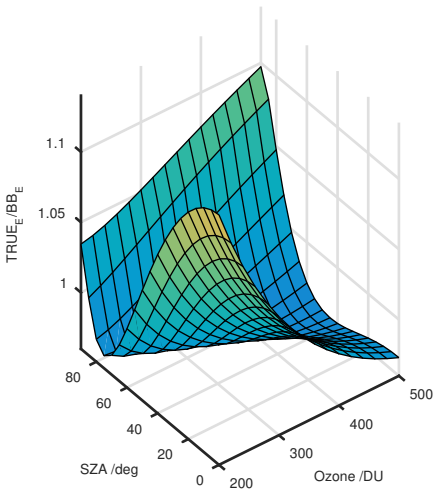

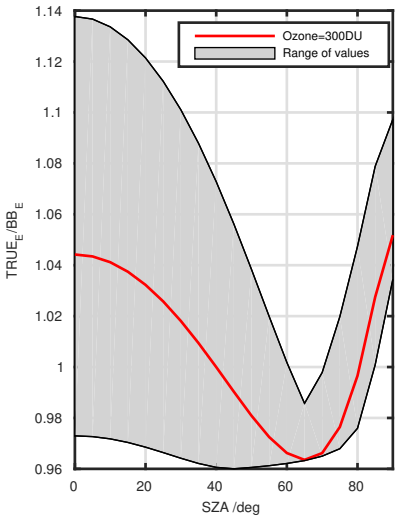

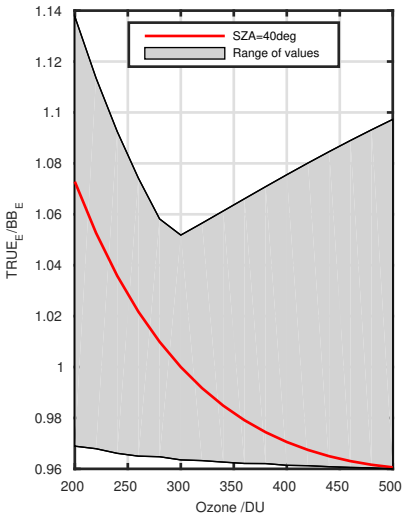

Calibration Results of KZ160177 (UVE)

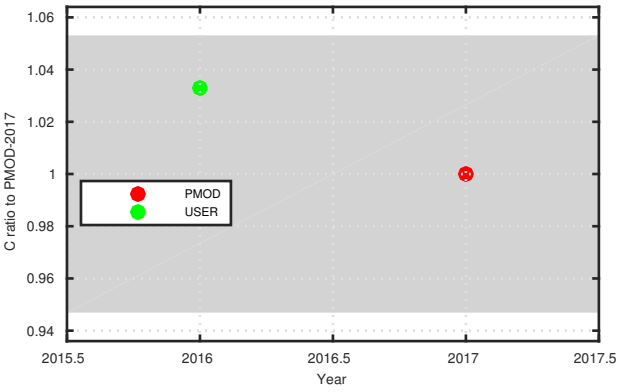

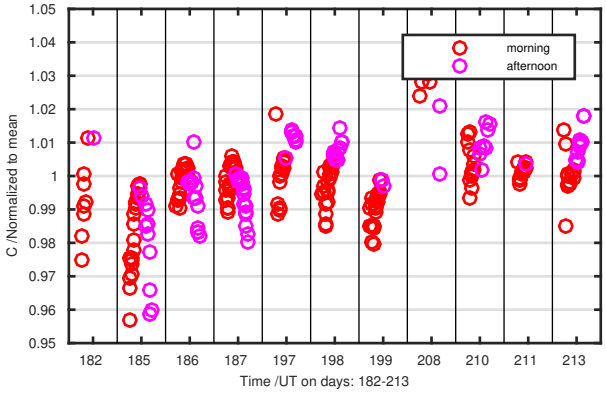

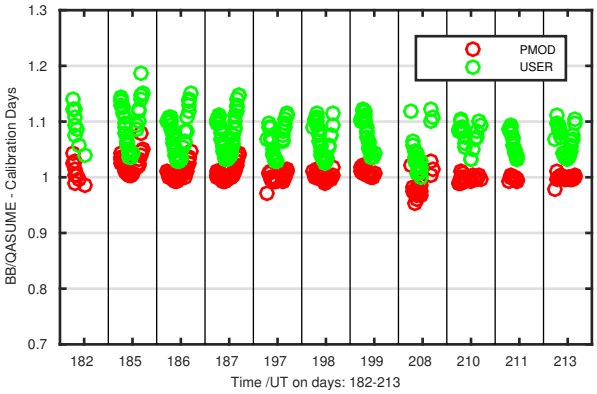

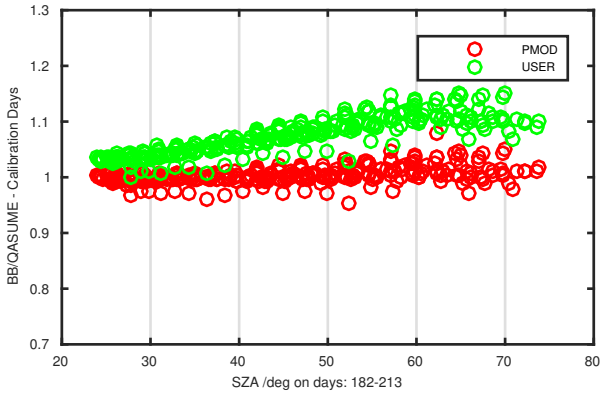

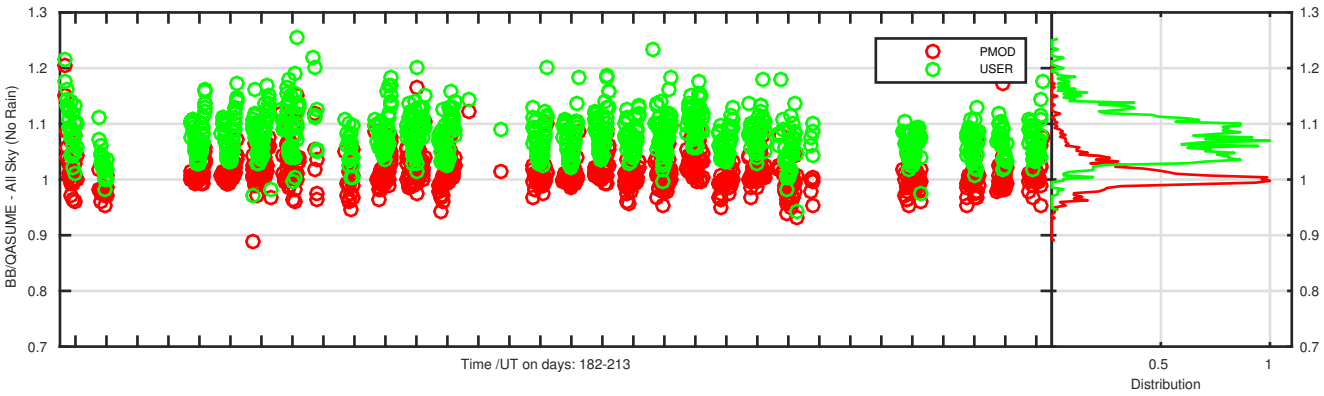

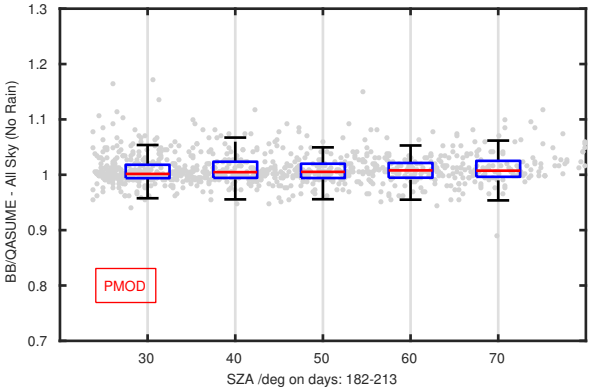

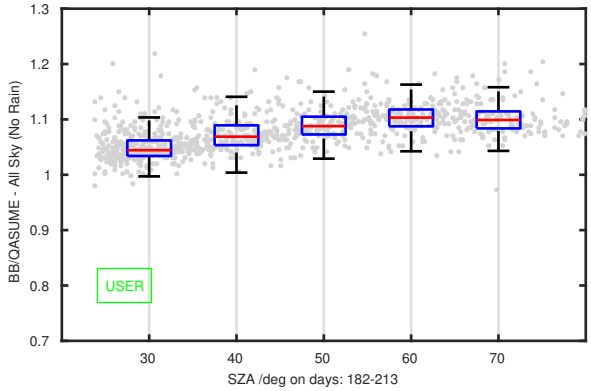

Calibration Results of KZ170204 (UVE)

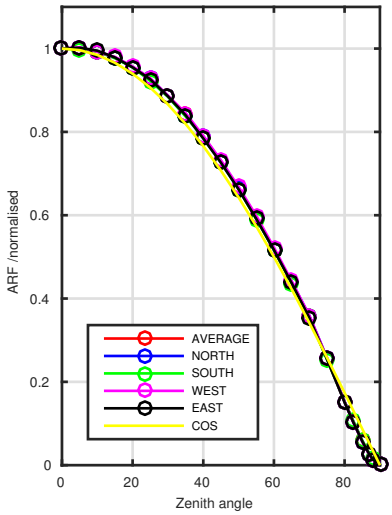

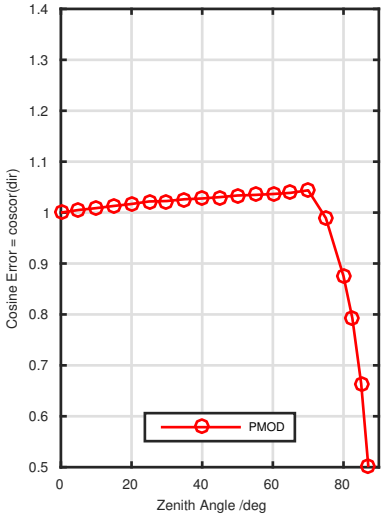

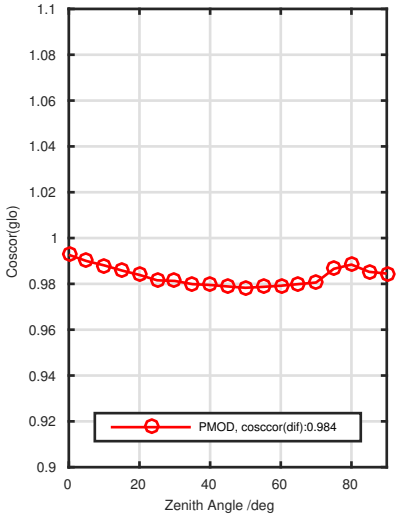

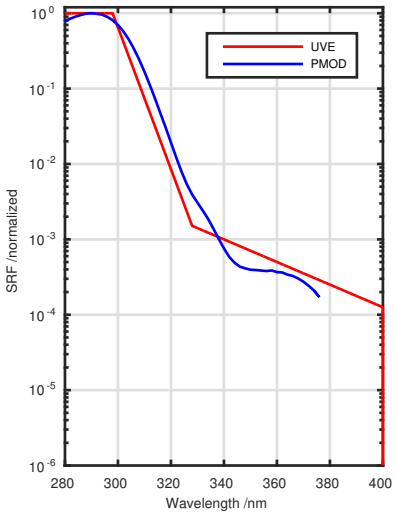

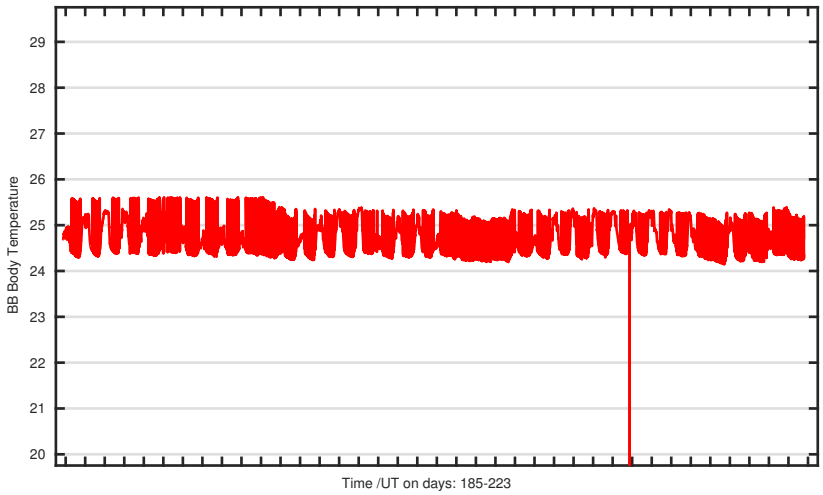

Calibration Matrix fn; Model sdisortREFms2009; f0=0.5380

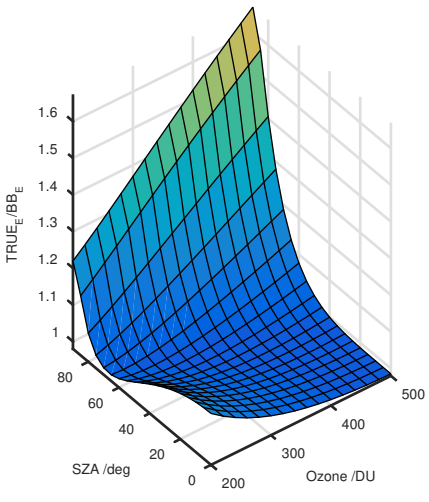

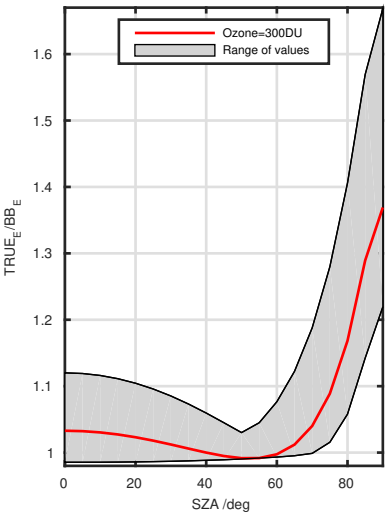

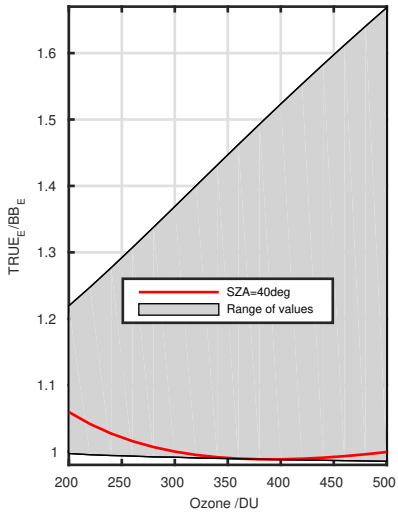

Calibration Results of KZ170204 (UVE)

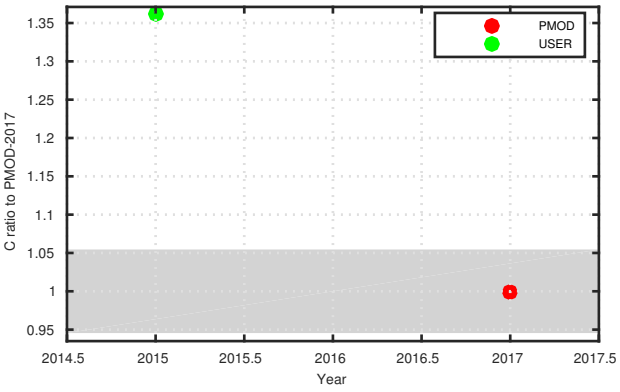

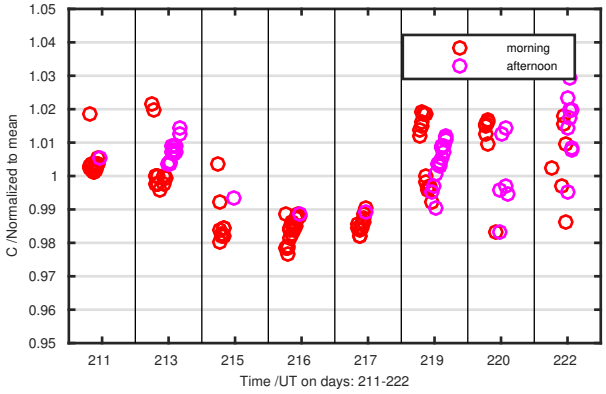

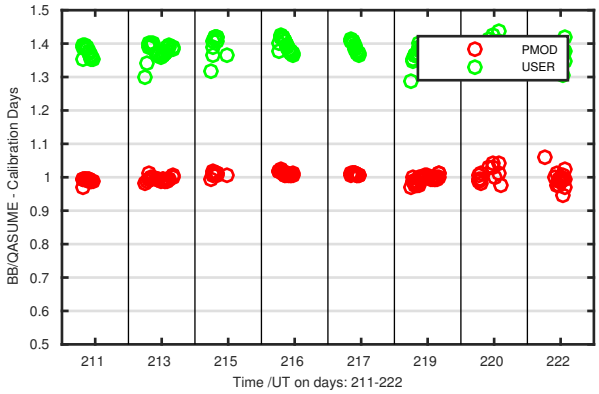

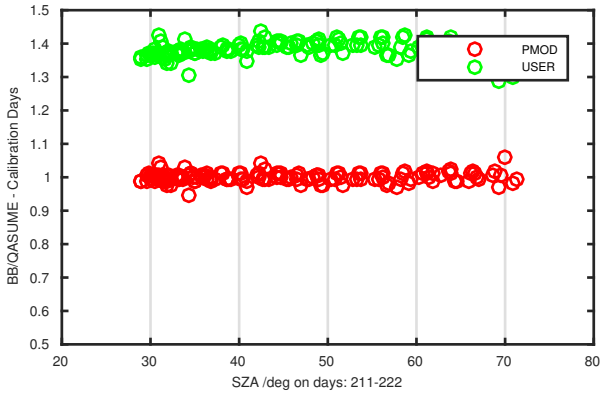

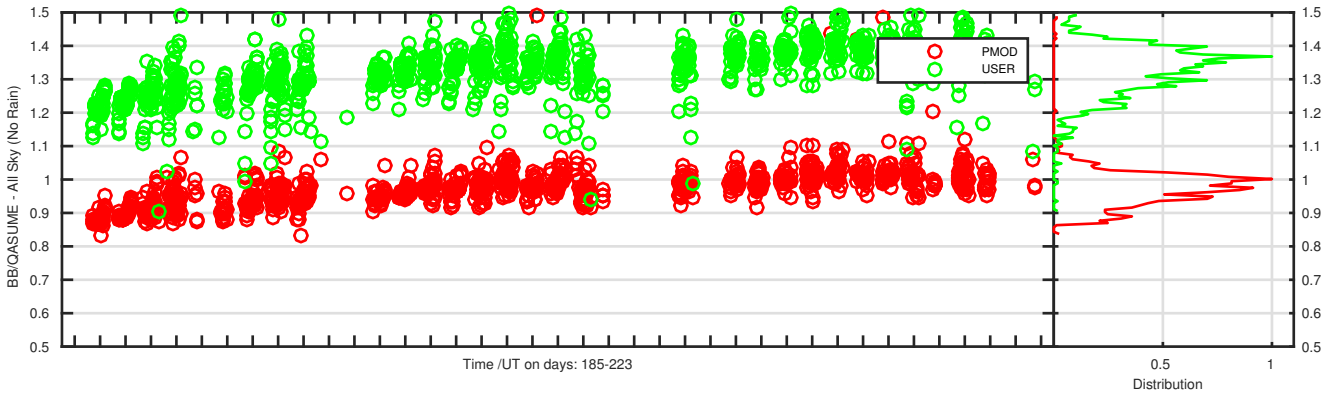

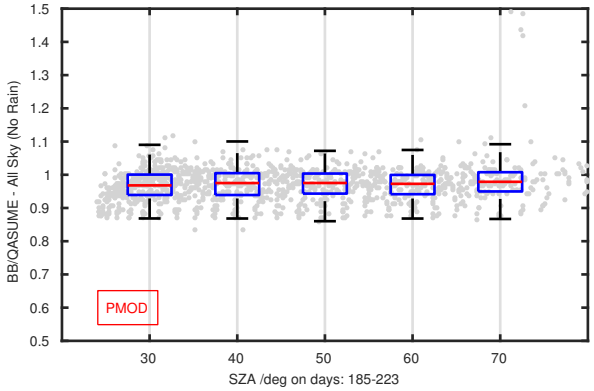

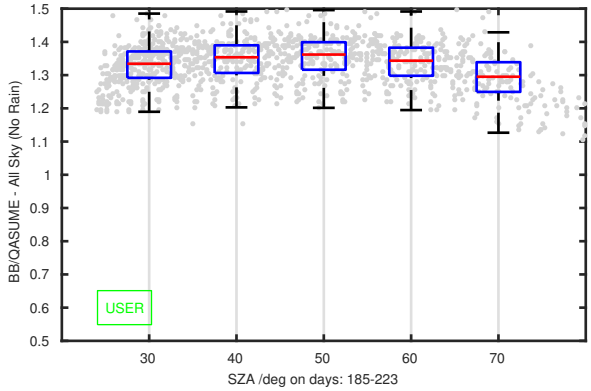

Calibration Results of SCI00341 (UVE)

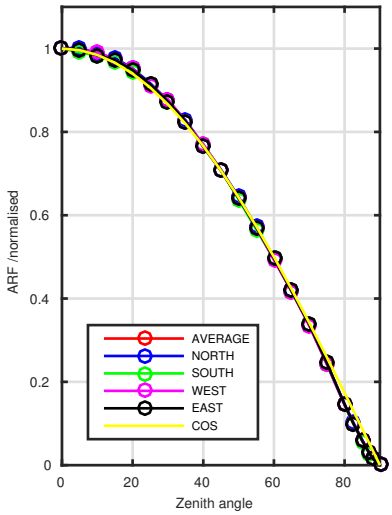

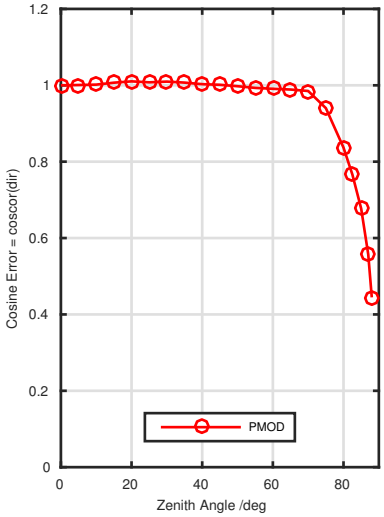

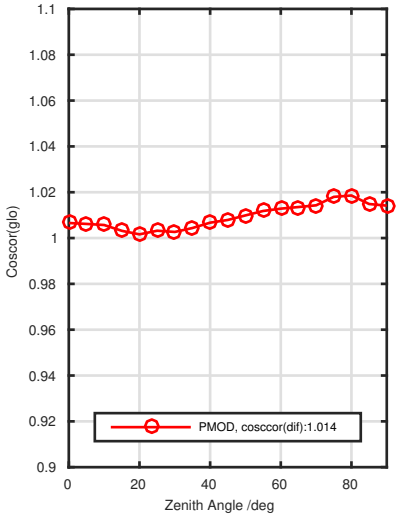

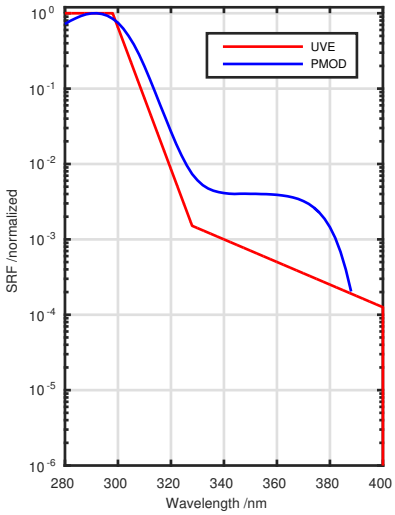

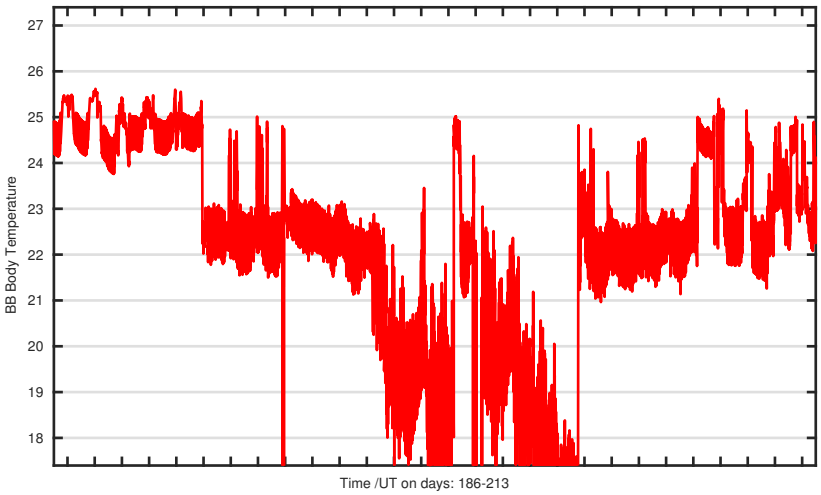

Calibration Matrix fn; Model sdisortREFms2009; f0=0.3545

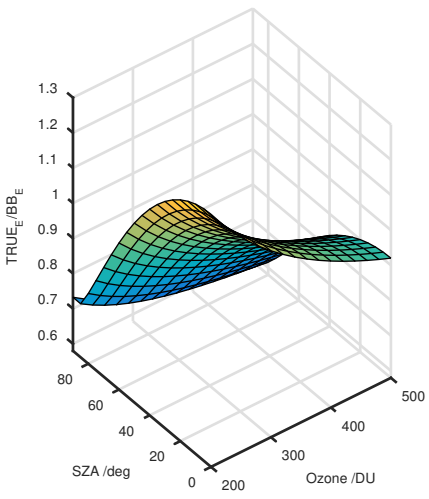

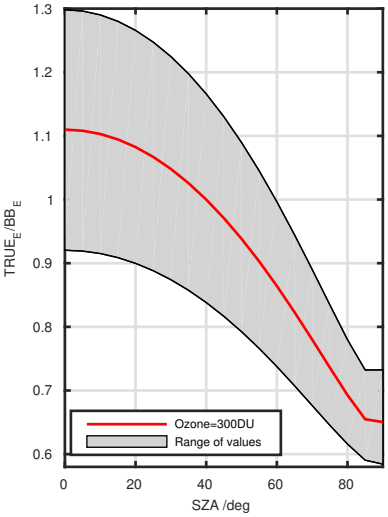

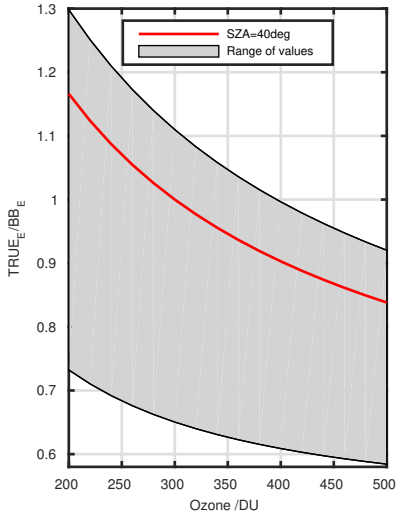

Calibration Results of SCI00341 (UVE)

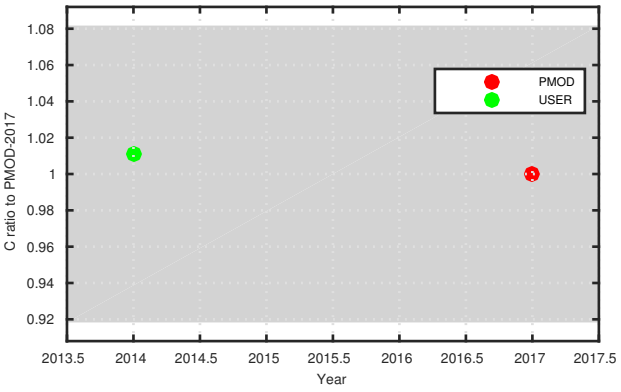

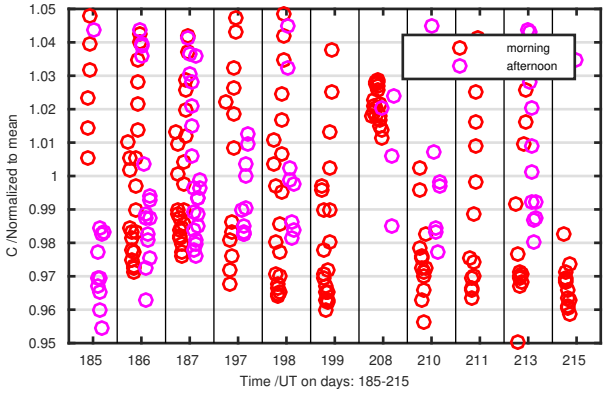

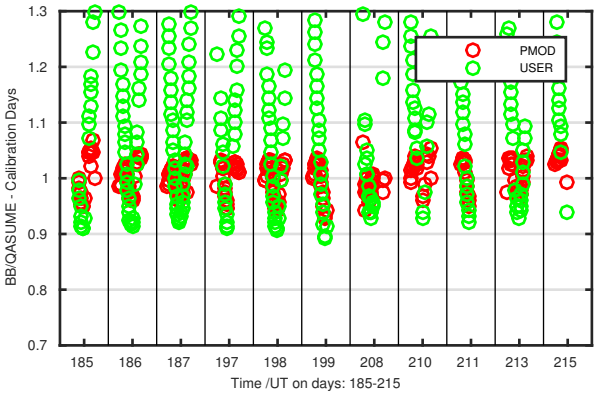

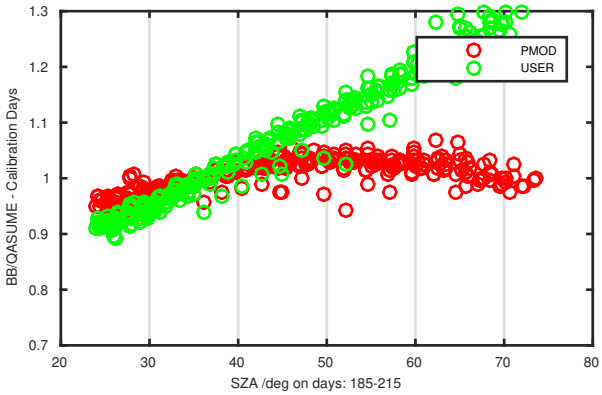

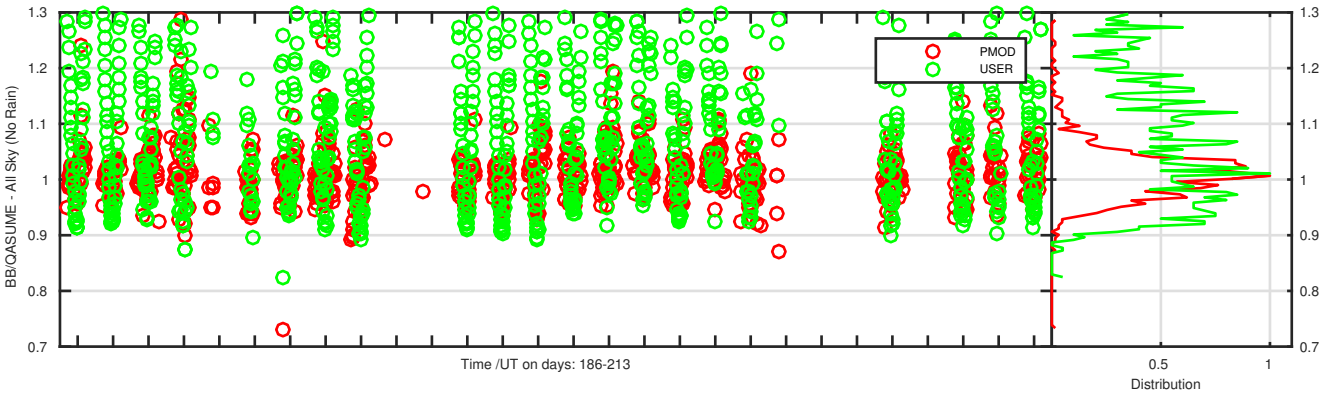

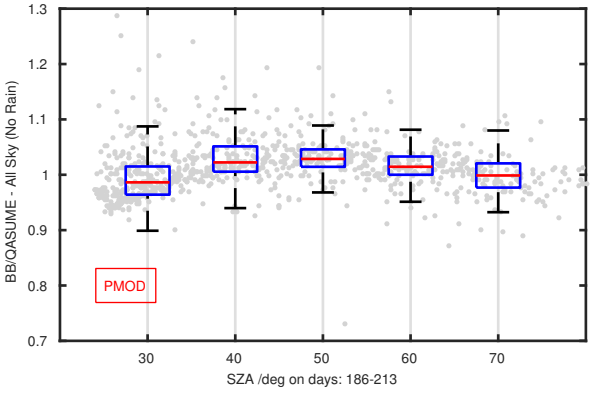

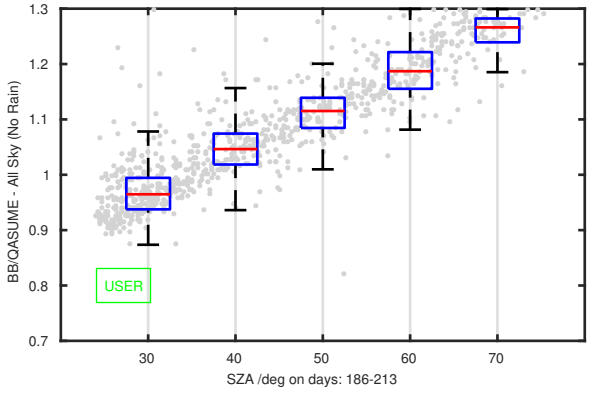

Calibration Results of SCI00400 (UVA)

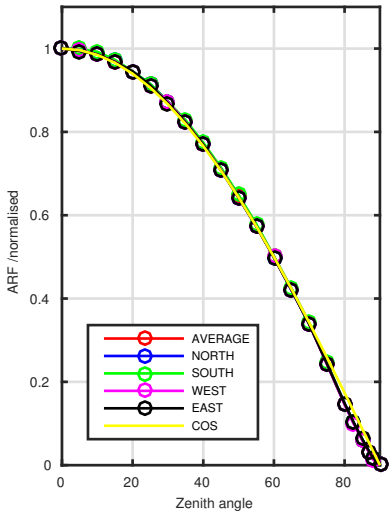

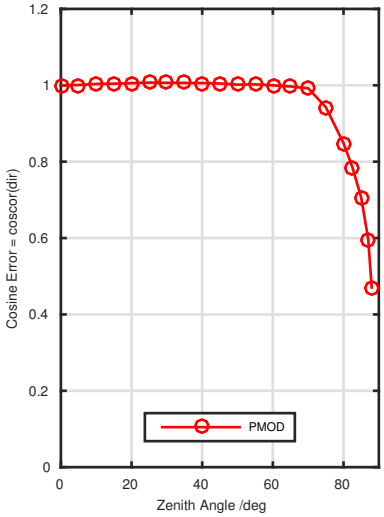

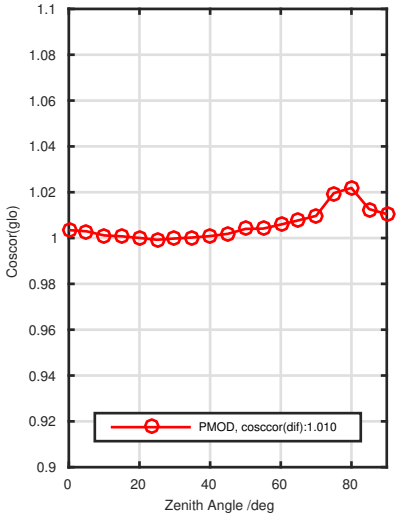

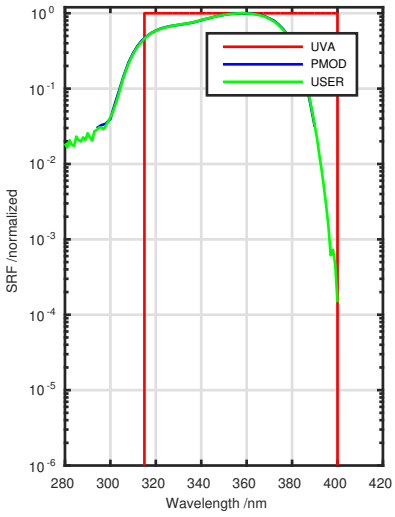

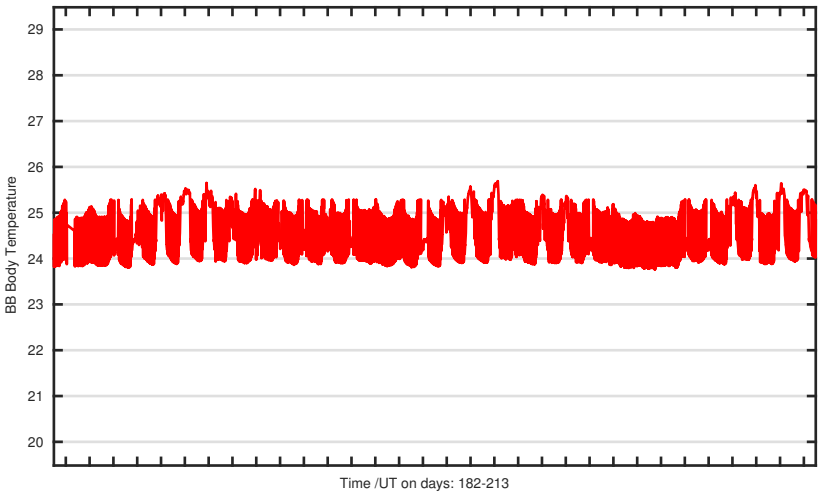

Calibration Matrix fn; Model sdisortREFms2009; f0=1.6419

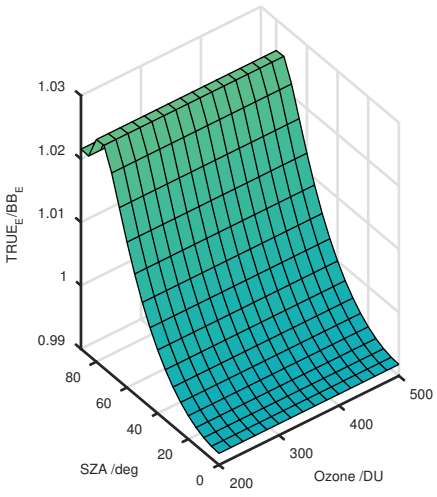

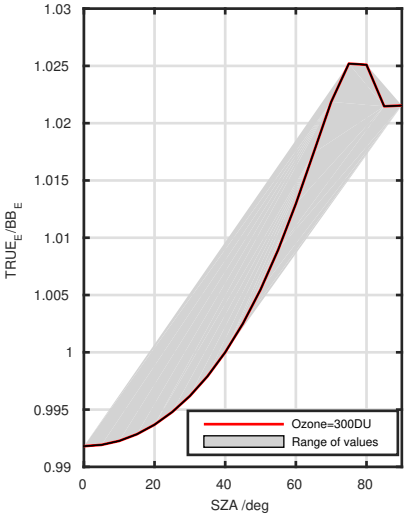

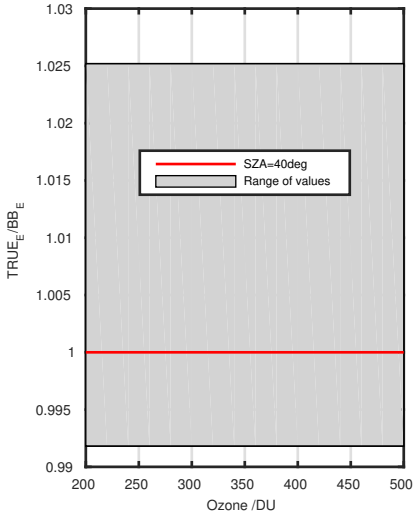

Calibration Results of SCI00400 (UVA)

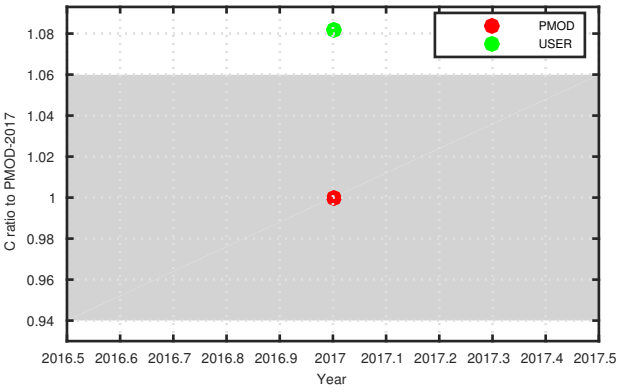

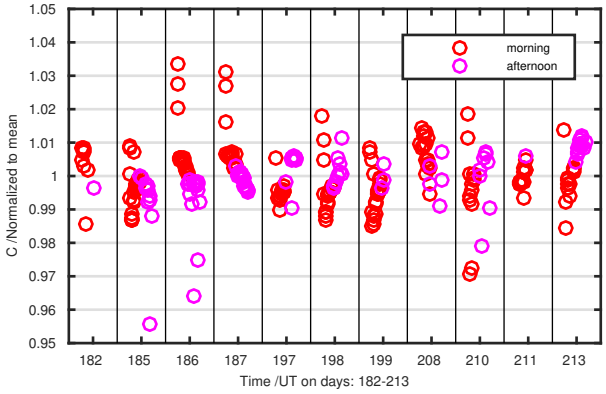

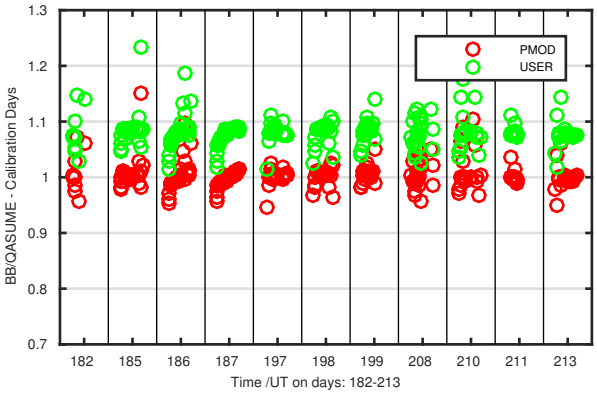

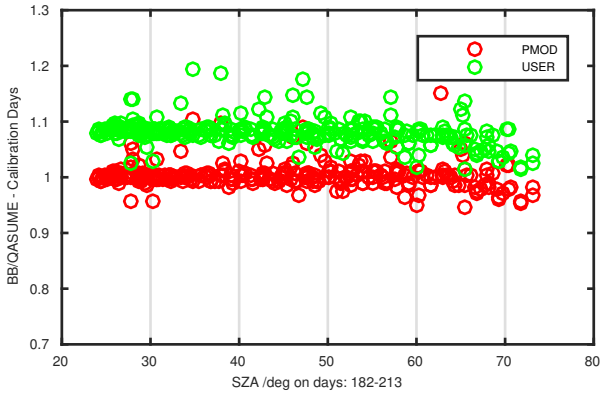

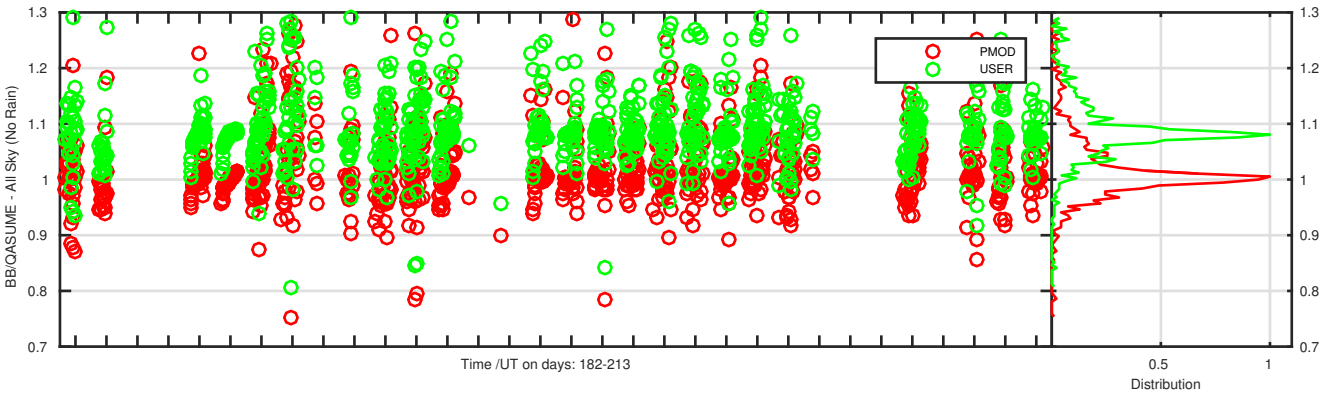

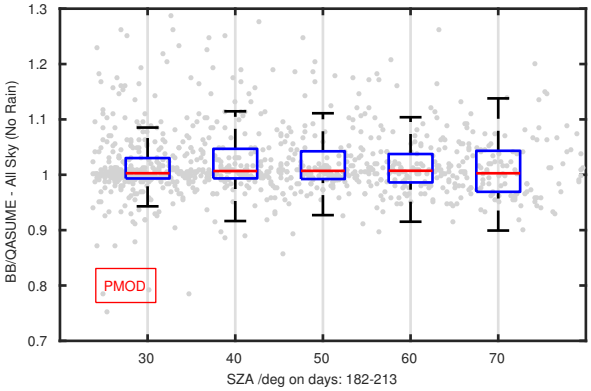

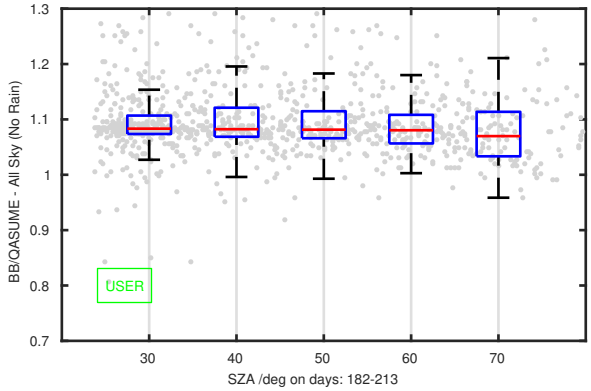

Calibration Results of SCI00400 (UVE)

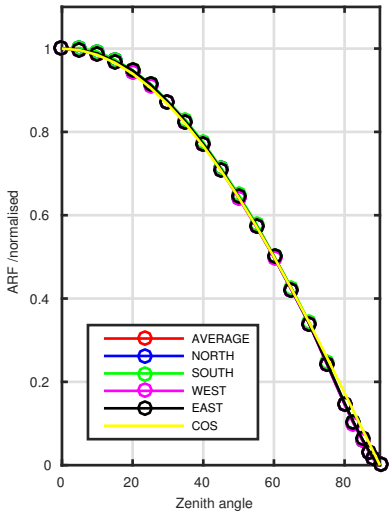

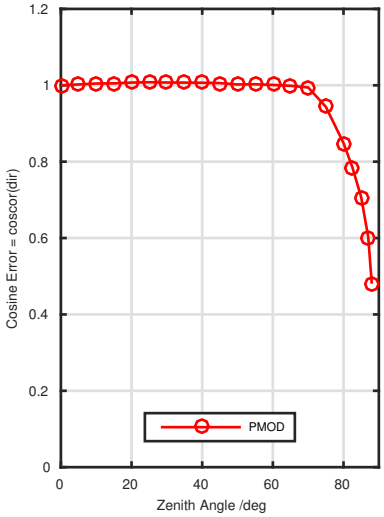

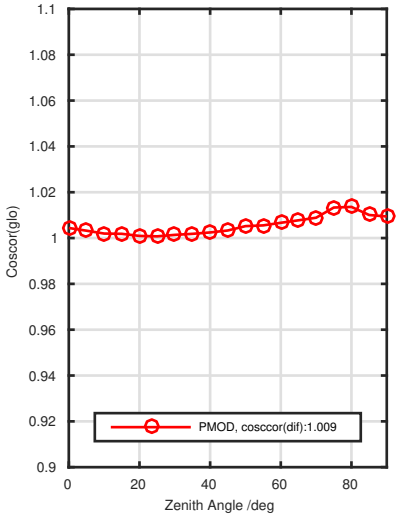

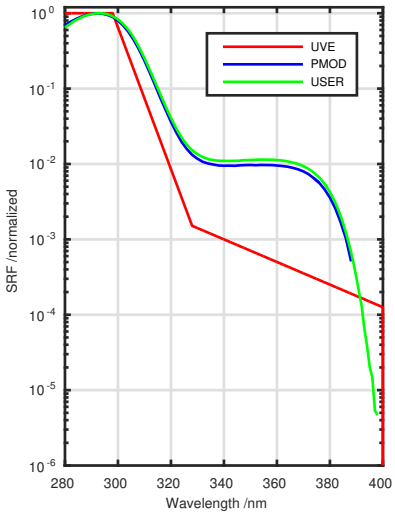

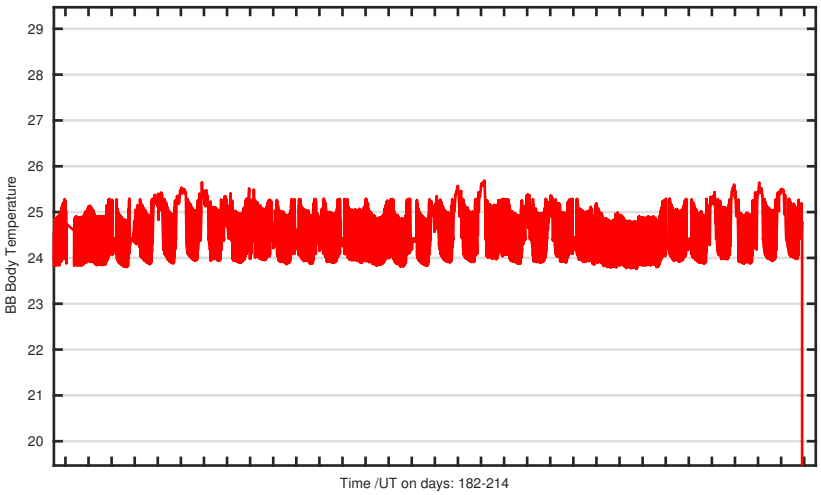

Calibration Matrix fn; Model sdisortREFms2009; f0=0.2352

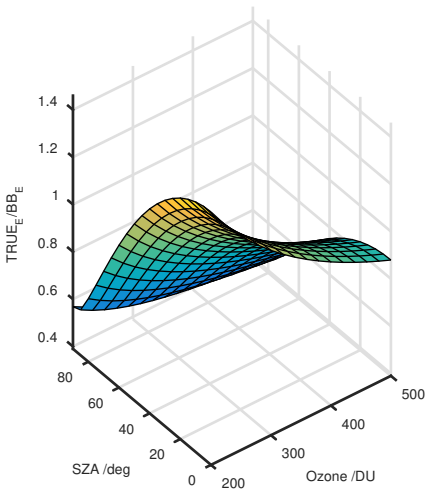

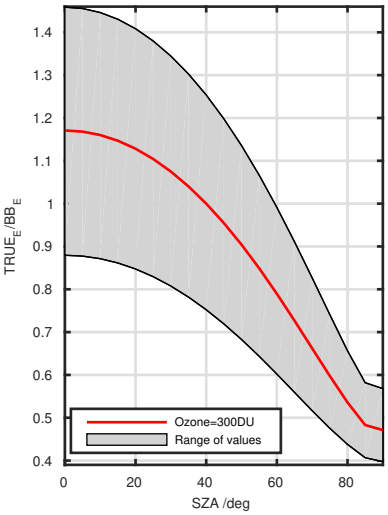

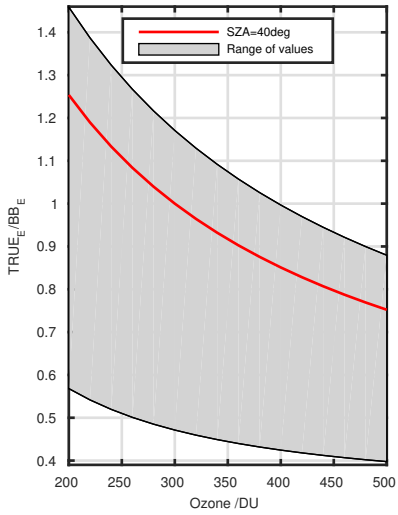

Calibration Results of SCI00400 (UVE)

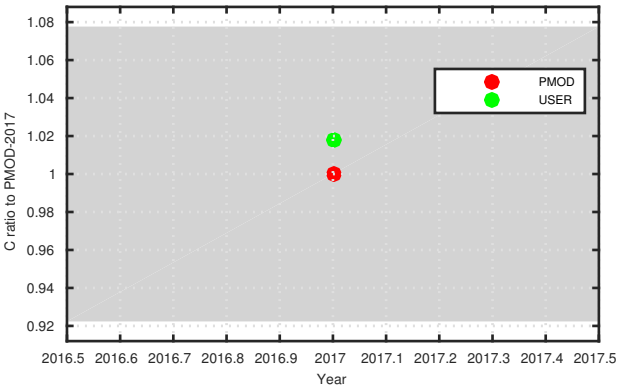

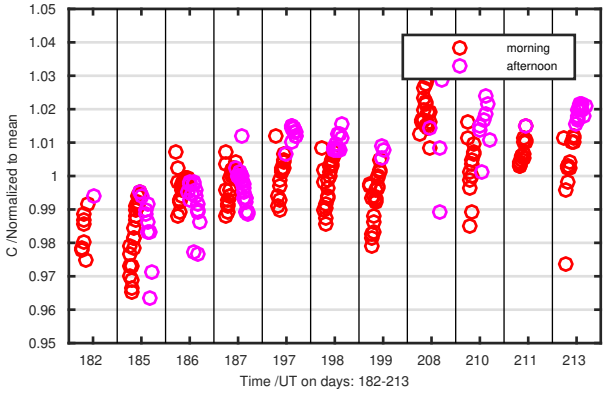

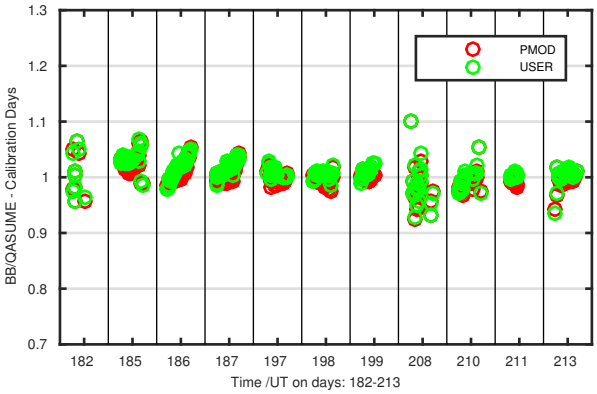

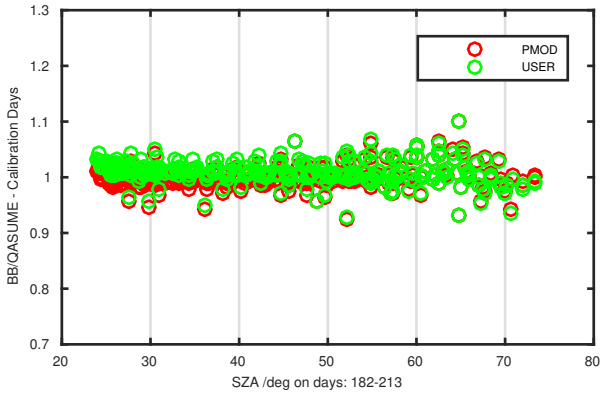

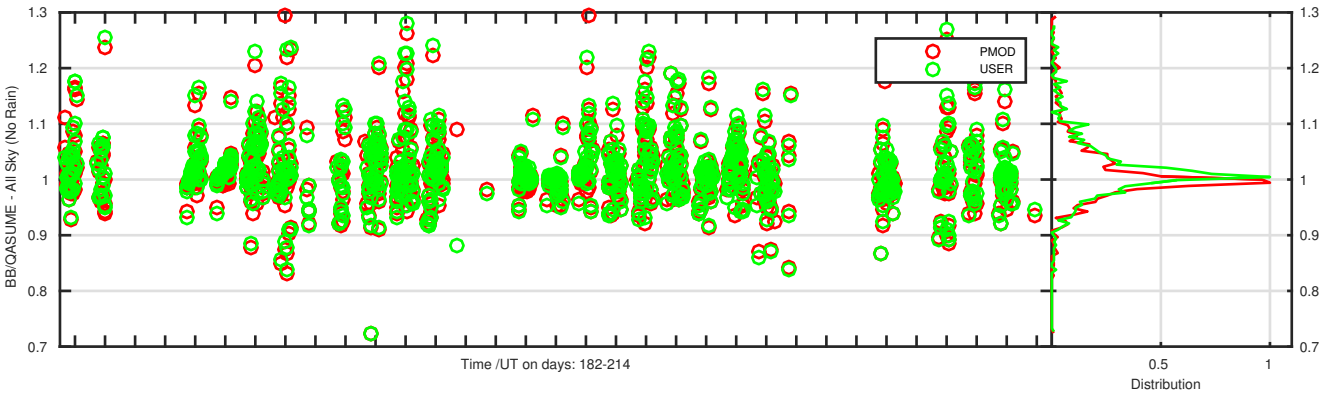

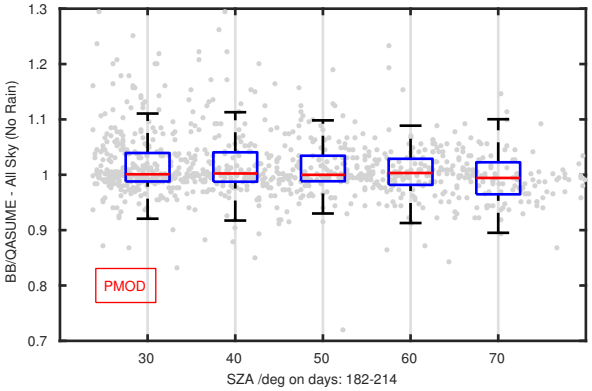

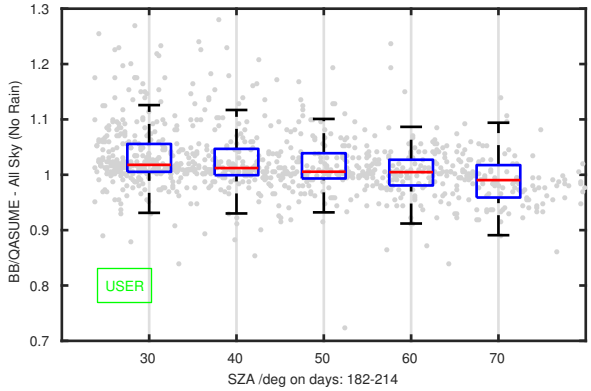

Calibration Results of SCI00407 (UVE)

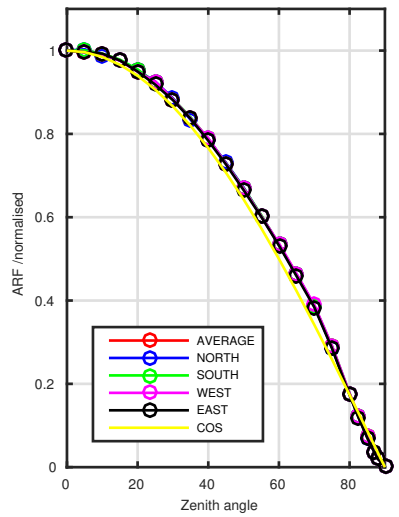

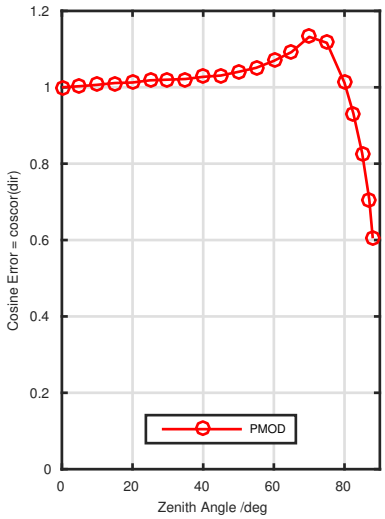

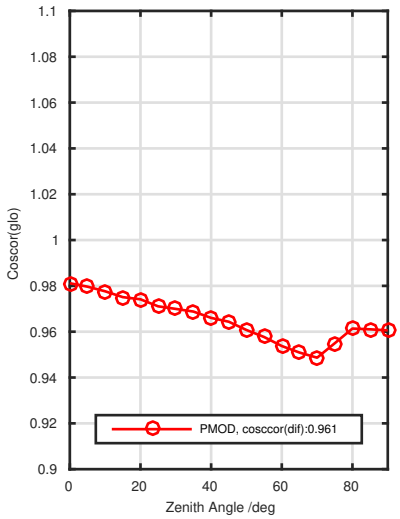

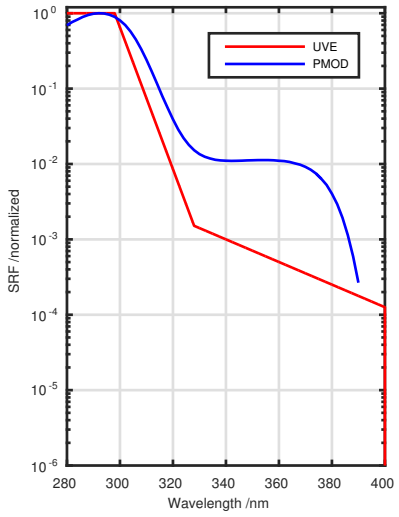

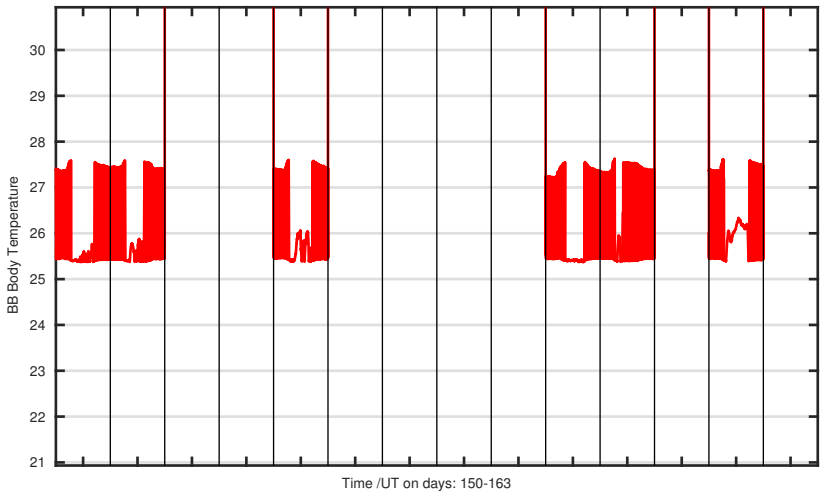

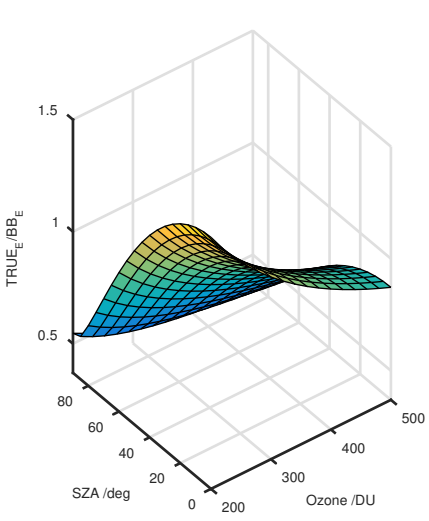

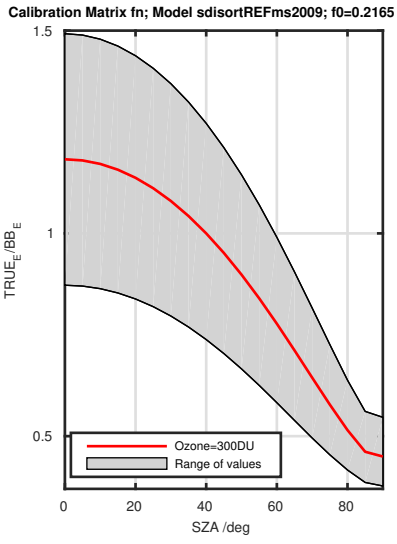

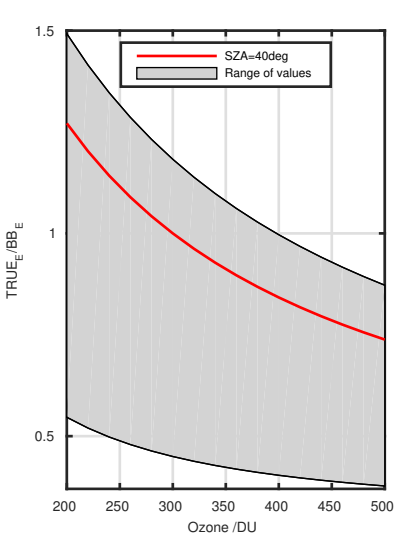

Calibration Results of SCI00407 (UVE)

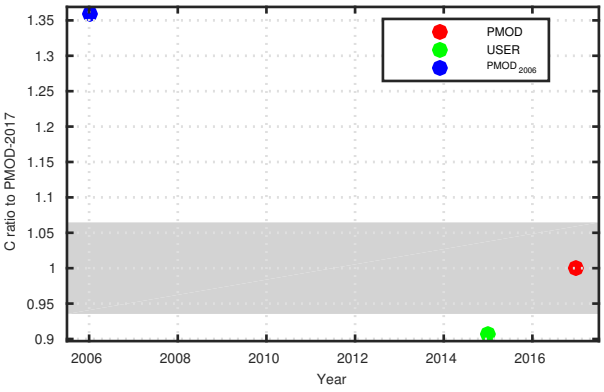

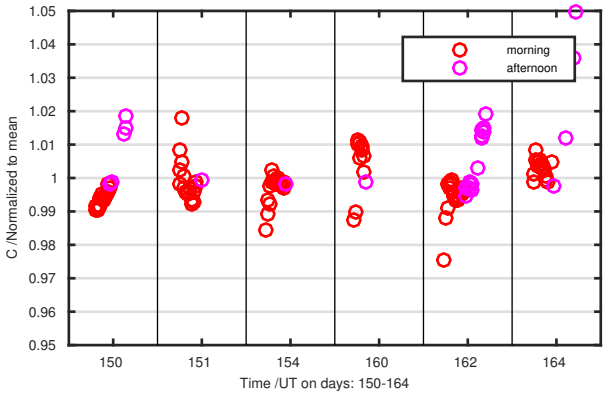

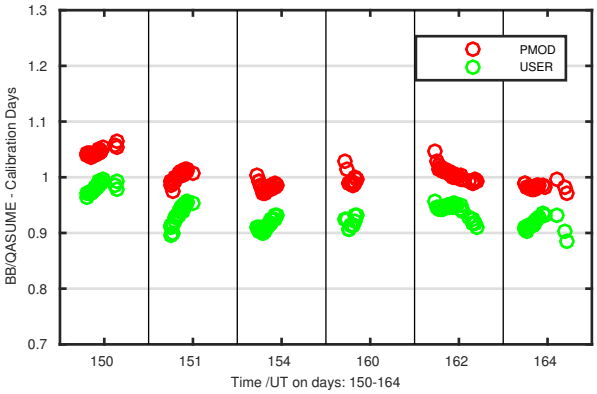

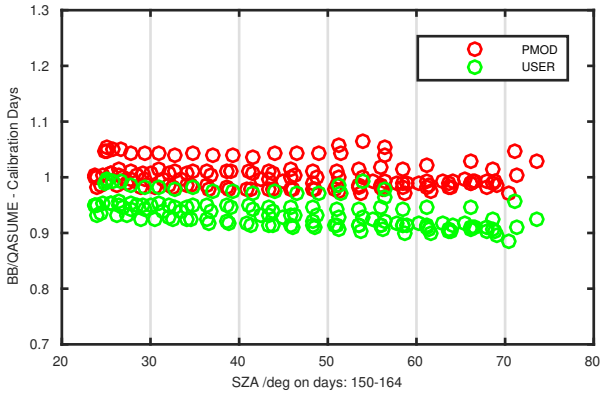

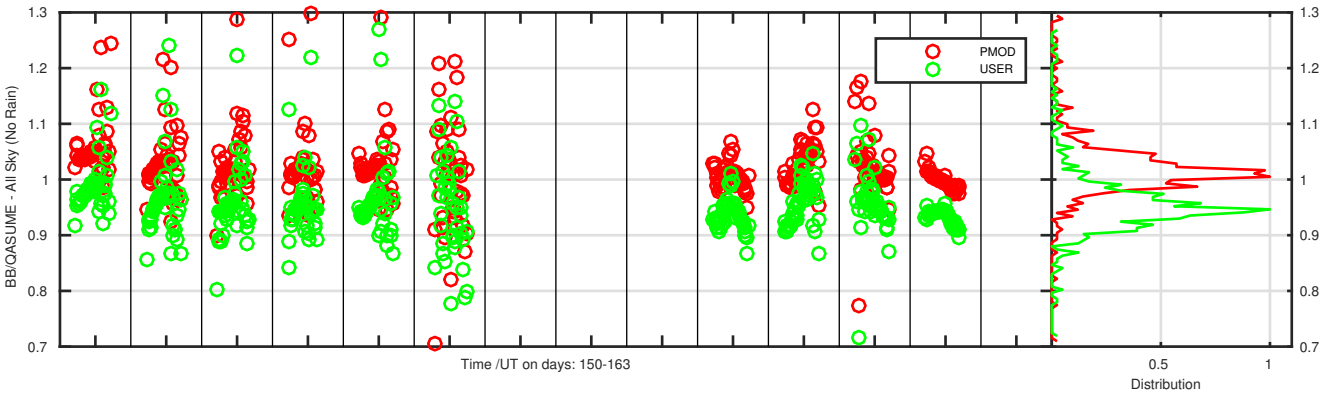

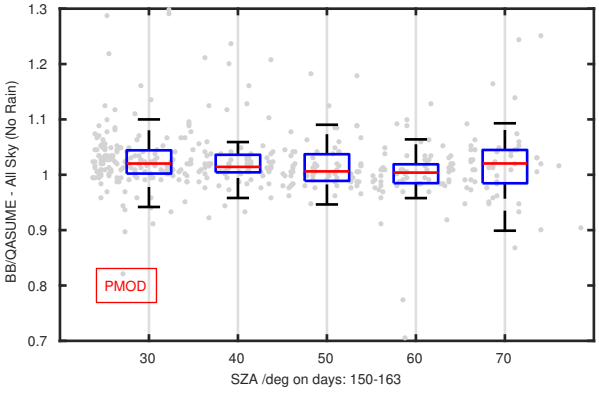

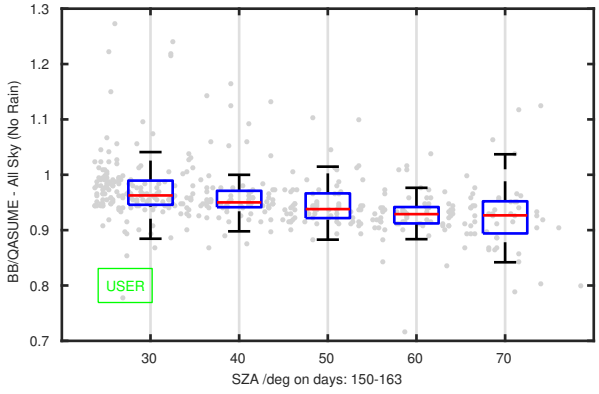

Calibration Results of SL1453 (UVE)

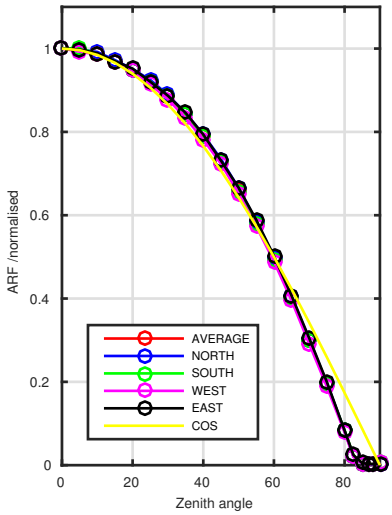

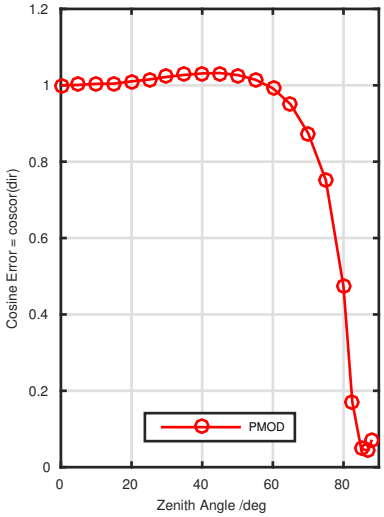

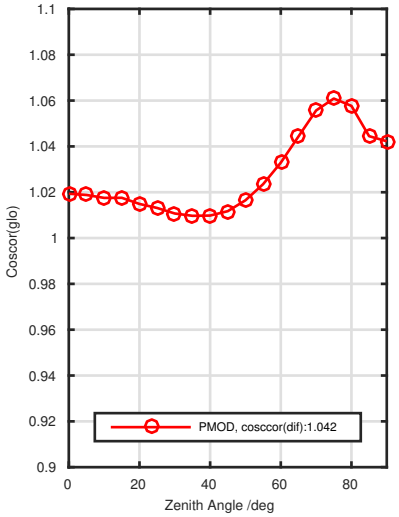

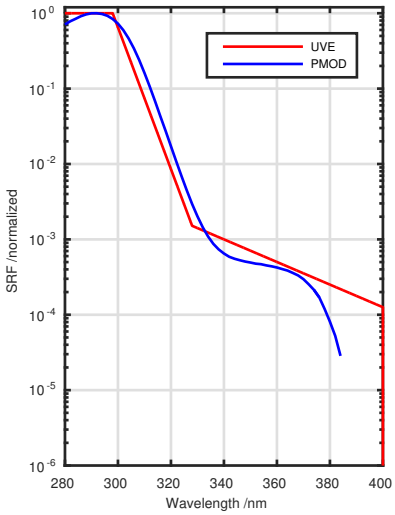

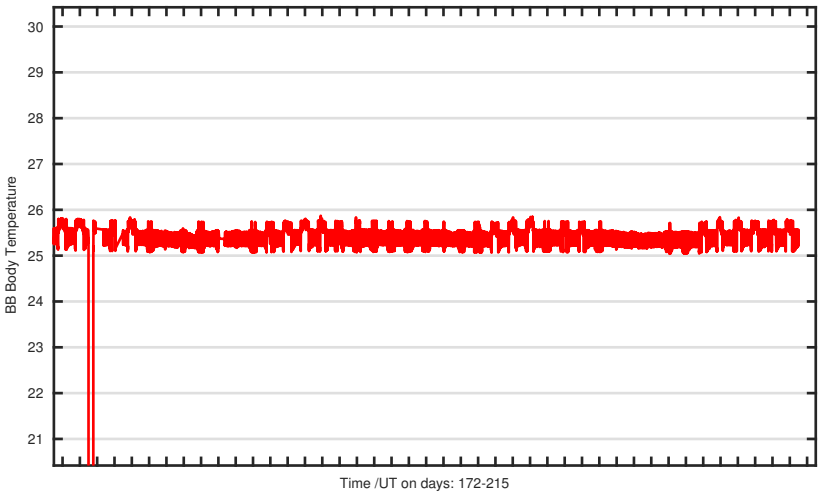

Calibration Matrix fn; Model sdisortREFms2009; f0=0.5634

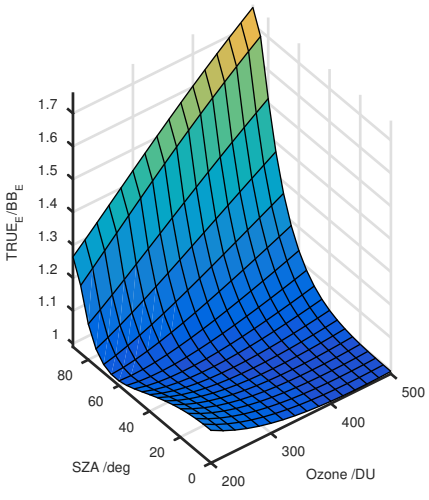

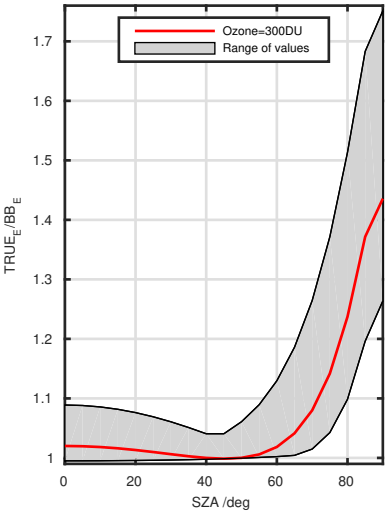

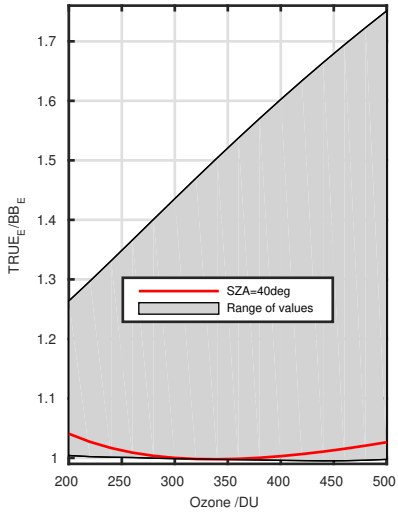

Calibration Results of SL1453 (UVE)

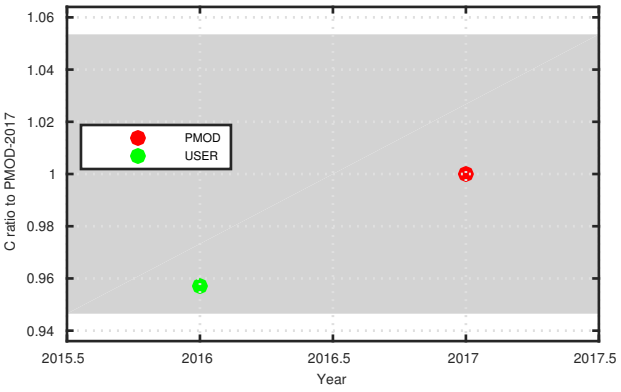

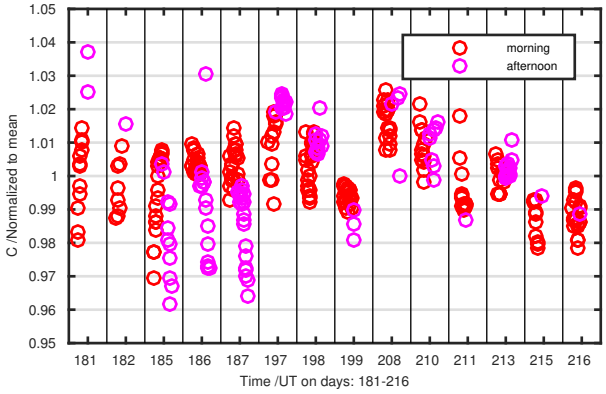

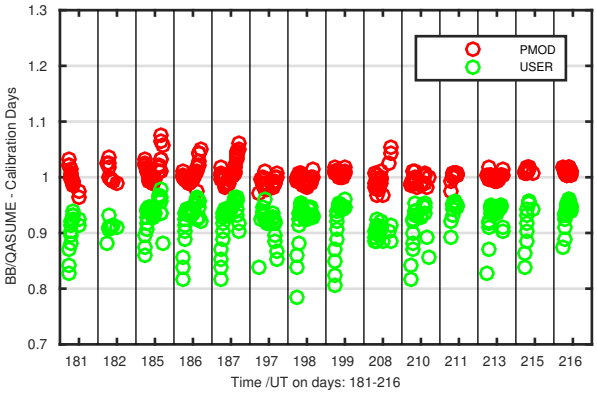

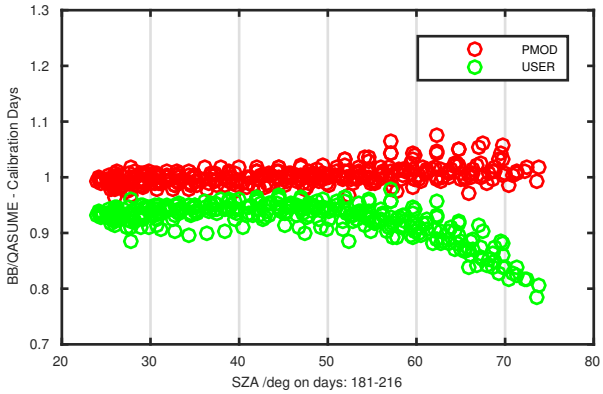

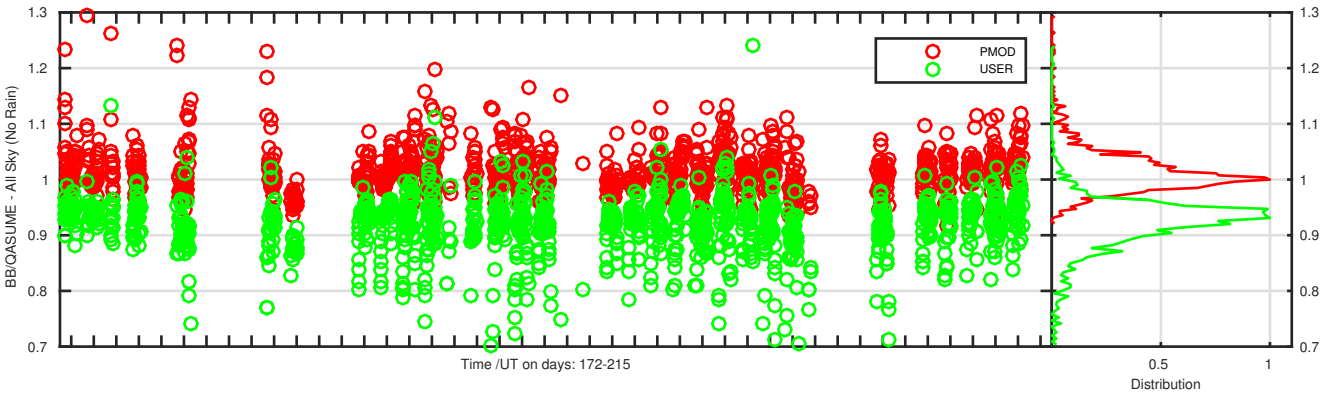

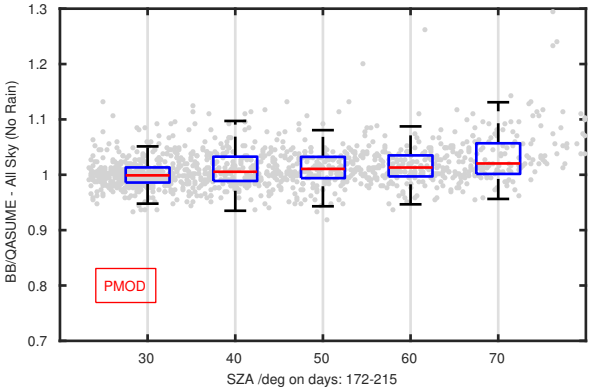

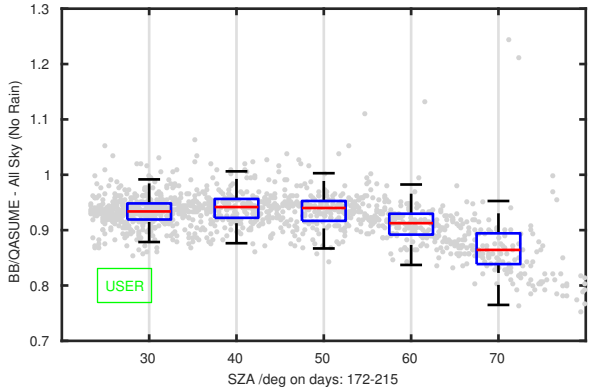

Calibration Results of SL1492 (UVE)

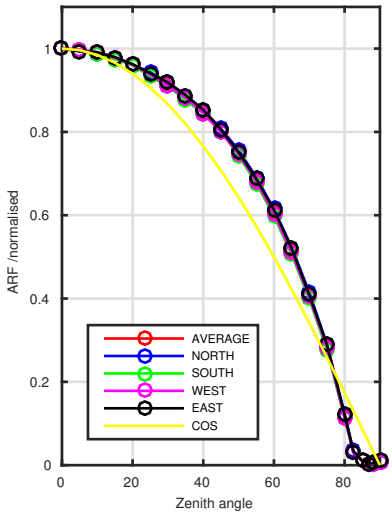

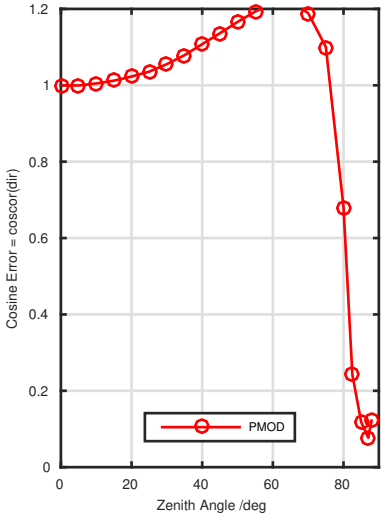

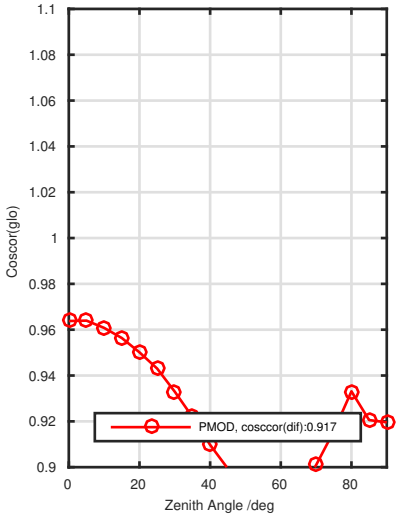

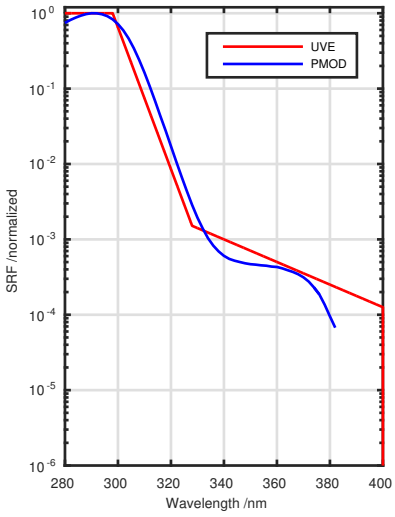

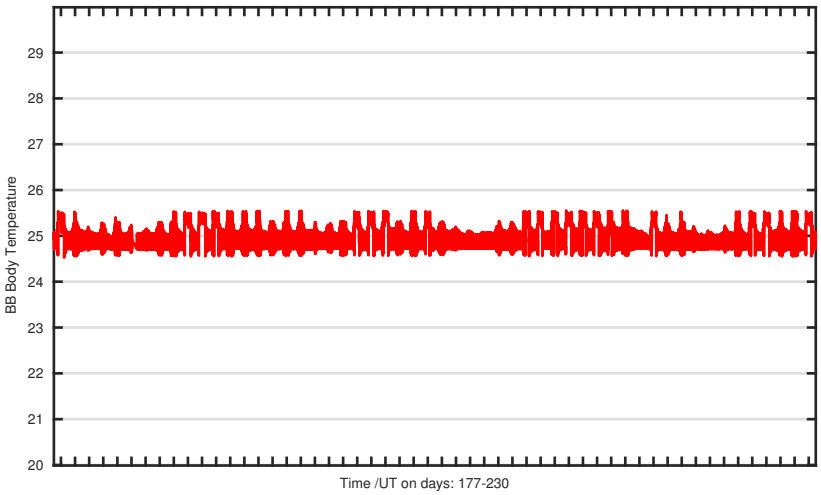

Calibration Matrix fn; Model sdisortPMODmsO3; f0=0.5635

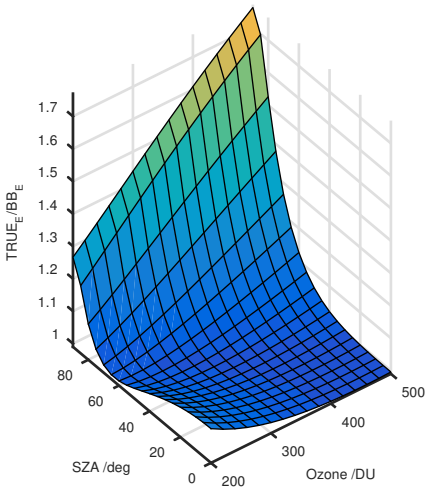

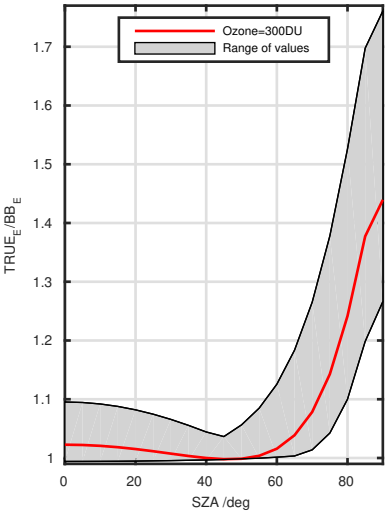

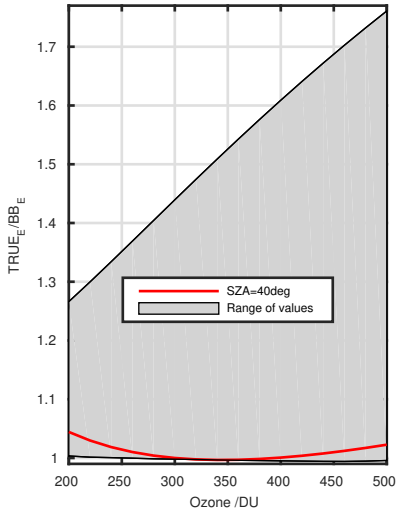

Calibration Results of SL1492 (UVE)

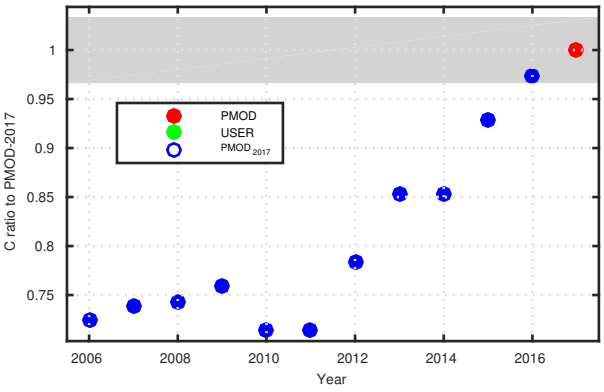

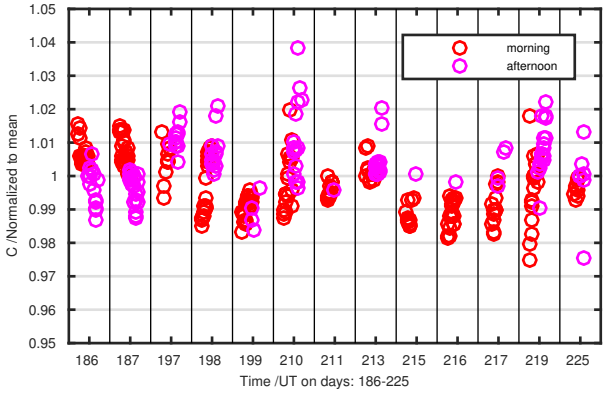

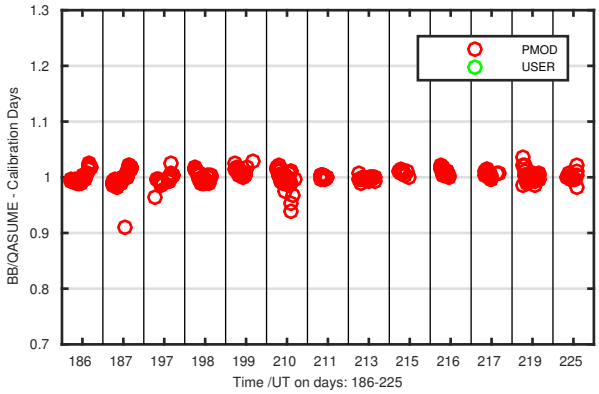

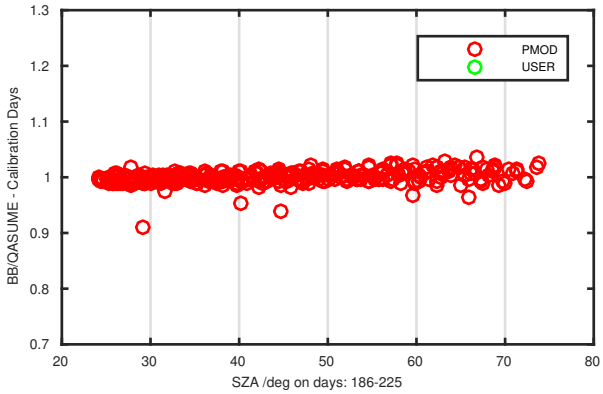

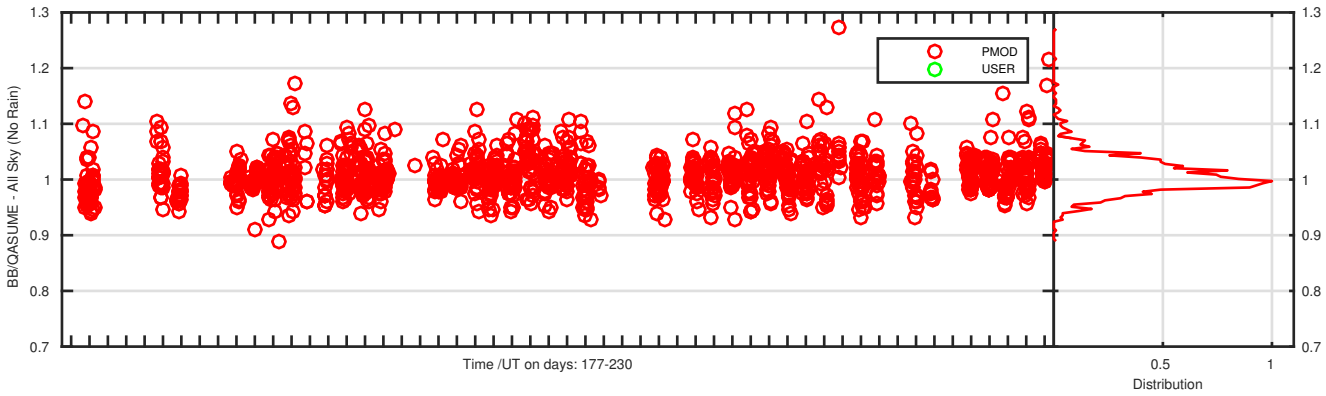

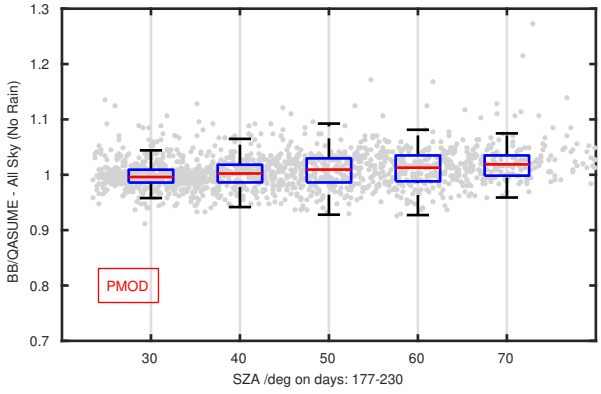

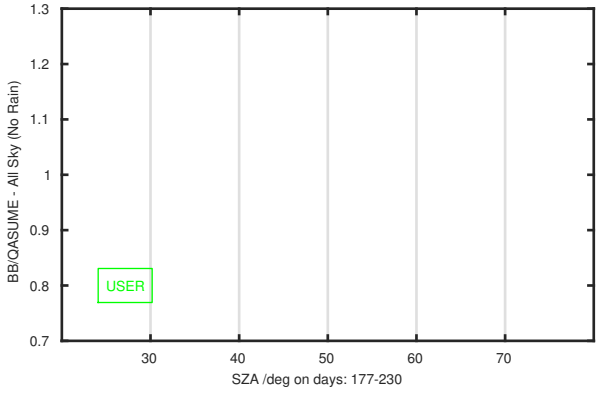

Calibration Results of SL1493 (UVE)

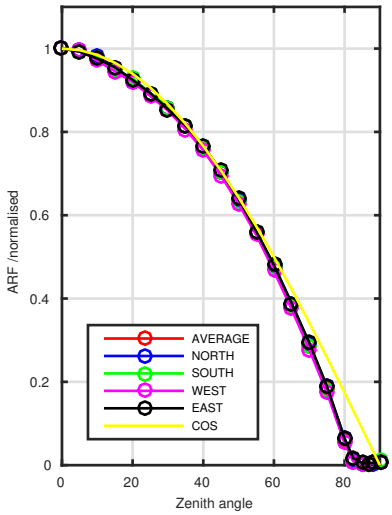

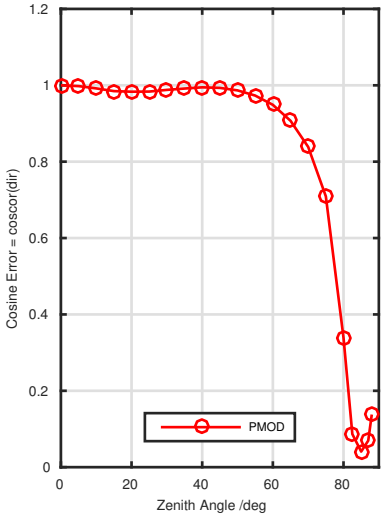

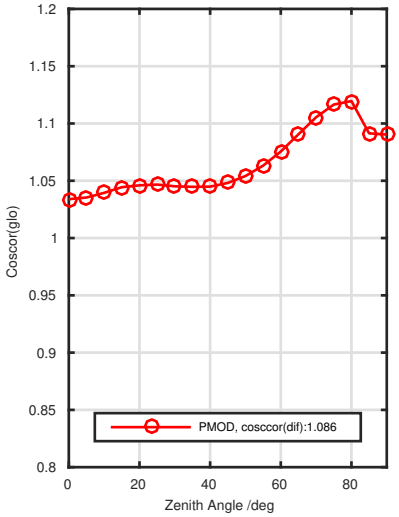

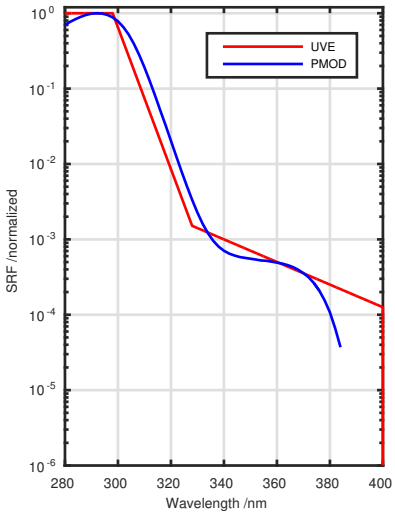

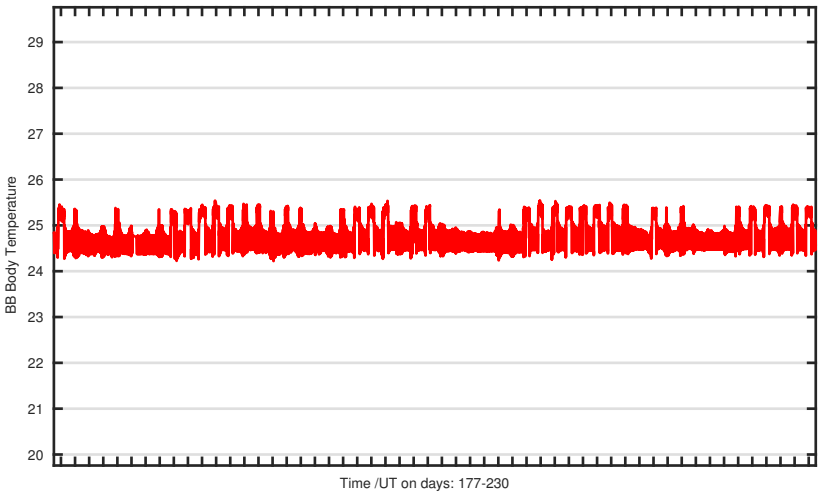

Calibration Matrix fn; Model sdisortPMODmsO3; f0=0.4860

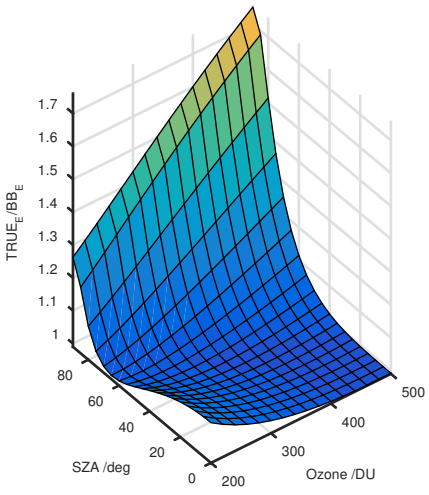

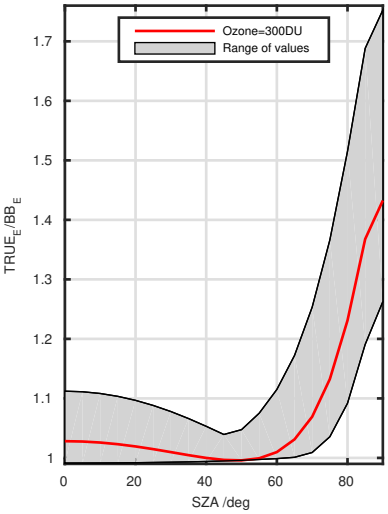

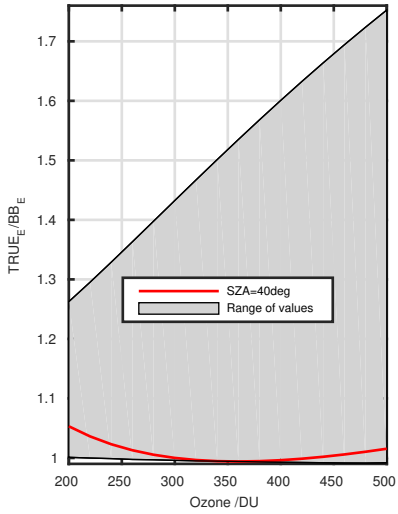

Calibration Results of SL1493 (UVE)

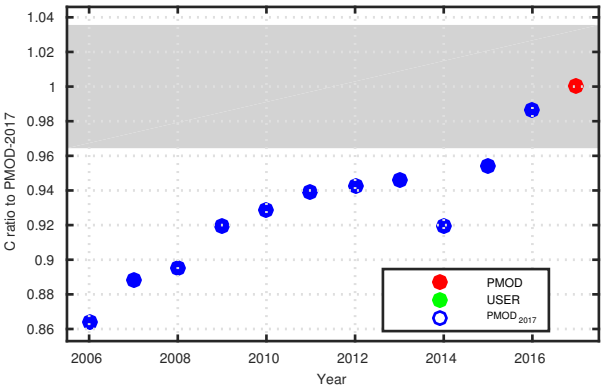

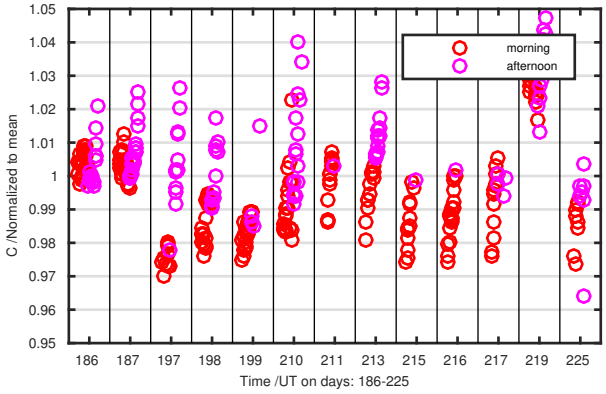

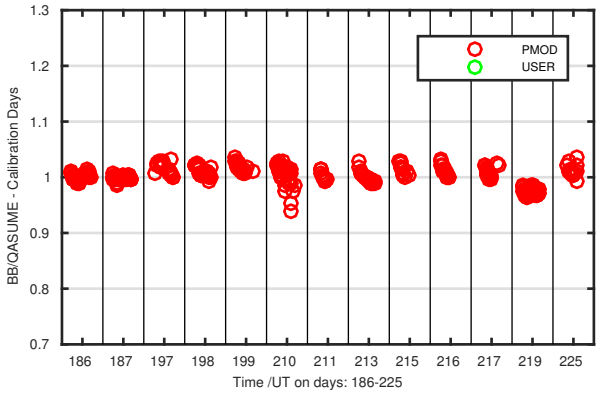

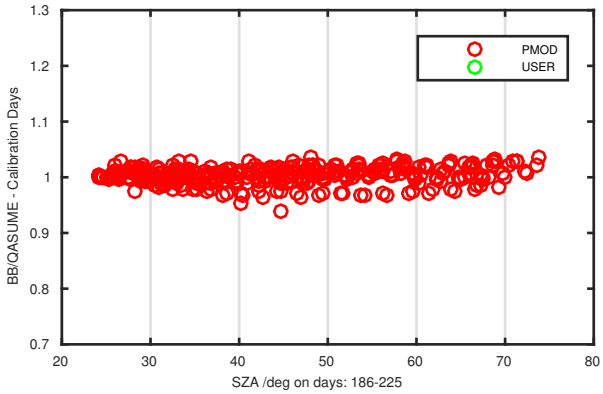

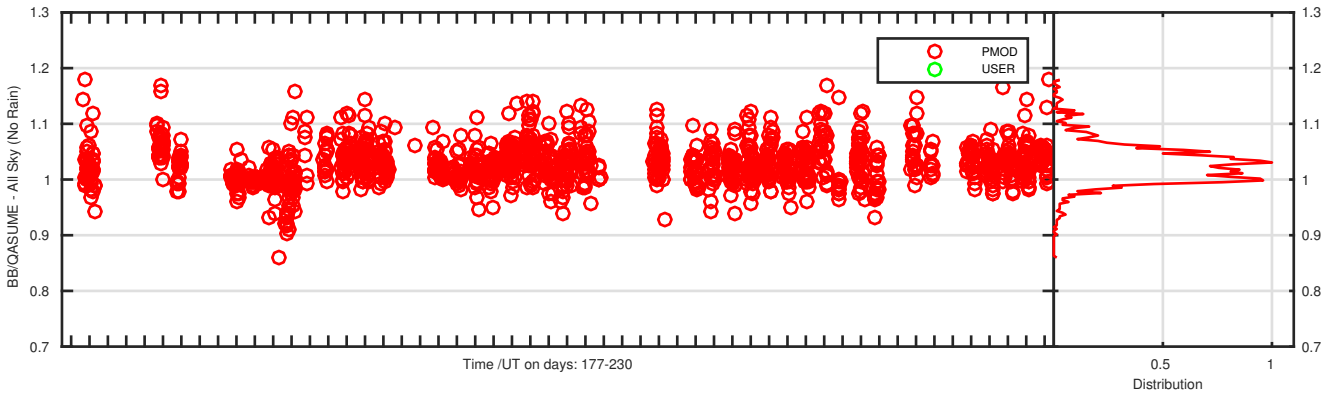

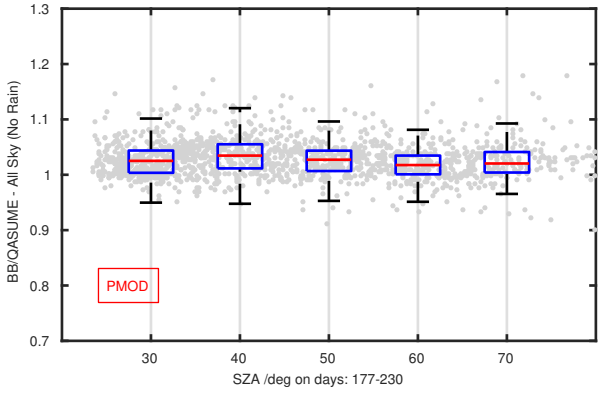

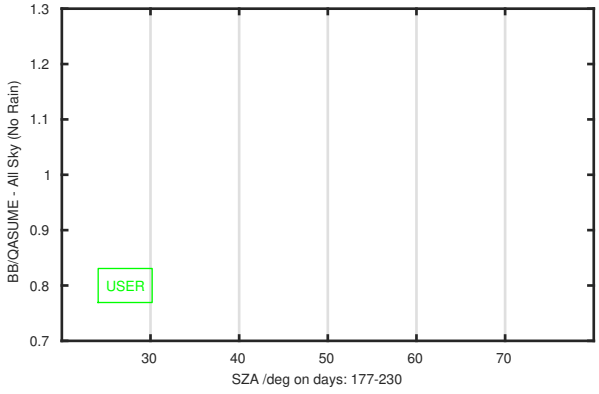

Calibration Results of SL1890 (UVE)

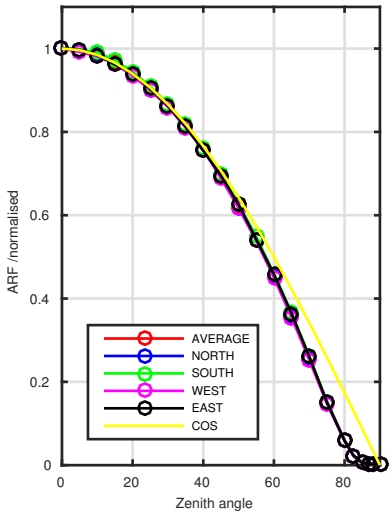

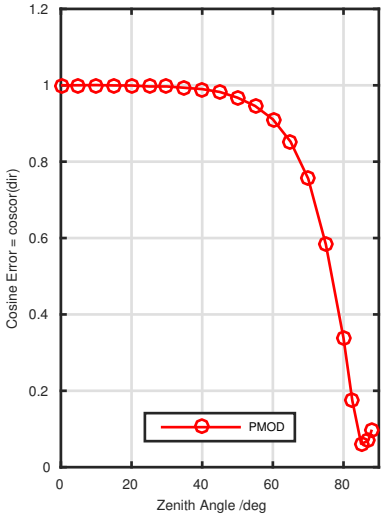

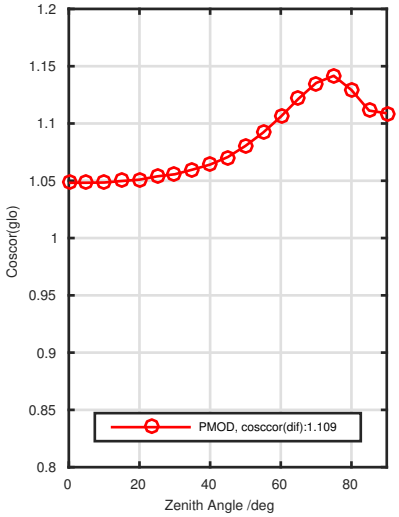

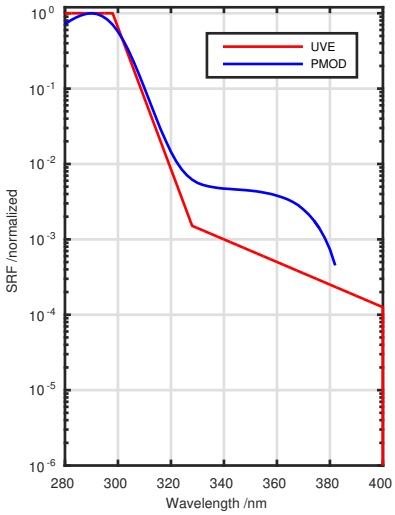

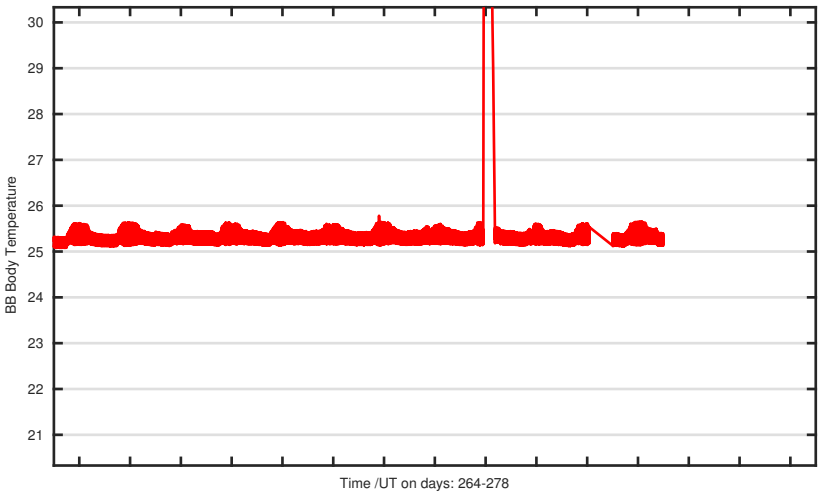

Calibration Matrix fn; Model sdisortREFms2009; f0=0.5373

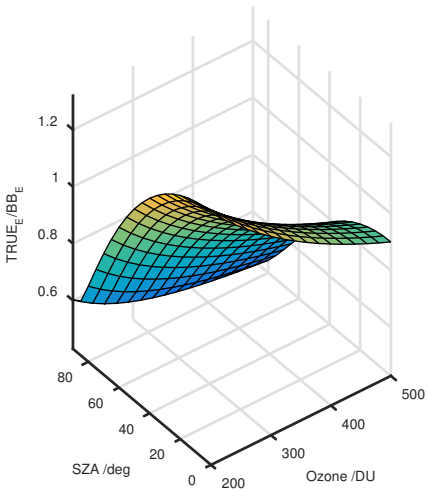

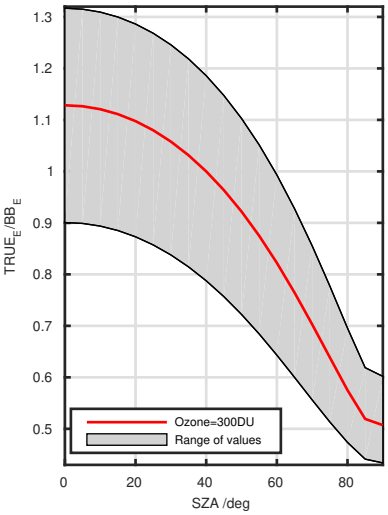

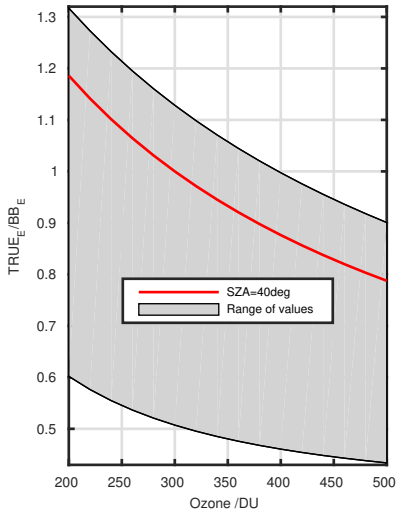

Calibration Results of SL1890 (UVE)

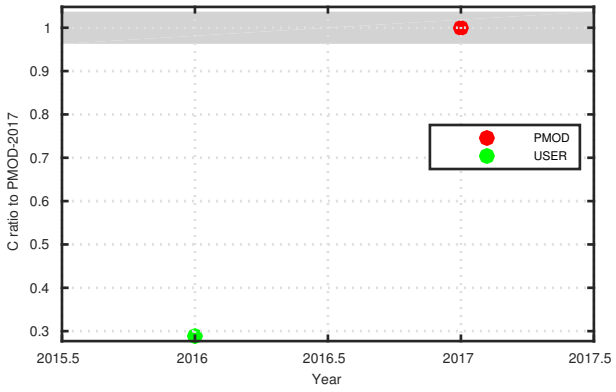

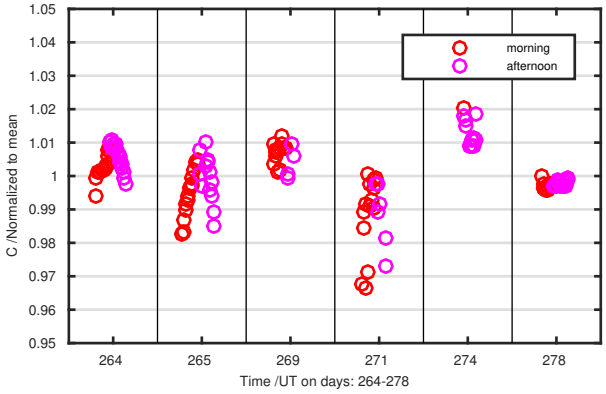

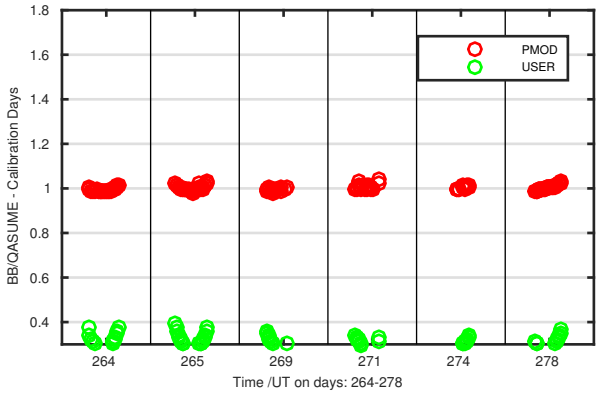

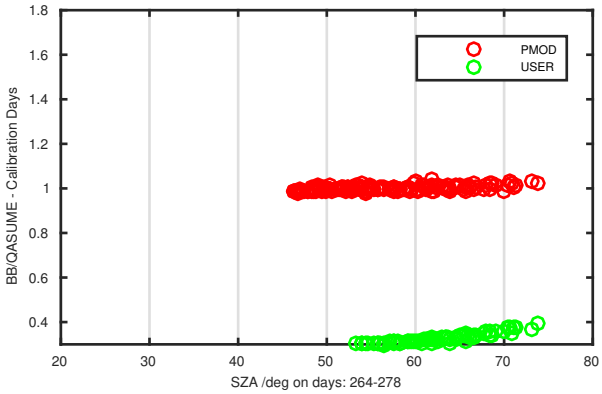

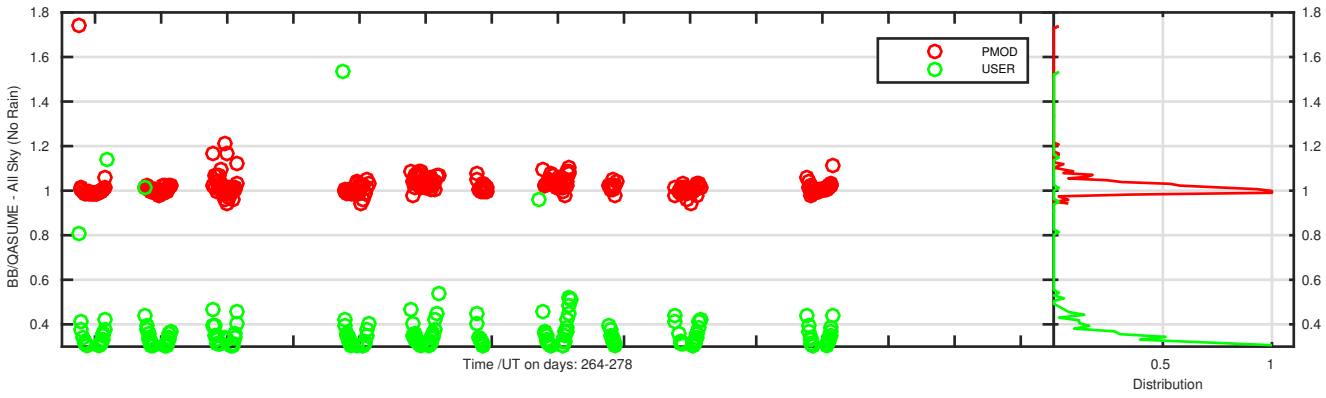

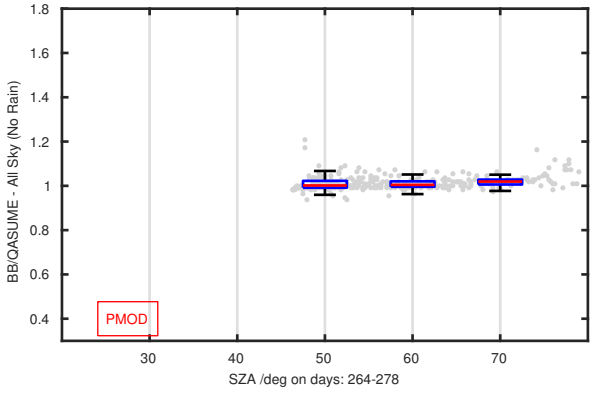

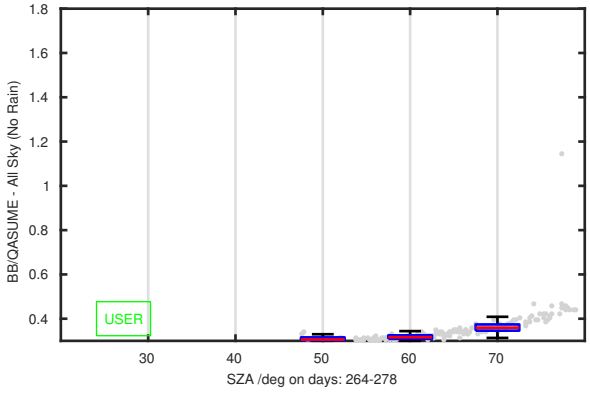

Calibration Results of SL1903 (UVE)

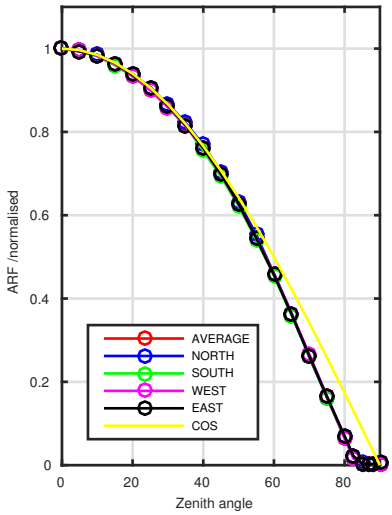

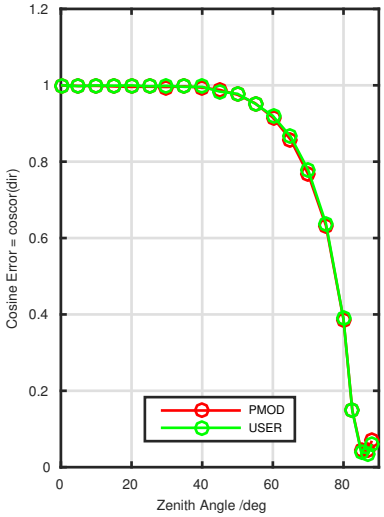

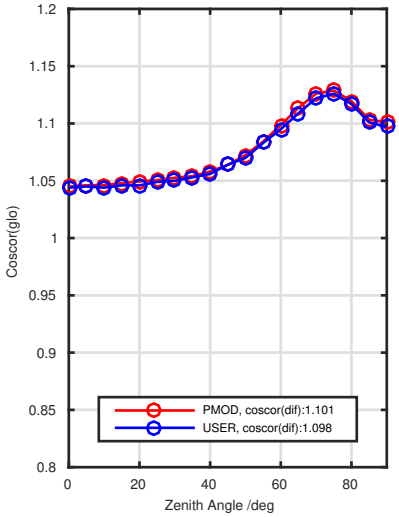

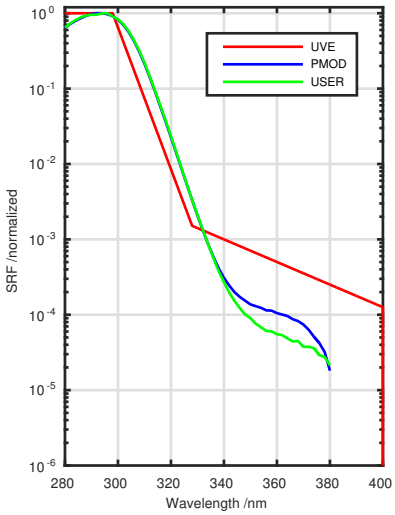

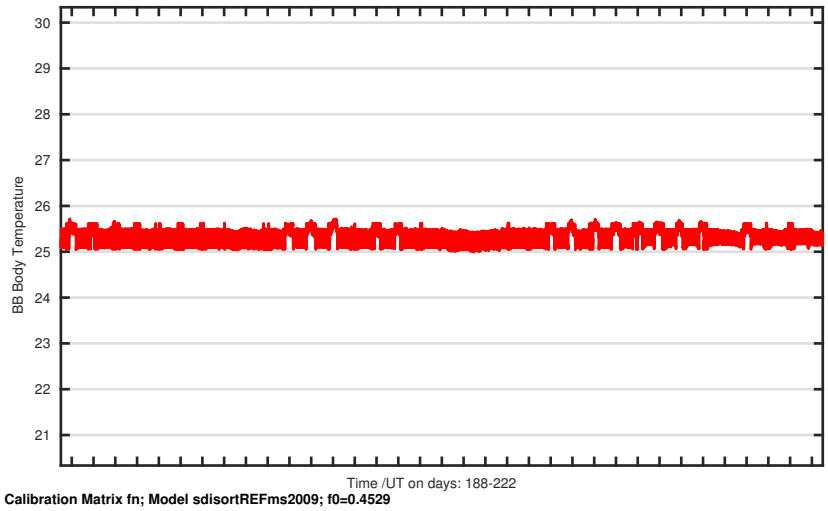

Calibration Matrix fn; Model sdisortREFms2009; f0=0.4529

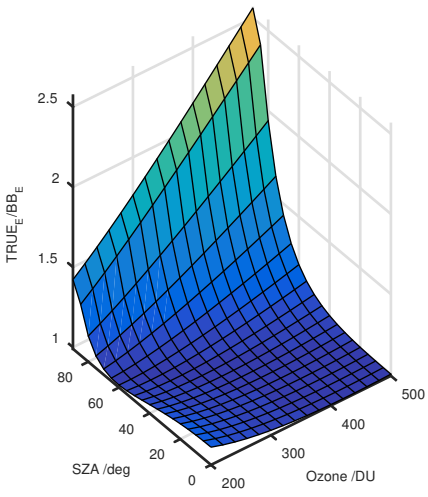

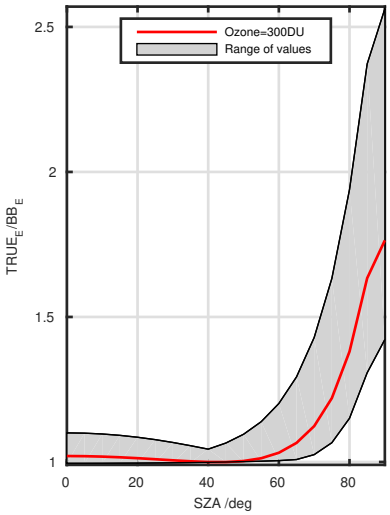

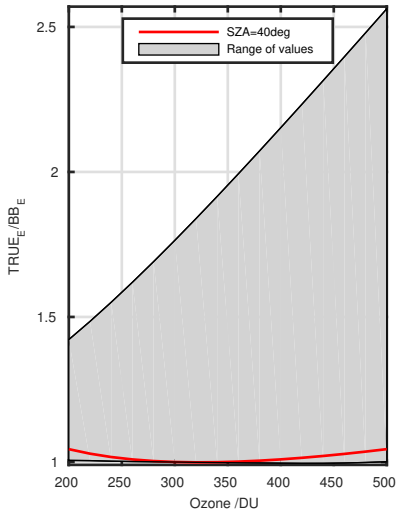

Calibration Results of SL1903 (UVE)

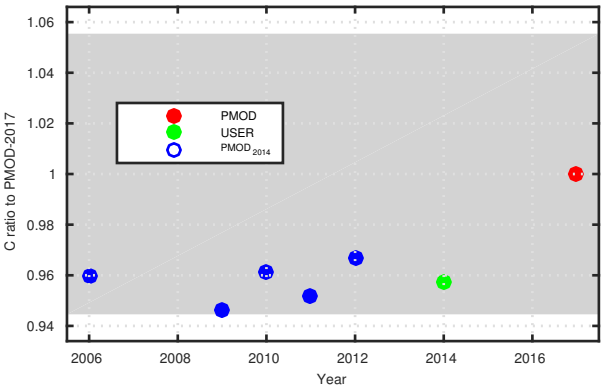

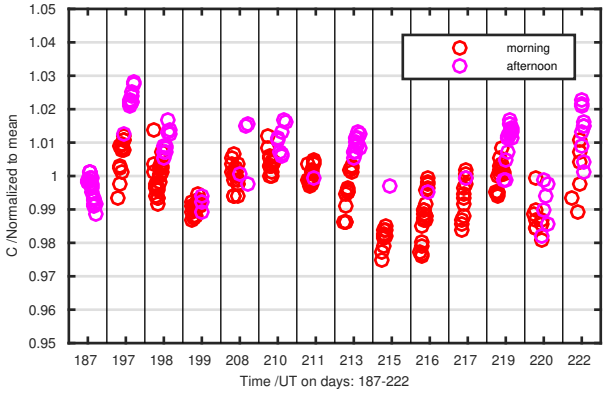

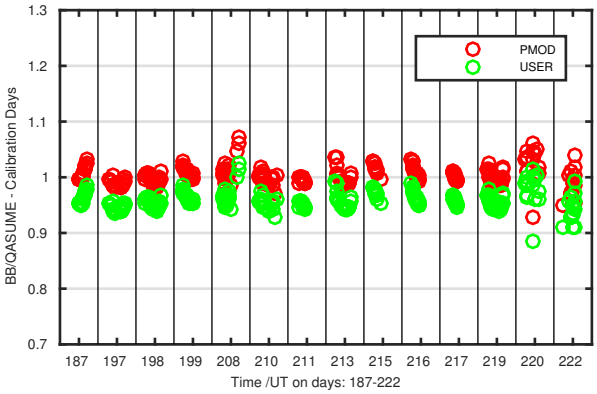

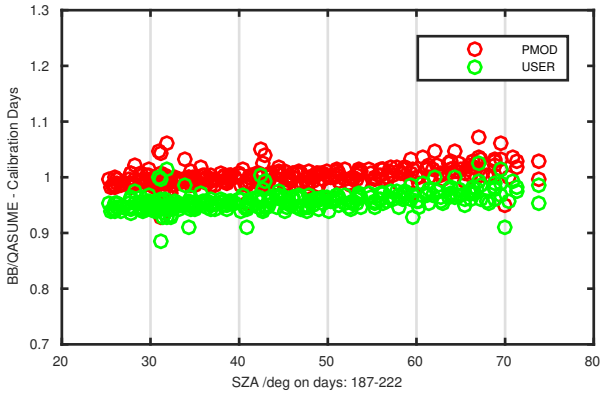

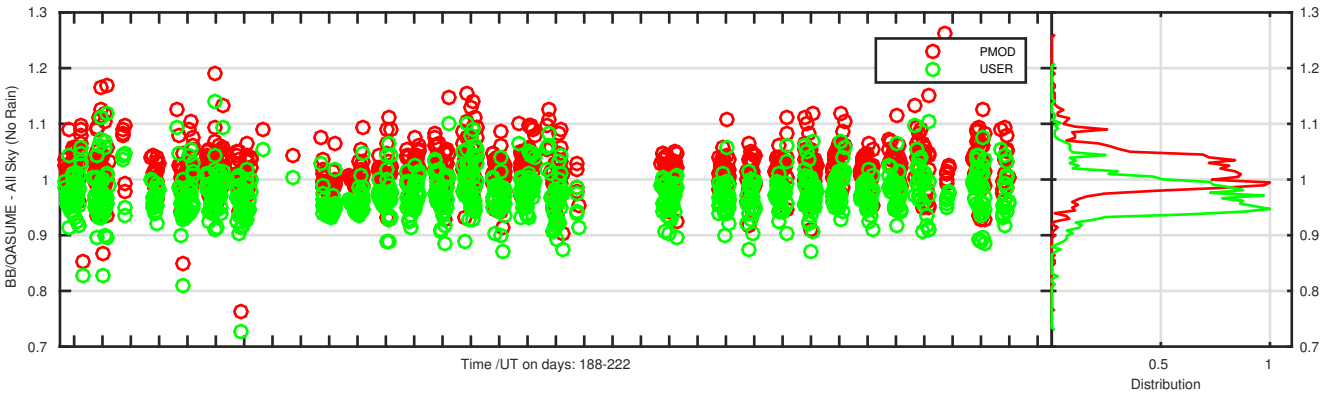

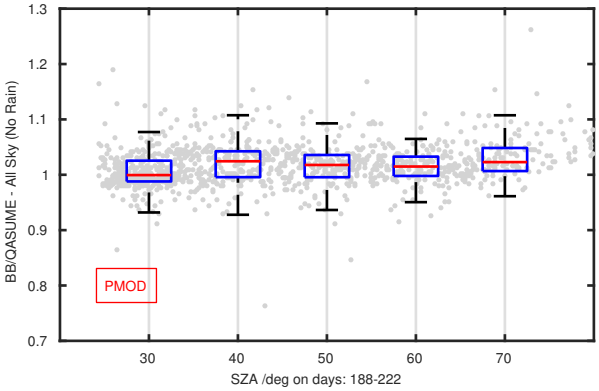

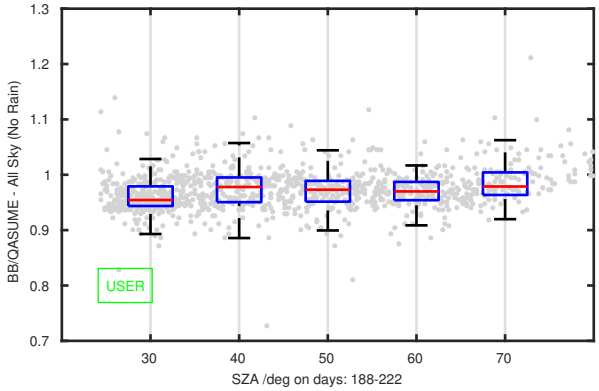

Calibration Results of SL2875 (UVA)

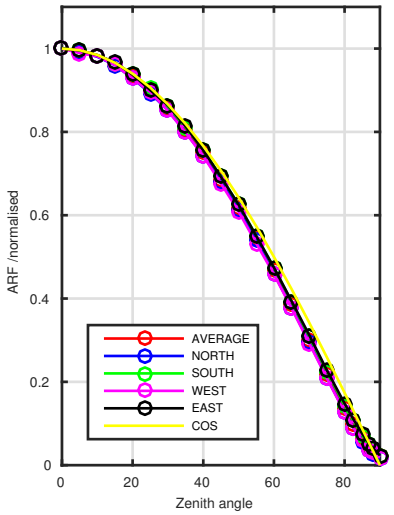

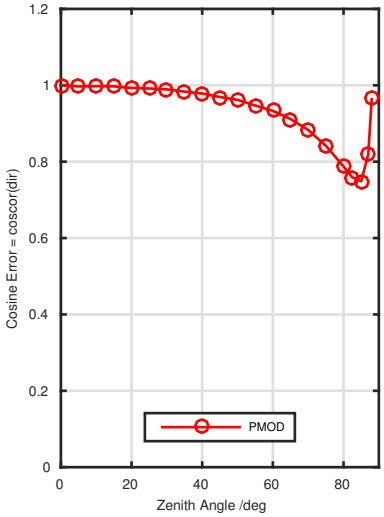

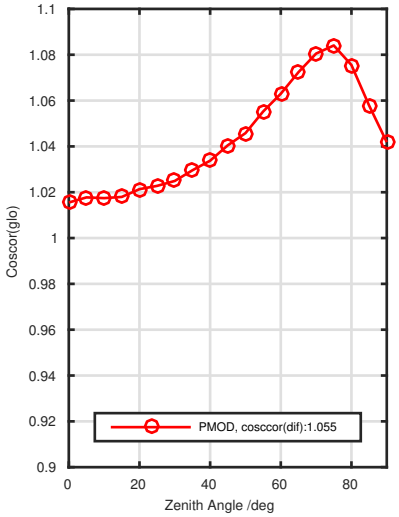

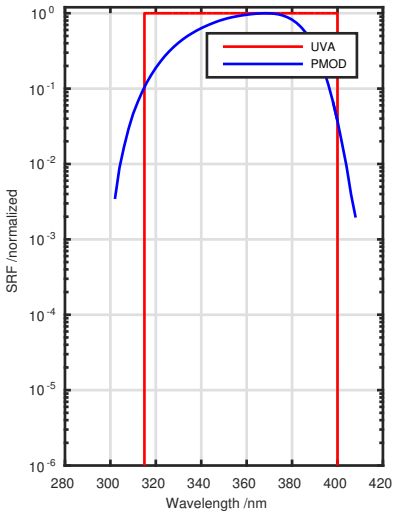

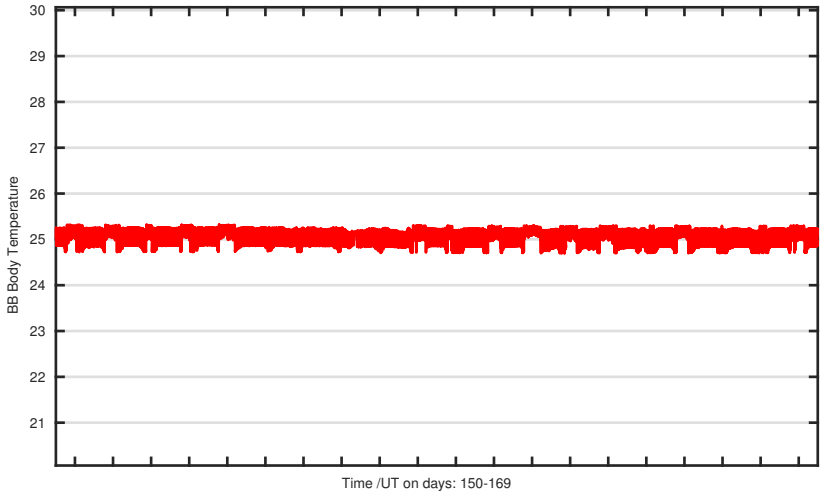

Calibration Matrix fn; Model sdisortPMODmsO3; f0=1.5578

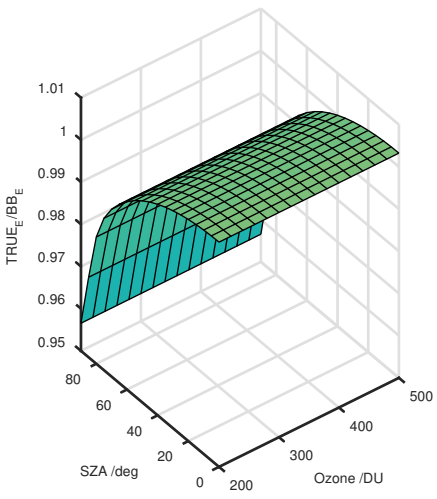

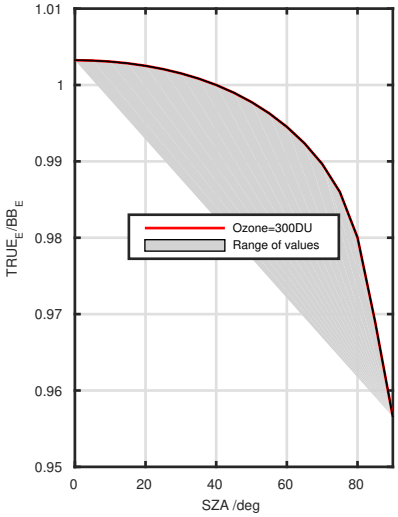

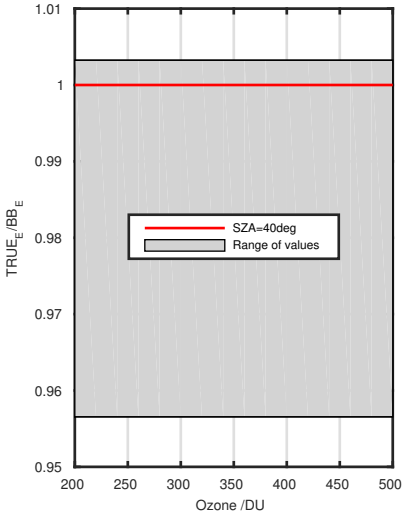

Calibration Results of SL2875 (UVA)

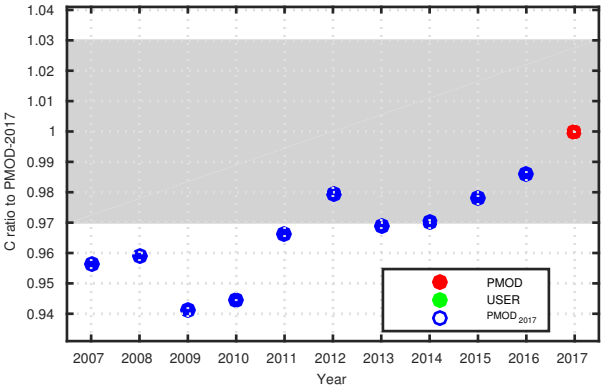

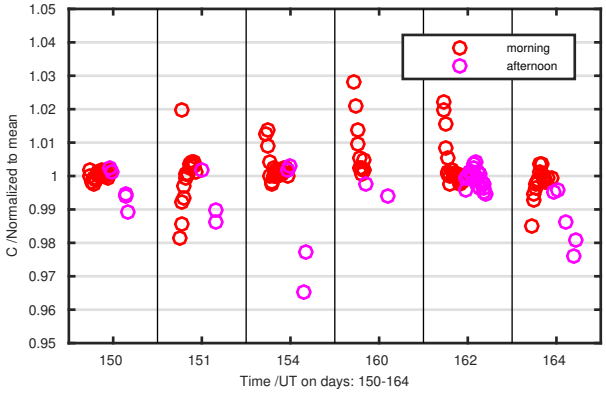

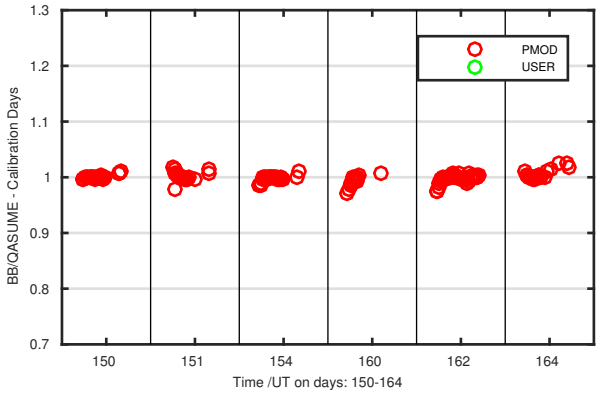

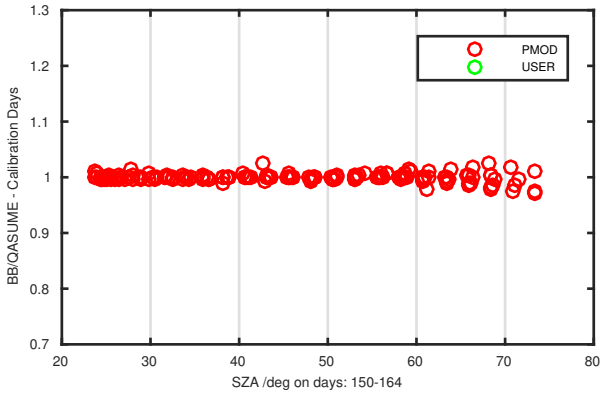

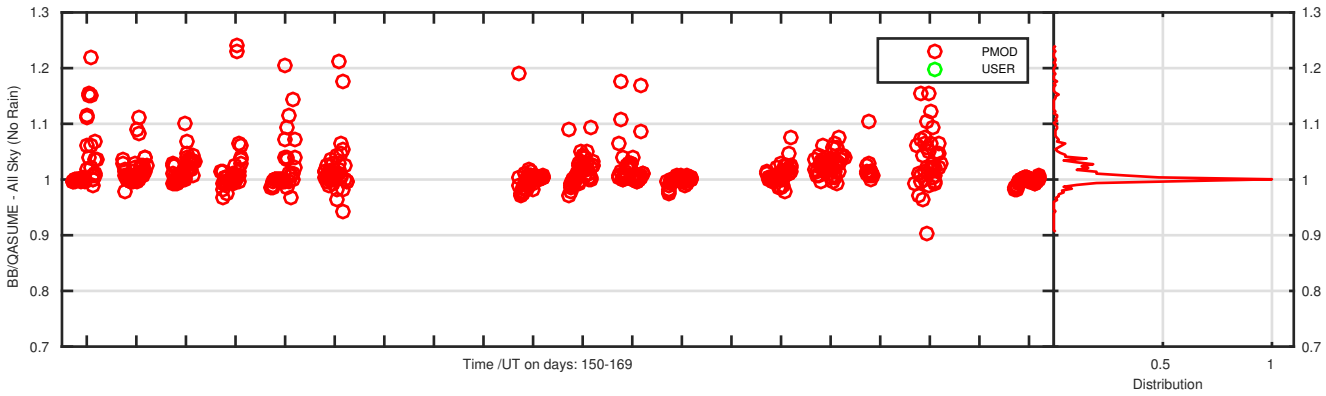

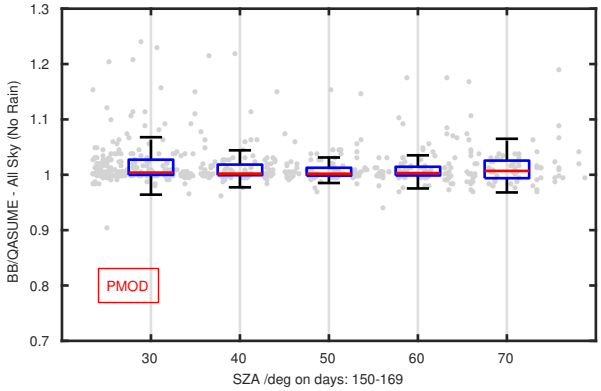

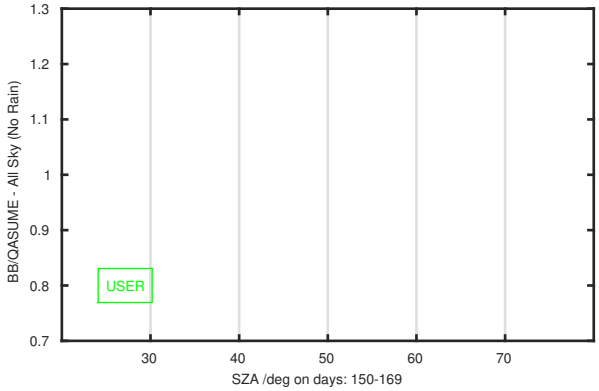

Calibration Results of SL2839 (UVE)

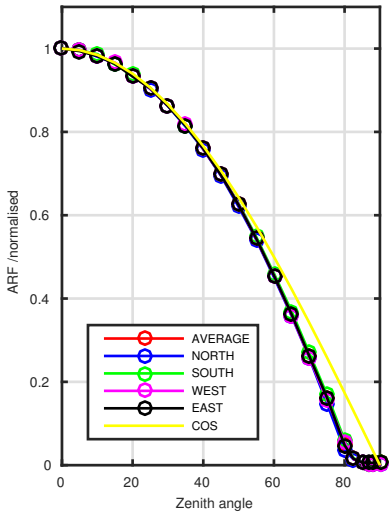

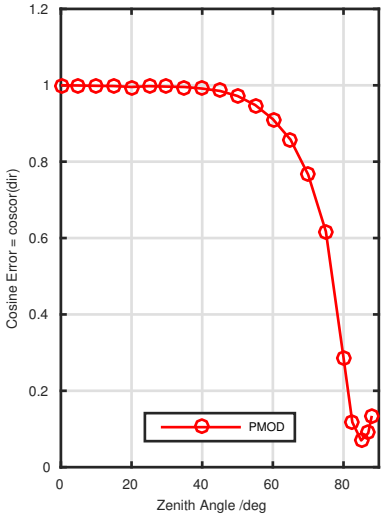

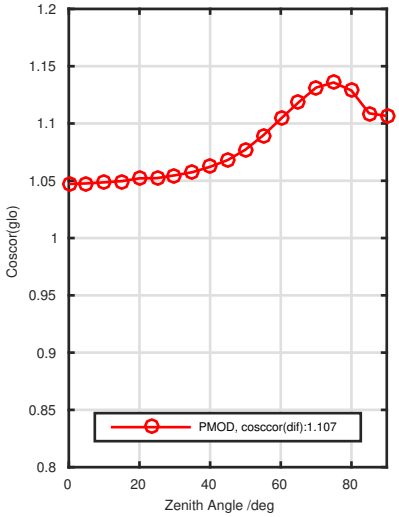

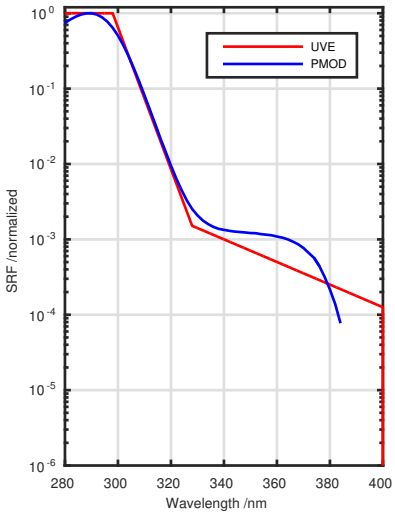

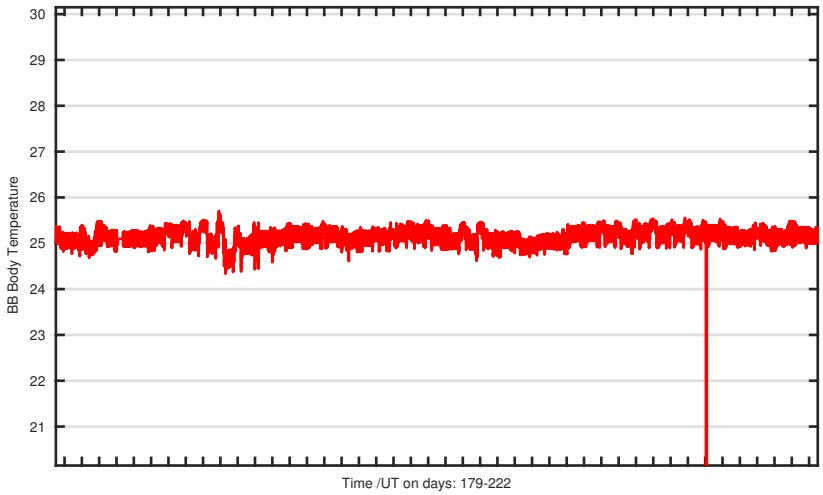

Calibration Matrix fn; Model sdisortREFms2009; f0=0.8984

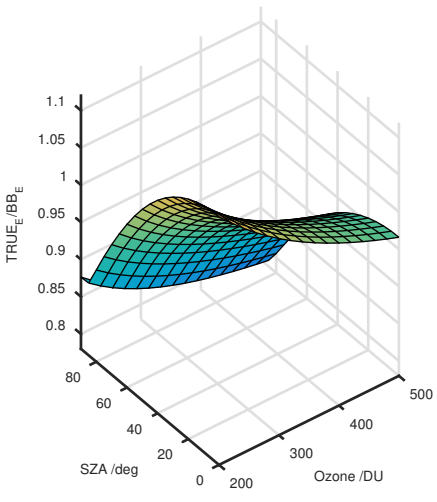

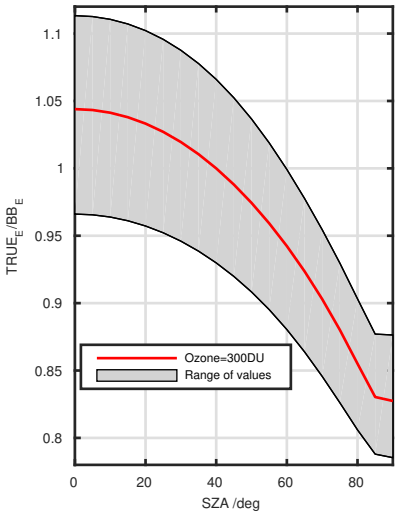

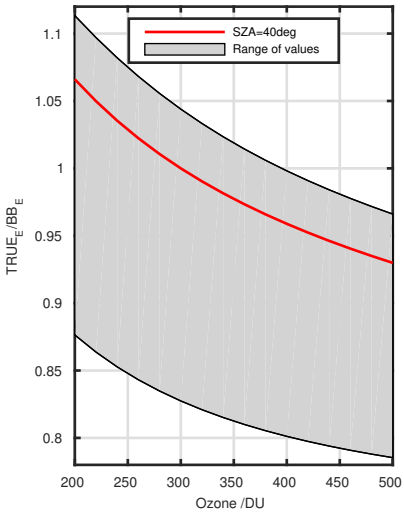

Calibration Results of SL2839 (UVE)

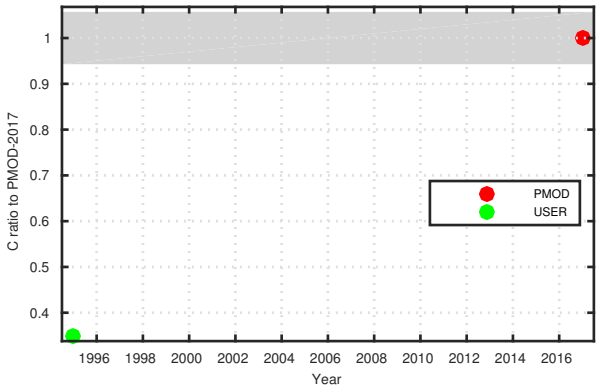

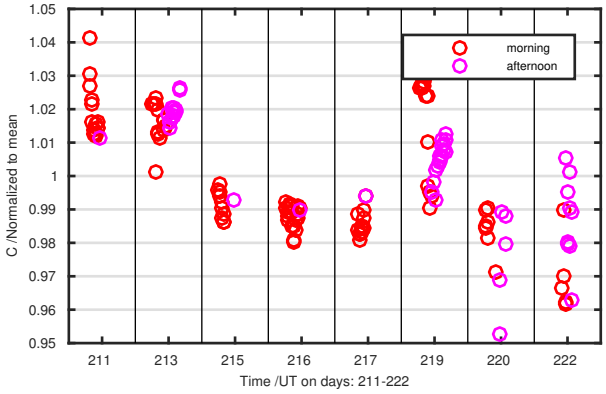

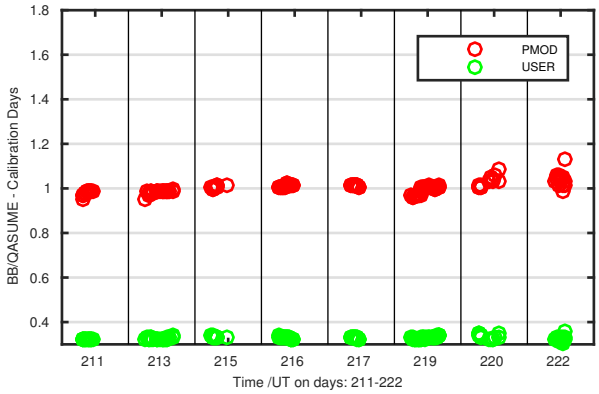

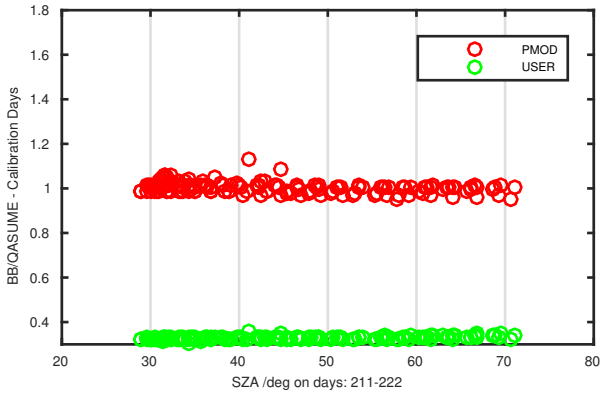

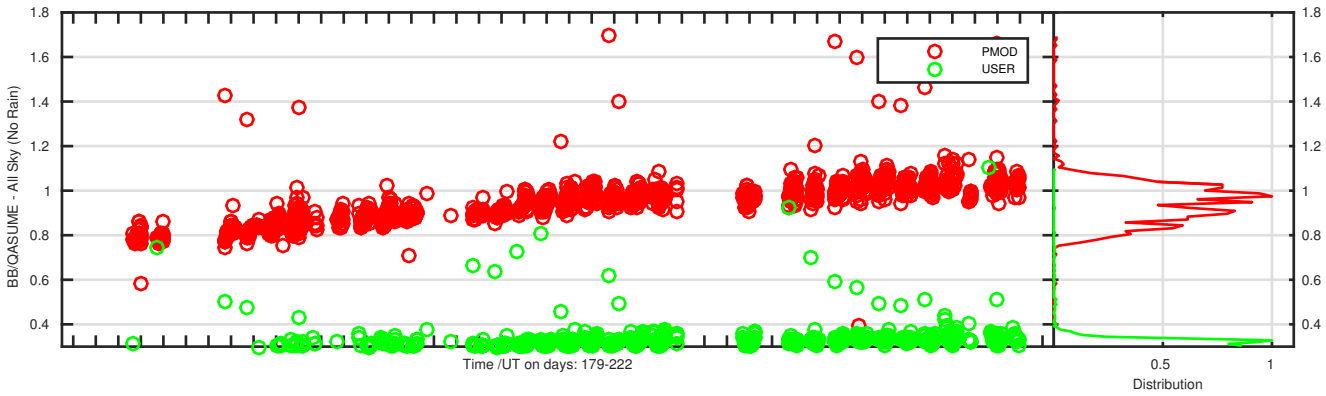

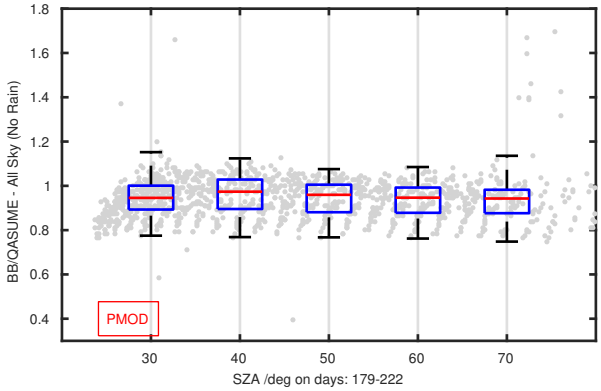

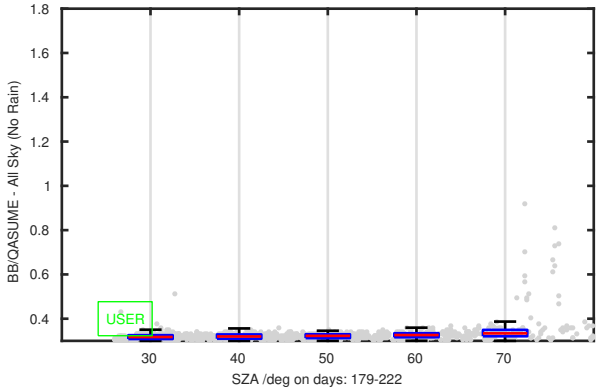

Calibration Results of SL3564 (UVA)

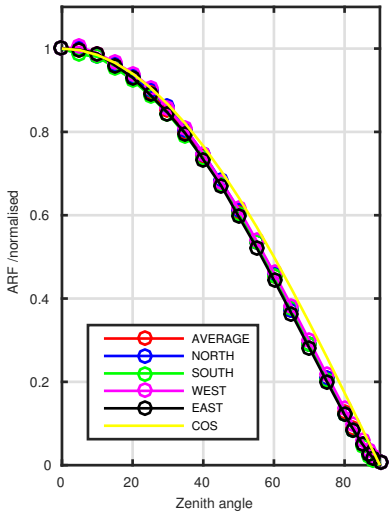

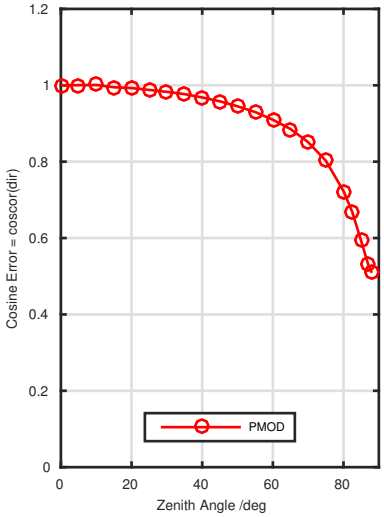

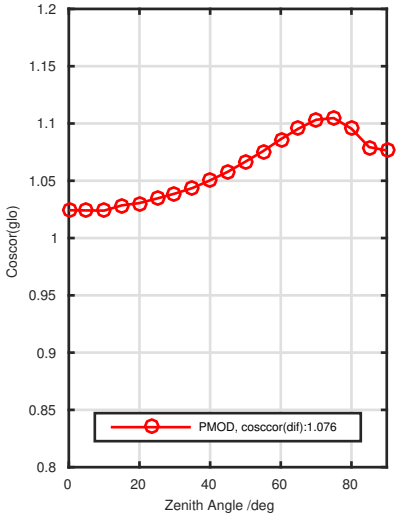

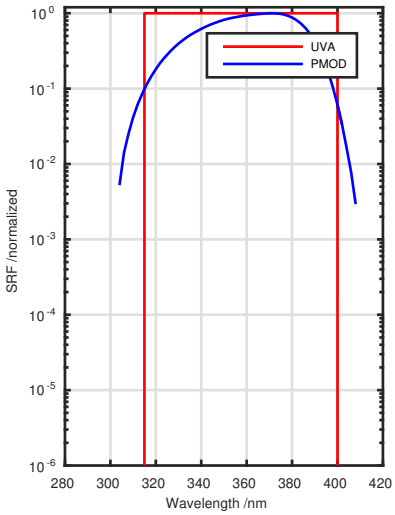

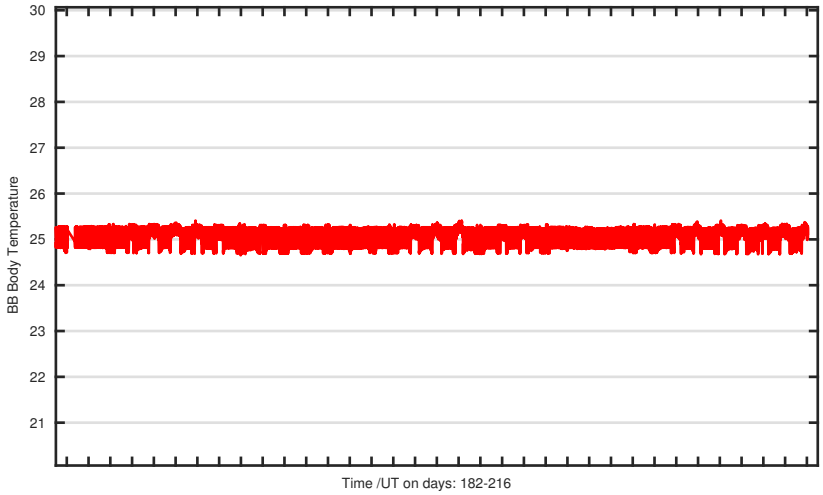

Calibration Matrix fn; Model sdisortREFms2009; f0=1.5192

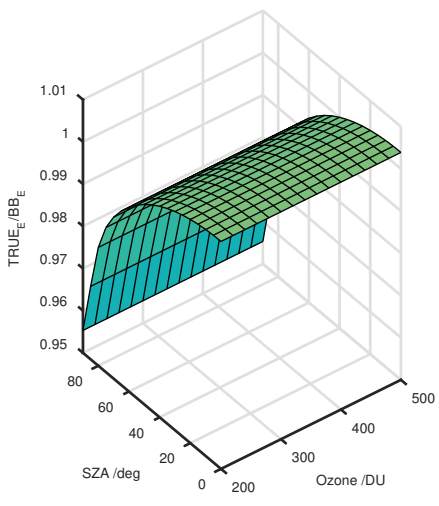

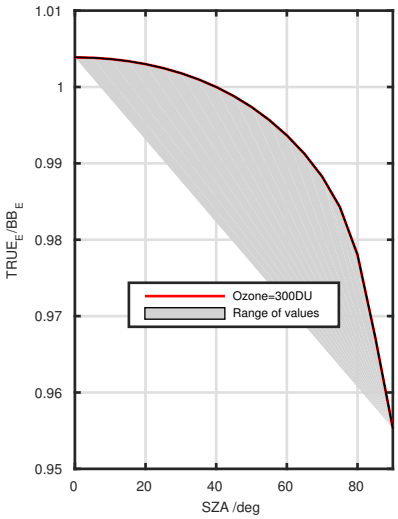

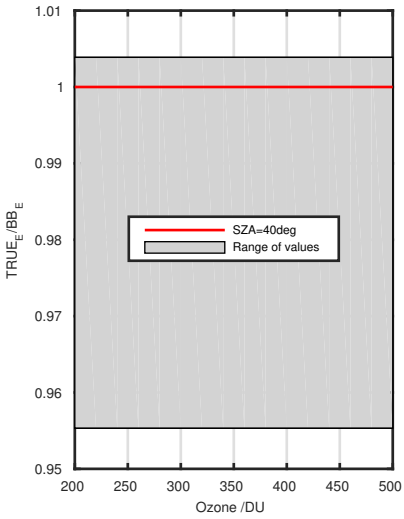

Calibration Results of SL3564 (UVA)

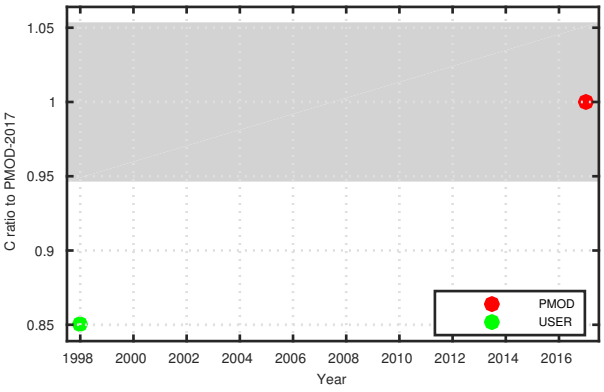

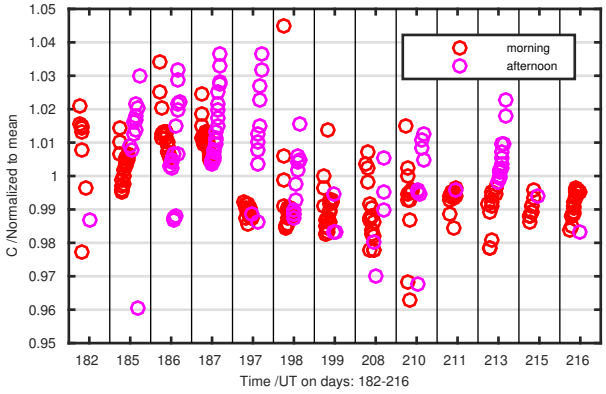

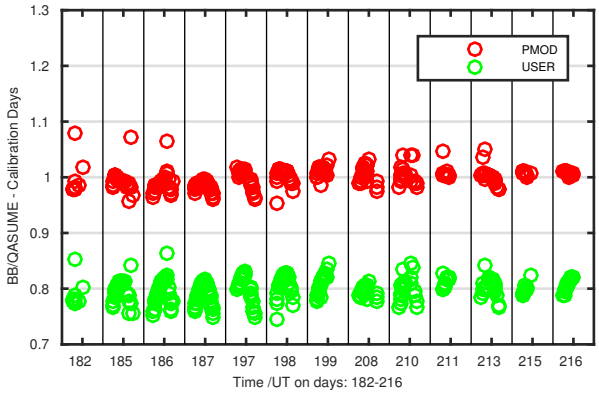

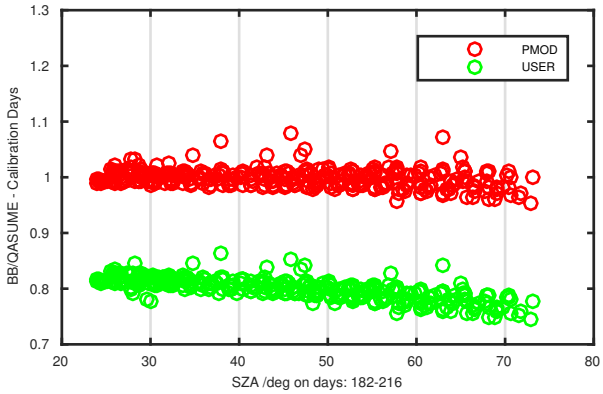

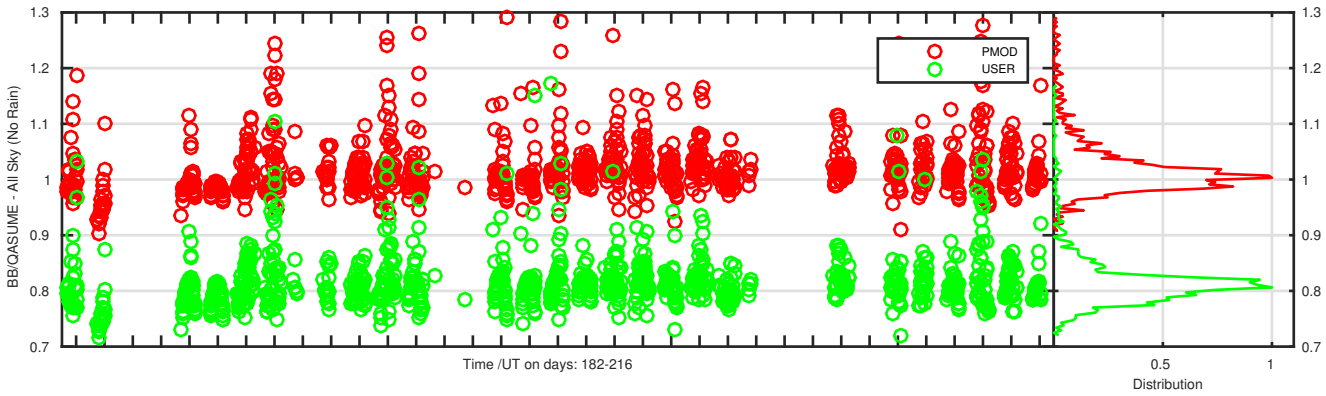

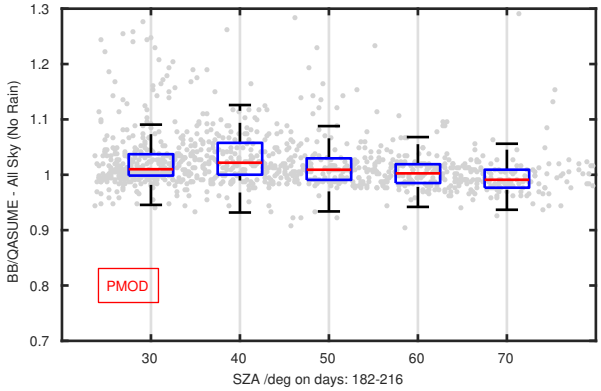

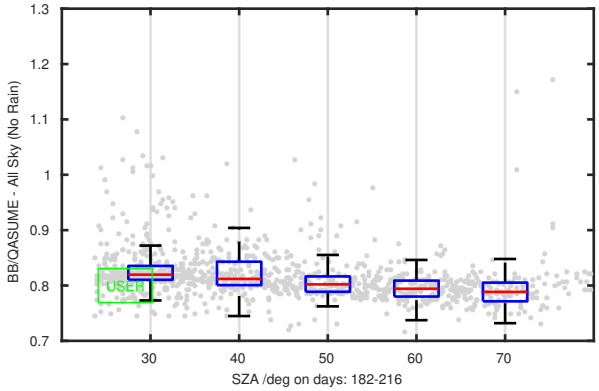

Calibration Results of SL3860 (UVE)

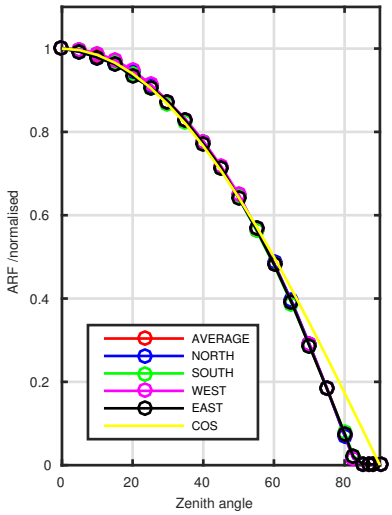

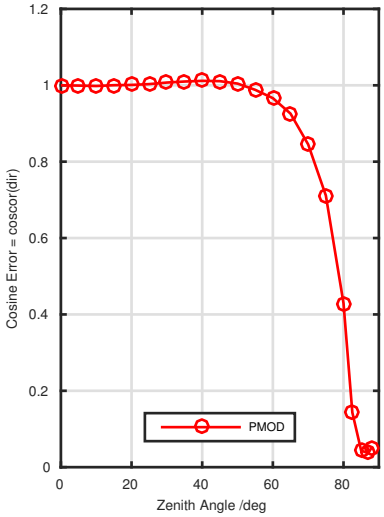

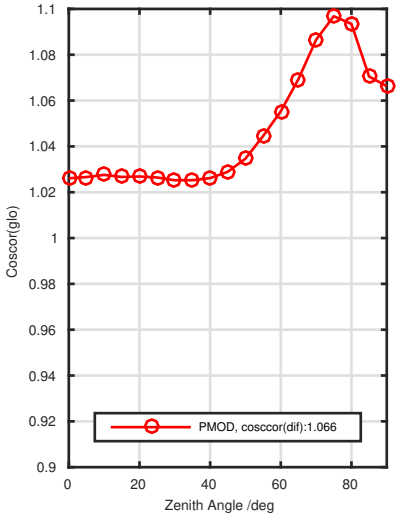

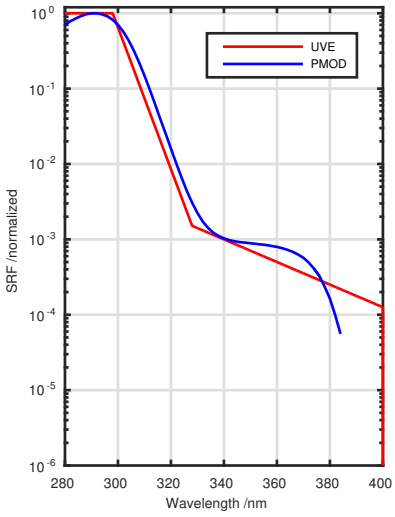

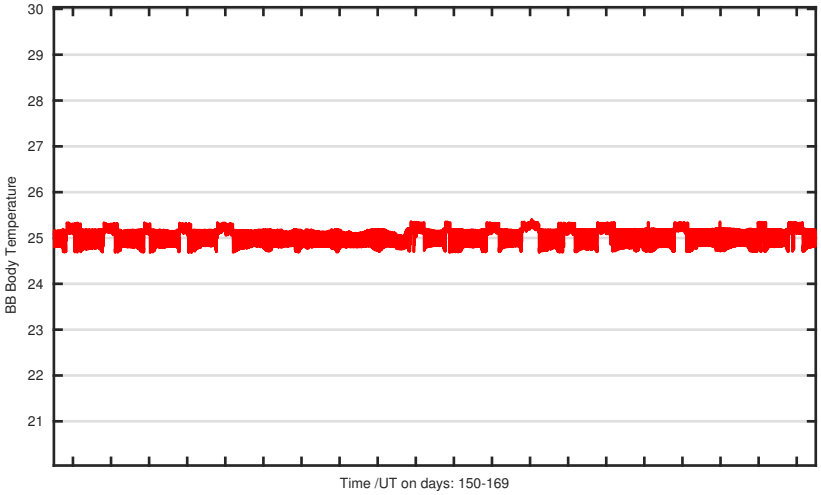

Calibration Matrix fn; Model sdisortPMODmsO3; f0=0.5831

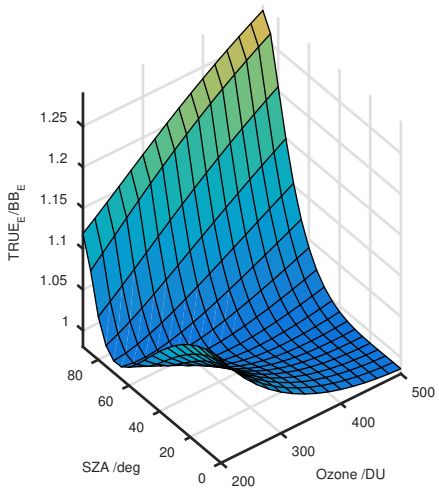

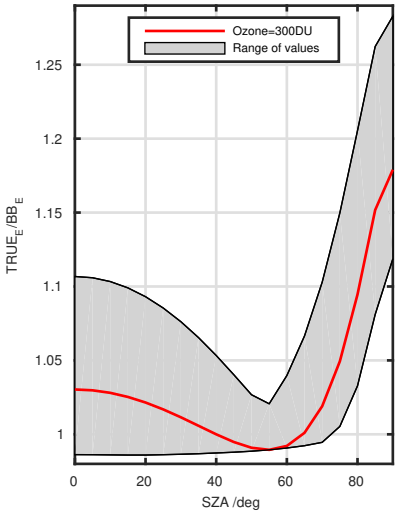

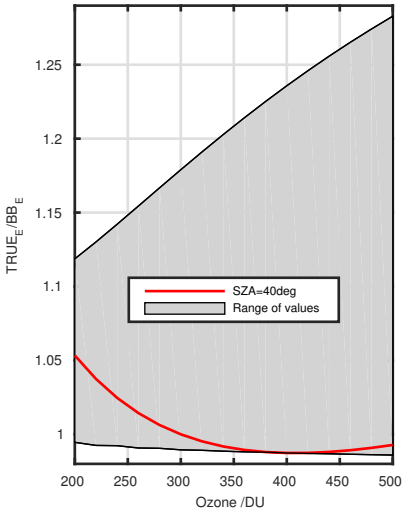

Calibration Results of SL3860 (UVE)

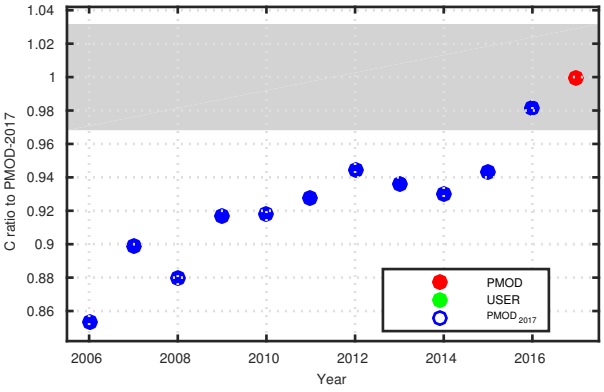

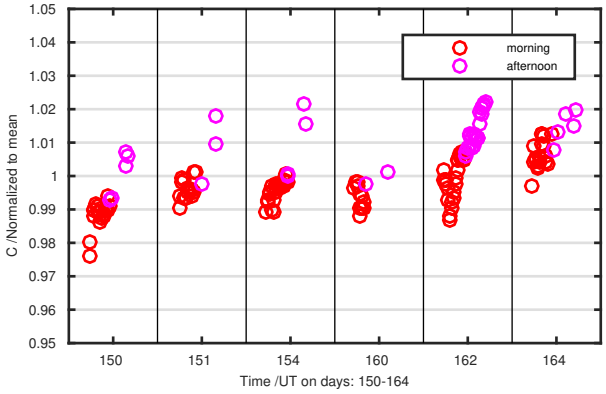

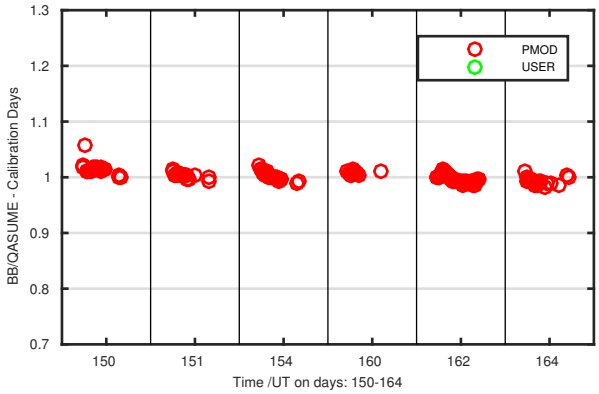

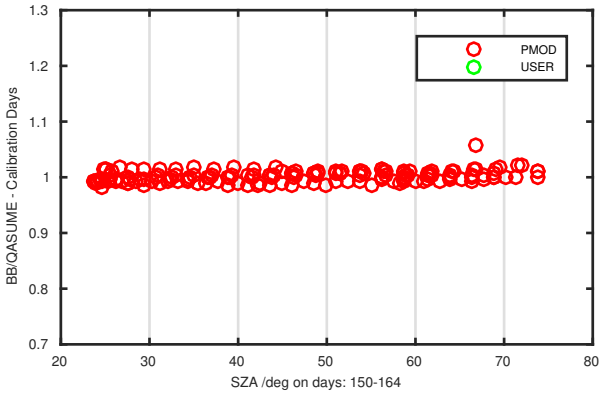

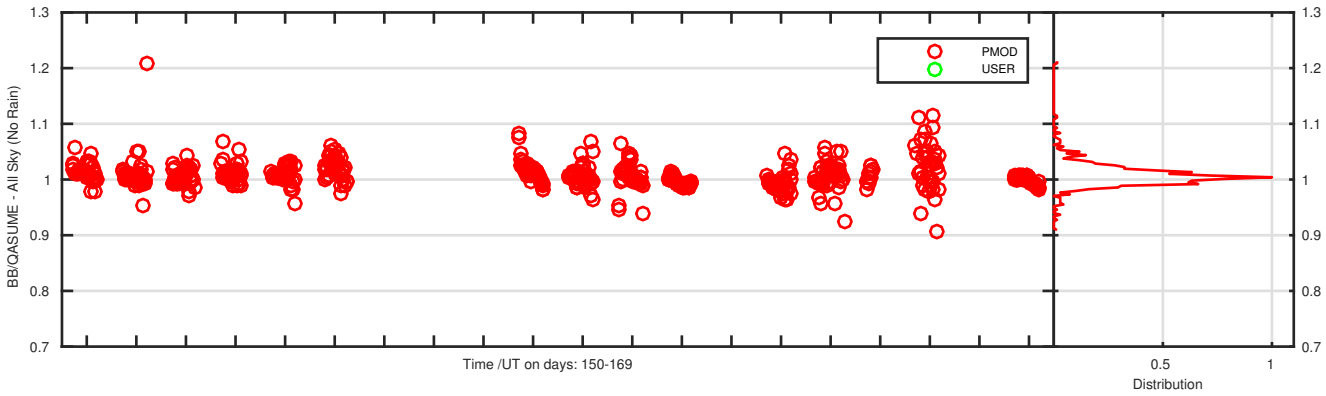

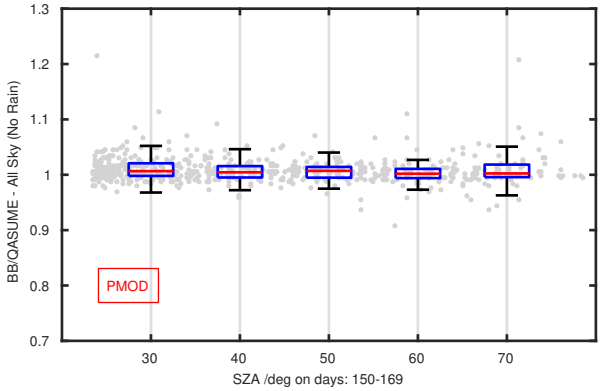

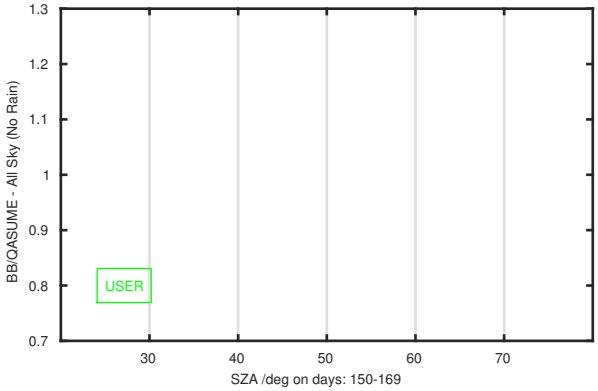

Calibration Results of SL4402 (UVA)

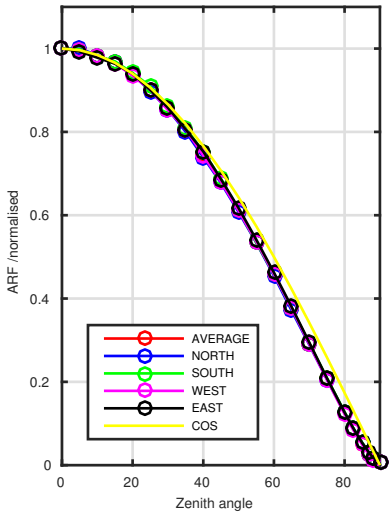

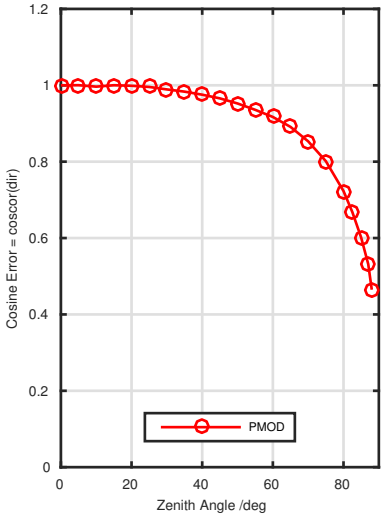

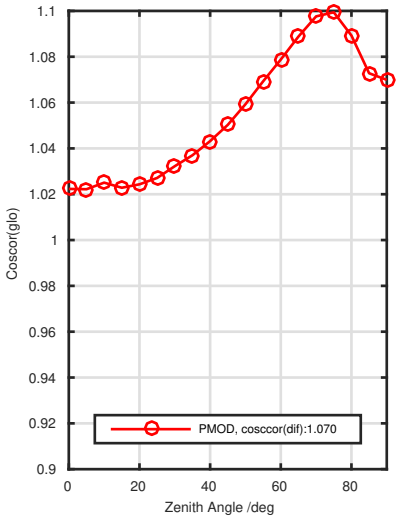

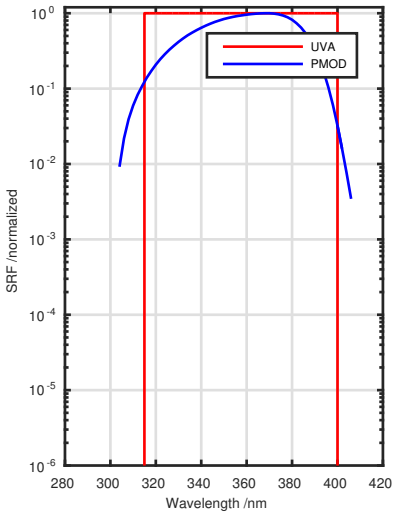

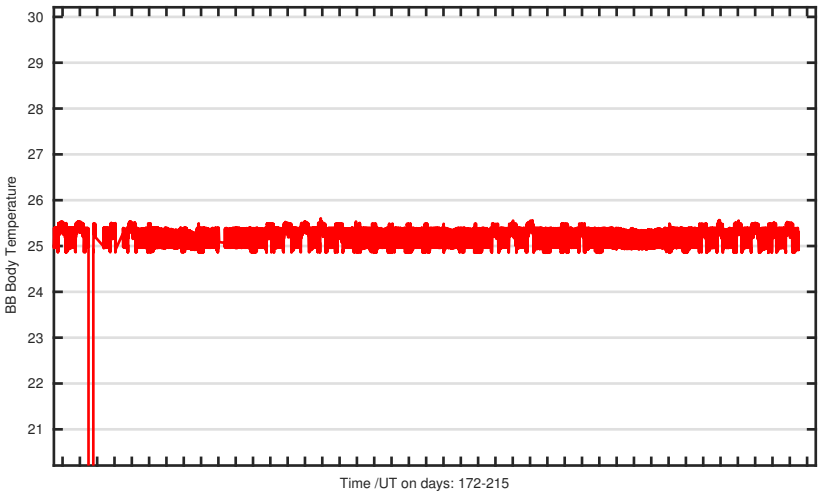

Calibration Matrix fn; Model sdisortREFms2009; f0=1.5542

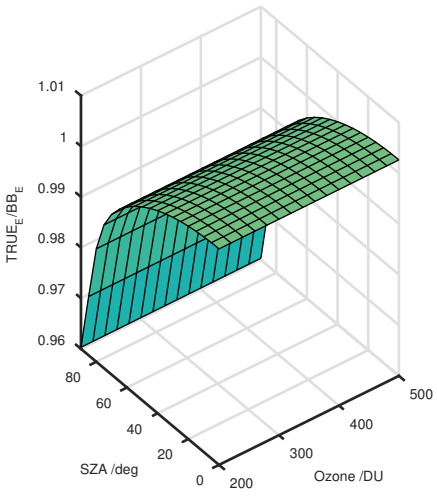

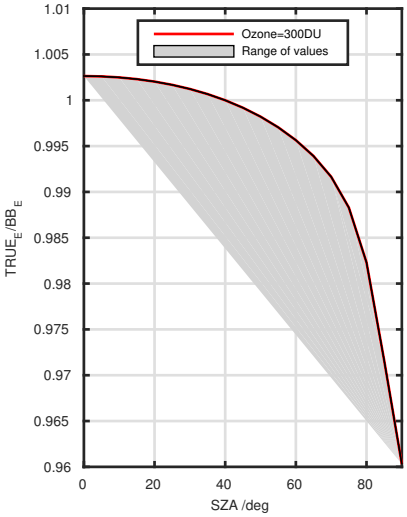

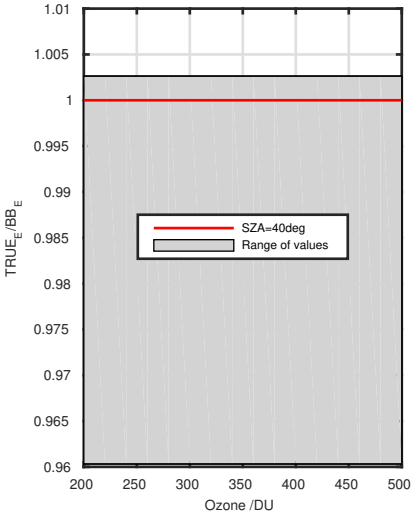

Calibration Results of SL4402 (UVA)

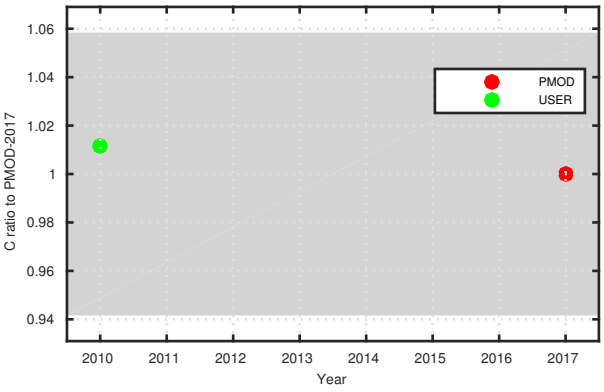

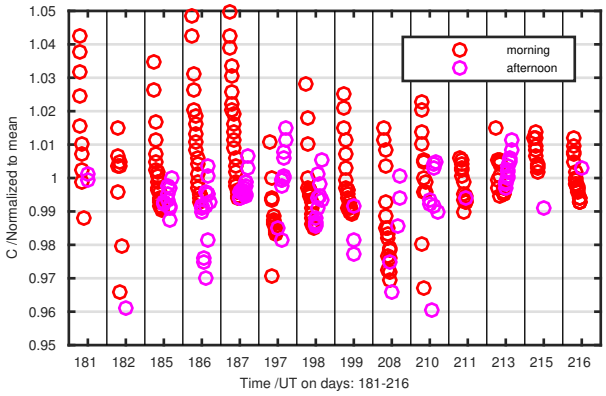

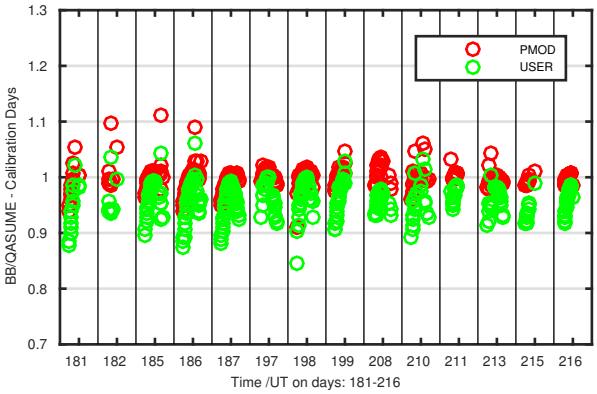

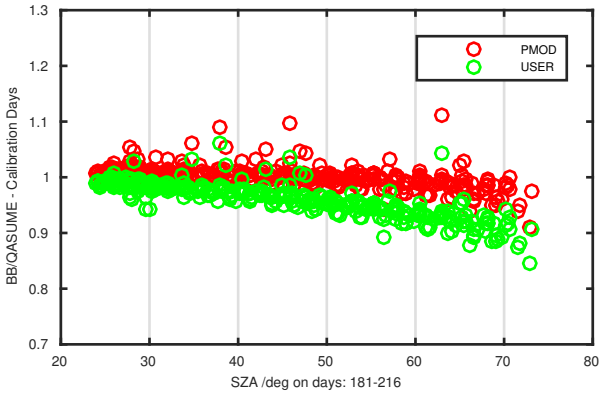

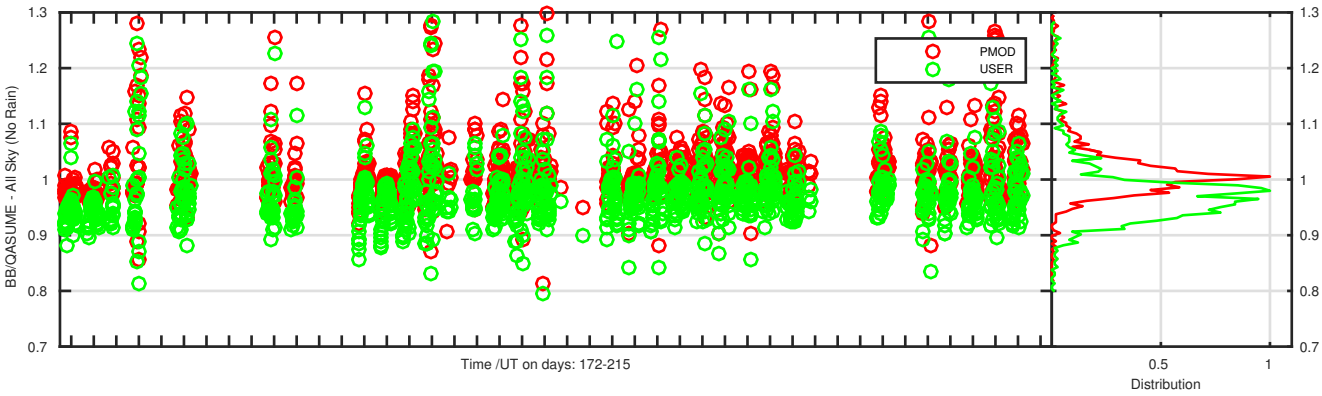

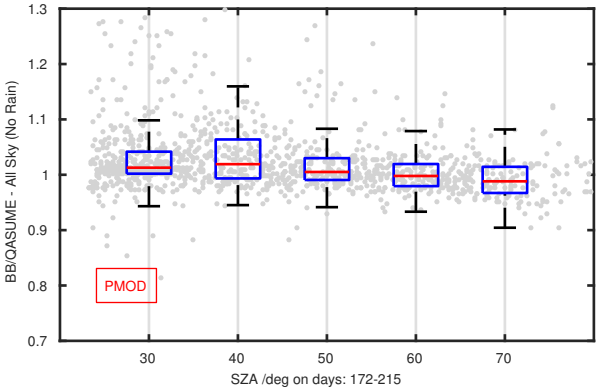

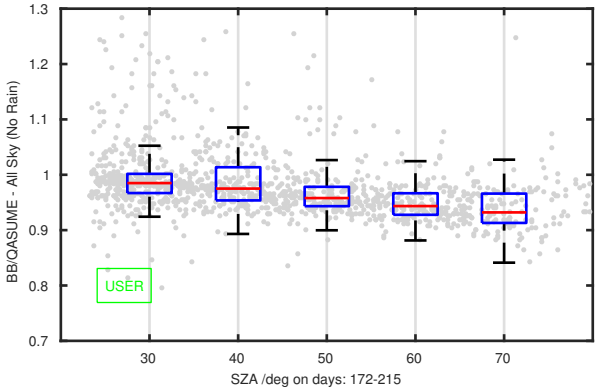

Calibration Results of SL4405 (UVE)

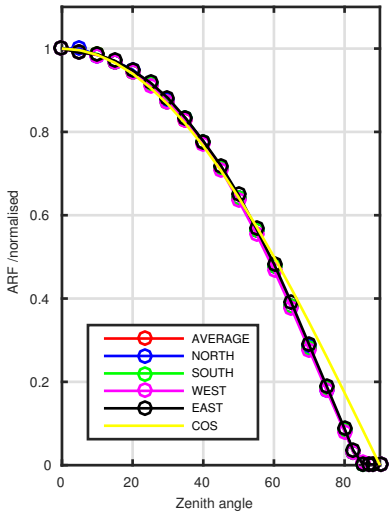

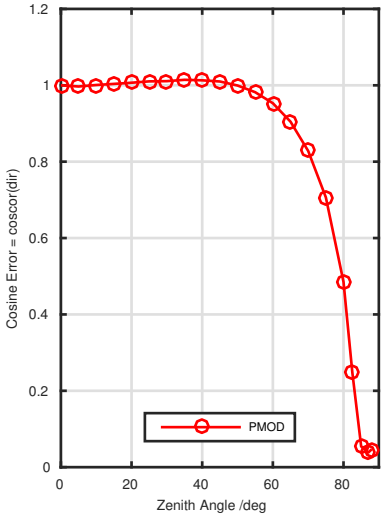

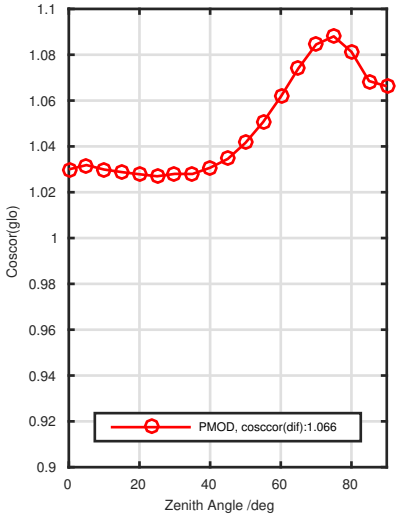

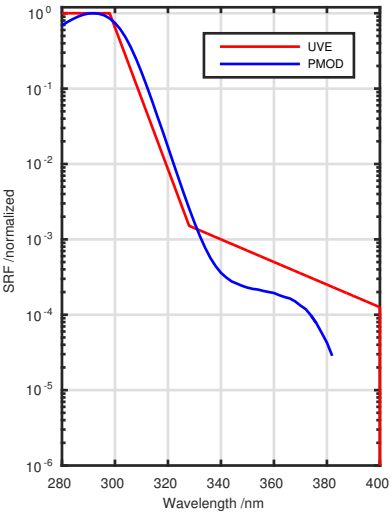

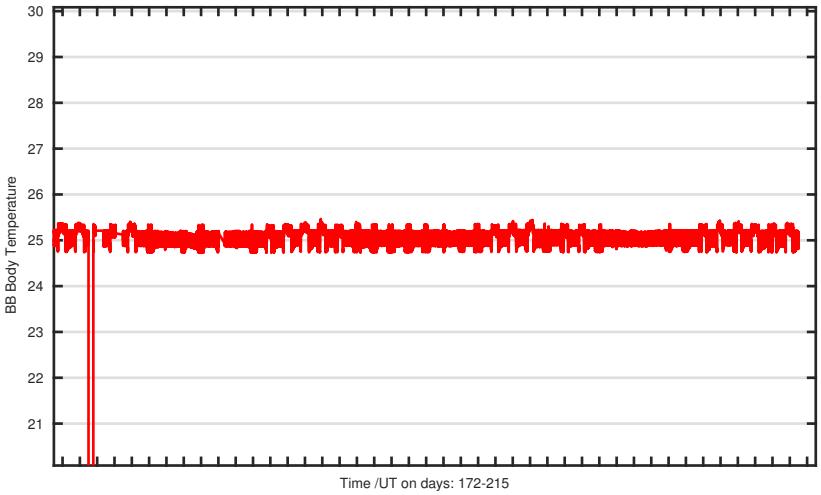

Calibration Matrix fn; Model sdisortREFms2009; f0=0.5684

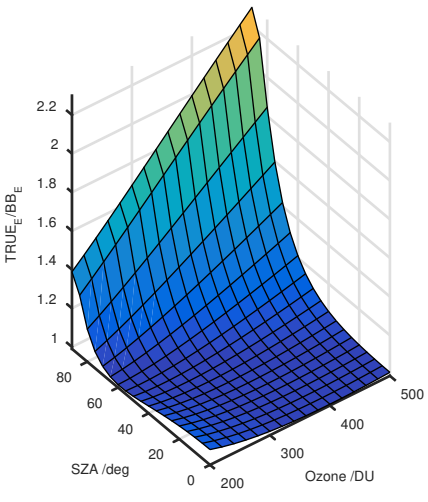

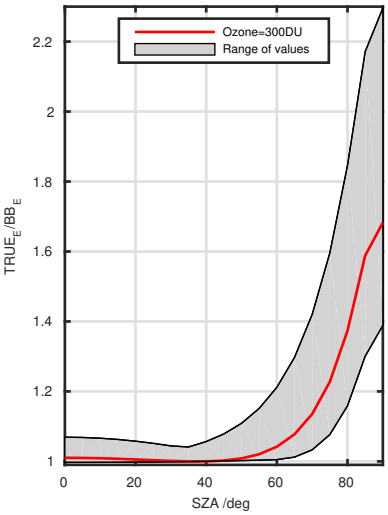

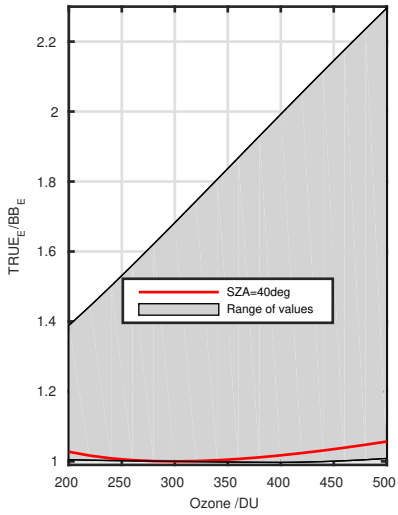

Calibration Results of SL4405 (UVE)

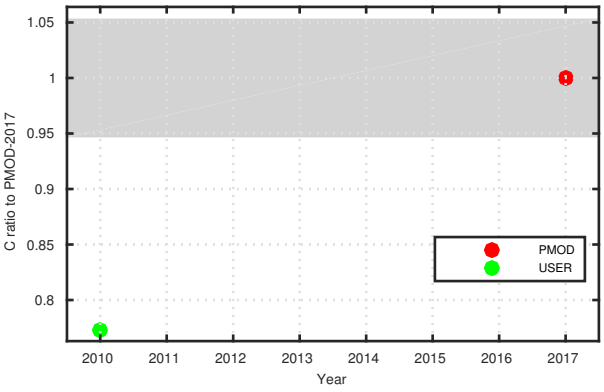

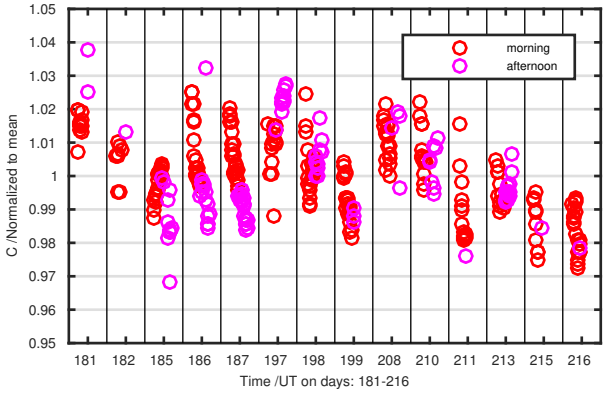

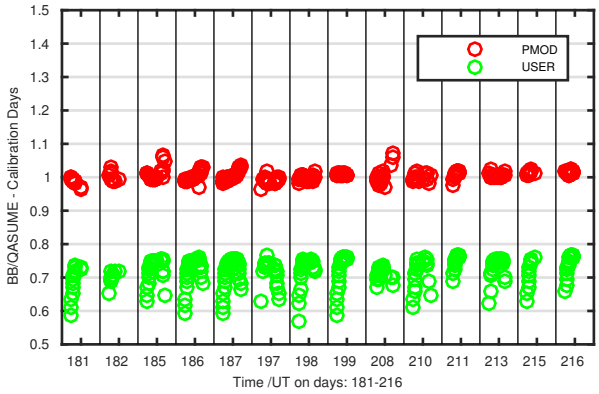

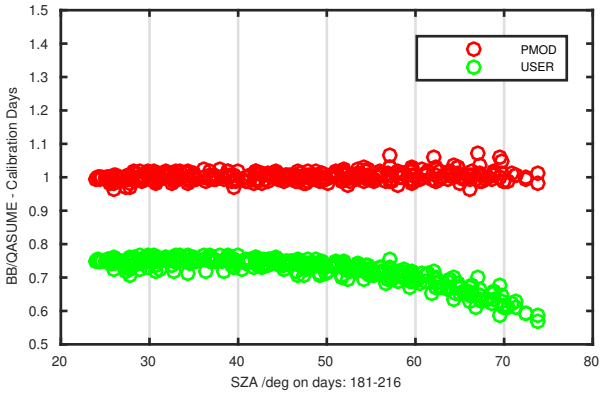

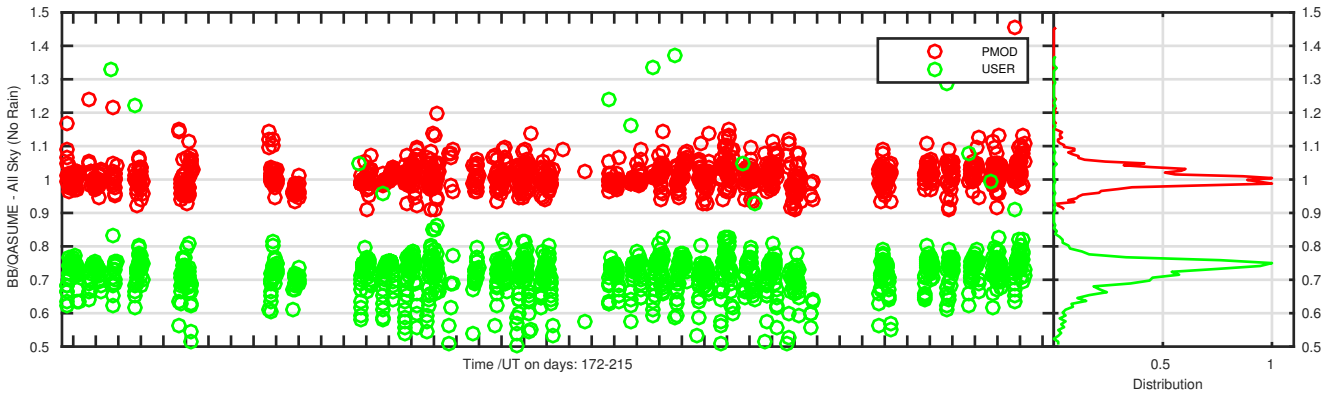

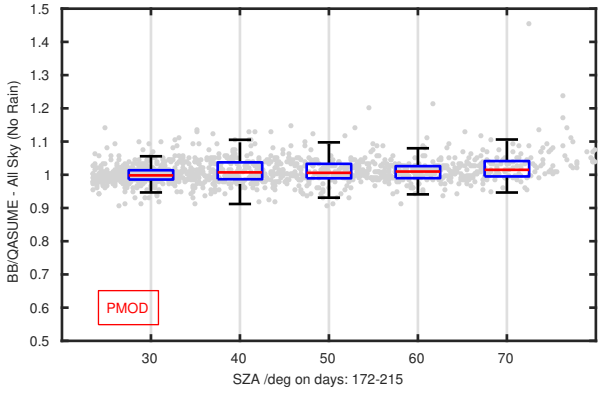

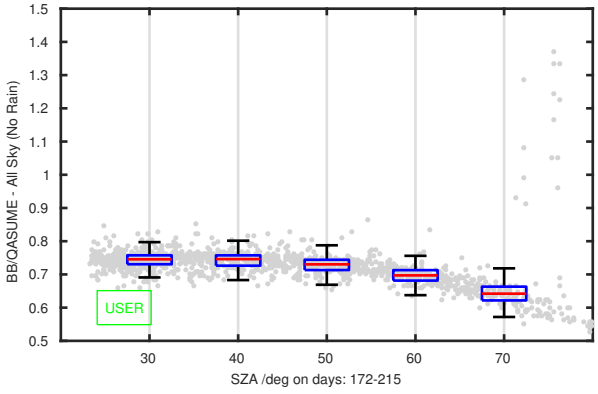

Calibration Results of SL4433 (UVE)

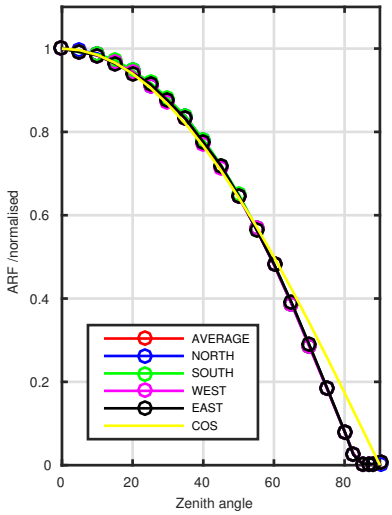

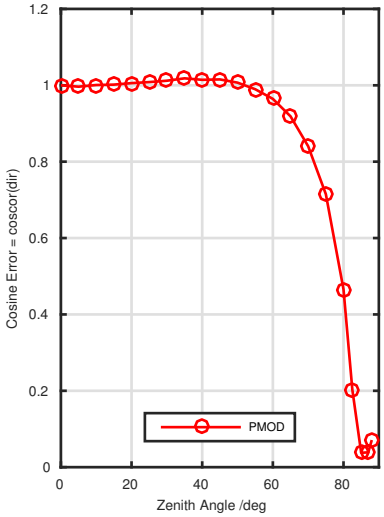

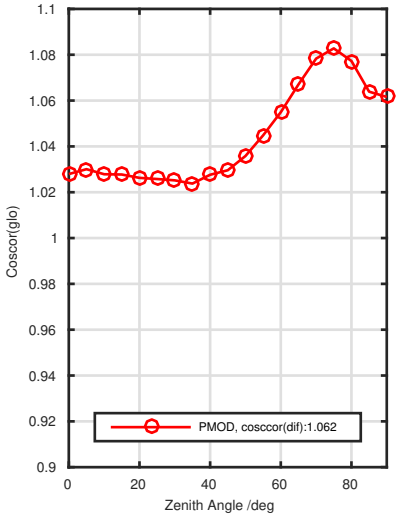

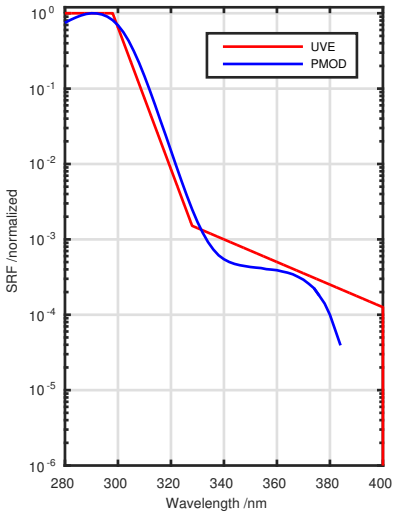

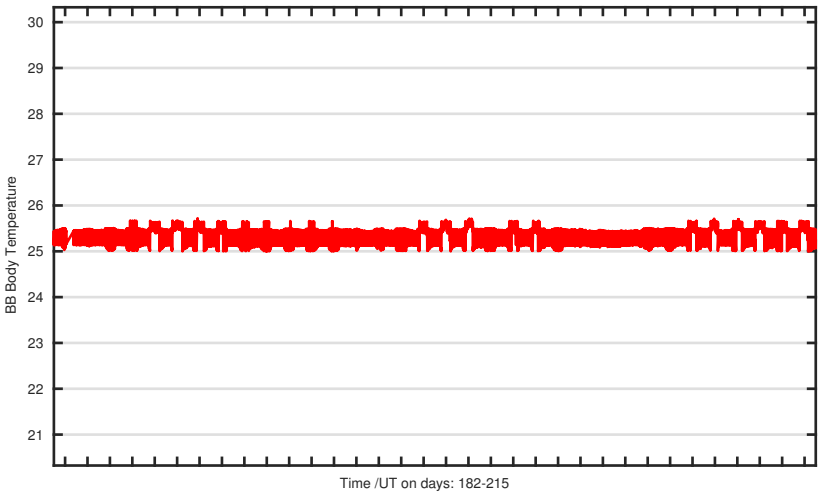

Calibration Matrix fn; Model sdisortREFms2009; f0=0.6230

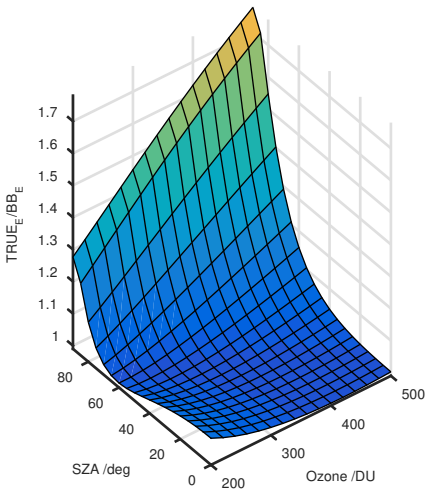

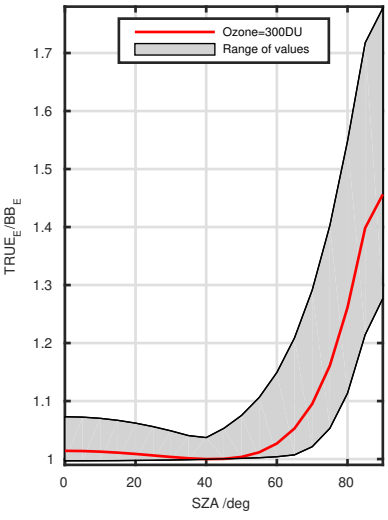

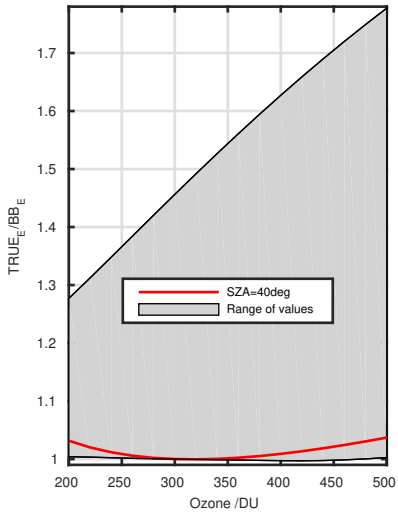

Calibration Results of SL4433 (UVE)

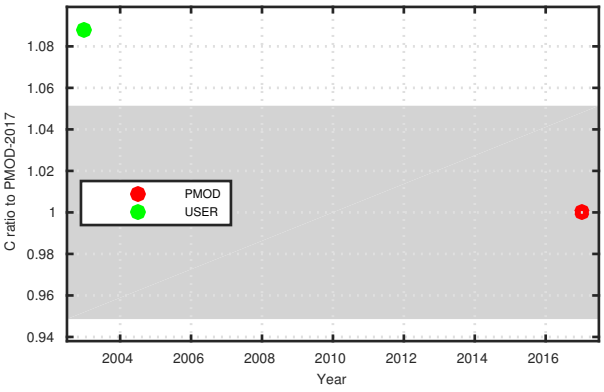

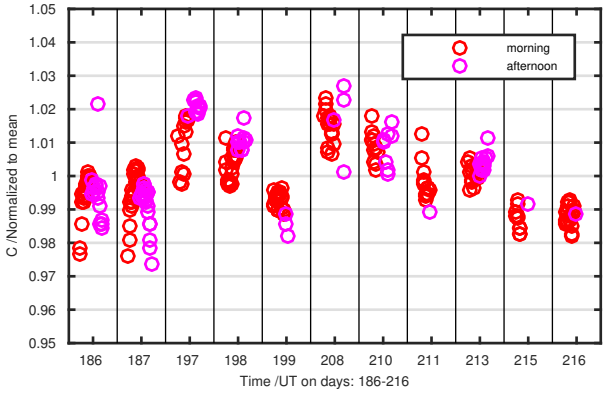

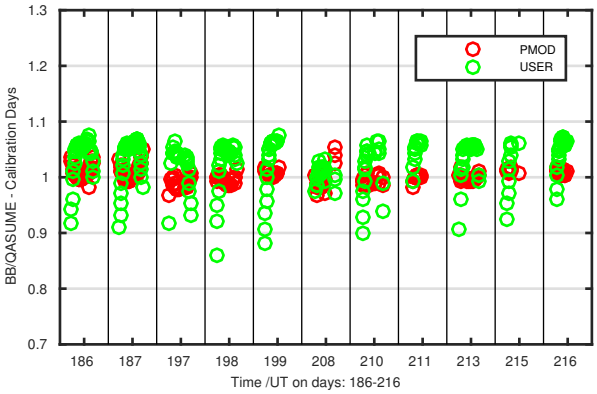

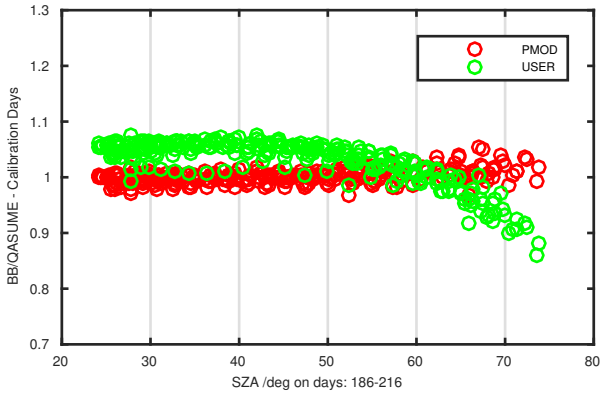

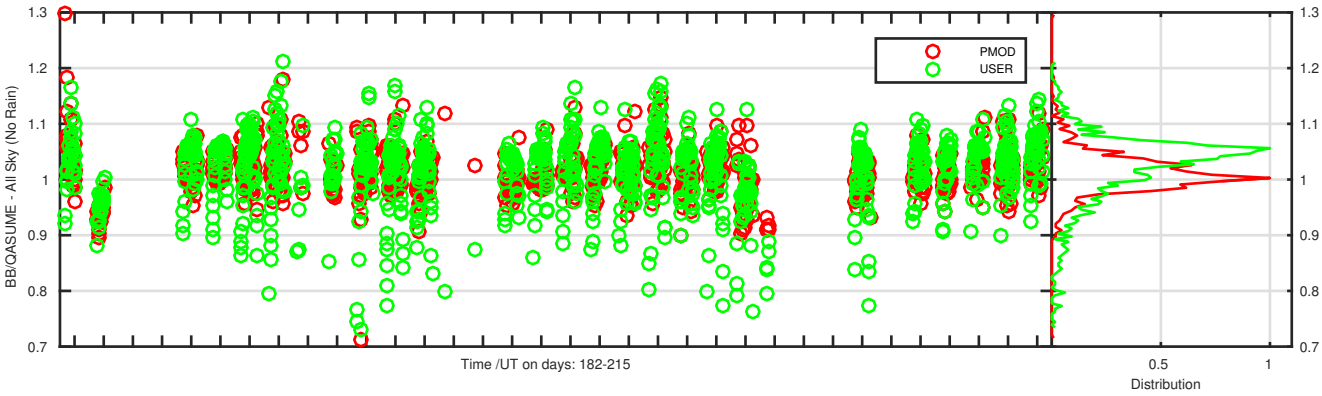

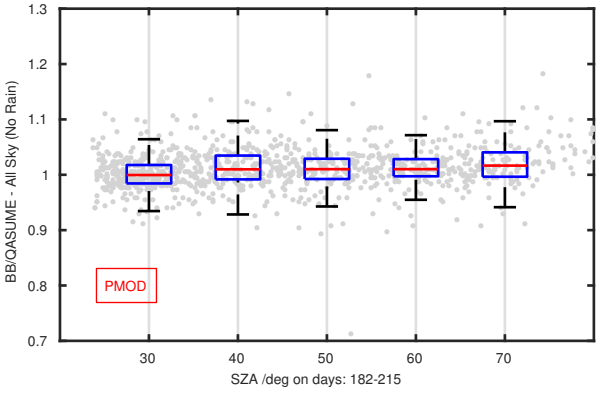

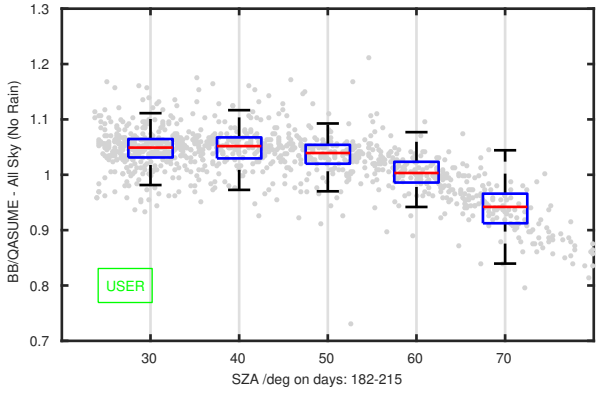

Calibration Results of SL5760 (UVE)

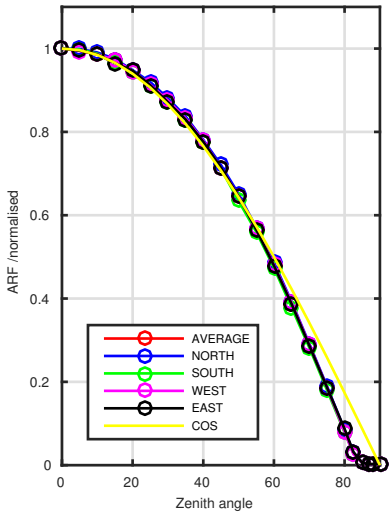

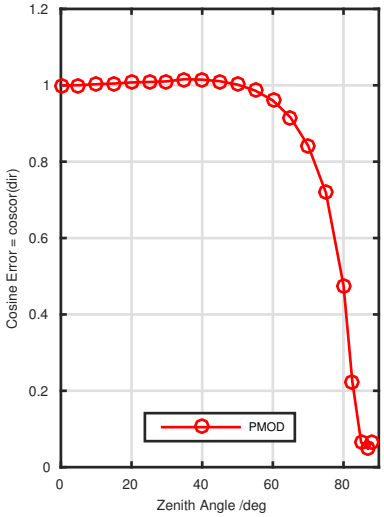

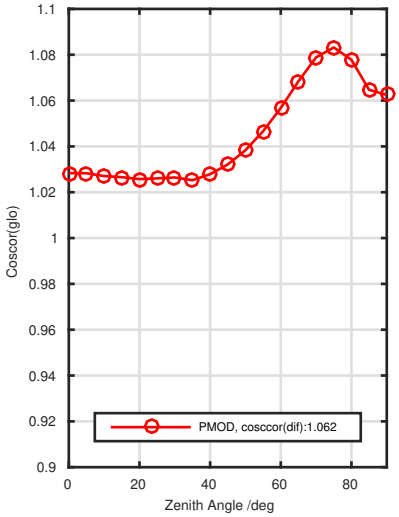

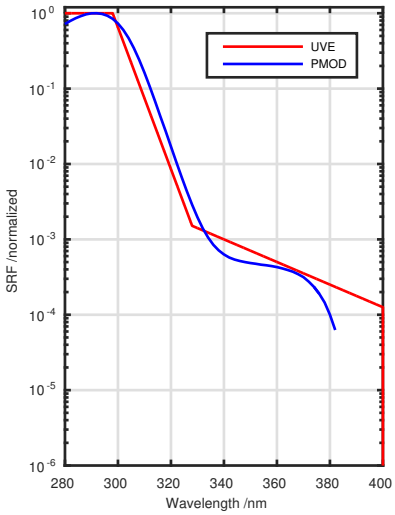

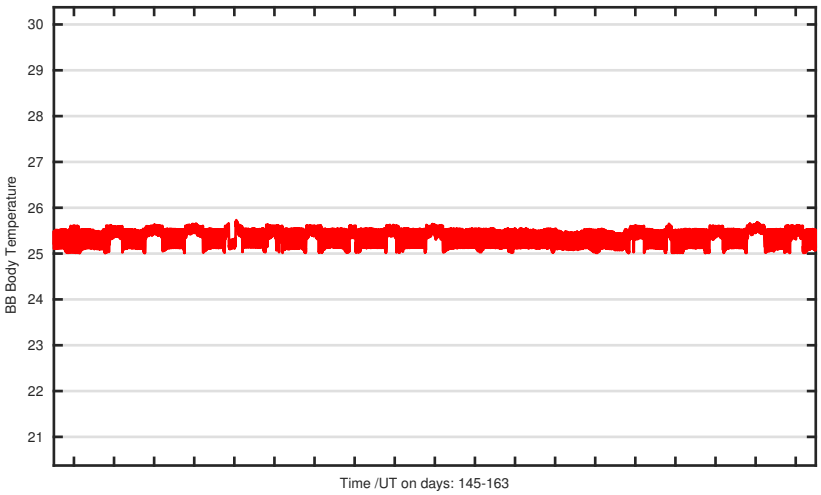

Calibration Matrix fn; Model sdisortREFms2009; f0=0.5608

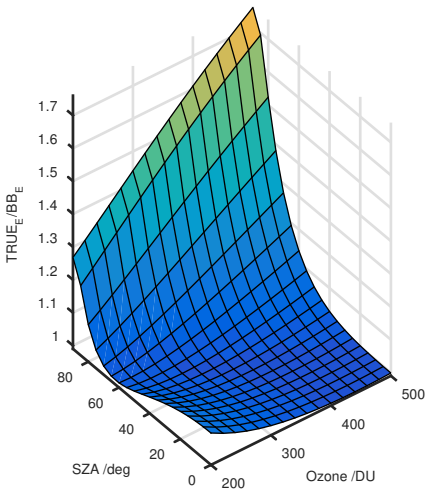

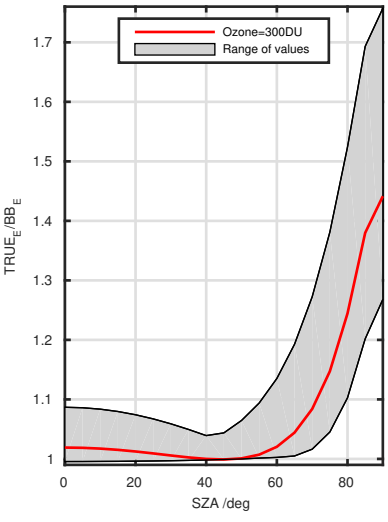

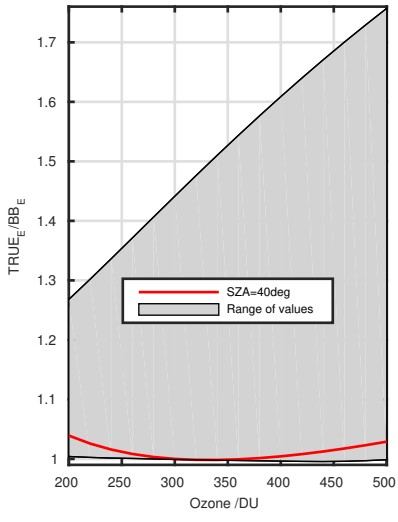

Calibration Results of SL5760 (UVE)

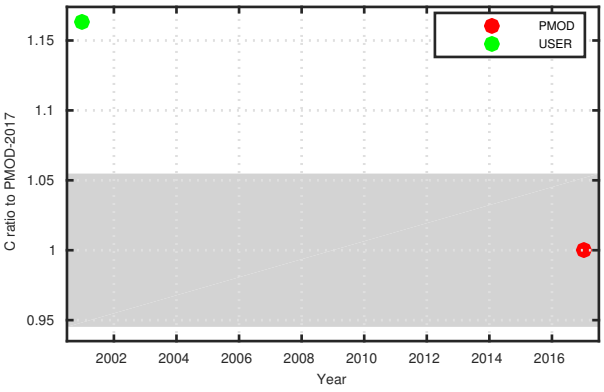

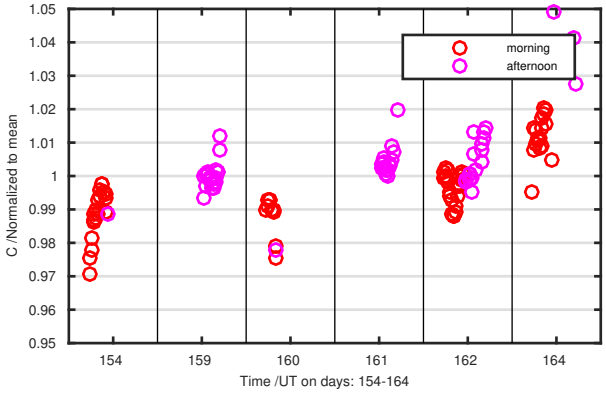

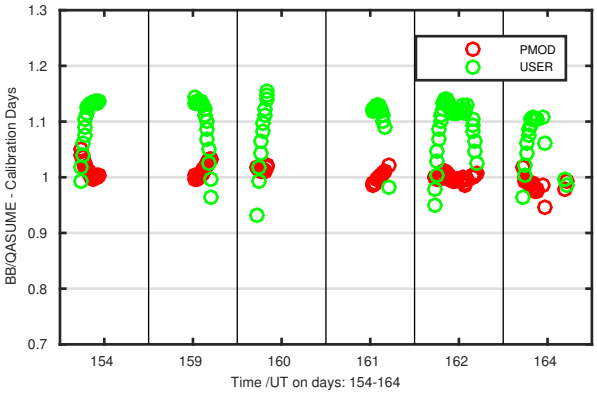

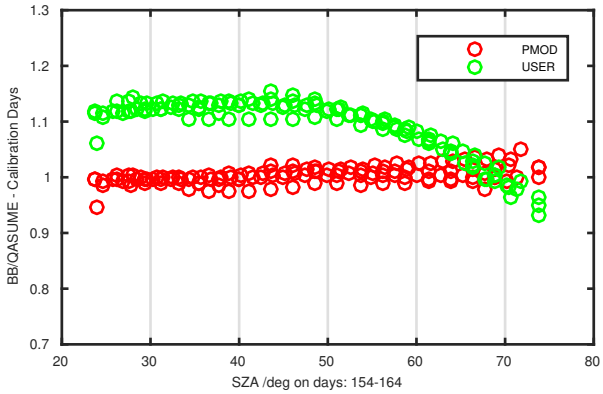

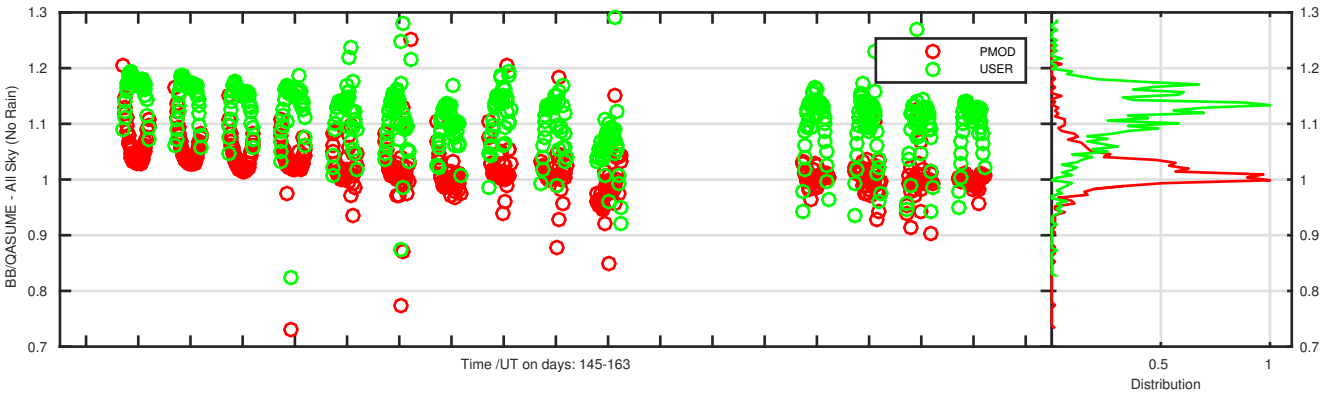

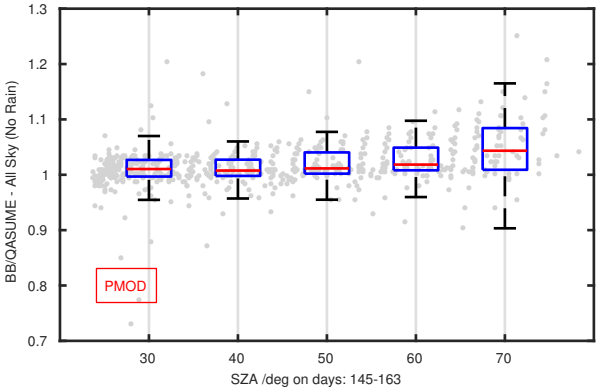

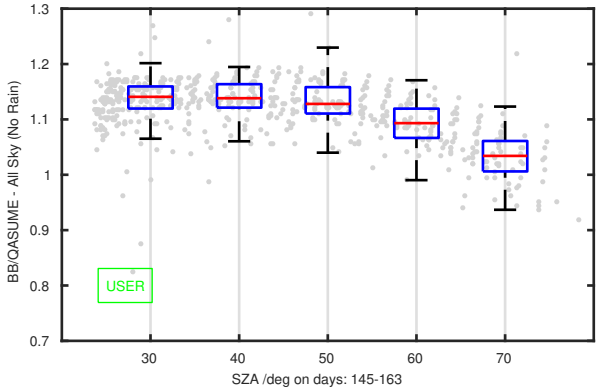

Calibration Results of SL5790 (UVE)

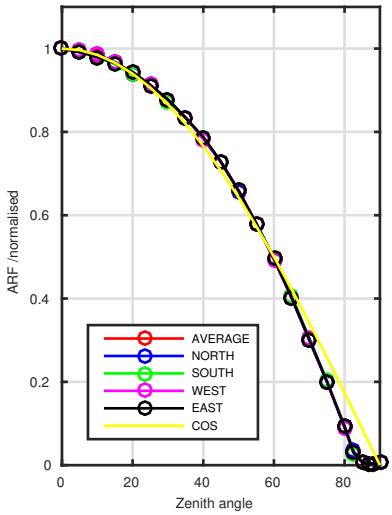

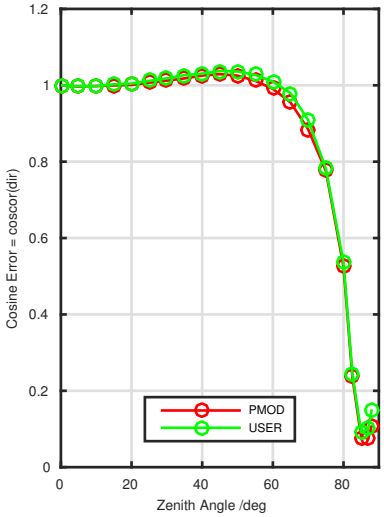

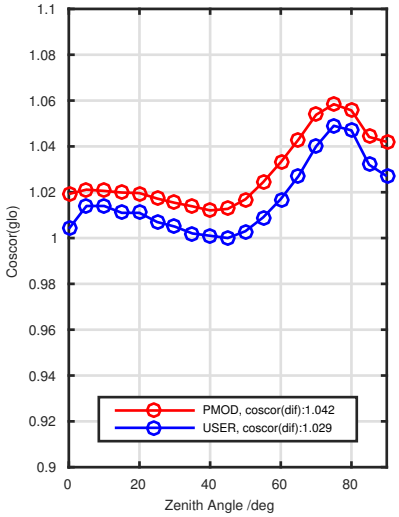

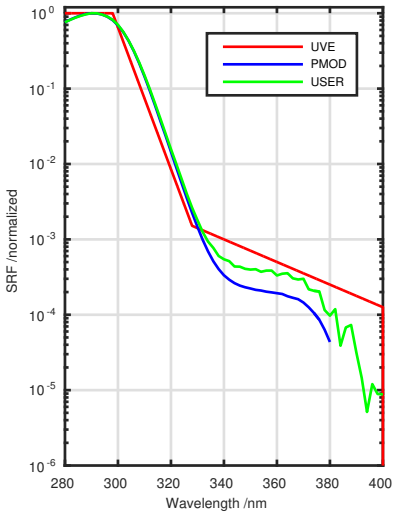

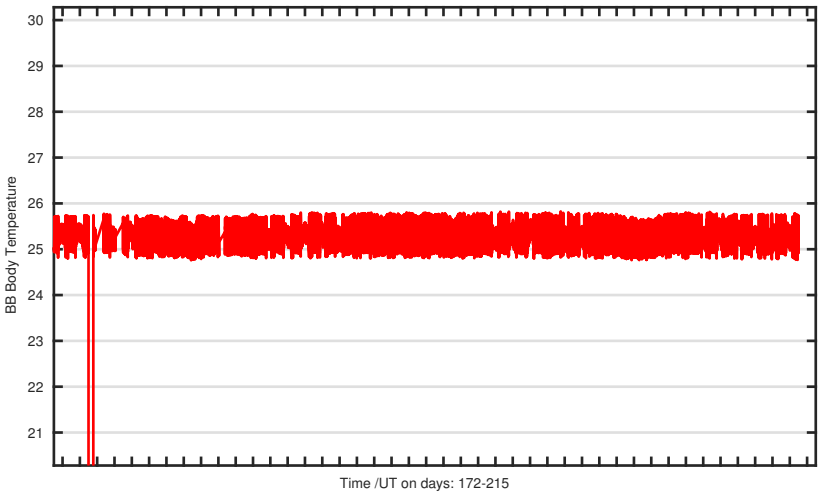

Calibration Matrix fn; Model sdisortREFms2009; f0=0.6433

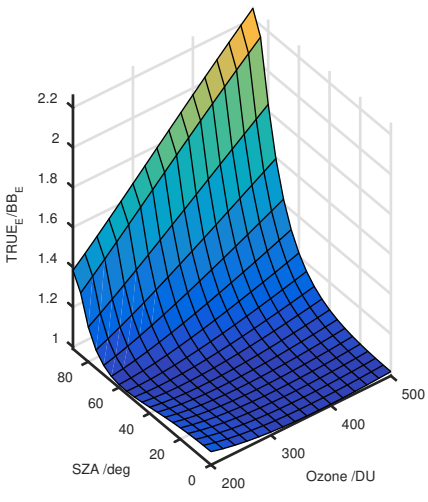

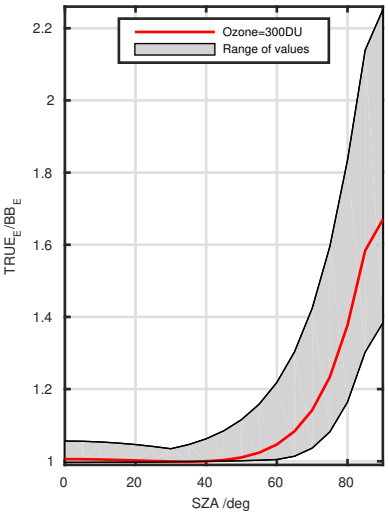

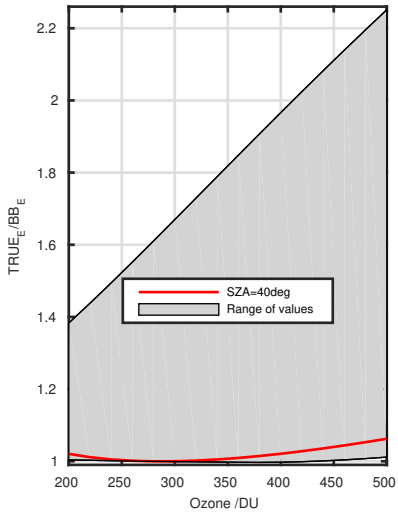

Calibration Results of SL5790 (UVE)

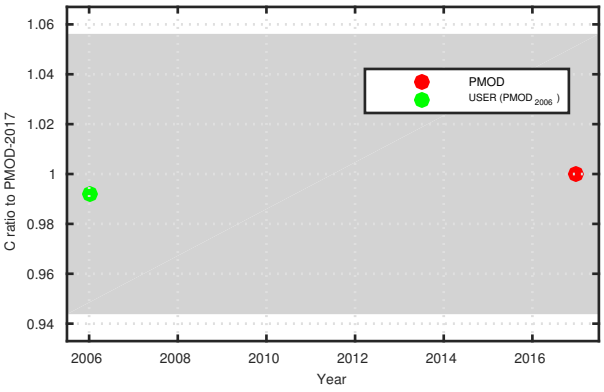

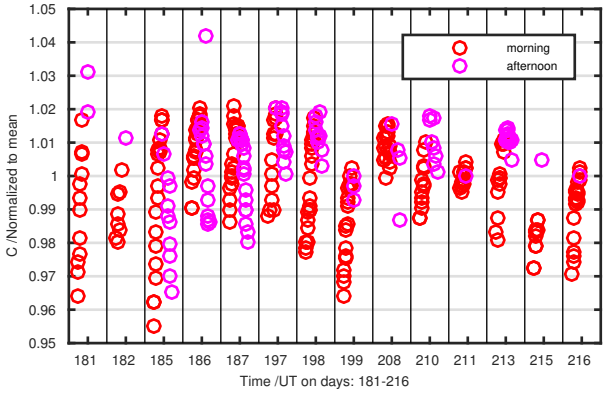

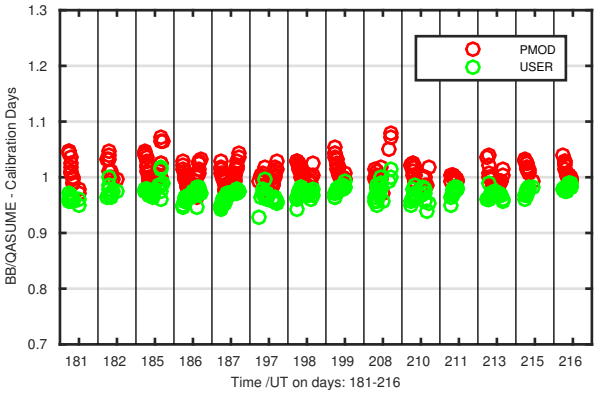

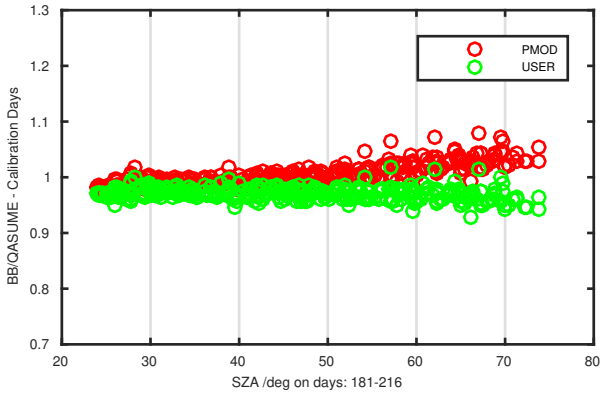

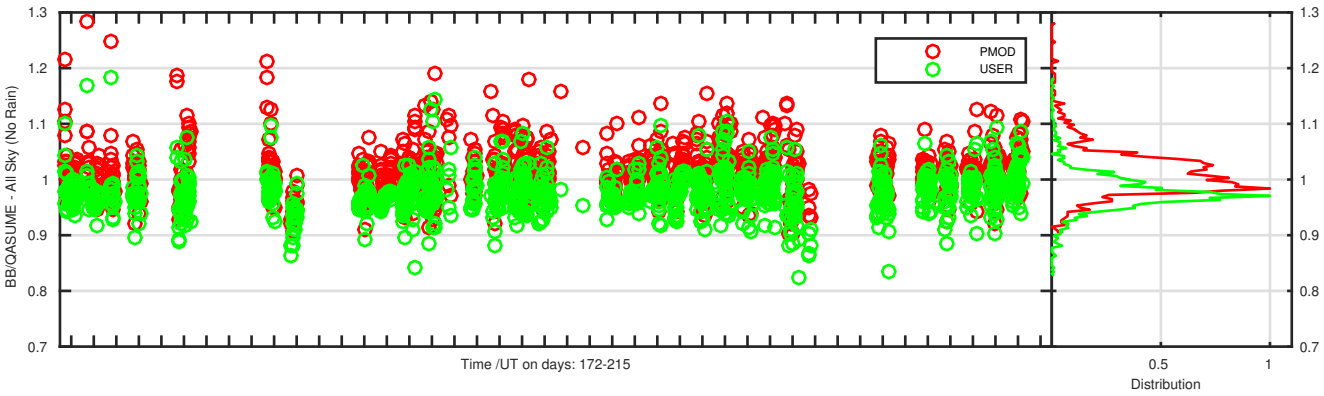

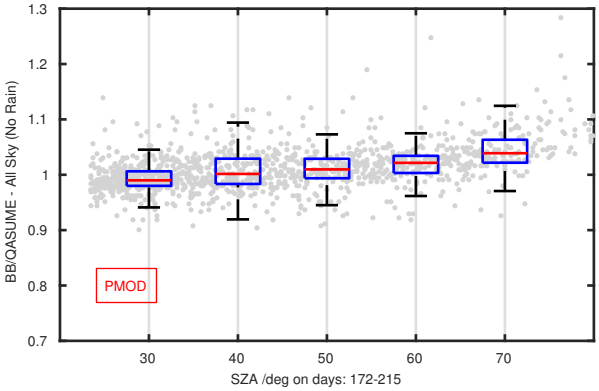

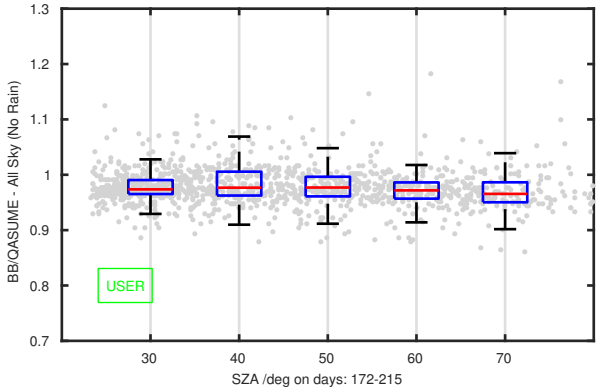

Calibration Results of SL8887 (UVE)

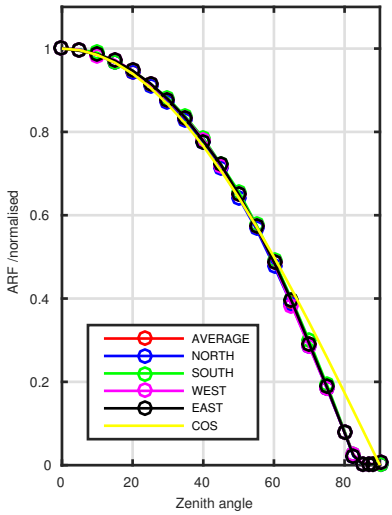

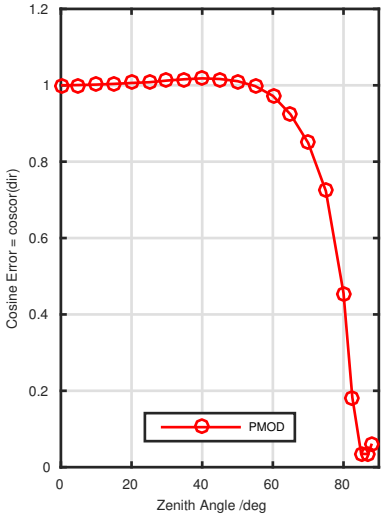

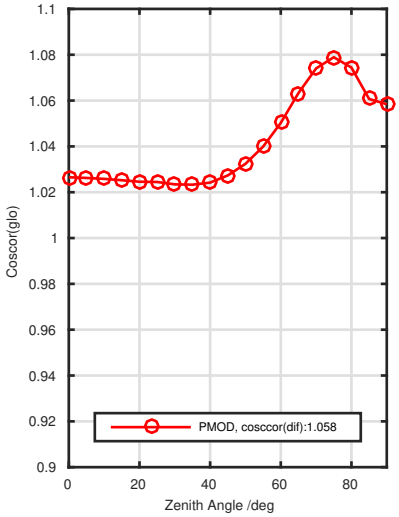

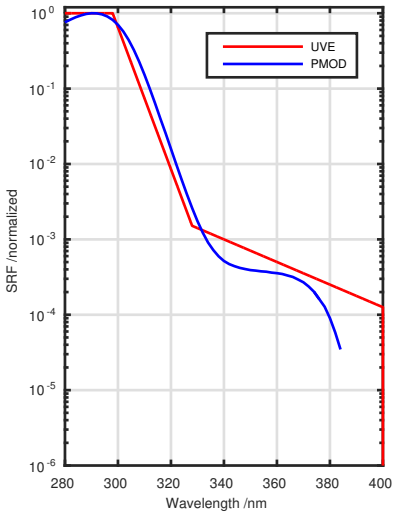

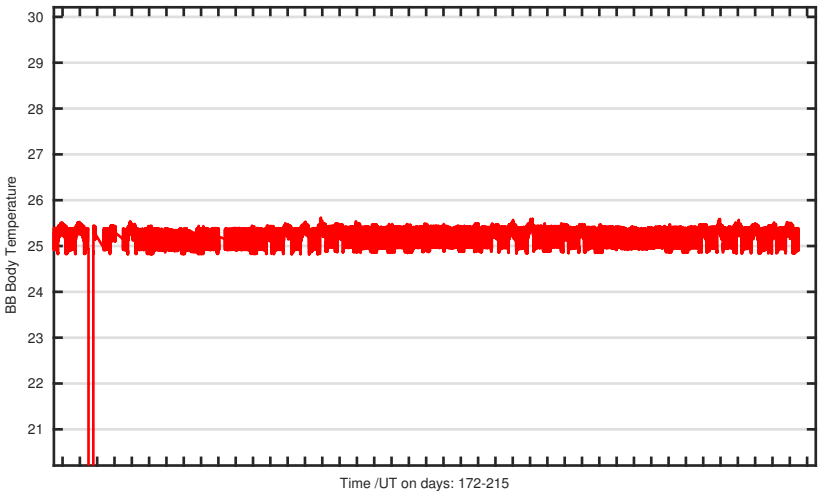

Calibration Matrix fn; Model sdisortREFms2009; f0=0.6002

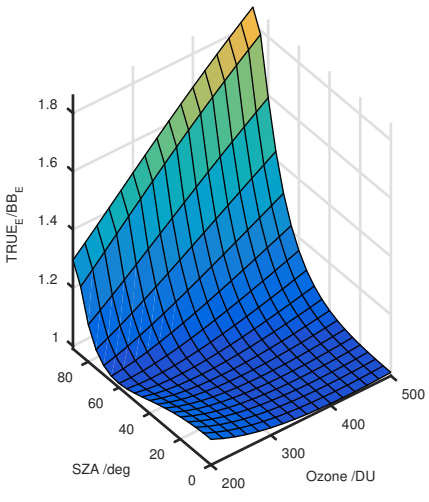

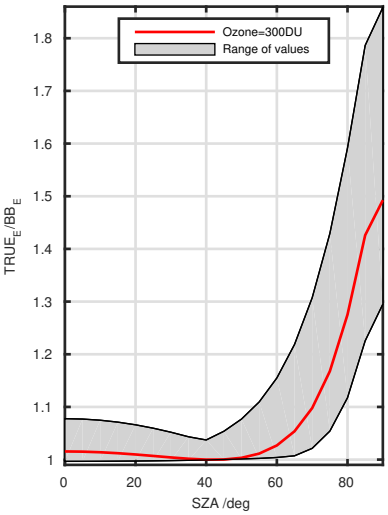

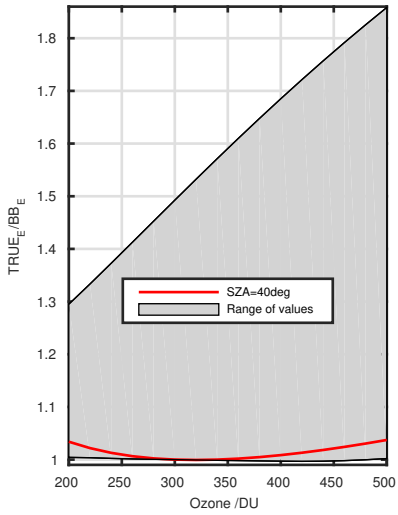

Calibration Results of SL8887 (UVE)

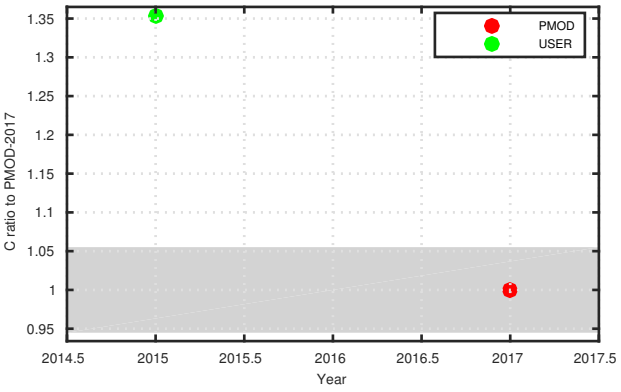

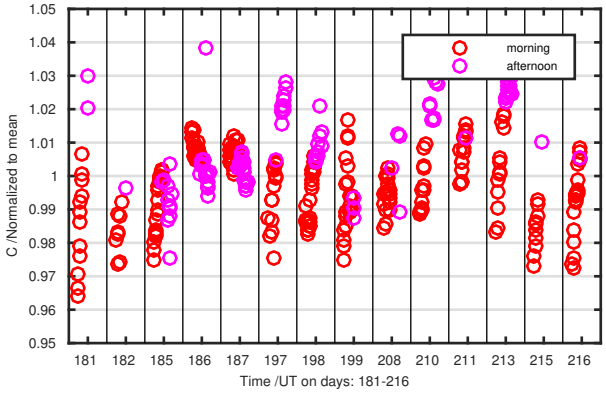

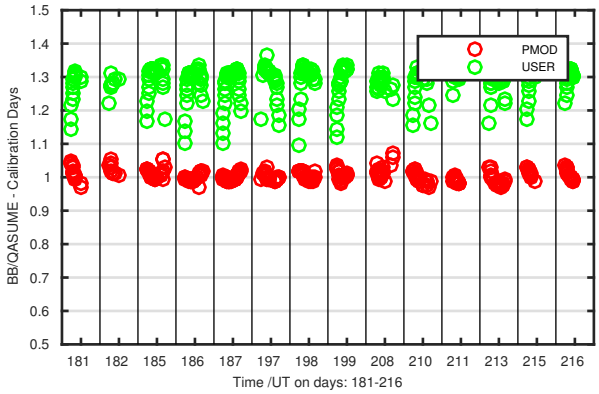

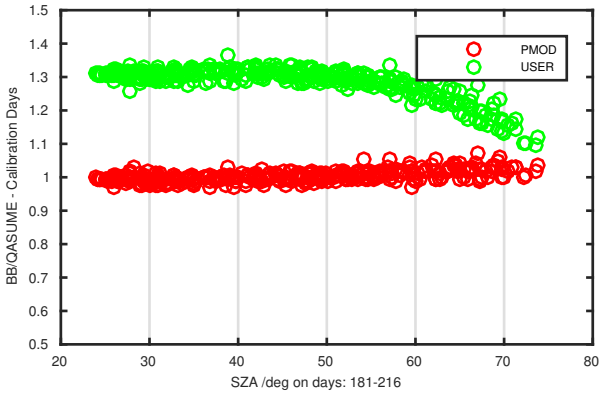

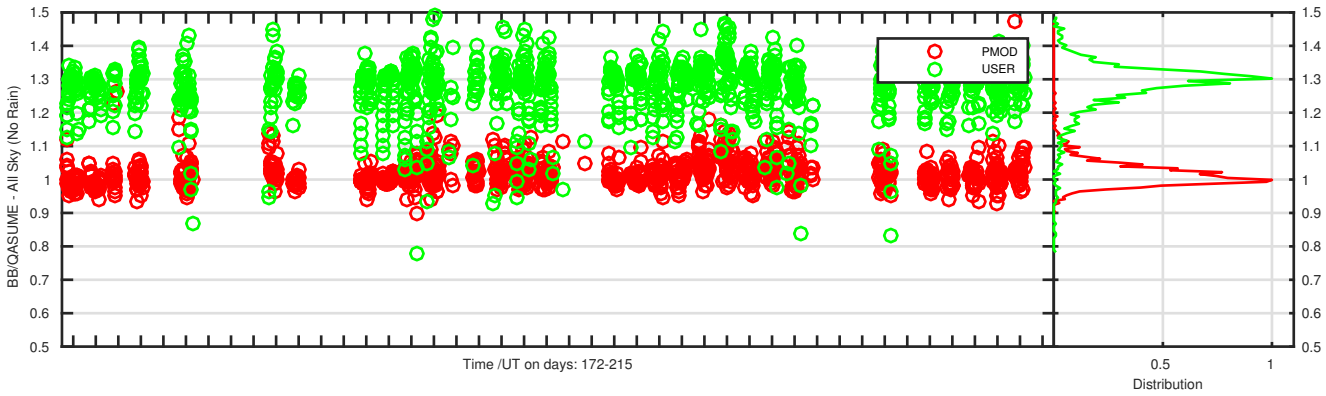

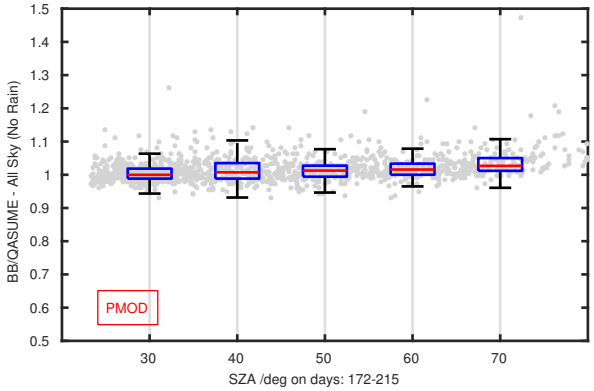

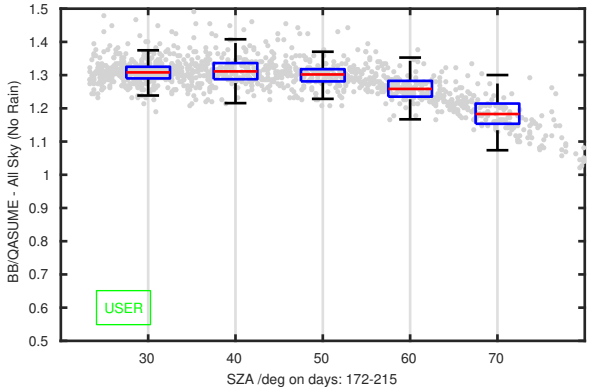

Calibration Results of SL19474 (UVE)

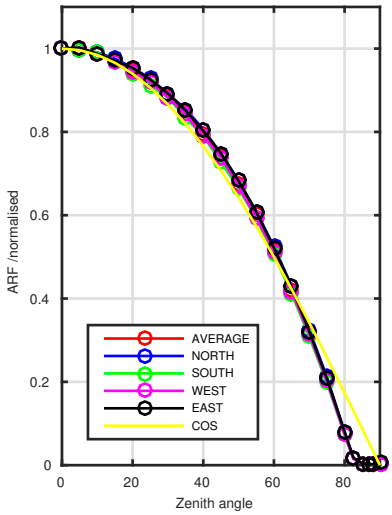

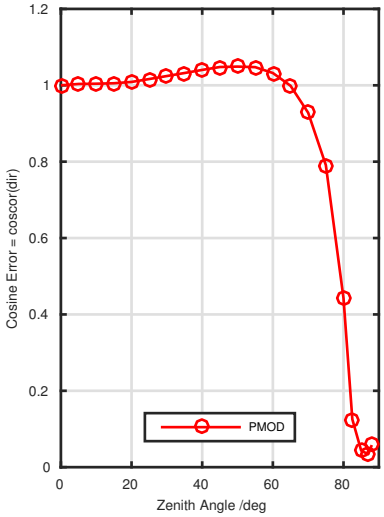

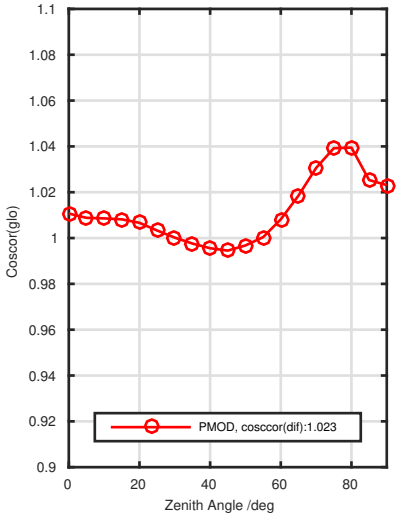

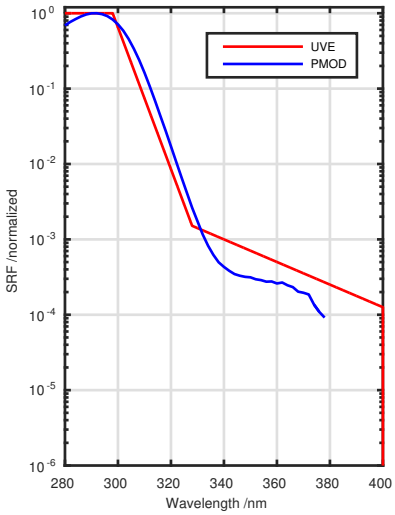

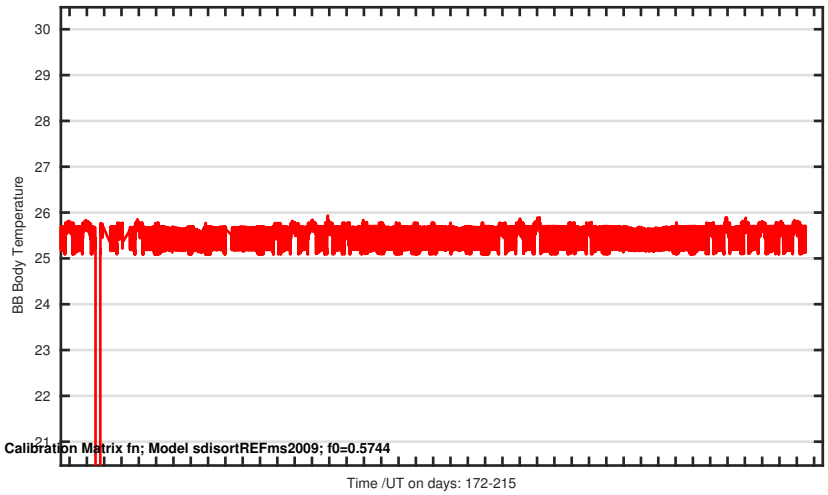

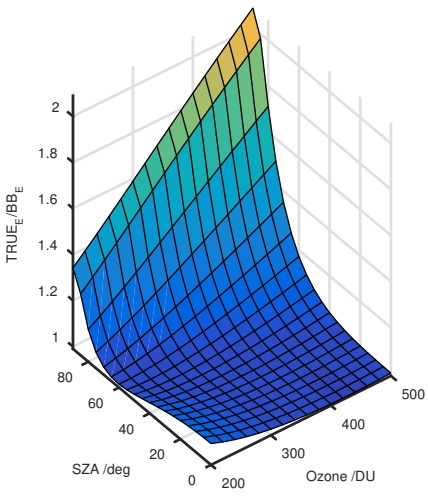

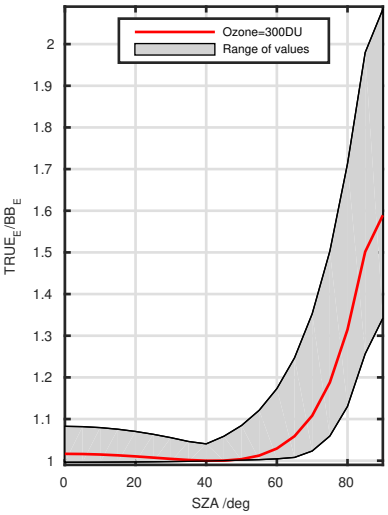

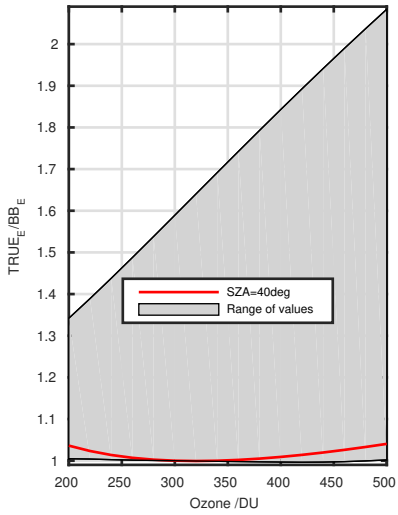

Calibration Results of SL19474 (UVE)

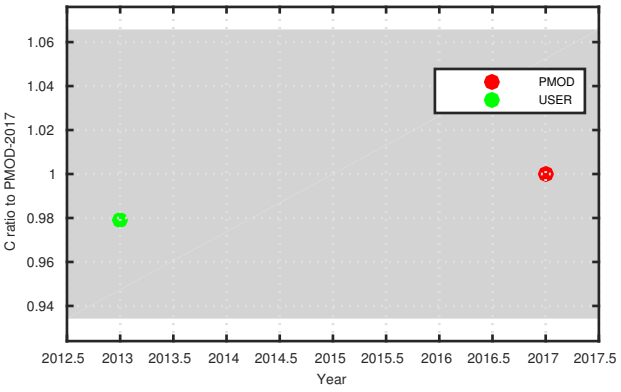

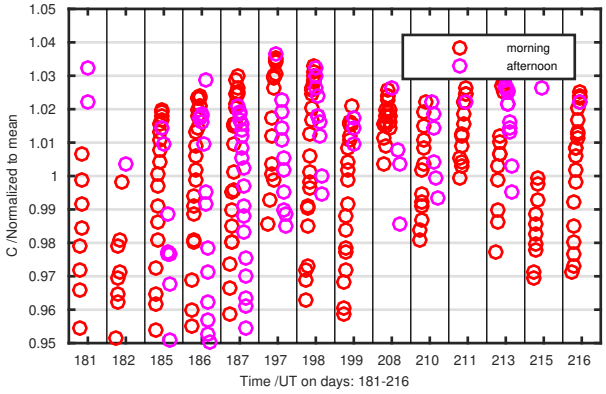

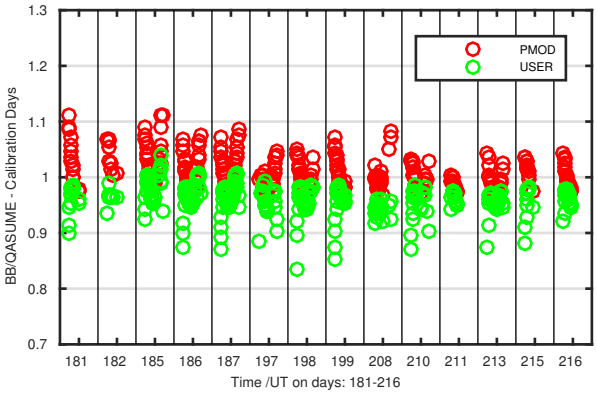

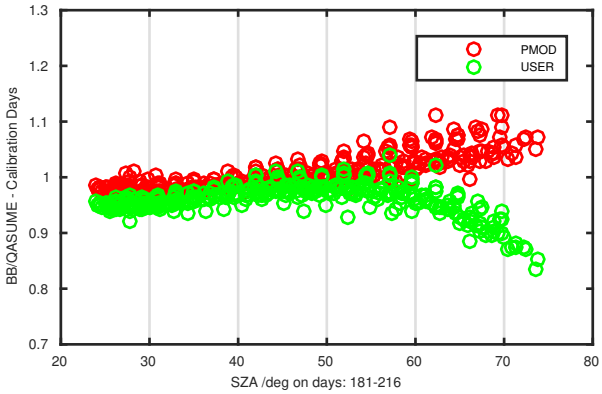

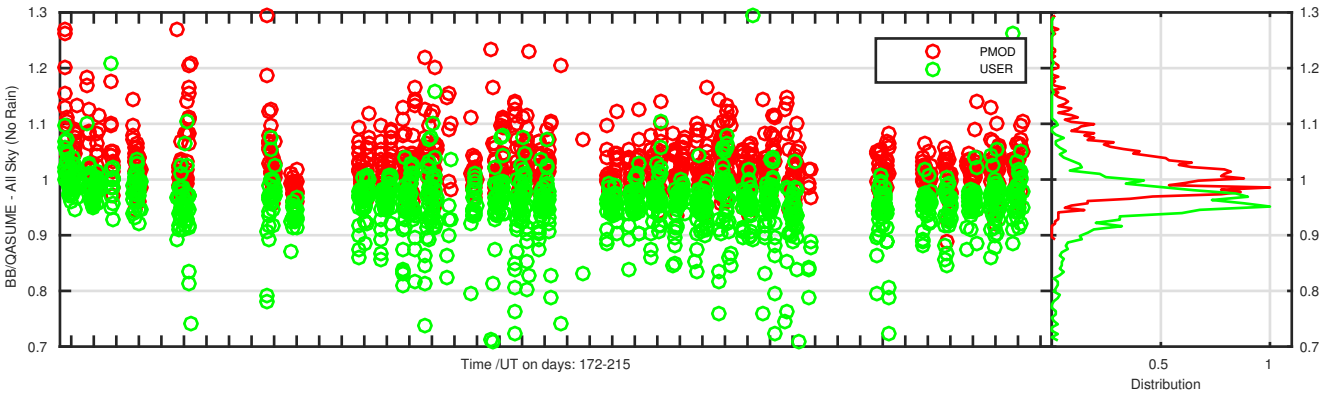

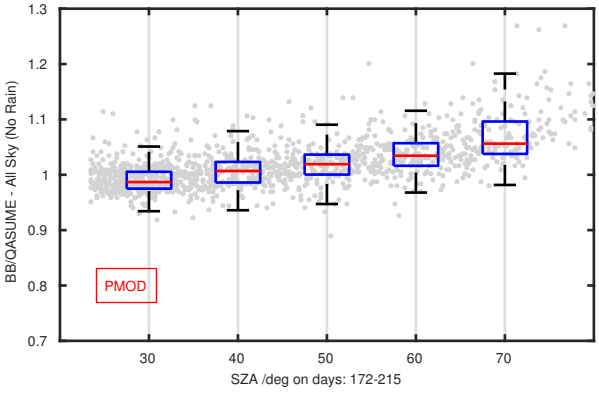

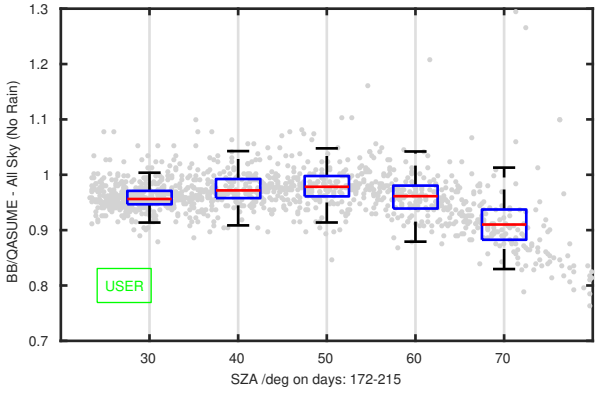

Calibration Results of SL19488 (UVE)

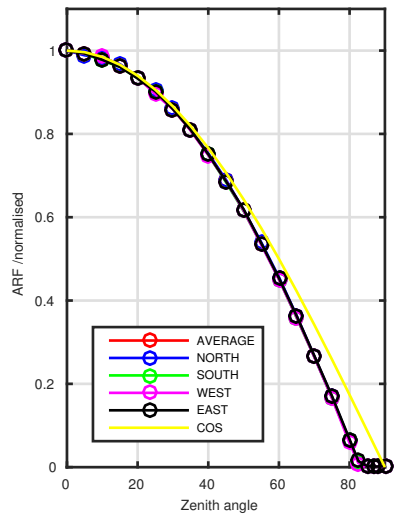

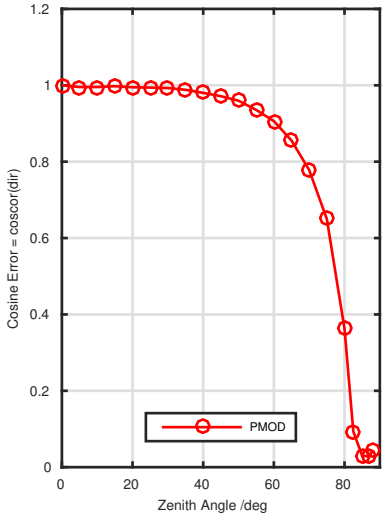

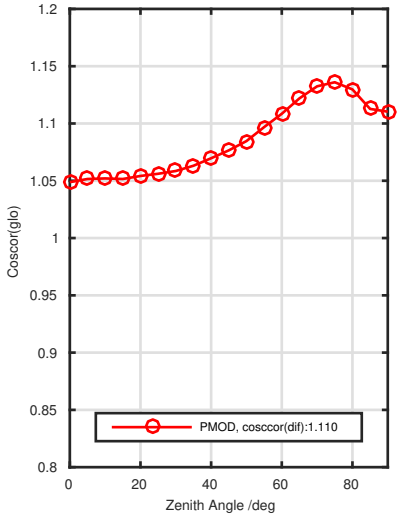

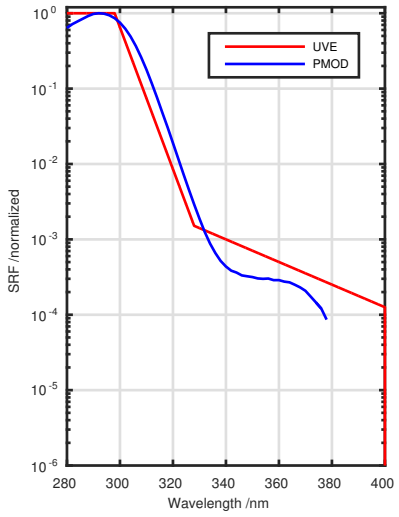

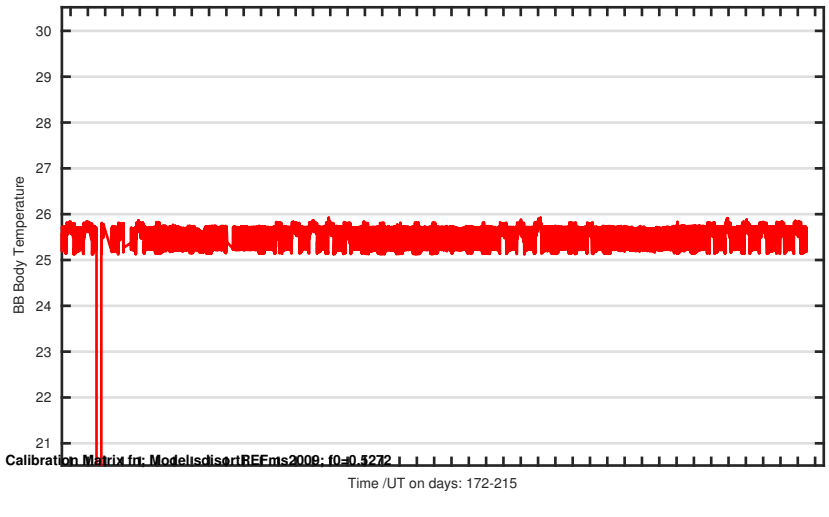

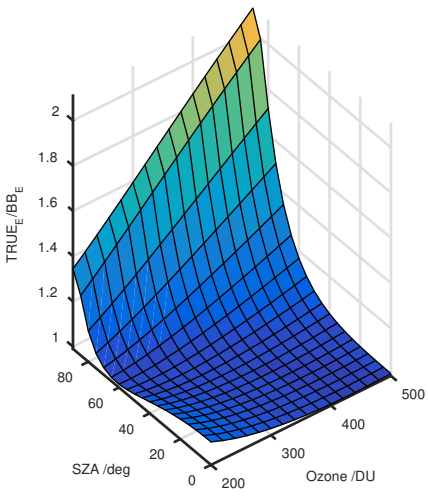

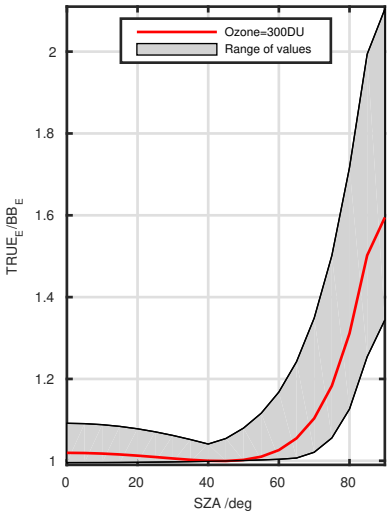

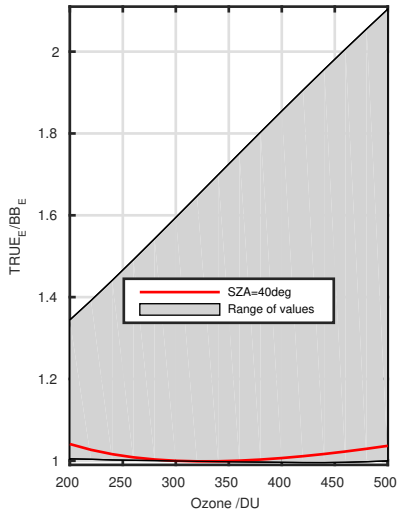

Calibration Results of SL19488 (UVE)

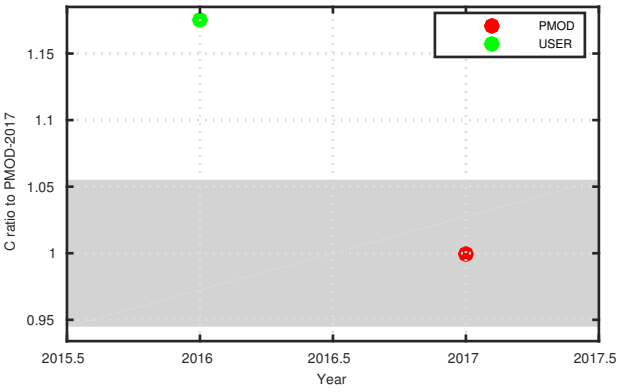

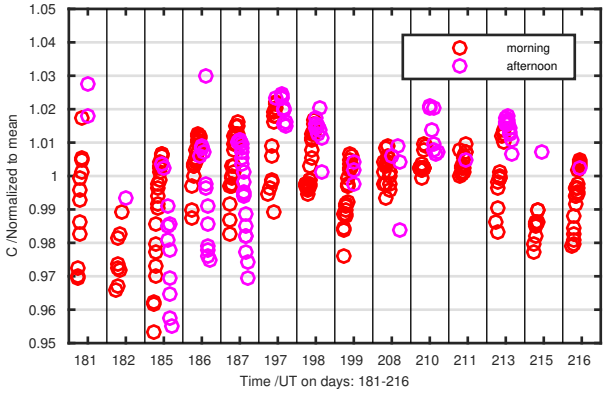

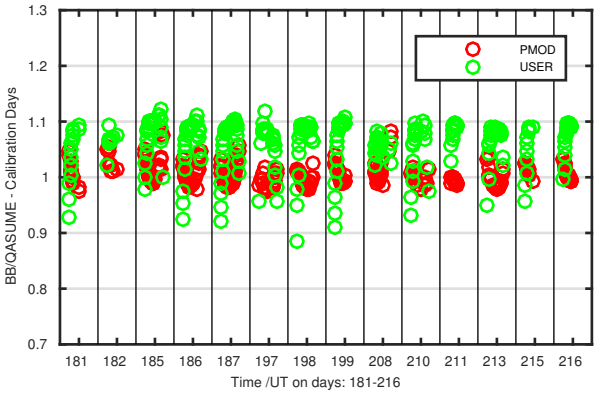

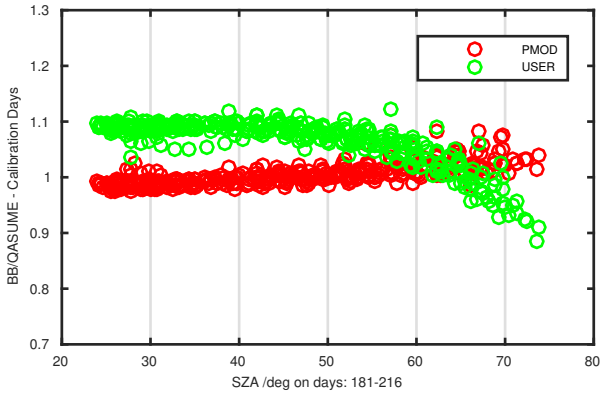

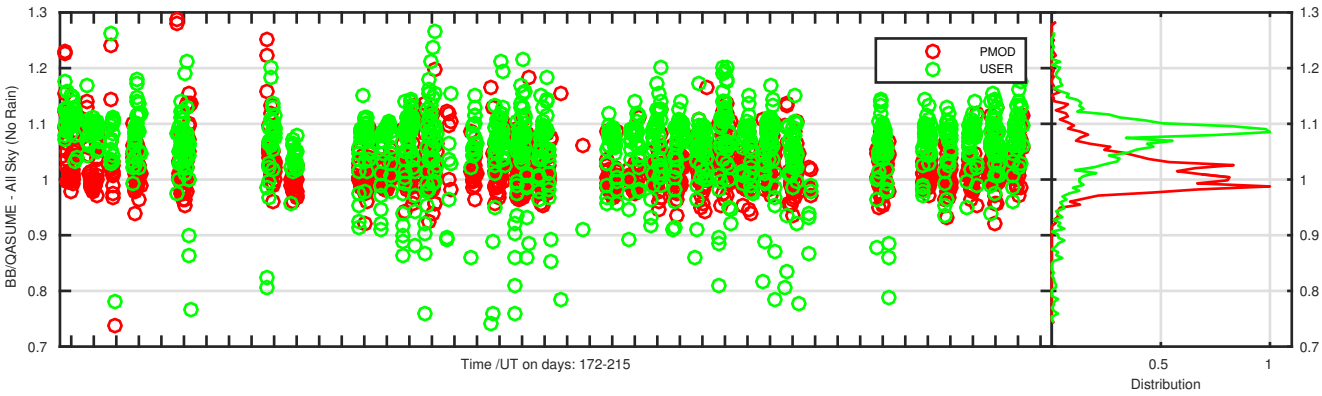

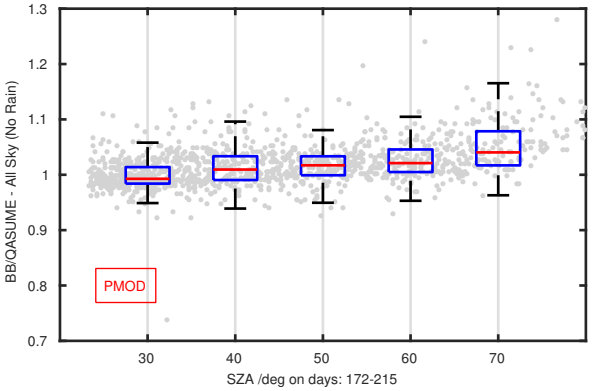

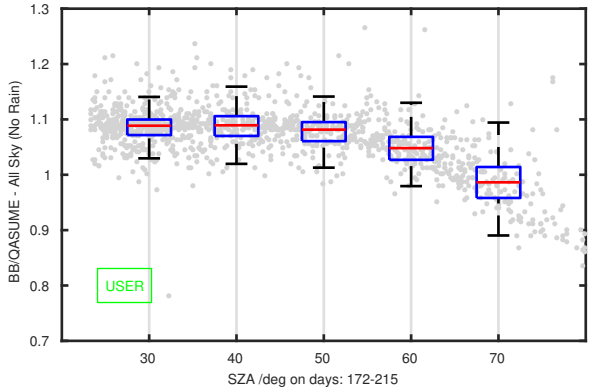

Calibration Results of SL19507 (UVE)

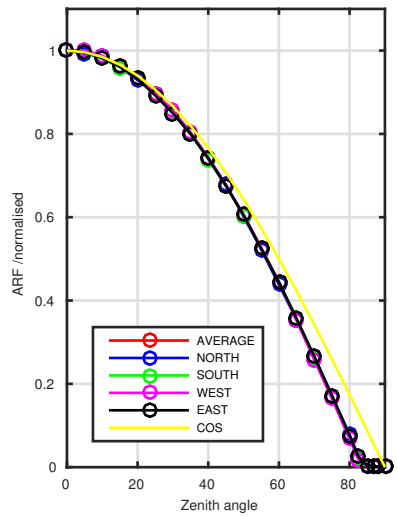

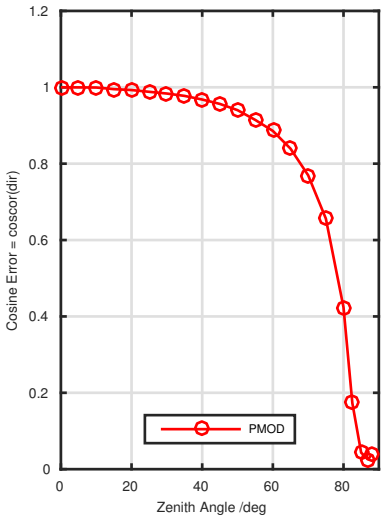

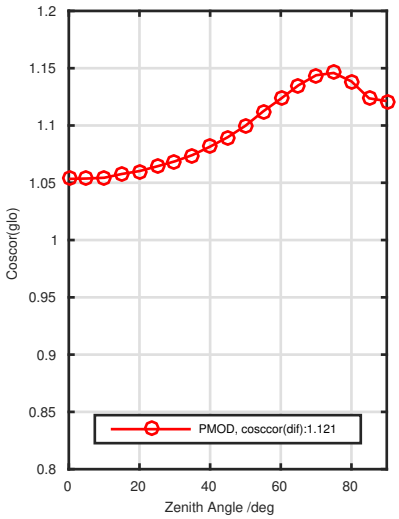

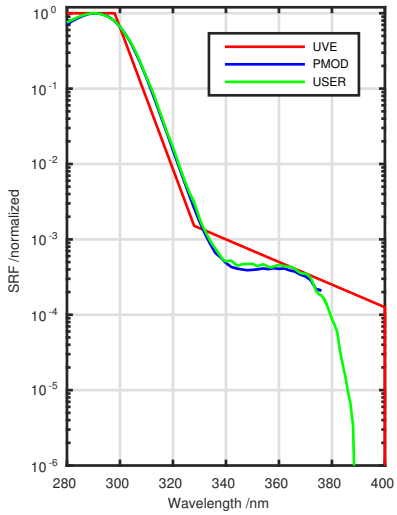

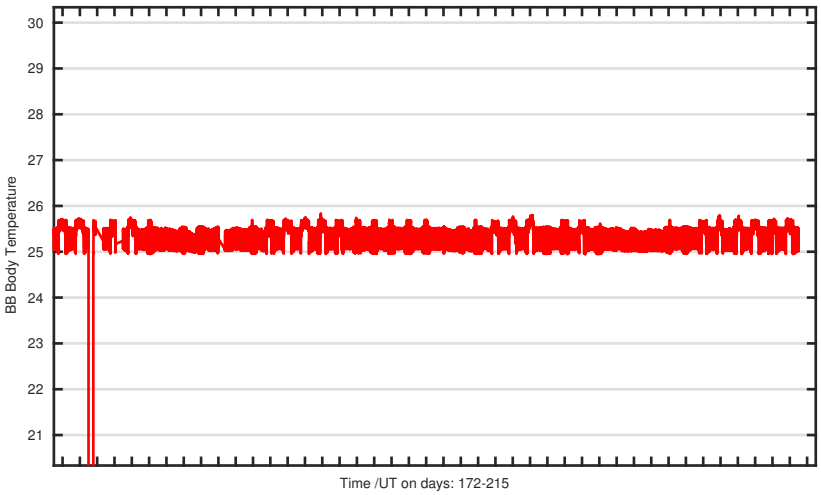

Calibration Matrix fn; Model sdisortREFms2009; f0=0.6467

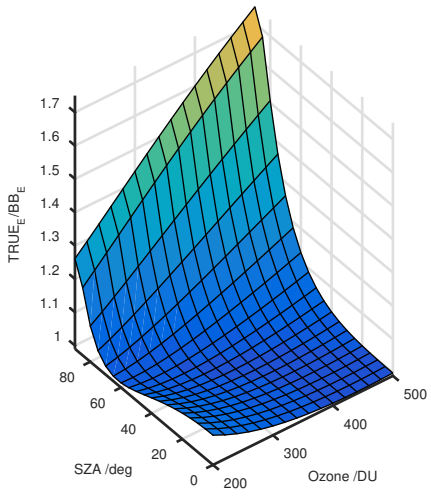

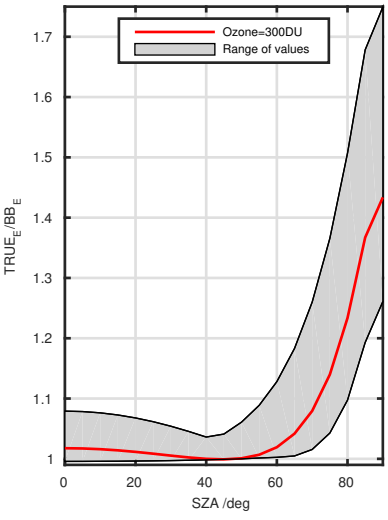

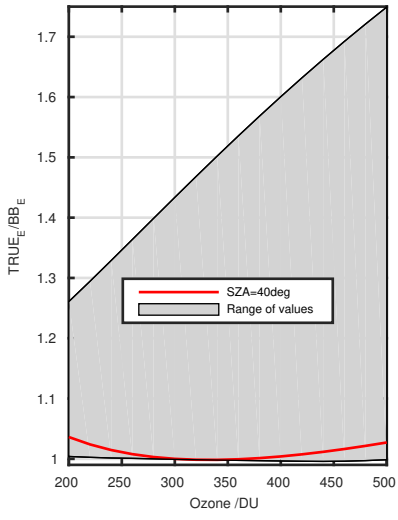

Calibration Results of SL19507 (UVE)

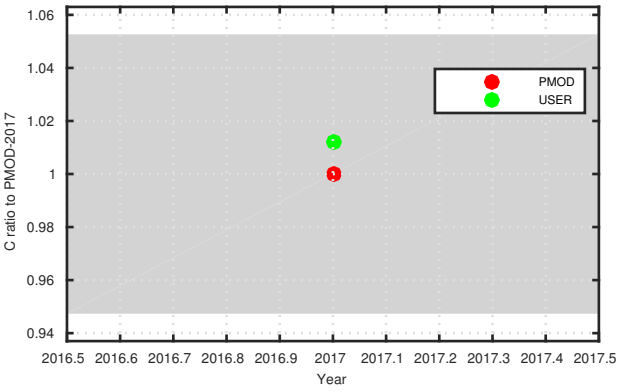

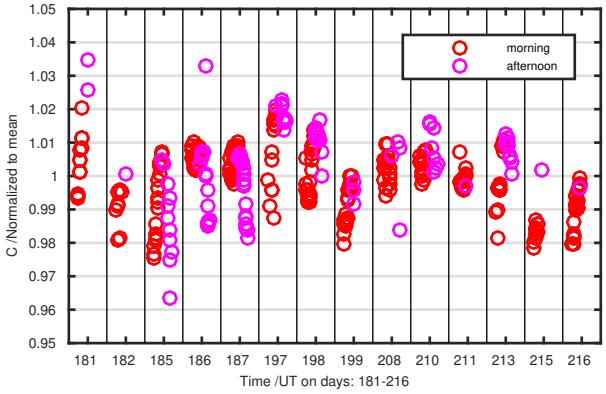

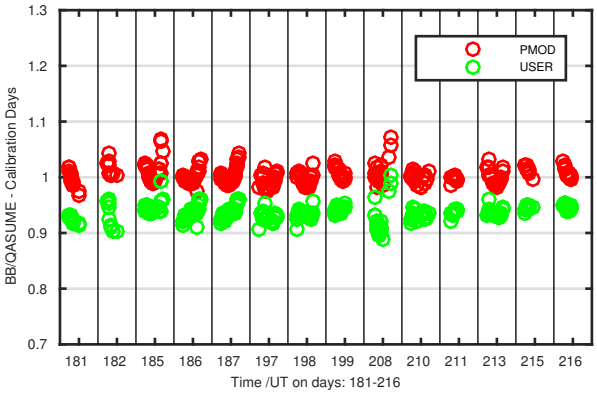

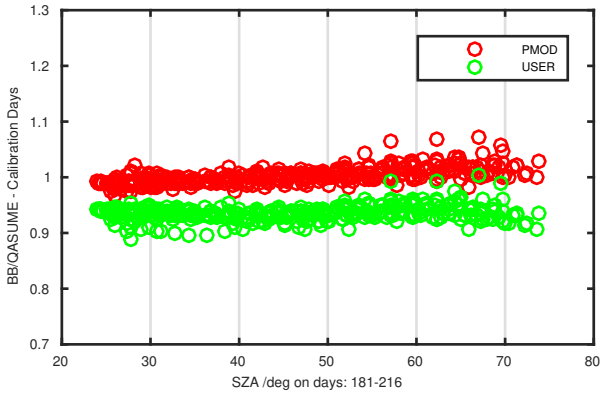

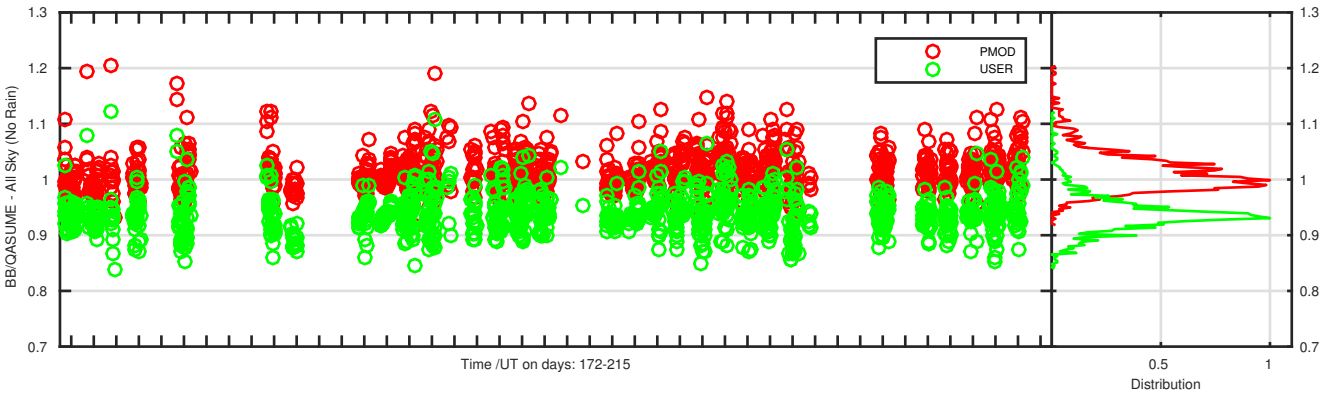

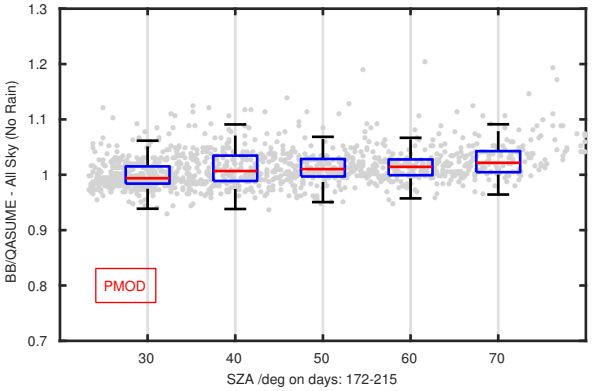

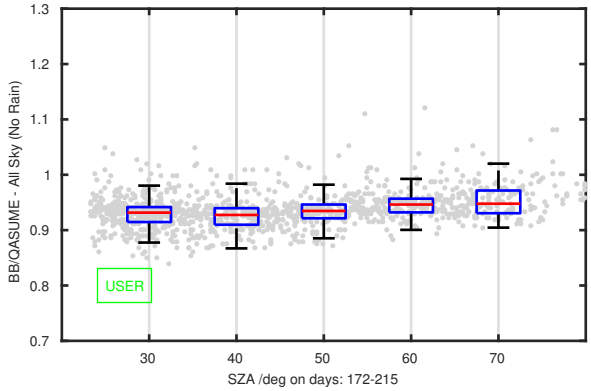

Calibration Results of SL23148 (UVE)

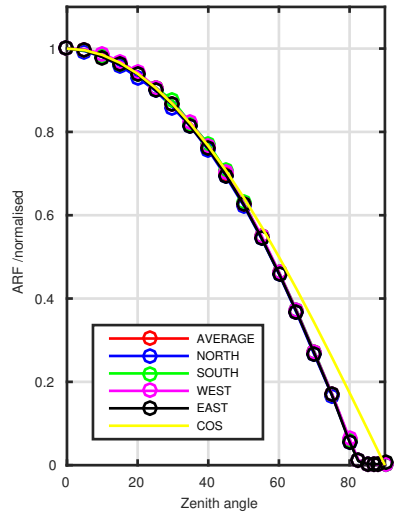

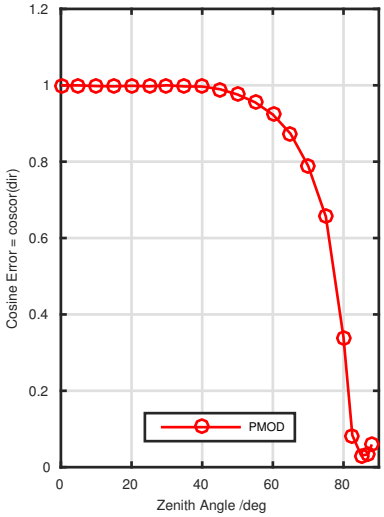

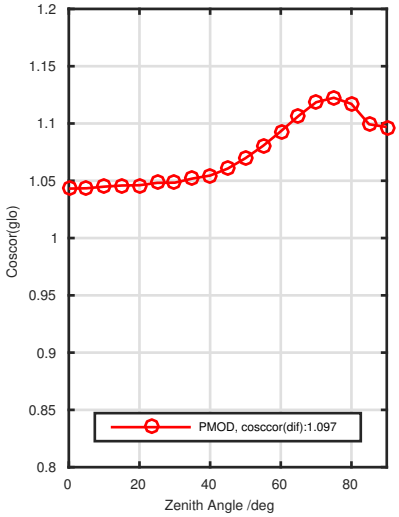

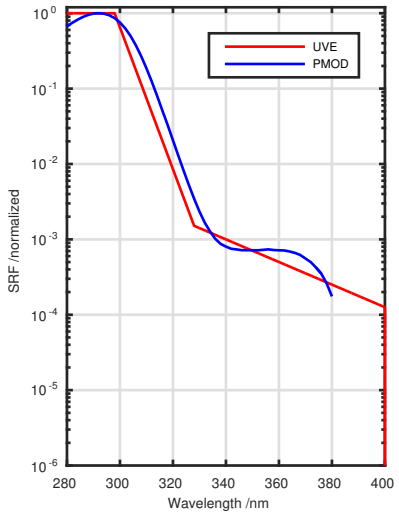

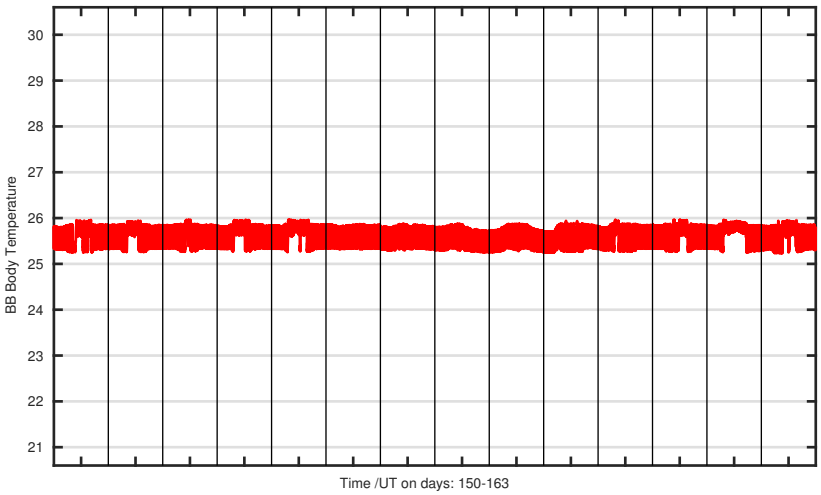

Calibration Matrix fn; Model sdisortREFms2009; f0=0.4874

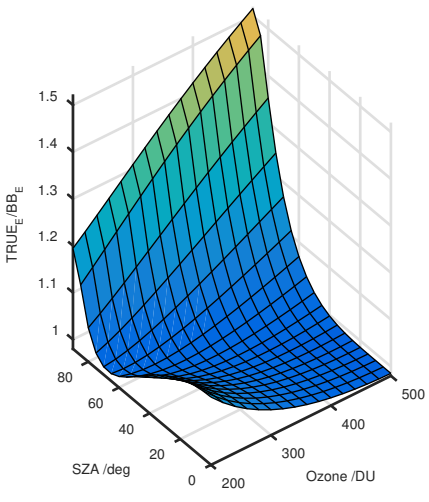

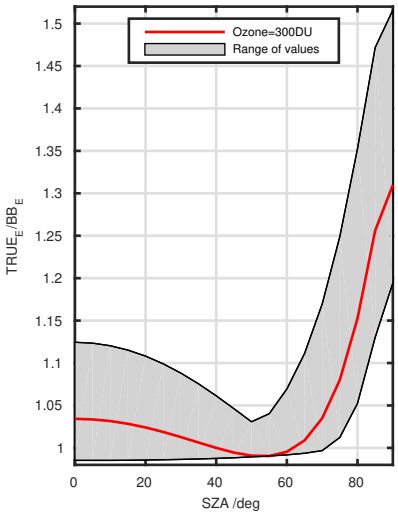

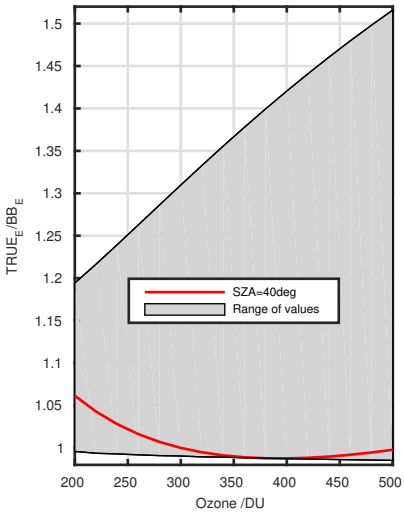

Calibration Results of SL23148 (UVE)

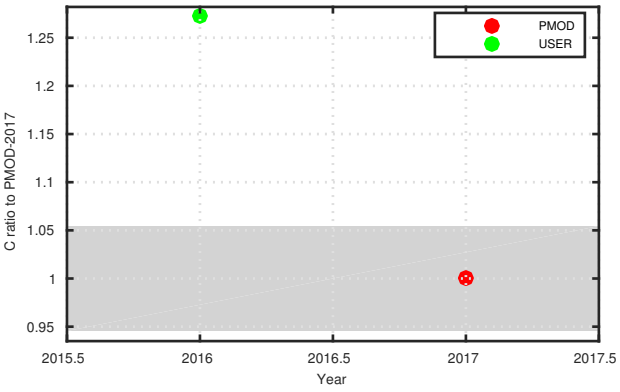

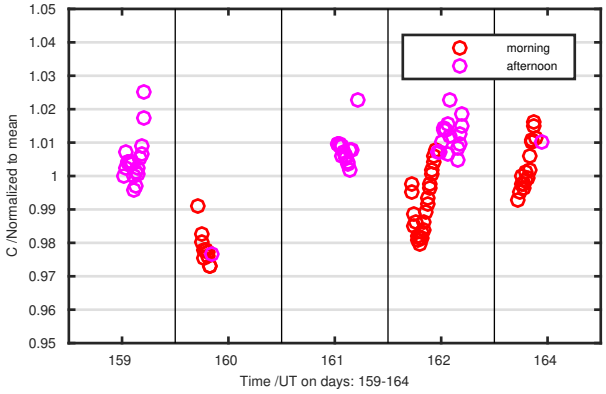

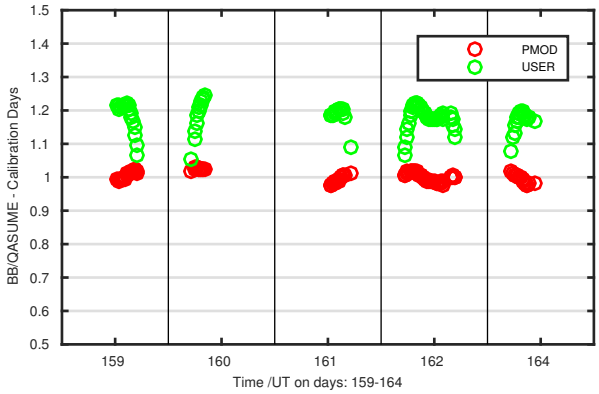

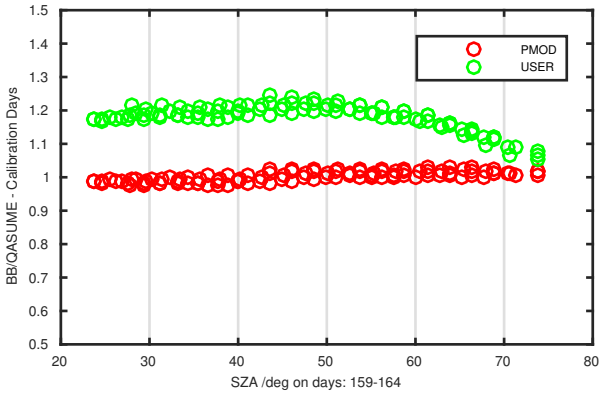

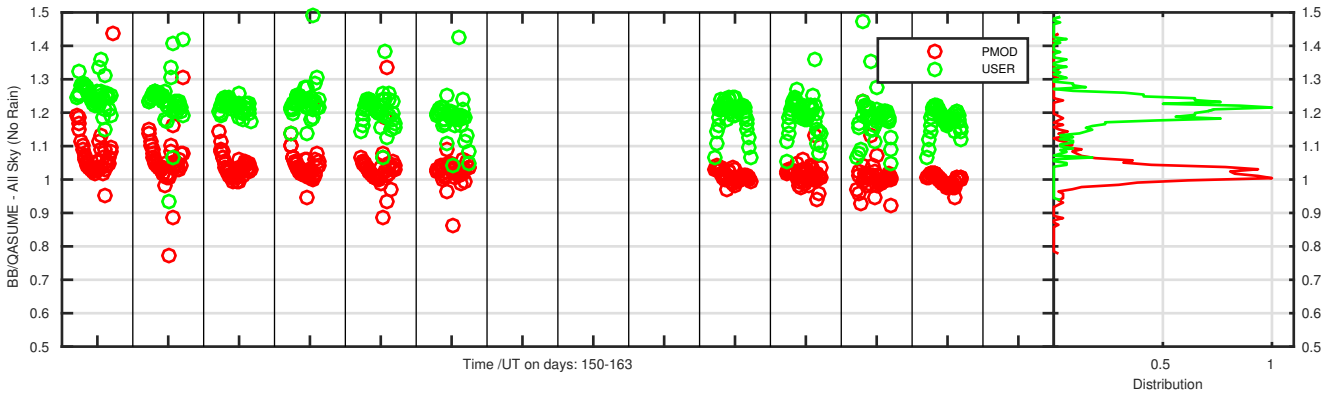

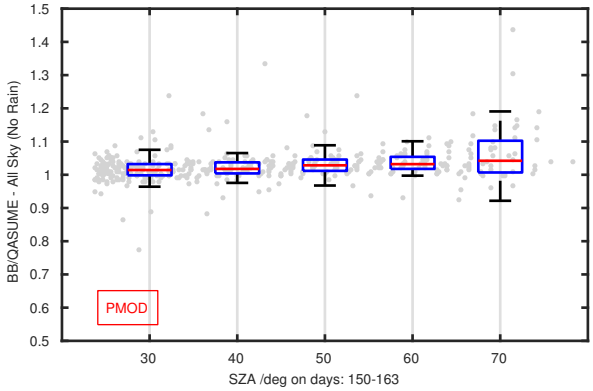

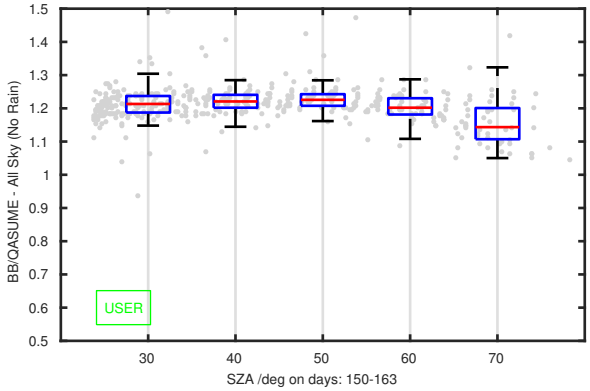

Calibration Results of SL0922 (UVE)

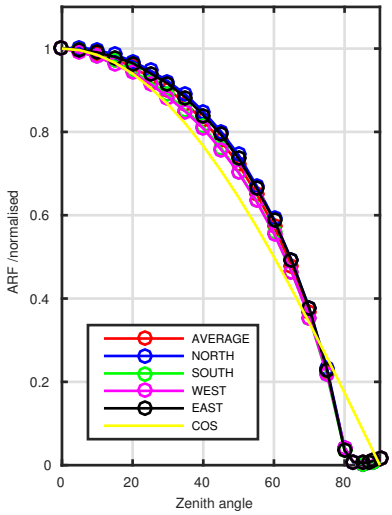

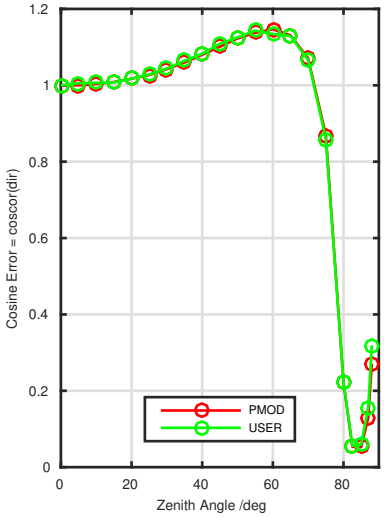

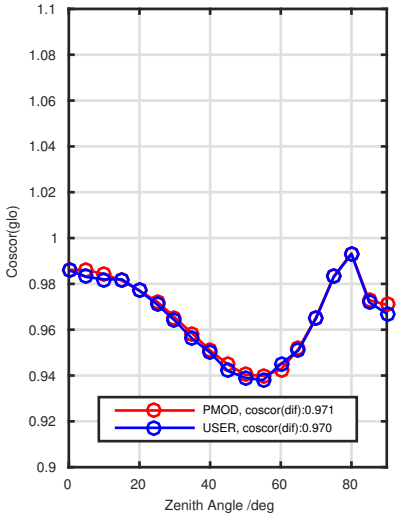

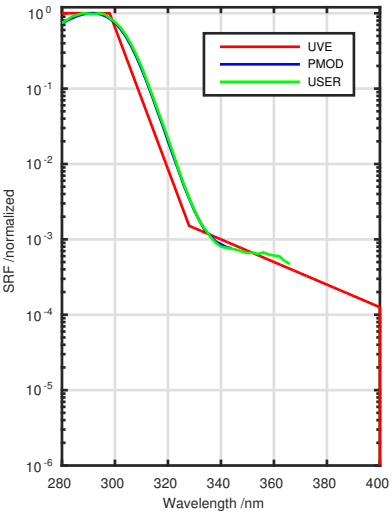

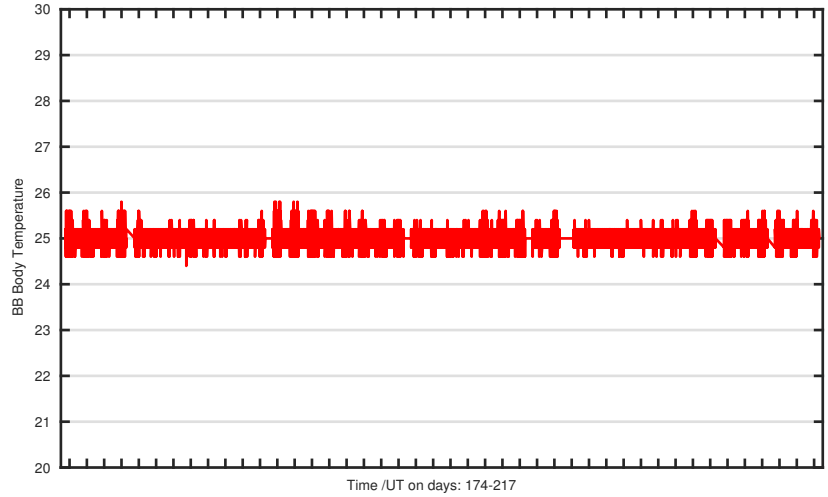

Calibration Matrix fn; Model sdisortREFms2009; f0=0.5098

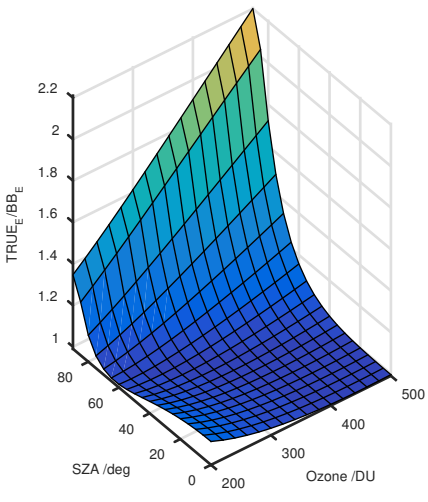

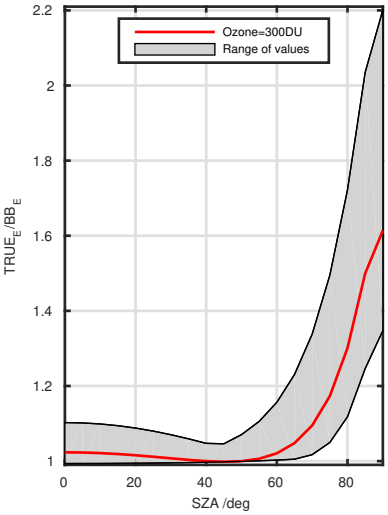

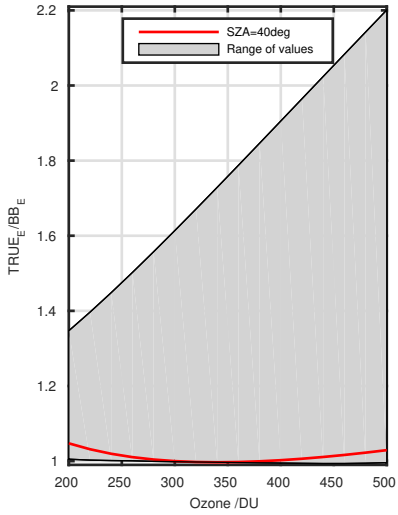

Calibration Results of SL0922 (UVE)

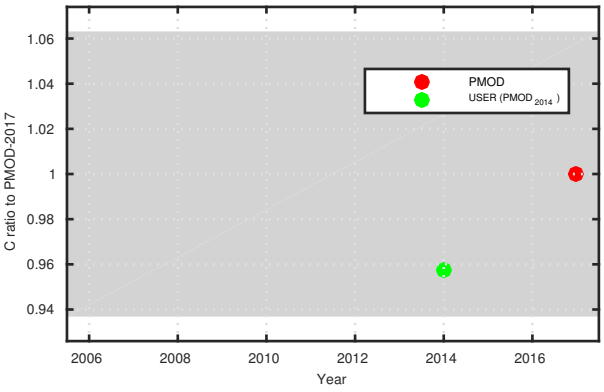

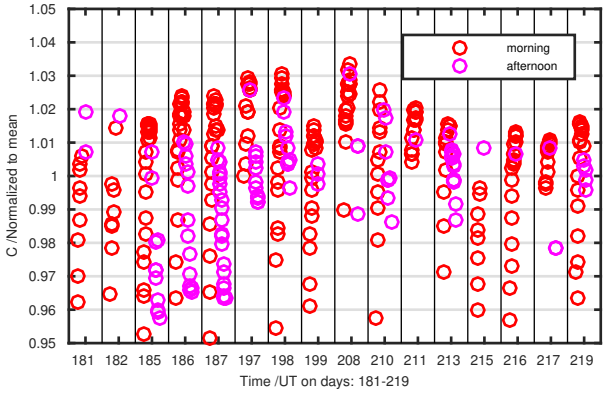

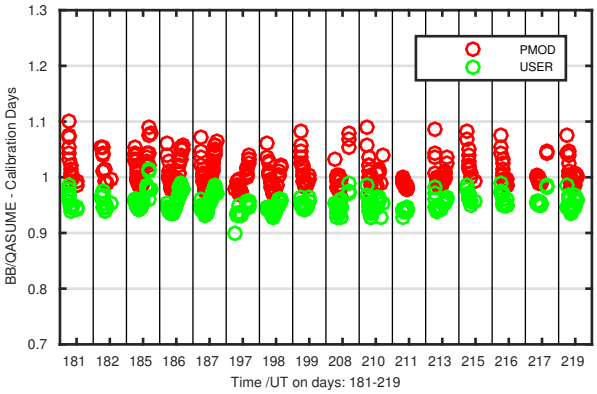

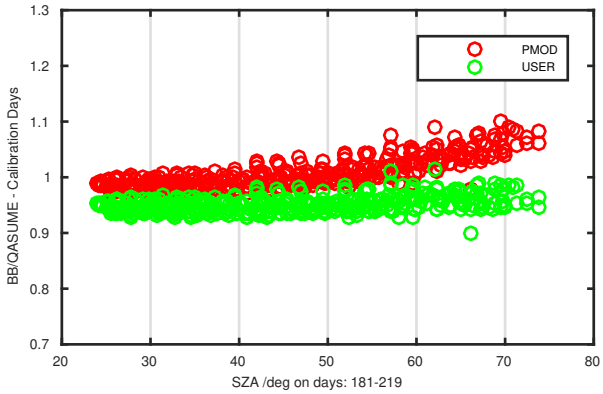

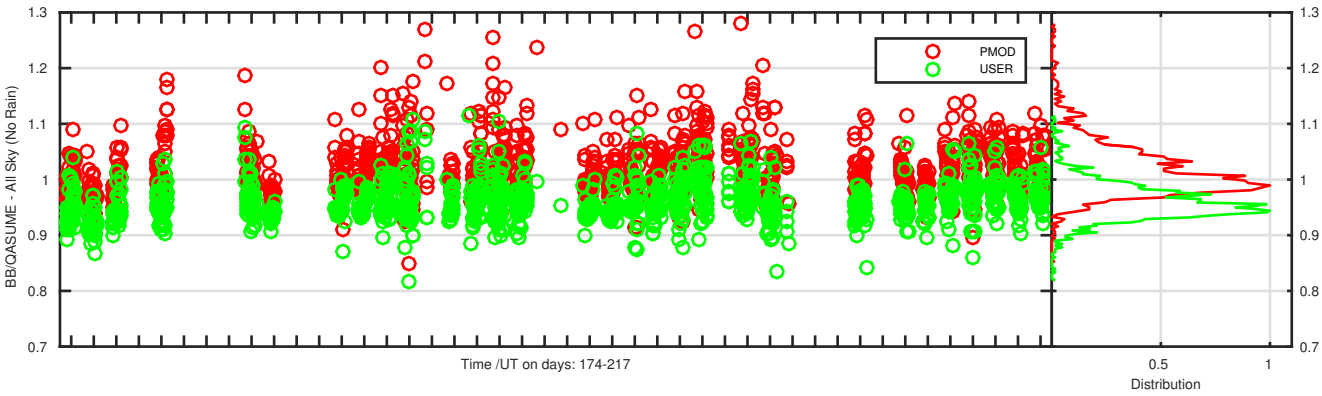

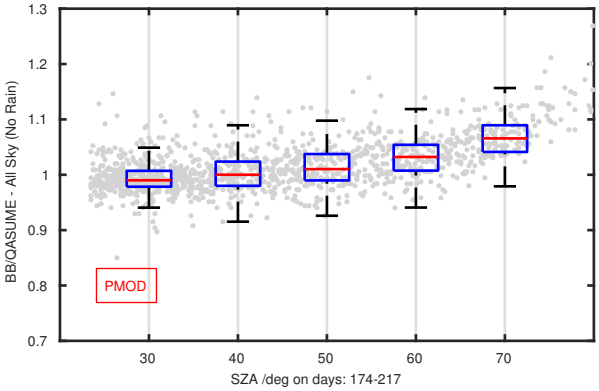

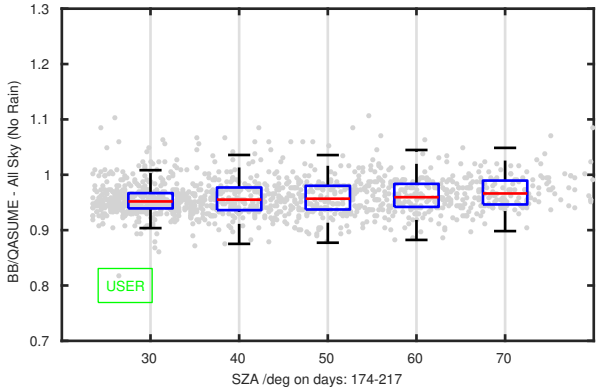

Calibration Results of SL0936 (UVE)

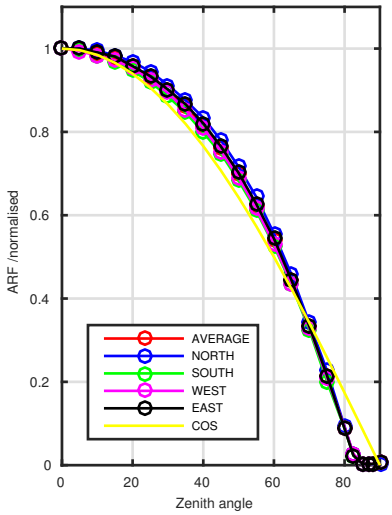

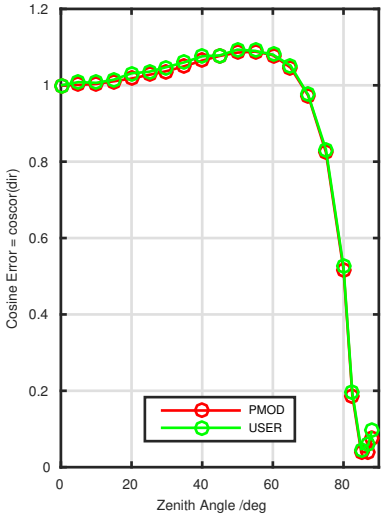

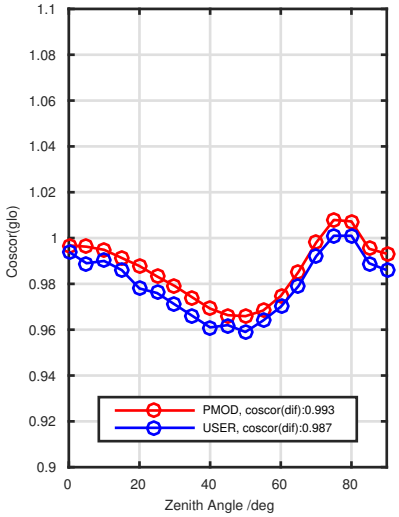

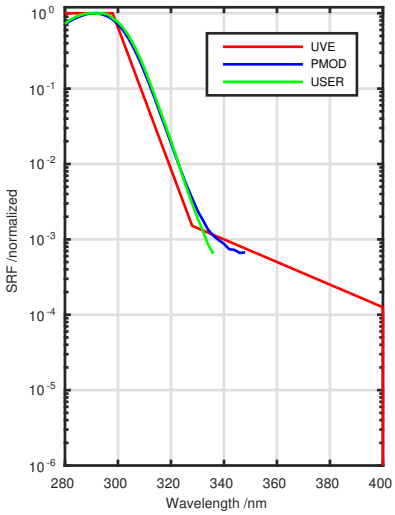

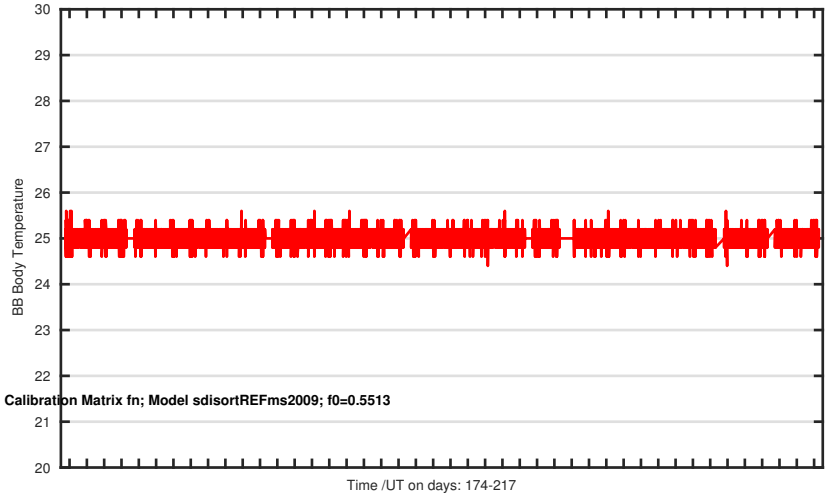

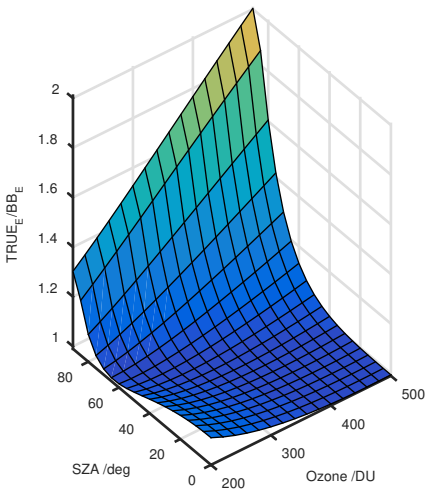

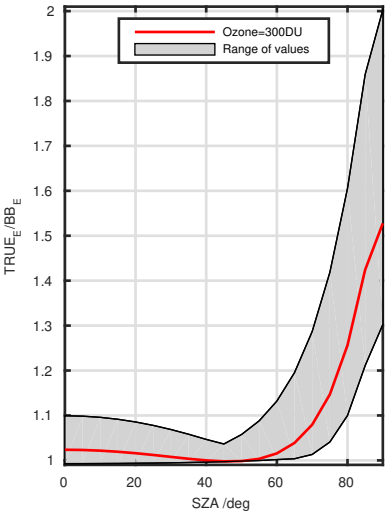

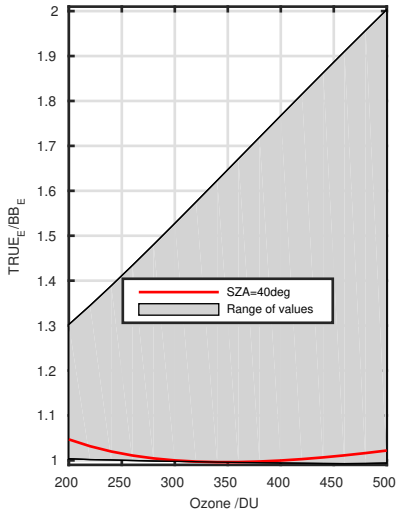

Calibration Results of SL0936 (UVE)

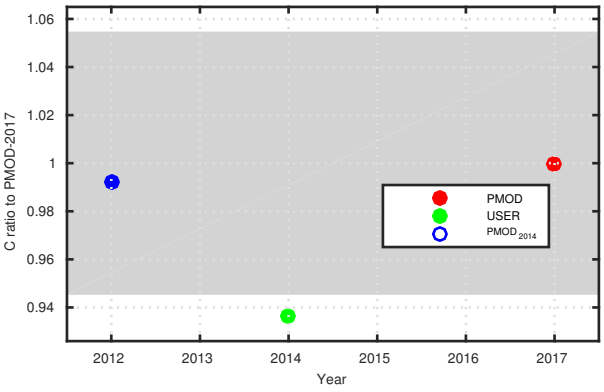

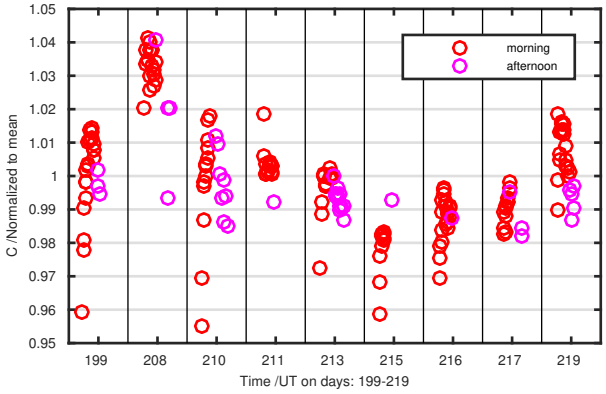

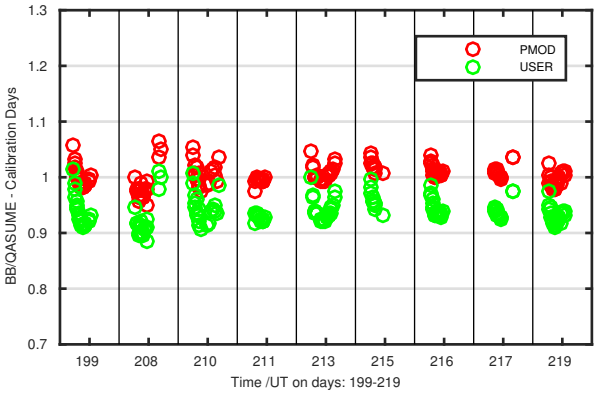

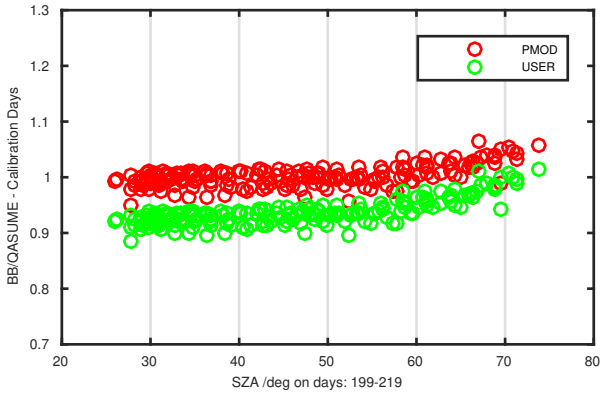

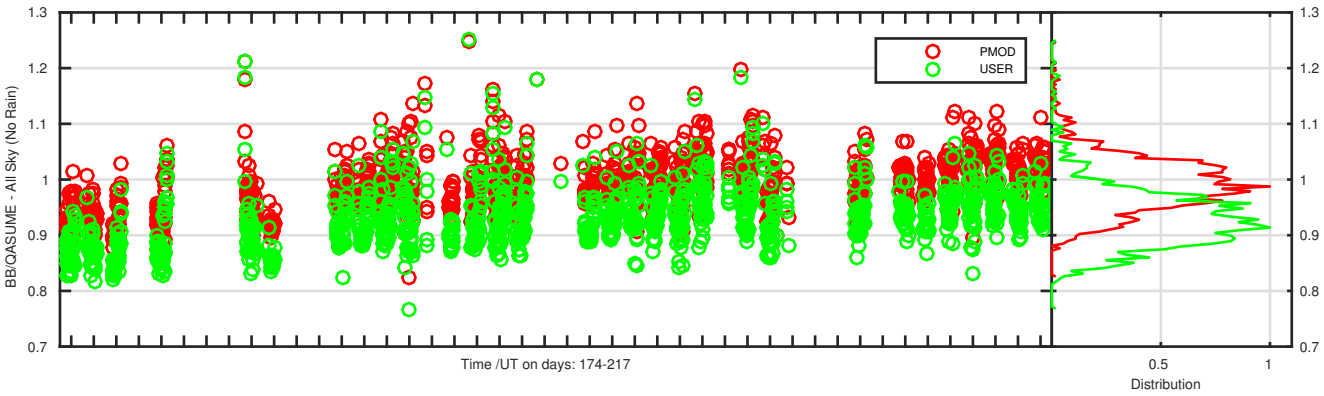

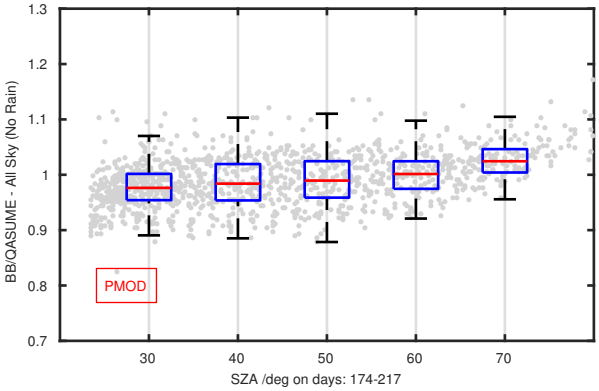

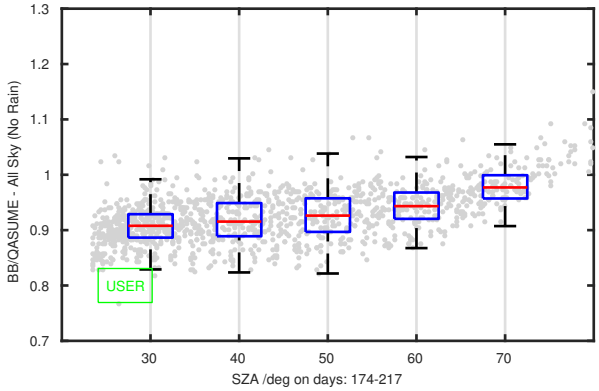

Calibration Results of SL1119 (UVE)

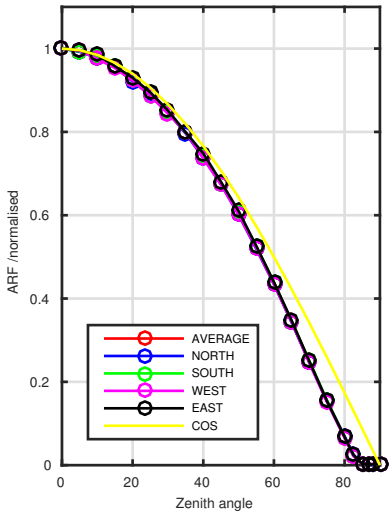

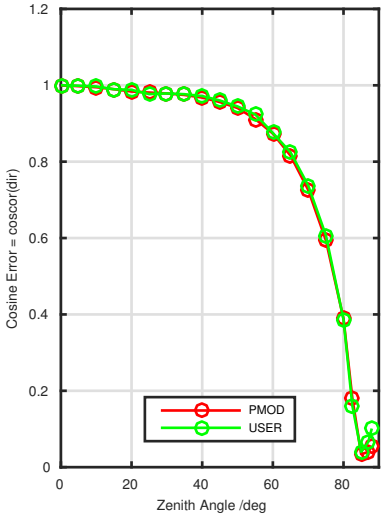

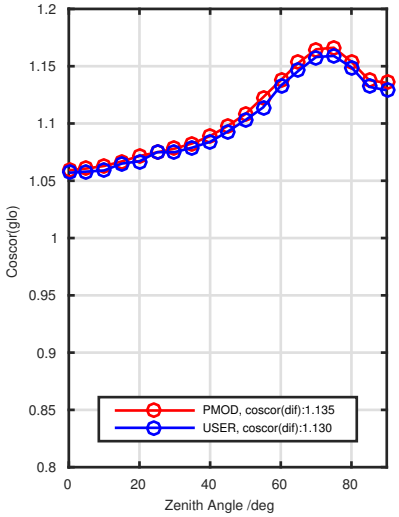

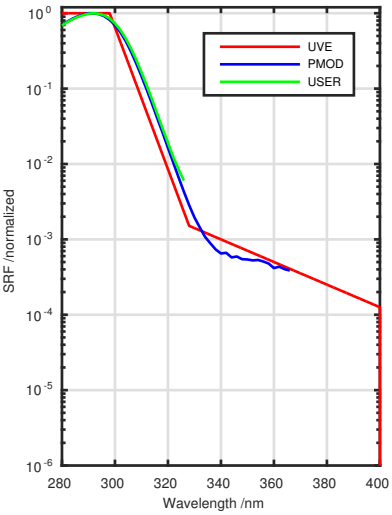

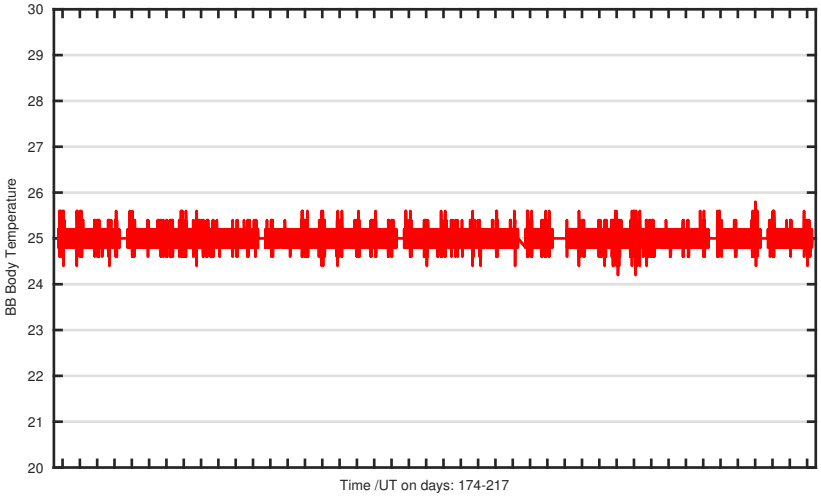

Calibration Matrix fn; Model sdisortREFms2009; f0=0.6097

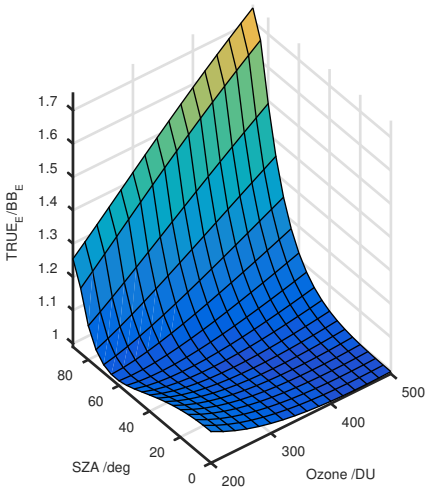

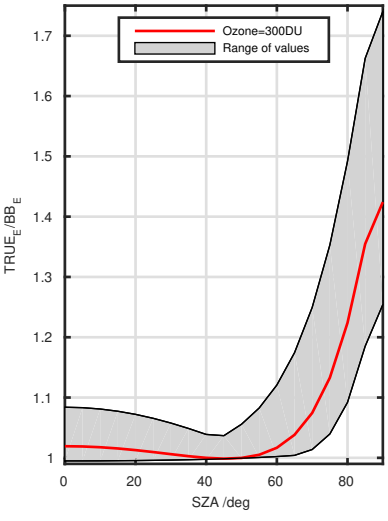

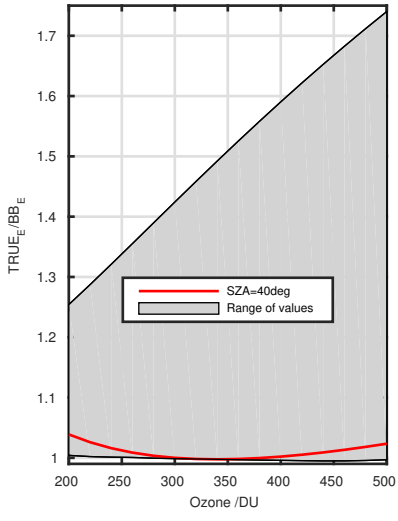

Calibration Results of SL1119 (UVE)

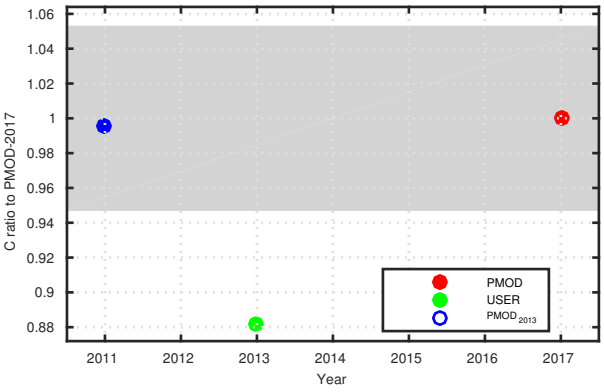

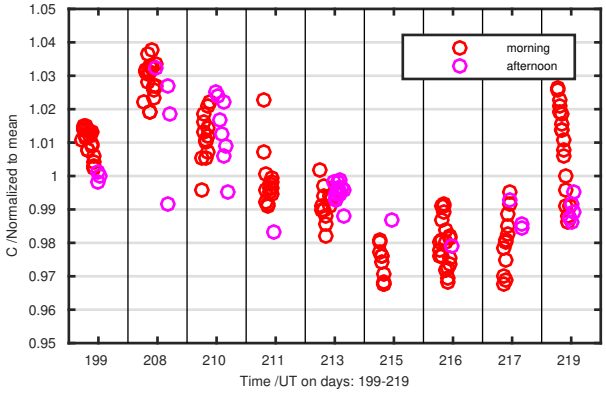

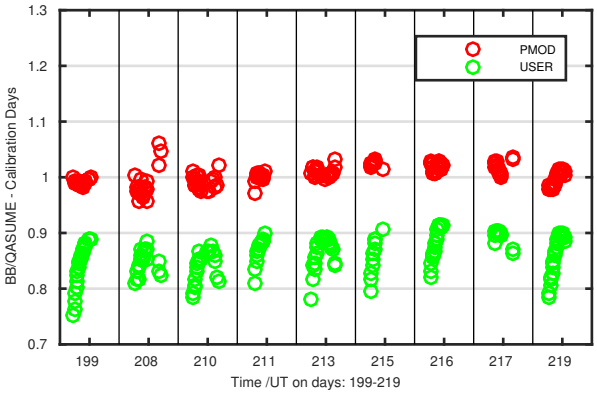

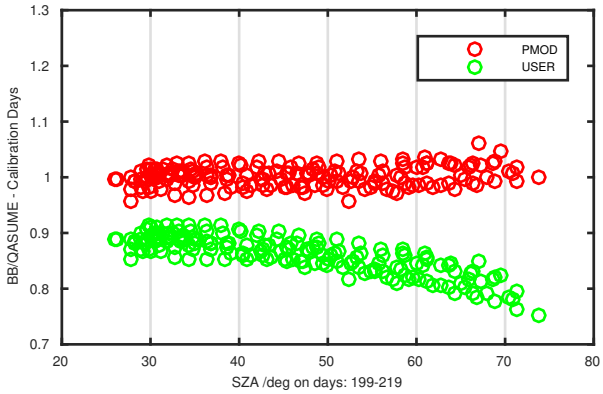

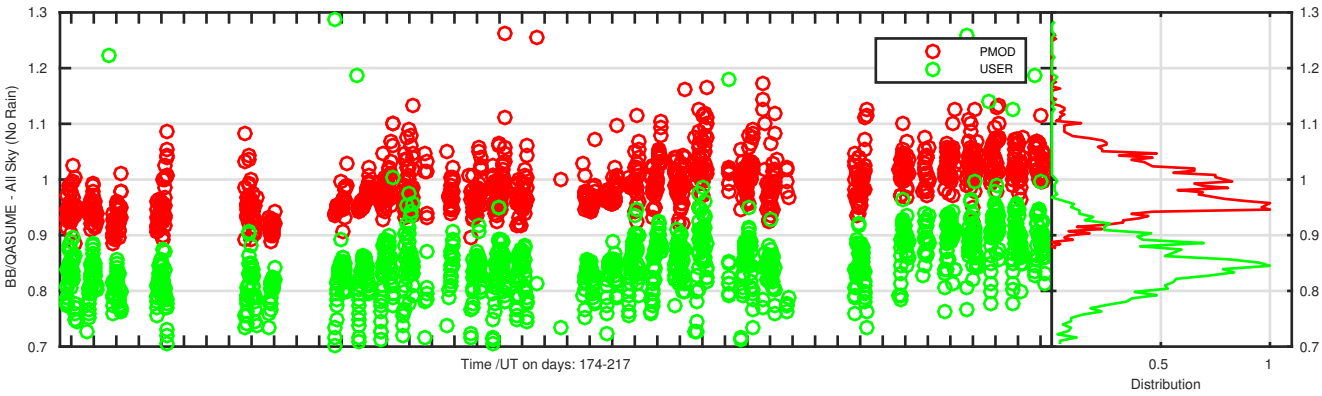

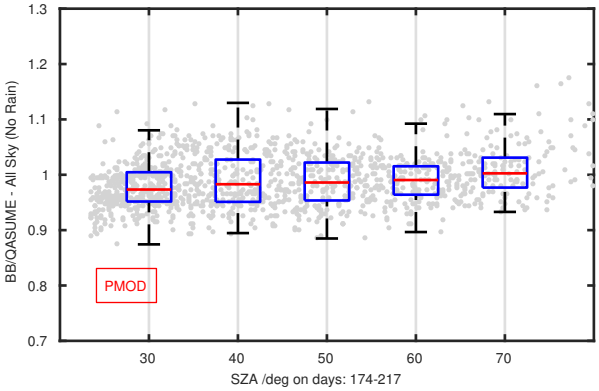

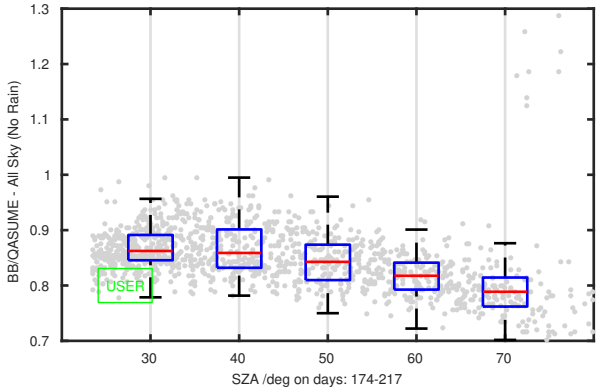

Calibration Results of SL2733 (UVE)

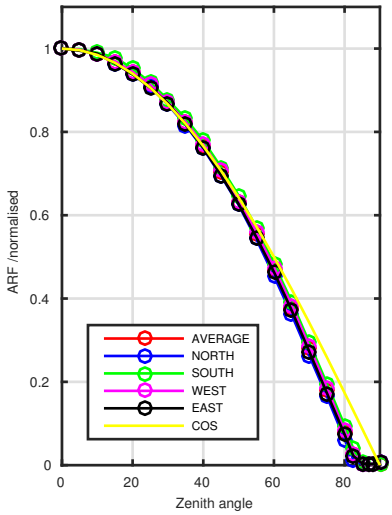

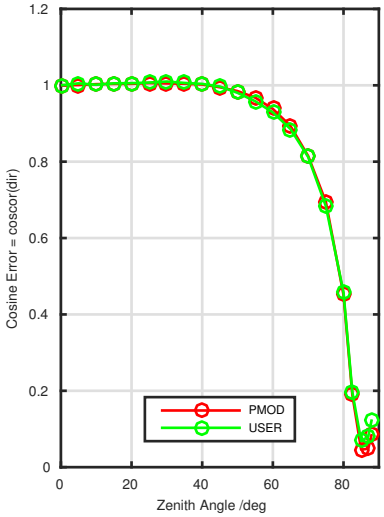

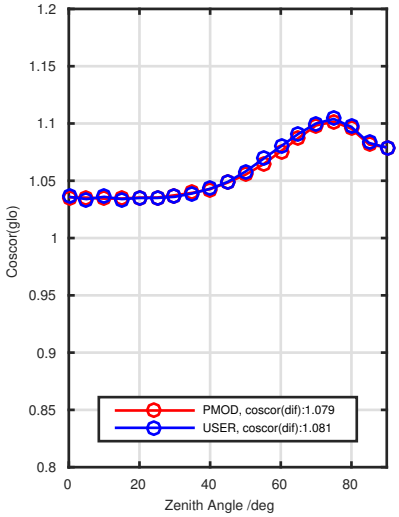

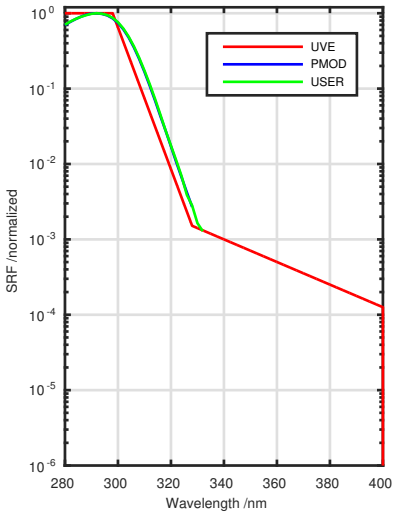

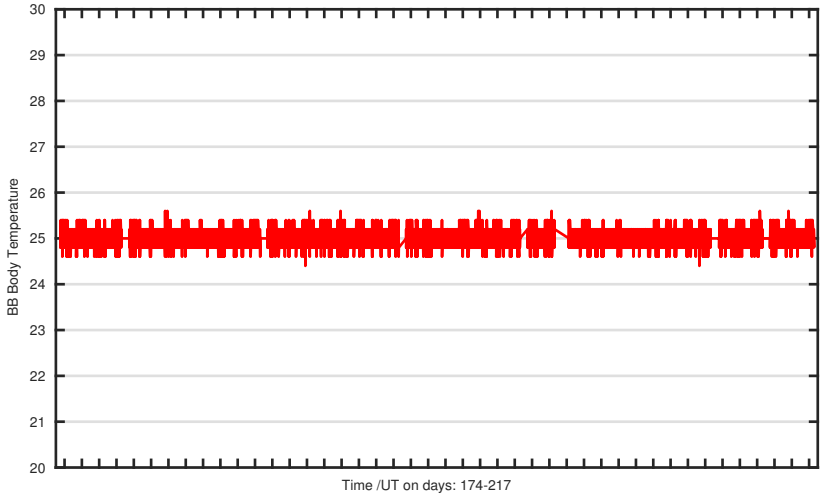

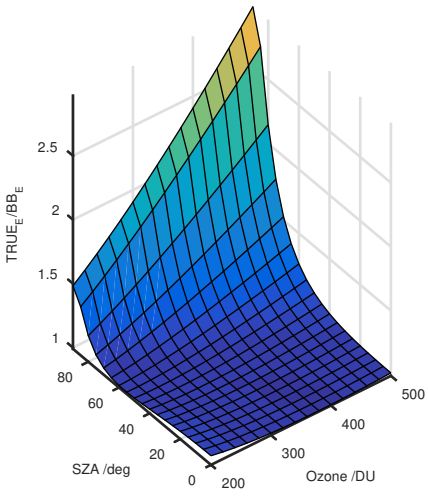

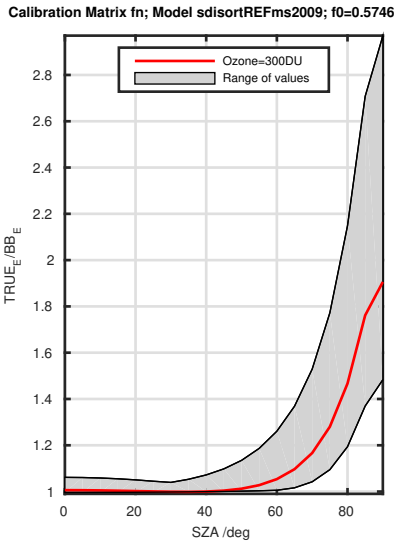

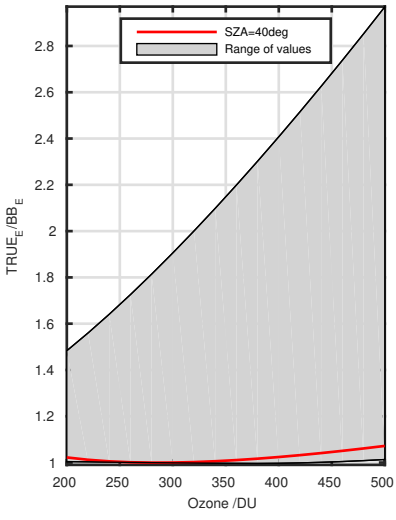

Calibration Results of SL2733 (UVE)

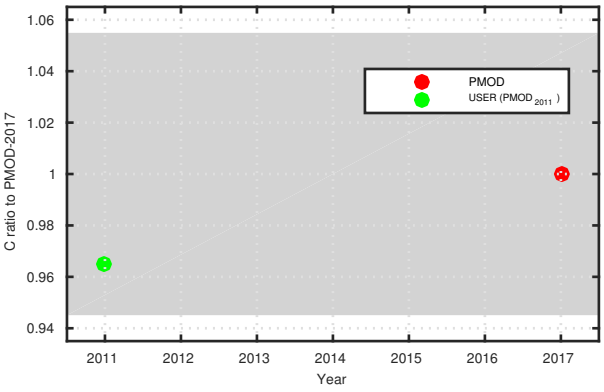

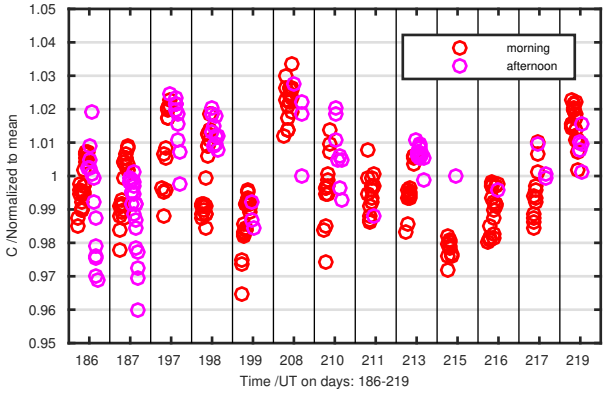

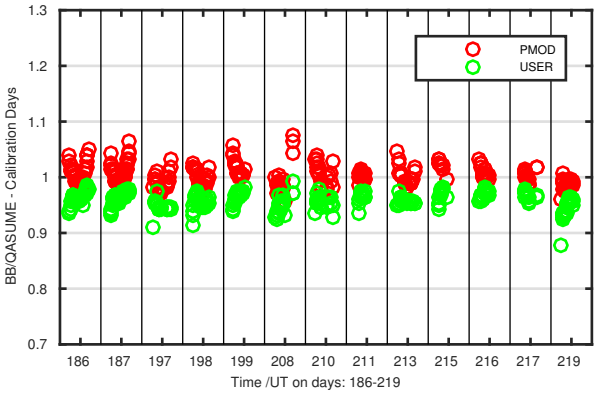

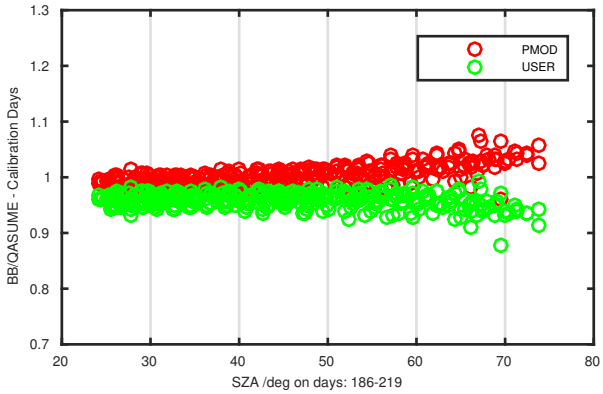

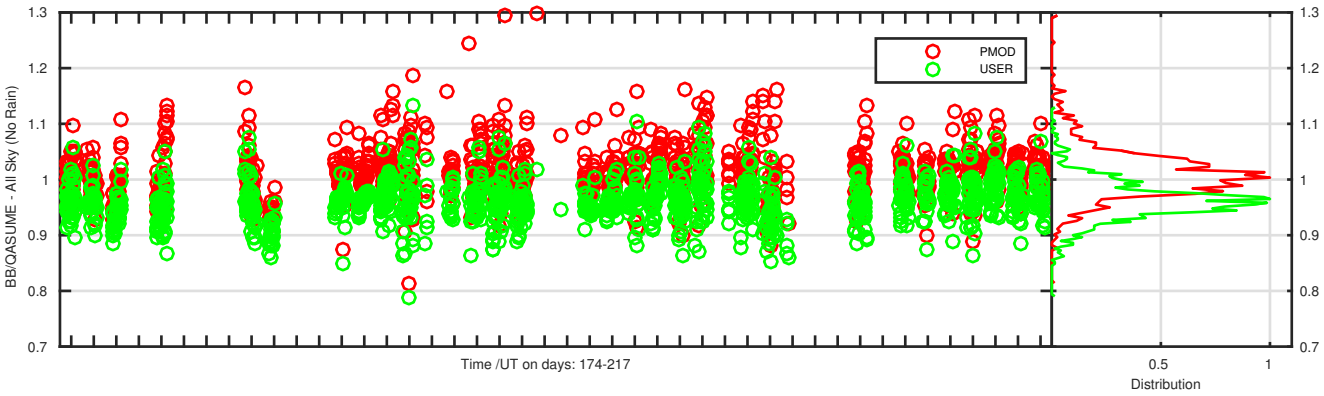

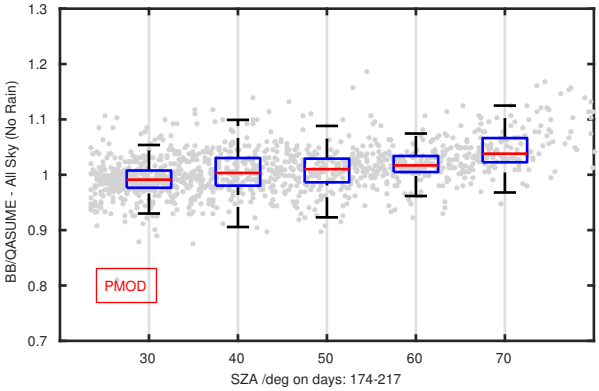

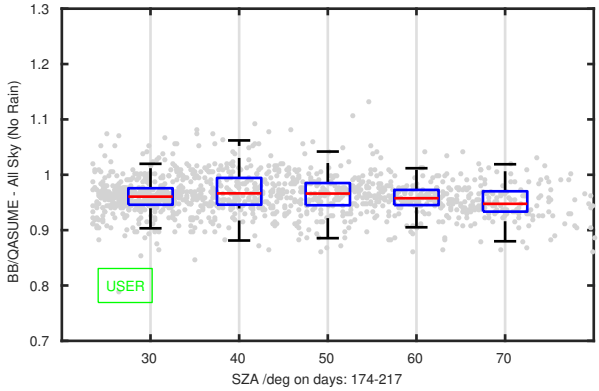

Calibration Results of SL4811 (UVE)

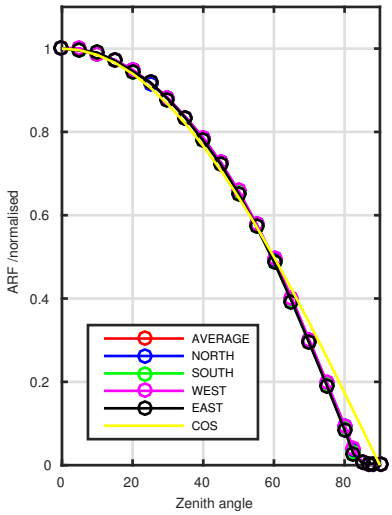

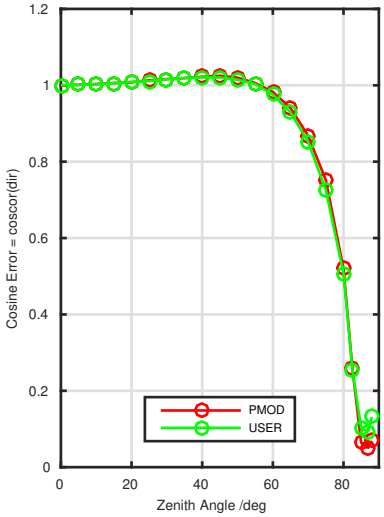

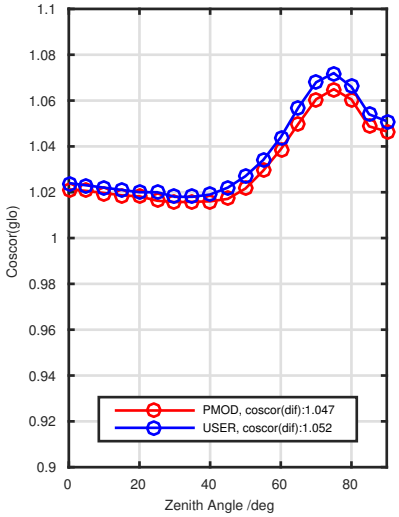

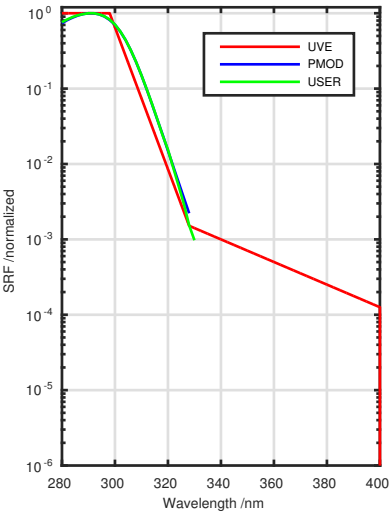

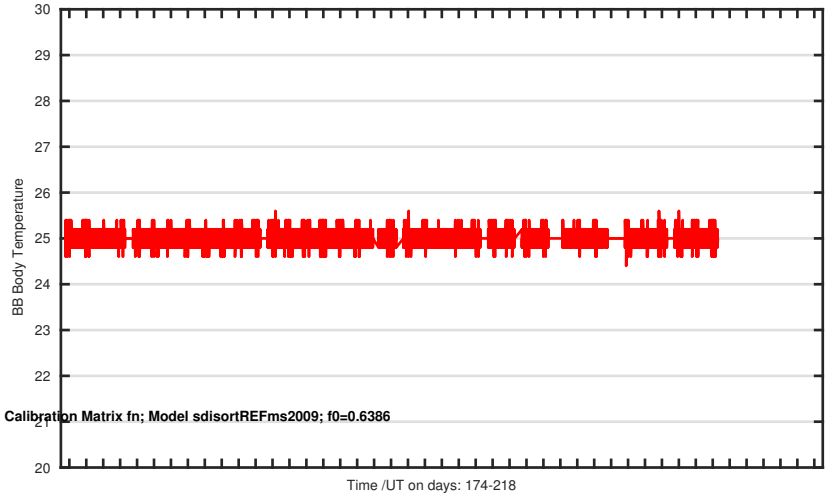

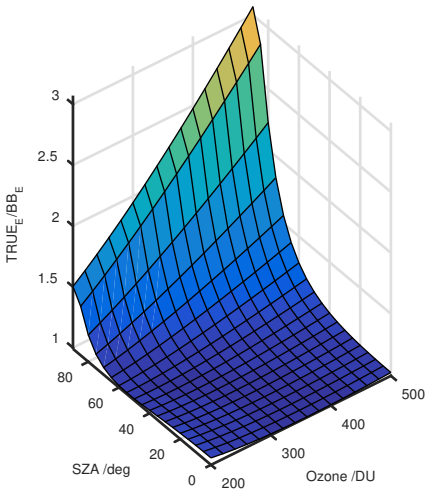

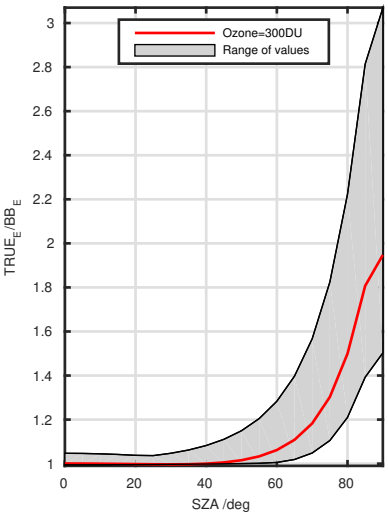

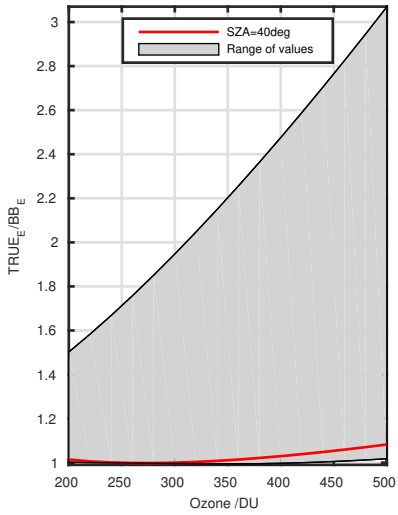

Calibration Results of SL4811 (UVE)

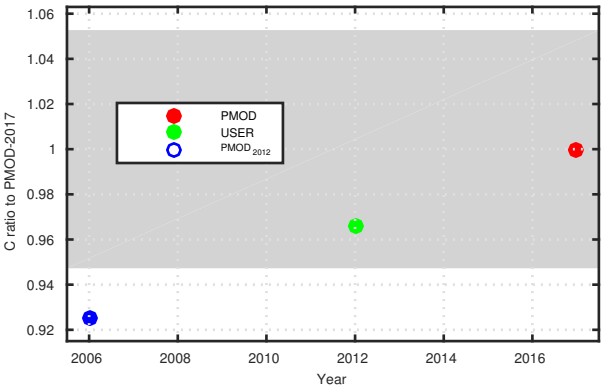

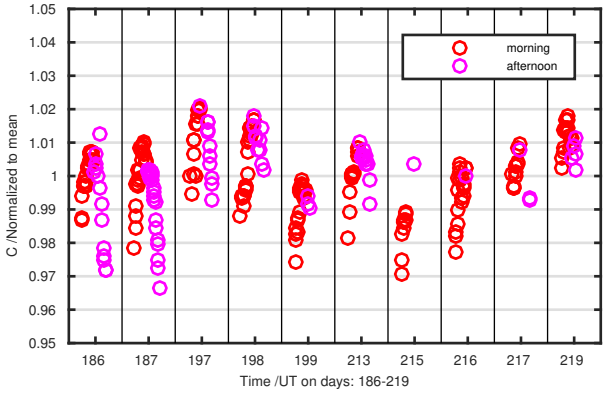

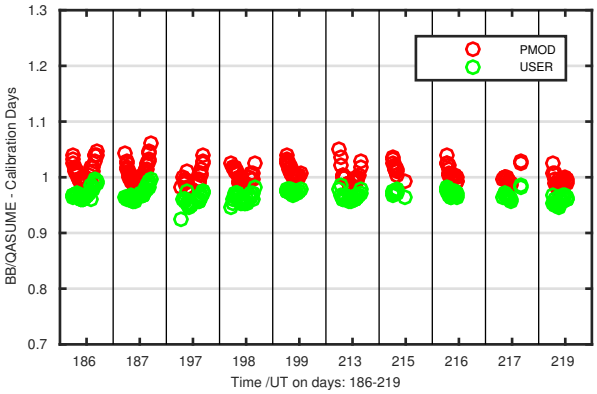

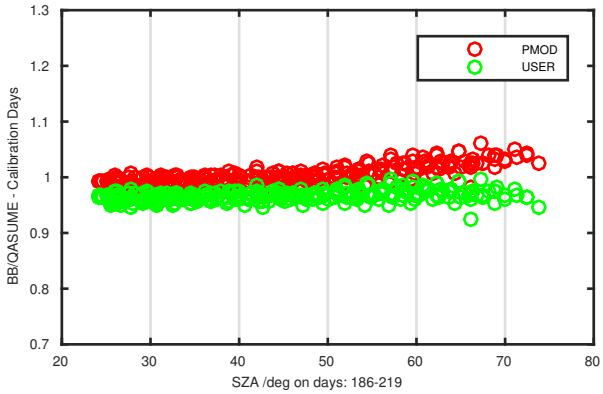

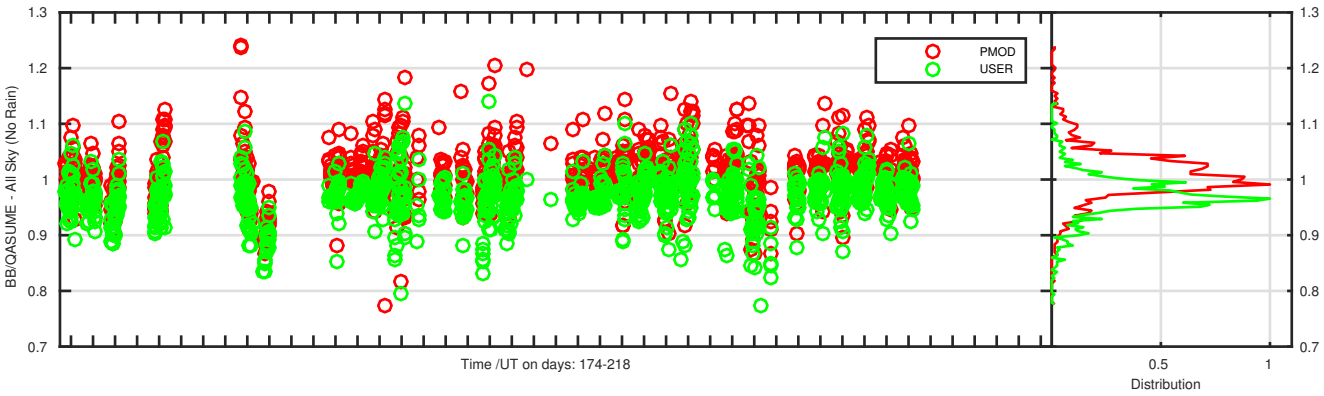

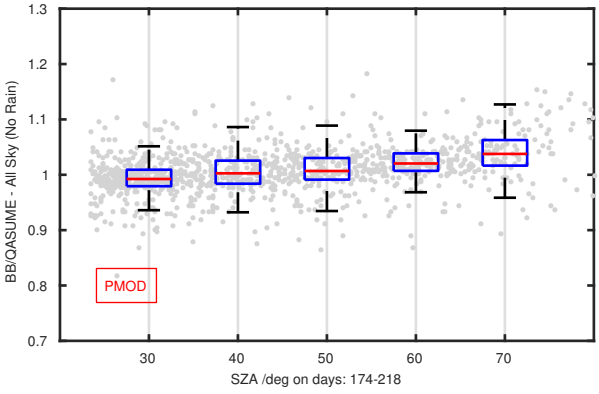

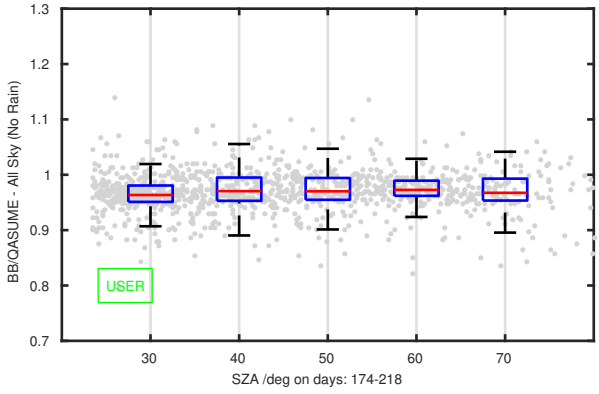

Calibration Results of SL4834 (UVE)

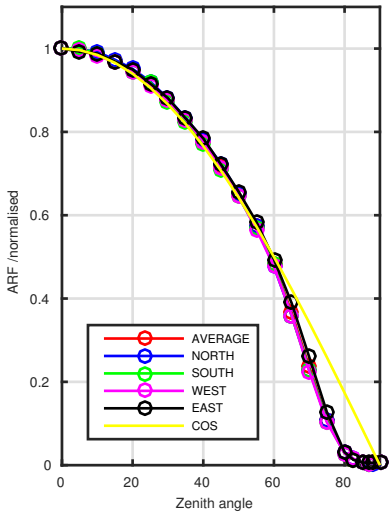

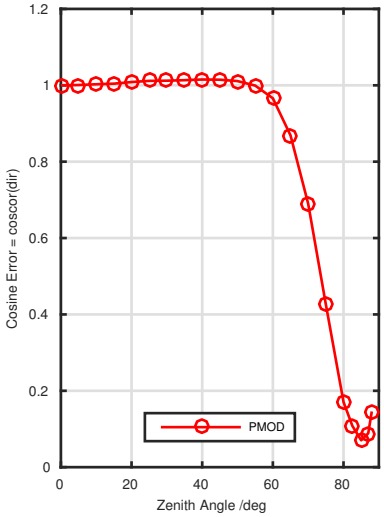

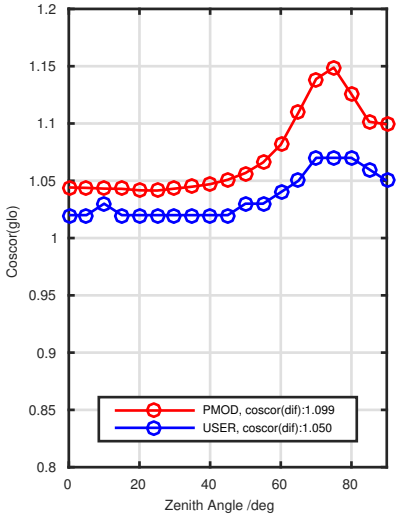

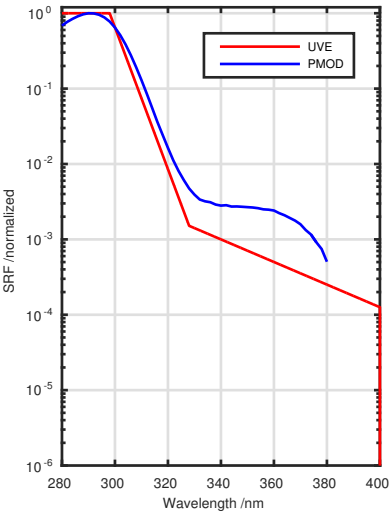

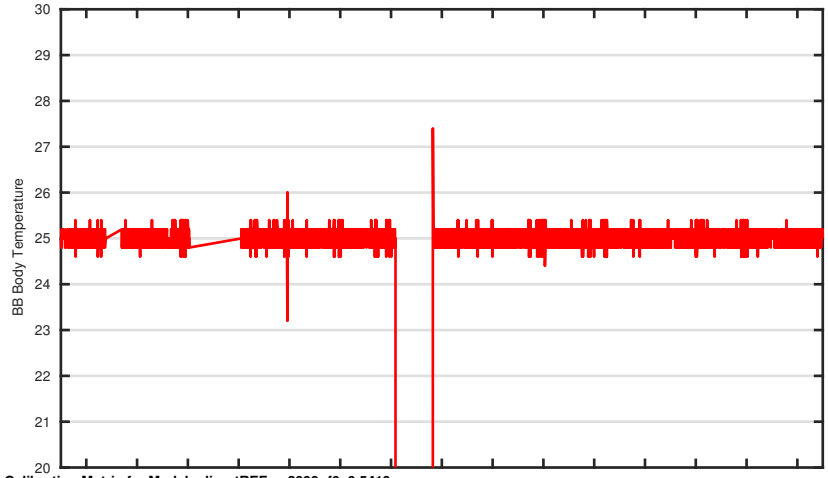

Calibration Matrix fn; Model sdisortREFms2009; f0=0.5419

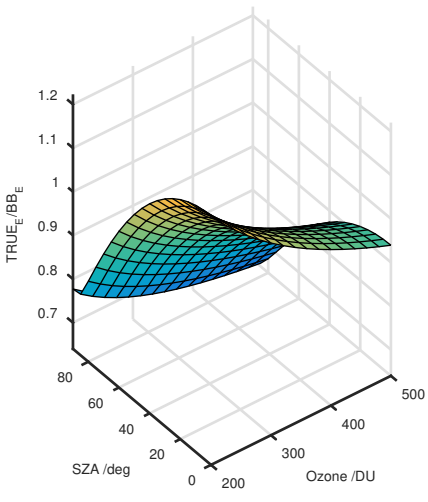

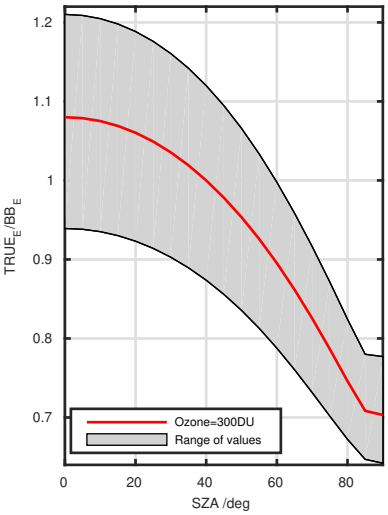

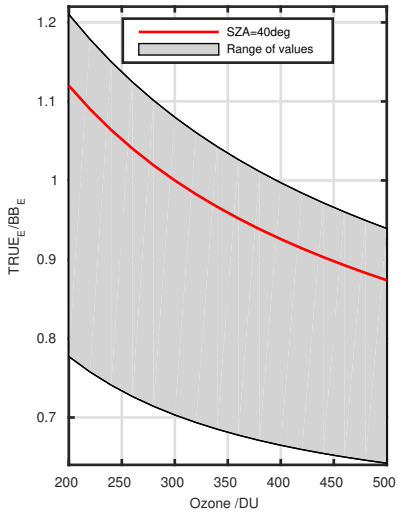

Calibration Results of SL4834 (UVE)

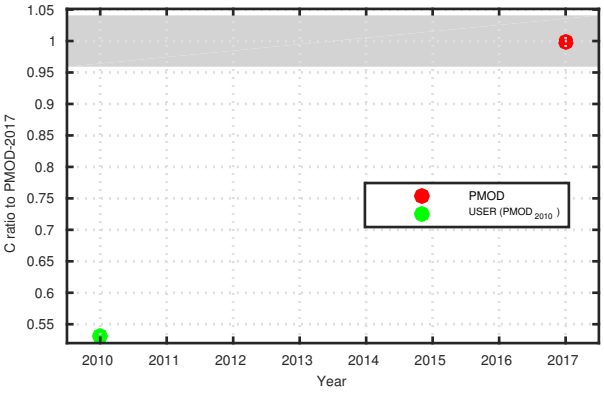

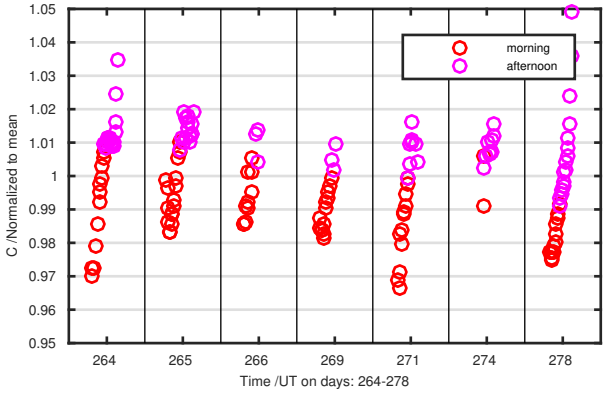

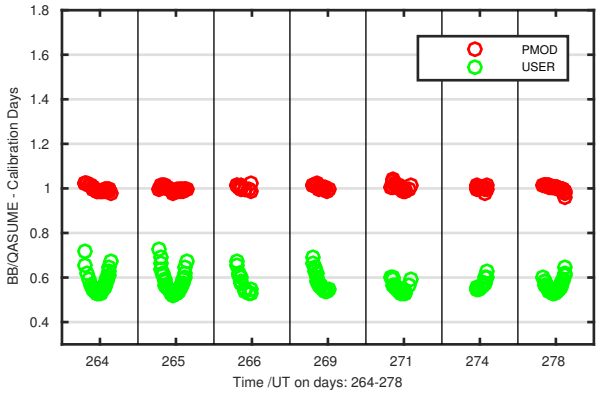

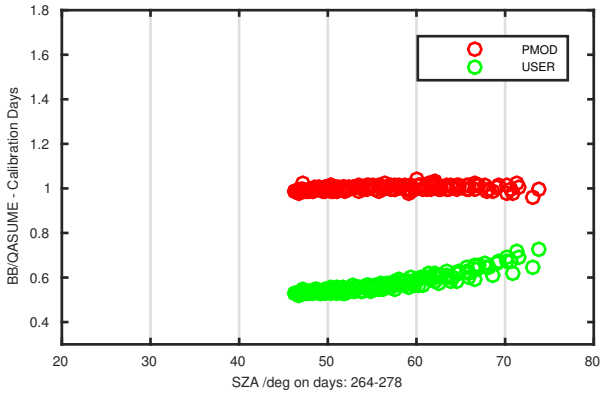

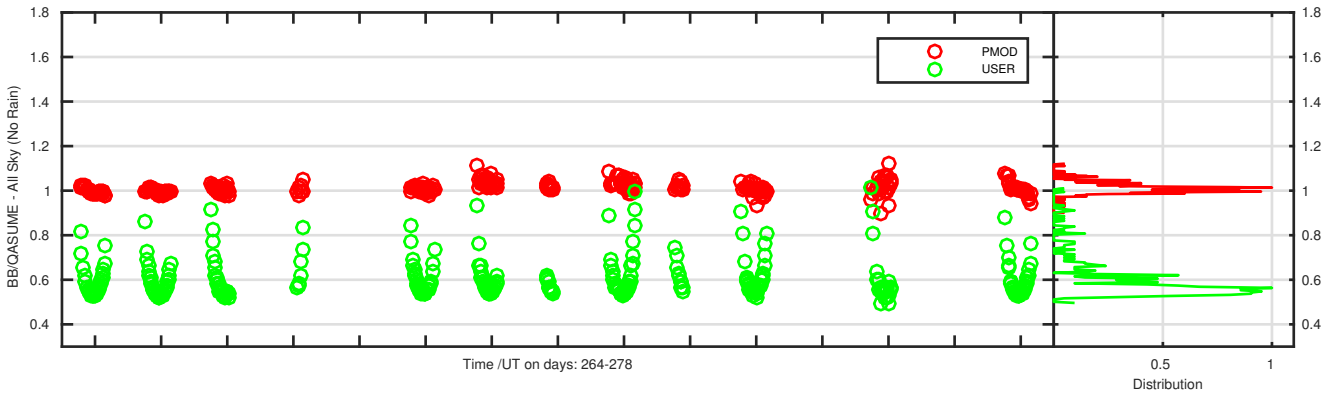

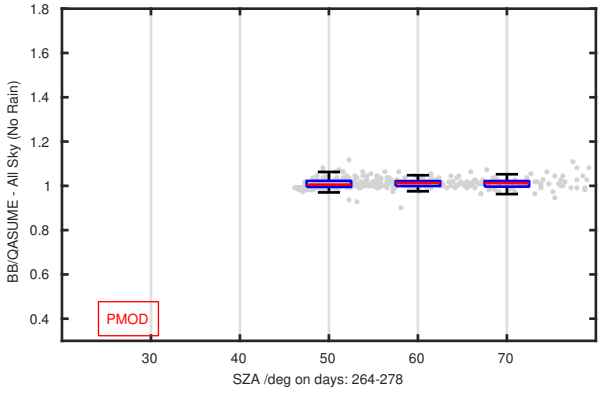

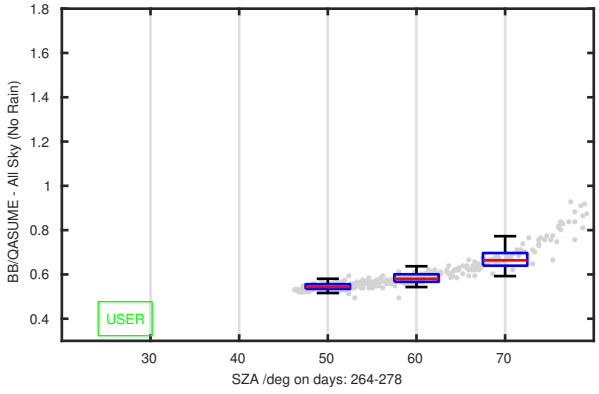

Calibration Results of SL10403 (UVE)

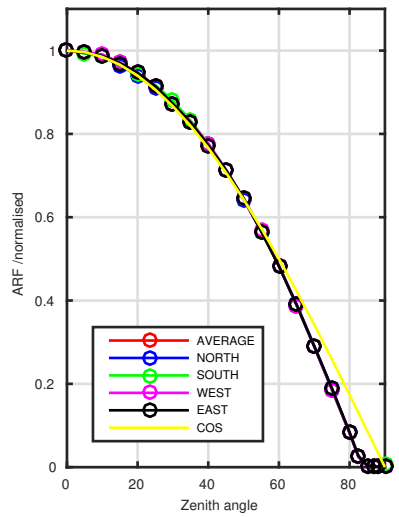

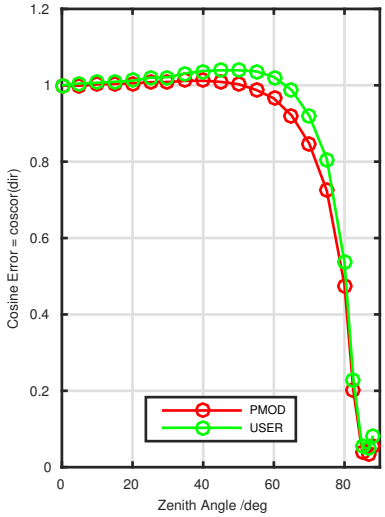

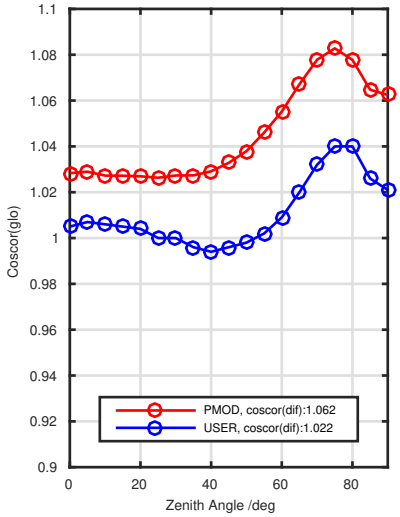

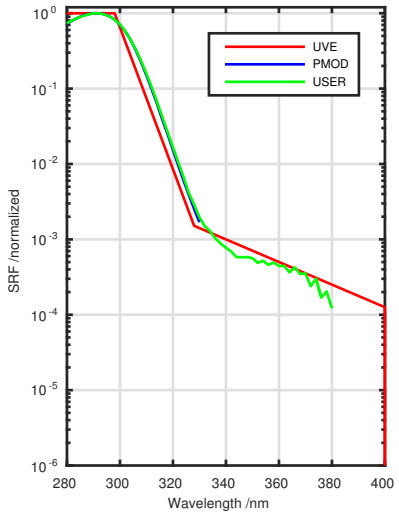

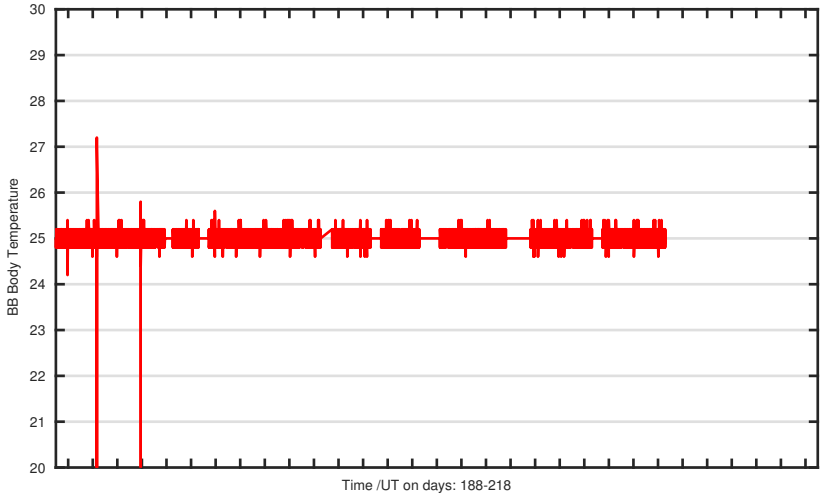

Calibration Matrix fn; Model sdisortREFms2009; f0=0.6326

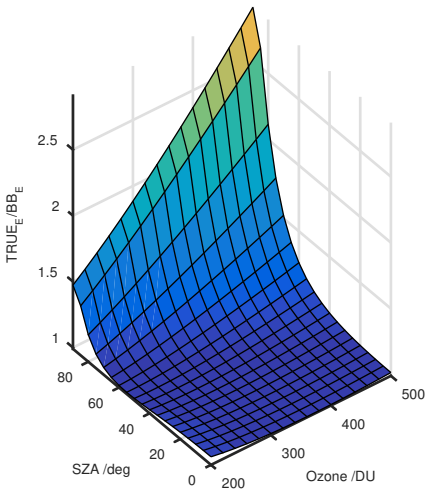

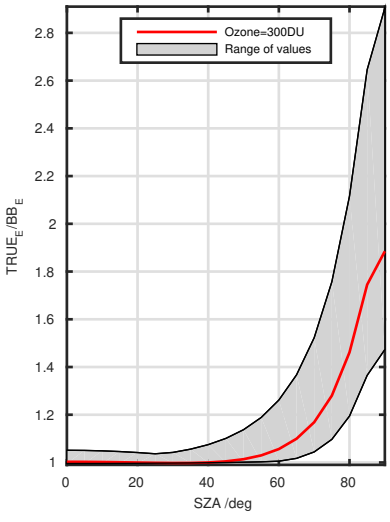

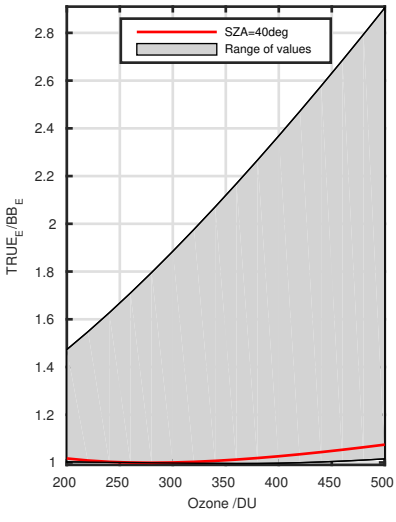

Calibration Results of SL10403 (UVE)

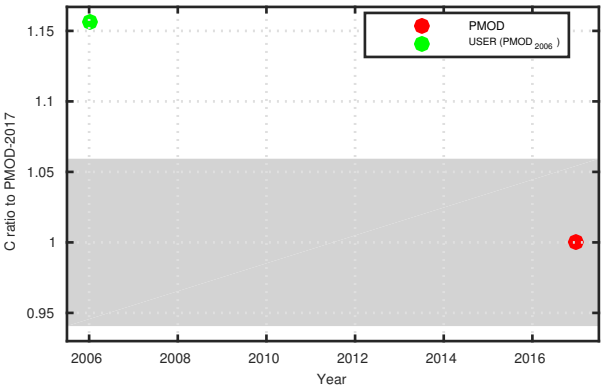

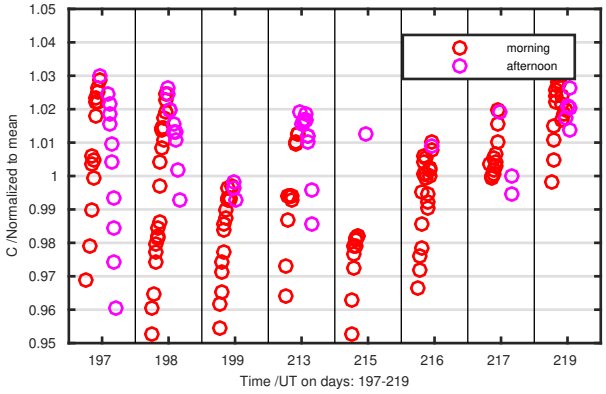

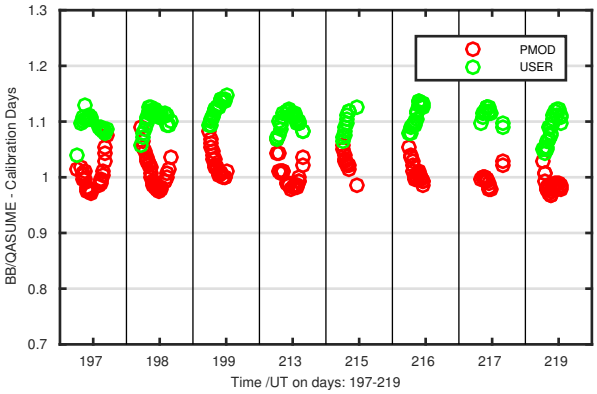

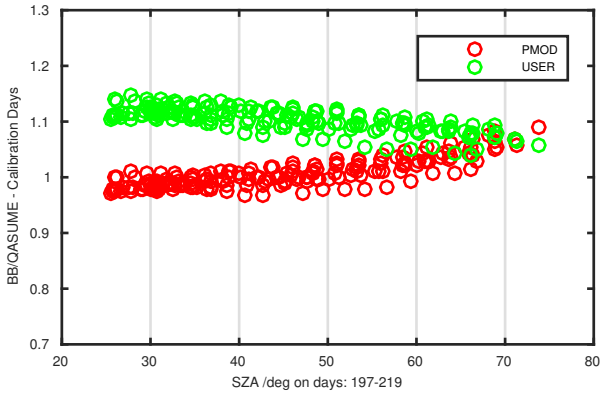

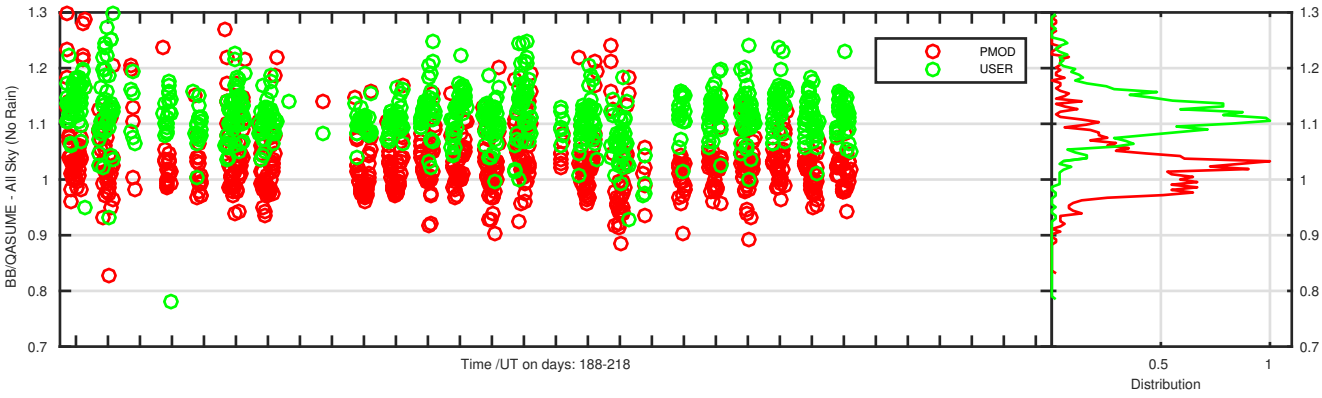

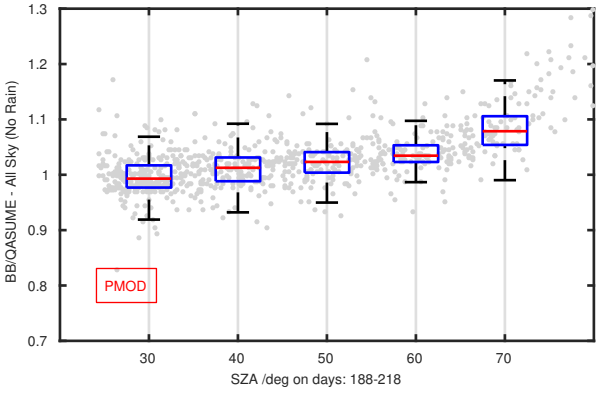

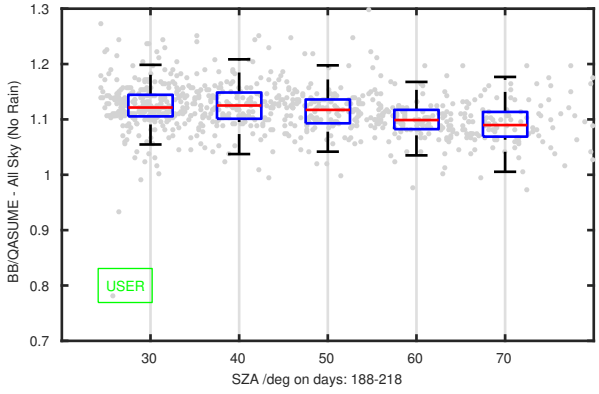

Calibration Results of SL14078 (UVE)

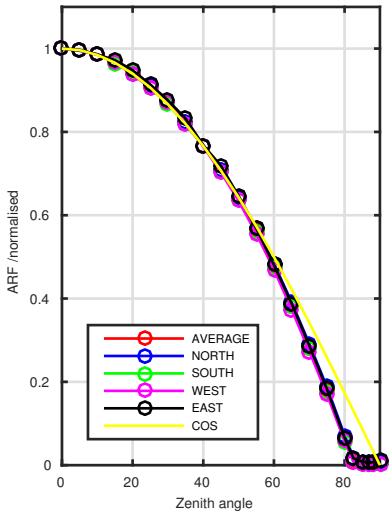

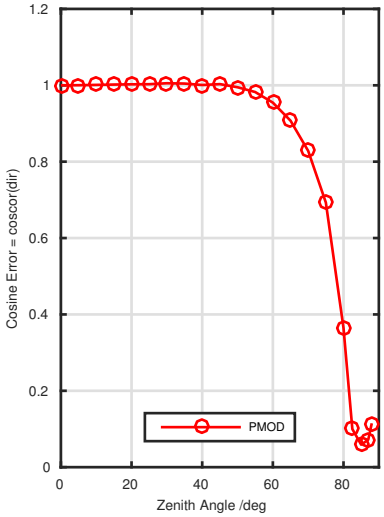

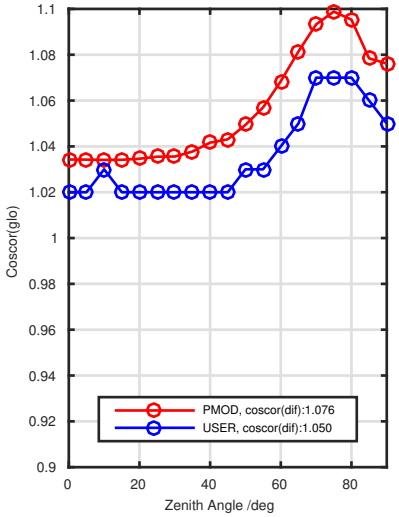

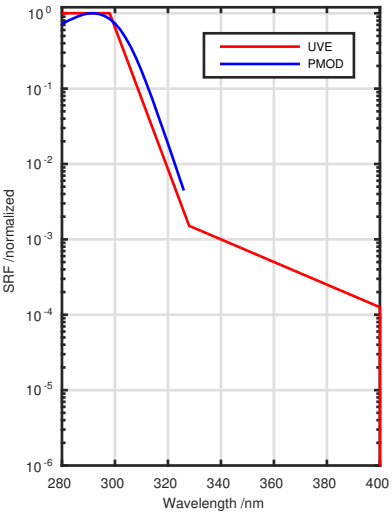

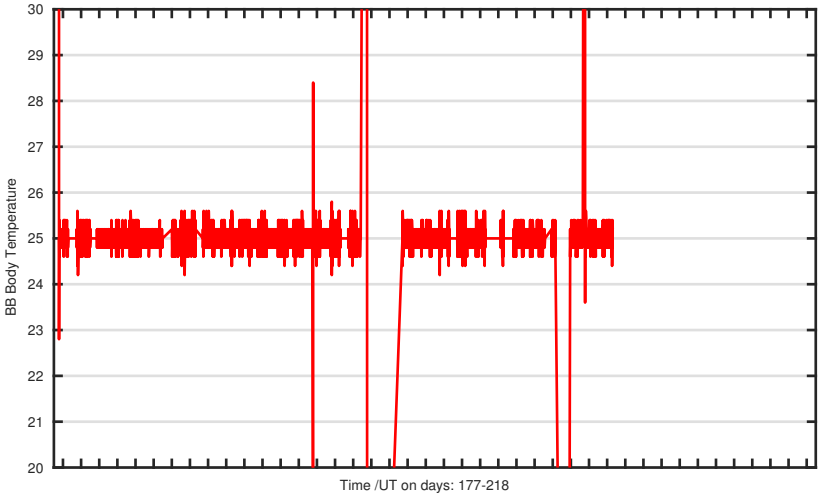

Calibration Matrix fn; Model sdisortREFms2009; f0=0.5562

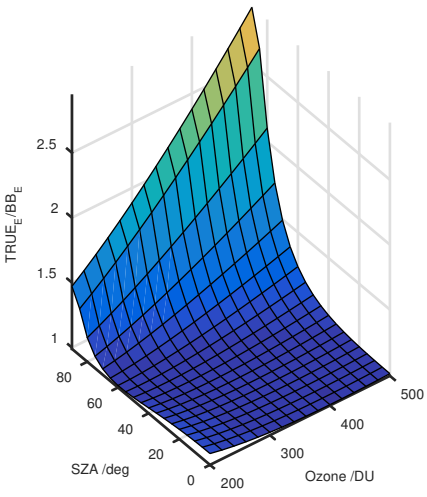

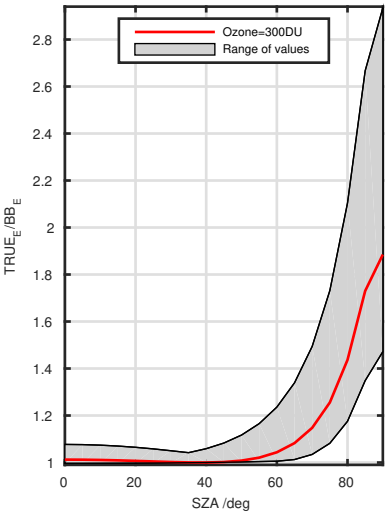

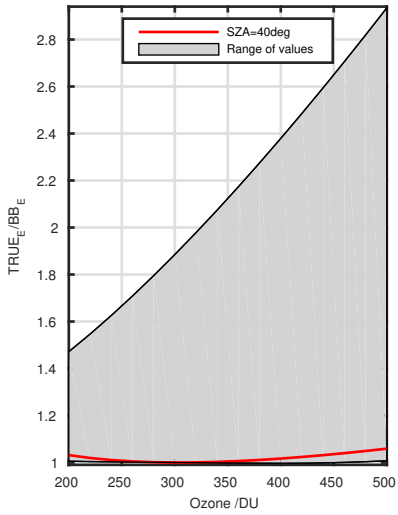

Calibration Results of SL14078 (UVE)

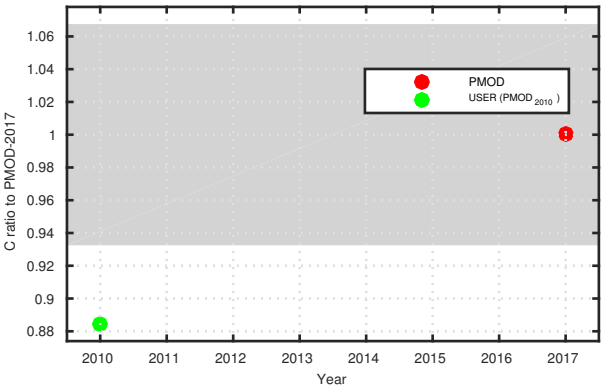

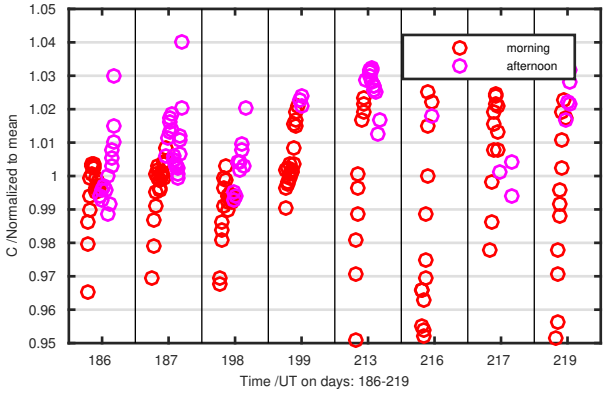

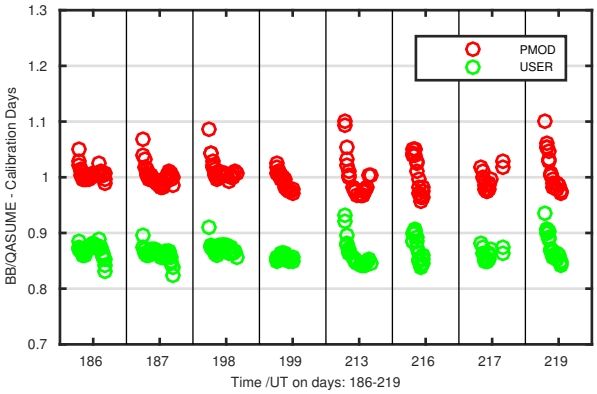

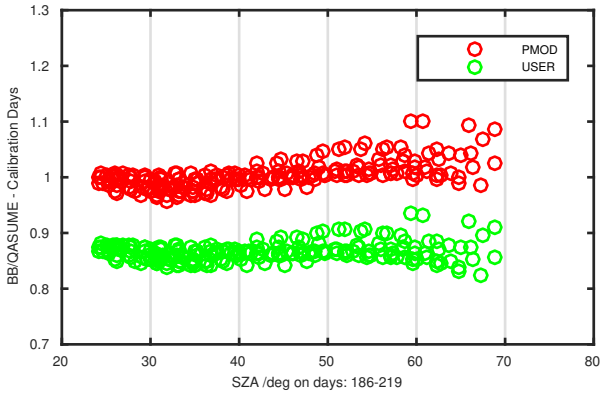

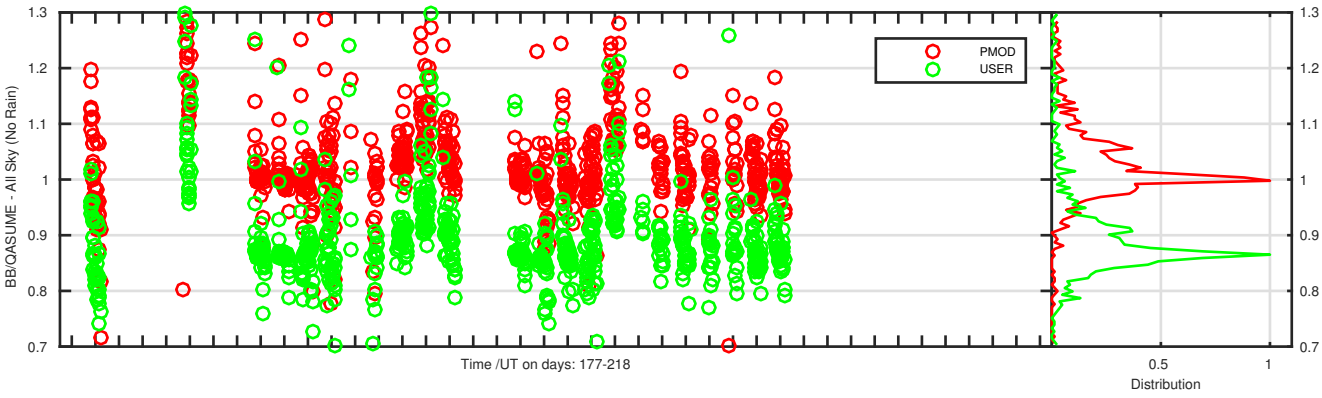

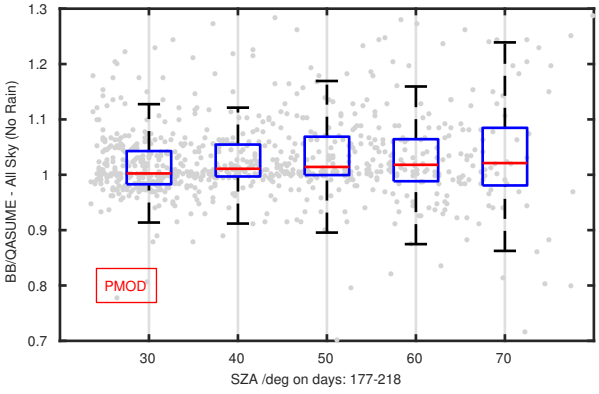

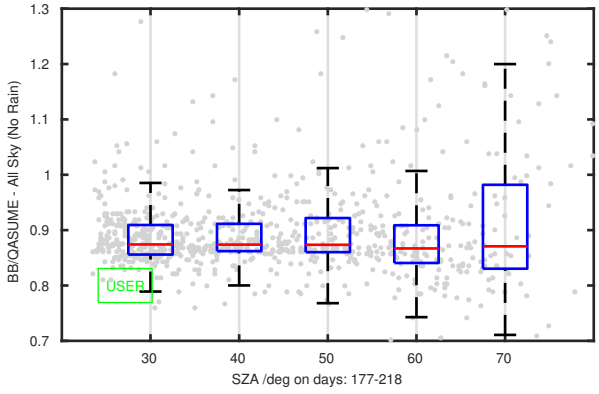

Calibration Results of SL16721 (UVE)

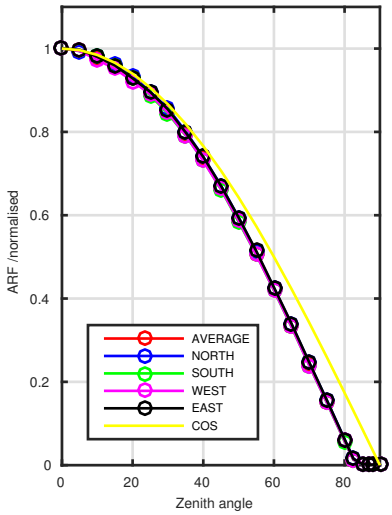

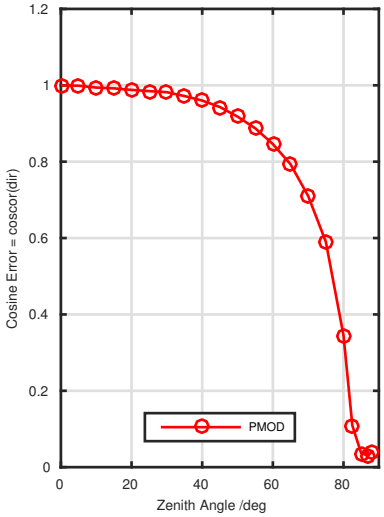

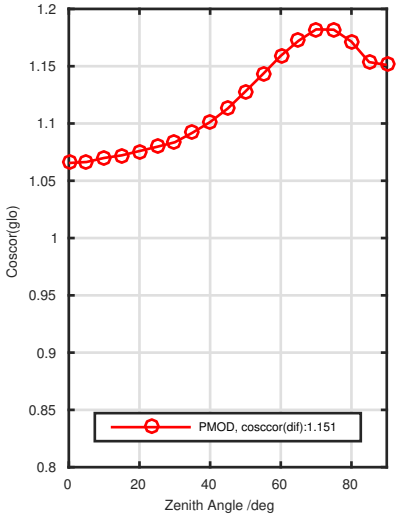

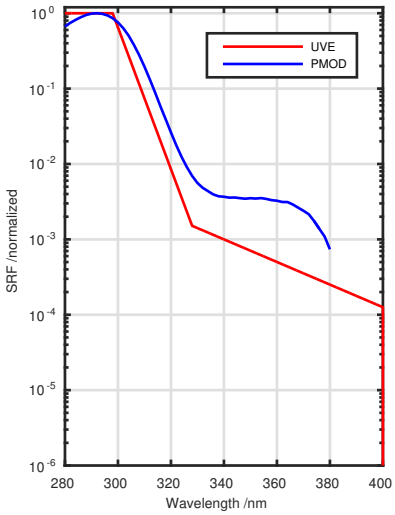

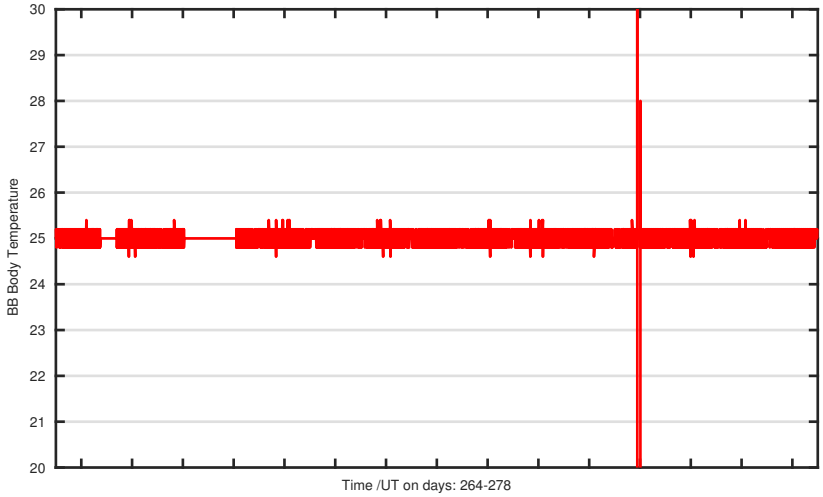

Calibration Matrix fn; Model sdisortREFms2009; f0=0.3736

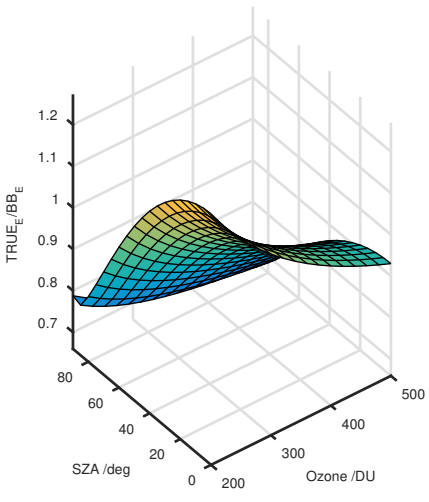

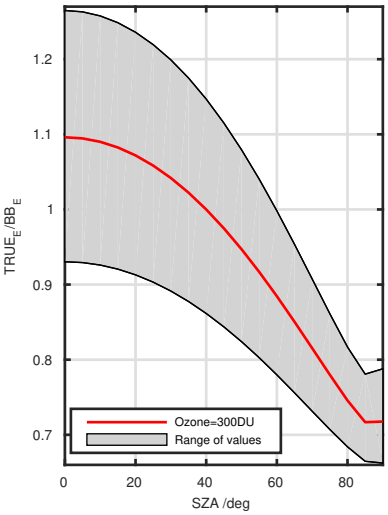

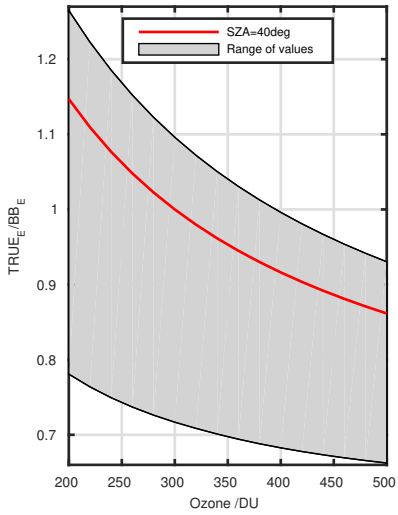

Calibration Results of SL16721 (UVE)

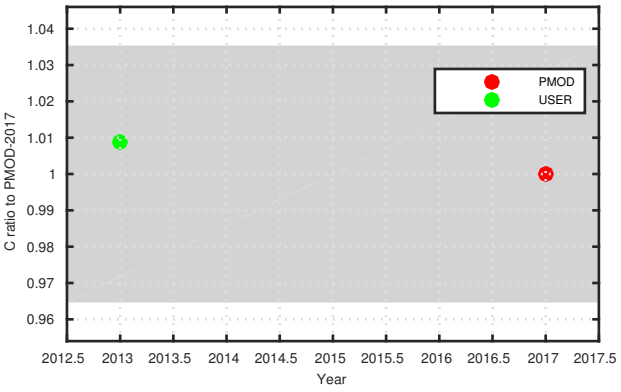

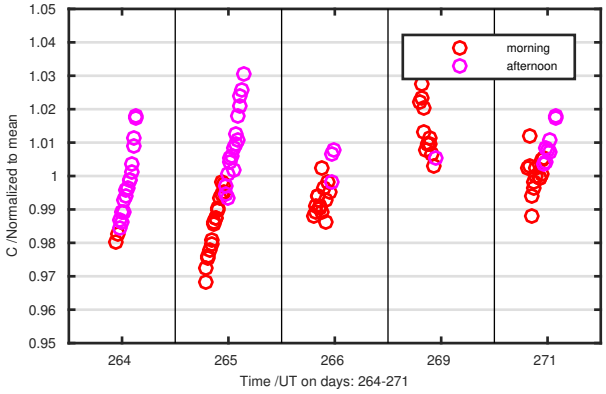

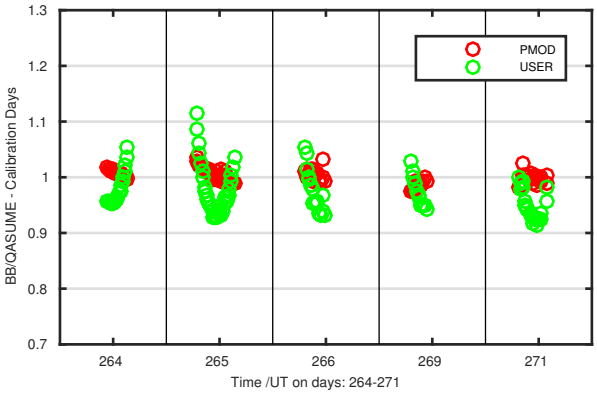

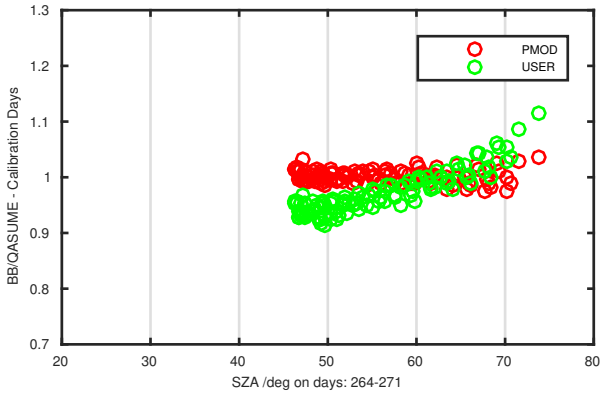

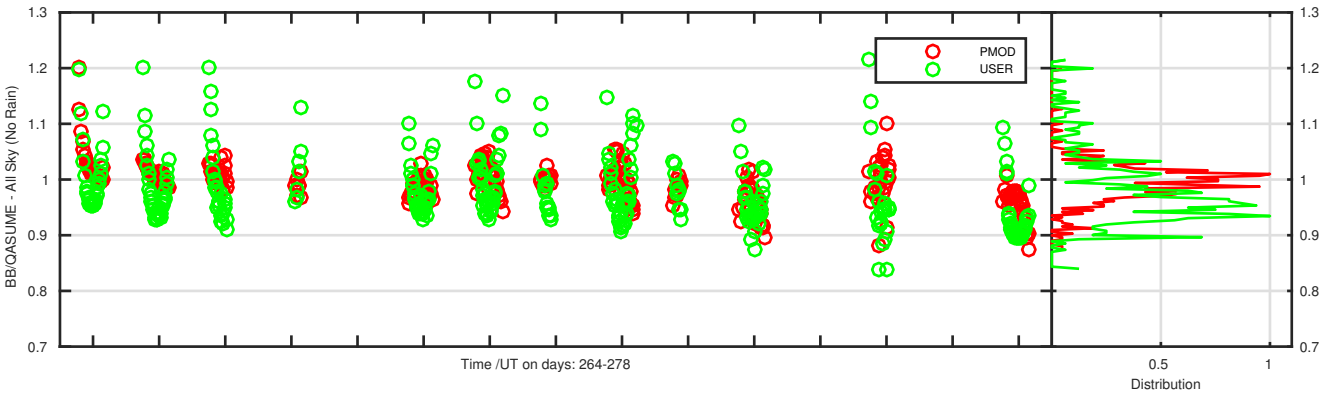

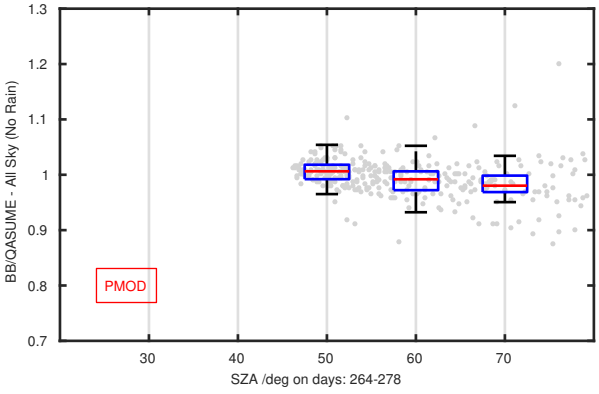

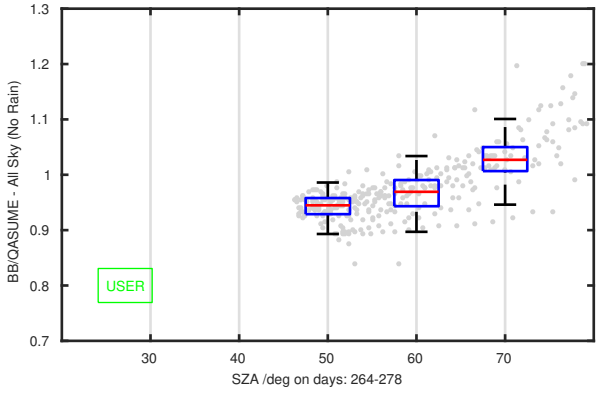

Calibration Results of YES000904 (UVE)

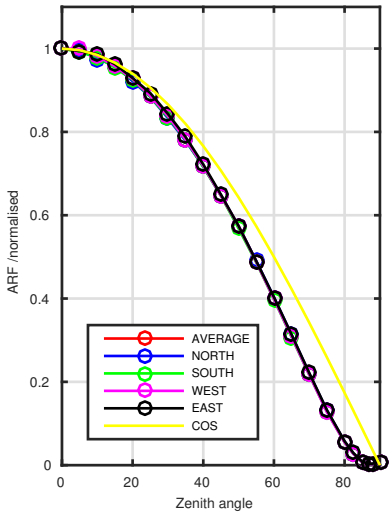

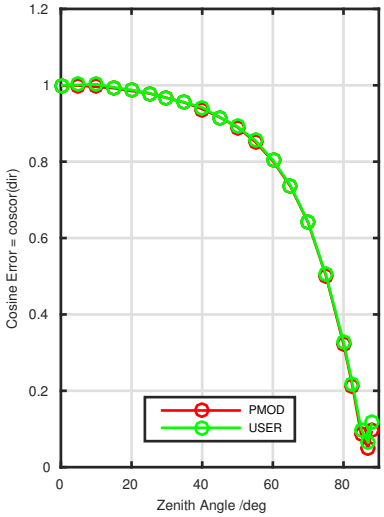

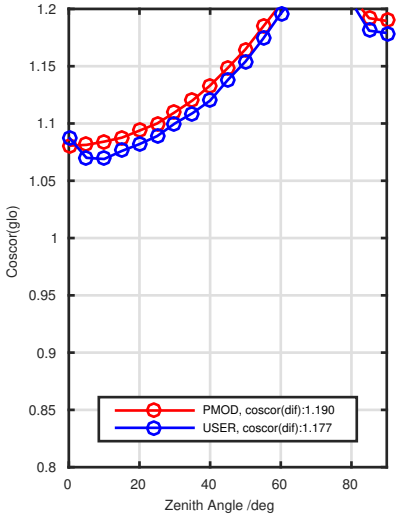

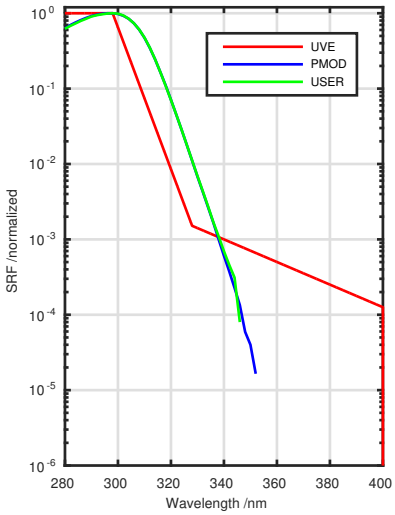

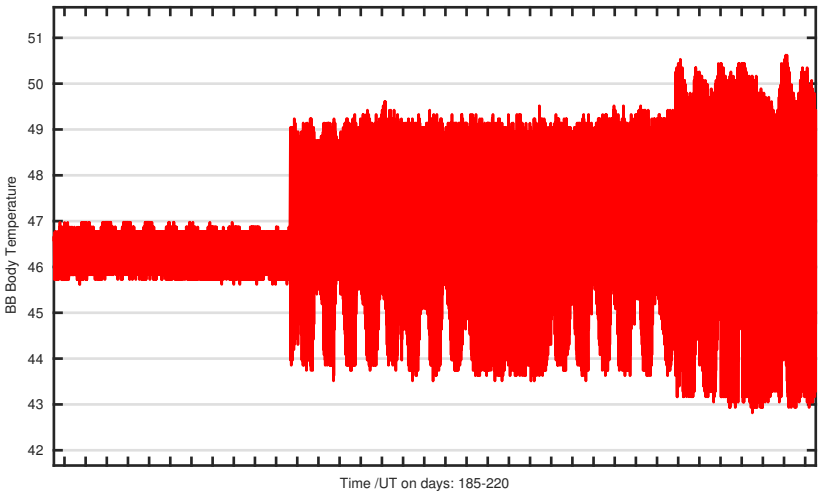

Calibration Matrix fn; Model sdisortREFms2009; f0=0.2026

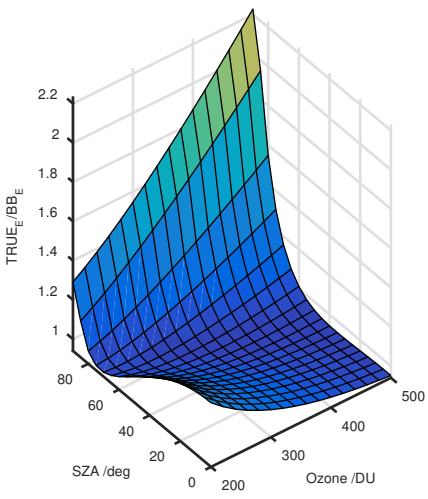

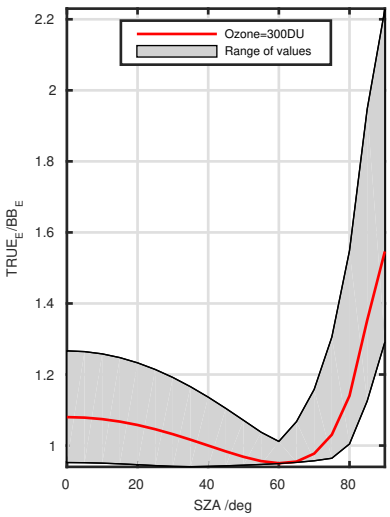

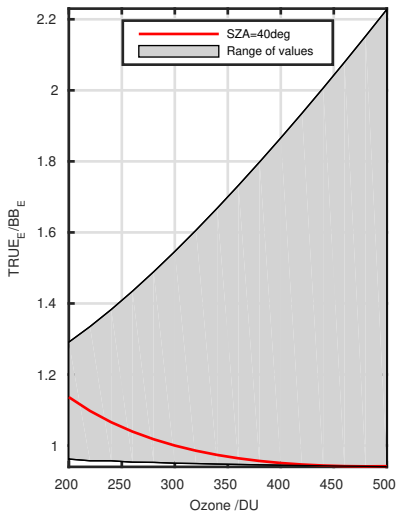

Calibration Results of YES000904 (UVE)

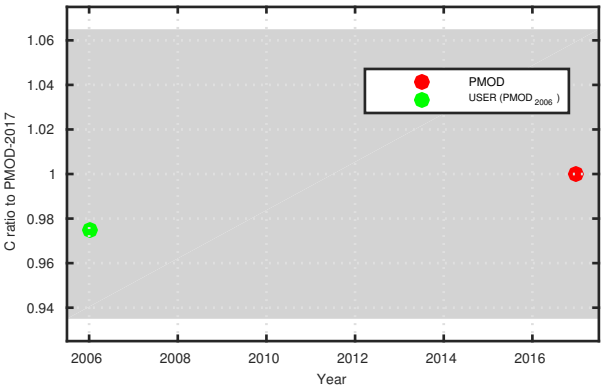

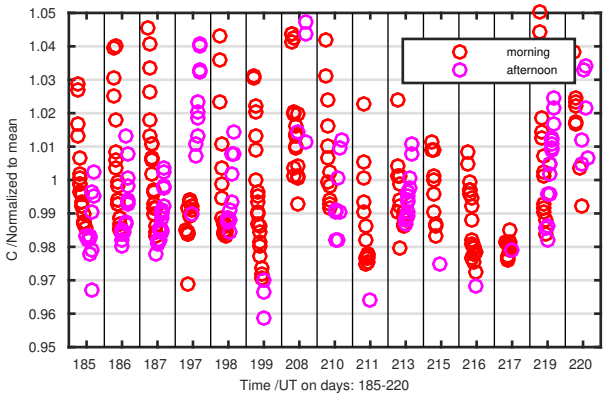

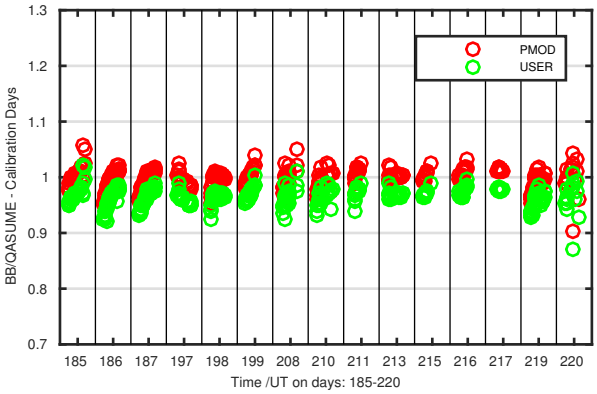

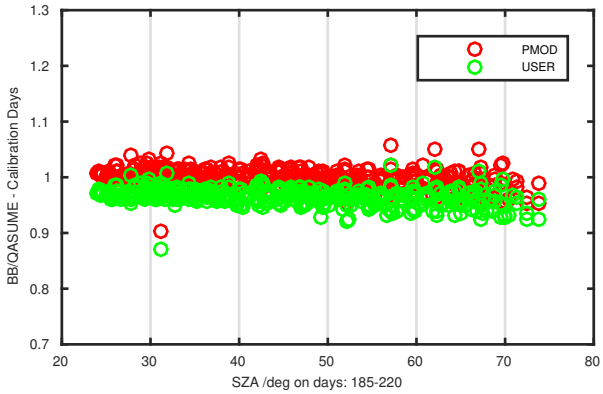

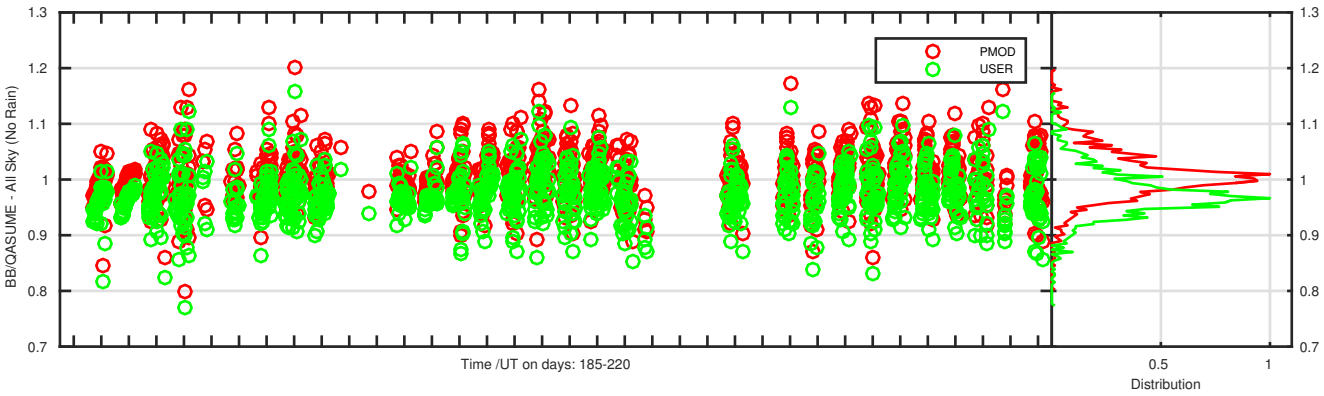

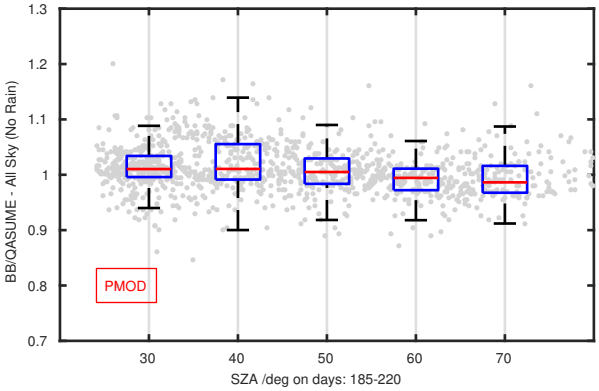

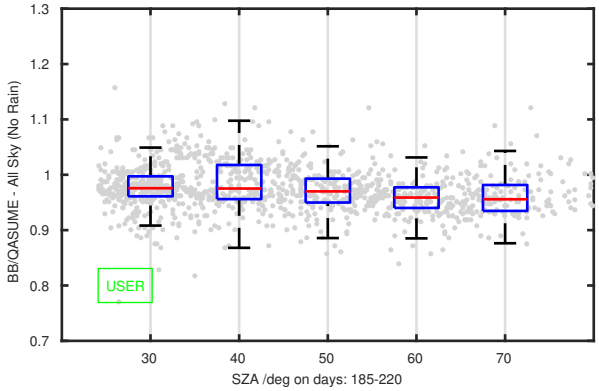

Calibration Results of YES010938 (UVE)

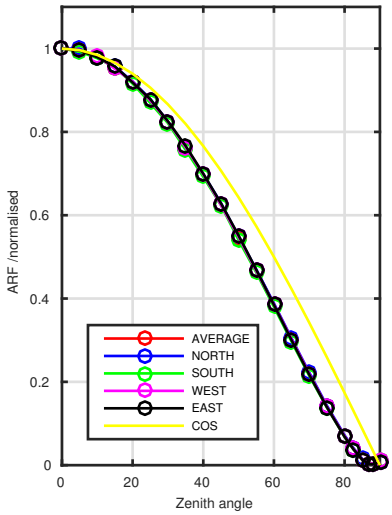

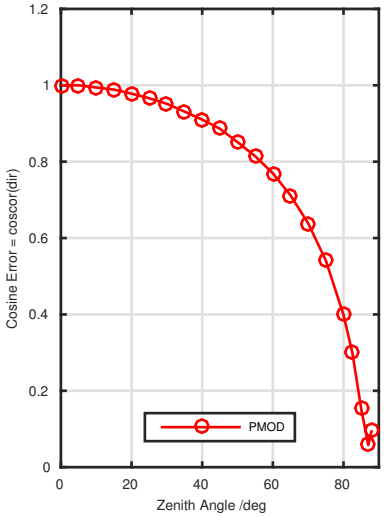

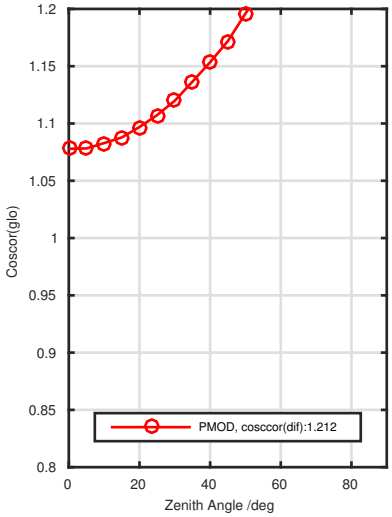

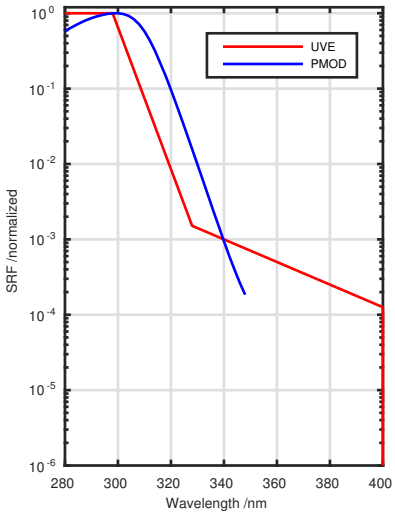

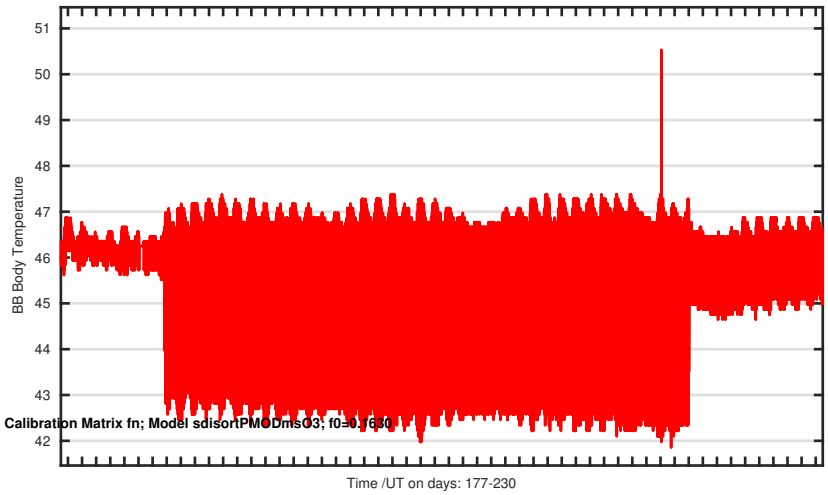

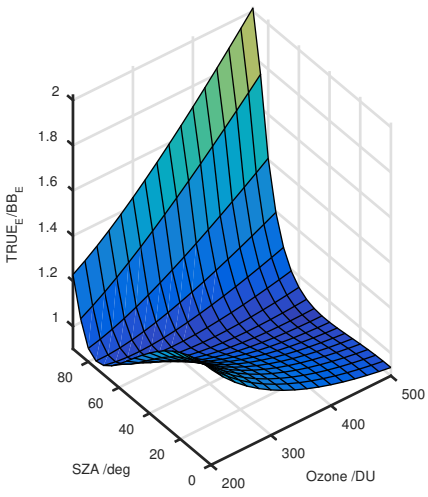

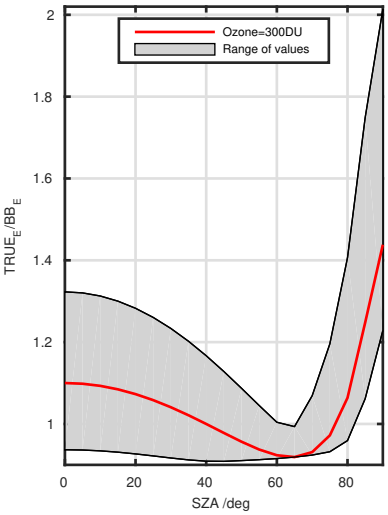

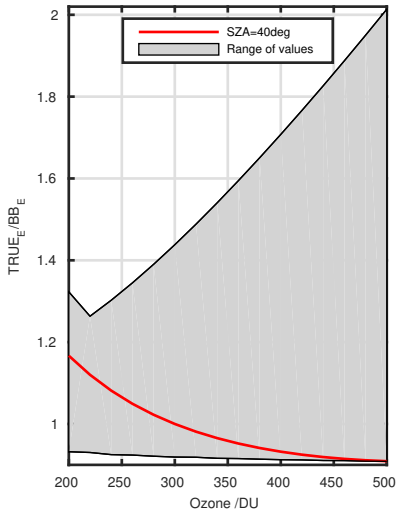

Calibration Results of YES010938 (UVE)

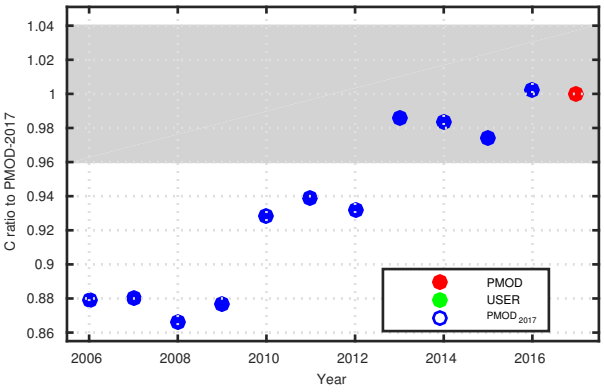

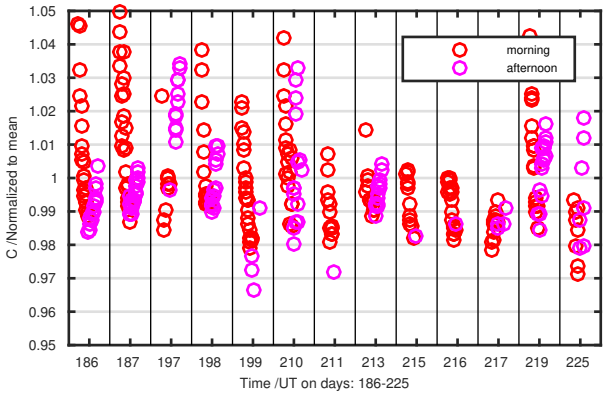

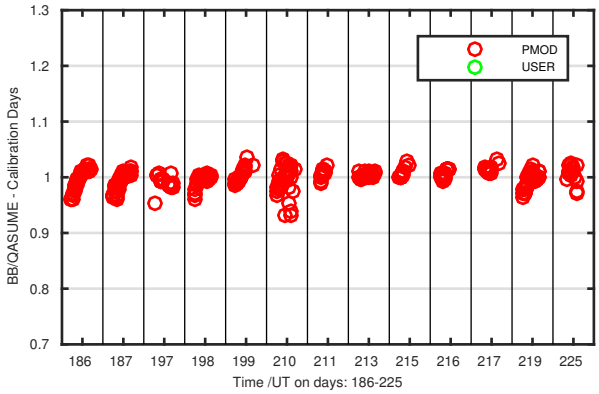

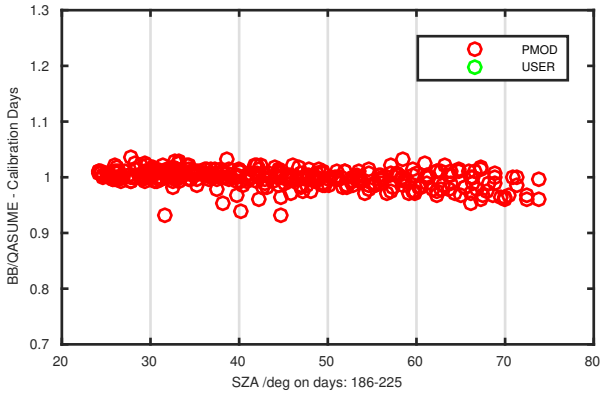

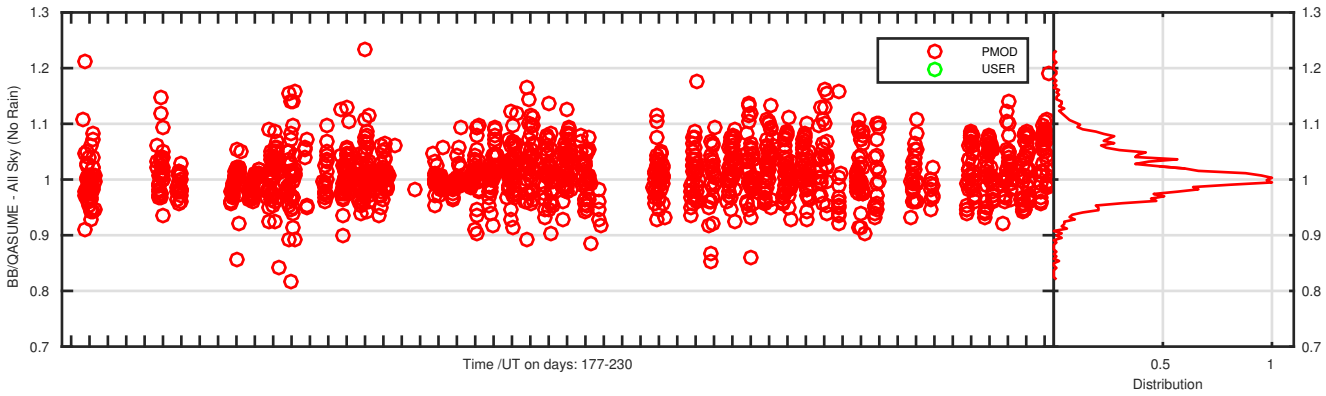

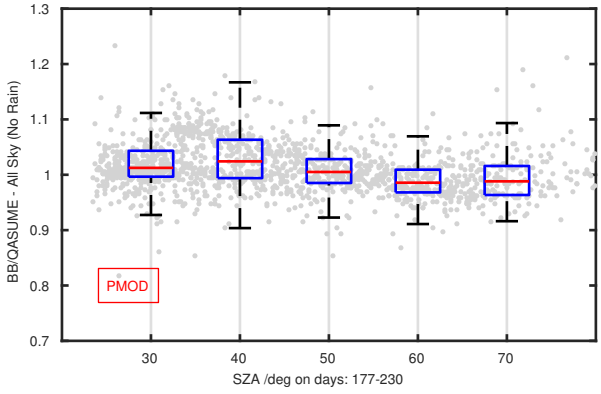

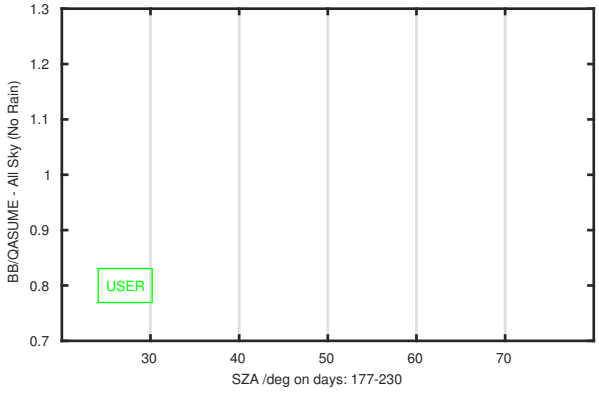

Calibration Results of YES030520 (UVE)

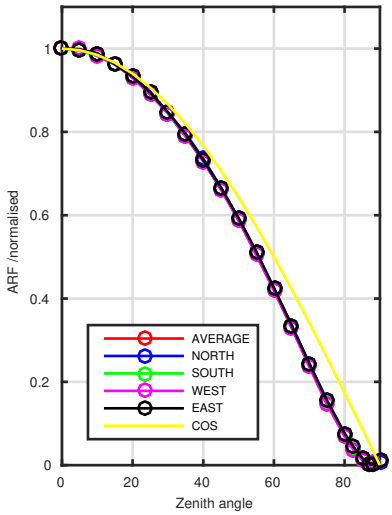

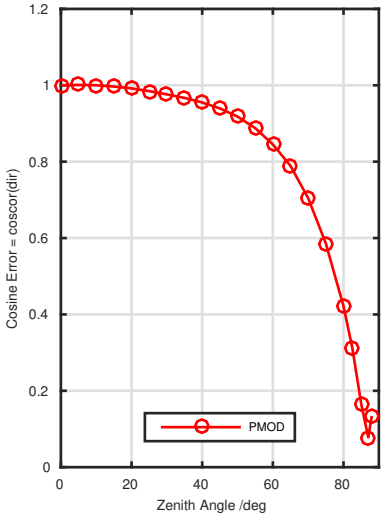

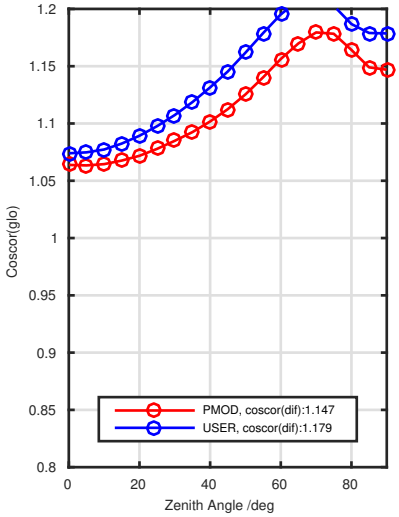

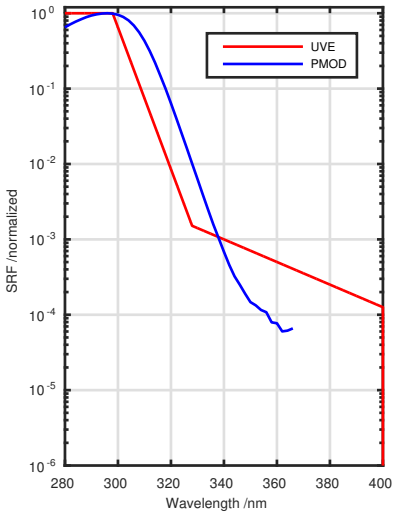

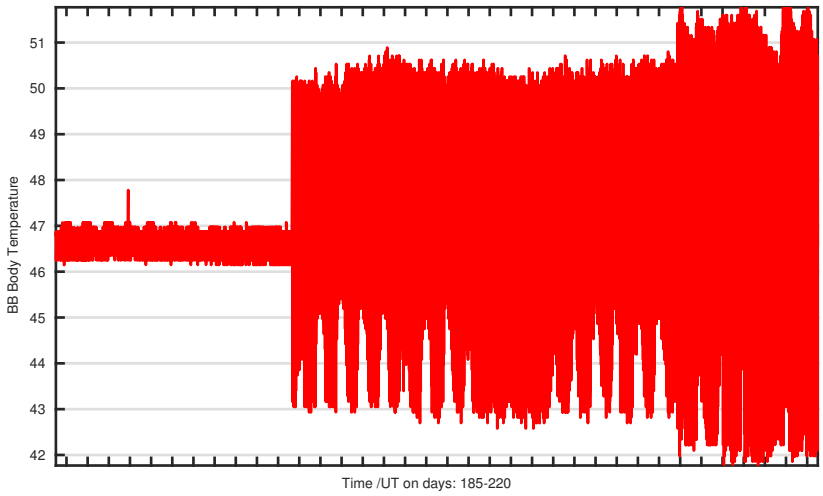

Calibration Matrix fn; Model sdisortREFms2009; f0=0.2212

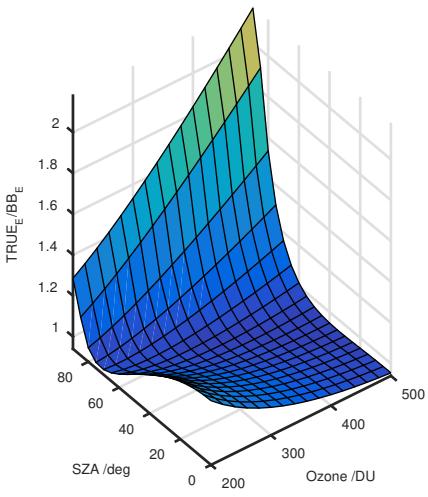

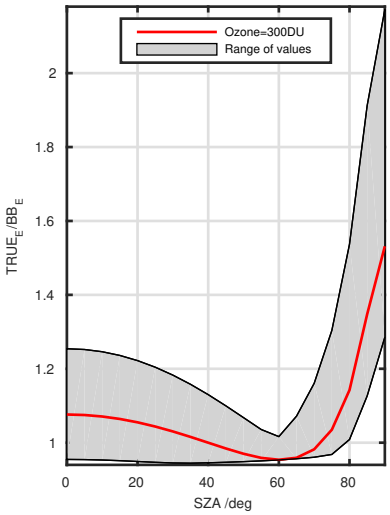

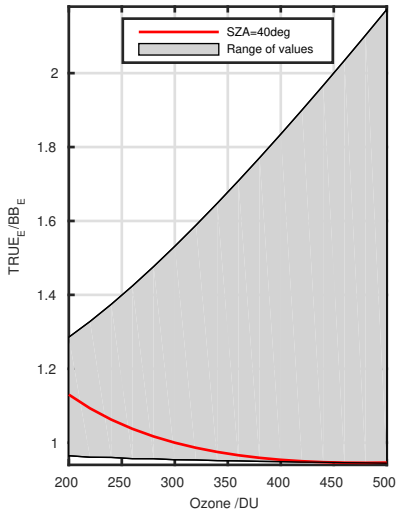

Calibration Results of YES030520 (UVE)

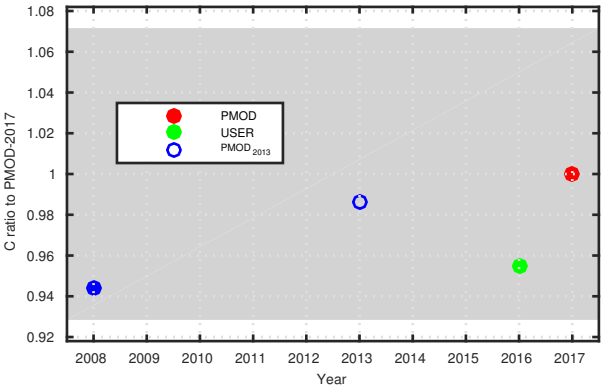

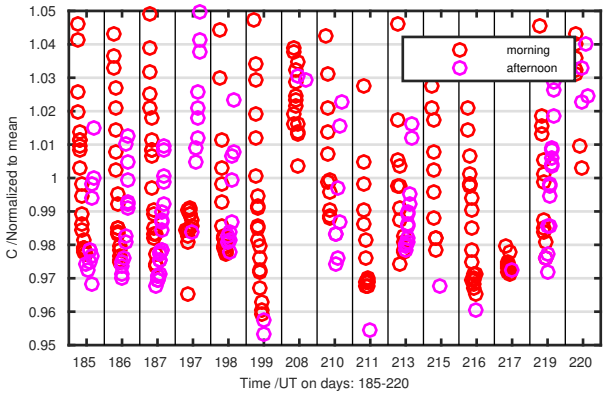

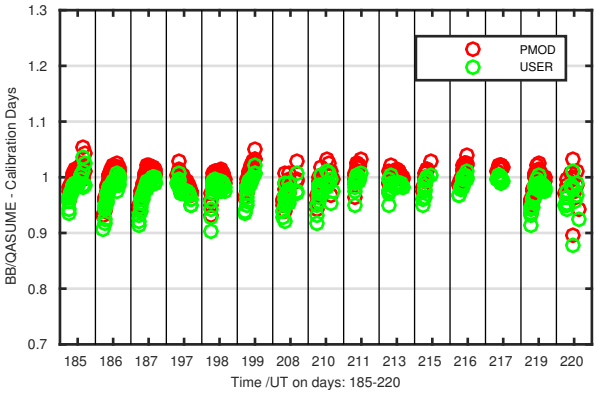

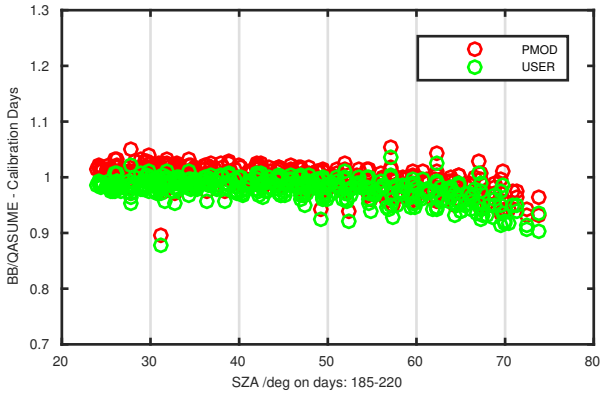

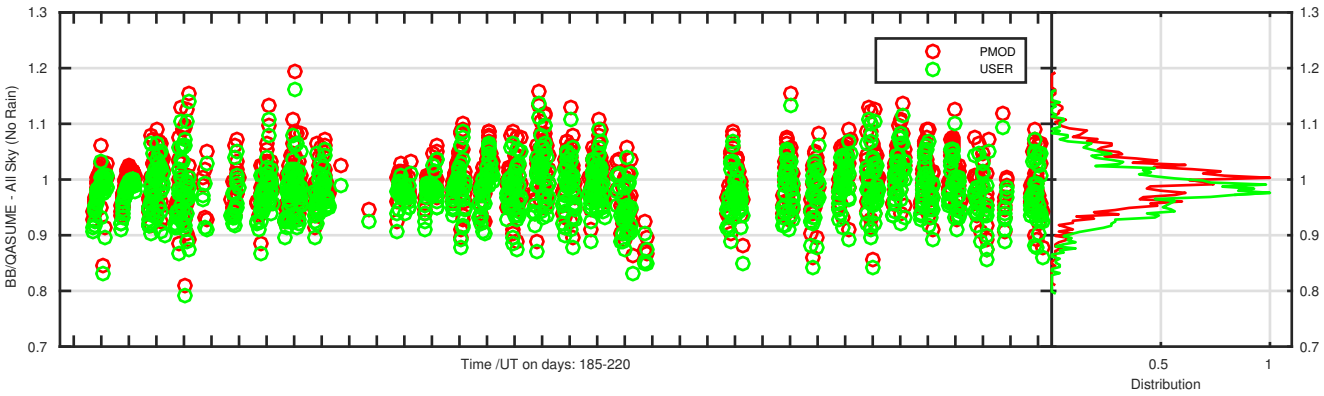

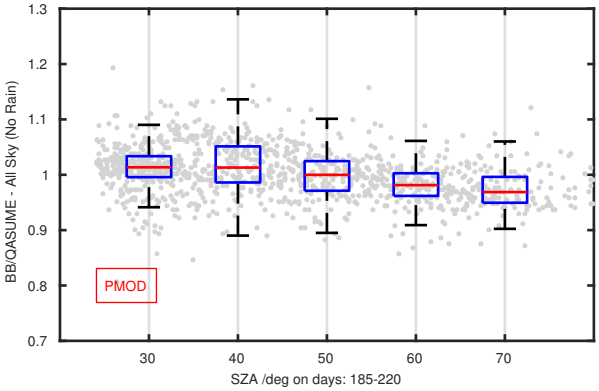

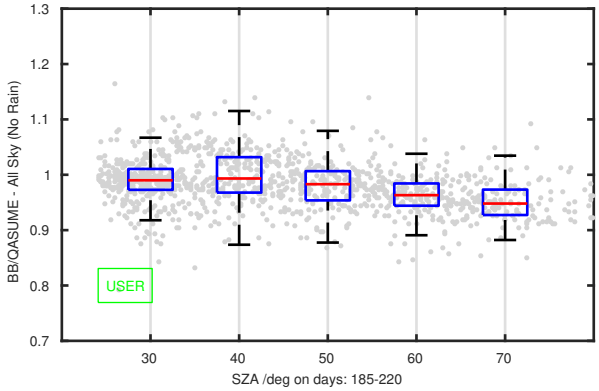

Calibration Results of YES030525 (UVB320)

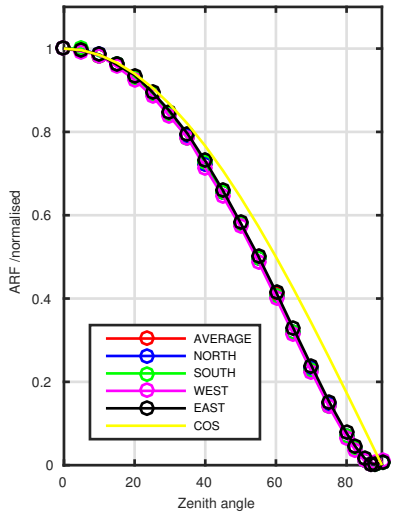

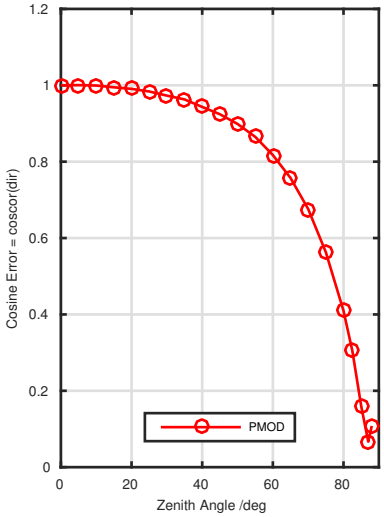

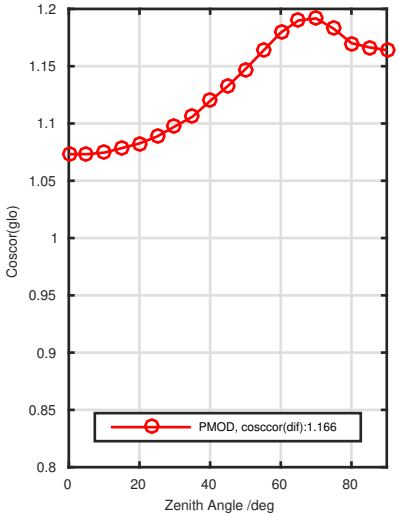

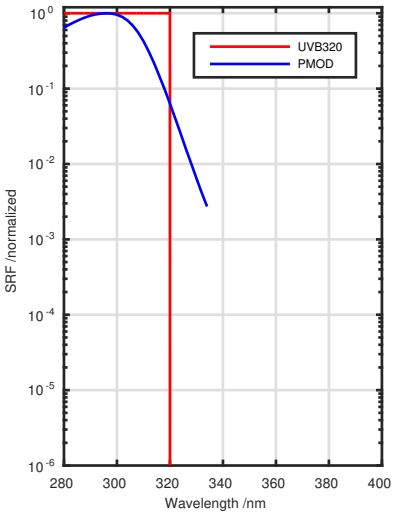

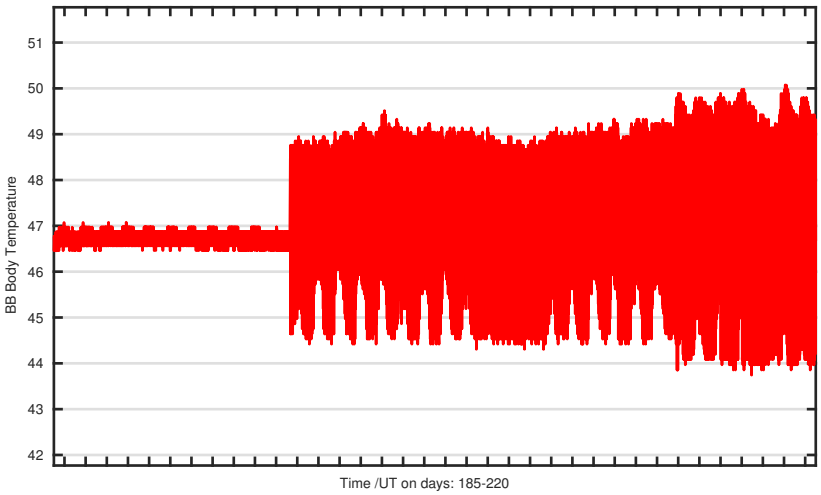

Calibration Matrix fn; Model sdisortREFms2009; f0=3.3448

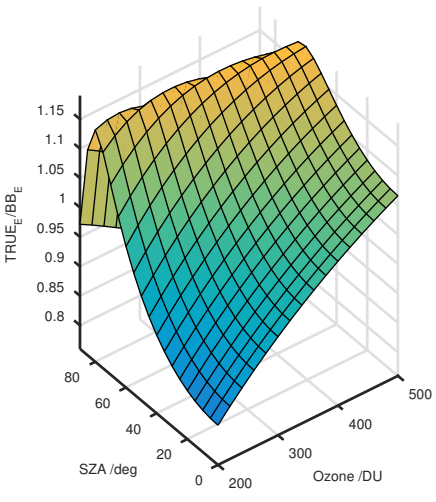

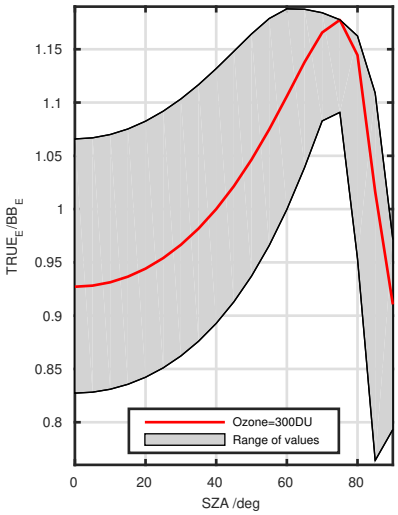

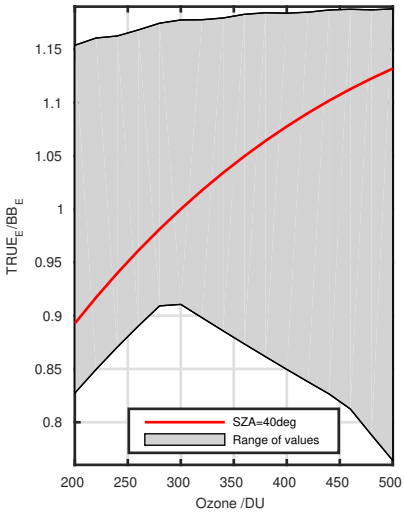

Calibration Results of YES030525 (UVB320)

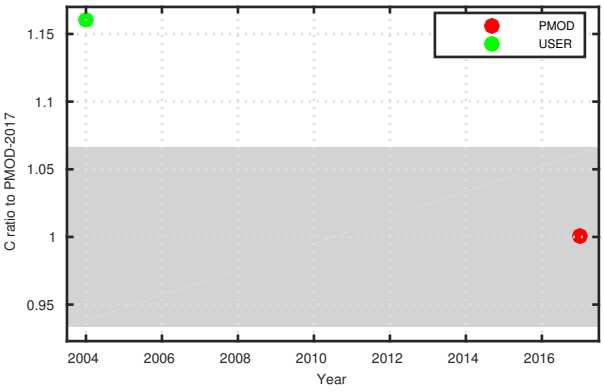

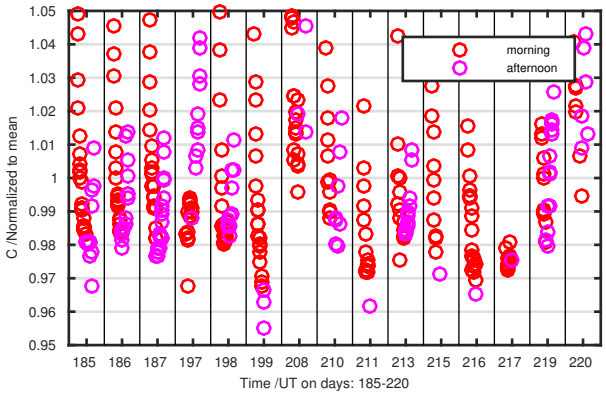

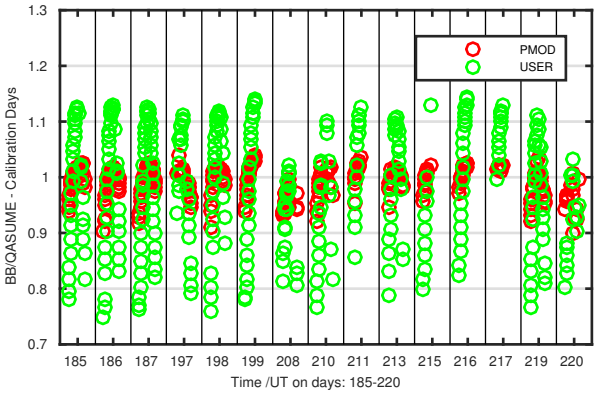

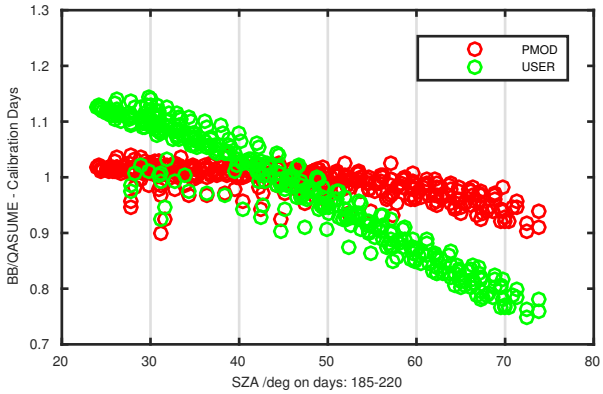

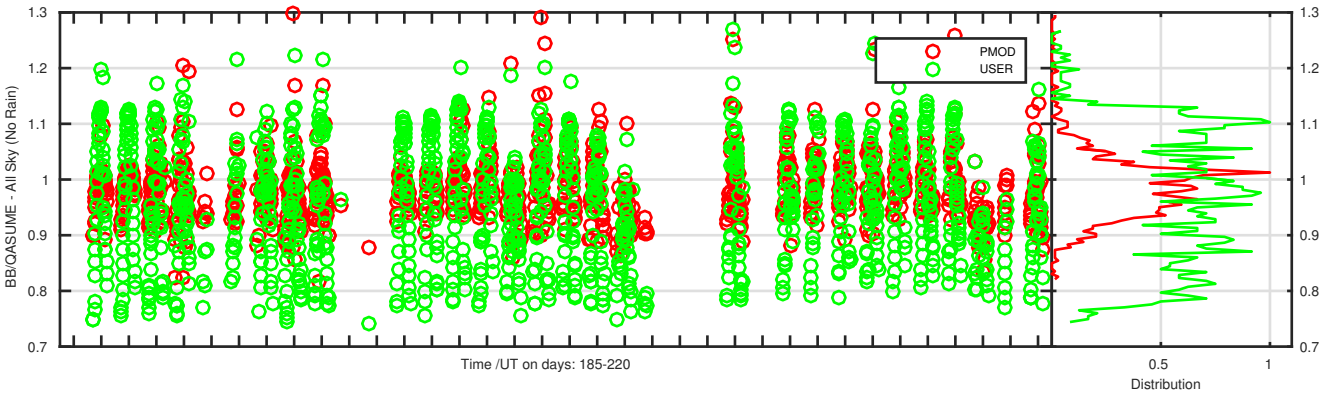

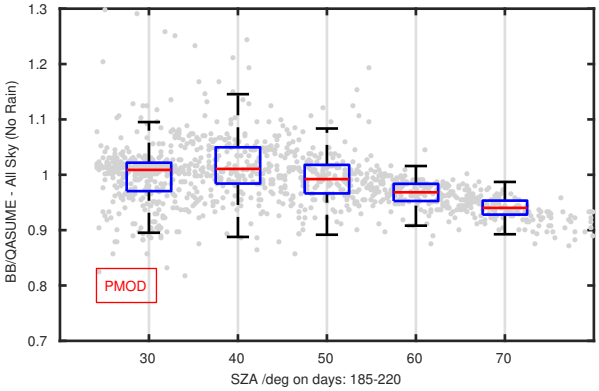

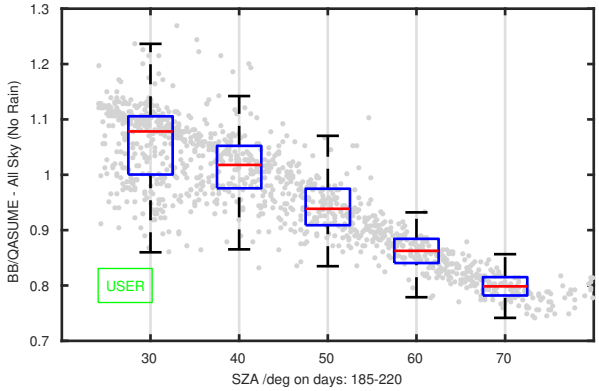

Calibration Results of YES090703 (UVB320)

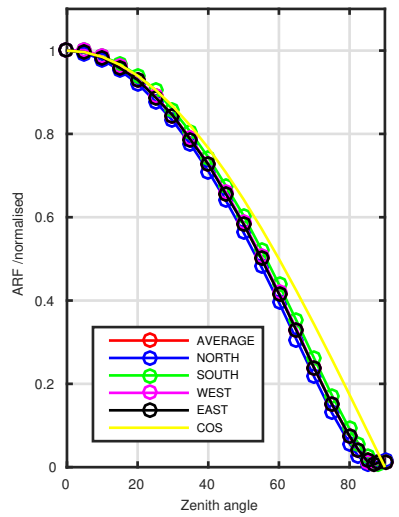

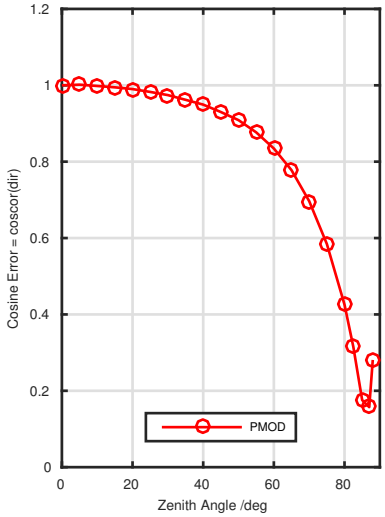

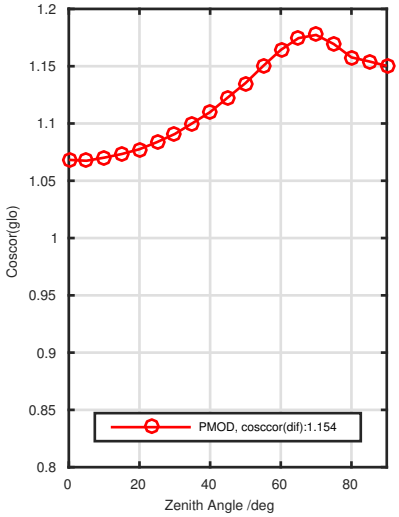

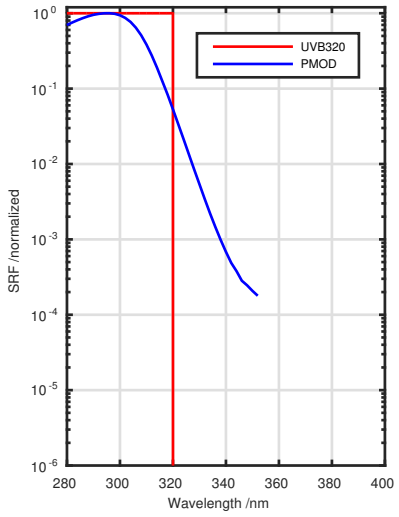

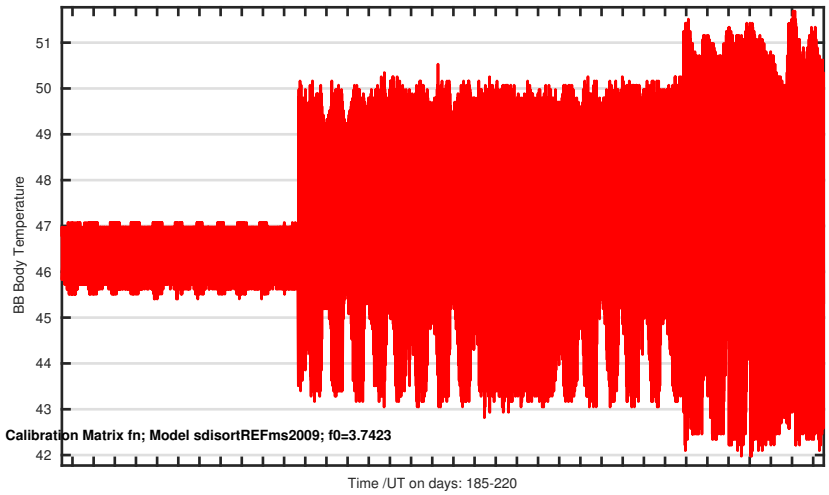

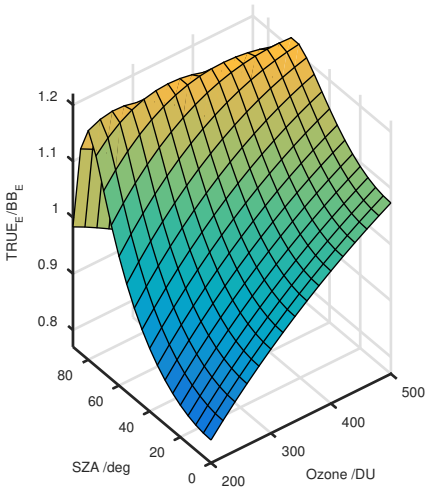

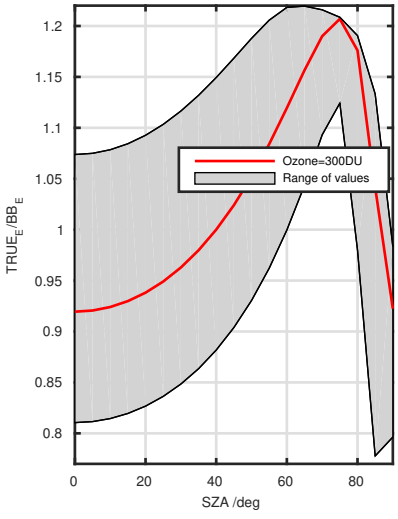

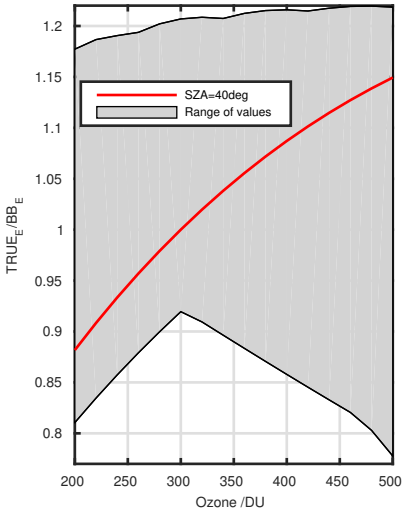

Calibration Results of YES090703 (UVB320)

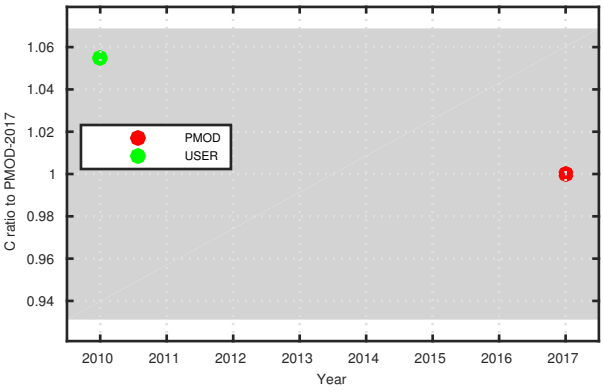

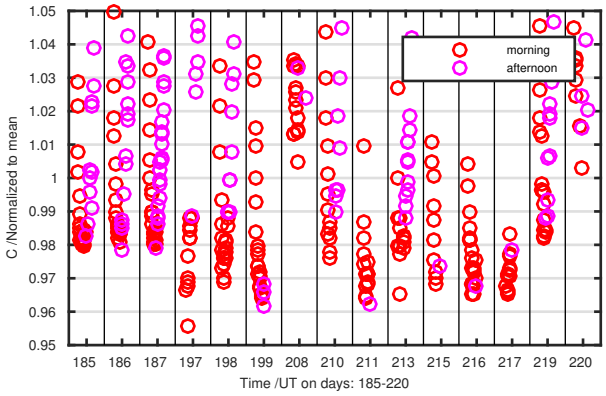

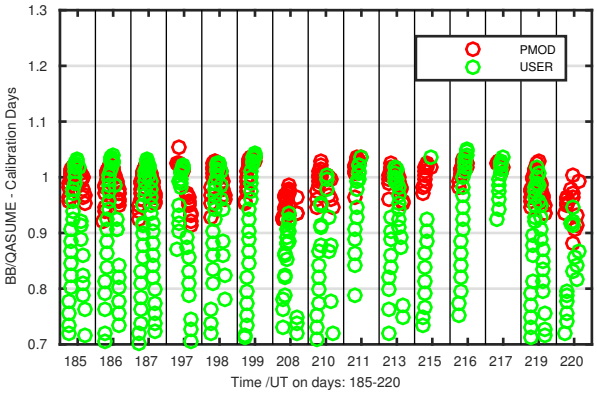

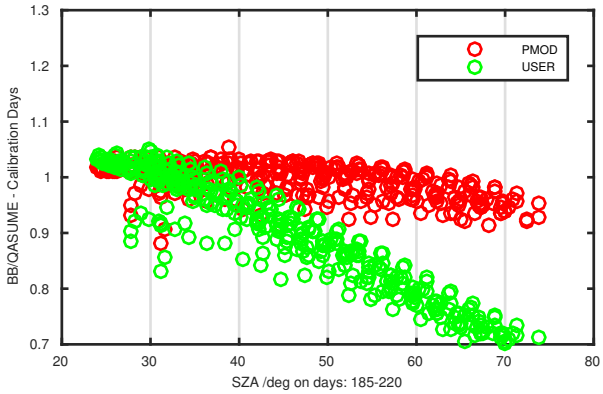

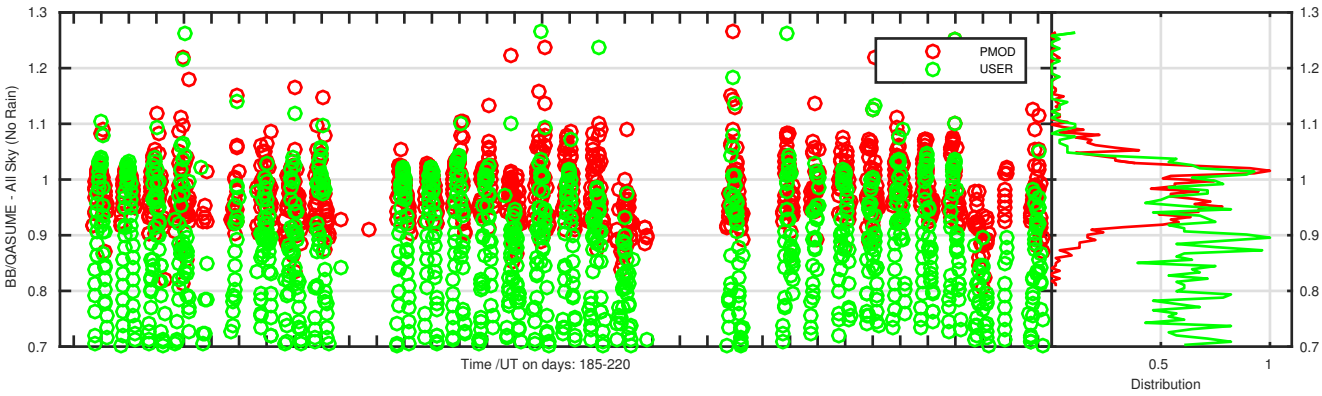

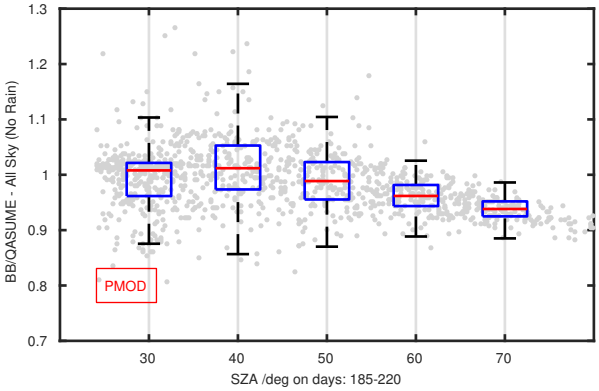

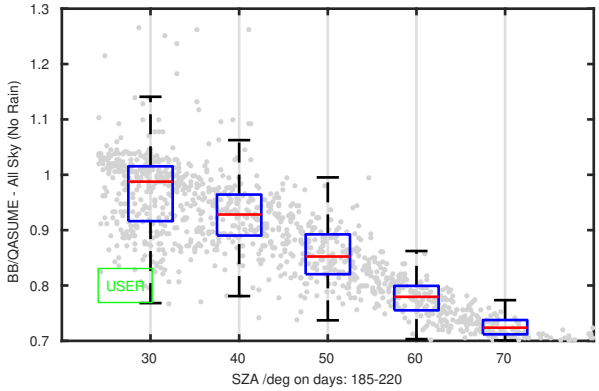

Calibration Results of YES921106 (UVB)

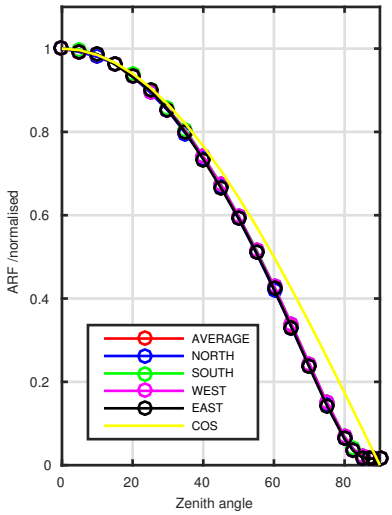

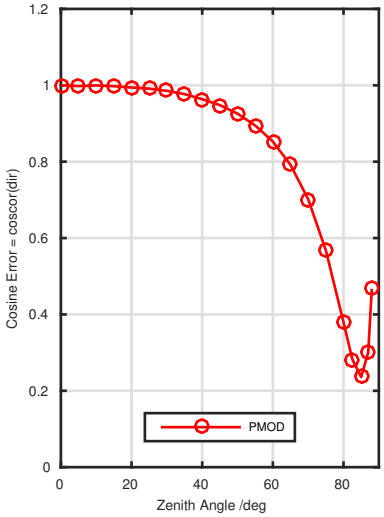

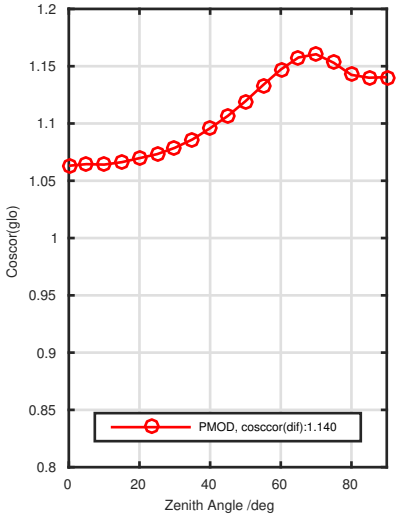

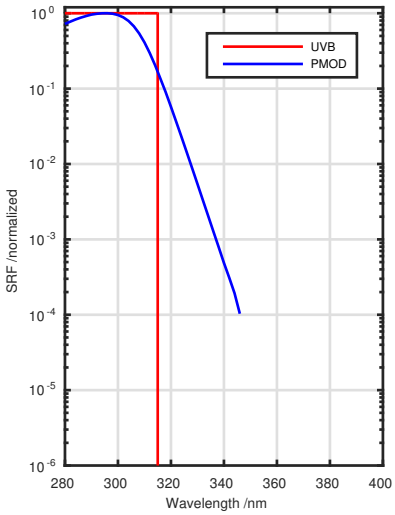

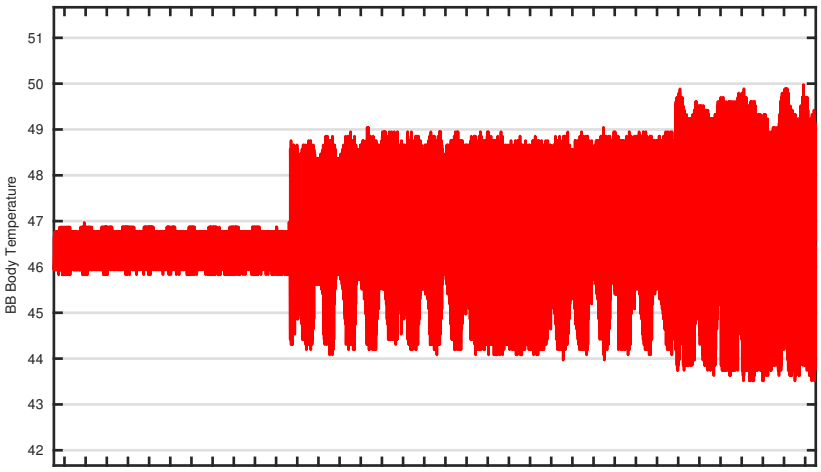

Calibration Matrix fn; Model sdisortREFms2009; f0=1.8175

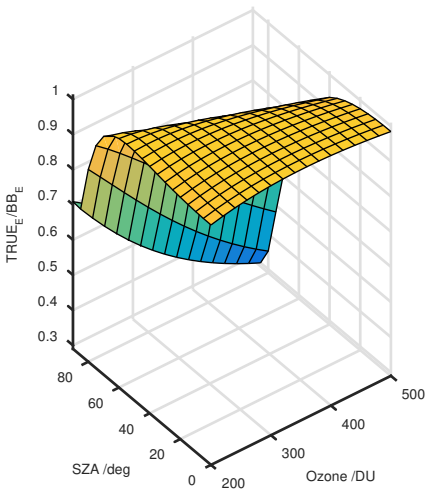

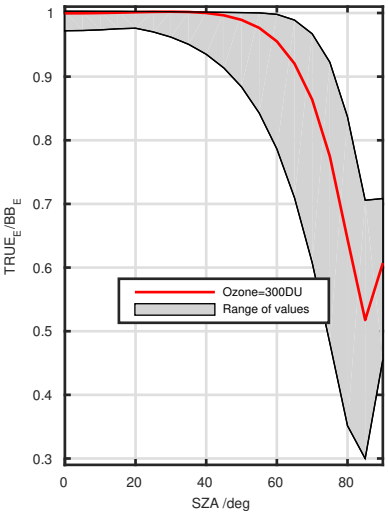

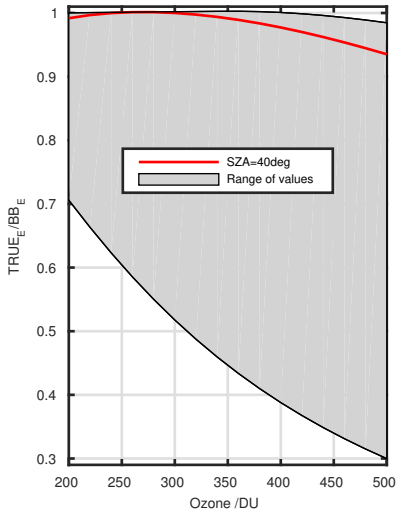

Calibration Results of YES921106 (UVB)

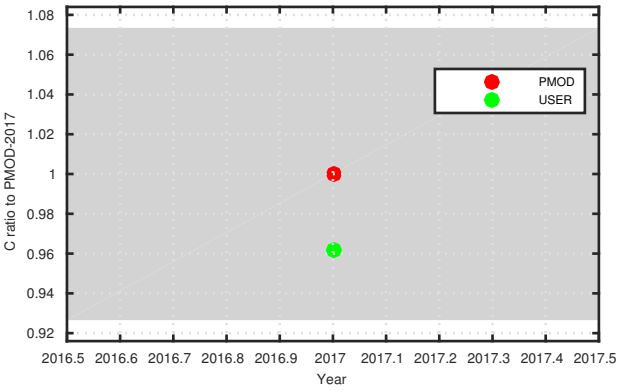

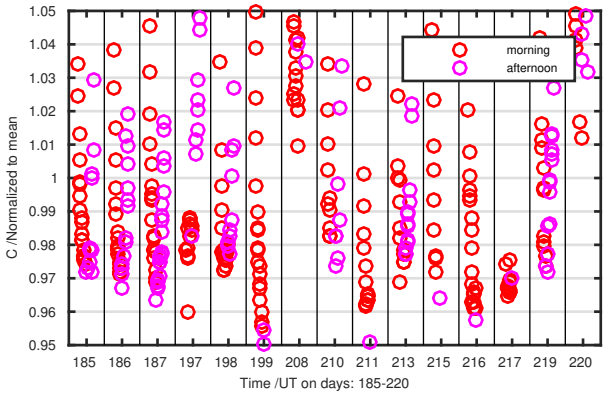

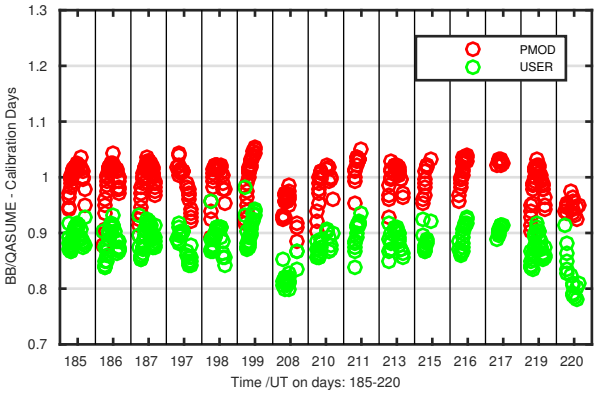

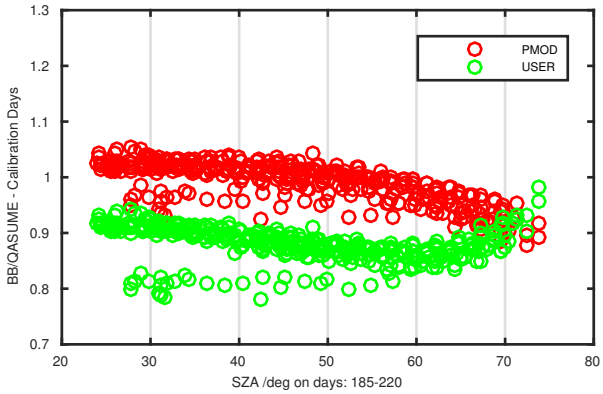

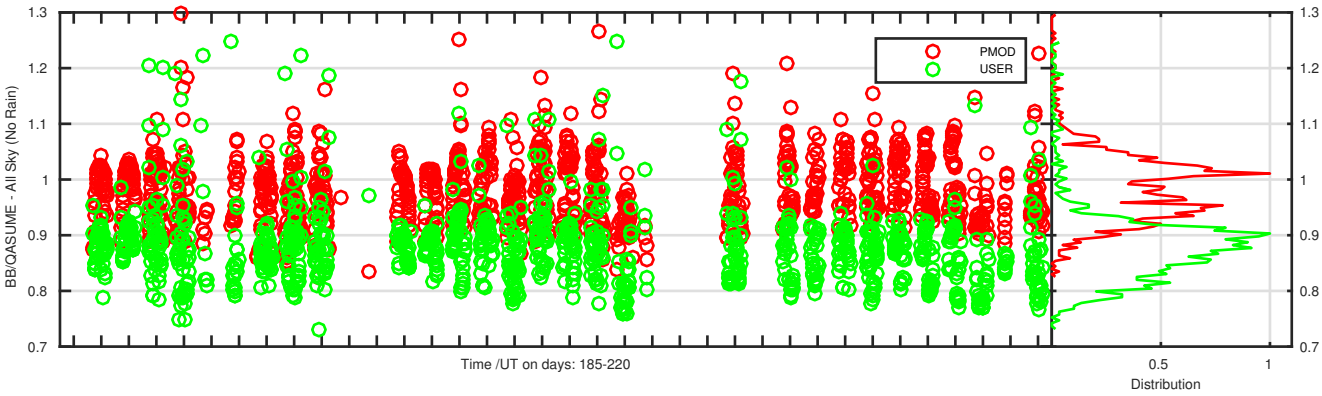

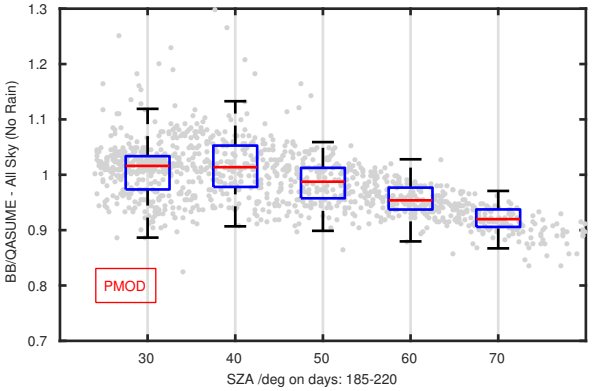

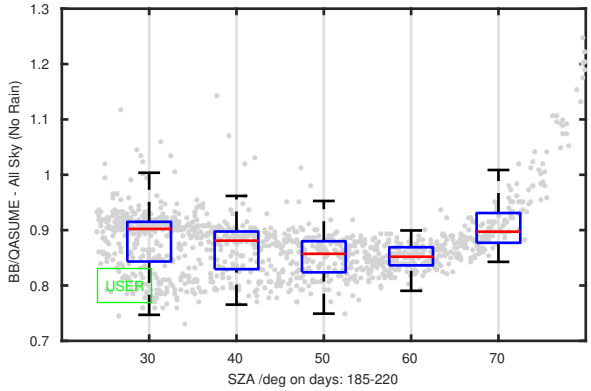

Calibration Results of YES921116 (UVE)

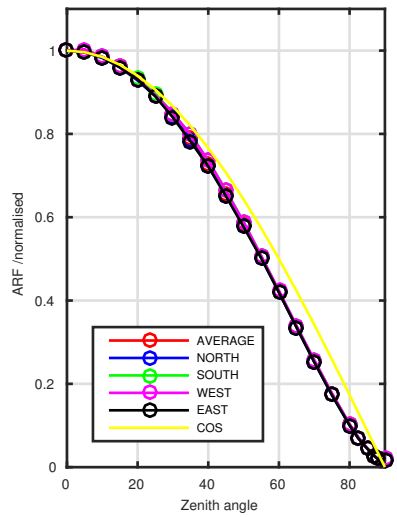

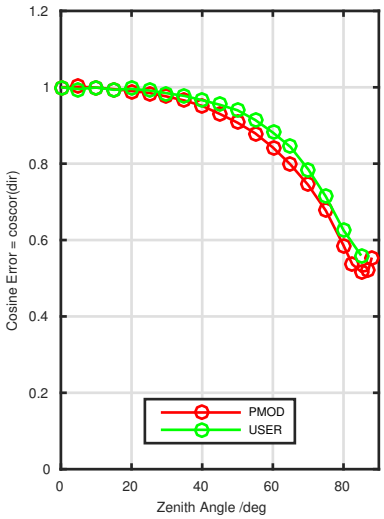

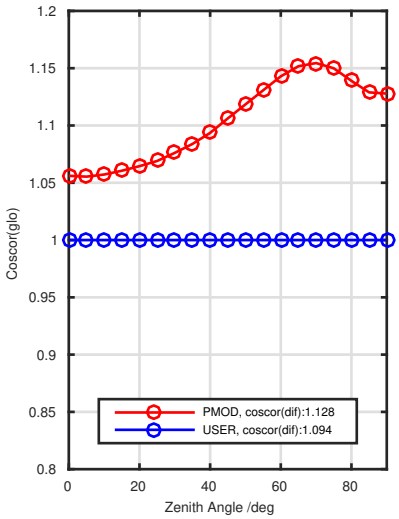

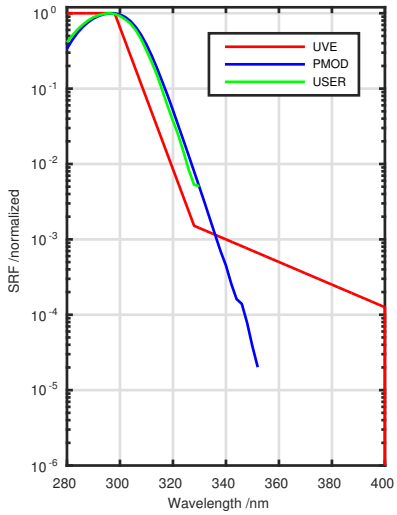

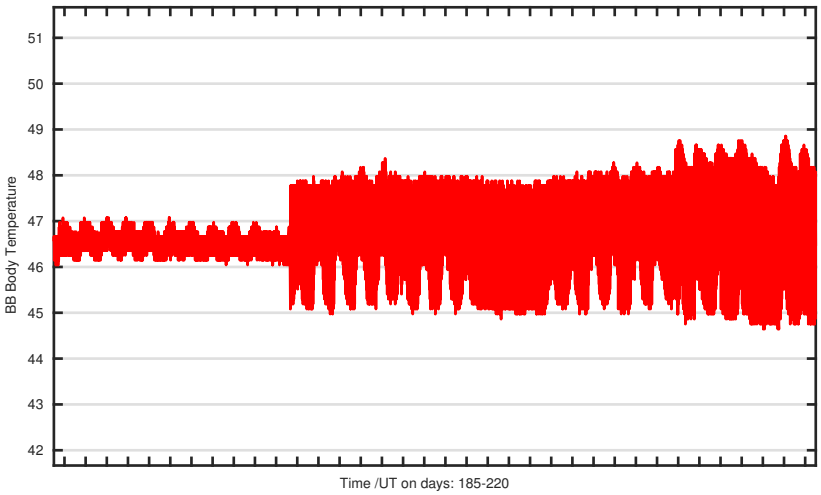

Calibration Matrix fn; Model sdisortREFms2009; f0=0.2525

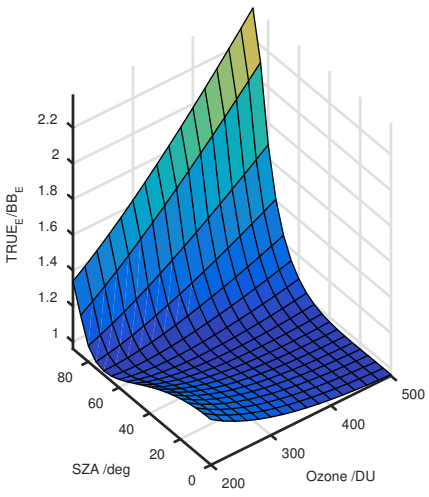

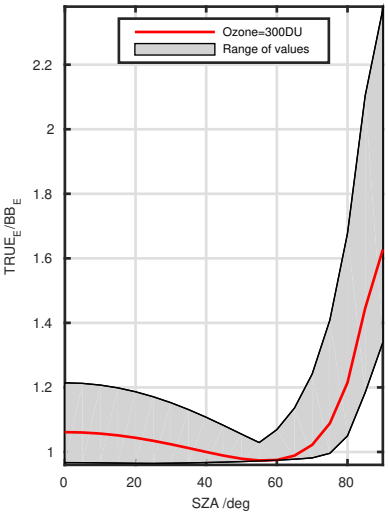

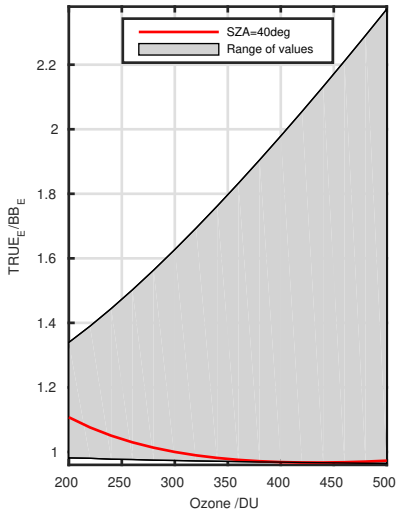

Calibration Results of YES921116 (UVE)

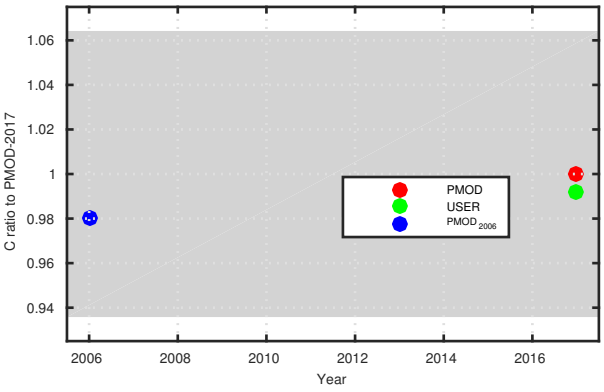

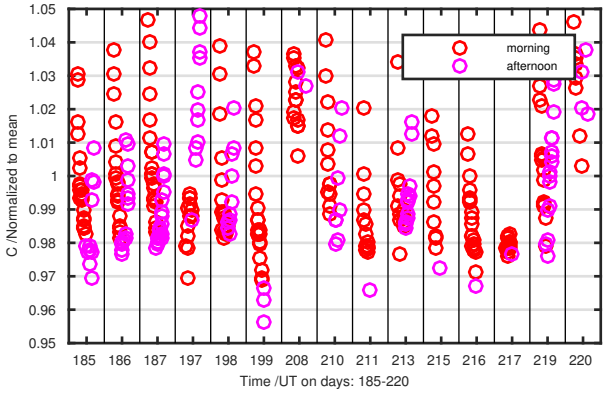

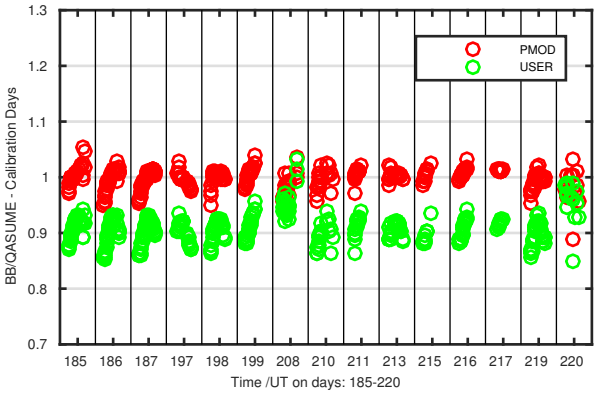

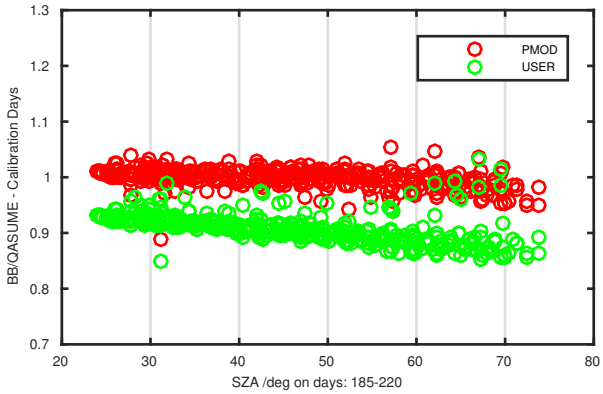

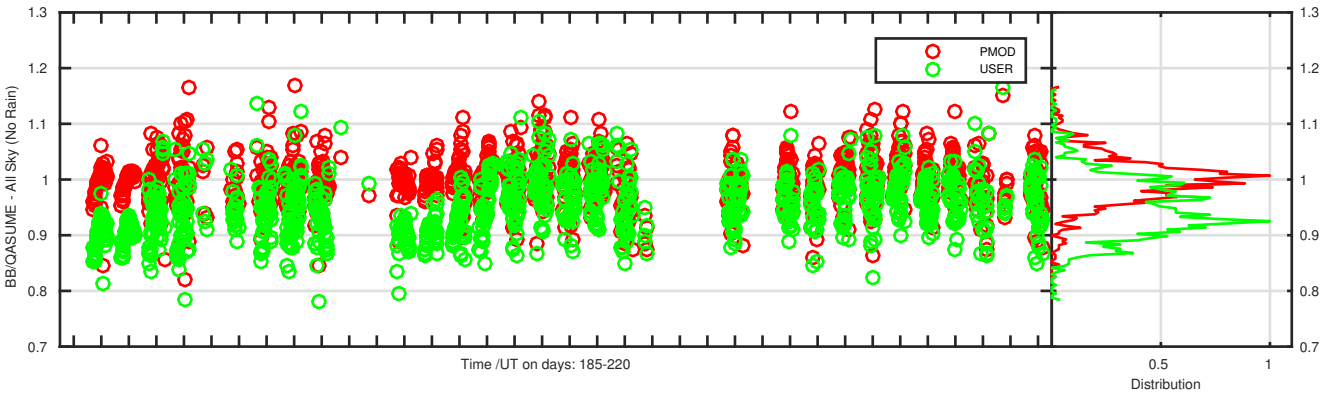

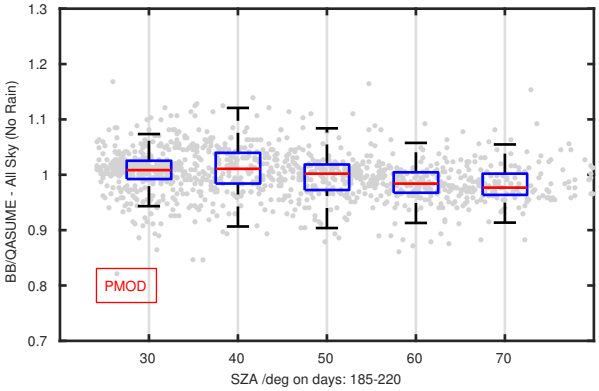

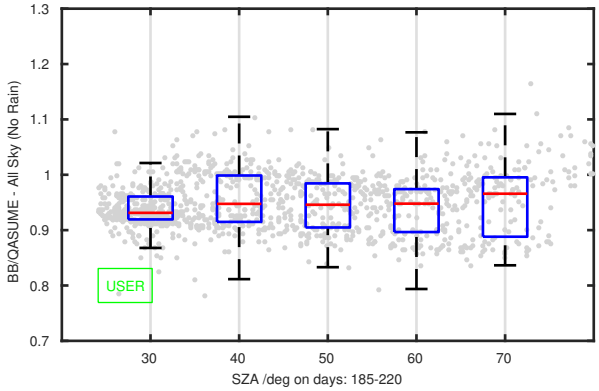

Calibration Results of YES930204 (UVB)

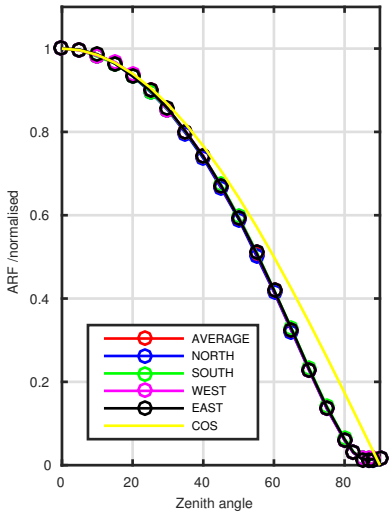

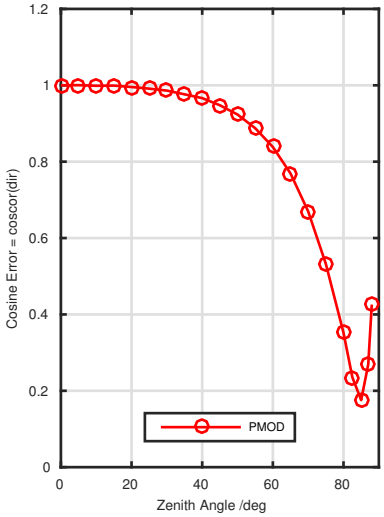

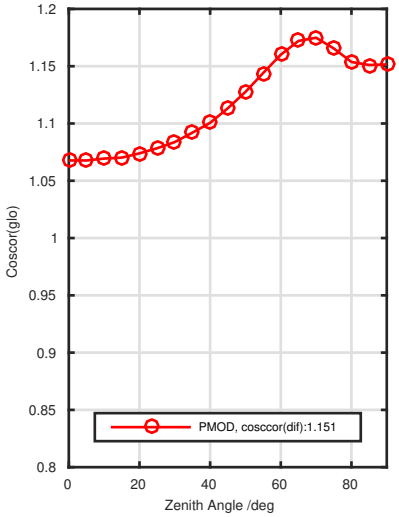

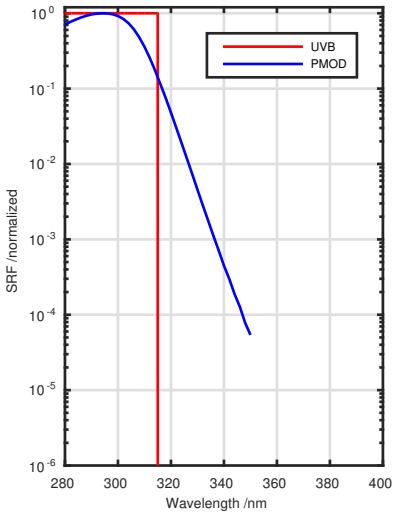

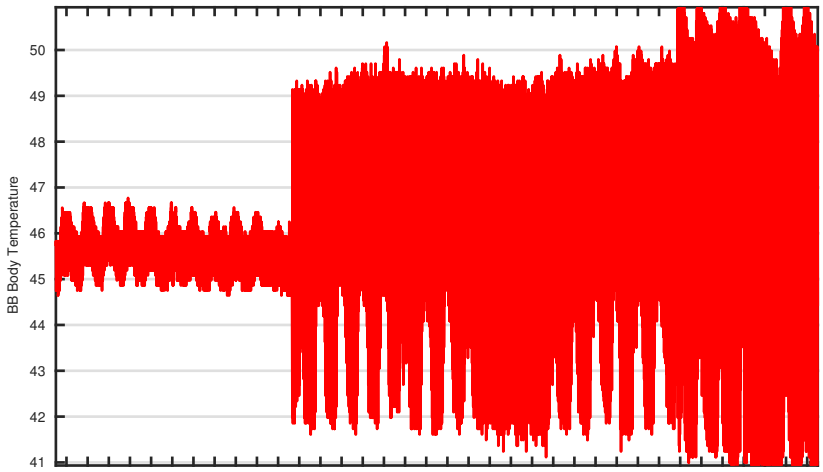

Calibration Matrix fn; Model sdisortREFms2009; f0=2.0782

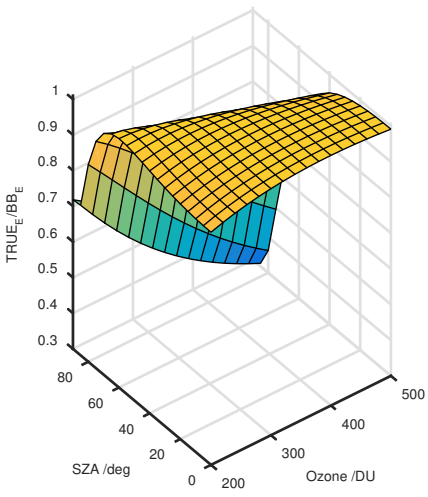

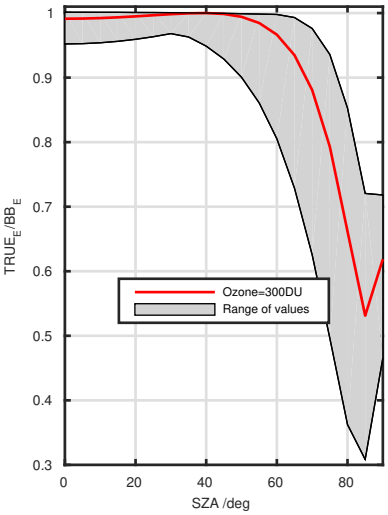

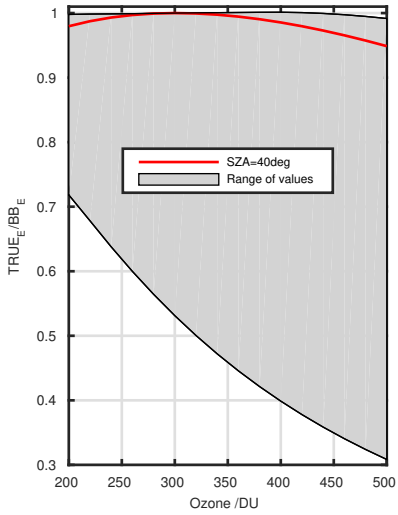

Calibration Results of YES930204 (UVB)

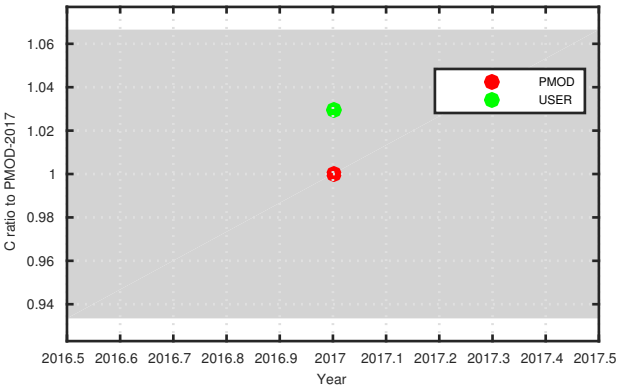

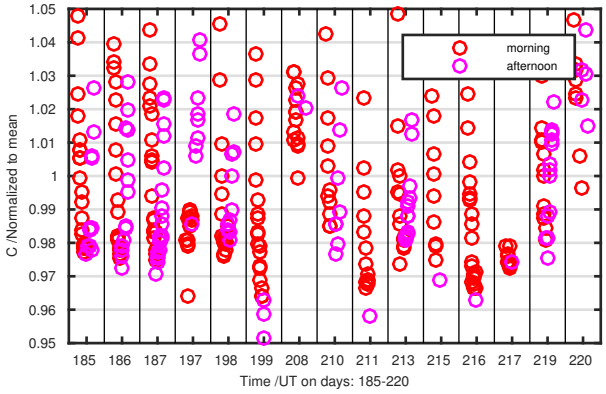

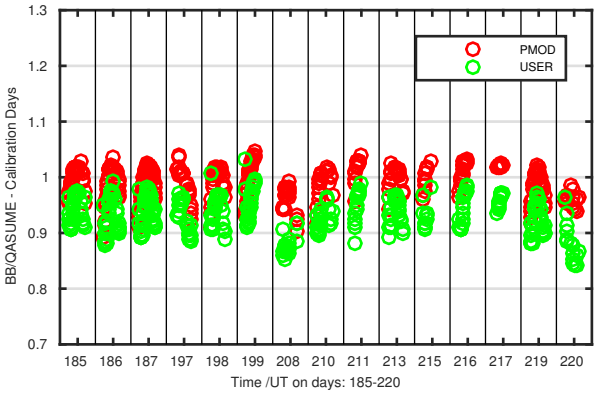

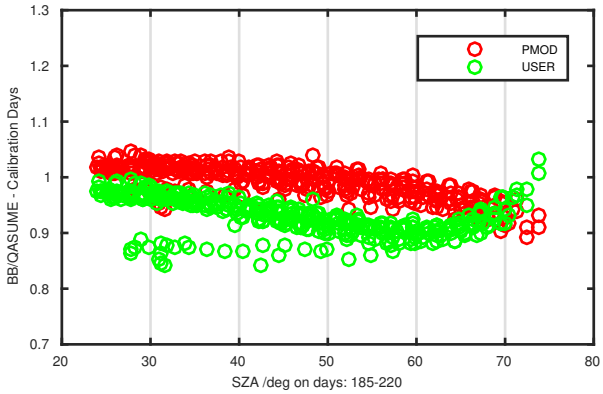

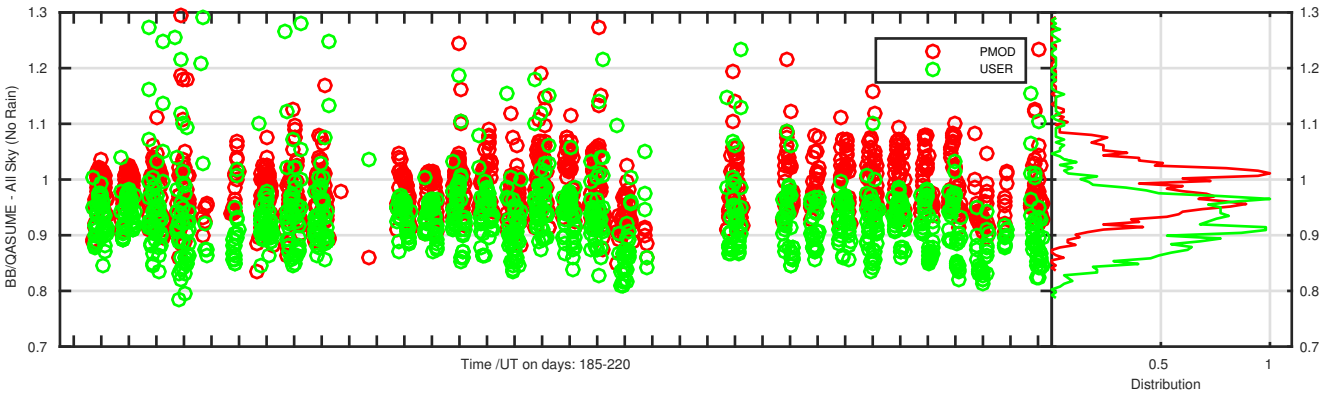

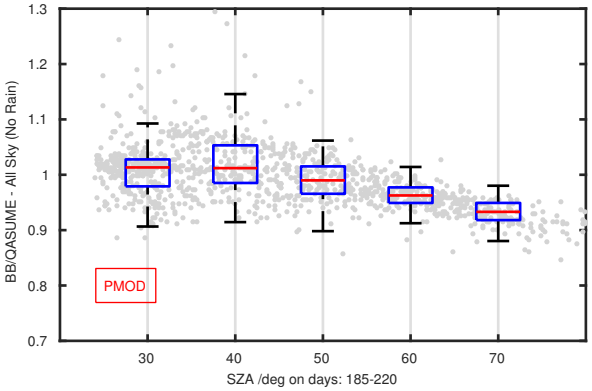

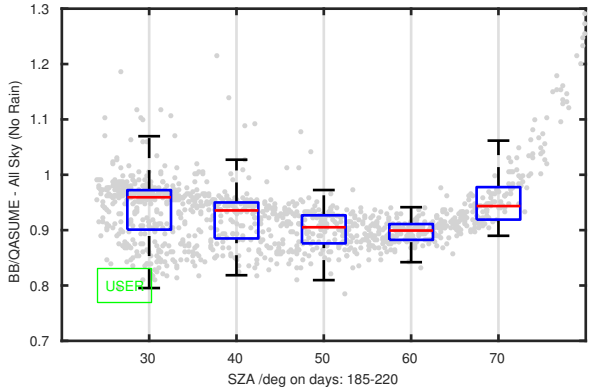

Calibration Results of YES960819 (UVB)

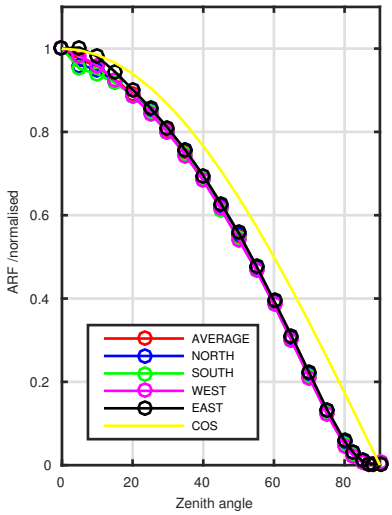

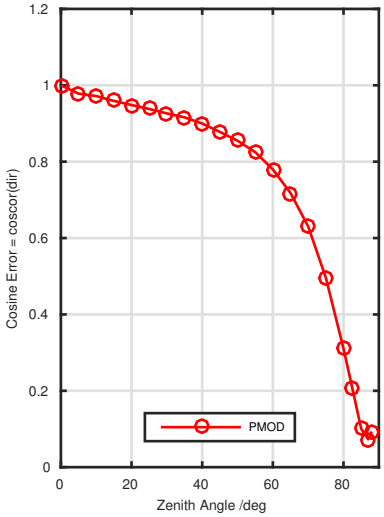

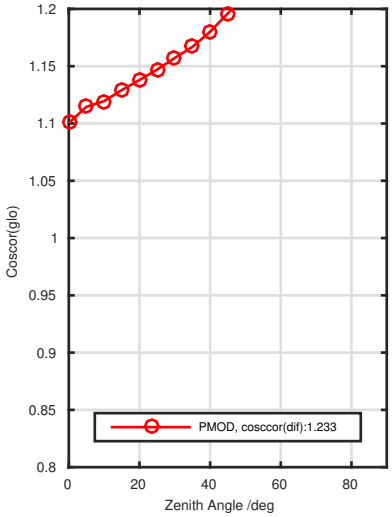

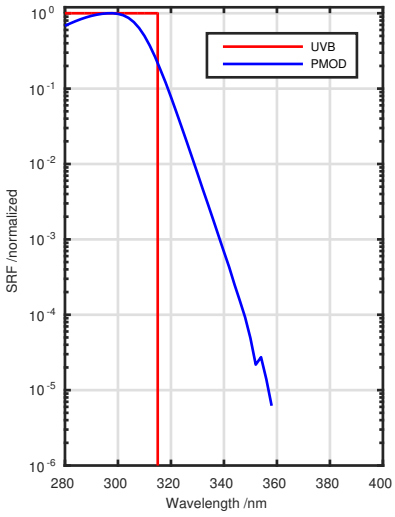

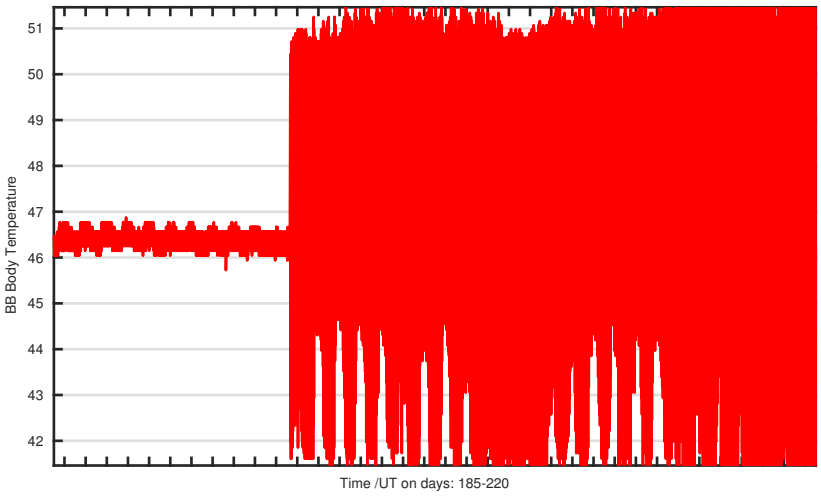

Calibration Matrix fn; Model sdisortREFms2009; f0=1.4661

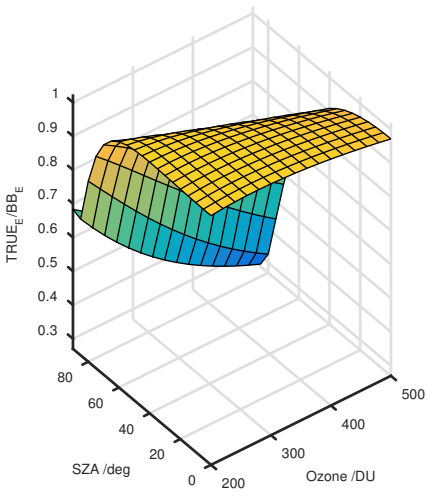

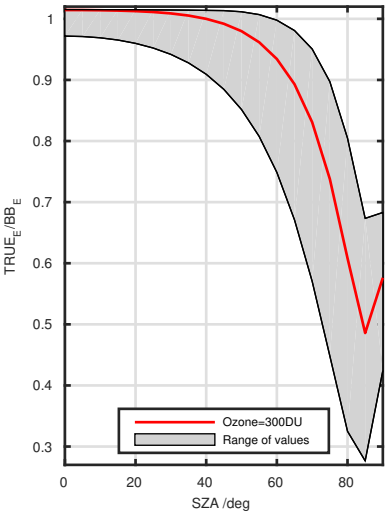

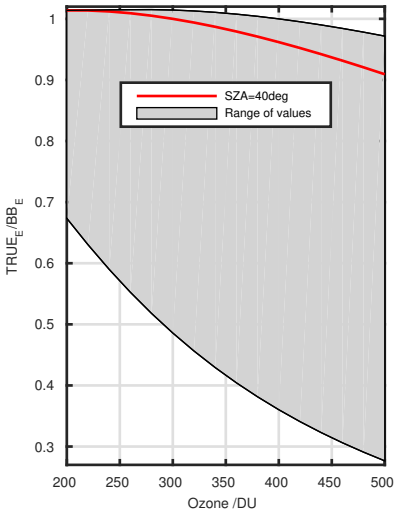

Calibration Results of YES960819 (UVB)

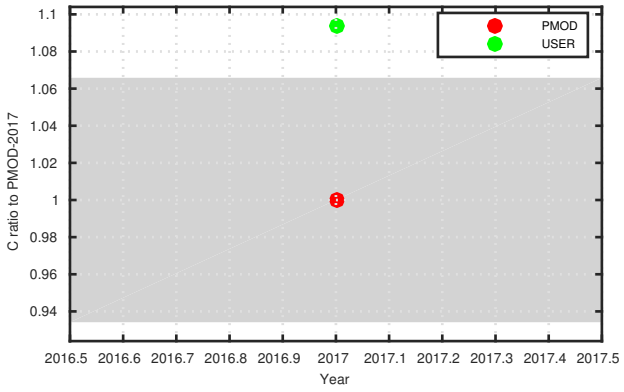

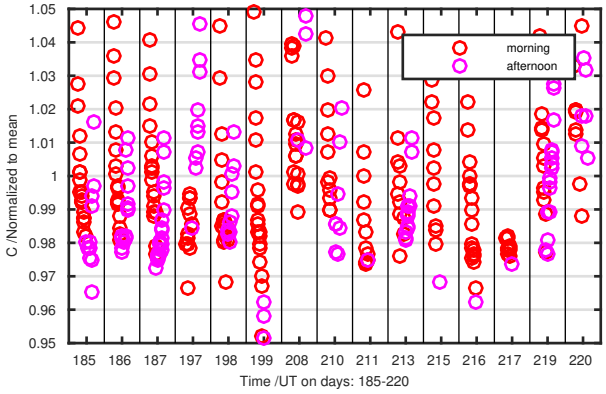

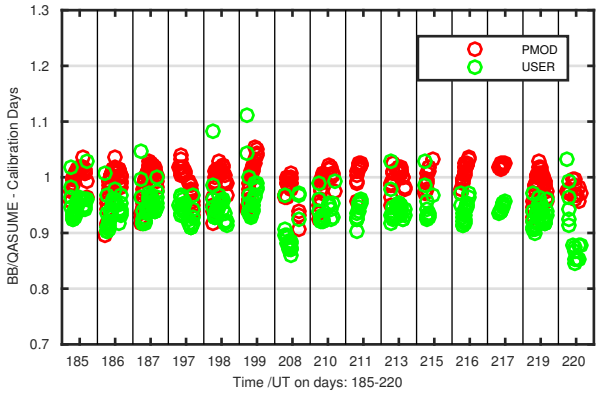

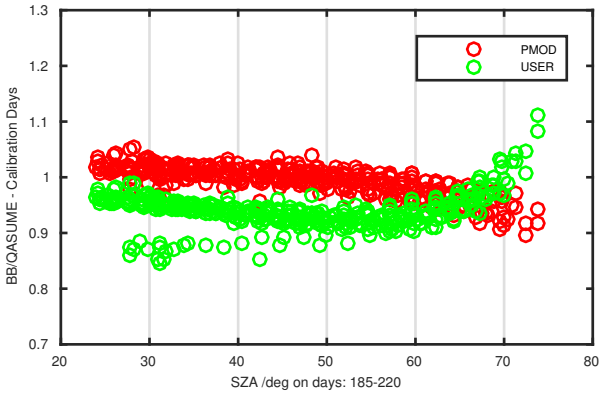

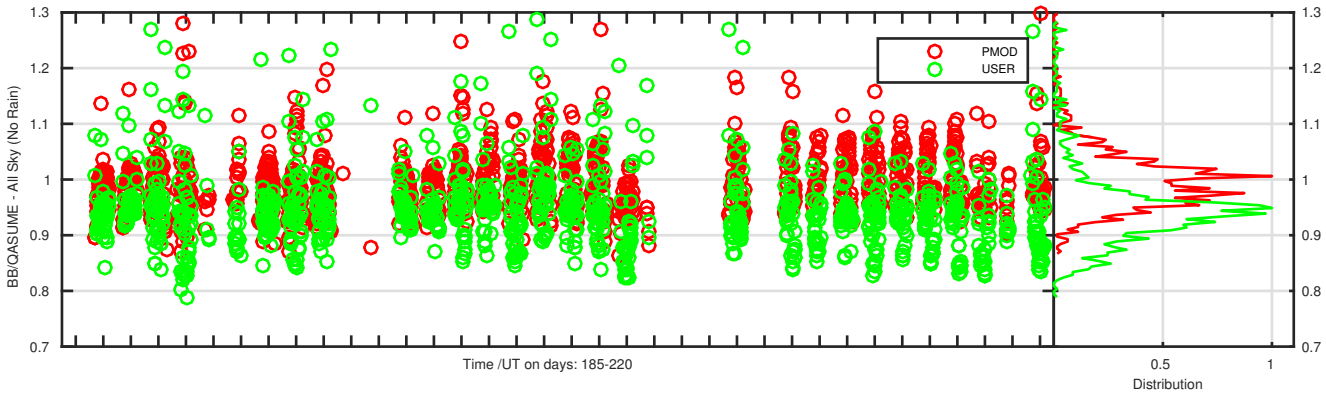

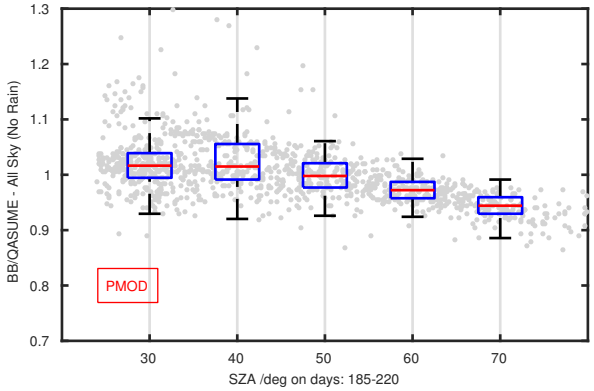

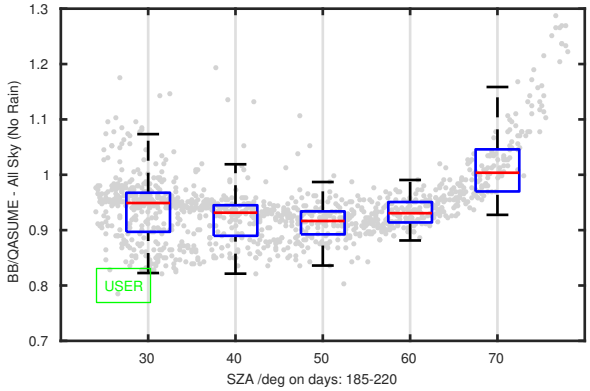

Calibration Results of YES990608 (UVE)

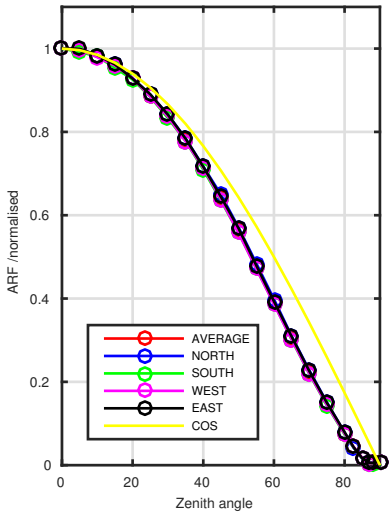

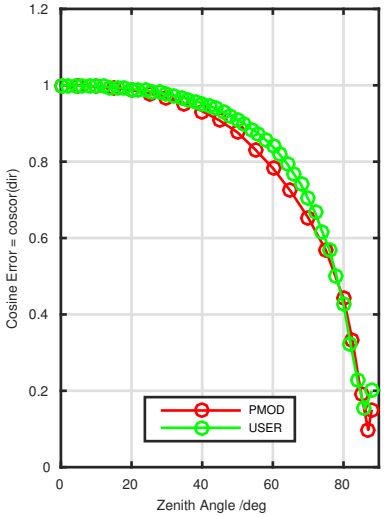

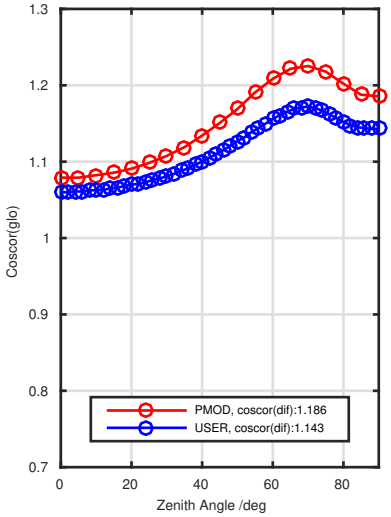

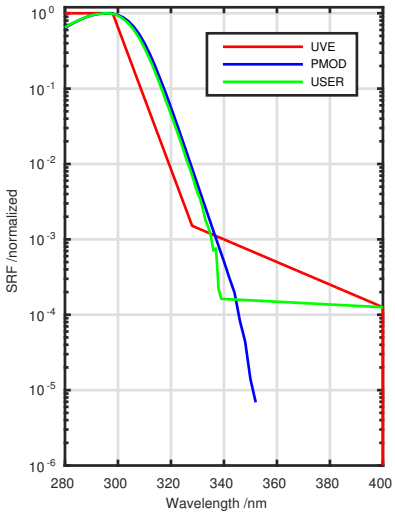

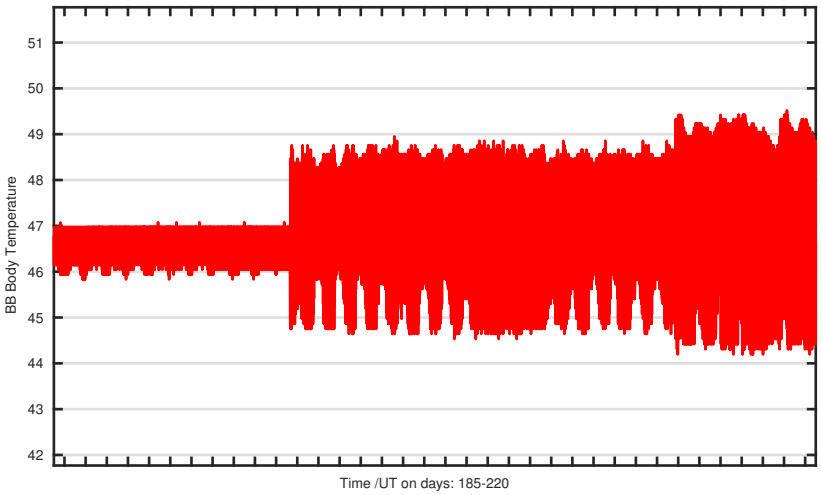

Calibration Matrix fn; Model sdisortREFms2009; f0=0.2407

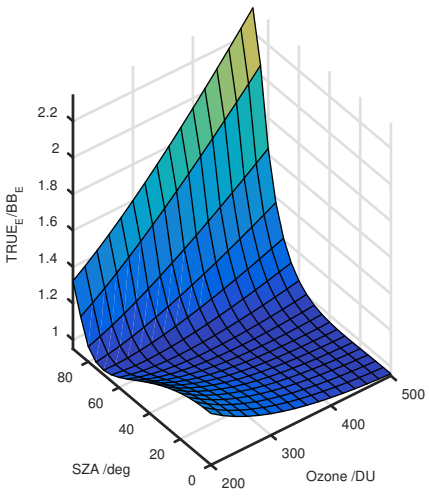

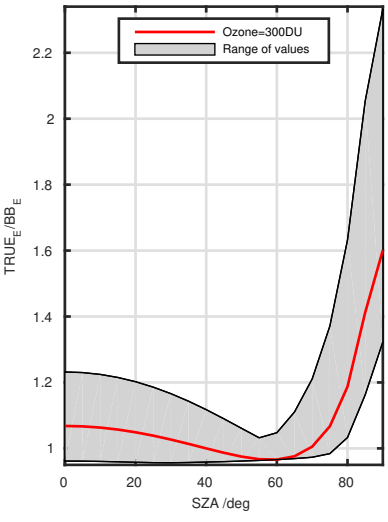

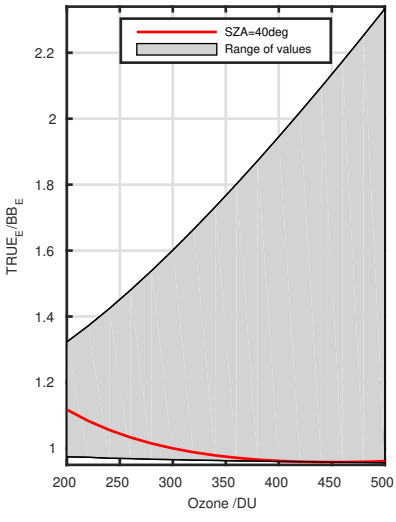

Calibration Results of YES990608 (UVE)

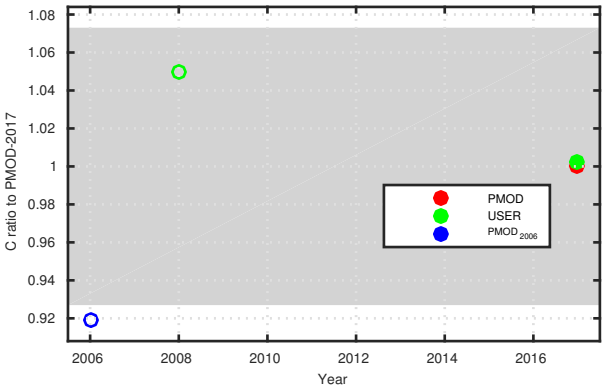

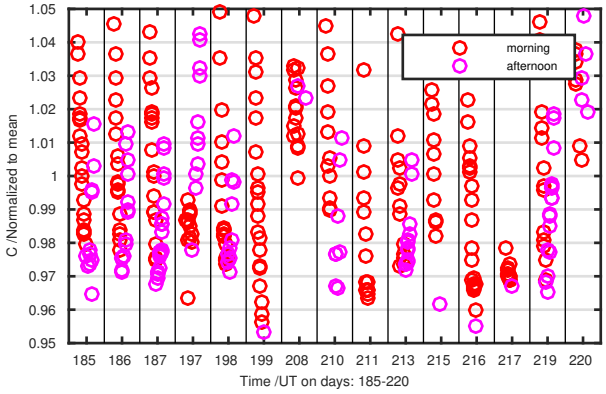

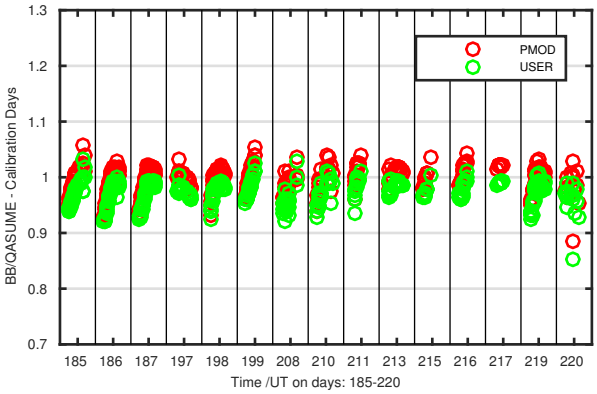

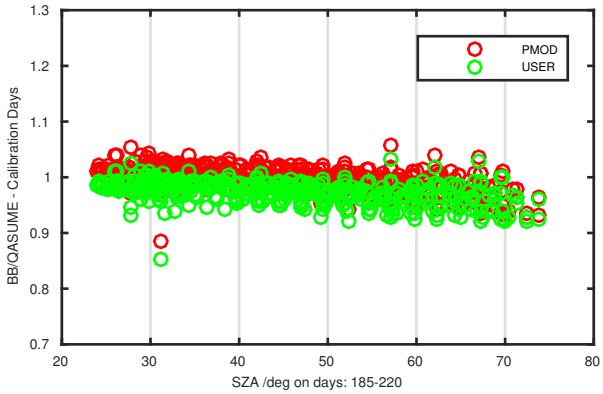

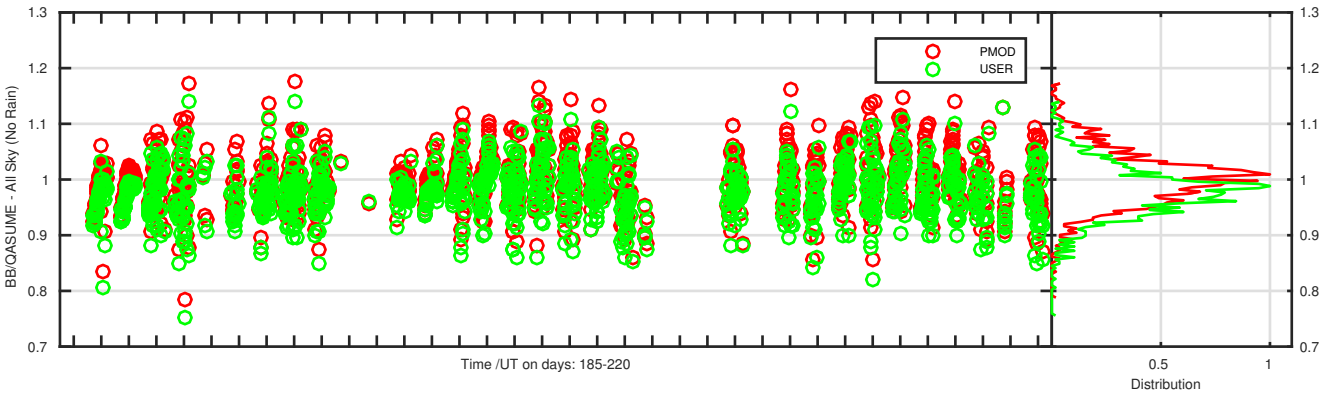

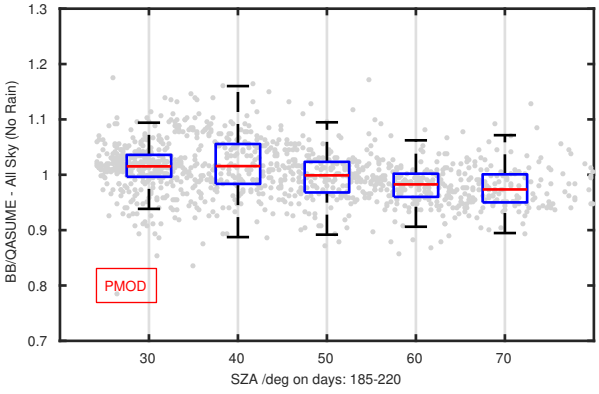

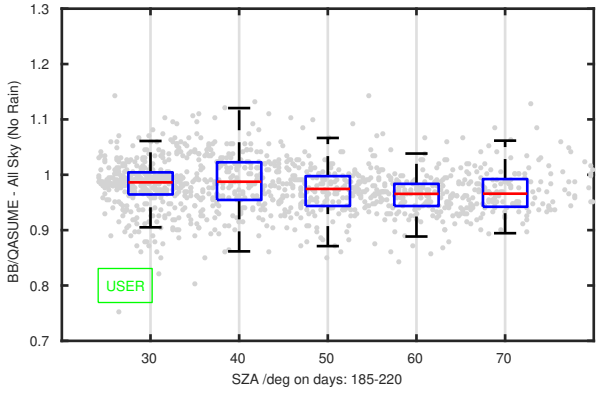

Calibration Results of YES990703 (UVB320)

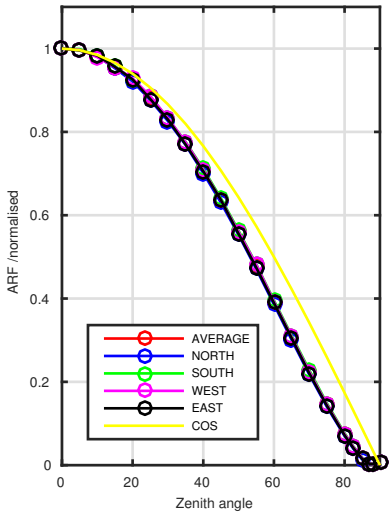

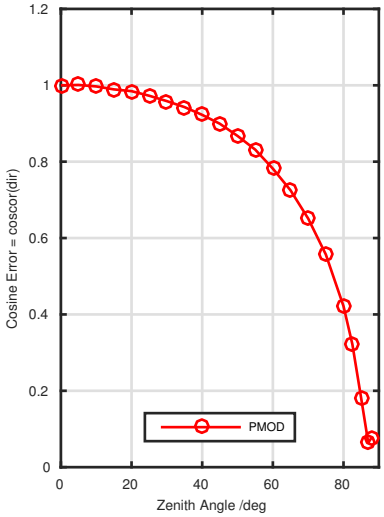

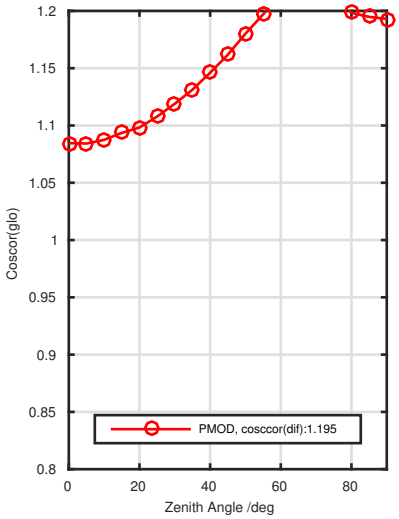

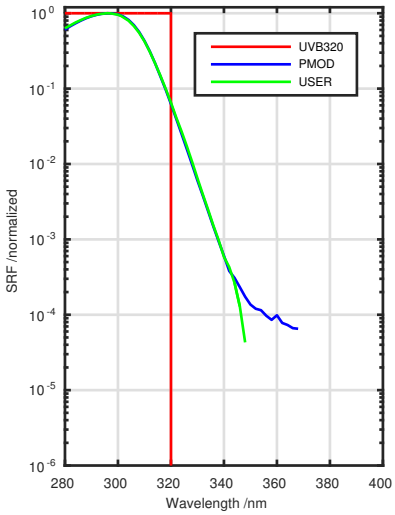

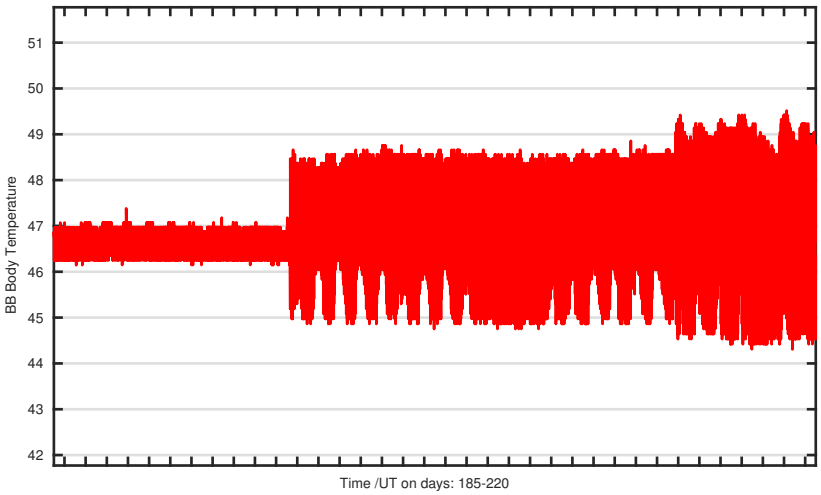

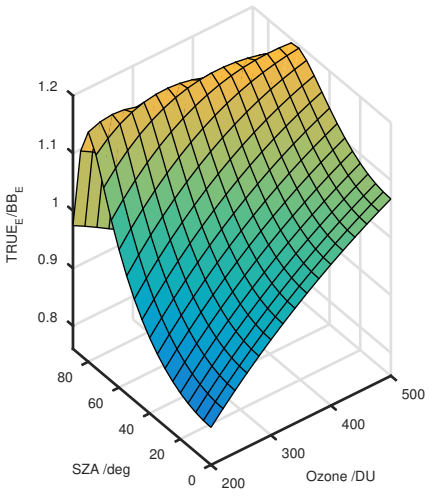

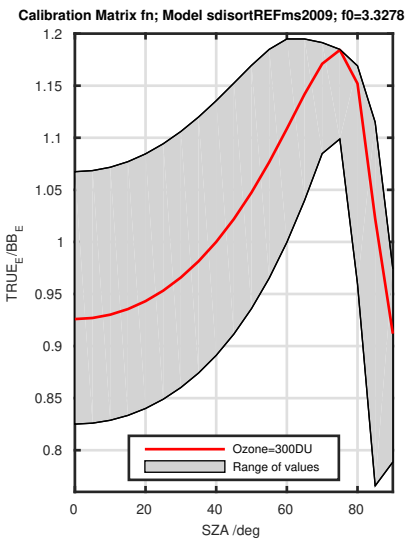

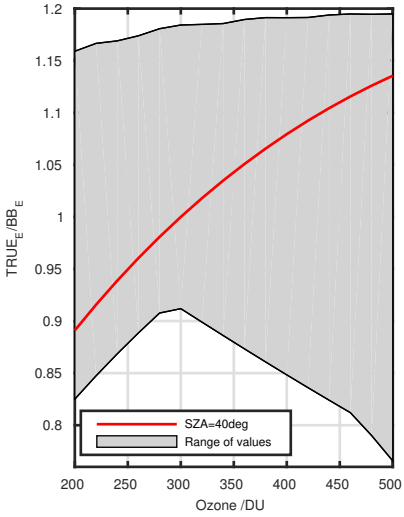

Calibration Results of YES990703 (UVB320)

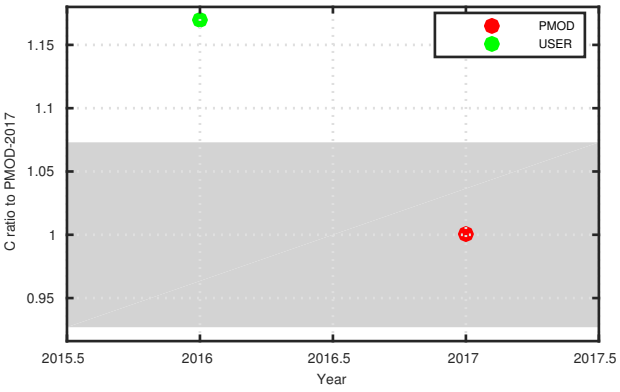

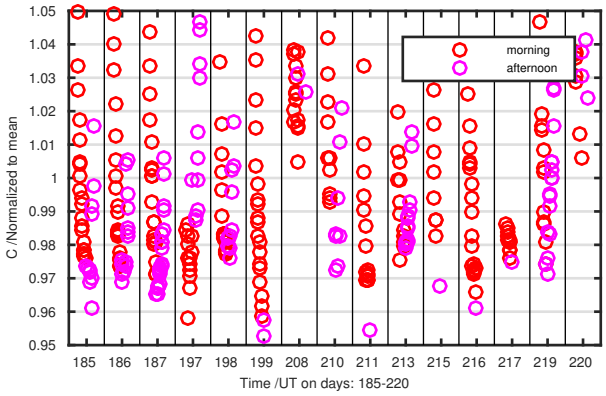

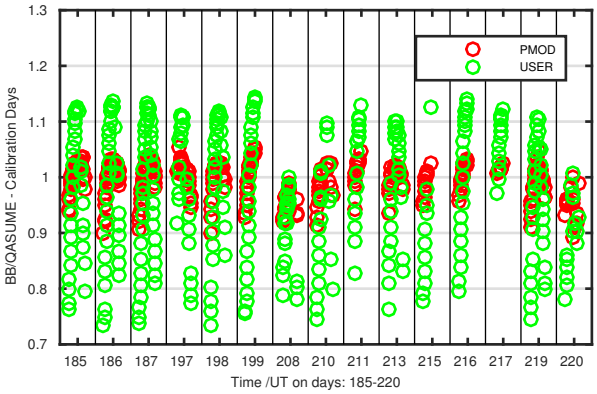

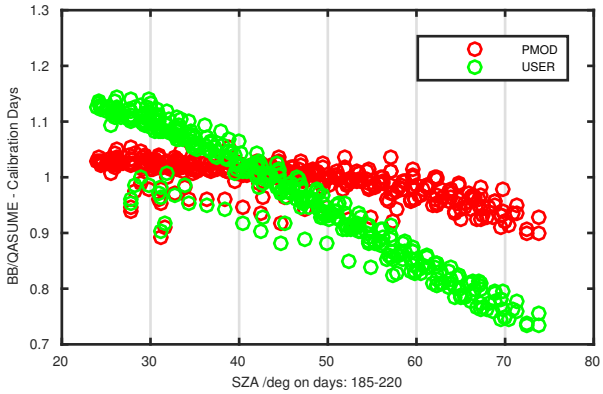

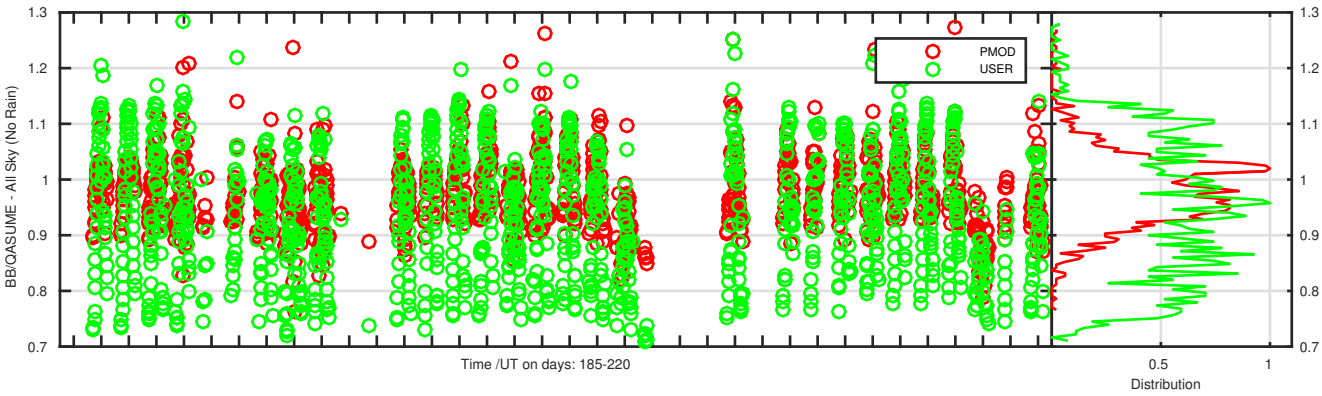

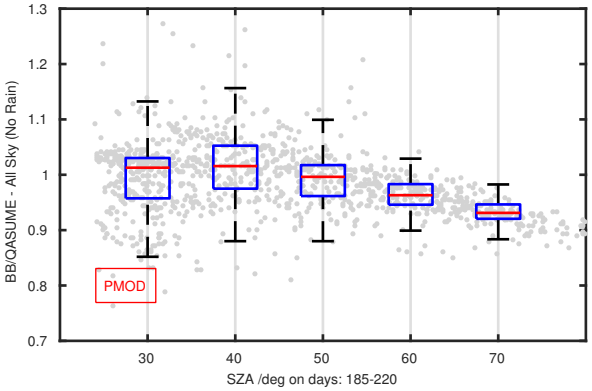

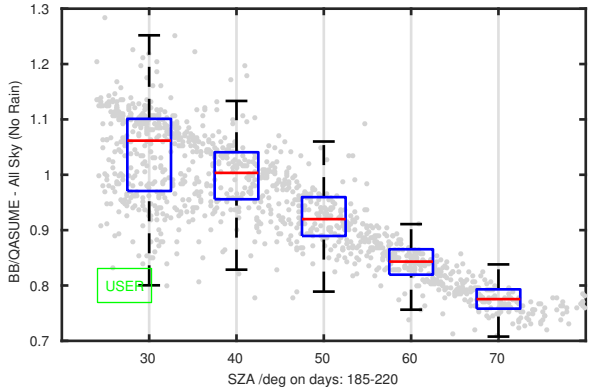

Calibration Results of DELTA15010872 (UVE)

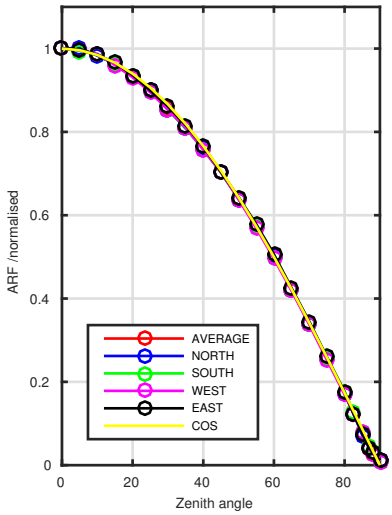

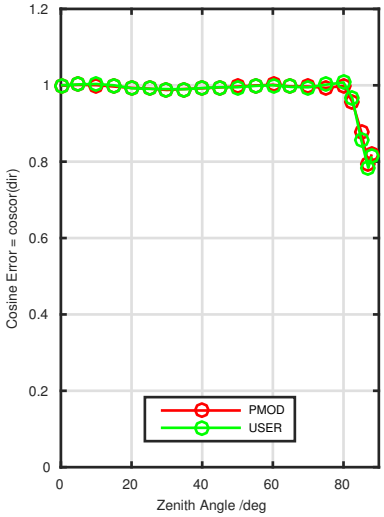

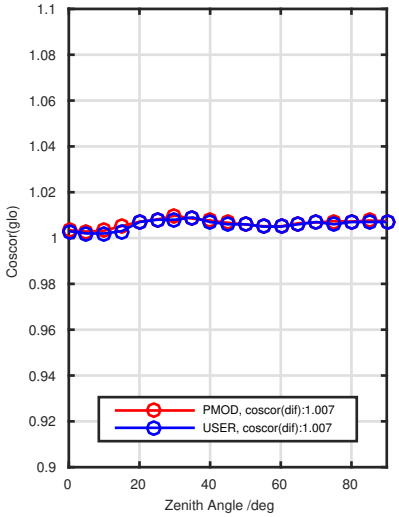

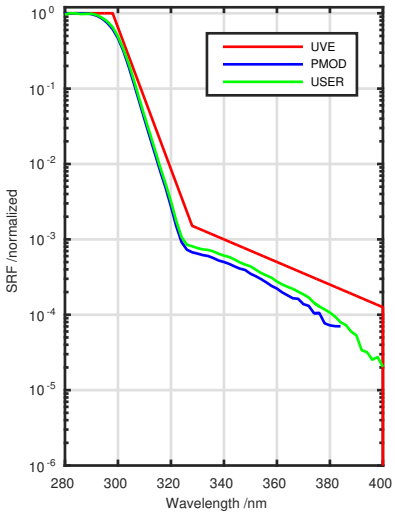

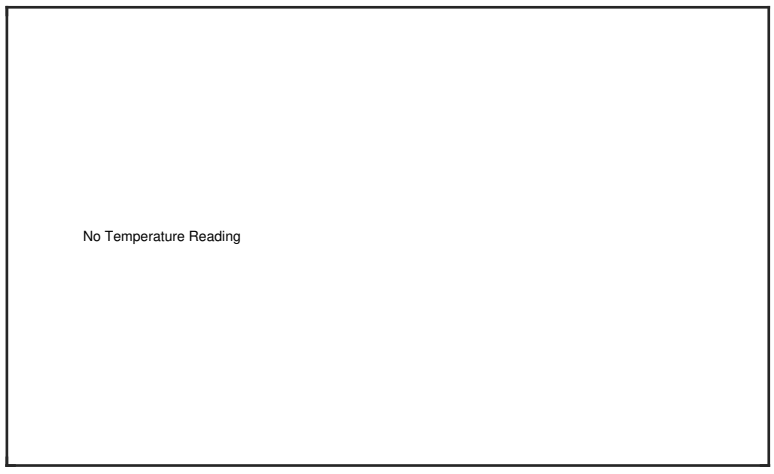

Calibration Matrix fn; Model sdisortREFms2009; f0=1.8656

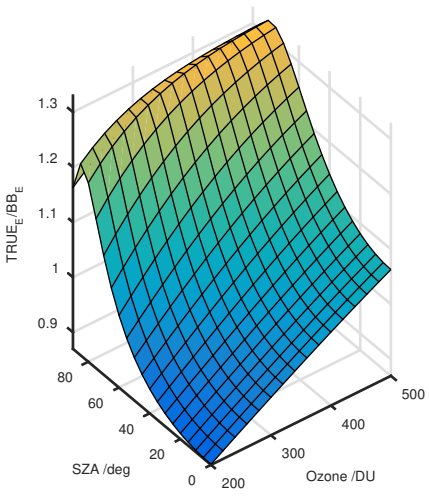

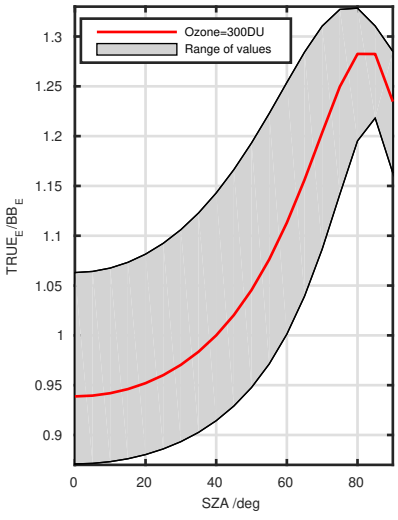

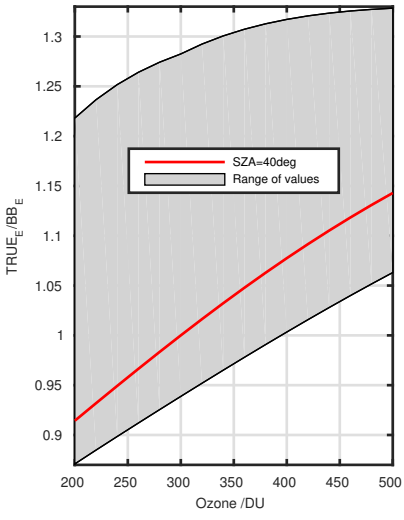

Calibration Results of DELTA15010872 (UVE)

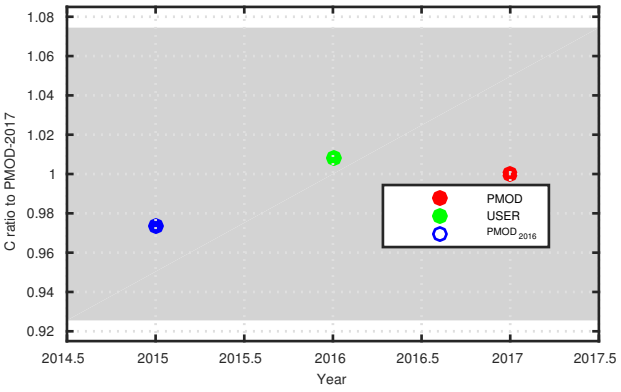

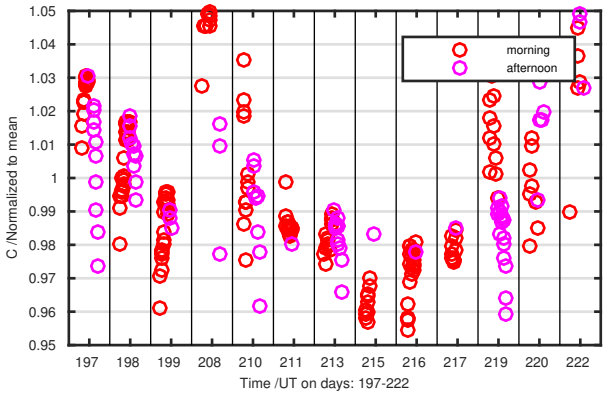

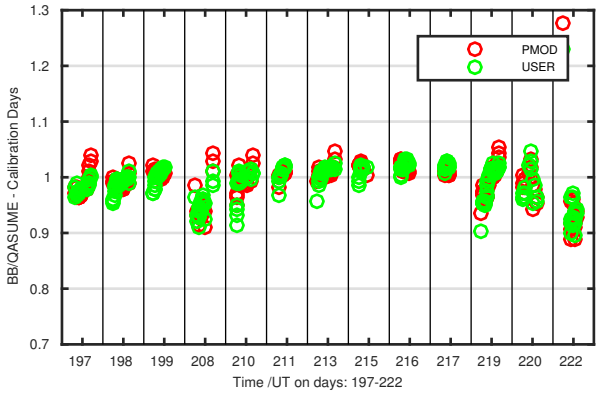

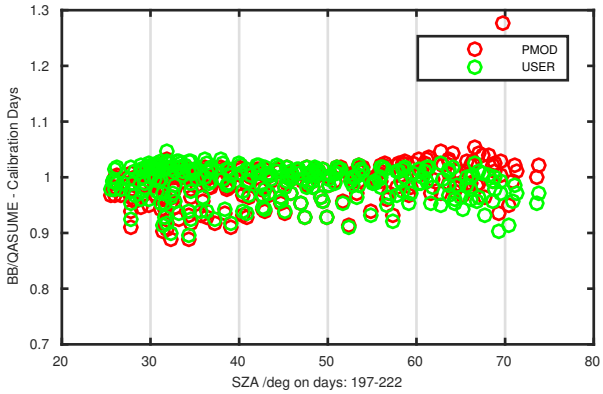

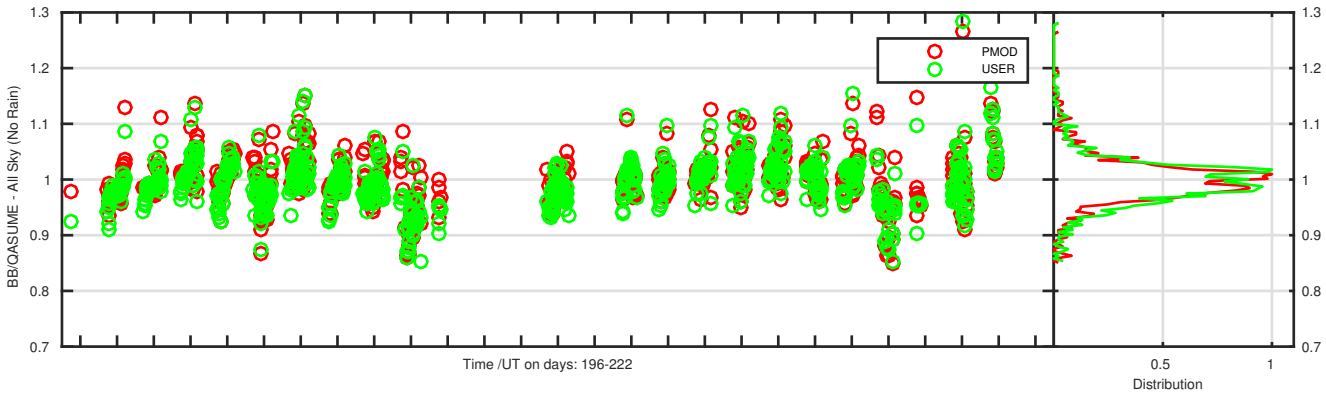

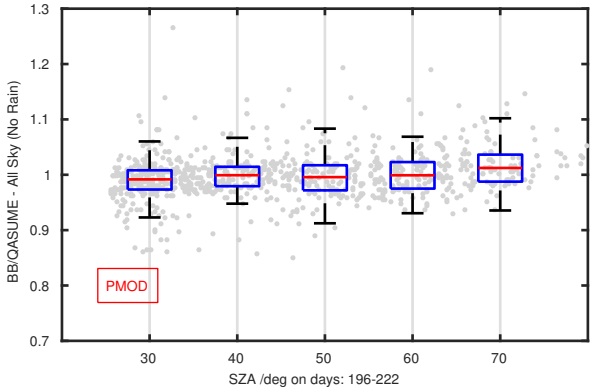

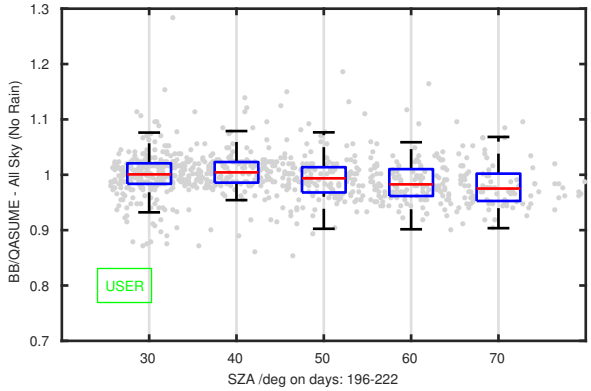

Calibration Results of DELTA17010973 (UVE)

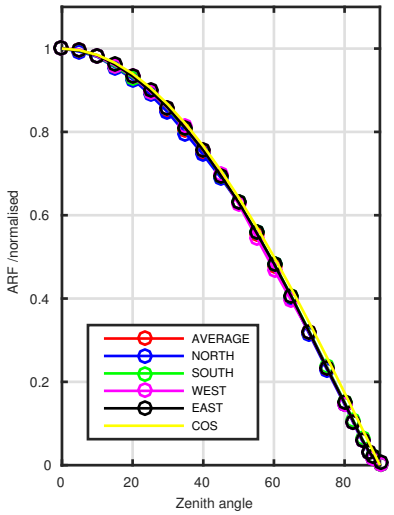

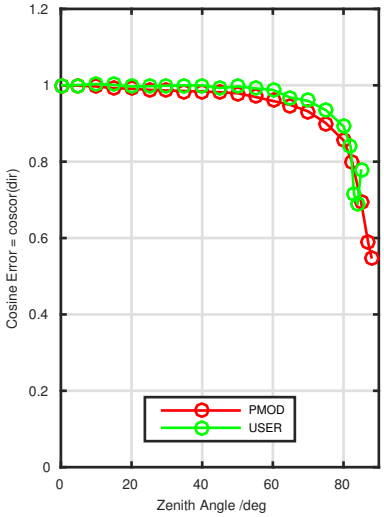

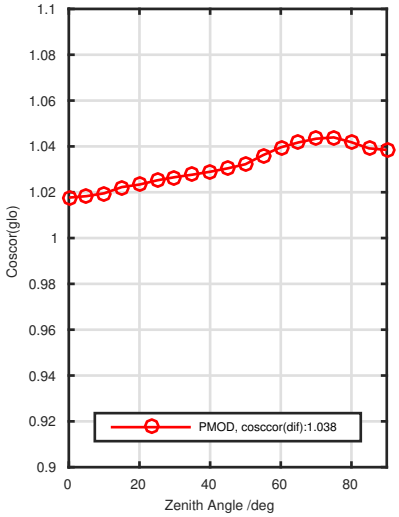

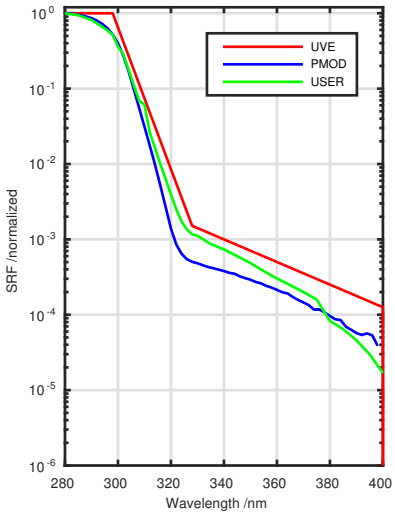

No Temperature Reading

Calibration Matrix fn; Model sdisortREFms2009; f0=2.3204

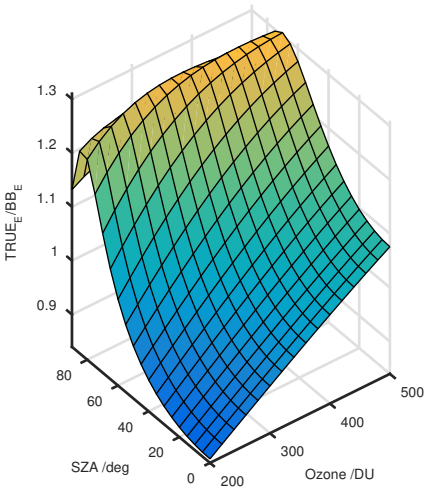

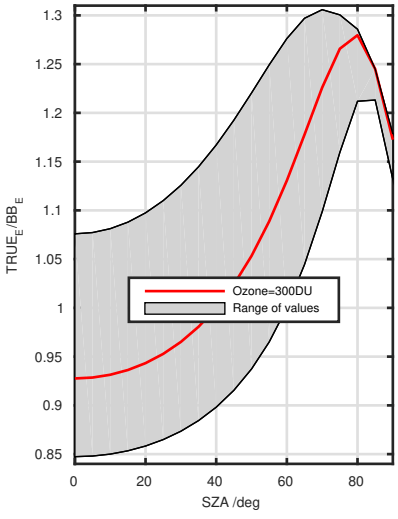

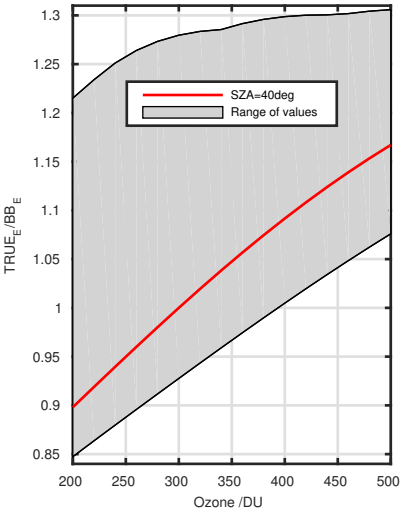

Calibration Results of DELTA17010973 (UVE)

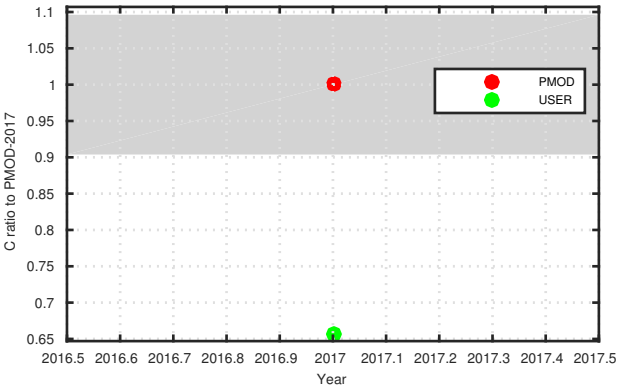

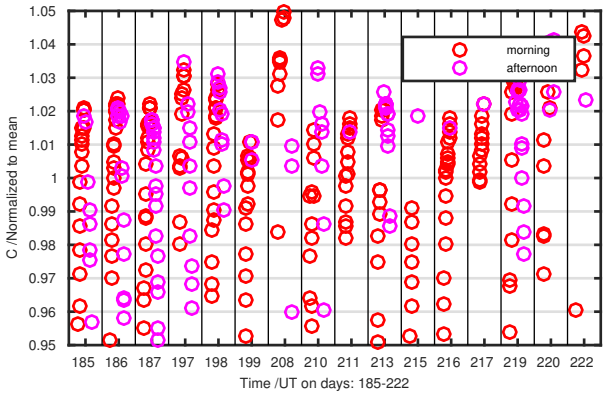

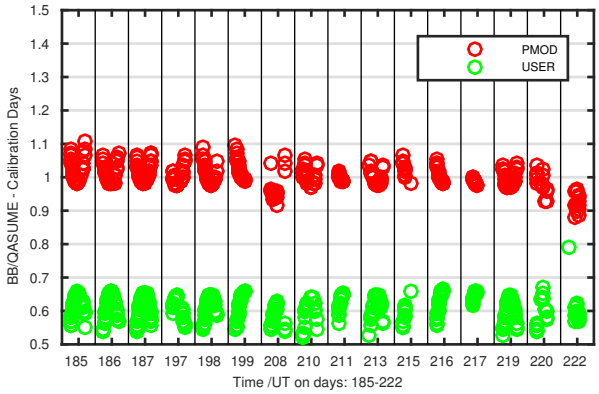

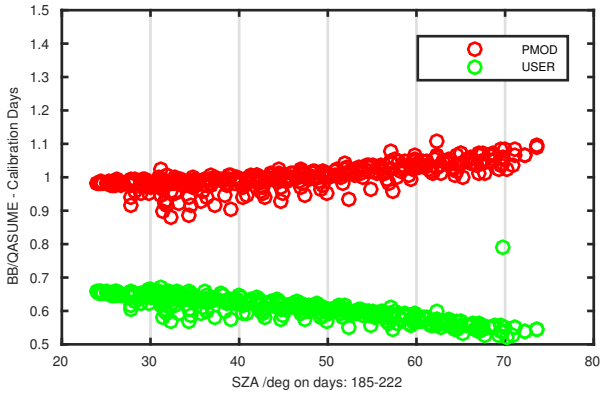

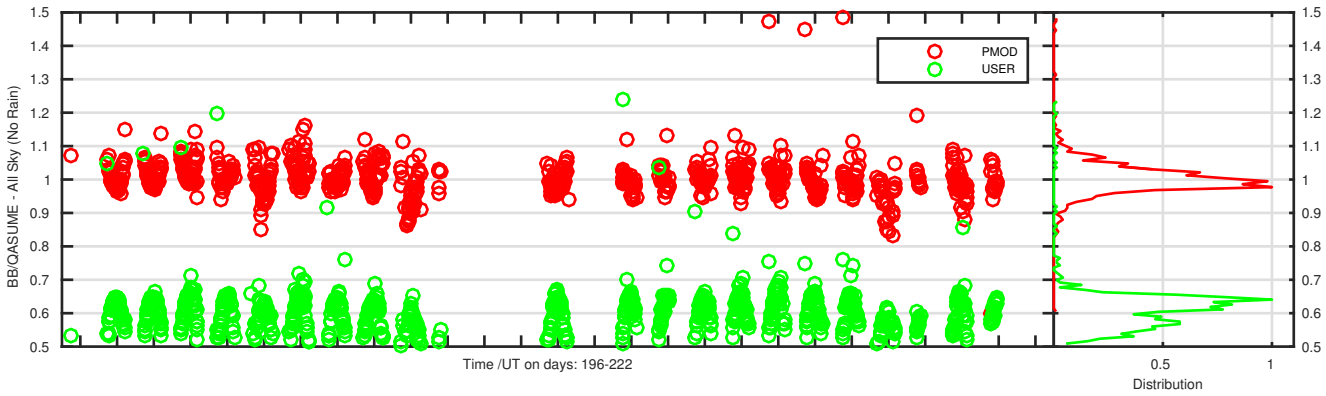

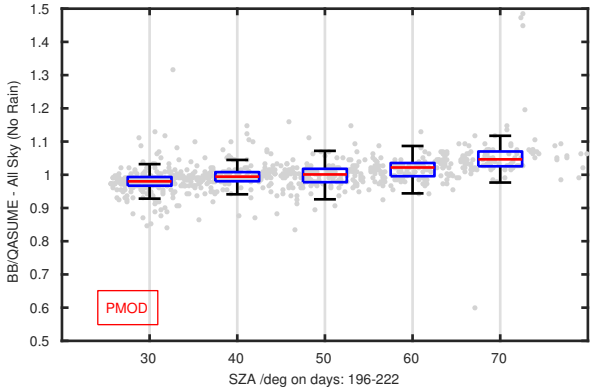

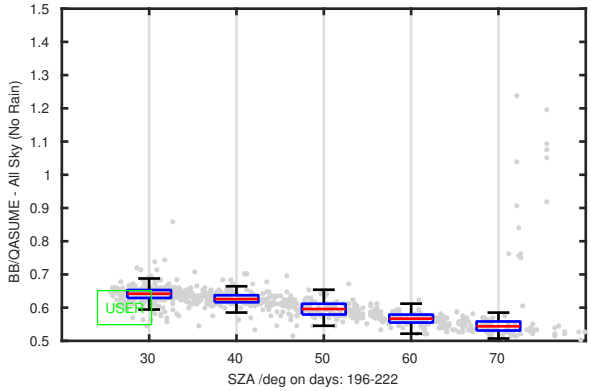

Calibration Results of IS1268817 (UVE)

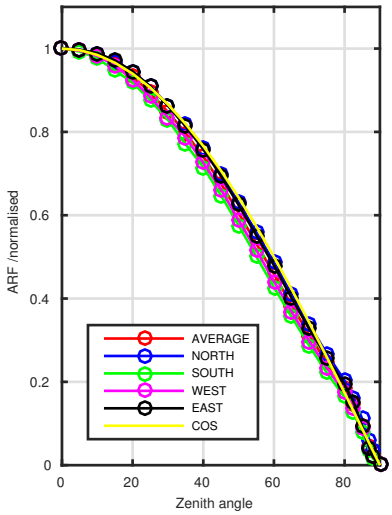

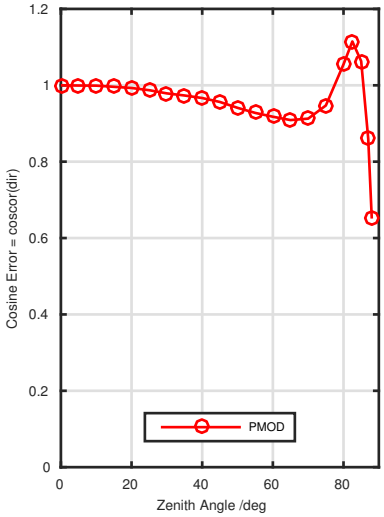

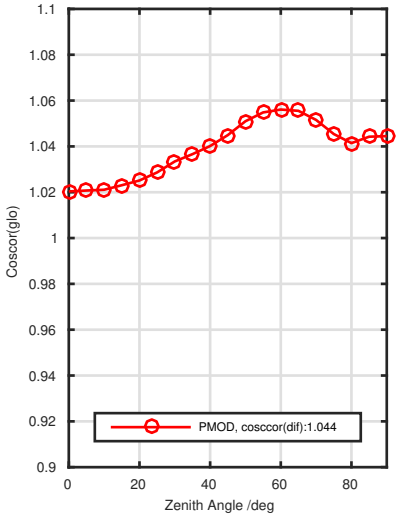

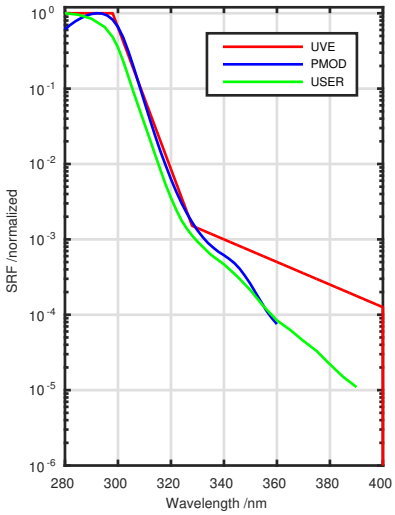

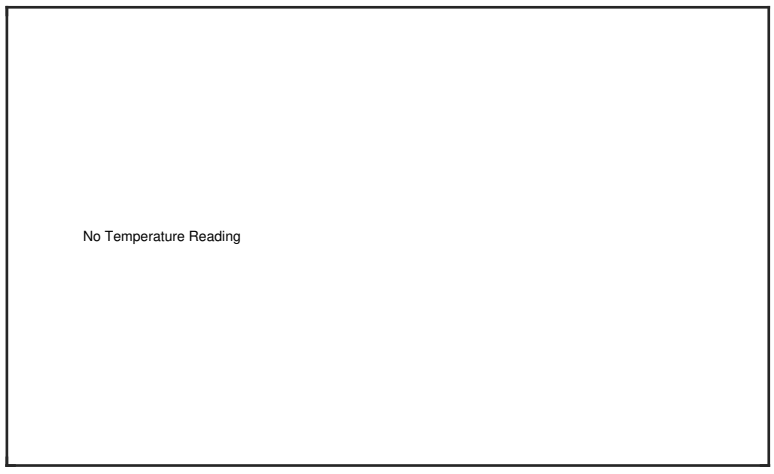

Calibration Matrix fn; Model sdisortREFms2009; f0=1.1610

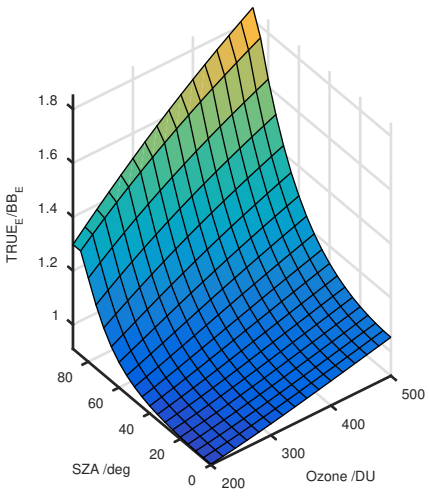

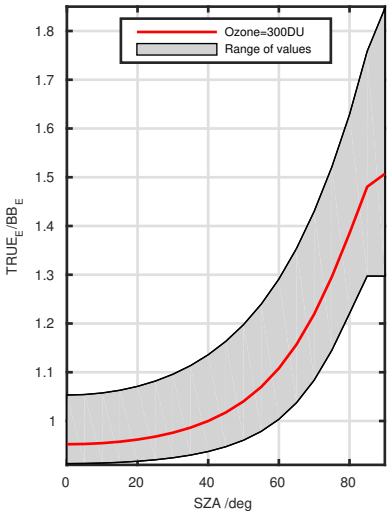

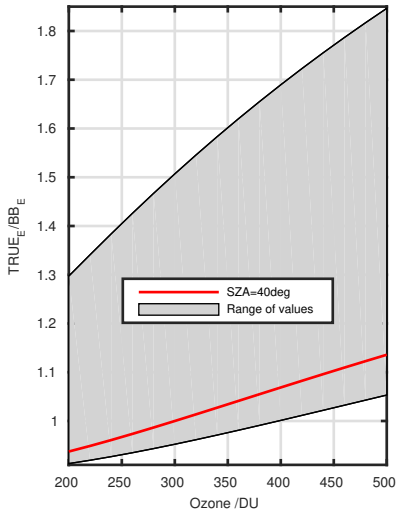

Calibration Results of IS1268817 (UVE)

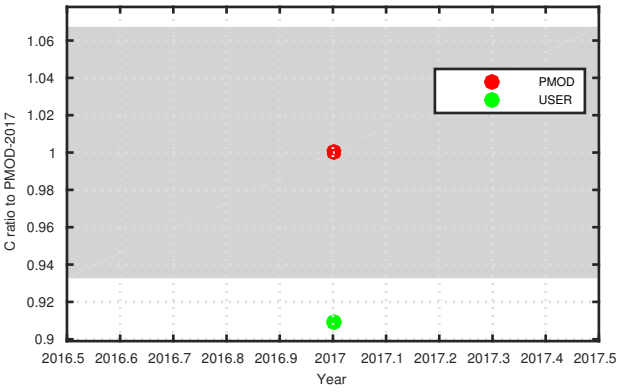

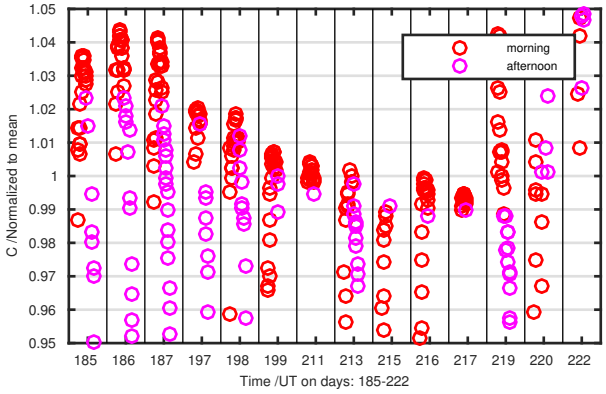

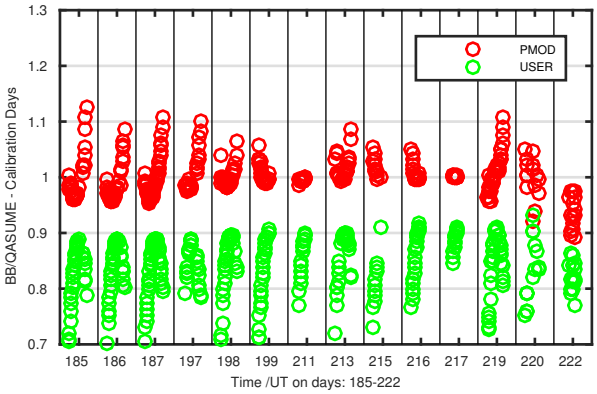

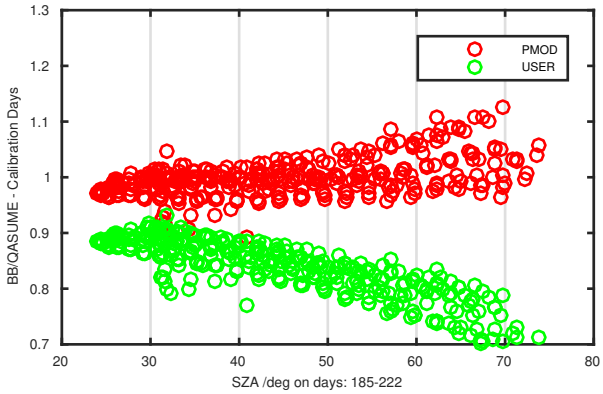

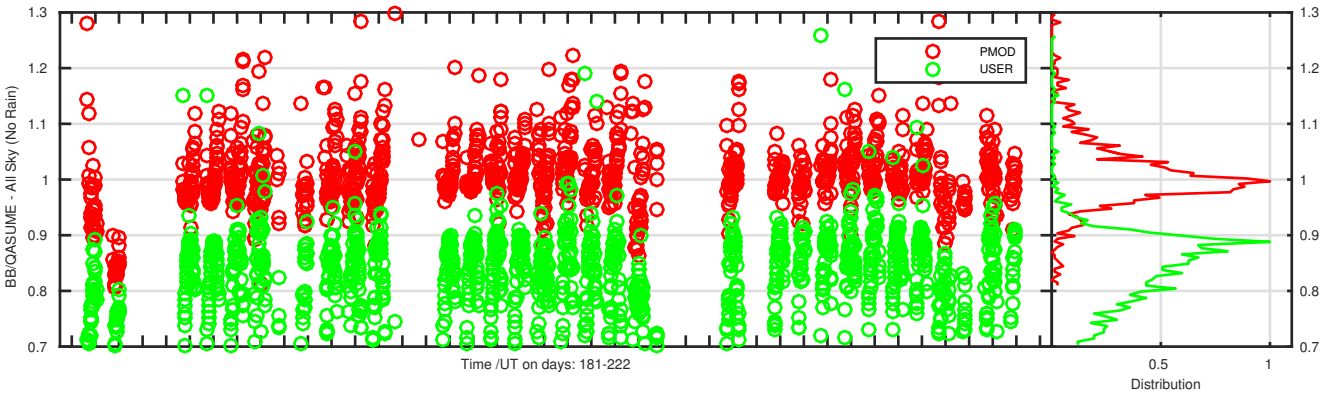

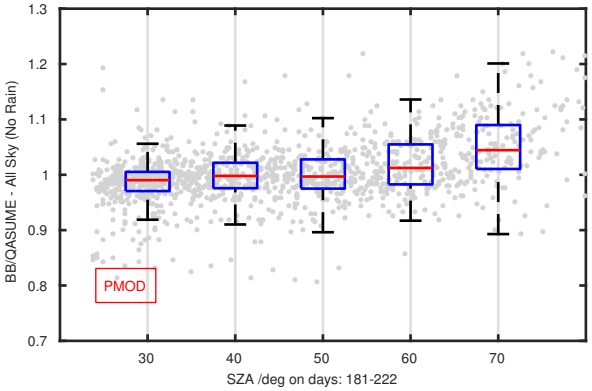

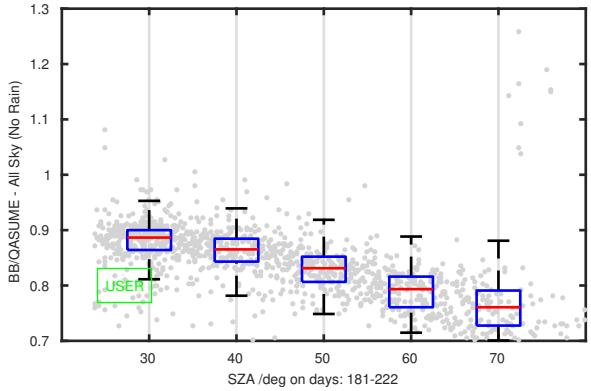

Calibration Results of GENIC586 (UVE)

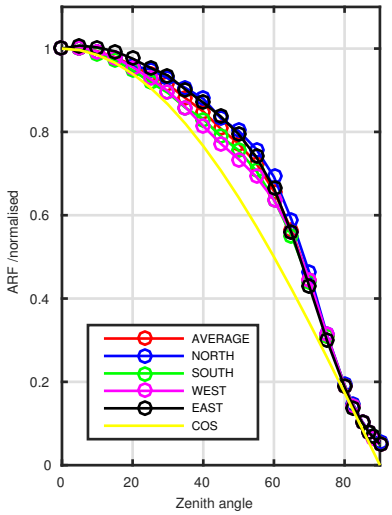

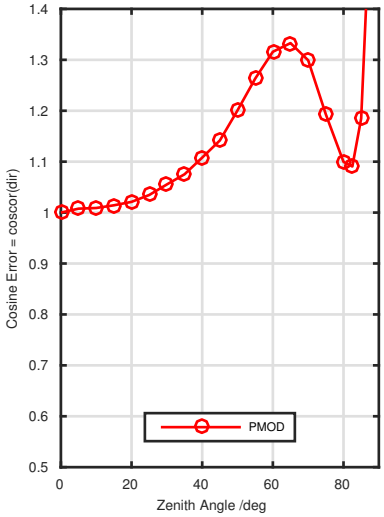

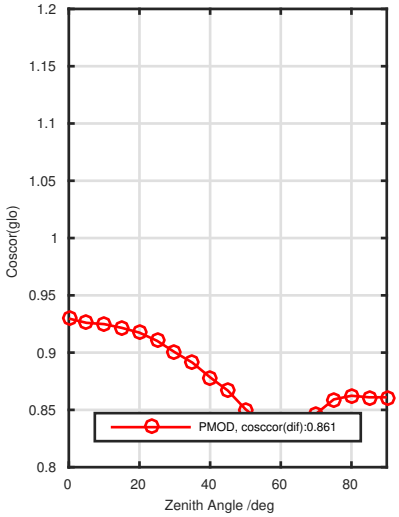

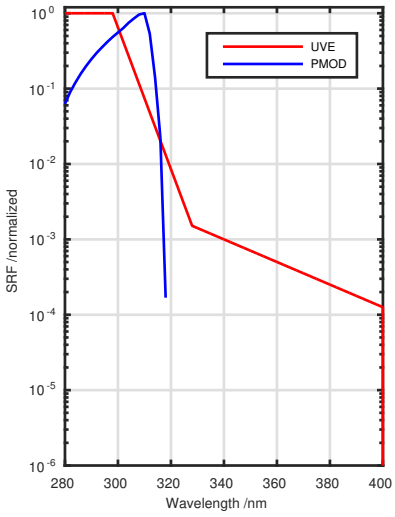

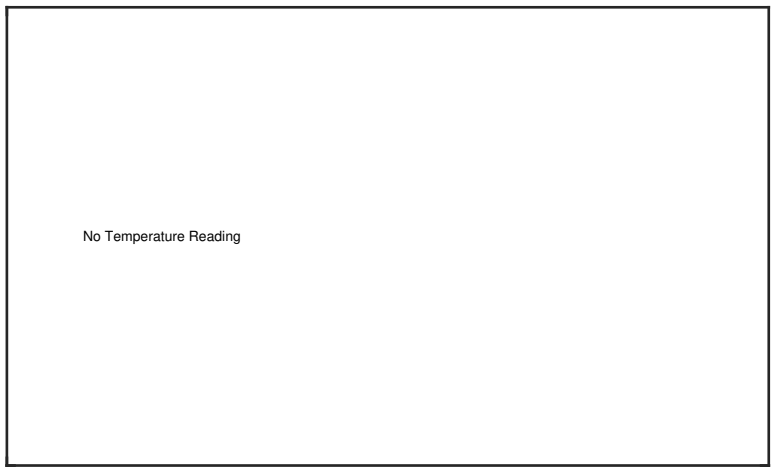

Calibration Matrix fn; Model sdisortREFms2009; f0=0.2271

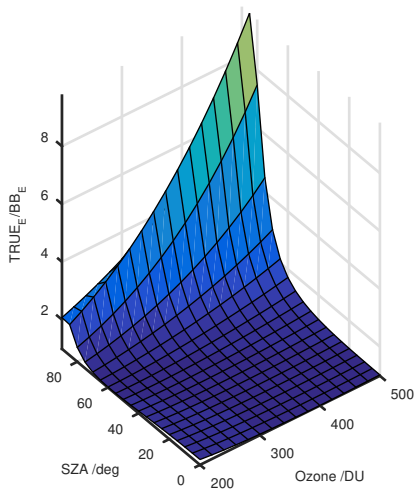

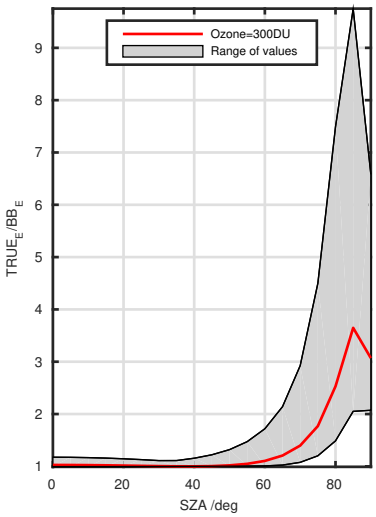

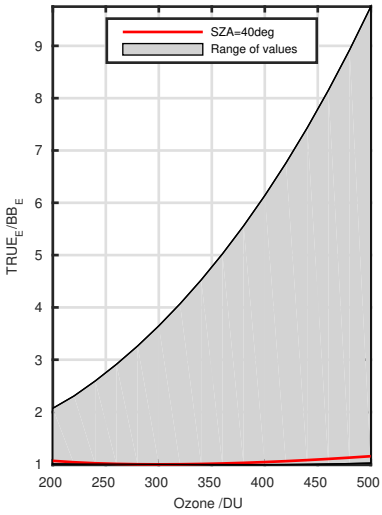

Calibration Results of GENIC586 (UVE)

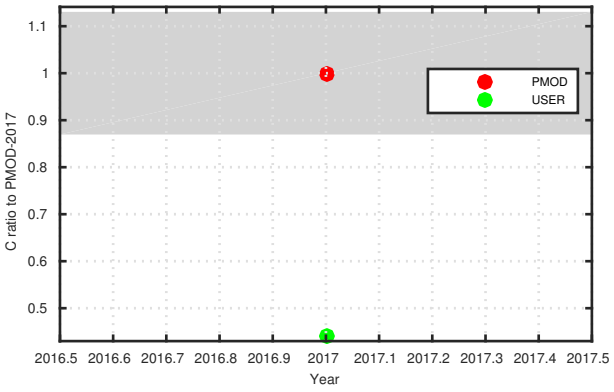

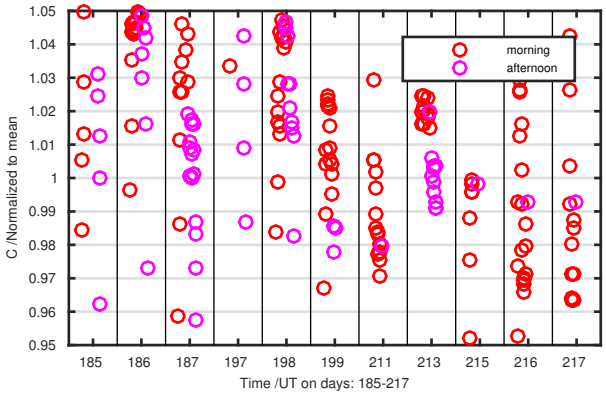

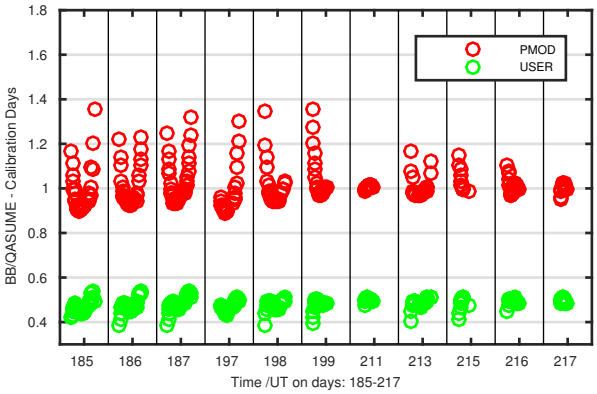

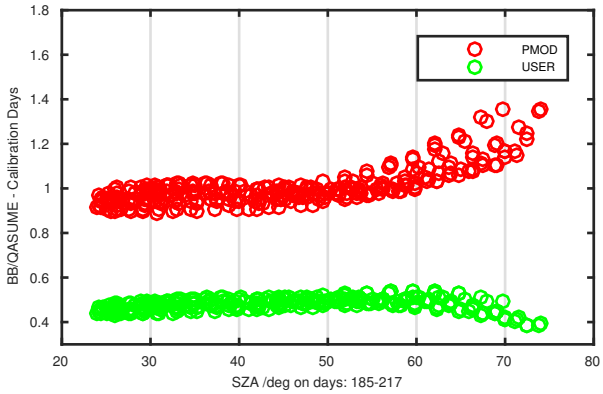

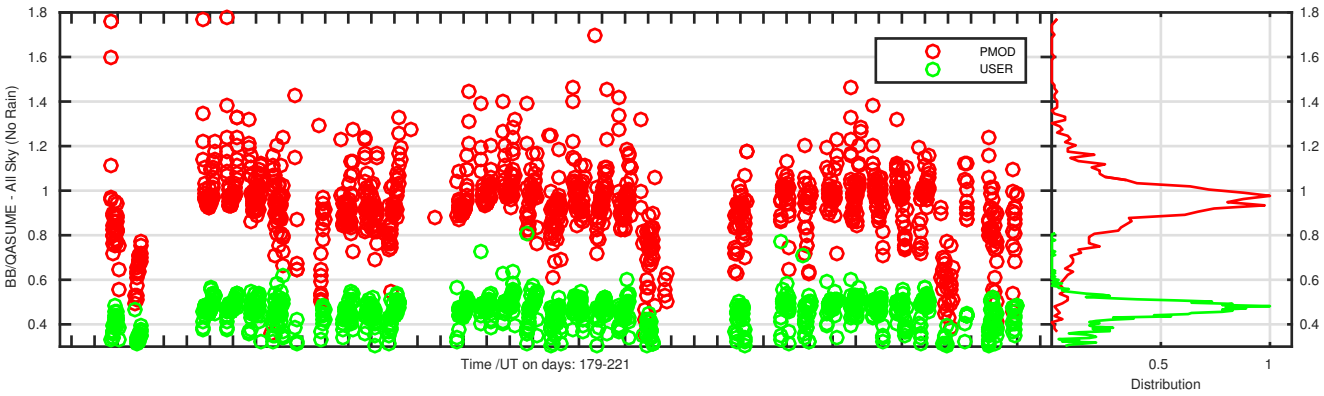

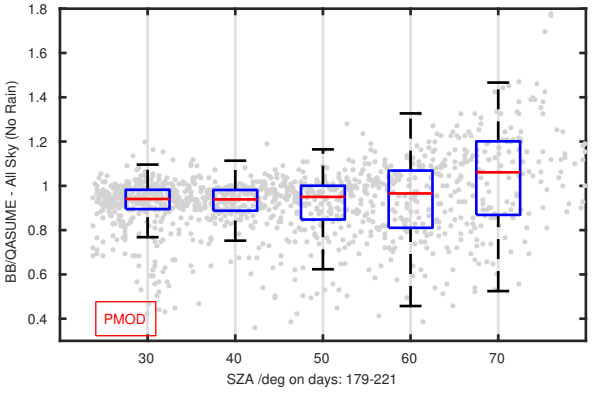

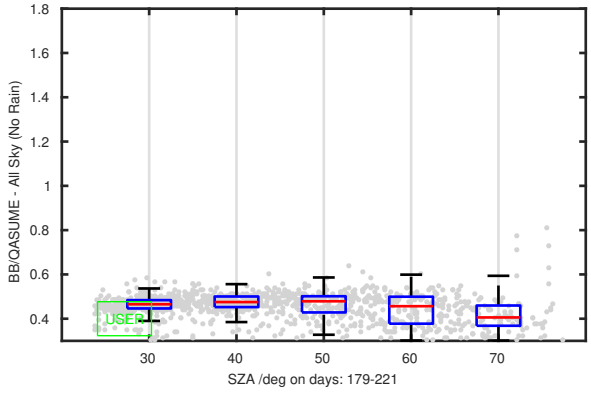

Calibration Results of EPPLEY26919 (UV290385)

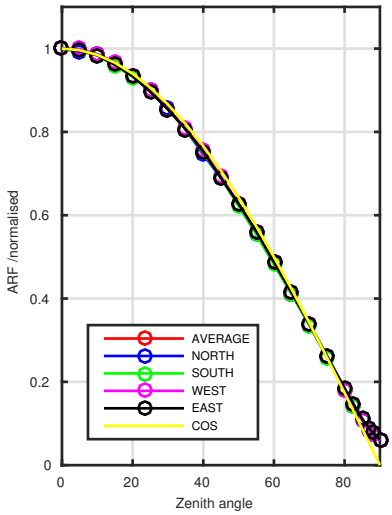

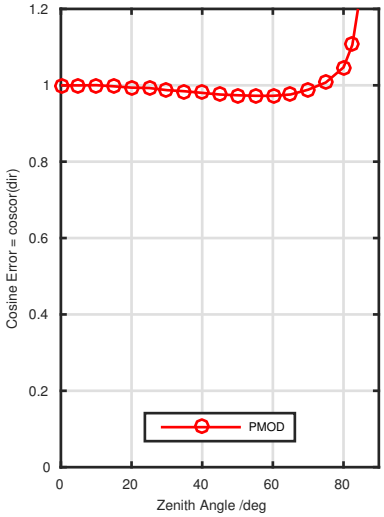

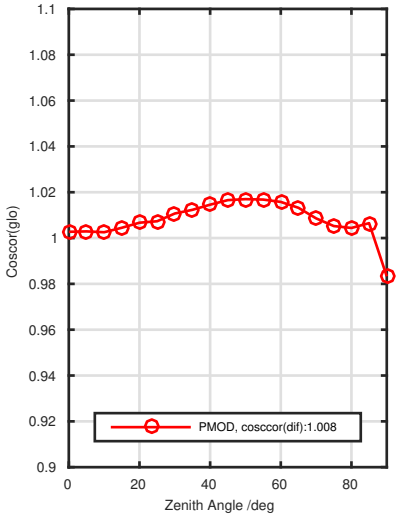

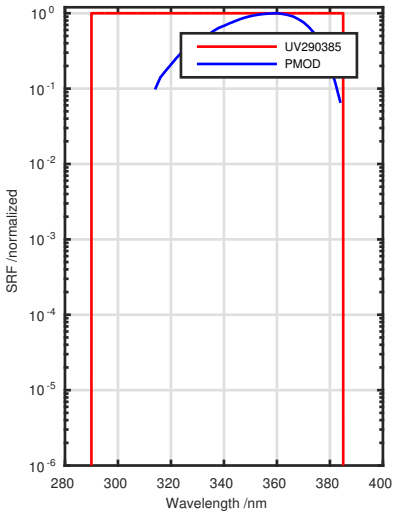

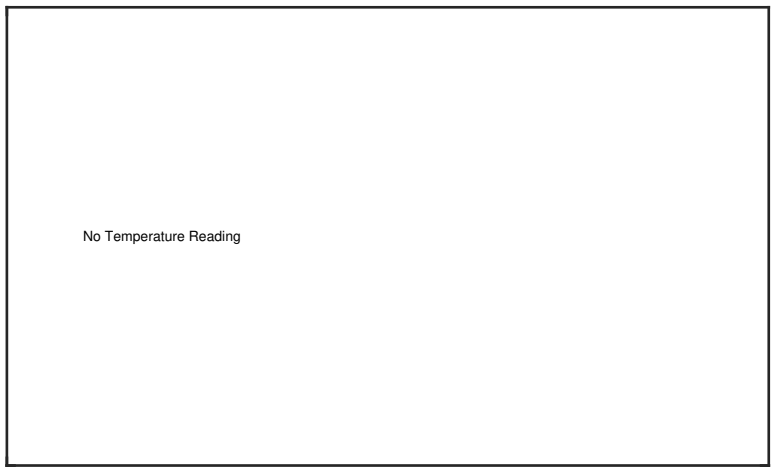

Calibration Matrix fn; Model sdisortREFms2009; f0=1.6392

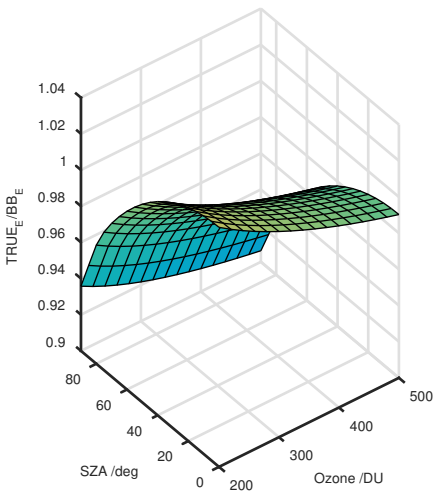

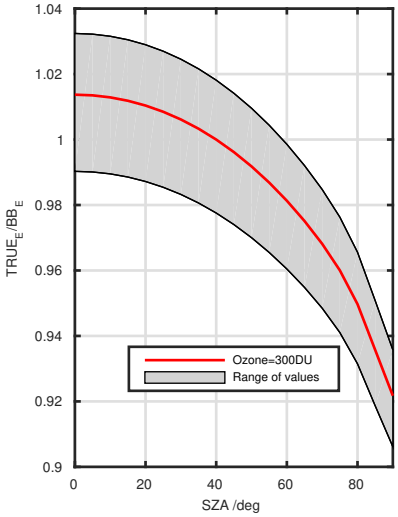

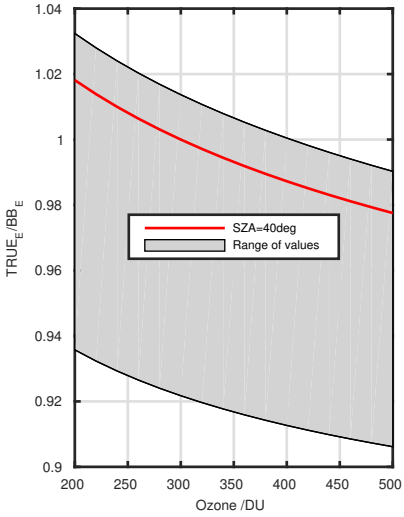

Calibration Results of EPPLEY26919 (UV290385)

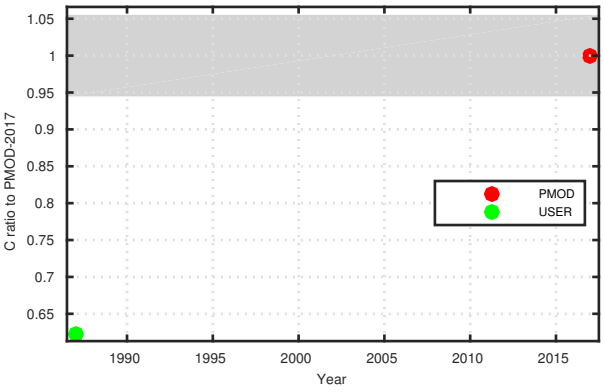

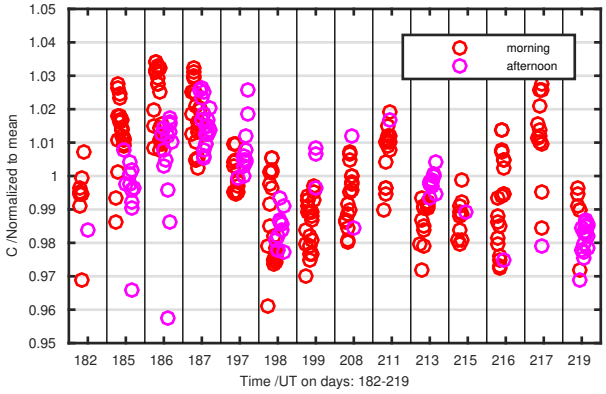

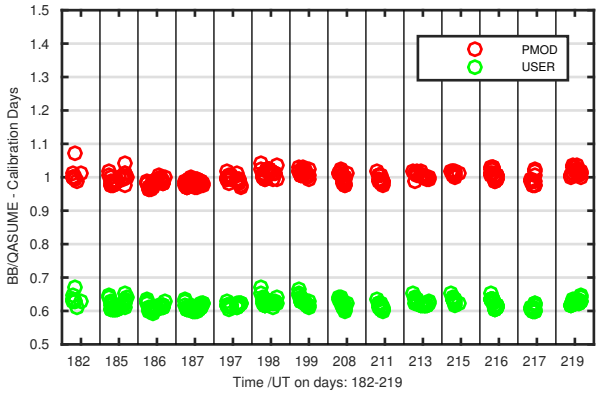

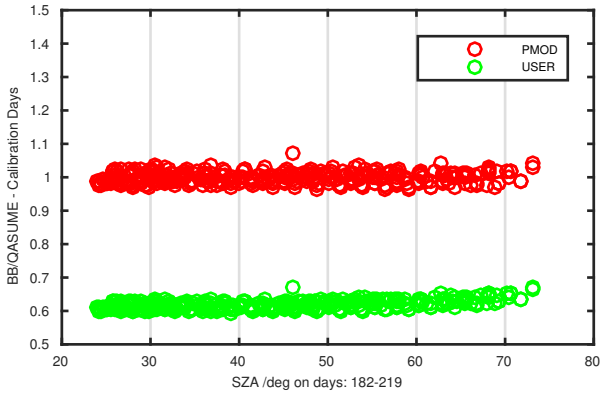

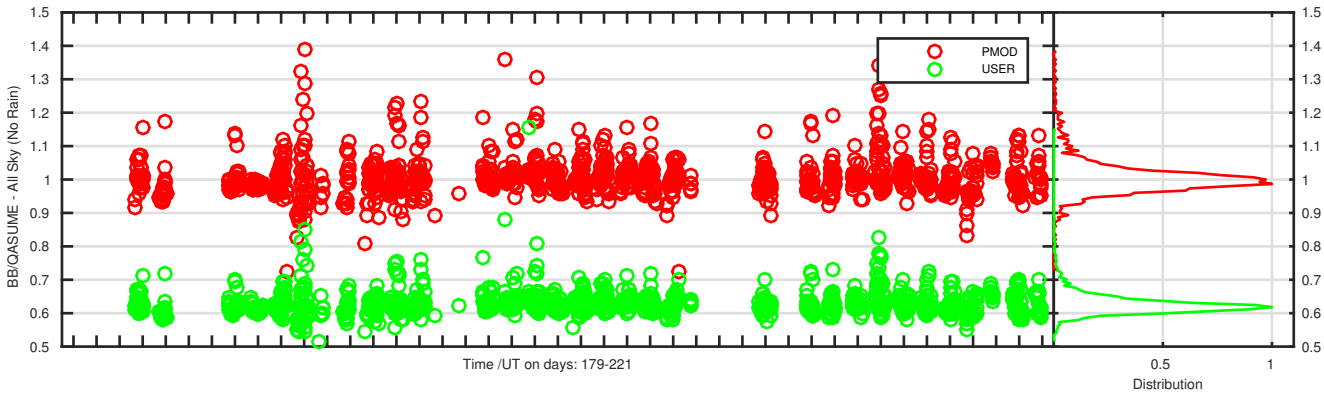

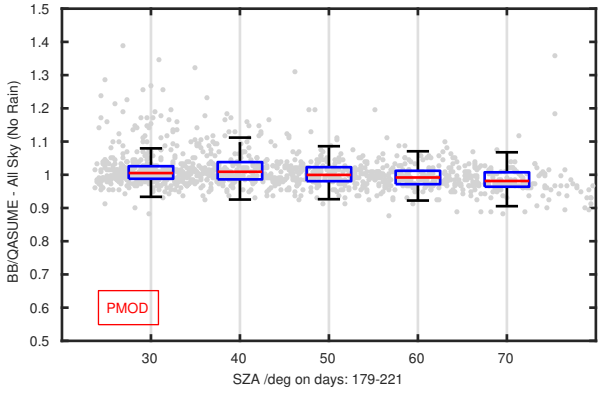

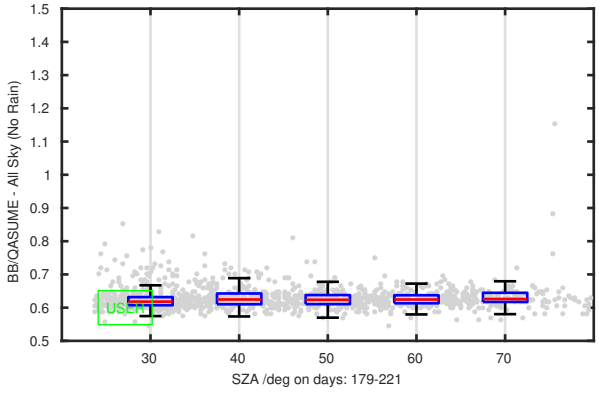

Calibration Results of EKO1113204 (UVE)

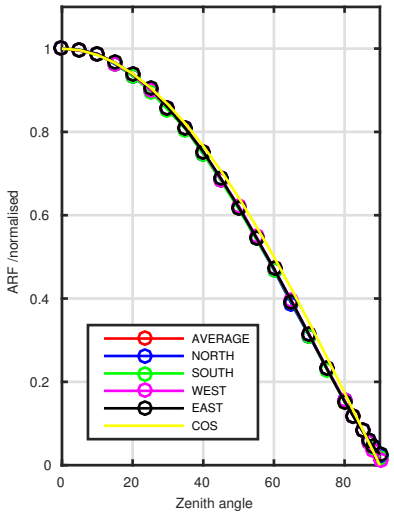

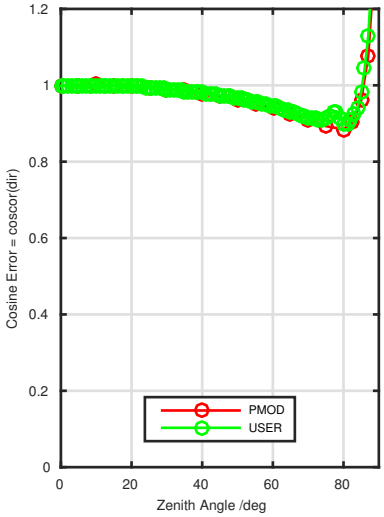

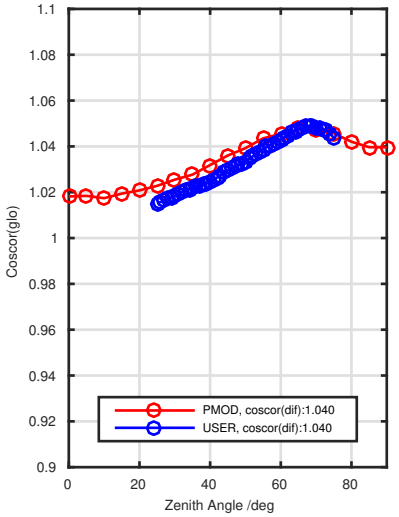

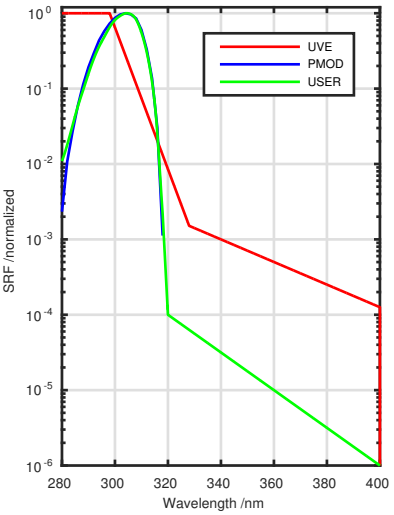

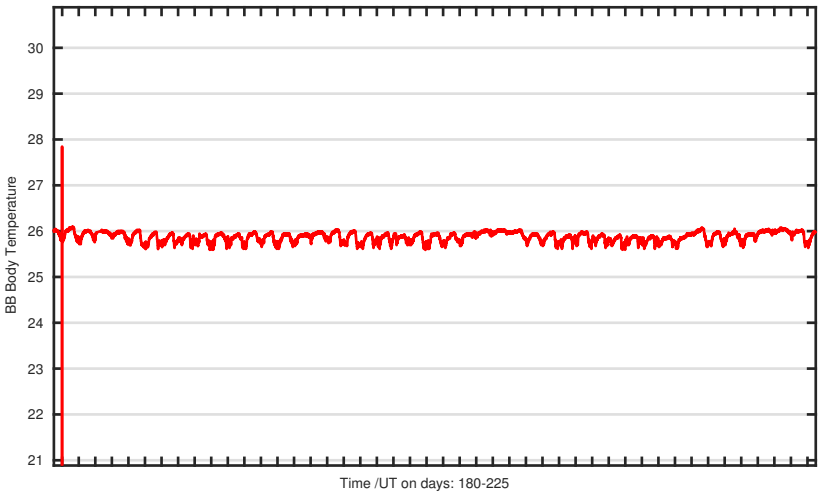

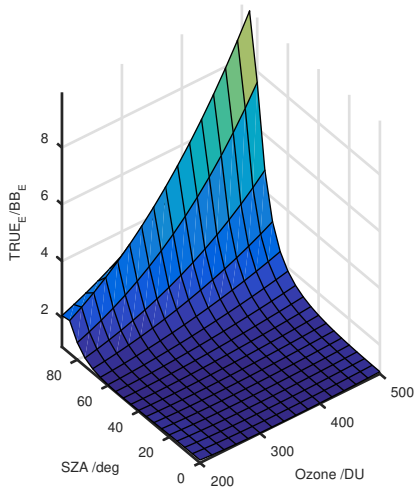

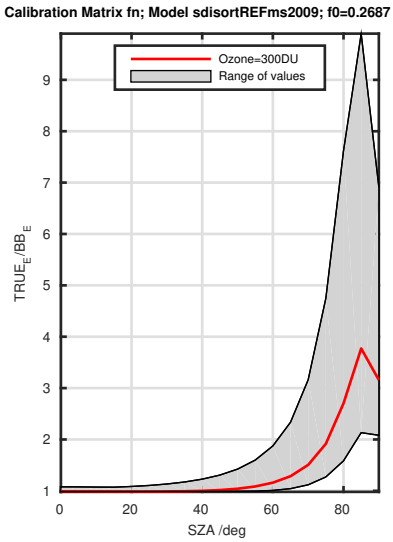

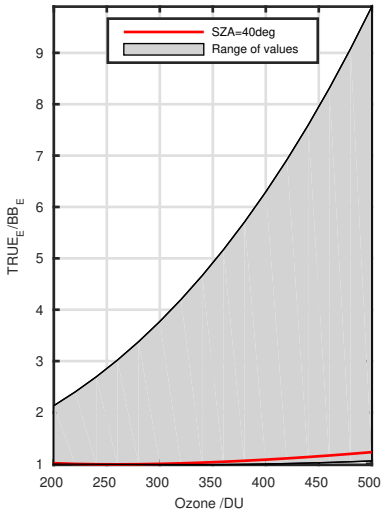

Calibration Results of EKO1113204 (UVE)

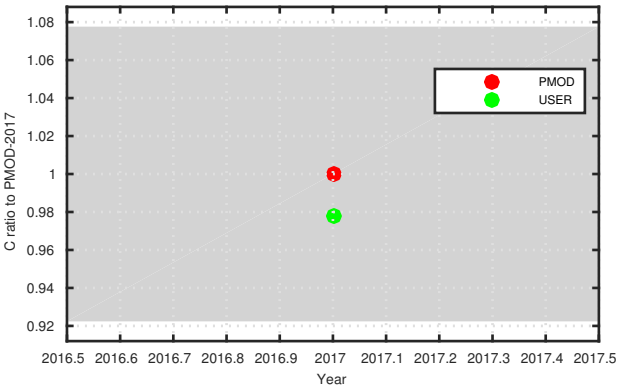

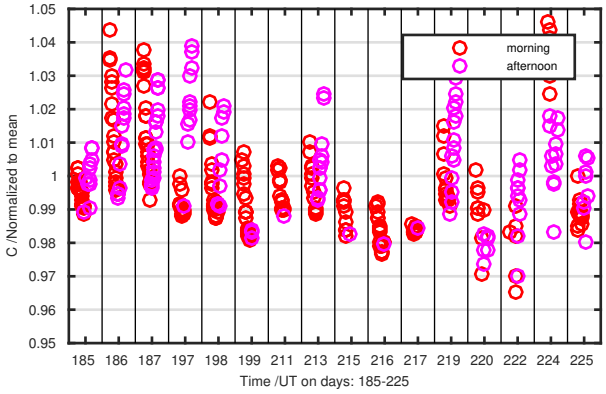

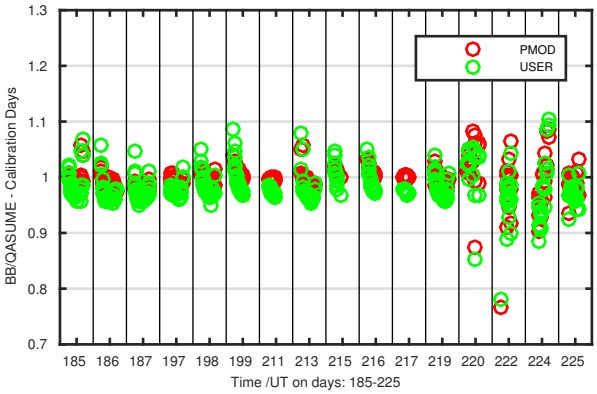

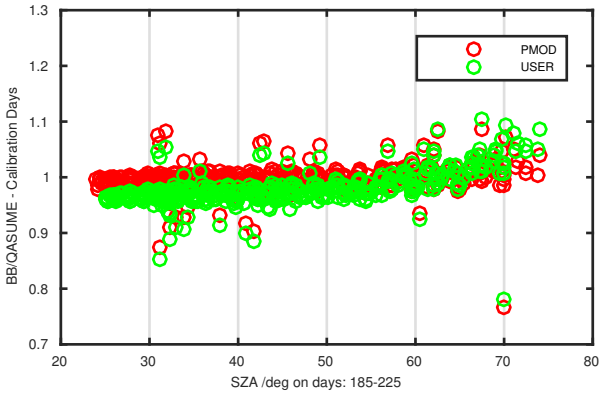

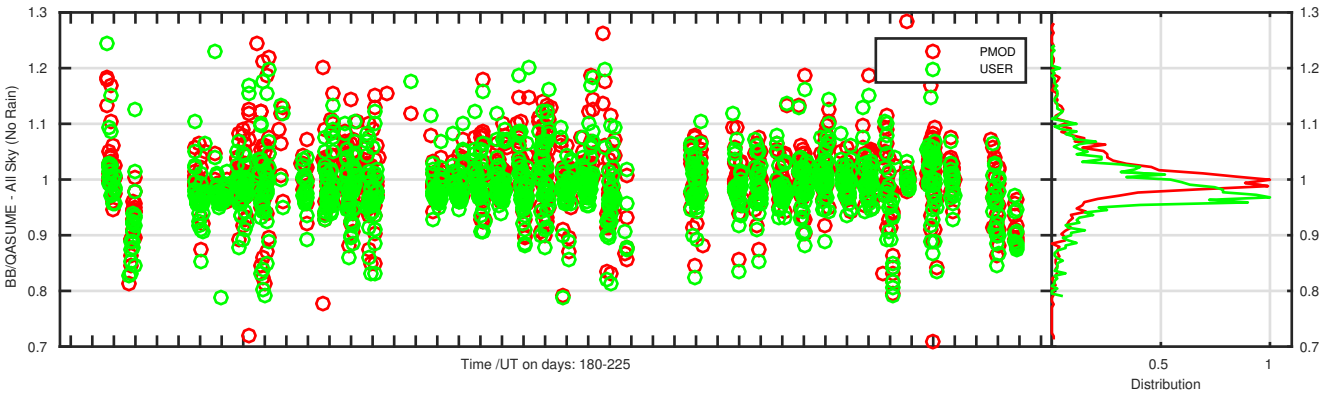

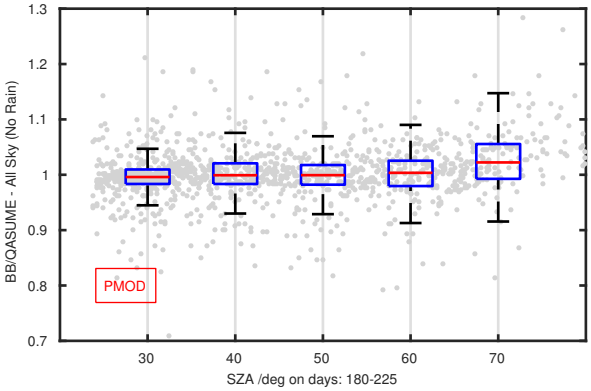

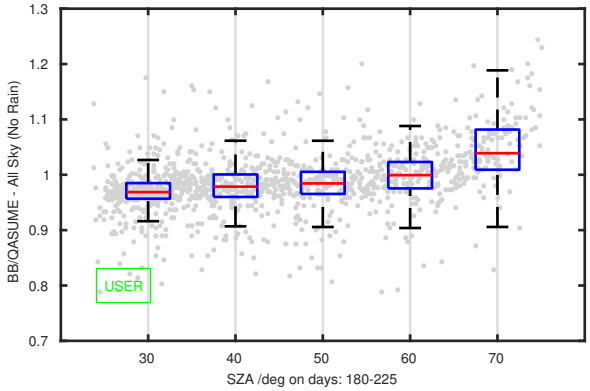

Calibration Results of EKO1700802 (UVB)

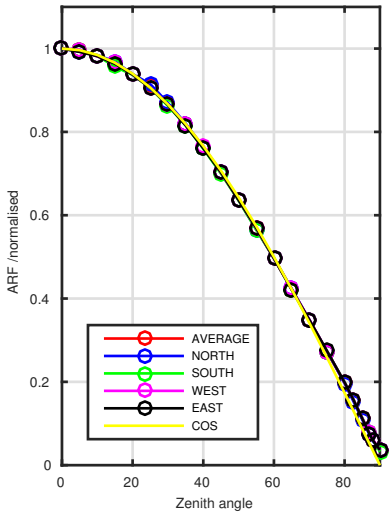

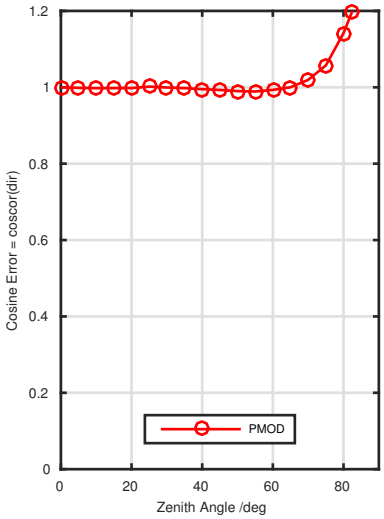

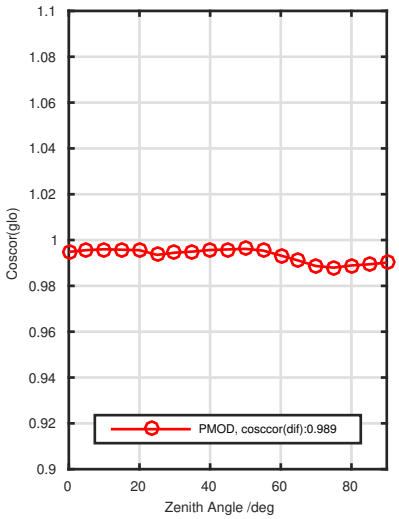

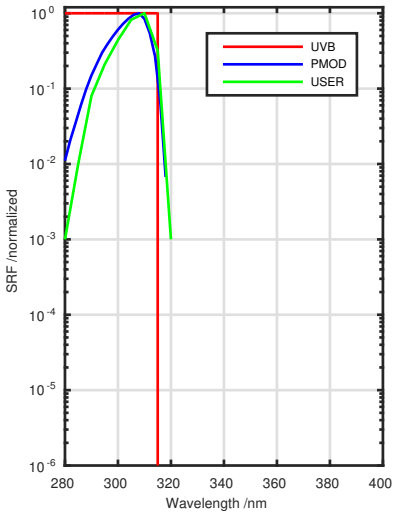

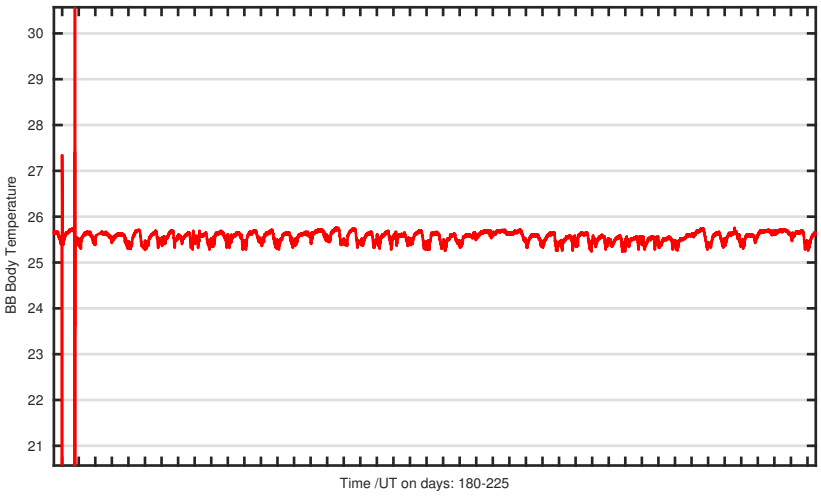

Calibration Matrix fn; Model sdisortREFms2009; f0=1.5770

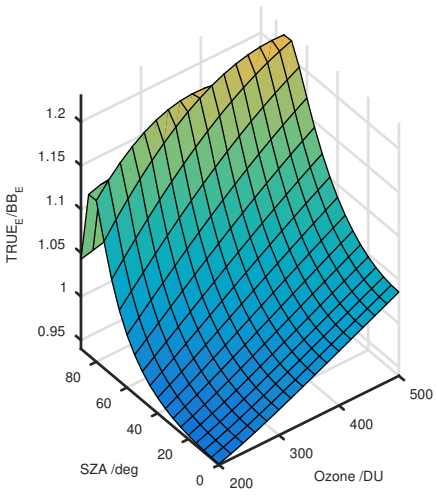

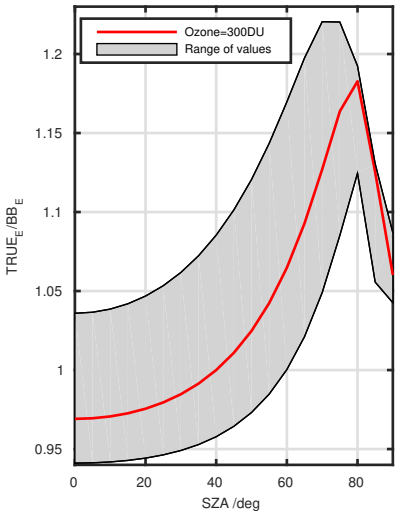

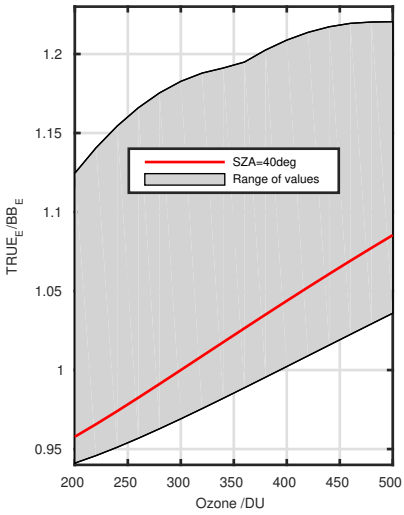

Calibration Results of EKO1700802 (UVB)

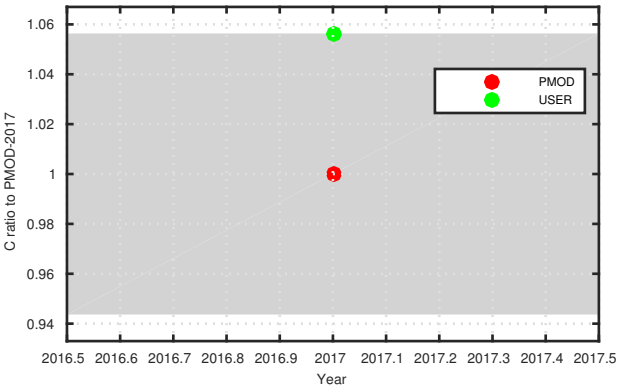

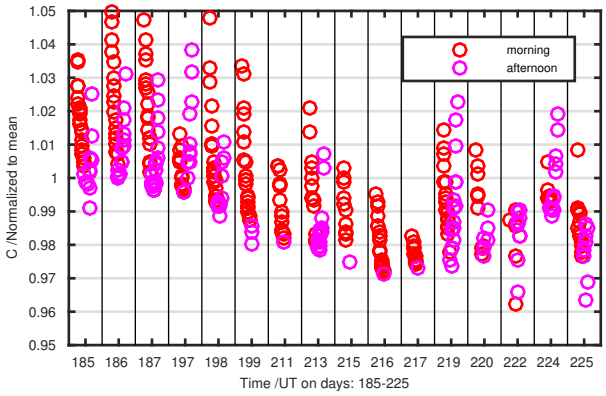

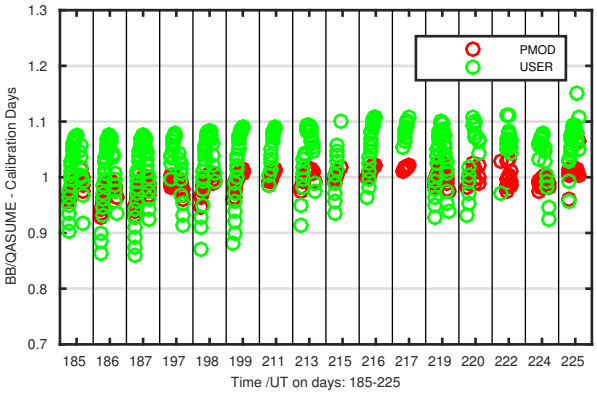

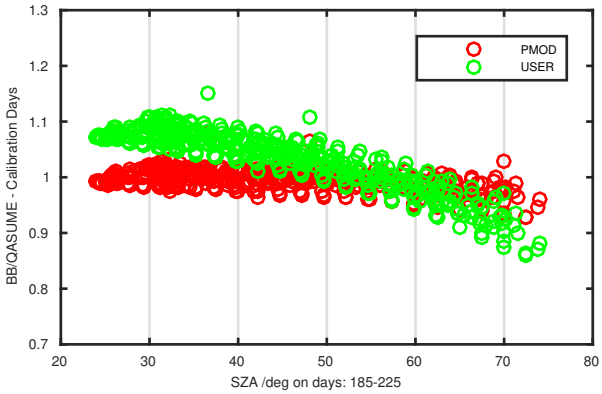

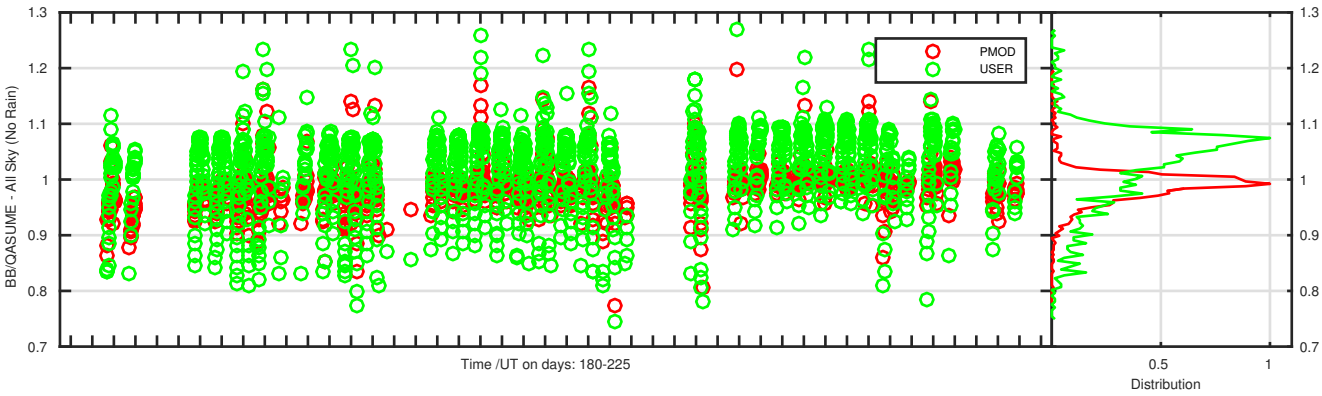

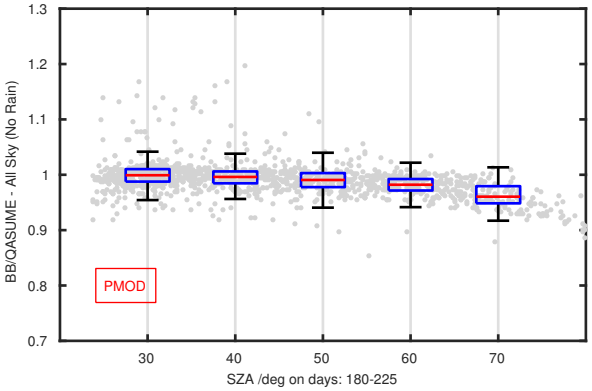

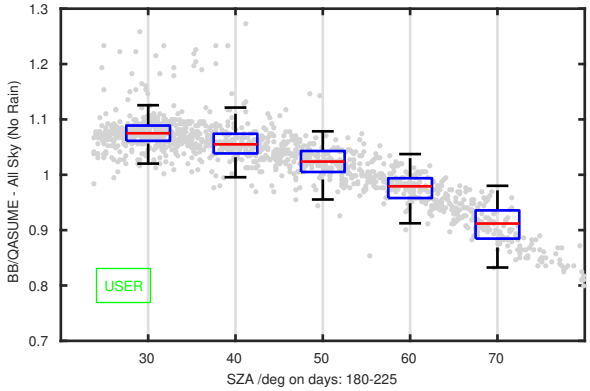

Calibration Results of MS5089 (UVB)

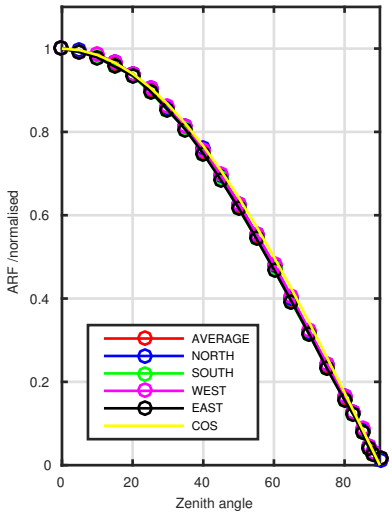

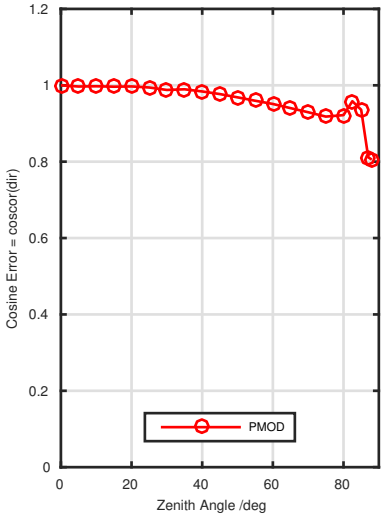

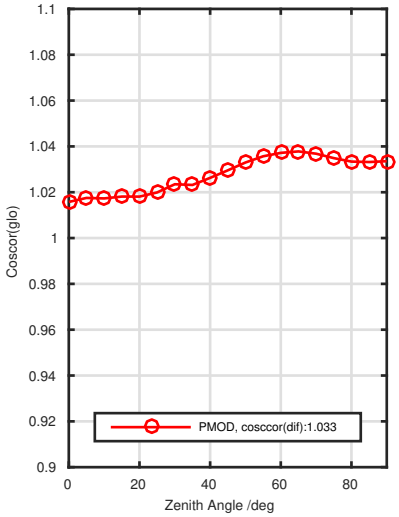

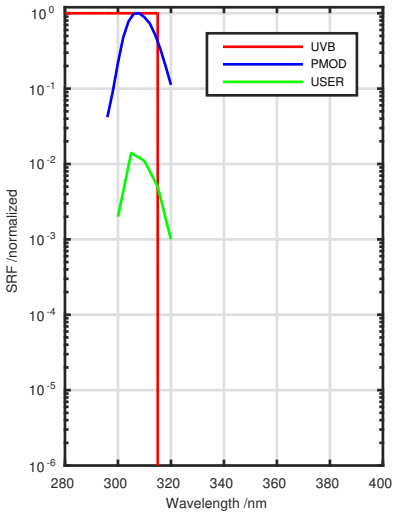

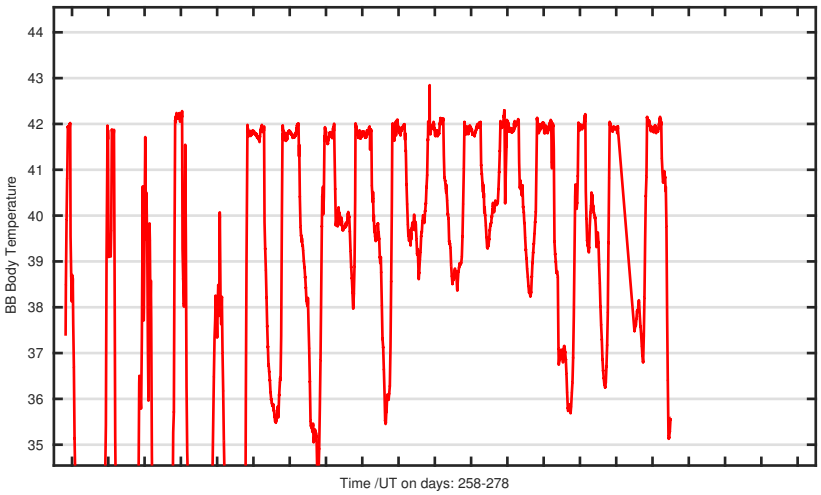

Calibration Matrix fn; Model sdisortREFms2009; f0=0.9418

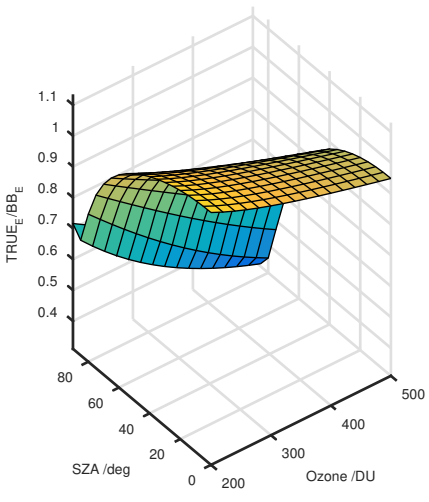

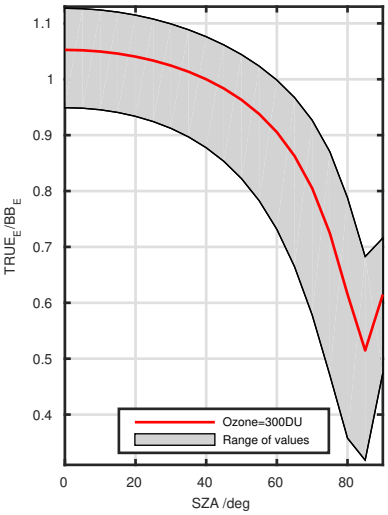

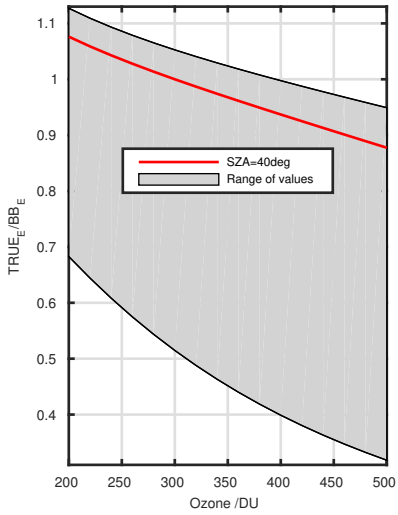
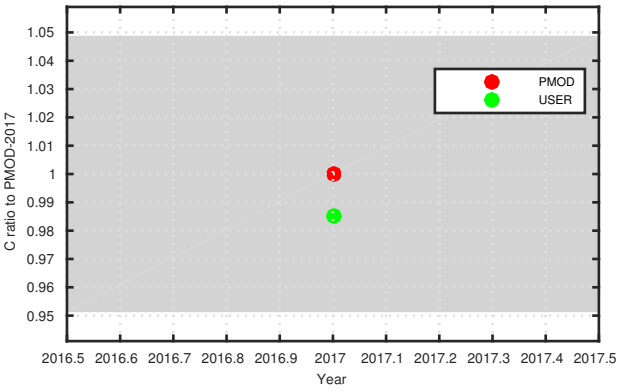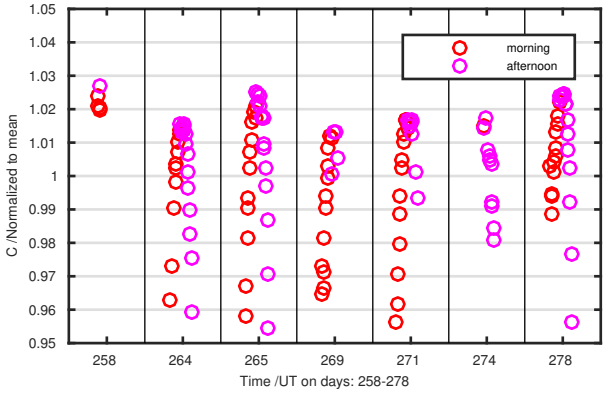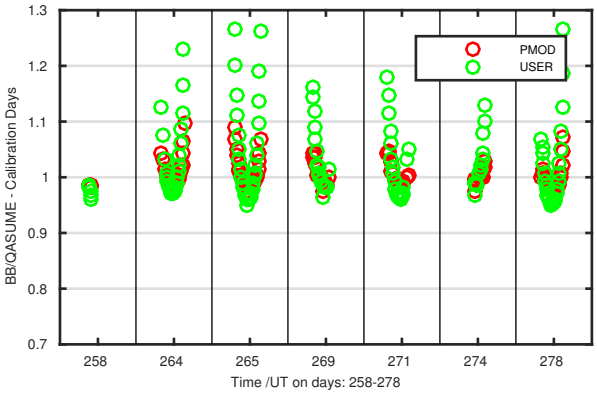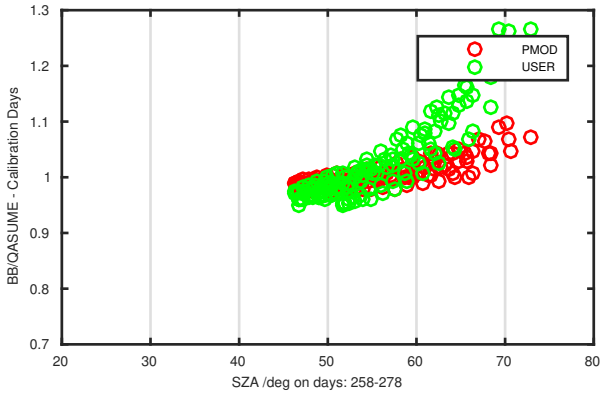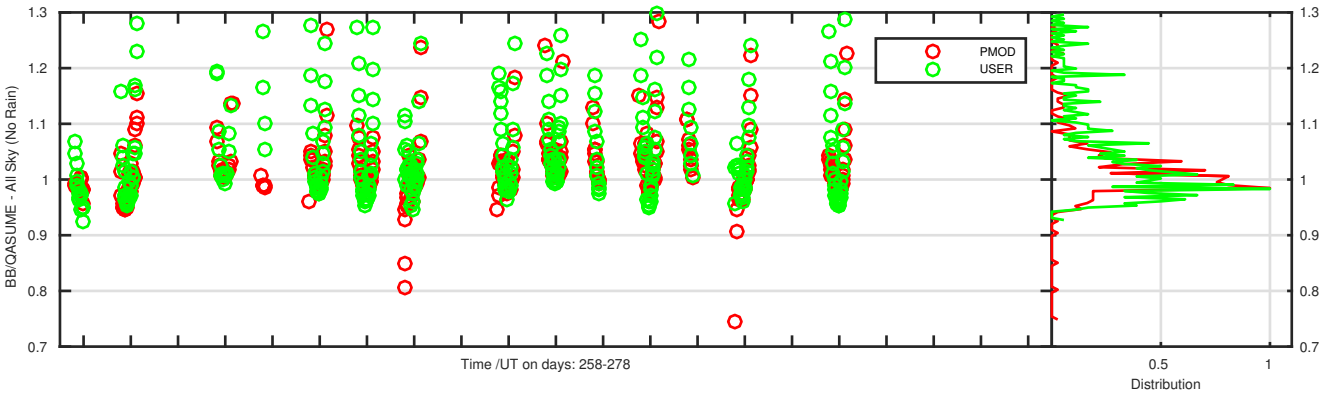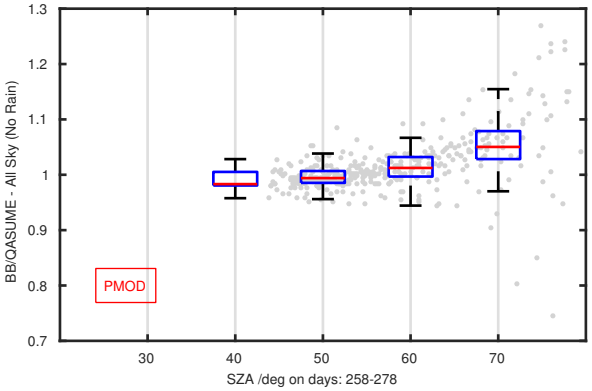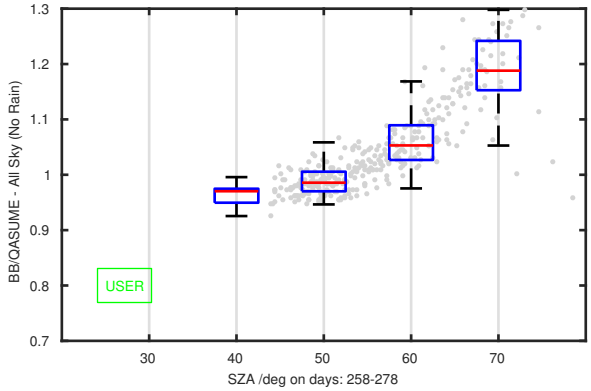
Calibration Results of MS5089 (UVB)